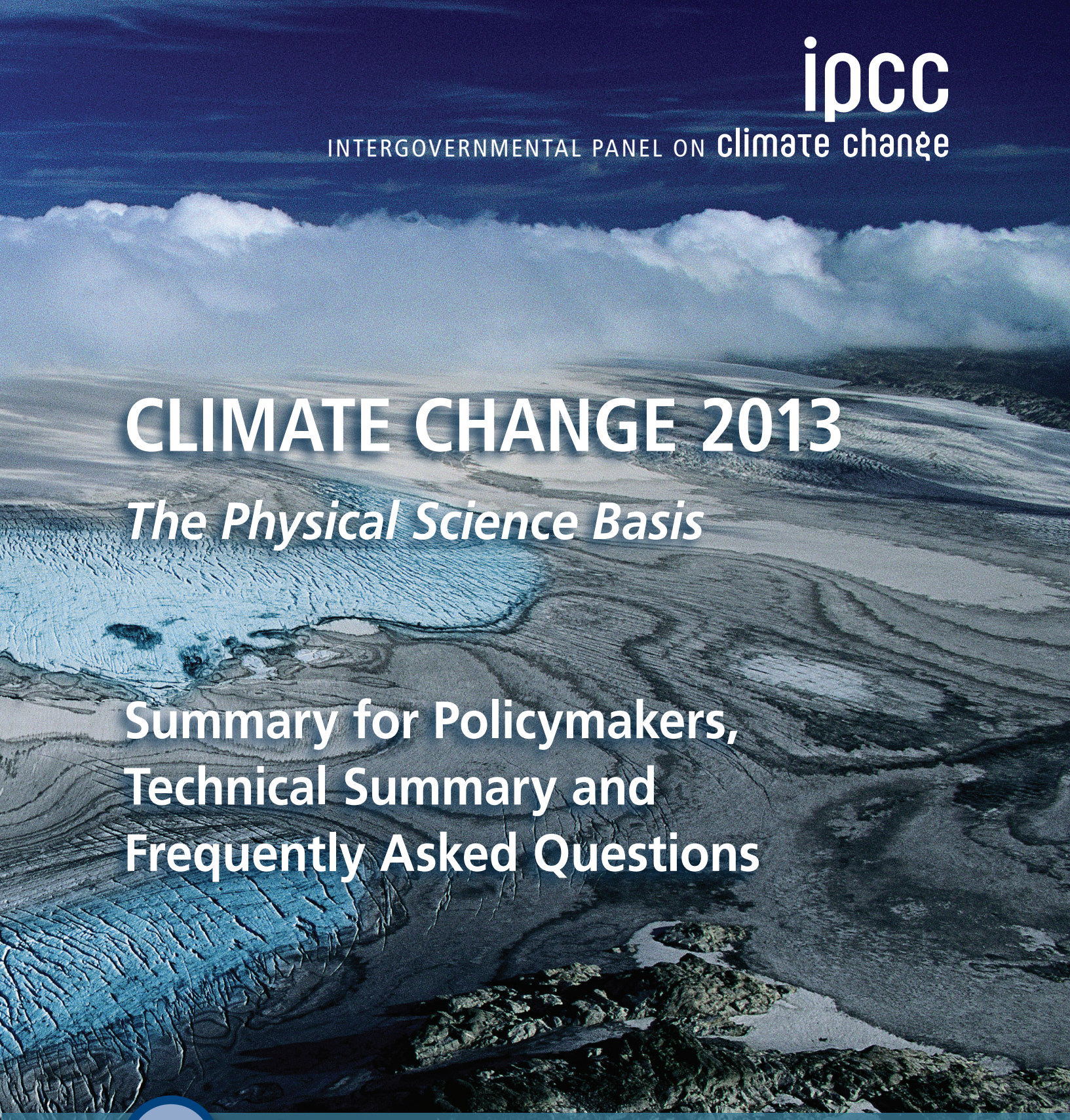

ipcc

INTERGOVERNMENTAL PANEL ON climate change

CLIMATE CHANGE 2013

The Physical Science Basis

Summary for Policymakers, Technical Summary and Frequently Asked Questions

WG I

WORKING GROUP I CONTRIBUTION TO THE
FIFTH ASSESSMENT REPORT OF THE
INTERGOVERNMENTAL PANEL ON CLIMATE CHANGE

WMO UNEP

Climate Change 2013
The Physical Science Basis

Summary for Policymakers

A report of Working Group I of the IPCC

Technical Summary

A report accepted by Working Group I of the IPCC but not approved in detail

and

Frequently Asked Questions

Part of the Working Group I Contribution to the Fifth Assessment Report of the Intergovernmental Panel on Climate Change

Edited by

Thomas F. Stocker
Working Group I Co-Chair
University of Bern

Dahe Qin
Working Group I Co-Chair
China Meteorological Administration

Gian-Kasper Plattner
Director of Science

Melinda M.B. Tignor
Director of Operations

Simon K. Allen
Senior Science Officer

Judith Boschung
Administrative Assistant

Alexander Nauels
Science Assistant

Yu Xia
Science Officer

Vincent Bex
IT Officer

Pauline M. Midgley
Head

Working Group I Technical Support Unit

ISBN 978-92-9169-138-8

Cover photo: Folgefonna glacier on the high plateaus of Sørfjorden, Norway (60°03' N - 6°20' E) © Yann Arthus-Bertrand / Altitude.

Foreword, Preface and Dedication

Foreword

"Climate Change 2013: The Physical Science Basis" presents clear and robust conclusions in a global assessment of climate change science—not the least of which is that the science now shows with 95 percent certainty that human activity is the dominant cause of observed warming since the mid-20th century. The report confirms that warming in the climate system is unequivocal, with many of the observed changes unprecedented over decades to millennia: warming of the atmosphere and the ocean, diminishing snow and ice, rising sea levels and increasing concentrations of greenhouse gases. Each of the last three decades has been successively warmer at the Earth's surface than any preceding decade since 1850.

These and other findings confirm and enhance our scientific understanding of the climate system and the role of greenhouse gas emissions; as such, the report demands the urgent attention of both policymakers and the general public.

As an intergovernmental body jointly established in 1988 by the World Meteorological Organization (WMO) and the United Nations Environment Programme (UNEP), the Intergovernmental Panel on Climate Change (IPCC) has provided policymakers with the most authoritative and objective scientific and technical assessments. Beginning in 1990, this series of IPCC Assessment Reports, Special Reports, Technical Papers, Methodology Reports and other products have become standard works of reference.

This Working Group I contribution to the IPCC's Fifth Assessment Report contains important new scientific knowledge that can be used to produce climate information and services for assisting society to act to address the challenges of climate change. The timing is particularly significant, as this information provides a new impetus, through clear and indisputable physical science, to those negotiators responsible for concluding a new agreement under the United Nations Framework Convention on Climate Change in 2015.

Climate change is a long-term challenge, but one that requires urgent action given the pace and the scale by which greenhouse gases are accumulating in the atmosphere and the risks of a more than 2 degree Celsius temperature rise. Today we need to focus on the fundamentals and on the actions otherwise the risks we run will get higher with every year.

This Working Group I assessment was made possible thanks to the commitment and dedication of many hundreds of experts worldwide, representing a wide range of disciplines. WMO and UNEP are proud that so many of the experts belong to their communities and networks. We express our deep gratitude to all authors, review editors and expert reviewers for devoting their knowledge, expertise and time. We would like to thank the staff of the Working Group I Technical Support Unit and the IPCC Secretariat for their dedication.

We are also grateful to the governments that supported their scientists' participation in developing this report and that contributed to the IPCC Trust Fund to provide for the essential participation of experts from developing countries and countries with economies in transition. We would like to express our appreciation to the government of Italy for hosting the scoping meeting for the IPCC's Fifth Assessment Report, to the governments of China, France, Morocco and Australia for hosting drafting sessions of the Working Group I contribution and to the government of Sweden for hosting the Twelfth Session of Working Group I in Stockholm for approval of the Working Group I Report. The generous financial support by the government of Switzerland, and the logistical support by the University of Bern (Switzerland), enabled the smooth operation of the Working Group I Technical Support Unit. This is gratefully acknowledged.

We would particularly like to thank Dr. Rajendra Pachauri, Chairman of the IPCC, for his direction and guidance of the IPCC and we express our deep gratitude to Professor Qin Dahe and Professor Thomas Stocker, the Co-Chairs of Working Group I for their tireless leadership throughout the development and production of this report.

M. Jarraud
Secretary-General
World Meteorological Organization

A. Steiner
Executive Director
United Nations Environment Programme

Preface

The Working Group I contribution to the Fifth Assessment Report of the Intergovernmental Panel on Climate Change (IPCC) provides a comprehensive assessment of the physical science basis of climate change. It builds upon the Working Group I contribution to the IPCC's Fourth Assessment Report in 2007 and incorporates subsequent new findings from the Special Report on Managing the Risks of Extreme Events and Disasters to Advance Climate Change Adaptation, as well as from research published in the extensive scientific and technical literature. The assessment considers new evidence of past, present and projected future climate change based on many independent scientific analyses from observations of the climate system, paleoclimate archives, theoretical studies of climate processes and simulations using climate models.

Scope of the Report

During the process of scoping and approving the outline of its Fifth Assessment Report, the IPCC focussed on those aspects of the current understanding of the science of climate change that were judged to be most relevant to policymakers.

In this report, Working Group I has extended coverage of future climate change compared to earlier reports by assessing near-term projections and predictability as well as long-term projections and irreversibility in two separate chapters. Following the decisions made by the Panel during the scoping and outline approval, a set of new scenarios, the Representative Concentration Pathways, are used across all three Working Groups for projections of climate change over the 21st century. The coverage of regional information in the Working Group I report is expanded by specifically assessing climate phenomena such as monsoon systems and their relevance to future climate change in the regions.

The Working Group I Report is an assessment, not a review or a text book of climate science, and is based on the published scientific and technical literature available up to 15 March 2013. Underlying all aspects of the report is a strong commitment to assessing the science comprehensively, without bias and in a way that is relevant to policy but not policy prescriptive.

Structure of the Report

This report consists of a short Summary for Policymakers, a longer Technical Summary and fourteen thematic chapters plus annexes. An innovation in this Working Group I assessment is the Atlas of Global and Regional Climate Projections (Annex I) containing time series and maps of temperature and precipitation projections for 35 regions of the world, which enhances accessibility for stakeholders and users.

The Summary for Policymakers and Technical Summary of this report follow a parallel structure and each includes cross-references to the chapter and section where the material being summarised can be found in the underlying report. In this way, these summary components of the report provide a road-map to the contents of the entire report and a traceable account of every major finding.

In order to facilitate the accessibility of the findings of the Working Group I assessment for a wide readership and to enhance their usability for stakeholders, each section of the Summary for Policymakers has a highlighted headline statement. Taken together, these 19 headline statements provide an overarching summary in simple and quotable language that is supported by the scientists and approved by the member governments of the IPCC. Another innovative feature of this report is the presentation of Thematic Focus Elements in the Technical Summary that provide end to end assessments of important cross-cutting issues in the physical science basis of climate change.

Introduction (Chapter 1): This chapter provides information on the progress in climate change science since the First Assessment Report of the IPCC in 1990 and gives an overview of key concepts, indicators of climate change, the treatment of uncertainties and advances in measurement and modelling capabilities. This includes a description of the future scenarios and in particular the Representative Concentration Pathway scenarios used across all Working Groups for the IPCC's Fifth Assessment Report.

Observations and Paleoclimate Information (Chapters 2, 3, 4, 5): These chapters assess information from all climate system components on climate variability and change as obtained from instrumental records and climate archives. They cover all relevant aspects of the atmosphere including the stratosphere, the land surface, the oceans and the cryosphere. Timescales from days to decades (Chapters 2, 3 and 4) and from centuries to many millennia (Chapter 5) are considered.

Process Understanding (Chapters 6 and 7): These chapters cover all relevant aspects from observations and process understanding to projections from global to regional scales for two key topics. Chapter 6 covers the carbon cycle and its interactions with other biogeochemical cycles, in particular the nitrogen cycle, as well as feedbacks on the climate system. For the first time, there is a chapter dedicated to the assessment of the physical science basis of clouds and aerosols, their interactions and chemistry, and the role of water vapour, as well as their role in feedbacks on the climate system (Chapter 7).

From Forcing to Attribution of Climate Change (Chapters 8, 9, 10): All the information on the different drivers (natural and anthropogenic) of climate change is collected, expressed in terms of Radiative Forcing and assessed in Chapter 8. In Chapter 9, the hierarchy of climate models used in simulating past and present climate change is assessed and evaluated against observations and paleoclimate reconstructions.

Information regarding detection of changes on global to regional scales and their attribution to the increase in anthropogenic greenhouse gases is assessed in Chapter 10.

Future Climate Change, Predictability and Irreversibility (Chapters 11 and 12): These chapters assess projections of future climate change derived from climate models on time scales from decades to centuries at both global and regional scales, including mean changes, variability and extremes. Fundamental questions related to the predictability of climate as well as long term climate change, climate change commitments and inertia in the climate system are addressed. Knowledge on irreversible changes and surprises in the climate system is also assessed.

Integration (Chapters 13 and 14): These chapters synthesise all relevant information for two key topics of this assessment: sea level change (Chapter 13) and climate phenomena across the regions (Chapter 14). Chapter 13 presents an end to end assessment of information on sea level change based on paleoclimate reconstructions, observations and process understanding, and provides projections from global to regional scales. Chapter 14 assesses the most important modes of variability in the climate system, such as El Niño-Southern Oscillation, monsoon and many others, as well as extreme events. Furthermore, this chapter deals with interconnections between the climate phenomena, their regional expressions and their relevance for future regional climate change.

Maps assessed in Chapter 14, together with Chapters 11 and 12, form the basis of the Atlas of Global and Regional Climate Projections in Annex I, which is also available in digital format. Radiative forcings and estimates of future atmospheric concentrations from Chapters 7, 8, 11 and 12 form the basis of the Climate System Scenario Tables presented in Annex II. All material including high-resolution versions of the figures, underlying data and Supplementary Material to the chapters is also available online: www.climatechange2013.org.

The scientific community and the climate modelling centres around the world brought together their activities in the Coordinated Modelling Intercomparison Project Phase 5 (CMIP5), providing the basis for most of the assessment of future climate change in this report. Their efforts enable Working Group I to deliver comprehensive scientific information for the policymakers and the users of this report, as well as for the specific assessments of impacts carried out by IPCC Working Group II, and of costs and mitigation strategies, carried out by IPCC Working Group III.

Following the successful introduction in the previous Working Group I assessment in 2007, all chapters contain Frequently Asked Questions. In these the authors provide scientific answers to a range of general questions in a form that will be accessible to a broad readership and serves as a resource for teaching purposes. Finally, the report is accompanied by extensive Supplementary Material which is made available in the online versions of the report to provide an additional level of detail, such as description of datasets, models, or methodologies used in chapter analyses, as well as material supporting the figures in the Summary for Policymakers.

The Process

This Working Group I Assessment Report represents the combined efforts of hundreds of leading experts in the field of climate science and has been prepared in accordance with rules and procedures established by the IPCC. A scoping meeting for the Fifth Assessment Report was held in July 2009 and the outlines for the contributions of the three Working Groups were approved at the 31st Session of the Panel in November 2009. Governments and IPCC observer organisations nominated experts for the author team. The team of 209 Coordinating Lead Authors and Lead Authors plus 50 Review Editors selected by the Working Group I Bureau was accepted at the 41st Session of the IPCC Bureau in May 2010. In addition, more than 600 Contributing Authors provided draft text and information to the author teams at their request. Drafts prepared by the authors were subject to two rounds of formal review and revision followed by a final round of government comments on the Summary for Policymakers. A total of 54,677 written review comments were submitted by 1089 individual expert reviewers and 38 governments. The Review Editors for each chapter monitored the review process to ensure that all substantive review comments received appropriate consideration. The Summary for Policymakers was approved line-by-line and the underlying chapters were then accepted at the 12th Session of IPCC Working Group I from 23–27 September 2007.

Acknowledgements

We are very grateful for the expertise, hard work, commitment to excellence and integrity shown throughout by the Coordinating Lead Authors and Lead Authors with important help by the many Contributing Authors. The Review Editors have played a critical role in assisting the author teams and ensuring the integrity of the review process. We express our sincere appreciation to all the expert and government reviewers. We would also like to thank the members of the Bureau of Working Group I: Jean Jouzel, Abdalah Mokssit, Fatemeh Rahimizadeh, Fredolin Tangang, David Wratt and Francis Zwiers, for their thoughtful advice and support throughout the preparation of the report.

We gratefully acknowledge the long-term efforts of the scientific community, organized and facilitated through the World Climate Research Programme, in particular CMIP5. In this effort by climate modelling centres around the world, more than 2 million gigabytes of numerical data have been produced, which were archived and distributed under the stewardship of the Program for Climate Model Diagnosis and Intercomparison. This represents an unprecedented concerted effort by the scientific community and their funding institutions.

Our sincere thanks go to the hosts and organizers of the four Working Group I Lead Author Meetings and the 12th Session of Working Group I. We gratefully acknowledge the support from the host countries: China, France, Morocco, Australia and Sweden. The support for their scientists provided by many governments as well as through the IPCC Trust Fund is much appreciated. The efficient operation of the Working Group I Technical Support Unit was made possible by the generous financial support provided by the government of Switzerland and logistical support from the University of Bern (Switzerland).

We would also like to thank Renate Christ, Secretary of the IPCC, and the staff of the IPCC Secretariat: Gaetano Leone, Jonathan Lynn, Mary Jean Burer, Sophie Schlingemann, Judith Ewa, Jesbin Baidya, Werani Zabula, Joelle Fernandez, Annie Courtin, Laura Biagioni and Amy Smith. Thanks are due to Francis Hayes who served as the conference officer for the Working Group I Approval Session.

Finally our particular appreciation goes to the Working Group I Technical Support Unit: Gian-Kasper Plattner, Melinda Tignor, Simon Allen, Judith Boschung, Alexander Nauels, Yu Xia, Vincent Bex and Pauline Midgley for their professionalism, creativity and dedication. Their tireless efforts to coordinate the Working Group I Report ensured a final product of high quality. They were assisted in this by Adrien Michel and Flavio Lehner with further support from Zhou Botao and Sun Ying. In addition, the following contributions are gratefully acknowledged: David Hansford (editorial assistance with the Frequently Asked Questions), UNEP/GRID-Geneva and University of Geneva (graphics assistance with the Frequently Asked Questions), Theresa Kornak (copyedit), Marilyn Anderson (index) and Michael Shibao (design and layout).

Rajendra K. Pachauri
IPCC Chair

Qin Dahe
IPCC WGI Co-Chair

Thomas F. Stocker
IPCC WGI Co-Chair

Dedication

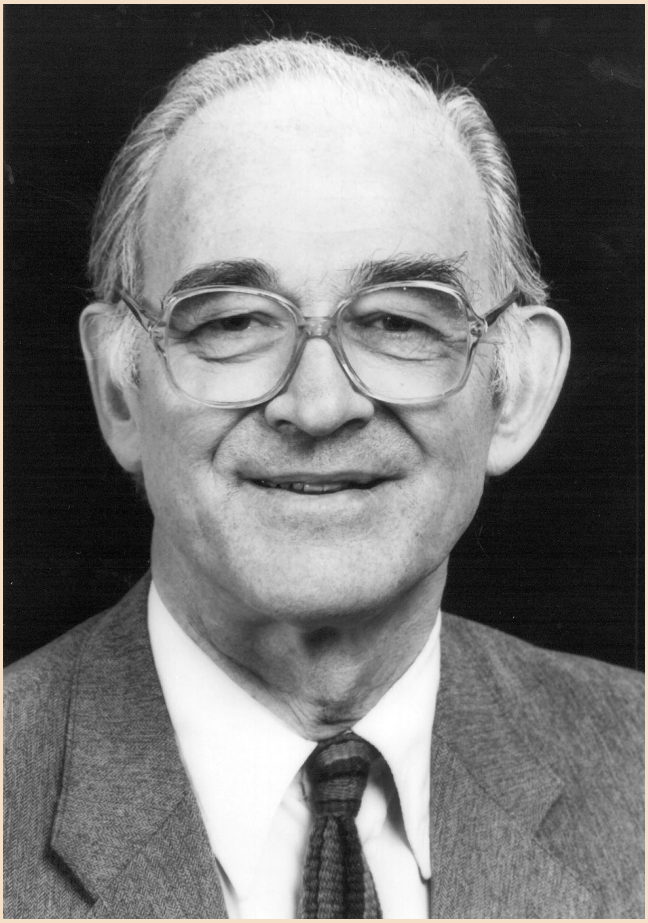

Bert Bolin
(15 May 1925 – 30 December 2007)

The Working Group I contribution to the Fifth Assessment Report of the Intergovernmental Panel on Climate Change (IPCC) *Climate Change 2013: The Physical Science Basis* is dedicated to the memory of Bert Bolin, the first Chair of the IPCC.

As an accomplished scientist who published on both atmospheric dynamics and the carbon cycle, including processes in the atmosphere, oceans and biosphere, Bert Bolin realised the complexity of the climate system and its sensitivity to anthropogenic perturbation. He made a fundamental contribution to the organisation of international cooperation in climate research, being involved in the establishment of a number of global programmes.

Bert Bolin played a key role in the creation of the IPCC and its assessments, which are carried out in a unique and formalized process in order to provide a robust scientific basis for informed decisions regarding one of the greatest challenges of our time. His vision and leadership of the Panel as the founding Chair from 1988 to 1997 laid the basis for subsequent assessments including this one and are remembered with deep appreciation.

Contents

Summary for Policymakers

SPM

Summary for Policymakers

Drafting Authors:

Lisa V. Alexander (Australia), Simon K. Allen (Switzerland/New Zealand), Nathaniel L. Bindoff (Australia), François-Marie Bréon (France), John A. Church (Australia), Ulrich Cubasch (Germany), Seita Emori (Japan), Piers Forster (UK), Pierre Friedlingstein (UK/Belgium), Nathan Gillett (Canada), Jonathan M. Gregory (UK), Dennis L. Hartmann (USA), Eystein Jansen (Norway), Ben Kirtman (USA), Reto Knutti (Switzerland), Krishna Kumar Kanikicharla (India), Peter Lemke (Germany), Jochem Marotzke (Germany), Valérie Masson-Delmotte (France), Gerald A. Meehl (USA), Igor I. Mokhov (Russian Federation), Shilong Piao (China), Gian-Kasper Plattner (Switzerland), Qin Dahe (China), Venkatachalam Ramaswamy (USA), David Randall (USA), Monika Rhein (Germany), Maisa Rojas (Chile), Christopher Sabine (USA), Drew Shindell (USA), Thomas F. Stocker (Switzerland), Lynne D. Talley (USA), David G. Vaughan (UK), Shang-Ping Xie (USA)

Draft Contributing Authors:

Myles R. Allen (UK), Olivier Boucher (France), Don Chambers (USA), Jens Hesselbjerg Christensen (Denmark), Philippe Ciais (France), Peter U. Clark (USA), Matthew Collins (UK), Josefino C. Comiso (USA), Viviane Vasconcellos de Menezes (Australia/Brazil), Richard A. Feely (USA), Thierry Fichefet (Belgium), Arlene M. Fiore (USA), Gregory Flato (Canada), Jan Fuglestvedt (Norway), Gabriele Hegerl (UK/Germany), Paul J. Hezel (Belgium/USA), Gregory C. Johnson (USA), Georg Kaser (Austria/Italy), Vladimir Kattsov (Russian Federation), John Kennedy (UK), Albert M. G. Klein Tank (Netherlands), Corinne Le Quéré (UK), Gunnar Myhre (Norway), Timothy Osborn (UK), Antony J. Payne (UK), Judith Perlwitz (USA), Scott Power (Australia), Michael Prather (USA), Stephen R. Rintoul (Australia), Joeri Rogelj (Switzerland/Belgium), Matilde Rusticucci (Argentina), Michael Schulz (Germany), Jan Sedláček (Switzerland), Peter A. Stott (UK), Rowan Sutton (UK), Peter W. Thorne (USA/Norway/UK), Donald Wuebbles (USA)

This Summary for Policymakers should be cited as:

IPCC, 2013: Summary for Policymakers. In: *Climate Change 2013: The Physical Science Basis. Contribution of Working Group I to the Fifth Assessment Report of the Intergovernmental Panel on Climate Change* [Stocker, T.F., D. Qin, G.-K. Plattner, M. Tignor, S.K. Allen, J. Boschung, A. Nauels, Y. Xia, V. Bex and P.M. Midgley (eds.)]. Cambridge University Press, Cambridge, United Kingdom and New York, NY, USA.

A. Introduction

The Working Group I contribution to the IPCC's Fifth Assessment Report (AR5) considers new evidence of climate change based on many independent scientific analyses from observations of the climate system, paleoclimate archives, theoretical studies of climate processes and simulations using climate models. It builds upon the Working Group I contribution to the IPCC's Fourth Assessment Report (AR4), and incorporates subsequent new findings of research. As a component of the fifth assessment cycle, the IPCC Special Report on Managing the Risks of Extreme Events and Disasters to Advance Climate Change Adaptation (SREX) is an important basis for information on changing weather and climate extremes.

This Summary for Policymakers (SPM) follows the structure of the Working Group I report. The narrative is supported by a series of overarching highlighted conclusions which, taken together, provide a concise summary. Main sections are introduced with a brief paragraph in italics which outlines the methodological basis of the assessment.

The degree of certainty in key findings in this assessment is based on the author teams' evaluations of underlying scientific understanding and is expressed as a qualitative level of confidence (from *very low* to *very high*) and, when possible, probabilistically with a quantified likelihood (from *exceptionally unlikely* to *virtually certain*). Confidence in the validity of a finding is based on the type, amount, quality, and consistency of evidence (e.g., data, mechanistic understanding, theory, models, expert judgment) and the degree of agreement[1]. Probabilistic estimates of quantified measures of uncertainty in a finding are based on statistical analysis of observations or model results, or both, and expert judgment[2]. Where appropriate, findings are also formulated as statements of fact without using uncertainty qualifiers. (See Chapter 1 and Box TS.1 for more details about the specific language the IPCC uses to communicate uncertainty).

The basis for substantive paragraphs in this Summary for Policymakers can be found in the chapter sections of the underlying report and in the Technical Summary. These references are given in curly brackets.

B. Observed Changes in the Climate System

Observations of the climate system are based on direct measurements and remote sensing from satellites and other platforms. Global-scale observations from the instrumental era began in the mid-19th century for temperature and other variables, with more comprehensive and diverse sets of observations available for the period 1950 onwards. Paleoclimate reconstructions extend some records back hundreds to millions of years. Together, they provide a comprehensive view of the variability and long-term changes in the atmosphere, the ocean, the cryosphere, and the land surface.

Warming of the climate system is unequivocal, and since the 1950s, many of the observed changes are unprecedented over decades to millennia. The atmosphere and ocean have warmed, the amounts of snow and ice have diminished, sea level has risen, and the concentrations of greenhouse gases have increased (see Figures SPM.1, SPM.2, SPM.3 and SPM.4). {2.2, 2.4, 3.2, 3.7, 4.2–4.7, 5.2, 5.3, 5.5–5.6, 6.2, 13.2}

[1] In this Summary for Policymakers, the following summary terms are used to describe the available evidence: limited, medium, or robust; and for the degree of agreement: low, medium, or high. A level of confidence is expressed using five qualifiers: very low, low, medium, high, and very high, and typeset in italics, e.g., *medium confidence*. For a given evidence and agreement statement, different confidence levels can be assigned, but increasing levels of evidence and degrees of agreement are correlated with increasing confidence (see Chapter 1 and Box TS.1 for more details).

[2] In this Summary for Policymakers, the following terms have been used to indicate the assessed likelihood of an outcome or a result: virtually certain 99–100% probability, very likely 90–100%, likely 66–100%, about as likely as not 33–66%, unlikely 0–33%, very unlikely 0–10%, exceptionally unlikely 0–1%. Additional terms (extremely likely: 95–100%, more likely than not >50–100%, and extremely unlikely 0–5%) may also be used when appropriate. Assessed likelihood is typeset in italics, e.g., *very likely* (see Chapter 1 and Box TS.1 for more details).

B.1 Atmosphere

Each of the last three decades has been successively warmer at the Earth's surface than any preceding decade since 1850 (see Figure SPM.1). In the Northern Hemisphere, 1983–2012 was *likely* the warmest 30-year period of the last 1400 years (*medium confidence*). {2.4, 5.3}

- The globally averaged combined land and ocean surface temperature data as calculated by a linear trend, show a warming of 0.85 [0.65 to 1.06] °C[3], over the period 1880 to 2012, when multiple independently produced datasets exist. The total increase between the average of the 1850–1900 period and the 2003–2012 period is 0.78 [0.72 to 0.85] °C, based on the single longest dataset available[4] (see Figure SPM.1). {2.4}

- For the longest period when calculation of regional trends is sufficiently complete (1901 to 2012), almost the entire globe has experienced surface warming (see Figure SPM.1). {2.4}

- In addition to robust multi-decadal warming, global mean surface temperature exhibits substantial decadal and interannual variability (see Figure SPM.1). Due to natural variability, trends based on short records are very sensitive to the beginning and end dates and do not in general reflect long-term climate trends. As one example, the rate of warming over the past 15 years (1998–2012; 0.05 [–0.05 to 0.15] °C per decade), which begins with a strong El Niño, is smaller than the rate calculated since 1951 (1951–2012; 0.12 [0.08 to 0.14] °C per decade)[5]. {2.4}

- Continental-scale surface temperature reconstructions show, with *high confidence*, multi-decadal periods during the Medieval Climate Anomaly (year 950 to 1250) that were in some regions as warm as in the late 20th century. These regional warm periods did not occur as coherently across regions as the warming in the late 20th century (*high confidence*). {5.5}

- It is *virtually certain* that globally the troposphere has warmed since the mid-20th century. More complete observations allow greater confidence in estimates of tropospheric temperature changes in the extratropical Northern Hemisphere than elsewhere. There is *medium confidence* in the rate of warming and its vertical structure in the Northern Hemisphere extra-tropical troposphere and *low confidence* elsewhere. {2.4}

- *Confidence* in precipitation change averaged over global land areas since 1901 is *low* prior to 1951 and *medium* afterwards. Averaged over the mid-latitude land areas of the Northern Hemisphere, precipitation has increased since 1901 (*medium confidence* before and *high confidence* after 1951). For other latitudes area-averaged long-term positive or negative trends have *low confidence* (see Figure SPM.2). {TS TFE.1, Figure 2; 2.5}

- Changes in many extreme weather and climate events have been observed since about 1950 (see Table SPM.1 for details). It is *very likely* that the number of cold days and nights has decreased and the number of warm days and nights has increased on the global scale[6]. It is *likely* that the frequency of heat waves has increased in large parts of Europe, Asia and Australia. There are *likely* more land regions where the number of heavy precipitation events has increased than where it has decreased. The frequency or intensity of heavy precipitation events has *likely* increased in North America and Europe. In other continents, *confidence* in changes in heavy precipitation events is at most *medium*. {2.6}

---

[3] In the WGI contribution to the AR5, uncertainty is quantified using 90% uncertainty intervals unless otherwise stated. The 90% uncertainty interval, reported in square brackets, is expected to have a 90% likelihood of covering the value that is being estimated. Uncertainty intervals are not necessarily symmetric about the corresponding best estimate. A best estimate of that value is also given where available.

[4] Both methods presented in this bullet were also used in AR4. The first calculates the difference using a best fit linear trend of all points between 1880 and 2012. The second calculates the difference between averages for the two periods 1850–1900 and 2003–2012. Therefore, the resulting values and their 90% uncertainty intervals are not directly comparable. {2.4}

[5] Trends for 15-year periods starting in 1995, 1996, and 1997 are 0.13 [0.02 to 0.24] °C per decade, 0.14 [0.03 to 0.24] °C per decade, and, 0.07 [–0.02 to 0.18] °C per decade, respectively.

[6] See the Glossary for the definition of these terms: cold days/cold nights, warm days/warm nights, heat waves.

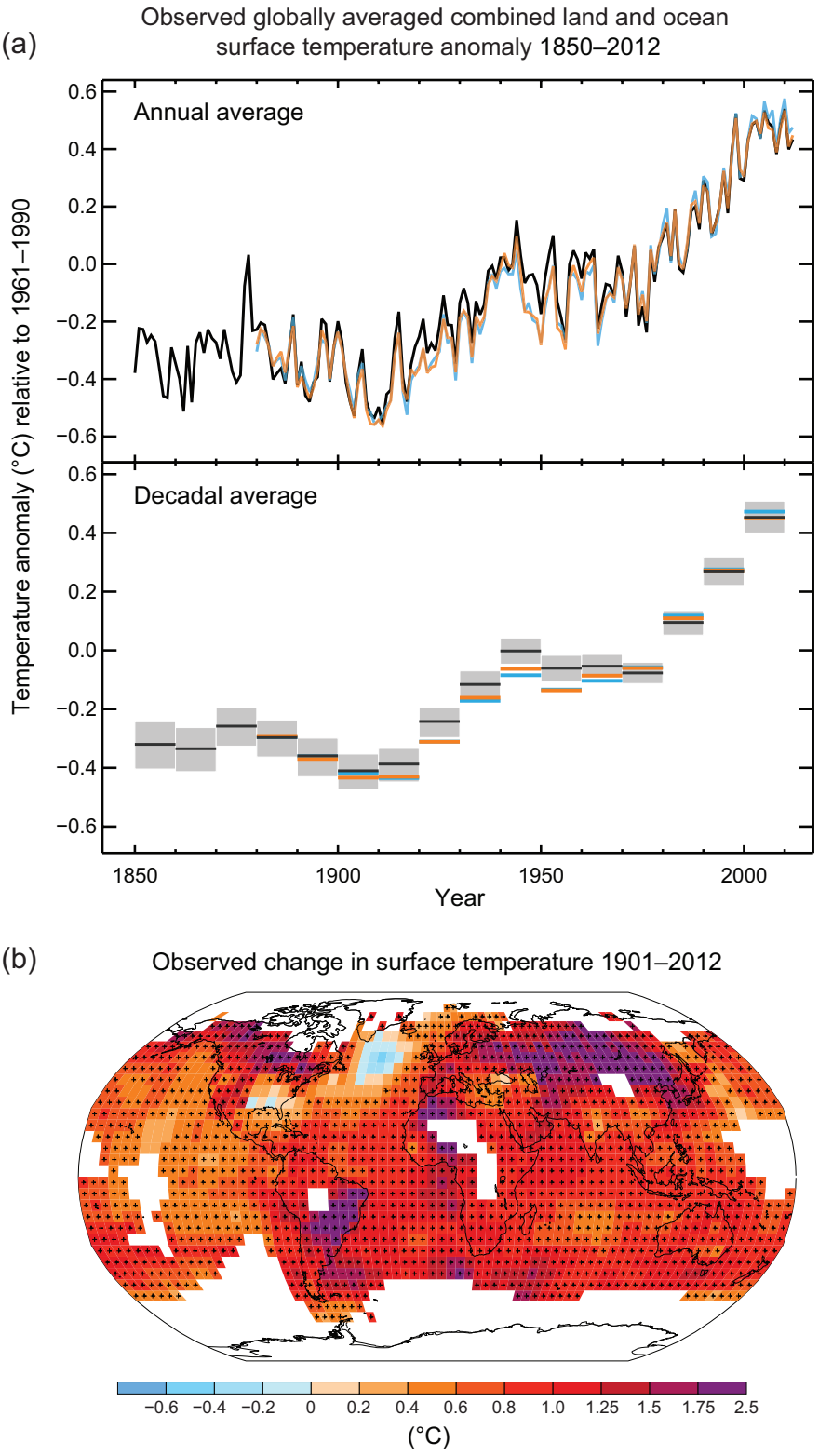

Figure SPM.1 | (a) Observed global mean combined land and ocean surface temperature anomalies, from 1850 to 2012 from three data sets. Top panel: annual mean values. Bottom panel: decadal mean values including the estimate of uncertainty for one dataset (black). Anomalies are relative to the mean of 1961–1990. (b) Map of the observed surface temperature change from 1901 to 2012 derived from temperature trends determined by linear regression from one dataset (orange line in panel a). Trends have been calculated where data availability permits a robust estimate (i.e., only for grid boxes with greater than 70% complete records and more than 20% data availability in the first and last 10% of the time period). Other areas are white. Grid boxes where the trend is significant at the 10% level are indicated by a + sign. For a listing of the datasets and further technical details see the Technical Summary Supplementary Material. {Figures 2.19–2.21; Figure TS.2}

Table SPM.1 | Extreme weather and climate events: Global-scale assessment of recent observed changes, human contribution to the changes, and projected further changes for the early (2016–2035) and late (2081–2100) 21st century. Bold indicates where the AR5 (black) provides a revised* global-scale assessment from the SREX (blue) or AR4 (red). Projections for early 21st century were not provided in previous assessment reports. Projections in the AR5 are relative to the reference period of 1986–2005, and use the new Representative Concentration Pathway (RCP) scenarios (see Box SPM.1) unless otherwise specified. See the Glossary for definitions of extreme weather and climate events.

Phenomenon and direction of trend	Assessment that changes occurred (typically since 1950 unless otherwise indicated)	Assessment of a human contribution to observed changes	Likelihood of further changes	
			Early 21st century	Late 21st century
Warmer and/or fewer cold days and nights over most land areas	*Very likely* {2.6} *Very likely* *Very likely*	***Very likely*** {10.6} *Likely* *Likely*	*Likely* {11.3}	*Virtually certain* {12.4} *Virtually certain* *Virtually certain*
Warmer and/or more frequent hot days and nights over most land areas	*Very likely* {2.6} *Very likely* *Very likely*	***Very likely*** {10.6} *Likely* *Likely* (nights only)	*Likely* {11.3}	*Virtually certain* {12.4} *Virtually certain* *Virtually certain*
Warm spells/heat waves. Frequency and/or duration increases over most land areas	***Medium confidence*** on a global scale *Likely* in large parts of Europe, Asia and Australia {2.6} *Medium confidence* in many (but not all) regions *Likely*	***Likely***[a] {10.6} Not formally assessed *More likely than not*	Not formally assessed[b] {11.3}	*Very likely* {12.4} *Very likely* *Very likely*
Heavy precipitation events. Increase in the frequency, intensity, and/or amount of heavy precipitation	*Likely* more land areas with increases than decreases[c] {2.6} *Likely* more land areas with increases than decreases *Likely* over most land areas	***Medium confidence*** {7.6, 10.6} *Medium confidence* *More likely than not*	*Likely* over many land areas {11.3}	***Very likely*** over most of the mid-latitude land masses and over wet tropical regions {12.4} *Likely* over many areas *Very likely* over most land areas
Increases in intensity and/or duration of drought	***Low confidence*** on a global scale *Likely* changes in some regions[d] {2.6} *Medium confidence* in some regions *Likely* in many regions, since 1970[e]	***Low confidence*** {10.6} *Medium confidence*[f] *More likely than not*	*Low confidence*[g] {11.3}	***Likely*** *(medium confidence)* on a regional to global scale[h] {12.4} *Medium confidence* in some regions *Likely*[e]
Increases in intense tropical cyclone activity	***Low confidence*** in long term (centennial) changes *Virtually certain* in North Atlantic since 1970 {2.6} *Low confidence* *Likely* in some regions, since 1970	***Low confidence***[i] {10.6} *Low confidence* *More likely than not*	*Low confidence* {11.3}	***More likely than not*** in the Western North Pacific and North Atlantic[j] {14.6} *More likely than not* in some basins *Likely*
Increased incidence and/or magnitude of extreme high sea level	*Likely* (since 1970) {3.7} *Likely* (late 20th century) *Likely*	***Likely***[k] {3.7} *Likely*[k] *More likely than not*[k]	*Likely*[l] {13.7}	***Very likely***[l] {13.7} *Very likely*[m] *Likely*

* The direct comparison of assessment findings between reports is difficult. For some climate variables, different aspects have been assessed, and the revised guidance note on uncertainties has been used for the SREX and AR5. The availability of new information, improved scientific understanding, continued analyses of data and models, and specific differences in methodologies applied in the assessed studies, all contribute to revised assessment findings.

Notes:

[a] Attribution is based on available case studies. It is *likely* that human influence has more than doubled the probability of occurrence of some observed heat waves in some locations.

[b] Models project near-term increases in the duration, intensity and spatial extent of heat waves and warm spells.

[c] In most continents, *confidence* in trends is not higher than *medium* except in North America and Europe where there have been *likely* increases in either the frequency or intensity of heavy precipitation with some seasonal and/or regional variation. It is *very likely* that there have been increases in central North America.

[d] The frequency and intensity of drought has *likely* increased in the Mediterranean and West Africa, and *likely* decreased in central North America and north-west Australia.

[e] AR4 assessed the area affected by drought.

[f] SREX assessed *medium confidence* that anthropogenic influence had contributed to some changes in the drought patterns observed in the second half of the 20th century, based on its attributed impact on precipitation and temperature changes. SREX assessed *low confidence* in the attribution of changes in droughts at the level of single regions.

[g] There is *low confidence* in projected changes in soil moisture.

[h] Regional to global-scale projected decreases in soil moisture and increased agricultural drought are *likely (medium confidence)* in presently dry regions by the end of this century under the RCP8.5 scenario. Soil moisture drying in the Mediterranean, Southwest US and southern African regions is consistent with projected changes in Hadley circulation and increased surface temperatures, so there is *high confidence* in *likely* surface drying in these regions by the end of this century under the RCP8.5 scenario.

[i] There is *medium confidence* that a reduction in aerosol forcing over the North Atlantic has contributed at least in part to the observed increase in tropical cyclone activity since the 1970s in this region.

[j] Based on expert judgment and assessment of projections which use an SRES A1B (or similar) scenario.

[k] Attribution is based on the close relationship between observed changes in extreme and mean sea level.

[l] There is *high confidence* that this increase in extreme high sea level will primarily be the result of an increase in mean sea level. There is *low confidence* in region-specific projections of storminess and associated storm surges.

[m] SREX assessed it to be *very likely* that mean sea level rise will contribute to future upward trends in extreme coastal high water levels.

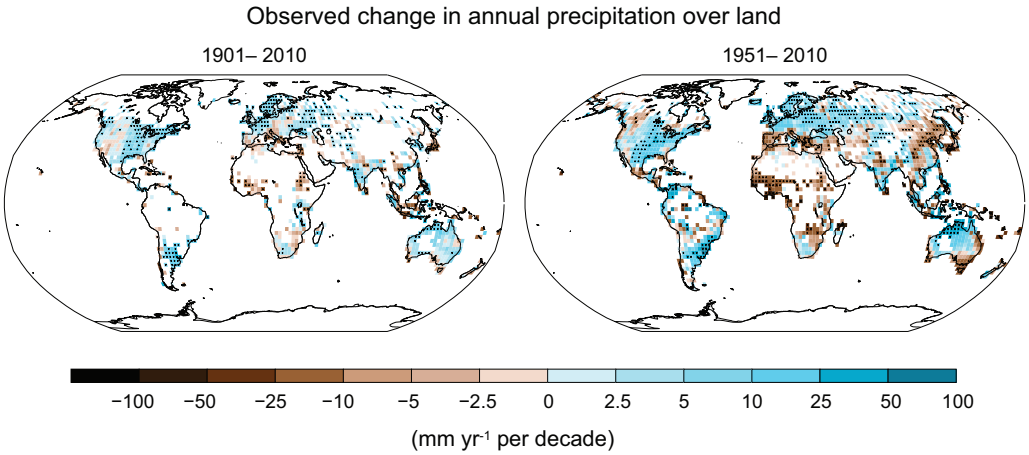

Figure SPM.2 | Maps of observed precipitation change from 1901 to 2010 and from 1951 to 2010 (trends in annual accumulation calculated using the same criteria as in Figure SPM.1) from one data set. For further technical details see the Technical Summary Supplementary Material. {TS TFE.1, Figure 2; Figure 2.29}

B.2 Ocean

Ocean warming dominates the increase in energy stored in the climate system, accounting for more than 90% of the energy accumulated between 1971 and 2010 (*high confidence*). It is *virtually certain* that the upper ocean (0–700 m) warmed from 1971 to 2010 (see Figure SPM.3), and it *likely* warmed between the 1870s and 1971. {3.2, Box 3.1}

- On a global scale, the ocean warming is largest near the surface, and the upper 75 m warmed by 0.11 [0.09 to 0.13] °C per decade over the period 1971 to 2010. Since AR4, instrumental biases in upper-ocean temperature records have been identified and reduced, enhancing confidence in the assessment of change. {3.2}

- It is *likely* that the ocean warmed between 700 and 2000 m from 1957 to 2009. Sufficient observations are available for the period 1992 to 2005 for a global assessment of temperature change below 2000 m. There were *likely* no significant observed temperature trends between 2000 and 3000 m for this period. It is *likely* that the ocean warmed from 3000 m to the bottom for this period, with the largest warming observed in the Southern Ocean. {3.2}

- More than 60% of the net energy increase in the climate system is stored in the upper ocean (0–700 m) during the relatively well-sampled 40-year period from 1971 to 2010, and about 30% is stored in the ocean below 700 m. The increase in upper ocean heat content during this time period estimated from a linear trend is *likely* 17 [15 to 19] × 10^{22} J [7] (see Figure SPM.3). {3.2, Box 3.1}

- It is *about as likely as not* that ocean heat content from 0–700 m increased more slowly during 2003 to 2010 than during 1993 to 2002 (see Figure SPM.3). Ocean heat uptake from 700–2000 m, where interannual variability is smaller, *likely* continued unabated from 1993 to 2009. {3.2, Box 9.2}

- It is *very likely* that regions of high salinity where evaporation dominates have become more saline, while regions of low salinity where precipitation dominates have become fresher since the 1950s. These regional trends in ocean salinity provide indirect evidence that evaporation and precipitation over the oceans have changed (*medium confidence*). {2.5, 3.3, 3.5}

- There is no observational evidence of a trend in the Atlantic Meridional Overturning Circulation (AMOC), based on the decade-long record of the complete AMOC and longer records of individual AMOC components. {3.6}

[7] A constant supply of heat through the ocean surface at the rate of 1 W m^{-2} for 1 year would increase the ocean heat content by 1.1 × 10^{22} J.

B.3 Cryosphere

Over the last two decades, the Greenland and Antarctic ice sheets have been losing mass, glaciers have continued to shrink almost worldwide, and Arctic sea ice and Northern Hemisphere spring snow cover have continued to decrease in extent (*high confidence*) (see Figure SPM.3). {4.2–4.7}

- The average rate of ice loss[8] from glaciers around the world, excluding glaciers on the periphery of the ice sheets[9], was *very likely* 226 [91 to 361] Gt yr^{-1} over the period 1971 to 2009, and *very likely* 275 [140 to 410] Gt yr^{-1} over the period 1993 to 2009[10]. {4.3}

- The average rate of ice loss from the Greenland ice sheet has *very likely* substantially increased from 34 [–6 to 74] Gt yr^{-1} over the period 1992 to 2001 to 215 [157 to 274] Gt yr^{-1} over the period 2002 to 2011. {4.4}

- The average rate of ice loss from the Antarctic ice sheet has *likely* increased from 30 [–37 to 97] Gt yr^{-1} over the period 1992–2001 to 147 [72 to 221] Gt yr^{-1} over the period 2002 to 2011. There is *very high confidence* that these losses are mainly from the northern Antarctic Peninsula and the Amundsen Sea sector of West Antarctica. {4.4}

- The annual mean Arctic sea ice extent decreased over the period 1979 to 2012 with a rate that was *very likely* in the range 3.5 to 4.1% per decade (range of 0.45 to 0.51 million km^2 per decade), and *very likely* in the range 9.4 to 13.6% per decade (range of 0.73 to 1.07 million km^2 per decade) for the summer sea ice minimum (perennial sea ice). The average decrease in decadal mean extent of Arctic sea ice has been most rapid in summer (*high confidence*); the spatial extent has decreased in every season, and in every successive decade since 1979 (*high confidence*) (see Figure SPM.3). There is *medium confidence* from reconstructions that over the past three decades, Arctic summer sea ice retreat was unprecedented and sea surface temperatures were anomalously high in at least the last 1,450 years. {4.2, 5.5}

- It is *very likely* that the annual mean Antarctic sea ice extent increased at a rate in the range of 1.2 to 1.8% per decade (range of 0.13 to 0.20 million km^2 per decade) between 1979 and 2012. There is *high confidence* that there are strong regional differences in this annual rate, with extent increasing in some regions and decreasing in others. {4.2}

- There is *very high confidence* that the extent of Northern Hemisphere snow cover has decreased since the mid-20th century (see Figure SPM.3). Northern Hemisphere snow cover extent decreased 1.6 [0.8 to 2.4] % per decade for March and April, and 11.7 [8.8 to 14.6] % per decade for June, over the 1967 to 2012 period. During this period, snow cover extent in the Northern Hemisphere did not show a statistically significant increase in any month. {4.5}

- There is *high confidence* that permafrost temperatures have increased in most regions since the early 1980s. Observed warming was up to 3°C in parts of Northern Alaska (early 1980s to mid-2000s) and up to 2°C in parts of the Russian European North (1971 to 2010). In the latter region, a considerable reduction in permafrost thickness and areal extent has been observed over the period 1975 to 2005 (*medium confidence*). {4.7}

- Multiple lines of evidence support very substantial Arctic warming since the mid-20th century. {Box 5.1, 10.3}

[8] All references to 'ice loss' or 'mass loss' refer to net ice loss, i.e., accumulation minus melt and iceberg calving.

[9] For methodological reasons, this assessment of ice loss from the Antarctic and Greenland ice sheets includes change in the glaciers on the periphery. These peripheral glaciers are thus excluded from the values given for glaciers.

[10] 100 Gt yr^{-1} of ice loss is equivalent to about 0.28 mm yr^{-1} of global mean sea level rise.

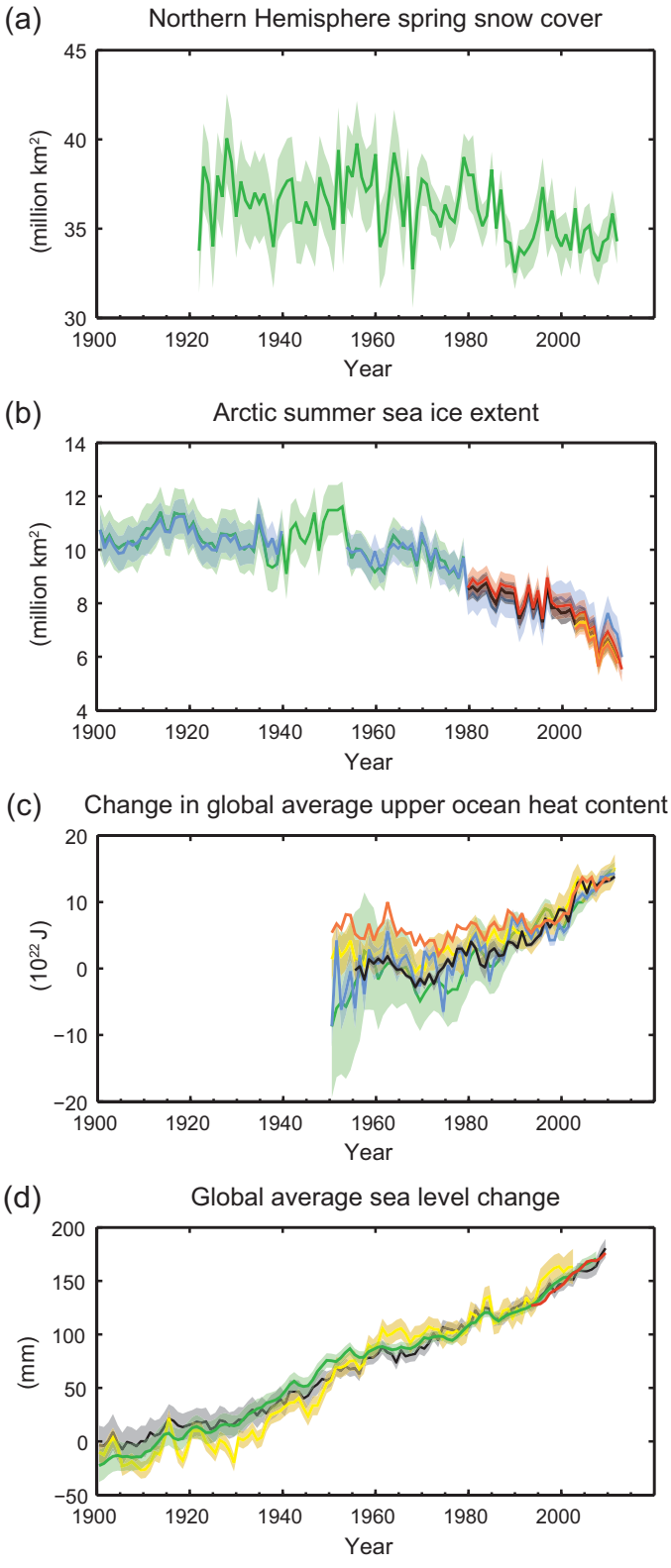

Figure SPM.3 | Multiple observed indicators of a changing global climate: (a) Extent of Northern Hemisphere March-April (spring) average snow cover; (b) extent of Arctic July-August-September (summer) average sea ice; (c) change in global mean upper ocean (0–700 m) heat content aligned to 2006–2010, and relative to the mean of all datasets for 1970; (d) global mean sea level relative to the 1900–1905 mean of the longest running dataset, and with all datasets aligned to have the same value in 1993, the first year of satellite altimetry data. All time-series (coloured lines indicating different data sets) show annual values, and where assessed, uncertainties are indicated by coloured shading. See Technical Summary Supplementary Material for a listing of the datasets. {Figures 3.2, 3.13, 4.19, and 4.3; FAQ 2.1, Figure 2; Figure TS.1}

B.4 Sea Level

The rate of sea level rise since the mid-19th century has been larger than the mean rate during the previous two millennia (*high confidence*). Over the period 1901 to 2010, global mean sea level rose by 0.19 [0.17 to 0.21] m (see Figure SPM.3). {3.7, 5.6, 13.2}

- Proxy and instrumental sea level data indicate a transition in the late 19th to the early 20th century from relatively low mean rates of rise over the previous two millennia to higher rates of rise (*high confidence*). It is *likely* that the rate of global mean sea level rise has continued to increase since the early 20th century. {3.7, 5.6, 13.2}

- It is *very likely* that the mean rate of global averaged sea level rise was 1.7 [1.5 to 1.9] mm yr^{-1} between 1901 and 2010, 2.0 [1.7 to 2.3] mm yr^{-1} between 1971 and 2010, and 3.2 [2.8 to 3.6] mm yr^{-1} between 1993 and 2010. Tide-gauge and satellite altimeter data are consistent regarding the higher rate of the latter period. It is *likely* that similarly high rates occurred between 1920 and 1950. {3.7}

- Since the early 1970s, glacier mass loss and ocean thermal expansion from warming together explain about 75% of the observed global mean sea level rise (*high confidence*). Over the period 1993 to 2010, global mean sea level rise is, with *high confidence*, consistent with the sum of the observed contributions from ocean thermal expansion due to warming (1.1 [0.8 to 1.4] mm yr^{-1}), from changes in glaciers (0.76 [0.39 to 1.13] mm yr^{-1}), Greenland ice sheet (0.33 [0.25 to 0.41] mm yr^{-1}), Antarctic ice sheet (0.27 [0.16 to 0.38] mm yr^{-1}), and land water storage (0.38 [0.26 to 0.49] mm yr^{-1}). The sum of these contributions is 2.8 [2.3 to 3.4] mm yr^{-1}. {13.3}

- There is *very high confidence* that maximum global mean sea level during the last interglacial period (129,000 to 116,000 years ago) was, for several thousand years, at least 5 m higher than present, and *high confidence* that it did not exceed 10 m above present. During the last interglacial period, the Greenland ice sheet *very likely* contributed between 1.4 and 4.3 m to the higher global mean sea level, implying with *medium confidence* an additional contribution from the Antarctic ice sheet. This change in sea level occurred in the context of different orbital forcing and with high-latitude surface temperature, averaged over several thousand years, at least 2°C warmer than present (*high confidence*). {5.3, 5.6}

B.5 Carbon and Other Biogeochemical Cycles

The atmospheric concentrations of carbon dioxide, methane, and nitrous oxide have increased to levels unprecedented in at least the last 800,000 years. Carbon dioxide concentrations have increased by 40% since pre-industrial times, primarily from fossil fuel emissions and secondarily from net land use change emissions. The ocean has absorbed about 30% of the emitted anthropogenic carbon dioxide, causing ocean acidification (see Figure SPM.4). {2.2, 3.8, 5.2, 6.2, 6.3}

- The atmospheric concentrations of the greenhouse gases carbon dioxide (CO_2), methane (CH_4), and nitrous oxide (N_2O) have all increased since 1750 due to human activity. In 2011 the concentrations of these greenhouse gases were 391 ppm[11], 1803 ppb, and 324 ppb, and exceeded the pre-industrial levels by about 40%, 150%, and 20%, respectively. {2.2, 5.2, 6.1, 6.2}

- Concentrations of CO_2, CH_4, and N_2O now substantially exceed the highest concentrations recorded in ice cores during the past 800,000 years. The mean rates of increase in atmospheric concentrations over the past century are, with *very high confidence*, unprecedented in the last 22,000 years. {5.2, 6.1, 6.2}

[11] ppm (parts per million) or ppb (parts per billion, 1 billion = 1,000 million) is the ratio of the number of gas molecules to the total number of molecules of dry air. For example, 300 ppm means 300 molecules of a gas per million molecules of dry air.

- Annual CO_2 emissions from fossil fuel combustion and cement production were 8.3 [7.6 to 9.0] GtC[12] yr^{-1} averaged over 2002–2011 (*high confidence*) and were 9.5 [8.7 to 10.3] GtC yr^{-1} in 2011, 54% above the 1990 level. Annual net CO_2 emissions from anthropogenic land use change were 0.9 [0.1 to 1.7] GtC yr^{-1} on average during 2002 to 2011 (*medium confidence*). {6.3}

- From 1750 to 2011, CO_2 emissions from fossil fuel combustion and cement production have released 375 [345 to 405] GtC to the atmosphere, while deforestation and other land use change are estimated to have released 180 [100 to 260] GtC. This results in cumulative anthropogenic emissions of 555 [470 to 640] GtC. {6.3}

- Of these cumulative anthropogenic CO_2 emissions, 240 [230 to 250] GtC have accumulated in the atmosphere, 155 [125 to 185] GtC have been taken up by the ocean and 160 [70 to 250] GtC have accumulated in natural terrestrial ecosystems (i.e., the cumulative residual land sink). {Figure TS.4, 3.8, 6.3}

- Ocean acidification is quantified by decreases in pH[13]. The pH of ocean surface water has decreased by 0.1 since the beginning of the industrial era (*high confidence*), corresponding to a 26% increase in hydrogen ion concentration (see Figure SPM.4). {3.8, Box 3.2}

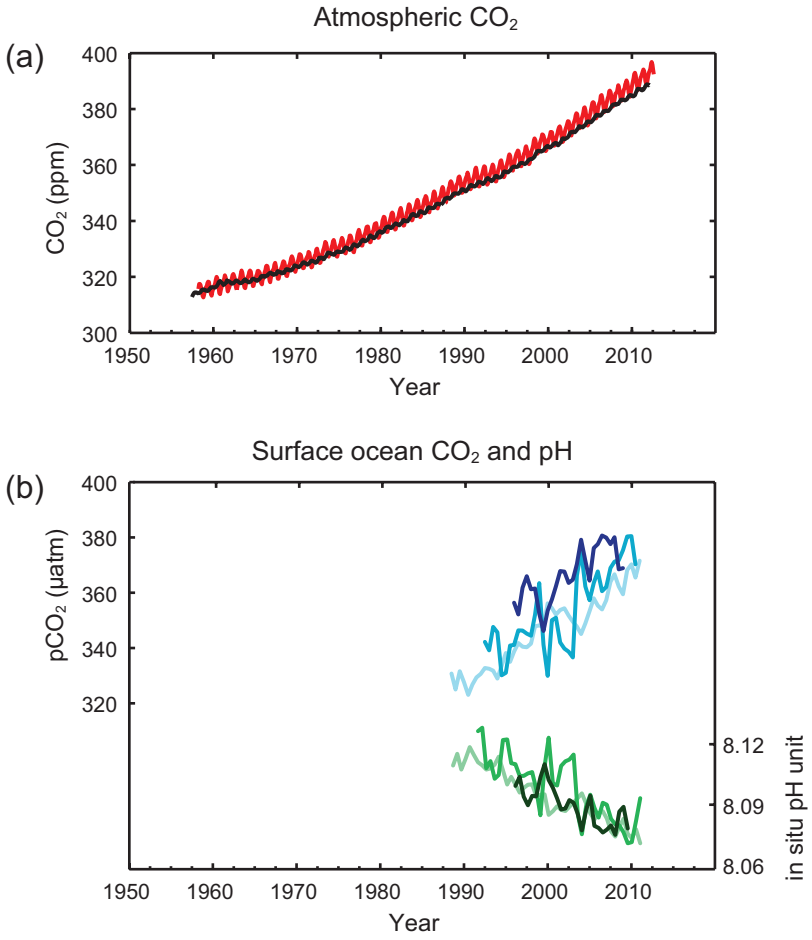

Figure SPM.4 | Multiple observed indicators of a changing global carbon cycle: (a) atmospheric concentrations of carbon dioxide (CO_2) from Mauna Loa (19°32'N, 155°34'W – red) and South Pole (89°59'S, 24°48'W – black) since 1958; (b) partial pressure of dissolved CO_2 at the ocean surface (blue curves) and in situ pH (green curves), a measure of the acidity of ocean water. Measurements are from three stations from the Atlantic (29°10'N, 15°30'W – dark blue/dark green; 31°40'N, 64°10'W – blue/green) and the Pacific Oceans (22°45'N, 158°00'W – light blue/light green). Full details of the datasets shown here are provided in the underlying report and the Technical Summary Supplementary Material. {Figures 2.1 and 3.18; Figure TS.5}

[12] 1 Gigatonne of carbon = 1 GtC = 10^{15} grams of carbon. This corresponds to 3.667 $GtCO_2$.

[13] pH is a measure of acidity using a logarithmic scale: a pH decrease of 1 unit corresponds to a 10-fold increase in hydrogen ion concentration, or acidity.

C. Drivers of Climate Change

Natural and anthropogenic substances and processes that alter the Earth's energy budget are drivers of climate change. Radiative forcing[14] (RF) quantifies the change in energy fluxes caused by changes in these drivers for 2011 relative to 1750, unless otherwise indicated. Positive RF leads to surface warming, negative RF leads to surface cooling. RF is estimated based on in-situ and remote observations, properties of greenhouse gases and aerosols, and calculations using numerical models representing observed processes. Some emitted compounds affect the atmospheric concentration of other substances. The RF can be reported based on the concentration changes of each substance[15]. Alternatively, the emission-based RF of a compound can be reported, which provides a more direct link to human activities. It includes contributions from all substances affected by that emission. The total anthropogenic RF of the two approaches are identical when considering all drivers. Though both approaches are used in this Summary for Policymakers, emission-based RFs are emphasized.

Total radiative forcing is positive, and has led to an uptake of energy by the climate system. The largest contribution to total radiative forcing is caused by the increase in the atmospheric concentration of CO_2 since 1750 (see Figure SPM.5). {3.2, Box 3.1, 8.3, 8.5}

- The total anthropogenic RF for 2011 relative to 1750 is 2.29 [1.13 to 3.33] W m^{-2} (see Figure SPM.5), and it has increased more rapidly since 1970 than during prior decades. The total anthropogenic RF best estimate for 2011 is 43% higher than that reported in AR4 for the year 2005. This is caused by a combination of continued growth in most greenhouse gas concentrations and improved estimates of RF by aerosols indicating a weaker net cooling effect (negative RF). {8.5}

- The RF from emissions of well-mixed greenhouse gases (CO_2, CH_4, N_2O, and Halocarbons) for 2011 relative to 1750 is 3.00 [2.22 to 3.78] W m^{-2} (see Figure SPM.5). The RF from changes in concentrations in these gases is 2.83 [2.26 to 3.40] W m^{-2}. {8.5}

- Emissions of CO_2 alone have caused an RF of 1.68 [1.33 to 2.03] W m^{-2} (see Figure SPM.5). Including emissions of other carbon-containing gases, which also contributed to the increase in CO_2 concentrations, the RF of CO_2 is 1.82 [1.46 to 2.18] W m^{-2}. {8.3, 8.5}

- Emissions of CH_4 alone have caused an RF of 0.97 [0.74 to 1.20] W m^{-2} (see Figure SPM.5). This is much larger than the concentration-based estimate of 0.48 [0.38 to 0.58] W m^{-2} (unchanged from AR4). This difference in estimates is caused by concentration changes in ozone and stratospheric water vapour due to CH_4 emissions and other emissions indirectly affecting CH_4. {8.3, 8.5}

- Emissions of stratospheric ozone-depleting halocarbons have caused a net positive RF of 0.18 [0.01 to 0.35] W m^{-2} (see Figure SPM.5). Their own positive RF has outweighed the negative RF from the ozone depletion that they have induced. The positive RF from all halocarbons is similar to the value in AR4, with a reduced RF from CFCs but increases from many of their substitutes. {8.3, 8.5}

- Emissions of short-lived gases contribute to the total anthropogenic RF. Emissions of carbon monoxide (CO) are *virtually certain* to have induced a positive RF, while emissions of nitrogen oxides (NO_x) are *likely* to have induced a net negative RF (see Figure SPM.5). {8.3, 8.5}

- The RF of the total aerosol effect in the atmosphere, which includes cloud adjustments due to aerosols, is –0.9 [–1.9 to –0.1] W m^{-2} (*medium confidence*), and results from a negative forcing from most aerosols and a positive contribution

[14] The strength of drivers is quantified as Radiative Forcing (RF) in units watts per square metre (W m^{-2}) as in previous IPCC assessments. RF is the change in energy flux caused by a driver, and is calculated at the tropopause or at the top of the atmosphere. In the traditional RF concept employed in previous IPCC reports all surface and tropospheric conditions are kept fixed. In calculations of RF for well-mixed greenhouse gases and aerosols in this report, physical variables, except for the ocean and sea ice, are allowed to respond to perturbations with rapid adjustments. The resulting forcing is called Effective Radiative Forcing (ERF) in the underlying report. This change reflects the scientific progress from previous assessments and results in a better indication of the eventual temperature response for these drivers. For all drivers other than well-mixed greenhouse gases and aerosols, rapid adjustments are less well characterized and assumed to be small, and thus the traditional RF is used. {8.1}

[15] This approach was used to report RF in the AR4 Summary for Policymakers.

from black carbon absorption of solar radiation. There is *high confidence* that aerosols and their interactions with clouds have offset a substantial portion of global mean forcing from well-mixed greenhouse gases. They continue to contribute the largest uncertainty to the total RF estimate. {7.5, 8.3, 8.5}

- The forcing from stratospheric volcanic aerosols can have a large impact on the climate for some years after volcanic eruptions. Several small eruptions have caused an RF of –0.11 [–0.15 to –0.08] W m^{-2} for the years 2008 to 2011, which is approximately twice as strong as during the years 1999 to 2002. {8.4}

- The RF due to changes in solar irradiance is estimated as 0.05 [0.00 to 0.10] W m^{-2} (see Figure SPM.5). Satellite observations of total solar irradiance changes from 1978 to 2011 indicate that the last solar minimum was lower than the previous two. This results in an RF of –0.04 [–0.08 to 0.00] W m^{-2} between the most recent minimum in 2008 and the 1986 minimum. {8.4}

- The total natural RF from solar irradiance changes and stratospheric volcanic aerosols made only a small contribution to the net radiative forcing throughout the last century, except for brief periods after large volcanic eruptions. {8.5}

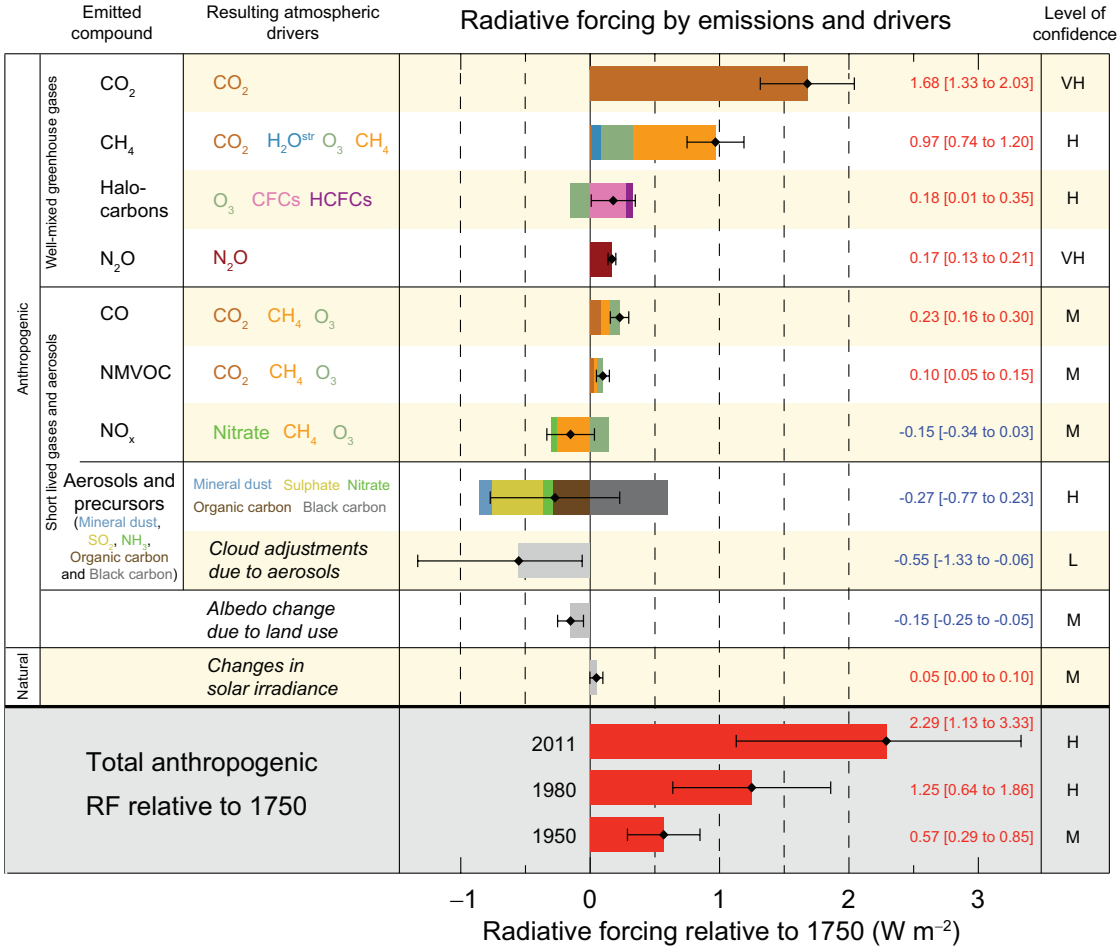

Figure SPM.5 | Radiative forcing estimates in 2011 relative to 1750 and aggregated uncertainties for the main drivers of climate change. Values are global average radiative forcing (RF[14]), partitioned according to the emitted compounds or processes that result in a combination of drivers. The best estimates of the net radiative forcing are shown as black diamonds with corresponding uncertainty intervals; the numerical values are provided on the right of the figure, together with the confidence level in the net forcing (VH – *very high*, H – *high*, M – *medium*, L – *low*, VL – *very low*). Albedo forcing due to black carbon on snow and ice is included in the black carbon aerosol bar. Small forcings due to contrails (0.05 W m^{-2}, including contrail induced cirrus), and HFCs, PFCs and SF_6 (total 0.03 W m^{-2}) are not shown. Concentration-based RFs for gases can be obtained by summing the like-coloured bars. Volcanic forcing is not included as its episodic nature makes is difficult to compare to other forcing mechanisms. Total anthropogenic radiative forcing is provided for three different years relative to 1750. For further technical details, including uncertainty ranges associated with individual components and processes, see the Technical Summary Supplementary Material. {8.5; Figures 8.14–8.18; Figures TS.6 and TS.7}

D. Understanding the Climate System and its Recent Changes

Understanding recent changes in the climate system results from combining observations, studies of feedback processes, and model simulations. Evaluation of the ability of climate models to simulate recent changes requires consideration of the state of all modelled climate system components at the start of the simulation and the natural and anthropogenic forcing used to drive the models. Compared to AR4, more detailed and longer observations and improved climate models now enable the attribution of a human contribution to detected changes in more climate system components.

Human influence on the climate system is clear. This is evident from the increasing greenhouse gas concentrations in the atmosphere, positive radiative forcing, observed warming, and understanding of the climate system. {2–14}

D.1 Evaluation of Climate Models

Climate models have improved since the AR4. Models reproduce observed continental-scale surface temperature patterns and trends over many decades, including the more rapid warming since the mid-20th century and the cooling immediately following large volcanic eruptions (*very high confidence*). {9.4, 9.6, 9.8}

- The long-term climate model simulations show a trend in global-mean surface temperature from 1951 to 2012 that agrees with the observed trend (*very high confidence*). There are, however, differences between simulated and observed trends over periods as short as 10 to 15 years (e.g., 1998 to 2012). {9.4, Box 9.2}

- The observed reduction in surface warming trend over the period 1998 to 2012 as compared to the period 1951 to 2012, is due in roughly equal measure to a reduced trend in radiative forcing and a cooling contribution from natural internal variability, which includes a possible redistribution of heat within the ocean (*medium confidence*). The reduced trend in radiative forcing is primarily due to volcanic eruptions and the timing of the downward phase of the 11-year solar cycle. However, there is *low confidence* in quantifying the role of changes in radiative forcing in causing the reduced warming trend. There is *medium confidence* that natural internal decadal variability causes to a substantial degree the difference between observations and the simulations; the latter are not expected to reproduce the timing of natural internal variability. There may also be a contribution from forcing inadequacies and, in some models, an overestimate of the response to increasing greenhouse gas and other anthropogenic forcing (dominated by the effects of aerosols). {9.4, Box 9.2, 10.3, Box 10.2, 11.3}

- On regional scales, the confidence in model capability to simulate surface temperature is less than for the larger scales. However, there is *high confidence* that regional-scale surface temperature is better simulated than at the time of the AR4. {9.4, 9.6}

- There has been substantial progress in the assessment of extreme weather and climate events since AR4. Simulated global-mean trends in the frequency of extreme warm and cold days and nights over the second half of the 20th century are generally consistent with observations. {9.5}

- There has been some improvement in the simulation of continental-scale patterns of precipitation since the AR4. At regional scales, precipitation is not simulated as well, and the assessment is hampered by observational uncertainties. {9.4, 9.6}

- Some important climate phenomena are now better reproduced by models. There is *high confidence* that the statistics of monsoon and El Niño-Southern Oscillation (ENSO) based on multi-model simulations have improved since AR4. {9.5}

- Climate models now include more cloud and aerosol processes, and their interactions, than at the time of the AR4, but there remains *low confidence* in the representation and quantification of these processes in models. {7.3, 7.6, 9.4, 9.7}

- There is robust evidence that the downward trend in Arctic summer sea ice extent since 1979 is now reproduced by more models than at the time of the AR4, with about one-quarter of the models showing a trend as large as, or larger than, the trend in the observations. Most models simulate a small downward trend in Antarctic sea ice extent, albeit with large inter-model spread, in contrast to the small upward trend in observations. {9.4}

- Many models reproduce the observed changes in upper-ocean heat content (0–700 m) from 1961 to 2005 (*high confidence*), with the multi-model mean time series falling within the range of the available observational estimates for most of the period. {9.4}

- Climate models that include the carbon cycle (Earth System Models) simulate the global pattern of ocean-atmosphere CO_2 fluxes, with outgassing in the tropics and uptake in the mid and high latitudes. In the majority of these models the sizes of the simulated global land and ocean carbon sinks over the latter part of the 20th century are within the range of observational estimates. {9.4}

D.2 Quantification of Climate System Responses

Observational and model studies of temperature change, climate feedbacks and changes in the Earth's energy budget together provide confidence in the magnitude of global warming in response to past and future forcing. {Box 12.2, Box 13.1}

- The net feedback from the combined effect of changes in water vapour, and differences between atmospheric and surface warming is *extremely likely* positive and therefore amplifies changes in climate. The net radiative feedback due to all cloud types combined is *likely* positive. Uncertainty in the sign and magnitude of the cloud feedback is due primarily to continuing uncertainty in the impact of warming on low clouds. {7.2}

- The equilibrium climate sensitivity quantifies the response of the climate system to constant radiative forcing on multi-century time scales. It is defined as the change in global mean surface temperature at equilibrium that is caused by a doubling of the atmospheric CO_2 concentration. Equilibrium climate sensitivity is *likely* in the range 1.5°C to 4.5°C (*high confidence*), *extremely unlikely* less than 1°C (*high confidence*), and *very unlikely* greater than 6°C (*medium confidence*)[16]. The lower temperature limit of the assessed *likely* range is thus less than the 2°C in the AR4, but the upper limit is the same. This assessment reflects improved understanding, the extended temperature record in the atmosphere and ocean, and new estimates of radiative forcing. {TS TFE.6, Figure 1; Box 12.2}

- The rate and magnitude of global climate change is determined by radiative forcing, climate feedbacks and the storage of energy by the climate system. Estimates of these quantities for recent decades are consistent with the assessed *likely* range of the equilibrium climate sensitivity to within assessed uncertainties, providing strong evidence for our understanding of anthropogenic climate change. {Box 12.2, Box 13.1}

- The transient climate response quantifies the response of the climate system to an increasing radiative forcing on a decadal to century timescale. It is defined as the change in global mean surface temperature at the time when the atmospheric CO_2 concentration has doubled in a scenario of concentration increasing at 1% per year. The transient climate response is *likely* in the range of 1.0°C to 2.5°C (*high confidence*) and *extremely unlikely* greater than 3°C. {Box 12.2}

- A related quantity is the transient climate response to cumulative carbon emissions (TCRE). It quantifies the transient response of the climate system to cumulative carbon emissions (see Section E.8). TCRE is defined as the global mean

[16] No best estimate for equilibrium climate sensitivity can now be given because of a lack of agreement on values across assessed lines of evidence and studies.

surface temperature change per 1000 GtC emitted to the atmosphere. TCRE is *likely* in the range of 0.8°C to 2.5°C per 1000 GtC and applies for cumulative emissions up to about 2000 GtC until the time temperatures peak (see Figure SPM.10). {12.5, Box 12.2}

- Various metrics can be used to compare the contributions to climate change of emissions of different substances. The most appropriate metric and time horizon will depend on which aspects of climate change are considered most important to a particular application. No single metric can accurately compare all consequences of different emissions, and all have limitations and uncertainties. The Global Warming Potential is based on the cumulative radiative forcing over a particular time horizon, and the Global Temperature Change Potential is based on the change in global mean surface temperature at a chosen point in time. Updated values are provided in the underlying Report. {8.7}

D.3 Detection and Attribution of Climate Change

Human influence has been detected in warming of the atmosphere and the ocean, in changes in the global water cycle, in reductions in snow and ice, in global mean sea level rise, and in changes in some climate extremes (see Figure SPM.6 and Table SPM.1). This evidence for human influence has grown since AR4. It is *extremely likely* that human influence has been the dominant cause of the observed warming since the mid-20th century. {10.3–10.6, 10.9}

- It is *extremely likely* that more than half of the observed increase in global average surface temperature from 1951 to 2010 was caused by the anthropogenic increase in greenhouse gas concentrations and other anthropogenic forcings together. The best estimate of the human-induced contribution to warming is similar to the observed warming over this period. {10.3}

- Greenhouse gases contributed a global mean surface warming *likely* to be in the range of 0.5°C to 1.3°C over the period 1951 to 2010, with the contributions from other anthropogenic forcings, including the cooling effect of aerosols, *likely* to be in the range of –0.6°C to 0.1°C. The contribution from natural forcings is *likely* to be in the range of –0.1°C to 0.1°C, and from natural internal variability is *likely* to be in the range of –0.1°C to 0.1°C. Together these assessed contributions are consistent with the observed warming of approximately 0.6°C to 0.7°C over this period. {10.3}

- Over every continental region except Antarctica, anthropogenic forcings have *likely* made a substantial contribution to surface temperature increases since the mid-20th century (see Figure SPM.6). For Antarctica, large observational uncertainties result in *low confidence* that anthropogenic forcings have contributed to the observed warming averaged over available stations. It is *likely* that there has been an anthropogenic contribution to the very substantial Arctic warming since the mid-20th century. {2.4, 10.3}

- It is *very likely* that anthropogenic influence, particularly greenhouse gases and stratospheric ozone depletion, has led to a detectable observed pattern of tropospheric warming and a corresponding cooling in the lower stratosphere since 1961. {2.4, 9.4, 10.3}

- It is *very likely* that anthropogenic forcings have made a substantial contribution to increases in global upper ocean heat content (0–700 m) observed since the 1970s (see Figure SPM.6). There is evidence for human influence in some individual ocean basins. {3.2, 10.4}

- It is *likely* that anthropogenic influences have affected the global water cycle since 1960. Anthropogenic influences have contributed to observed increases in atmospheric moisture content in the atmosphere (*medium confidence*), to global-scale changes in precipitation patterns over land (*medium confidence*), to intensification of heavy precipitation over land regions where data are sufficient (*medium confidence*), and to changes in surface and sub-surface ocean salinity (*very likely*). {2.5, 2.6, 3.3, 7.6, 10.3, 10.4}

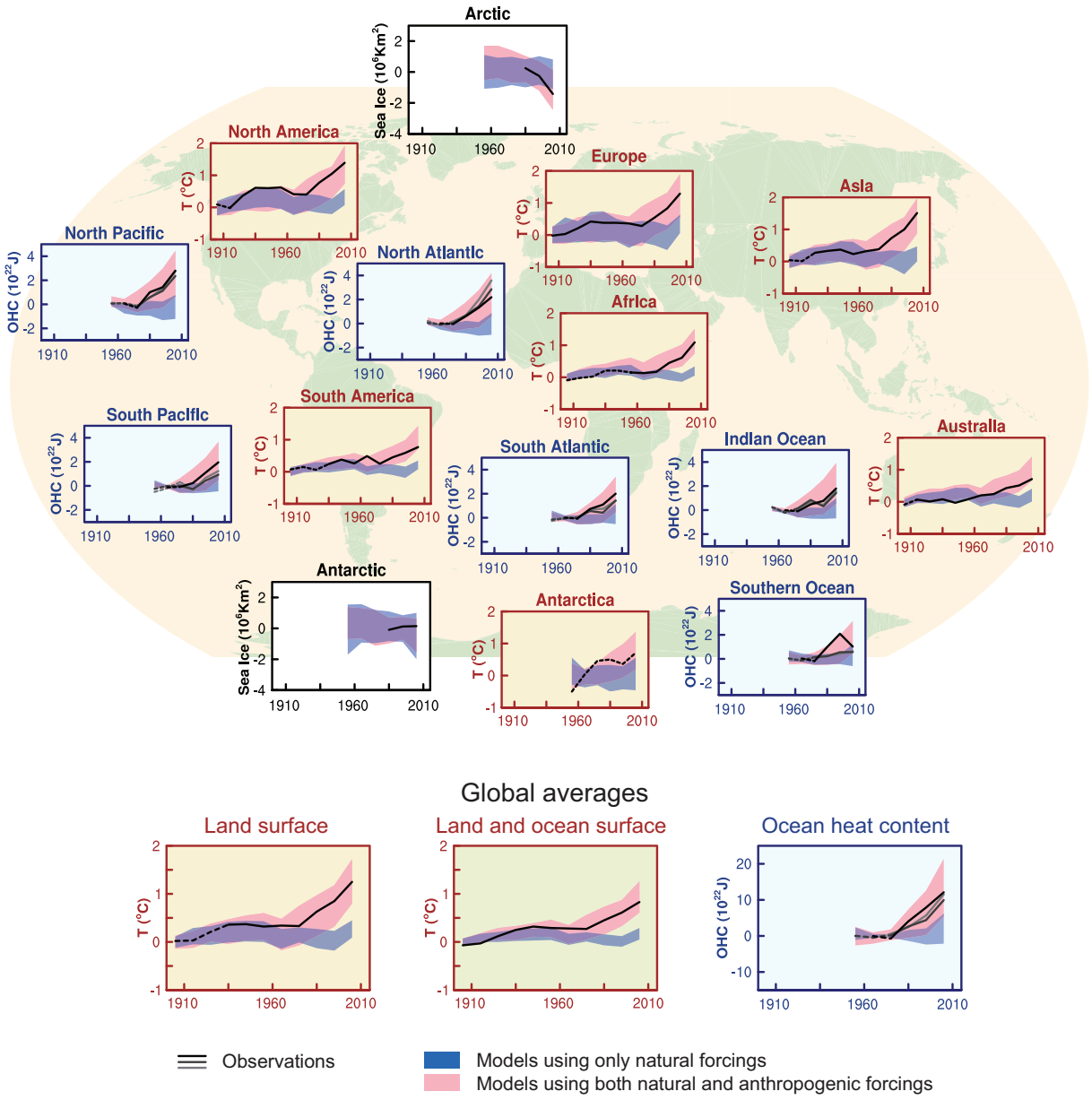

Figure SPM.6 | Comparison of observed and simulated climate change based on three large-scale indicators in the atmosphere, the cryosphere and the ocean: change in continental land surface air temperatures (yellow panels), Arctic and Antarctic September sea ice extent (white panels), and upper ocean heat content in the major ocean basins (blue panels). Global average changes are also given. Anomalies are given relative to 1880–1919 for surface temperatures, 1960–1980 for ocean heat content and 1979–1999 for sea ice. All time-series are decadal averages, plotted at the centre of the decade. For temperature panels, observations are dashed lines if the spatial coverage of areas being examined is below 50%. For ocean heat content and sea ice panels the solid line is where the coverage of data is good and higher in quality, and the dashed line is where the data coverage is only adequate, and thus, uncertainty is larger. Model results shown are Coupled Model Intercomparison Project Phase 5 (CMIP5) multi-model ensemble ranges, with shaded bands indicating the 5 to 95% confidence intervals. For further technical details, including region definitions see the Technical Summary Supplementary Material. {Figure 10.21; Figure TS.12}

- There has been further strengthening of the evidence for human influence on temperature extremes since the SREX. It is now *very likely* that human influence has contributed to observed global scale changes in the frequency and intensity of daily temperature extremes since the mid-20th century, and *likely* that human influence has more than doubled the probability of occurrence of heat waves in some locations (see Table SPM.1). {10.6}

- Anthropogenic influences have *very likely* contributed to Arctic sea ice loss since 1979. There is *low confidence* in the scientific understanding of the small observed increase in Antarctic sea ice extent due to the incomplete and competing scientific explanations for the causes of change and *low confidence* in estimates of natural internal variability in that region (see Figure SPM.6). {10.5}

- Anthropogenic influences *likely* contributed to the retreat of glaciers since the 1960s and to the increased surface mass loss of the Greenland ice sheet since 1993. Due to a low level of scientific understanding there is *low confidence* in attributing the causes of the observed loss of mass from the Antarctic ice sheet over the past two decades. {4.3, 10.5}

- It is *likely* that there has been an anthropogenic contribution to observed reductions in Northern Hemisphere spring snow cover since 1970. {10.5}

- It is *very likely* that there is a substantial anthropogenic contribution to the global mean sea level rise since the 1970s. This is based on the *high confidence* in an anthropogenic influence on the two largest contributions to sea level rise, that is thermal expansion and glacier mass loss. {10.4, 10.5, 13.3}

- There is *high confidence* that changes in total solar irradiance have not contributed to the increase in global mean surface temperature over the period 1986 to 2008, based on direct satellite measurements of total solar irradiance. There is *medium confidence* that the 11-year cycle of solar variability influences decadal climate fluctuations in some regions. No robust association between changes in cosmic rays and cloudiness has been identified. {7.4, 10.3, Box 10.2}

E. Future Global and Regional Climate Change

Projections of changes in the climate system are made using a hierarchy of climate models ranging from simple climate models, to models of intermediate complexity, to comprehensive climate models, and Earth System Models. These models simulate changes based on a set of scenarios of anthropogenic forcings. A new set of scenarios, the Representative Concentration Pathways (RCPs), was used for the new climate model simulations carried out under the framework of the Coupled Model Intercomparison Project Phase 5 (CMIP5) of the World Climate Research Programme. In all RCPs, atmospheric CO_2 concentrations are higher in 2100 relative to present day as a result of a further increase of cumulative emissions of CO_2 to the atmosphere during the 21st century (see Box SPM.1). Projections in this Summary for Policymakers are for the end of the 21st century (2081–2100) given relative to 1986–2005, unless otherwise stated. To place such projections in historical context, it is necessary to consider observed changes between different periods. Based on the longest global surface temperature dataset available, the observed change between the average of the period 1850–1900 and of the AR5 reference period is 0.61 [0.55 to 0.67] °C. However, warming has occurred beyond the average of the AR5 reference period. Hence this is not an estimate of historical warming to present (see Chapter 2) .

Continued emissions of greenhouse gases will cause further warming and changes in all components of the climate system. Limiting climate change will require substantial and sustained reductions of greenhouse gas emissions. {6, 11–14}

- Projections for the next few decades show spatial patterns of climate change similar to those projected for the later 21st century but with smaller magnitude. Natural internal variability will continue to be a major influence on climate, particularly in the near-term and at the regional scale. By the mid-21st century the magnitudes of the projected changes are substantially affected by the choice of emissions scenario (Box SPM.1). {11.3, Box 11.1, Annex I}

- Projected climate change based on RCPs is similar to AR4 in both patterns and magnitude, after accounting for scenario differences. The overall spread of projections for the high RCPs is narrower than for comparable scenarios used in AR4 because in contrast to the SRES emission scenarios used in AR4, the RCPs used in AR5 are defined as concentration pathways and thus carbon cycle uncertainties affecting atmospheric CO_2 concentrations are not considered in the concentration-driven CMIP5 simulations. Projections of sea level rise are larger than in the AR4, primarily because of improved modelling of land-ice contributions.{11.3, 12.3, 12.4, 13.4, 13.5}

E.1 Atmosphere: Temperature

Global surface temperature change for the end of the 21st century is *likely* to exceed 1.5°C relative to 1850 to 1900 for all RCP scenarios except RCP2.6. It is *likely* to exceed 2°C for RCP6.0 and RCP8.5, and *more likely than not* to exceed 2°C for RCP4.5. Warming will continue beyond 2100 under all RCP scenarios except RCP2.6. Warming will continue to exhibit interannual-to-decadal variability and will not be regionally uniform (see Figures SPM.7 and SPM.8). {11.3, 12.3, 12.4, 14.8}

- The global mean surface temperature change for the period 2016–2035 relative to 1986–2005 will *likely* be in the range of 0.3°C to 0.7°C (*medium confidence*). This assessment is based on multiple lines of evidence and assumes there will be no major volcanic eruptions or secular changes in total solar irradiance. Relative to natural internal variability, near-term increases in seasonal mean and annual mean temperatures are expected to be larger in the tropics and subtropics than in mid-latitudes (*high confidence*). {11.3}

- Increase of global mean surface temperatures for 2081–2100 relative to 1986–2005 is projected to *likely* be in the ranges derived from the concentration-driven CMIP5 model simulations, that is, 0.3°C to 1.7°C (RCP2.6), 1.1°C to 2.6°C (RCP4.5), 1.4°C to 3.1°C (RCP6.0), 2.6°C to 4.8°C (RCP8.5). The Arctic region will warm more rapidly than the global mean, and mean warming over land will be larger than over the ocean (*very high confidence*) (see Figures SPM.7 and SPM.8, and Table SPM.2). {12.4, 14.8}

- Relative to the average from year 1850 to 1900, global surface temperature change by the end of the 21st century is projected to *likely* exceed 1.5°C for RCP4.5, RCP6.0 and RCP8.5 (*high confidence*). Warming is *likely* to exceed 2°C for RCP6.0 and RCP8.5 (*high confidence*), *more likely than not* to exceed 2°C for RCP4.5 (*high confidence*), but *unlikely* to exceed 2°C for RCP2.6 (*medium confidence*). Warming is *unlikely* to exceed 4°C for RCP2.6, RCP4.5 and RCP6.0 (*high confidence*) and is *about as likely as not* to exceed 4°C for RCP8.5 (*medium confidence*). {12.4}

- It is *virtually certain* that there will be more frequent hot and fewer cold temperature extremes over most land areas on daily and seasonal timescales as global mean temperatures increase. It is *very likely* that heat waves will occur with a higher frequency and duration. Occasional cold winter extremes will continue to occur (see Table SPM.1). {12.4}

E.2 Atmosphere: Water Cycle

Changes in the global water cycle in response to the warming over the 21st century will not be uniform. The contrast in precipitation between wet and dry regions and between wet and dry seasons will increase, although there may be regional exceptions (see Figure SPM.8). {12.4, 14.3}

- Projected changes in the water cycle over the next few decades show similar large-scale patterns to those towards the end of the century, but with smaller magnitude. Changes in the near-term, and at the regional scale will be strongly influenced by natural internal variability and may be affected by anthropogenic aerosol emissions. {11.3}

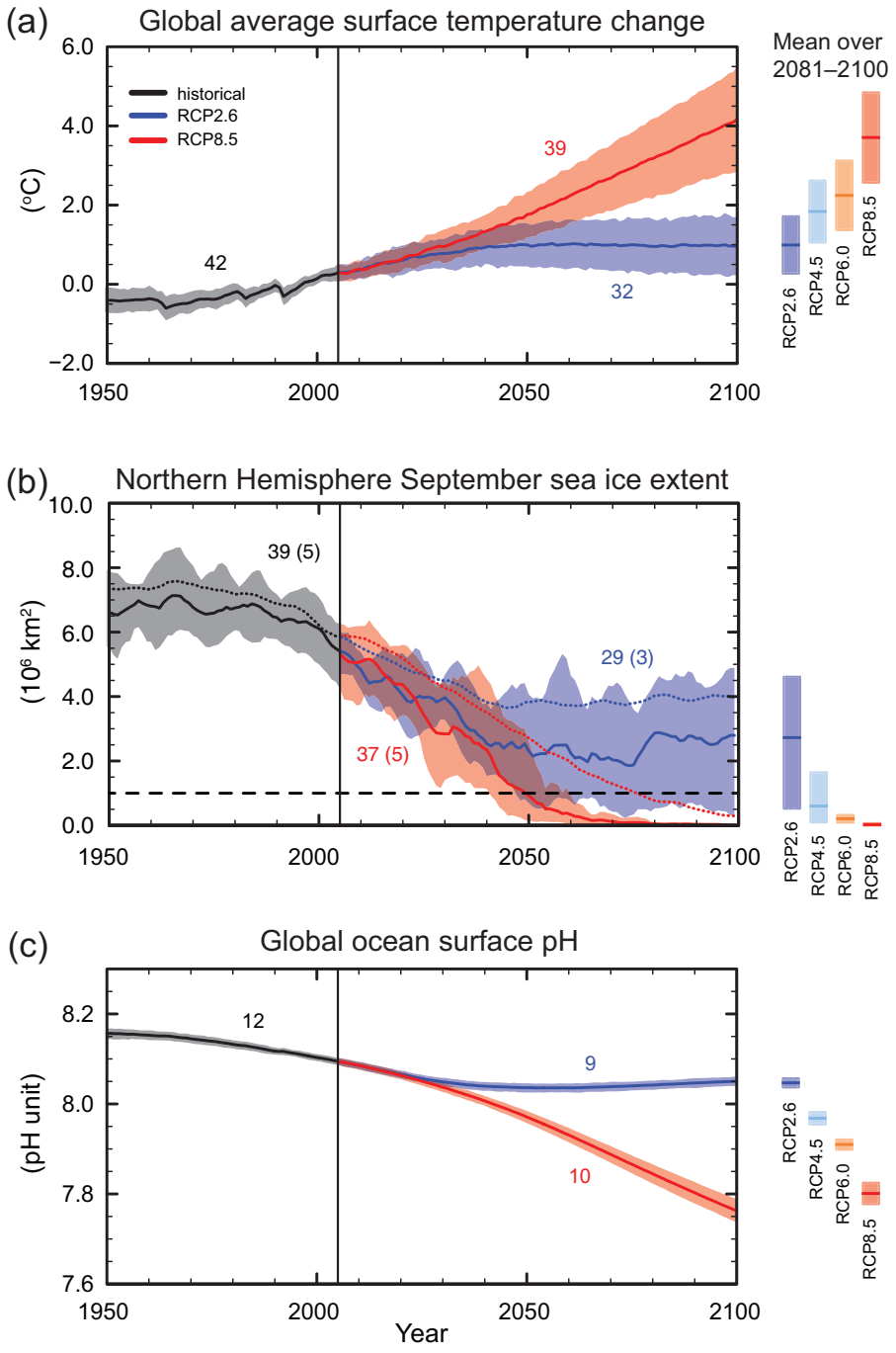

Figure SPM.7 | CMIP5 multi-model simulated time series from 1950 to 2100 for (a) change in global annual mean surface temperature relative to 1986–2005, (b) Northern Hemisphere September sea ice extent (5-year running mean), and (c) global mean ocean surface pH. Time series of projections and a measure of uncertainty (shading) are shown for scenarios RCP2.6 (blue) and RCP8.5 (red). Black (grey shading) is the modelled historical evolution using historical reconstructed forcings. The mean and associated uncertainties averaged over 2081–2100 are given for all RCP scenarios as colored vertical bars. The numbers of CMIP5 models used to calculate the multi-model mean is indicated. For sea ice extent (b), the projected mean and uncertainty (minimum-maximum range) of the subset of models that most closely reproduce the climatological mean state and 1979 to 2012 trend of the Arctic sea ice is given (number of models given in brackets). For completeness, the CMIP5 multi-model mean is also indicated with dotted lines. The dashed line represents nearly ice-free conditions (i.e., when sea ice extent is less than 10^6 km^2 for at least five consecutive years). For further technical details see the Technical Summary Supplementary Material {Figures 6.28, 12.5, and 12.28–12.31; Figures TS.15, TS.17, and TS.20}

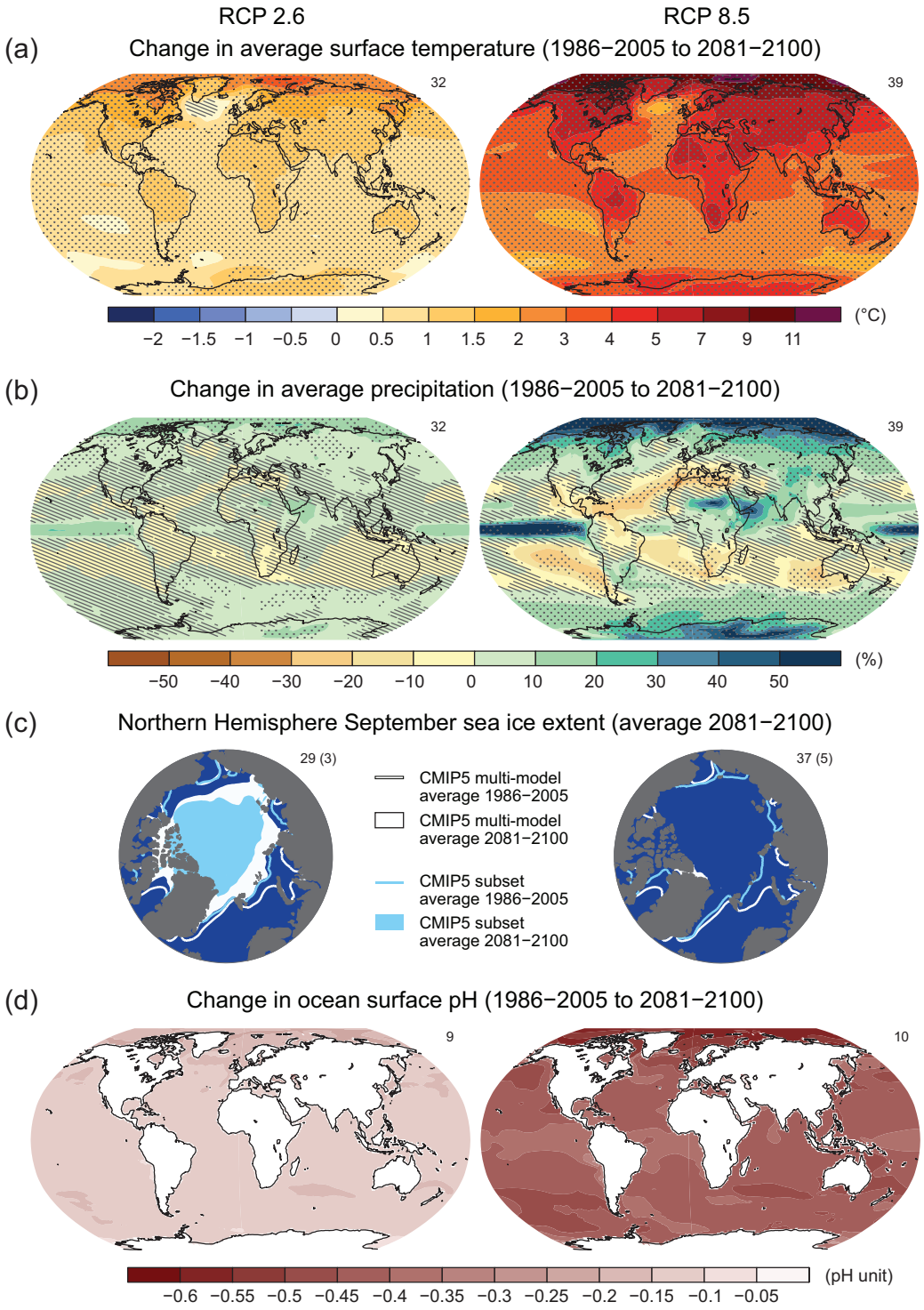

Figure SPM.8 | Maps of CMIP5 multi-model mean results for the scenarios RCP2.6 and RCP8.5 in 2081–2100 of (a) annual mean surface temperature change, (b) average percent change in annual mean precipitation, (c) Northern Hemisphere September sea ice extent, and (d) change in ocean surface pH. Changes in panels (a), (b) and (d) are shown relative to 1986–2005. The number of CMIP5 models used to calculate the multi-model mean is indicated in the upper right corner of each panel. For panels (a) and (b), hatching indicates regions where the multi-model mean is small compared to natural internal variability (i.e., less than one standard deviation of natural internal variability in 20-year means). Stippling indicates regions where the multi-model mean is large compared to natural internal variability (i.e., greater than two standard deviations of natural internal variability in 20-year means) and where at least 90% of models agree on the sign of change (see Box 12.1). In panel (c), the lines are the modelled means for 1986–2005; the filled areas are for the end of the century. The CMIP5 multi-model mean is given in white colour, the projected mean sea ice extent of a subset of models (number of models given in brackets) that most closely reproduce the climatological mean state and 1979 to 2012 trend of the Arctic sea ice extent is given in light blue colour. For further technical details see the Technical Summary Supplementary Material. {Figures 6.28, 12.11, 12.22, and 12.29; Figures TS.15, TS.16, TS.17, and TS.20}

- The high latitudes and the equatorial Pacific Ocean are *likely* to experience an increase in annual mean precipitation by the end of this century under the RCP8.5 scenario. In many mid-latitude and subtropical dry regions, mean precipitation will *likely* decrease, while in many mid-latitude wet regions, mean precipitation will *likely* increase by the end of this century under the RCP8.5 scenario (see Figure SPM.8). {7.6, 12.4, 14.3}

- Extreme precipitation events over most of the mid-latitude land masses and over wet tropical regions will *very likely* become more intense and more frequent by the end of this century, as global mean surface temperature increases (see Table SPM.1). {7.6, 12.4}

- Globally, it is *likely* that the area encompassed by monsoon systems will increase over the 21st century. While monsoon winds are *likely* to weaken, monsoon precipitation is *likely* to intensify due to the increase in atmospheric moisture. Monsoon onset dates are *likely* to become earlier or not to change much. Monsoon retreat dates will *likely* be delayed, resulting in lengthening of the monsoon season in many regions. {14.2}

- There is *high confidence* that the El Niño-Southern Oscillation (ENSO) will remain the dominant mode of interannual variability in the tropical Pacific, with global effects in the 21st century. Due to the increase in moisture availability, ENSO-related precipitation variability on regional scales will *likely* intensify. Natural variations of the amplitude and spatial pattern of ENSO are large and thus *confidence* in any specific projected change in ENSO and related regional phenomena for the 21st century remains *low*. {5.4, 14.4}

Table SPM.2 | Projected change in global mean surface air temperature and global mean sea level rise for the mid- and late 21st century relative to the reference period of 1986–2005. {12.4; Table 12.2, Table 13.5}

		2046–2065		2081–2100	
	Scenario	**Mean**	***Likely* range[c]**	**Mean**	***Likely* range[c]**
Global Mean Surface Temperature Change (°C)[a]	RCP2.6	1.0	0.4 to 1.6	1.0	0.3 to 1.7
	RCP4.5	1.4	0.9 to 2.0	1.8	1.1 to 2.6
	RCP6.0	1.3	0.8 to 1.8	2.2	1.4 to 3.1
	RCP8.5	2.0	1.4 to 2.6	3.7	2.6 to 4.8
	Scenario	**Mean**	***Likely* range[d]**	**Mean**	***Likely* range[d]**
Global Mean Sea Level Rise (m)[b]	RCP2.6	0.24	0.17 to 0.32	0.40	0.26 to 0.55
	RCP4.5	0.26	0.19 to 0.33	0.47	0.32 to 0.63
	RCP6.0	0.25	0.18 to 0.32	0.48	0.33 to 0.63
	RCP8.5	0.30	0.22 to 0.38	0.63	0.45 to 0.82

Notes:

[a] Based on the CMIP5 ensemble; anomalies calculated with respect to 1986–2005. Using HadCRUT4 and its uncertainty estimate (5–95% confidence interval), the observed warming to the reference period 1986–2005 is 0.61 [0.55 to 0.67] °C from 1850–1900, and 0.11 [0.09 to 0.13] °C from 1980–1999, the reference period for projections used in AR4. *Likely* ranges have not been assessed here with respect to earlier reference periods because methods are not generally available in the literature for combining the uncertainties in models and observations. Adding projected and observed changes does not account for potential effects of model biases compared to observations, and for natural internal variability during the observational reference period {2.4; 11.2; Tables 12.2 and 12.3}

[b] Based on 21 CMIP5 models; anomalies calculated with respect to 1986–2005. Where CMIP5 results were not available for a particular AOGCM and scenario, they were estimated as explained in Chapter 13, Table 13.5. The contributions from ice sheet rapid dynamical change and anthropogenic land water storage are treated as having uniform probability distributions, and as largely independent of scenario. This treatment does not imply that the contributions concerned will not depend on the scenario followed, only that the current state of knowledge does not permit a quantitative assessment of the dependence. Based on current understanding, only the collapse of marine-based sectors of the Antarctic ice sheet, if initiated, could cause global mean sea level to rise substantially above the *likely* range during the 21st century. There is *medium confidence* that this additional contribution would not exceed several tenths of a meter of sea level rise during the 21st century.

[c] Calculated from projections as 5–95% model ranges. These ranges are then assessed to be *likely* ranges after accounting for additional uncertainties or different levels of confidence in models. For projections of global mean surface temperature change in 2046–2065 *confidence* is *medium*, because the relative importance of natural internal variability, and uncertainty in non-greenhouse gas forcing and response, are larger than for 2081–2100. The *likely* ranges for 2046–2065 do not take into account the possible influence of factors that lead to the assessed range for near-term (2016–2035) global mean surface temperature change that is lower than the 5–95% model range, because the influence of these factors on longer term projections has not been quantified due to insufficient scientific understanding. {11.3}

[d] Calculated from projections as 5–95% model ranges. These ranges are then assessed to be *likely* ranges after accounting for additional uncertainties or different levels of confidence in models. For projections of global mean sea level rise *confidence* is *medium* for both time horizons.

E.3 Atmosphere: Air Quality

- The range in projections of air quality (ozone and PM2.5[17] in near-surface air) is driven primarily by emissions (including CH_4), rather than by physical climate change (*medium confidence*). There is *high confidence* that globally, warming decreases background surface ozone. High CH_4 levels (as in RCP8.5) can offset this decrease, raising background surface ozone by year 2100 on average by about 8 ppb (25% of current levels) relative to scenarios with small CH_4 changes (as in RCP4.5 and RCP6.0) (*high confidence*). {11.3}

- Observational and modelling evidence indicates that, all else being equal, locally higher surface temperatures in polluted regions will trigger regional feedbacks in chemistry and local emissions that will increase peak levels of ozone and PM2.5 (*medium confidence*). For PM2.5, climate change may alter natural aerosol sources as well as removal by precipitation, but no confidence level is attached to the overall impact of climate change on PM2.5 distributions. {11.3}

E.4 Ocean

The global ocean will continue to warm during the 21st century. Heat will penetrate from the surface to the deep ocean and affect ocean circulation. {11.3, 12.4}

- The strongest ocean warming is projected for the surface in tropical and Northern Hemisphere subtropical regions. At greater depth the warming will be most pronounced in the Southern Ocean (*high confidence*). Best estimates of ocean warming in the top one hundred meters are about 0.6°C (RCP2.6) to 2.0°C (RCP8.5), and about 0.3°C (RCP2.6) to 0.6°C (RCP8.5) at a depth of about 1000 m by the end of the 21st century. {12.4, 14.3}

- It is *very likely* that the Atlantic Meridional Overturning Circulation (AMOC) will weaken over the 21st century. Best estimates and ranges[18] for the reduction are 11% (1 to 24%) in RCP2.6 and 34% (12 to 54%) in RCP8.5. It is *likely* that there will be some decline in the AMOC by about 2050, but there may be some decades when the AMOC increases due to large natural internal variability. {11.3, 12.4}

- It is *very unlikely* that the AMOC will undergo an abrupt transition or collapse in the 21st century for the scenarios considered. There is *low confidence* in assessing the evolution of the AMOC beyond the 21st century because of the limited number of analyses and equivocal results. However, a collapse beyond the 21st century for large sustained warming cannot be excluded. {12.5}

E.5 Cryosphere

It is *very likely* that the Arctic sea ice cover will continue to shrink and thin and that Northern Hemisphere spring snow cover will decrease during the 21st century as global mean surface temperature rises. Global glacier volume will further decrease. {12.4, 13.4}

- Year-round reductions in Arctic sea ice extent are projected by the end of the 21st century from multi-model averages. These reductions range from 43% for RCP2.6 to 94% for RCP8.5 in September and from 8% for RCP2.6 to 34% for RCP8.5 in February (*medium confidence*) (see Figures SPM.7 and SPM.8). {12.4}

[17] PM2.5 refers to particulate matter with a diameter of less than 2.5 micrometres, a measure of atmospheric aerosol concentration.

[18] The ranges in this paragraph indicate a CMIP5 model spread.

- Based on an assessment of the subset of models that most closely reproduce the climatological mean state and 1979 to 2012 trend of the Arctic sea ice extent, a nearly ice-free Arctic Ocean[19] in September before mid-century is *likely* for RCP8.5 (*medium confidence*) (see Figures SPM.7 and SPM.8). A projection of when the Arctic might become nearly ice-free in September in the 21st century cannot be made with confidence for the other scenarios. {11.3, 12.4, 12.5}

- In the Antarctic, a decrease in sea ice extent and volume is projected with *low confidence* for the end of the 21st century as global mean surface temperature rises. {12.4}

- By the end of the 21st century, the global glacier volume, excluding glaciers on the periphery of Antarctica, is projected to decrease by 15 to 55% for RCP2.6, and by 35 to 85% for RCP8.5 (*medium confidence*). {13.4, 13.5}

- The area of Northern Hemisphere spring snow cover is projected to decrease by 7% for RCP2.6 and by 25% in RCP8.5 by the end of the 21st century for the model average (*medium confidence*). {12.4}

- It is *virtually certain* that near-surface permafrost extent at high northern latitudes will be reduced as global mean surface temperature increases. By the end of the 21st century, the area of permafrost near the surface (upper 3.5 m) is projected to decrease by between 37% (RCP2.6) to 81% (RCP8.5) for the model average (*medium confidence*). {12.4}

E.6 Sea Level

Global mean sea level will continue to rise during the 21st century (see Figure SPM.9). Under all RCP scenarios, the rate of sea level rise will *very likely* exceed that observed during 1971 to 2010 due to increased ocean warming and increased loss of mass from glaciers and ice sheets. {13.3–13.5}

- Confidence in projections of global mean sea level rise has increased since the AR4 because of the improved physical understanding of the components of sea level, the improved agreement of process-based models with observations, and the inclusion of ice-sheet dynamical changes. {13.3–13.5}

- Global mean sea level rise for 2081–2100 relative to 1986–2005 will *likely* be in the ranges of 0.26 to 0.55 m for RCP2.6, 0.32 to 0.63 m for RCP4.5, 0.33 to 0.63 m for RCP6.0, and 0.45 to 0.82 m for RCP8.5 (*medium confidence*). For RCP8.5, the rise by the year 2100 is 0.52 to 0.98 m, with a rate during 2081 to 2100 of 8 to 16 mm yr^{-1} (*medium confidence*). These ranges are derived from CMIP5 climate projections in combination with process-based models and literature assessment of glacier and ice sheet contributions (see Figure SPM.9, Table SPM.2). {13.5}

- In the RCP projections, thermal expansion accounts for 30 to 55% of 21st century global mean sea level rise, and glaciers for 15 to 35%. The increase in surface melting of the Greenland ice sheet will exceed the increase in snowfall, leading to a positive contribution from changes in surface mass balance to future sea level (*high confidence*). While surface melting will remain small, an increase in snowfall on the Antarctic ice sheet is expected (*medium confidence*), resulting in a negative contribution to future sea level from changes in surface mass balance. Changes in outflow from both ice sheets combined will *likely* make a contribution in the range of 0.03 to 0.20 m by 2081–2100 (*medium confidence*). {13.3–13.5}

- Based on current understanding, only the collapse of marine-based sectors of the Antarctic ice sheet, if initiated, could cause global mean sea level to rise substantially above the *likely* range during the 21st century. However, there is *medium confidence* that this additional contribution would not exceed several tenths of a meter of sea level rise during the 21st century. {13.4, 13.5}

[19] Conditions in the Arctic Ocean are referred to as nearly ice-free when the sea ice extent is less than 10^6 km^2 for at least five consecutive years.

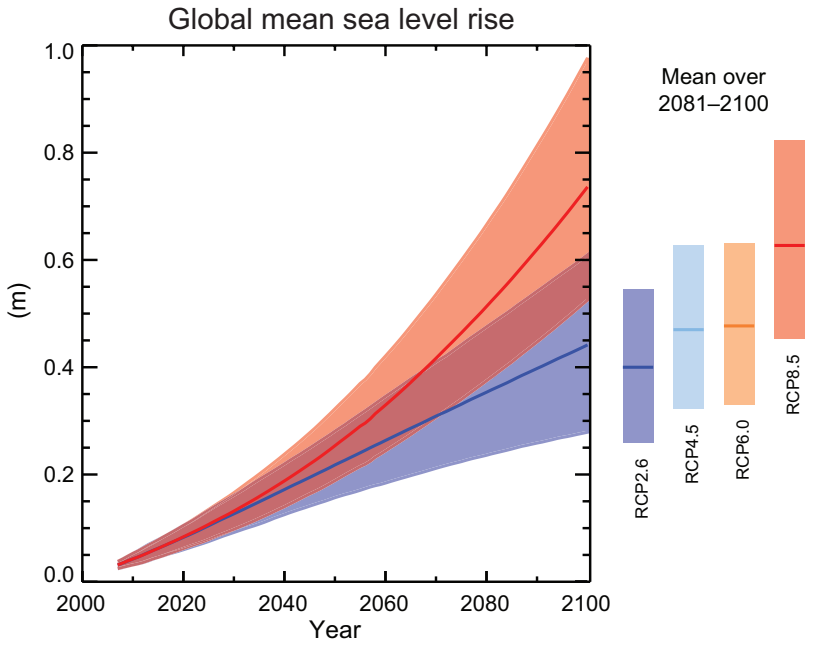

Figure SPM.9 | Projections of global mean sea level rise over the 21st century relative to 1986–2005 from the combination of the CMIP5 ensemble with process-based models, for RCP2.6 and RCP8.5. The assessed *likely* range is shown as a shaded band. The assessed *likely* ranges for the mean over the period 2081–2100 for all RCP scenarios are given as coloured vertical bars, with the corresponding median value given as a horizontal line. For further technical details see the Technical Summary Supplementary Material {Table 13.5, Figures 13.10 and 13.11; Figures TS.21 and TS.22}

- The basis for higher projections of global mean sea level rise in the 21st century has been considered and it has been concluded that there is currently insufficient evidence to evaluate the probability of specific levels above the assessed *likely* range. Many semi-empirical model projections of global mean sea level rise are higher than process-based model projections (up to about twice as large), but there is no consensus in the scientific community about their reliability and there is thus *low confidence* in their projections. {13.5}

- Sea level rise will not be uniform. By the end of the 21st century, it is *very likely* that sea level will rise in more than about 95% of the ocean area. About 70% of the coastlines worldwide are projected to experience sea level change within 20% of the global mean sea level change. {13.1, 13.6}

E.7 Carbon and Other Biogeochemical Cycles

Climate change will affect carbon cycle processes in a way that will exacerbate the increase of CO_2 in the atmosphere (*high confidence*). Further uptake of carbon by the ocean will increase ocean acidification. {6.4}

- Ocean uptake of anthropogenic CO_2 will continue under all four RCPs through to 2100, with higher uptake for higher concentration pathways (*very high confidence*). The future evolution of the land carbon uptake is less certain. A majority of models projects a continued land carbon uptake under all RCPs, but some models simulate a land carbon loss due to the combined effect of climate change and land use change. {6.4}

- Based on Earth System Models, there is *high confidence* that the feedback between climate and the carbon cycle is positive in the 21st century; that is, climate change will partially offset increases in land and ocean carbon sinks caused by rising atmospheric CO_2. As a result more of the emitted anthropogenic CO_2 will remain in the atmosphere. A positive feedback between climate and the carbon cycle on century to millennial time scales is supported by paleoclimate observations and modelling. {6.2, 6.4}

Table SPM.3 | Cumulative CO_2 emissions for the 2012 to 2100 period compatible with the RCP atmospheric concentrations simulated by the CMIP5 Earth System Models. {6.4, Table 6.12, Figure TS.19}

Scenario	Cumulative CO_2 Emissions 2012 to 2100[a]			
	GtC		$GtCO_2$	
	Mean	Range	Mean	Range
RCP2.6	270	140 to 410	990	510 to 1505
RCP4.5	780	595 to 1005	2860	2180 to 3690
RCP6.0	1060	840 to 1250	3885	3080 to 4585
RCP8.5	1685	1415 to 1910	6180	5185 to 7005

Notes:
[a] 1 Gigatonne of carbon = 1 GtC = 10^{15} grams of carbon. This corresponds to 3.667 $GtCO_2$.

- Earth System Models project a global increase in ocean acidification for all RCP scenarios. The corresponding decrease in surface ocean pH by the end of 21st century is in the range[18] of 0.06 to 0.07 for RCP2.6, 0.14 to 0.15 for RCP4.5, 0.20 to 0.21 for RCP6.0, and 0.30 to 0.32 for RCP8.5 (see Figures SPM.7 and SPM.8). {6.4}

- Cumulative CO_2 emissions[20] for the 2012 to 2100 period compatible with the RCP atmospheric CO_2 concentrations, as derived from 15 Earth System Models, range[18] from 140 to 410 GtC for RCP2.6, 595 to 1005 GtC for RCP4.5, 840 to 1250 GtC for RCP6.0, and 1415 to 1910 GtC for RCP8.5 (see Table SPM.3). {6.4}

- By 2050, annual CO_2 emissions derived from Earth System Models following RCP2.6 are smaller than 1990 emissions (by 14 to 96%). By the end of the 21st century, about half of the models infer emissions slightly above zero, while the other half infer a net removal of CO_2 from the atmosphere. {6.4, Figure TS.19}

- The release of CO_2 or CH_4 to the atmosphere from thawing permafrost carbon stocks over the 21st century is assessed to be in the range of 50 to 250 GtC for RCP8.5 (*low confidence*). {6.4}

E.8 Climate Stabilization, Climate Change Commitment and Irreversibility

Cumulative emissions of CO_2 largely determine global mean surface warming by the late 21st century and beyond (see Figure SPM.10). Most aspects of climate change will persist for many centuries even if emissions of CO_2 are stopped. This represents a substantial multi-century climate change commitment created by past, present and future emissions of CO_2. {12.5}

- Cumulative total emissions of CO_2 and global mean surface temperature response are approximately linearly related (see Figure SPM.10). Any given level of warming is associated with a range of cumulative CO_2 emissions[21], and therefore, e.g., higher emissions in earlier decades imply lower emissions later. {12.5}

- Limiting the warming caused by anthropogenic CO_2 emissions alone with a probability of >33%, >50%, and >66% to less than 2°C since the period 1861–1880[22], will require cumulative CO_2 emissions from all anthropogenic sources to stay between 0 and about 1570 GtC (5760 $GtCO_2$), 0 and about 1210 GtC (4440 $GtCO_2$), and 0 and about 1000 GtC (3670 $GtCO_2$) since that period, respectively[23]. These upper amounts are reduced to about 900 GtC (3300 $GtCO_2$), 820 GtC (3010 $GtCO_2$), and 790 GtC (2900 $GtCO_2$), respectively, when accounting for non-CO_2 forcings as in RCP2.6. An amount of 515 [445 to 585] GtC (1890 [1630 to 2150] $GtCO_2$), was already emitted by 2011. {12.5}

[20] From fossil fuel, cement, industry, and waste sectors.

[21] Quantification of this range of CO_2 emissions requires taking into account non-CO_2 drivers.

[22] The first 20-year period available from the models.

[23] This is based on the assessment of the transient climate response to cumulative carbon emissions (TCRE, see Section D.2).

- A lower warming target, or a higher likelihood of remaining below a specific warming target, will require lower cumulative CO_2 emissions. Accounting for warming effects of increases in non-CO_2 greenhouse gases, reductions in aerosols, or the release of greenhouse gases from permafrost will also lower the cumulative CO_2 emissions for a specific warming target (see Figure SPM.10). {12.5}

- A large fraction of anthropogenic climate change resulting from CO_2 emissions is irreversible on a multi-century to millennial time scale, except in the case of a large net removal of CO_2 from the atmosphere over a sustained period. Surface temperatures will remain approximately constant at elevated levels for many centuries after a complete cessation of net anthropogenic CO_2 emissions. Due to the long time scales of heat transfer from the ocean surface to depth, ocean warming will continue for centuries. Depending on the scenario, about 15 to 40% of emitted CO_2 will remain in the atmosphere longer than 1,000 years. {Box 6.1, 12.4, 12.5}

- It is *virtually certain* that global mean sea level rise will continue beyond 2100, with sea level rise due to thermal expansion to continue for many centuries. The few available model results that go beyond 2100 indicate global mean sea level rise above the pre-industrial level by 2300 to be less than 1 m for a radiative forcing that corresponds to CO_2 concentrations that peak and decline and remain below 500 ppm, as in the scenario RCP2.6. For a radiative forcing that corresponds to a CO_2 concentration that is above 700 ppm but below 1500 ppm, as in the scenario RCP8.5, the projected rise is 1 m to more than 3 m (*medium confidence*). {13.5}

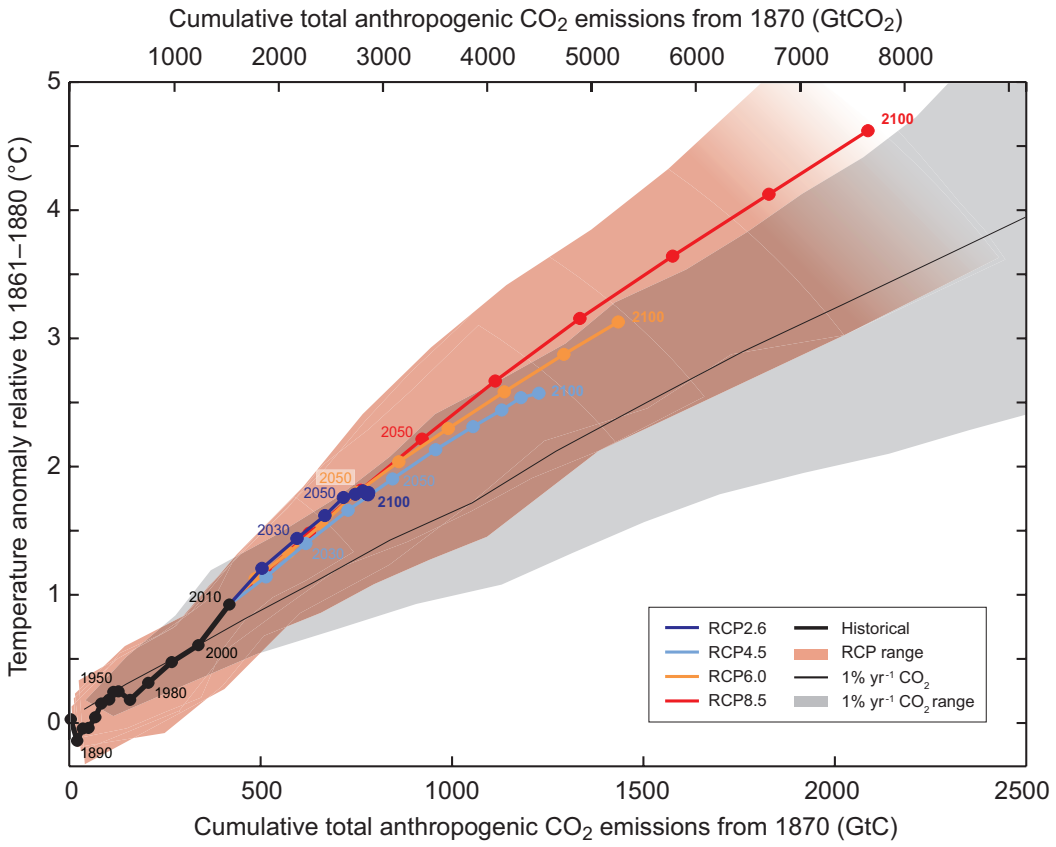

Figure SPM.10 | Global mean surface temperature increase as a function of cumulative total global CO_2 emissions from various lines of evidence. Multi-model results from a hierarchy of climate-carbon cycle models for each RCP until 2100 are shown with coloured lines and decadal means (dots). Some decadal means are labeled for clarity (e.g., 2050 indicating the decade 2040–2049). Model results over the historical period (1860 to 2010) are indicated in black. The coloured plume illustrates the multi-model spread over the four RCP scenarios and fades with the decreasing number of available models in RCP8.5. The multi-model mean and range simulated by CMIP5 models, forced by a CO_2 increase of 1% per year (1% yr^{-1} CO_2 simulations), is given by the thin black line and grey area. For a specific amount of cumulative CO_2 emissions, the 1% per year CO_2 simulations exhibit lower warming than those driven by RCPs, which include additional non-CO_2 forcings. Temperature values are given relative to the 1861–1880 base period, emissions relative to 1870. Decadal averages are connected by straight lines. For further technical details see the Technical Summary Supplementary Material. {Figure 12.45; TS TFE.8, Figure 1}

- Sustained mass loss by ice sheets would cause larger sea level rise, and some part of the mass loss might be irreversible. There is *high confidence* that sustained warming greater than some threshold would lead to the near-complete loss of the Greenland ice sheet over a millennium or more, causing a global mean sea level rise of up to 7 m. Current estimates indicate that the threshold is greater than about 1°C (*low confidence*) but less than about 4°C (*medium confidence*) global mean warming with respect to pre-industrial. Abrupt and irreversible ice loss from a potential instability of marine-based sectors of the Antarctic ice sheet in response to climate forcing is possible, but current evidence and understanding is insufficient to make a quantitative assessment. {5.8, 13.4, 13.5}

- Methods that aim to deliberately alter the climate system to counter climate change, termed geoengineering, have been proposed. Limited evidence precludes a comprehensive quantitative assessment of both Solar Radiation Management (SRM) and Carbon D ioxide Removal (CDR) and their impact on the climate system. CDR methods have biogeochemical and technological limitations to their potential on a global scale. There is insufficient knowledge to quantify how much CO_2 emissions could be partially offset by CDR on a century timescale. Modelling indicates that SRM methods, if realizable, have the potential to substantially offset a global temperature rise, but they would also modify the global water cycle, and would not reduce ocean acidification. If SRM were terminated for any reason, there is *high confidence* that global surface temperatures would rise very rapidly to values consistent with the greenhouse gas forcing. CDR and SRM methods carry side effects and long-term consequences on a global scale. {6.5, 7.7}

Box SPM.1: Representative Concentration Pathways (RCPs)

Climate change projections in IPCC Working Group I require information about future emissions or concentrations of greenhouse gases, aerosols and other climate drivers. This information is often expressed as a scenario of human activities, which are not assessed in this report. Scenarios used in Working Group I have focused on anthropogenic emissions and do not include changes in natural drivers such as solar or volcanic forcing or natural emissions, for example, of CH_4 and N_2O.

For the Fifth Assessment Report of IPCC, the scientific community has defined a set of four new scenarios, denoted Representative Concentration Pathways (RCPs, see Glossary). They are identified by their approximate total radiative forcing in year 2100 relative to 1750: 2.6 W m^{-2} for RCP2.6, 4.5 W m^{-2} for RCP4.5, 6.0 W m^{-2} for RCP6.0, and 8.5 W m^{-2} for RCP8.5. For the Coupled Model Intercomparison Project Phase 5 (CMIP5) results, these values should be understood as indicative only, as the climate forcing resulting from all drivers varies between models due to specific model characteristics and treatment of short-lived climate forcers. These four RCPs include one mitigation scenario leading to a very low forcing level (RCP2.6), two stabilization scenarios (RCP4.5 and RCP6), and one scenario with very high greenhouse gas emissions (RCP8.5). The RCPs can thus represent a range of 21st century climate policies, as compared with the no-climate policy of the Special Report on Emissions Scenarios (SRES) used in the Third Assessment Report and the Fourth Assessment Report. For RCP6.0 and RCP8.5, radiative forcing does not peak by year 2100; for RCP2.6 it peaks and declines; and for RCP4.5 it stabilizes by 2100. Each RCP provides spatially resolved data sets of land use change and sector-based emissions of air pollutants, and it specifies annual greenhouse gas concentrations and anthropogenic emissions up to 2100. RCPs are based on a combination of integrated assessment models, simple climate models, atmospheric chemistry and global carbon cycle models. While the RCPs span a wide range of total forcing values, they do not cover the full range of emissions in the literature, particularly for aerosols.

Most of the CMIP5 and Earth System Model simulations were performed with prescribed CO_2 concentrations reaching 421 ppm (RCP2.6), 538 ppm (RCP4.5), 670 ppm (RCP6.0), and 936 ppm (RCP 8.5) by the year 2100. Including also the prescribed concentrations of CH_4 and N_2O, the combined CO_2-equivalent concentrations are 475 ppm (RCP2.6), 630 ppm (RCP4.5), 800 ppm (RCP6.0), and 1313 ppm (RCP8.5). For RCP8.5, additional CMIP5 Earth System Model simulations are performed with prescribed CO_2 emissions as provided by the integrated assessment models. For all RCPs, additional calculations were made with updated atmospheric chemistry data and models (including the Atmospheric Chemistry and Climate component of CMIP5) using the RCP prescribed emissions of the chemically reactive gases (CH_4, N_2O, HFCs, NO_x, CO, NMVOC). These simulations enable investigation of uncertainties related to carbon cycle feedbacks and atmospheric chemistry.

Technical Summary

TS Technical Summary

Coordinating Lead Authors:
Thomas F. Stocker (Switzerland), Qin Dahe (China), Gian-Kasper Plattner (Switzerland)

Lead Authors:
Lisa V. Alexander (Australia), Simon K. Allen (Switzerland/New Zealand), Nathaniel L. Bindoff (Australia), François-Marie Bréon (France), John A. Church (Australia), Ulrich Cubasch (Germany), Seita Emori (Japan), Piers Forster (UK), Pierre Friedlingstein (UK/Belgium), Nathan Gillett (Canada), Jonathan M. Gregory (UK), Dennis L. Hartmann (USA), Eystein Jansen (Norway), Ben Kirtman (USA), Reto Knutti (Switzerland), Krishna Kumar Kanikicharla (India), Peter Lemke (Germany), Jochem Marotzke (Germany), Valérie Masson-Delmotte (France), Gerald A. Meehl (USA), Igor I. Mokhov (Russian Federation), Shilong Piao (China), Venkatachalam Ramaswamy (USA), David Randall (USA), Monika Rhein (Germany), Maisa Rojas (Chile), Christopher Sabine (USA), Drew Shindell (USA), Lynne D. Talley (USA), David G. Vaughan (UK), Shang-Ping Xie (USA)

Contributing Authors:
Myles R. Allen (UK), Olivier Boucher (France), Don Chambers (USA), Jens Hesselbjerg Christensen (Denmark), Philippe Ciais (France), Peter U. Clark (USA), Matthew Collins (UK), Josefino C. Comiso (USA), Viviane Vasconcellos de Menezes (Australia/Brazil), Richard A. Feely (USA), Thierry Fichefet (Belgium), Gregory Flato (Canada), Jesús Fidel González Rouco (Spain), Ed Hawkins (UK), Paul J. Hezel (Belgium/USA), Gregory C. Johnson (USA), Simon A. Josey (UK), Georg Kaser (Austria/Italy), Albert M.G. Klein Tank (Netherlands), Janina Körper (Germany), Gunnar Myhre (Norway), Timothy Osborn (UK), Scott B. Power (Australia), Stephen R. Rintoul (Australia), Joeri Rogelj (Switzerland/Belgium), Matilde Rusticucci (Argentina), Michael Schulz (Germany), Jan Sedláček (Switzerland), Peter A. Stott (UK), Rowan Sutton (UK), Peter W. Thorne (USA/Norway/UK), Donald Wuebbles (USA)

Review Editors:
Sylvie Joussaume (France), Joyce Penner (USA), Fredolin Tangang (Malaysia)

This Technical Summary should be cited as:
Stocker, T.F., D. Qin, G.-K. Plattner, L.V. Alexander, S.K. Allen, N.L. Bindoff, F.-M. Bréon, J.A. Church, U. Cubasch, S. Emori, P. Forster, P. Friedlingstein, N. Gillett, J.M. Gregory, D.L. Hartmann, E. Jansen, B. Kirtman, R. Knutti, K. Krishna Kumar, P. Lemke, J. Marotzke, V. Masson-Delmotte, G.A. Meehl, I.I. Mokhov, S. Piao, V. Ramaswamy, D. Randall, M. Rhein, M. Rojas, C. Sabine, D. Shindell, L.D. Talley, D.G. Vaughan and S.-P. Xie, 2013: Technical Summary. In: *Climate Change 2013: The Physical Science Basis. Contribution of Working Group I to the Fifth Assessment Report of the Intergovernmental Panel on Climate Change* [Stocker, T.F., D. Qin, G.-K. Plattner, M. Tignor, S.K. Allen, J. Boschung, A. Nauels, Y. Xia, V. Bex and P.M. Midgley (eds.)]. Cambridge University Press, Cambridge, United Kingdom and New York, NY, USA.

Table of Contents

Supplementary Material

Supplementary Material is available in online versions of the report.

TS.1 Introduction

Climate Change 2013: The Physical Science Basis is the contribution of Working Group I (WGI) to the Fifth Assessment Report (AR5) of the Intergovernmental Panel on Climate Change (IPCC). This comprehensive assessment of the physical aspects of climate change puts a focus on those elements that are relevant to understand past, document current and project future climate change. The assessment builds on the IPCC Fourth Assessment Report (AR4)[1] and the recent Special Report on Managing the Risk of Extreme Events and Disasters to Advance Climate Change Adaptation (SREX)[2] and is presented in 14 chapters and 3 annexes. The chapters cover direct and proxy observations of changes in all components of the climate system; assess the current knowledge of various processes within, and interactions among, climate system components, which determine the sensitivity and response of the system to changes in forcing; and quantify the link between the changes in atmospheric constituents, and hence radiative forcing (RF)[3], and the consequent detection and attribution of climate change. Projections of changes in all climate system components are based on model simulations forced by a new set of scenarios. The Report also provides a comprehensive assessment of past and future sea level change in a dedicated chapter. Regional climate change information is presented in the form of an Atlas of Global and Regional Climate Projections (Annex I). This is complemented by Annex II: Climate System Scenario Tables and Annex III: Glossary.

The primary purpose of this Technical Summary (TS) is to provide the link between the complete assessment of the multiple lines of independent evidence presented in the 14 chapters of the main report and the highly condensed summary prepared as the WGI Summary for Policymakers (SPM). The Technical Summary thus serves as a starting point for those readers who seek the full information on more specific topics covered by this assessment. This purpose is facilitated by including pointers to the chapters and sections where the full assessment can be found. Policy-relevant topics, which cut across many chapters and involve many interlinked processes in the climate system, are presented here as Thematic Focus Elements (TFEs), allowing rapid access to this information.

An integral element of this report is the use of uncertainty language that permits a traceable account of the assessment (Box TS.1). The degree of certainty in key findings in this assessment is based on the author teams' evaluations of underlying scientific understanding and is expressed as a level of confidence that results from the type, amount, quality and consistency of evidence and the degree of agreement in the scientific studies considered[4]. Confidence is expressed qualitatively. Quantified measures of uncertainty in a finding are expressed probabilistically and are based on a combination of statistical analyses of observations or model results, or both, and expert judgement. Where appropriate, findings are also formulated as statements of fact without using uncertainty qualifiers (see Chapter 1 and Box TS.1 for more details).

The Technical Summary is structured into four main sections presenting the assessment results following the storyline of the WGI contribution to AR5: Section TS.2 covers the assessment of observations of changes in the climate system; Section TS.3 summarizes the information on the different drivers, natural and anthropogenic, expressed in terms of RF; Section TS.4 presents the assessment of the quantitative understanding of observed climate change; and Section TS.5 summarizes the assessment results for projections of future climate change over the 21st century and beyond from regional to global scale. Section TS.6 combines and lists key uncertainties from the WGI assessment from Sections TS.2 to TS.5. The overall nine TFEs, cutting across the various components of the WGI AR5, are dispersed throughout the four main TS sections, are visually distinct from the main text and should allow stand-alone reading.

The basis for substantive paragraphs in this Technical Summary can be found in the chapter sections of the underlying report. These references are given in curly brackets.

---

1 IPCC, 2007: *Climate Change 2007: The Physical Science Basis.* Contribution of Working Group I to the Fourth Assessment Report of the Intergovernmental Panel on Climate Change [Solomon, S., D. Qin, M. Manning, Z. Chen, M. Marquis, K.B. Averyt, M. Tignor and H.L. Miller (eds.)]. Cambridge University Press, Cambridge, United Kingdom and New York, NY, USA, 996 pp.

2 IPCC, 2012: *Managing the Risks of Extreme Events and Disasters to Advance Climate Change Adaptation*. A Special Report of Working Groups I and II of the Intergovernmental Panel on Climate Change [Field, C.B., V. Barros, T.F. Stocker, D. Qin, D.J. Dokken, K.L. Ebi, M.D. Mastrandrea, K.J. Mach, G.-K. Plattner, S.K. Allen, M. Tignor and P. M. Midgley (eds.)]. Cambridge University Press, Cambridge, UK, and New York, NY, USA, 582 pp.

3 Radiative forcing (RF) is a measure of the net change in the energy balance of the Earth system in response to some external perturbation. It is expressed in watts per square metre (W m^{-2}); see Box TS.2.

4 Mastrandrea, M.D., C.B. Field, T.F. Stocker, O. Edenhofer, K.L. Ebi, D.J. Frame, H. Held, E. Kriegler, K.J. Mach, P.R. Matschoss, G.-K. Plattner, G.W. Yohe, and F.W. Zwiers, 2010: *Guidance Note for Lead Authors of the IPCC Fifth Assessment Report on Consistent Treatment of Uncertainties*. Intergovernmental Panel on Climate Change (IPCC).

Box TS.1 | Treatment of Uncertainty

Based on the Guidance Note for Lead Authors of the IPCC Fifth Assessment Report on Consistent Treatment of Uncertainties, this WGI Technical Summary and the WGI Summary for Policymakers rely on two metrics for communicating the degree of certainty in key findings, which is based on author teams' evaluations of underlying scientific understanding:

- Confidence in the validity of a finding, based on the type, amount, quality and consistency of evidence (e.g., mechanistic understanding, theory, data, models, expert judgement) and the degree of agreement. Confidence is expressed qualitatively.
- Quantified measures of uncertainty in a finding expressed probabilistically (based on statistical analysis of observations or model results, or expert judgement).

The AR5 Guidance Note refines the guidance provided to support the IPCC Third and Fourth Assessment Reports. Direct comparisons between assessment of uncertainties in findings in this Report and those in the AR4 and the SREX are difficult, because of the application of the revised guidance note on uncertainties, as well as the availability of new information, improved scientific understanding, continued analyses of data and models and specific differences in methodologies applied in the assessed studies. For some climate variables, different aspects have been assessed and therefore a direct comparison would be inappropriate.

Each key finding is based on an author team's evaluation of associated evidence and agreement. The confidence metric provides a qualitative synthesis of an author team's judgement about the validity of a finding, as determined through evaluation of evidence and agreement. If uncertainties can be quantified probabilistically, an author team can characterize a finding using the calibrated likelihood language or a more precise presentation of probability. Unless otherwise indicated, high or very high confidence is associated with findings for which an author team has assigned a likelihood term.

The following summary terms are used to describe the available evidence: limited, medium, or robust; and for the degree of agreement: low, medium, or high. A level of confidence is expressed using five qualifiers very low, low, medium, high, and very high, and typeset in italics, e.g., *medium confidence.* Box TS.1, Figure 1 depicts summary statements for evidence and agreement and their relationship to confidence. There is flexibility in this relationship; for a given evidence and agreement statement, different confidence levels can be assigned, but increasing levels of evidence and degrees of agreement correlate with increasing confidence.

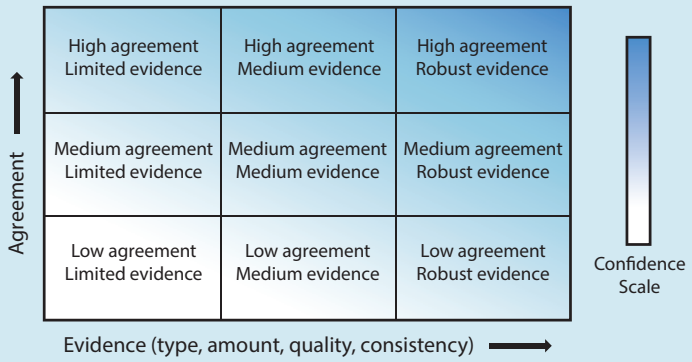

Box TS.1, Figure 1 | A depiction of evidence and agreement statements and their relationship to confidence. Confidence increases toward the top right corner as suggested by the increasing strength of shading. Generally, evidence is most robust when there are multiple, consistent independent lines of high quality. {Figure 1.11}

The following terms have been used to indicate the assessed likelihood, and typeset in italics:

Term*	**Likelihood of the outcome**
Virtually certain	99–100% probability
Very likely	90–100% probability
Likely	66–100% probability
About as likely as not	33–66% probability
Unlikely	0–33% probability
Very unlikely	0–10% probability
Exceptionally unlikely	0–1% probability

* Additional terms (*extremely likely*: 95–100% probability, *more likely than not*: >50–100% probability, and *extremely unlikely*: 0–5% probability) may also be used when appropriate.

TS.2 Observation of Changes in the Climate System

TS.2.1 Introduction

Observations of the climate system are based on direct physical and biogeochemical measurements, and remote sensing from ground stations and satellites; information derived from paleoclimate archives provides a long-term context. Global-scale observations from the instrumental era began in the mid-19th century, and paleoclimate reconstructions extend the record of some quantities back hundreds to millions of years. Together, they provide a comprehensive view of the variability and long-term changes in the atmosphere, the ocean, the cryosphere and at the land surface.

The assessment of observational evidence for climate change is summarized in this section. Substantial advancements in the availability, acquisition, quality and analysis of observational data sets for the atmosphere, land surface, ocean and cryosphere have occurred since the AR4. Many aspects of the climate system are showing evidence of a changing climate. {2, 3, 4, 5, 6, 13}

TS.2.2 Changes in Temperature

TS.2.2.1 Surface

It is certain that global mean surface temperature (GMST) has increased since the late 19th century (Figures TS.1 and TS.2). Each of the past three decades has been successively warmer at the Earth's surface than any the previous decades in the instrumental record, and the decade of the 2000's has been the warmest. The globally averaged combined land and ocean temperature data as calculated by a linear trend[5], show a warming of 0.85 [0.65 to 1.06] °C[6], over the period 1880–2012, when multiple independently produced datasets exist, about 0.89 [0.69 to 1.08] °C over the period 1901–2012, and about 0.72 [0.49 to 0.89] °C over the period 1951–2012 when based on three independently-produced data sets. The total increase between the average of the 1850–1900 period and the 2003–2012 period is 0.78 [0.72 to 0.85] °C, based on the Hadley Centre/Climatic Research Unit gridded surface temperature data set 4 (HadCRUT4), the global mean surface temperature dataset with the longest record of the three independently-produced data sets. The warming from 1850–1900 to 1986–2005 (reference period for the modelling chapters and the Atlas in Annex I) is 0.61 [0.55 to 0.67] °C, when calculated using HadCRUT4 and its uncertainty estimates. It is also *virtually certain* that maximum and minimum temperatures over land have increased on a global scale since 1950.[7] {2.4.1, 2.4.3; Chapter 2 Supplementary Material Section 2.SM.3}

Despite the robust multi-decadal warming, there exists substantial interannual to decadal variability in the rate of warming, with several periods exhibiting weaker trends (including the warming hiatus since 1998) (Figure TS.1). The rate of warming over the past 15 years (1998–2012; 0.05 [–0.05 to +0.15] °C per decade) is smaller than the trend since 1951 (1951–2012; 0.12[0.08 to 0.14] °C per decade). Trends for short periods are uncertain and very sensitive to the start and end years. For example, trends for 15-year periods starting in 1995, 1996, and 1997 are 0.13 [0.02 to 0.24] °C per decade, 0.14 [0.03 to 0.24] °C per decade and 0.07 [–0.02 to 0.18] °C per decade, respectively. Several independently analysed data records of global and regional land surface air temperature obtained from station observations are in broad agreement that land surface air temperatures have increased. Sea surface temperatures (SSTs) have also increased. Intercomparisons of new SST data records obtained by different measurement methods, including satellite data, have resulted in better understanding of errors and biases in the records. {2.4.1–2.4.3; Box 9.2}

It is *unlikely* that any uncorrected urban heat island effects and land use change effects have raised the estimated centennial globally averaged land surface air temperature trends by more than 10% of the reported trend. This is an average value; in some regions that have rapidly developed urban heat island and land use change impacts on regional trends may be substantially larger. {2.4.1}

There is *high confidence* that annual mean surface warming since the 20th century has reversed long-term cooling trends of the past 5000 years in mid-to-high latitudes of the Northern Hemisphere (NH). For average annual NH temperatures, the period 1983–2012 was *very likely* the warmest 30-year period of the last 800 years (*high confidence*) and *likely* the warmest 30-year period of the last 1400 years (*medium confidence*). This is supported by comparison of instrumental temperatures with multiple reconstructions from a variety of proxy data and statistical methods, and is consistent with AR4. Continental-scale surface temperature reconstructions show, with *high confidence*, multi-decadal periods during the Medieval Climate Anomaly (950–1250) that were in some regions as warm as in the mid-20th century and in others as warm as in the late 20th century. With *high confidence*, these regional warm periods were not as synchronous across regions as the warming since the mid-20th century. Based on the comparison between reconstructions and simulations, there is *high confidence* that not only external orbital, solar and volcanic forcing, but also internal

[5] The warming is reported as an unweighted average based on linear trend estimates calculated from Hadley Centre/Climatic Research Unit gridded surface temperature data set 4 (HadCRUT4), Merged Land–Ocean Surface Temperature Analysis (MLOST) and Goddard Institute for Space Studies Surface Temperature Analysis (GISTEMP) data sets (see Figure TS.2; Section 2.4.3).

[6] In the WGI contribution to the AR5, uncertainty is quantified using 90% uncertainty intervals unless otherwise stated. The 90% uncertainty interval, reported in square brackets, is expected to have a 90% likelihood of covering the value that is being estimated. The upper endpoint of the uncertainty interval has a 95% likelihood of exceeding the value that is being estimated and the lower endpoint has a 95% likelihood of being less than that value. A best estimate of that value is also given where available. Uncertainty intervals are not necessarily symmetric about the corresponding best estimate.

[7] Both methods presented in this paragraph to calculate temperature change were also used in AR4. The first calculates the difference using a best fit linear trend of all points between two years, e.g., 1880 and 2012. The second calculates the difference between averages for the two periods, e.g., 1850 to 1900 and 2003 to 2012. Therefore, the resulting values and their 90% uncertainty intervals are not directly comparable.

variability, contributed substantially to the spatial pattern and timing of surface temperature changes between the Medieval Climate Anomaly and the Little Ice Age (1450–1850). {5.3.5, 5.5.1}

TS.2.2.2 Troposphere and Stratosphere

Based on multiple independent analyses of measurements from radiosondes and satellite sensors, it is *virtually certain* that globally the troposphere has warmed and the stratosphere has cooled since the mid-20th century (Figure TS.1). Despite unanimous agreement on the sign of the trends, substantial disagreement exists between available estimates as to the rate of temperature changes, particularly outside the NH extratropical troposphere, which has been well sampled by radiosondes. Hence there is only *medium confidence* in the rate of change and its vertical structure in the NH extratropical troposphere and *low confidence* elsewhere. {2.4.4}

TS.2.2.3 Ocean

It is *virtually certain* that the upper ocean (above 700 m) has warmed from 1971 to 2010, and *likely* that it has warmed from the 1870s to 1971 (Figure TS.1). There is less certainty in changes prior to 1971 because of relatively sparse sampling in earlier time periods. Instrumental biases in historical upper ocean temperature measurements have been identified and reduced since AR4, diminishing artificial decadal variation in temperature and upper ocean heat content, most prominent during the 1970s and 1980s. {3.2.1–3.2.3, 3.5.3}

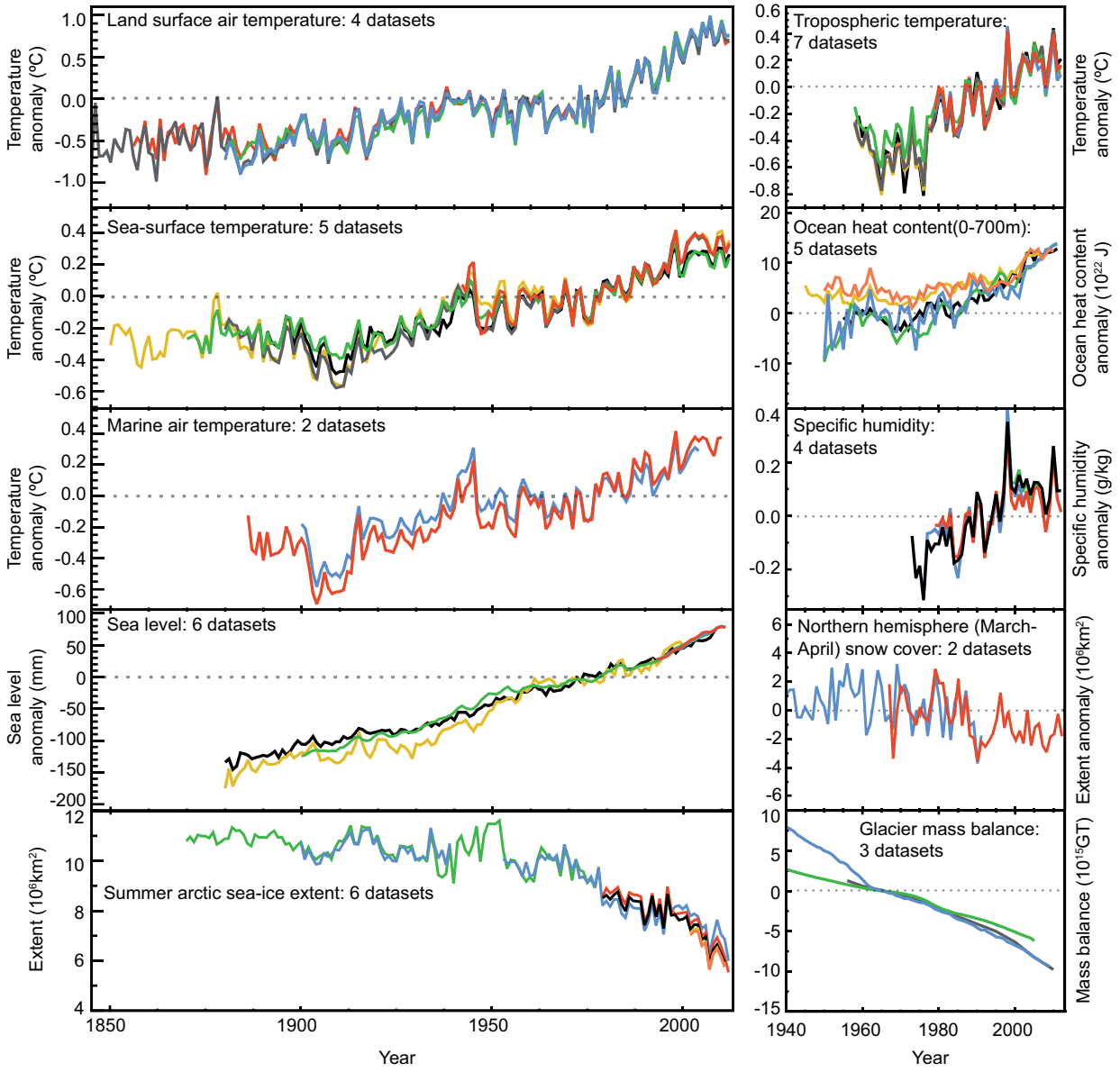

Figure TS.1 | Multiple complementary indicators of a changing global climate. Each line represents an independently derived estimate of change in the climate element. The times series presented are assessed in Chapters 2, 3 and 4. In each panel all data sets have been normalized to a common period of record. A full detailing of which source data sets go into which panel is given in Chapter 2 Supplementary Material Section 2.SM.5 and in the respective chapters. Further detail regarding the related Figure SPM.3 is given in the TS Supplementary Material. {FAQ 2.1, Figure 1; 2.4, 2.5, 3.2, 3.7, 4.5.2, 4.5.3}

It is *likely* that the ocean warmed between 700-2000 m from 1957 to 2009, based on 5-year averages. It is *likely* that the ocean warmed from 3000 m to the bottom from 1992 to 2005, while no significant trends in global average temperature were observed between 2000 and 3000 m depth from circa 1992 to 2005. Below 3000 m depth, the largest warming is observed in the Southern Ocean. {3.2.4, 3.5.1; Figures 3.2b, 3.3; FAQ 3.1}

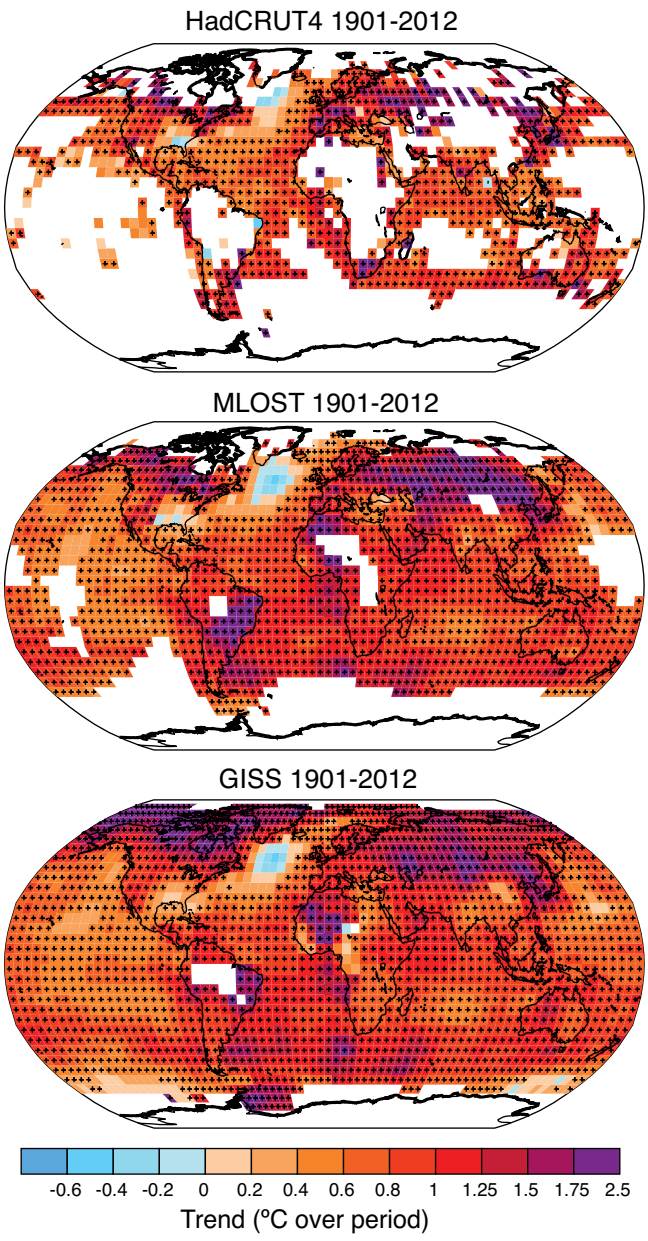

Figure TS.2 | Change in surface temperature over 1901–2012 as determined by linear trend for three data sets. White areas indicate incomplete or missing data. Trends have been calculated only for those grid boxes with greater than 70% complete records and more than 20% data availability in the first and last 10% of the time period. Black plus signs (+) indicate grid boxes where trends are significant (i.e., a trend of zero lies outside the 90% confidence interval). Differences in coverage primarily reflect the degree of interpolation to account for data void regions undertaken by the data set providers ranging from none beyond grid box averaging (Hadley Centre/Climatic Research Unit gridded surface temperature data set 4 (HadCRUT4)) to substantial (Goddard Institute for Space Studies Surface Temperature Analysis (GISTEMP)). Further detail regarding the related Figure SPM.1 is given in the TS Supplementary Material. {Figure 2.21}

TS.2.3 Changes in Energy Budget and Heat Content

The Earth has been in radiative imbalance, with more energy from the Sun entering than exiting the top of the atmosphere, since at least about 1970. It is *virtually certain* that the Earth has gained substantial energy from 1971 to 2010. The estimated increase in energy inventory between 1971 and 2010 is 274 [196 to 351] × 10^{21} J (*high confidence*), with a heating rate of 213 × 10^{12} W from a linear fit to the annual values over that time period (see also TFE.4). {Boxes 3.1, 13.1}

Ocean warming dominates that total heating rate, with full ocean depth warming accounting for about 93% (*high confidence*), and warming of the upper (0 to 700 m) ocean accounting for about 64%. Melting ice (including Arctic sea ice, ice sheets and glaciers) and warming of the continents each account for 3% of the total. Warming of the atmosphere makes up the remaining 1%. The 1971–2010 estimated rate of ocean energy gain is 199 × 10^{12} W from a linear fit to data over that time period, equivalent to 0.42 W m^{-2} heating applied continuously over the Earth's entire surface, and 0.55 W m^{-2} for the portion owing to ocean warming applied over the ocean's entire surface area. The Earth's estimated energy increase from 1993 to 2010 is 163 [127 to 201] × 10^{21} J with a trend estimate of 275 × 10^{15} W. The ocean portion of the trend for 1993–2010 is 257 × 10^{12} W, equivalent to a mean heat flux into the ocean of 0.71 W m^{-2}. {3.2.3, 3.2.4; Box 3.1}

It is *about as likely as not* that ocean heat content from 0–700 m increased more slowly during 2003 to 2010 than during 1993 to 2002 (Figure TS.1). Ocean heat uptake from 700–2000 m, where interannual variability is smaller, *likely* continued unabated from 1993 to 2009. {3.2.3, 3.2.4; Box 9.2}

TS.2.4 Changes in Circulation and Modes of Variability

Large variability on interannual to decadal time scales hampers robust conclusions on long-term changes in atmospheric circulation in many instances. *Confidence* is *high* that the increase of the northern mid-latitude westerly winds and the North Atlantic Oscillation (NAO) index from the 1950s to the 1990s, and the weakening of the Pacific Walker Circulation from the late 19th century to the 1990s, have been largely offset by recent changes. With *high confidence*, decadal and multi-decadal changes in the winter NAO index observed since the 20th century are not unprecedented in the context of the past 500 years. {2.7.2, 2.7.5, 2.7.8, 5.4.2; Box 2.5; Table 2.14}

It is *likely* that circulation features have moved poleward since the 1970s, involving a widening of the tropical belt, a poleward shift of storm tracks and jet streams and a contraction of the northern polar vortex. Evidence is more robust for the NH. It is *likely* that the Southern Annular Mode (SAM) has become more positive since the 1950s. The increase in the strength of the observed summer SAM since 1950 has been anomalous, with *medium confidence*, in the context of the past 400 years. {2.7.5, 2.7.6, 2.7.8, 5.4.2; Box 2.5; Table 2.14}

New results from high-resolution coral records document with *high confidence* that the El Niño-Southern Oscillation (ENSO) system has remained highly variable throughout the past 7000 years, showing no discernible evidence for an orbital modulation of ENSO. {5.4.1}

Recent observations have strengthened evidence for variability in major ocean circulation systems on time scales from years to decades. It is *very likely* that the subtropical gyres in the North Pacific and South Pacific have expanded and strengthened since 1993. Based on measurements of the full Atlantic Meridional Overturning Circulation (AMOC) and its individual components at various latitudes and different time periods, there is no evidence of a long-term trend. There is also no evidence for trends in the transports of the Indonesian Throughflow, the Antarctic Circumpolar Current (ACC) or in the transports between the Atlantic Ocean and Nordic Seas. However, a southward shift of the ACC by about 1° of latitude is observed in data spanning the time period 1950–2010 with *medium confidence*. {3.6}

TS.2.5 Changes in the Water Cycle and Cryosphere

TS.2.5.1 Atmosphere

Confidence in precipitation change averaged over global land areas is *low* prior to 1951 and *medium* afterwards because of insufficient data, particularly in the earlier part of the record (for an overview of observed and projected changes in the global water cycle see TFE.1). Further, when virtually all the land area is filled in using a reconstruction method, the resulting time series shows little change in land-based precipitation since 1901. NH mid-latitude land areas do show a *likely* overall increase in precipitation (*medium confidence* prior to 1951, but *high confidence* afterwards). For other latitudes area-averaged long-term positive or negative trends have *low confidence* (TFE.1, Figure 1). {2.5.1}

It is *very likely* that global near surface and tropospheric air specific humidity have increased since the 1970s. However, during recent years the near-surface moistening trend over land has abated (*medium confidence*) (Figure TS.1). As a result, fairly widespread decreases in relative humidity near the surface are observed over the land in recent years. {2.4.4, 2.5.5, 2.5.6}

Although trends of cloud cover are consistent between independent data sets in certain regions, substantial ambiguity and therefore *low confidence* remains in the observations of global-scale cloud variability and trends. {2.5.7}

TS.2.5.2 Ocean and Surface Fluxes

It is *very likely* that regional trends have enhanced the mean geographical contrasts in sea surface salinity since the 1950s: saline surface waters in the evaporation-dominated mid-latitudes have become more saline, while relatively fresh surface waters in rainfall-dominated tropical and polar regions have become fresher. The mean contrast between high- and low-salinity regions increased by 0.13 [0.08 to 0.17] from 1950 to 2008. It is *very likely* that the inter-basin contrast in freshwater content has increased: the Atlantic has become saltier and the Pacific and Southern Oceans have freshened. Although similar conclusions were reached in AR4, recent studies based on expanded data sets and new analysis approaches provide *high confidence* in this assessment. {3.3.2, 3.3.3, 3.9; FAQ 3.2}

The spatial patterns of the salinity trends, mean salinity and the mean distribution of evaporation minus precipitation are all similar (TFE.1, Figure 1). These similarities provide indirect evidence that the pattern of evaporation minus precipitation over the oceans has been enhanced since the 1950s (*medium confidence*). Uncertainties in currently available surface fluxes prevent the flux products from being reliably used to identify trends in the regional or global distribution of evaporation or precipitation over the oceans on the time scale of the observed salinity changes since the 1950s. {3.3.2–3.3.4, 3.4.2, 3.4.3, 3.9; FAQ 3.2}

TS.2.5.3 Sea Ice

Continuing the trends reported in AR4, there is *very high confidence* that the Arctic sea ice extent (annual, multi-year and perennial) decreased over the period 1979–2012 (Figure TS.1). The rate of the annual decrease was *very likely* between 3.5 and 4.1% per decade (range of 0.45 to 0.51 million km^2 per decade). The average decrease in decadal extent of annual Arctic sea ice has been most rapid in summer and autumn (*high confidence*), but the extent has decreased in every season, and in every successive decade since 1979 (*high confidence*). The extent of Arctic perennial and multi-year ice decreased between 1979 and 2012 (*very high confidence*). The rates are *very likely* 11.5 [9.4 to 13.6]% per decade (0.73 to 1.07 million km^2 per decade) for the sea ice extent at summer minimum (perennial ice) and *very likely* 13.5 [11 to 16] % per decade for multi-year ice. There is *medium confidence* from reconstructions that the current (1980–2012) Arctic summer sea ice retreat was unprecedented and SSTs were anomalously high in the perspective of at least the last 1,450 years. {4.2.2, 5.5.2}

It is *likely* that the annual period of surface melt on Arctic perennial sea ice lengthened by 5.7 [4.8 to 6.6] days per decade over the period 1979–2012. Over this period, in the region between the East Siberian Sea and the western Beaufort Sea, the duration of ice-free conditions increased by nearly 3 months. {4.2.2}

There is *high confidence* that the average winter sea ice thickness within the Arctic Basin decreased between 1980 and 2008. The average decrease was *likely* between 1.3 m and 2.3 m. *High confidence* in this assessment is based on observations from multiple sources: submarine, electromagnetic probes and satellite altimetry; and is consistent with the decline in multi-year and perennial ice extent. Satellite measurements made in the period 2010–2012 show a decrease in sea ice volume compared to those made over the period 2003–2008 (*medium confidence*). There is *high confidence* that in the Arctic, where the sea ice thickness has decreased, the sea ice drift speed has increased. {4.2.2}

It is *very likely* that the annual Antarctic sea ice extent increased at a rate of between 1.2 and 1.8% per decade (0.13 to 0.20 million km^2 per decade) between 1979 and 2012 (*very high confidence*). There was a greater increase in sea ice area, due to a decrease in the percentage of open water within the ice pack. There is *high confidence* that there are strong regional differences in this annual rate, with some regions increasing in extent/area and some decreasing. There are also contrasting regions around the Antarctic where the ice-free season has lengthened, and others where it has decreased over the satellite period (*high confidence*). {4.2.3}

TS.2.5.4 Glaciers and Ice Sheets

There is *very high confidence* that glaciers world-wide are persistently shrinking as revealed by the time series of measured changes in glacier length, area, volume and mass (Figures TS.1 and TS.3). The few exceptions are regionally and temporally limited. Measurements of glacier change have increased substantially in number since AR4. Most of the new data sets, along with a globally complete glacier inventory, have been derived from satellite remote sensing {4.3.1, 4.3.3}

There is *very high confidence* that, during the last decade, the largest contributions to global glacier ice loss were from glaciers in Alaska, the Canadian Arctic, the periphery of the Greenland ice sheet, the Southern Andes and the Asian mountains. Together these areas account for more than 80% of the total ice loss. Total mass loss from all glaciers in the world, excluding those on the periphery of the ice sheets, was *very likely* 226 [91 to 361] Gt yr^{-1} (sea level equivalent, 0.62 [0.25 to 0.99] mm yr^{-1}) in the period 1971–2009, 275 [140 to 410] Gt yr^{-1} (0.76 [0.39 to 1.13] mm yr^{-1}) in the period 1993–2009 and 301 [166 to 436] Gt yr^{-1} (0.83 [0.46 to 1.20] mm yr^{-1}) between 2005 and 2009[8]. {4.3.3; Tables 4.4, 4.5}

There is *high confidence* that current glacier extents are out of balance with current climatic conditions, indicating that glaciers will continue to shrink in the future even without further temperature increase. {4.3.3}

There is *very high confidence* that the Greenland ice sheet has lost ice during the last two decades. Combinations of satellite and airborne remote sensing together with field data indicate with *high confidence* that the ice loss has occurred in several sectors and that large rates of mass loss have spread to wider regions than reported in AR4 (Figure TS.3). There is *high confidence* that the mass loss of the Greenland ice sheet has accelerated since 1992: the average rate has *very likely* increased from 34 [–6 to 74] Gt yr^{-1} over the period 1992–2001 (sea level equivalent, 0.09 [–0.02 to 0.20] mm yr^{-1}), to 215 [157 to 274] Gt yr^{-1} over the period 2002–2011 (0.59 [0.43 to 0.76] mm yr^{-1}). There is *high confidence* that ice loss from Greenland resulted from increased surface melt and runoff and increased outlet glacier discharge, and these occurred in similar amounts. There is *high confidence* that the area subject to summer melt has increased over the last two decades. {4.4.2, 4.4.3}

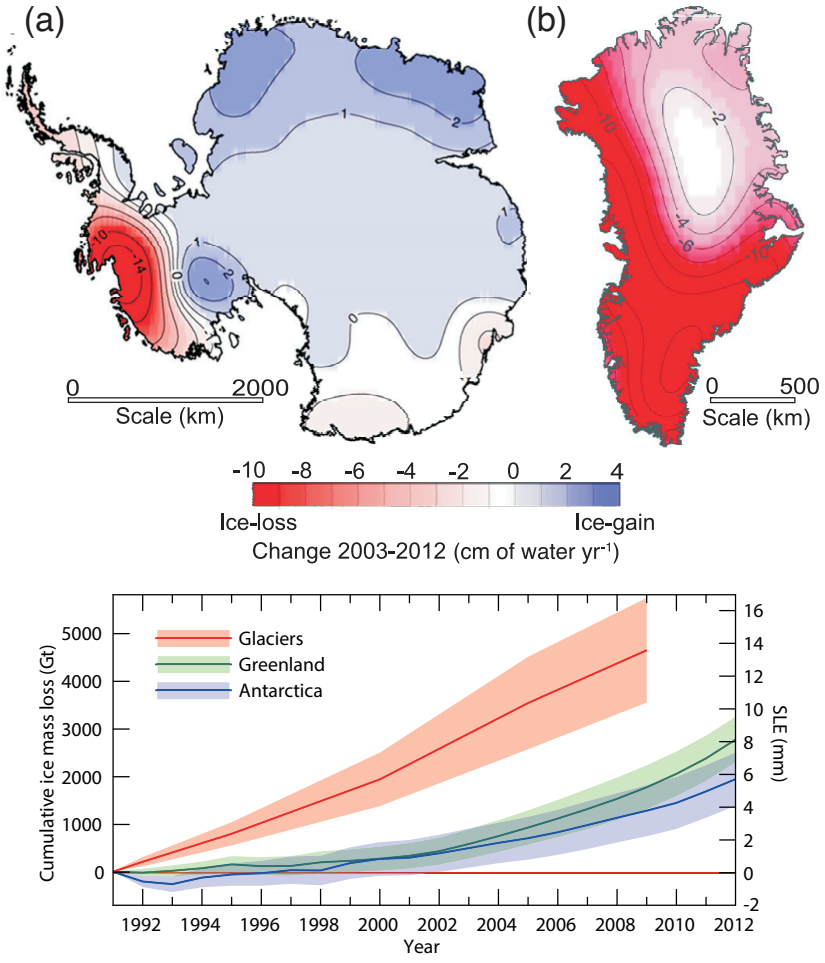

Figure TS.3 | (Upper) Distribution of ice loss determined from Gravity Recovery and Climate Experiment (GRACE) time-variable gravity for (a) Antarctica and (b) Greenland, shown in centimetres of water per year (cm of water yr^{-1}) for the period 2003–2012. (Lower) The assessment of the total loss of ice from glaciers and ice sheets in terms of mass (Gt) and sea level equivalent (mm). The contribution from glaciers excludes those on the periphery of the ice sheets. {4.3.4; Figures 4.12–4.14, 4.16, 4.17, 4.25}

[8] 100 Gt yr^{-1} of ice loss corresponds to about 0.28 mm yr^{-1} of sea level equivalent.

Thematic Focus Elements

TFE.1 | Water Cycle Change

The water cycle describes the continuous movement of water through the climate system in its liquid, solid and vapour forms, and storage in the reservoirs of ocean, cryosphere, land surface and atmosphere. In the atmosphere, water occurs primarily as a gas, water vapour, but it also occurs as ice and liquid water in clouds. The ocean is primarily liquid water, but the ocean is partly covered by ice in polar regions. Terrestrial water in liquid form appears as surface water (lakes, rivers), soil moisture and groundwater. Solid terrestrial water occurs in ice sheets, glaciers, snow and ice on the surface and permafrost. The movement of water in the climate system is essential to life on land, as much of the water that falls on land as precipitation and supplies the soil moisture and river flow has been evaporated from the ocean and transported to land by the atmosphere. Water that falls as snow in winter can provide soil moisture in springtime and river flow in summer and is essential to both natural and human systems. The movement of fresh water between the atmosphere and the ocean can also influence oceanic salinity, which is an important driver of the density and circulation of the ocean. The latent heat contained in water vapour in the atmosphere is critical to driving the circulation of the atmosphere on scales ranging from individual thunderstorms to the global circulation of the atmosphere. {12.4.5; FAQ 3.2, FAQ 12.2}

Observations of Water Cycle Change

Because the saturation vapour pressure of air increases with temperature, it is expected that the amount of water vapour in air will increase with a warming climate. Observations from surface stations, radiosondes, global positioning systems and satellite measurements indicate increases in tropospheric water vapour at large spatial scales (TFE.1, Figure 1). It is *very likely* that tropospheric specific humidity has increased since the 1970s. The magnitude of the observed global change in tropospheric water vapour of about 3.5% in the past 40 years is consistent with the observed temperature change of about 0.5°C during the same period, and the relative humidity has stayed approximately constant. The water vapour change can be attributed to human influence with *medium confidence*. {2.5.4, 10.3.2}

Changes in precipitation are harder to measure with the existing records, both because of the greater difficulty in sampling precipitation and also because it is expected that precipitation will have a smaller fractional change than the water vapour content of air as the climate warms. Some regional precipitation trends appear to be robust (TFE.1, Figure 2), but when virtually all the land area is filled in using a reconstruction method, the resulting time series of global mean land precipitation shows little change since 1900. At present there is *medium confidence* that there has been a significant human influence on global scale changes in precipitation patterns, including increases in Northern Hemisphere (NH) mid-to-high latitudes. Changes in the extremes of precipitation, and other climate extremes related to the water cycle are comprehensively discussed in TFE.9. {2.5.1, 10.3.2}

Although direct trends in precipitation and evaporation are difficult to measure with the available records, the observed oceanic surface salinity, which is strongly dependent on the difference between evaporation and precipitation, shows significant trends (TFE.1, Figure 1). The spatial patterns of the salinity trends since 1950 are very similar to the mean salinity and the mean distribution of evaporation minus precipitation: regions of high salinity where evaporation dominates have become more saline, while regions of low salinity where rainfall dominates have become fresher (TFE.1, Figure 1). This provides indirect evidence that the pattern of evaporation minus precipitation over the oceans has been enhanced since the 1950s (*medium confidence*). The inferred changes in evaporation minus precipitation are consistent with the observed increased water vapour content of the warmer air. It is *very likely* that observed changes in surface and subsurface salinity are due in part to anthropogenic climate forcings. {2.5, 3.3.2–3.3.4, 3.4, 3.9, 10.4.2; FAQ 3.2}

In most regions analysed, it is *likely* that decreasing numbers of snowfall events are occurring where increased winter temperatures have been observed. Both satellite and *in situ* observations show significant reductions in the NH snow cover extent over the past 90 years, with most of the reduction occurring in the 1980s. Snow cover decreased most in June when the average extent decreased *very likely* by 53% (40 to 66%) over the period 1967 to 2012. From 1922 to 2012 only data from March and April are available and show *very likely* a 7% (4.5 to 9.5%) decline. Because of earlier spring snowmelt, the duration of the NH snow season has declined by 5.3 days per decade since the 1972/1973 winter. It is *likely* that there has been an anthropogenic component to these observed reductions in snow cover since the 1970s. {4.5.2, 10.5.1, 10.5.3}

(continued on next page)

TFE.1 (continued)

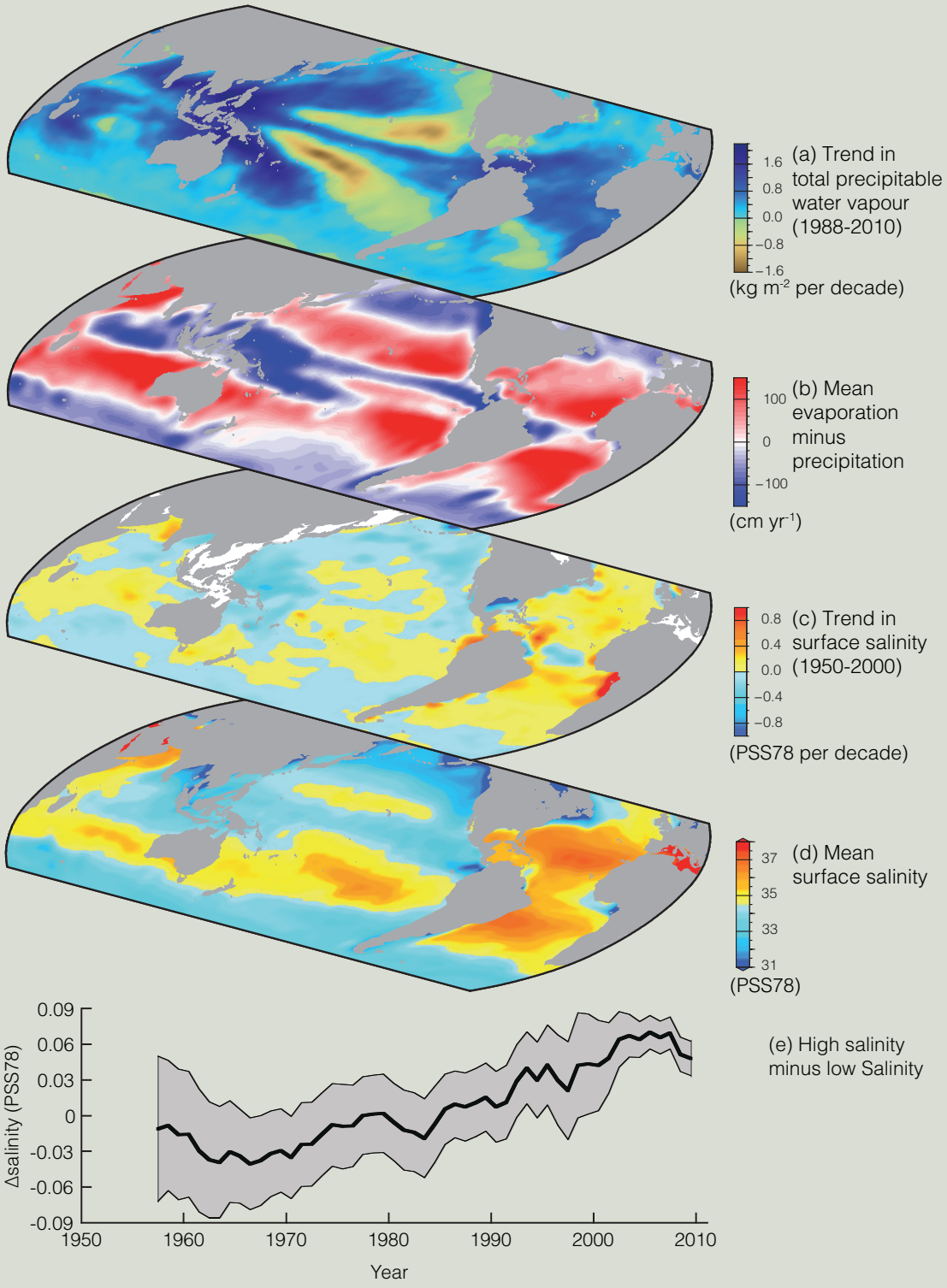

TFE.1, Figure 1 | Changes in sea surface salinity are related to the atmospheric patterns of evaporation minus precipitation ($E - P$) and trends in total precipitable water: (a) Linear trend (1988 to 2010) in total precipitable water (water vapour integrated from the Earth's surface up through the entire atmosphere) (kg m^{-2} per decade) from satellite observations. (b) The 1979–2005 climatological mean net evaporation minus precipitation (cm yr^{-1}) from meteorological reanalysis data. (c) Trend (1950–2000) in surface salinity (Practical Salinity Scale 78 (PSS78) per 50 years). (d) The climatological mean surface salinity (PSS78) (blues <35; yellows-reds >35). (e) Global difference between salinity averaged over regions where the sea surface salinity is greater than the global mean sea surface salinity ("High Salinity") and salinity averaged over regions with values below the global mean ('Low Salinity'). For details of data sources see Figure 3.21 and FAQ 3.2, Figure 1. {3.9}

TFE.1 (continued)

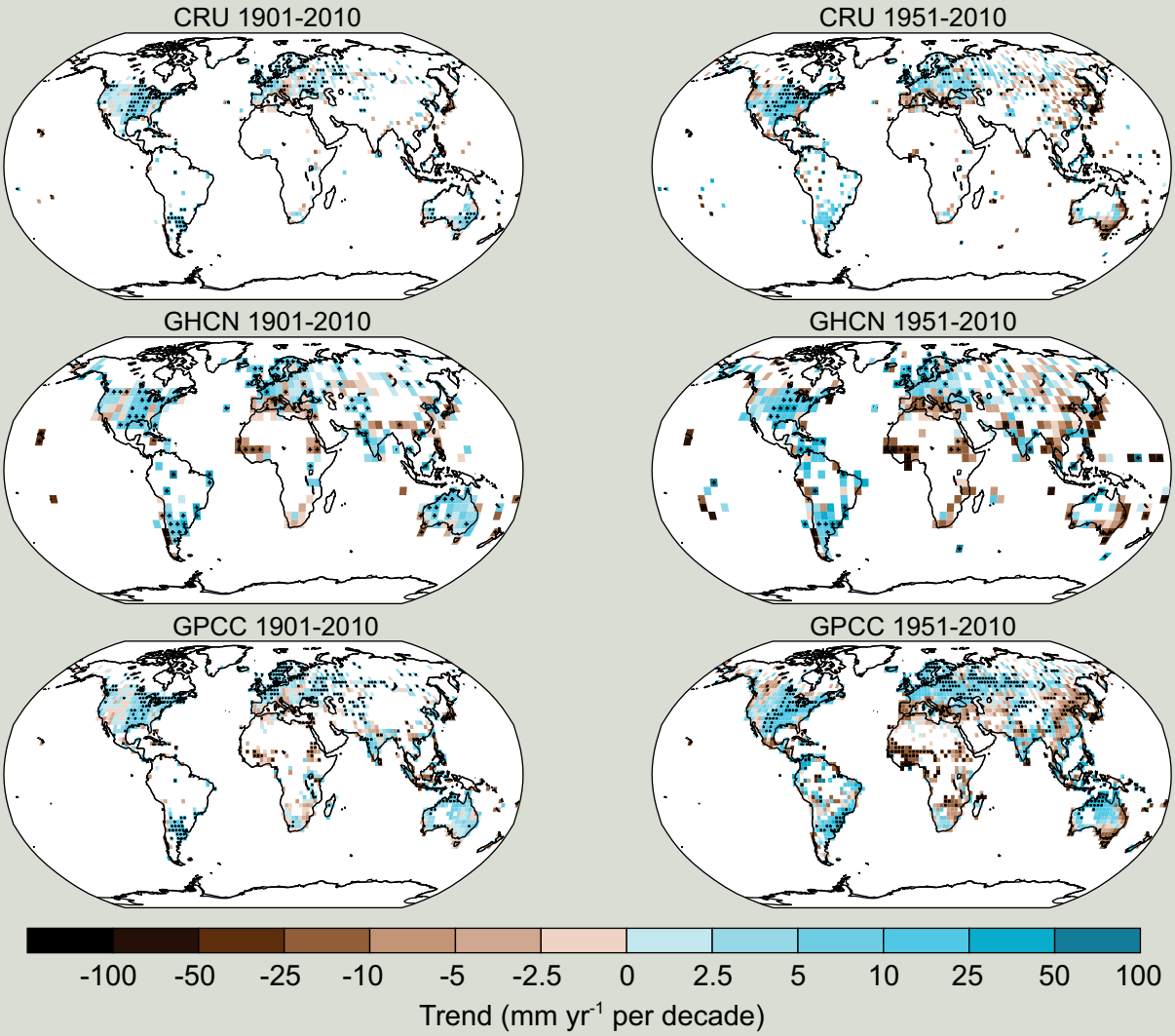

TFE.1, Figure 2 | Maps of observed precipitation change over land from 1901 to 2010 (left-hand panels) and 1951 to 2010 (right-hand panels) from the Climatic Research Unit (CRU), Global Historical Climatology Network (GHCN) and Global Precipitation Climatology Centre (GPCC) data sets. Trends in annual accumulation have been calculated only for those grid boxes with greater than 70% complete records and more than 20% data availability in first and last decile of the period. White areas indicate incomplete or missing data. Black plus signs (+) indicate grid boxes where trends are significant (i.e., a trend of zero lies outside the 90% confidence interval). Further detail regarding the related Figure SPM.2 is given in the TS Supplementary Material. {Figure 2.29; 2.5.1}

The most recent and most comprehensive analyses of river runoff do not support the IPCC Fourth Assessment Report (AR4) conclusion that global runoff has increased during the 20th century. New results also indicate that the AR4 conclusions regarding global increasing trends in droughts since the 1970s are no longer supported. {2.5.2, 2.6.2}

Projections of Future Changes

Changes in the water cycle are projected to occur in a warming climate (TFE.1, Figure 3, see also TS 4.6, TS 5.6, Annex I). Global-scale precipitation is projected to gradually increase in the 21st century. The precipitation increase is projected to be much smaller (about 2% K^{-1}) than the rate of lower tropospheric water vapour increase (about 7% K^{-1}), due to global energetic constraints. Changes of average precipitation in a much warmer world will not be uniform, with some regions experiencing increases, and others with decreases or not much change at all. The high latitude land masses are *likely* to experience greater amounts of precipitation due to the additional water carrying capacity of the warmer troposphere. Many mid-latitude and subtropical arid and semi-arid regions will *likely* experience less precipitation. The largest precipitation changes over northern Eurasia and North America are projected to occur during the winter. {12.4.5, Annex I}

(continued on next page)

TFE.1 (continued)

Regional to global-scale projections of soil moisture and drought remain relatively uncertain compared to other aspects of the water cycle. Nonetheless, drying in the Mediterranean, southwestern USA and southern African regions are consistent with projected changes in the Hadley Circulation, so drying in these regions as global temperatures increase is *likely* for several degrees of warming under the Representative Concentration Pathway RCP8.5. Decreases in runoff are *likely* in southern Europe and the Middle East. Increased runoff is *likely* in high northern latitudes, and consistent with the projected precipitation increases there. {12.4.5}

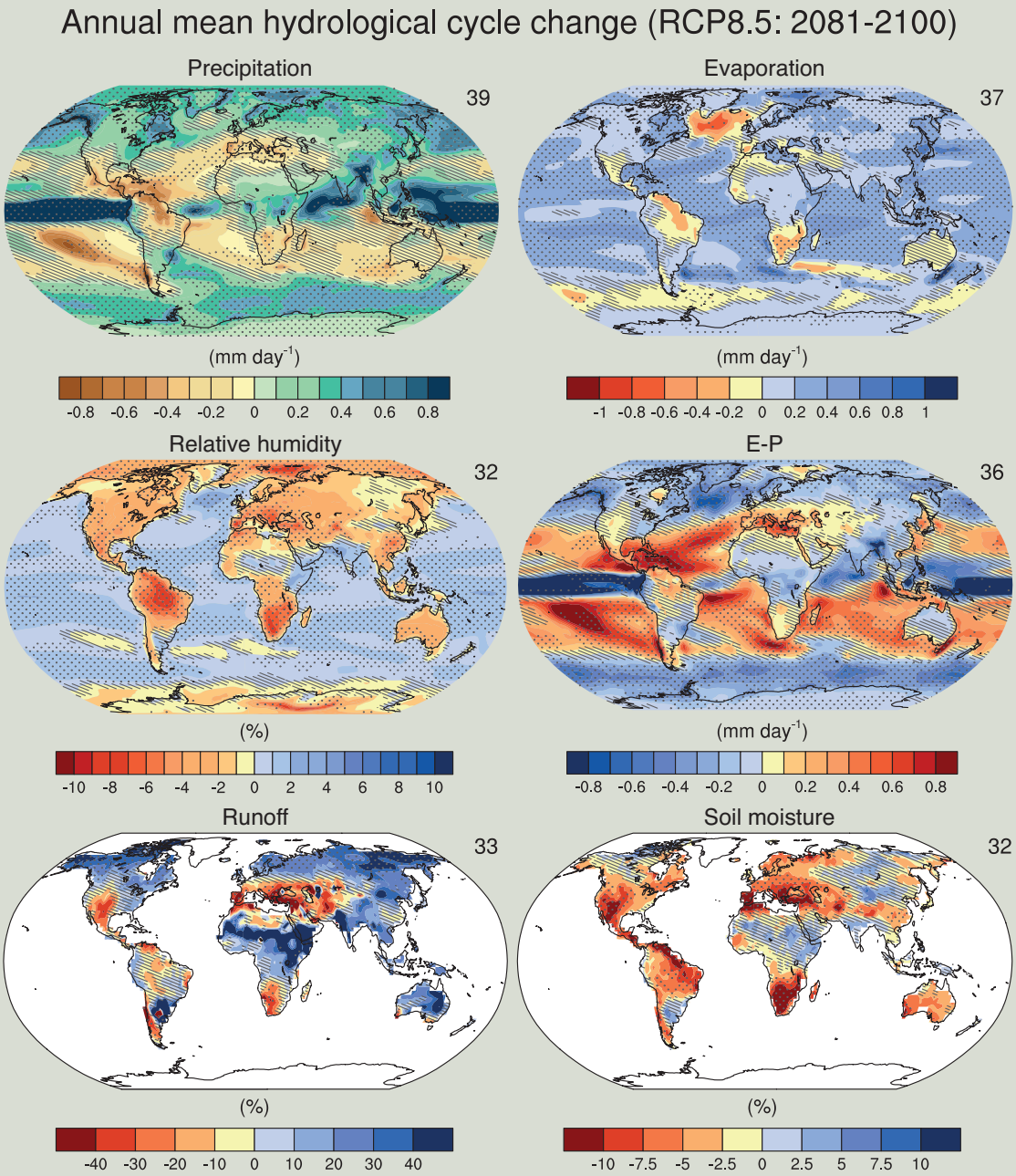

TFE.1, Figure 3 | Annual mean changes in precipitation (*P*), evaporation (*E*), relative humidity, *E* – *P*, runoff and soil moisture for 2081–2100 relative to 1986–2005 under the Representative Concentration Pathway RCP8.5 (see Box TS.6). The number of Coupled Model Intercomparison Project Phase 5 (CMIP5) models to calculate the multi-model mean is indicated in the upper right corner of each panel. Hatching indicates regions where the multi-model mean change is less than one standard deviation of internal variability. Stippling indicates regions where the multi-model mean change is greater than two standard deviations of internal variability and where 90% of models agree on the sign of change (see Box 12.1). {Figures 12.25–12.27}

There is *high confidence* that the Antarctic ice sheet has been losing ice during the last two decades (Figure TS.3). There is *very high confidence* that these losses are mainly from the northern Antarctic Peninsula and the Amundsen Sea sector of West Antarctica and *high confidence* that they result from the acceleration of outlet glaciers. The average rate of ice loss from Antarctica *likely* increased from 30 [–37 to 97] Gt yr^{-1} (sea level equivalent, 0.08 [–0.10 to 0.27] mm yr^{-1}) over the period 1992–2001, to 147 [72 to 221] Gt yr^{-1} over the period 2002–2011 (0.40 [0.20 to 0.61] mm yr^{-1}). {4.4.2, 4.4.3}

There is *high confidence* that in parts of Antarctica floating ice shelves are undergoing substantial changes. There is *medium confidence* that ice shelves are thinning in the Amundsen Sea region of West Antarctica, and *low confidence* that this is due to high ocean heat flux. There is *high confidence* that ice shelves around the Antarctic Peninsula continue a long-term trend of retreat and partial collapse that began decades ago. {4.4.2, 4.4.5}

TS.2.5.5 Snow Cover, Freshwater Ice and Frozen Ground

There is *very high confidence* that snow cover extent has decreased in the NH, especially in spring (Figure TS.1). Satellite records indicate that over the period 1967–2012, snow cover extent *very likely* decreased; the largest change, –53% [–40 to –66%], occurred in June. No month had statistically significant increases. Over the longer period, 1922–2012, data are available only for March and April, but these show *very likely* a 7% [4.5 to 9.5%] decline and a negative correlation (–0.76) with March to April 40°N to 60°N land temperature. In the Southern Hemisphere (SH), evidence is too limited to conclude whether changes have occurred. {4.5.2, 4.5.3}

Permafrost temperatures have increased in most regions around the world since the early 1980s (*high confidence*). These increases were in response to increased air temperature and to changes in the timing and thickness of snow cover (*high confidence*). The temperature increase for colder permafrost was generally greater than for warmer permafrost (*high confidence*). {4.7.2; Table 4.8}

TS.2.6 Changes in Sea Level

The primary contributions to changes in the volume of water in the ocean are the expansion of the ocean water as it warms and the transfer to the ocean of water currently stored on land, particularly from glaciers and ice sheets. Water impoundment in reservoirs and ground water depletion (and its subsequent runoff to the ocean) also affect sea level. Change in sea level relative to the land (relative sea level) can be significantly different from the global mean sea level (GMSL) change because of changes in the distribution of water in the ocean, vertical movement of the land and changes in the Earth's gravitational field. For an overview on the scientific understanding and uncertainties associated with recent (and projected) sea level change see TFE.2. {3.7.3, 13.1}

During warm intervals of the mid Pliocene (3.3 to 3.0 Ma), when there is *medium confidence* that GMSTs were 1.9°C to 3.6°C warmer than for pre-industrial climate and carbon dioxide (CO_2) levels were between 350 and 450 ppm, there is *high confidence* that GMSL was above present, implying reduced volume of polar ice sheets. The best estimates from various methods imply with *high confidence* that sea level has not exceeded +20 m during the warmest periods of the Pliocene, due to deglaciation of the Greenland and West Antarctic ice sheets and areas of the East Antarctic ice sheet. {5.6.1, 13.2}

There is *very high confidence* that maximum GMSL during the last interglacial period (129 to 116 ka) was, for several thousand years, at least 5 m higher than present and *high confidence* that it did not exceed 10 m above present, implying substantial contributions from the Greenland and Antarctic ice sheets. This change in sea level occurred in the context of different orbital forcing and with high-latitude surface temperature, averaged over several thousand years, at least 2°C warmer than present (*high confidence*). Based on ice sheet model simulations consistent with elevation changes derived from a new Greenland ice core, the Greenland ice sheet *very likely* contributed between 1.4 m and 4.3 m sea level equivalent, implying with *medium confidence* a contribution from the Antarctic ice sheet to the GMSL during the Last Interglacial Period. {5.3.4, 5.6.2, 13.2.1}

Proxy and instrumental sea level data indicate a transition in the late 19th to the early 20th century from relatively low mean rates of rise over the previous two millennia to higher rates of rise (*high confidence*) {3.7, 3.7.4, 5.6.3, 13.2}

GMSL has risen by 0.19 [0.17 to 0.21] m, estimated from a linear trend over the period 1901–2010, based on tide gauge records and additionally on satellite data since 1993. It is *very likely* that the mean rate of sea level rise was 1.7 [1.5 to 1.9] mm yr^{-1} between 1901 and 2010. Between 1993 and 2010, the rate was *very likely* higher at 3.2 [2.8 to 3.6] mm yr^{-1}; similarly high rates *likely* occurred between 1920 and 1950. The rate of GMSL rise has *likely* increased since the early 1900s, with estimates ranging from 0.000 [–0.002 to 0.002] to 0.013 [–0.007 to 0.019] mm yr^{-2}. {3.7, 5.6.3, 13.2}

TS.2.7 Changes in Extremes

TS.2.7.1 Atmosphere

Recent analyses of extreme events generally support the AR4 and SREX conclusions (see TFE.9 and in particular TFE.9, Table 1, for a synthesis). It is *very likely* that the number of cold days and nights has decreased and the number of warm days and nights has increased on the global scale between 1951 and 2010. Globally, there is *medium confidence* that the length and frequency of warm spells, including heat waves, has increased since the middle of the 20th century, mostly owing to lack of data or studies in Africa and South America. However, it is *likely* that heat wave frequency has increased over this period in large parts of Europe, Asia and Australia. {2.6.1; Tables 2.12, 2.13}

It is *likely* that since about 1950 the number of heavy precipitation events over land has increased in more regions than it has decreased. Confidence is highest for North America and Europe where there have been *likely* increases in either the frequency or intensity of heavy precipitation with some seasonal and regional variations. It is *very likely* that there have been trends towards heavier precipitation events in central North America. {2.6.2; Table 2.13}

Thematic Focus Elements

TFE.2 | Sea Level Change: Scientific Understanding and Uncertainties

After the Last Glacial Maximum, global mean sea levels (GMSLs) reached close to present-day values several thousand years ago. Since then, it is *virtually certain* that the rate of sea level rise has increased from low rates of sea level change during the late Holocene (order tenths of mm yr^{-1}) to 20th century rates (order mm yr^{-1}, Figure TS1). {3.7, 5.6, 13.2}

Ocean thermal expansion and glacier mass loss are the dominant contributors to GMSL rise during the 20th century (*high confidence*). It is *very likely* that warming of the ocean has contributed 0.8 [0.5 to 1.1] mm yr^{-1} of sea level change during 1971–2010, with the majority of the contribution coming from the upper 700 m. The model mean rate of ocean thermal expansion for 1971–2010 is close to observations. {3.7, 13.3}

Observations, combined with improved methods of analysis, indicate that the global glacier contribution (excluding the peripheral glaciers around Greenland and Antarctica) to sea level was 0.25 to 0.99 mm yr^{-1} sea level equivalent during 1971–2010. *Medium confidence* in global glacier mass balance models used for projections of glacier changes arises from the process-based understanding of glacier surface mass balance, the consistency of observations and models of glacier changes, and the evidence that Atmosphere–Ocean General Circulation Model (AOGCM) climate simulations can provide realitistic climate input. A simulation using observed climate data shows a larger rate of glacier mass loss during the 1930s than the simulations using AOGCM input, possibly a result of an episode of warming in Greenland associated with unforced regional climate variability. {4.3, 13.3}

Observations indicate that the Greenland ice sheet has *very likely* experienced a net loss of mass due to both increased surface melting and runoff, and increased ice discharge over the last two decades (Figure TS.3). Regional climate models indicate that Greenland ice sheet surface mass balance showed no significant trend from the 1960s to the 1980s, but melting and consequent runoff has increased since the early 1990s. This tendency is related to pronounced regional warming, which may be attributed to a combination of anomalous regional variability in recent years and anthropogenic climate change. *High confidence* in projections of future warming in Greenland and increased surface melting is based on the qualitative agreements of models in projecting amplified warming at high northern latitudes for well-understood physical reasons. {4.4, 13.3}

There is *high confidence* that the Antarctic ice sheet is in a state of net mass loss and its contribution to sea level is also *likely* to have increased over the last two decades. Acceleration in ice outflow has been observed since the 1990s, especially in the Amundsen Sea sector of West Antarctica. Interannual variability in accumulation is large and as a result no significant trend is present in accumulation since 1979 in either models or observations. Surface melting is currently negligible in Antarctica. {4.4, 13.3}

Model-based estimates of climate-related changes in water storage on land (as snow cover, surface water, soil moisture and ground water) do not show significant long-term contributions to sea level change for recent decades. However, human-induced changes (reservoir impoundment and groundwater depletion) have each contributed at least several tenths of mm yr^{-1} to sea level change. Reservoir impoundment exceeded groundwater depletion for the majority of the 20th century but the rate of groundwater depletion has increased and now exceeds the rate of impoundment. Their combined net contribution for the 20th century is estimated to be small. {13.3}

The observed GMSL rise for 1993–2010 is consistent with the sum of the observationally estimated contributions (TFE.2, Figure 1e). The closure of the observational budget for recent periods within uncertainties represents a significant advance since the IPCC Fourth Assessment Report in physical understanding of the causes of past GMSL change, and provides an improved basis for critical evaluation of models of these contributions in order to assess their reliability for making projections. {13.3}

The sum of modelled ocean thermal expansion and glacier contributions and the estimated change in land water storage (which is relatively small) accounts for about 65% of the observed GMSL rise for 1901–1990, and 90% for 1971–2010 and 1993–2010 (TFE.2, Figure 1). After inclusion of small long-term contributions from ice sheets and the possible greater mass loss from glaciers during the 1930s due to unforced climate variability, the sum of the modelled contribution is close to the observed rise. The addition of the observed ice sheet contribution since 1993 improves the agreement further between the observed and modelled sea level rise (TFE.2, Figure 1). The evidence now available gives a clearer account than in previous IPCC assessments of 20th century sea level change. {13.3}

(continued on next page)

TFE.2 (continued)

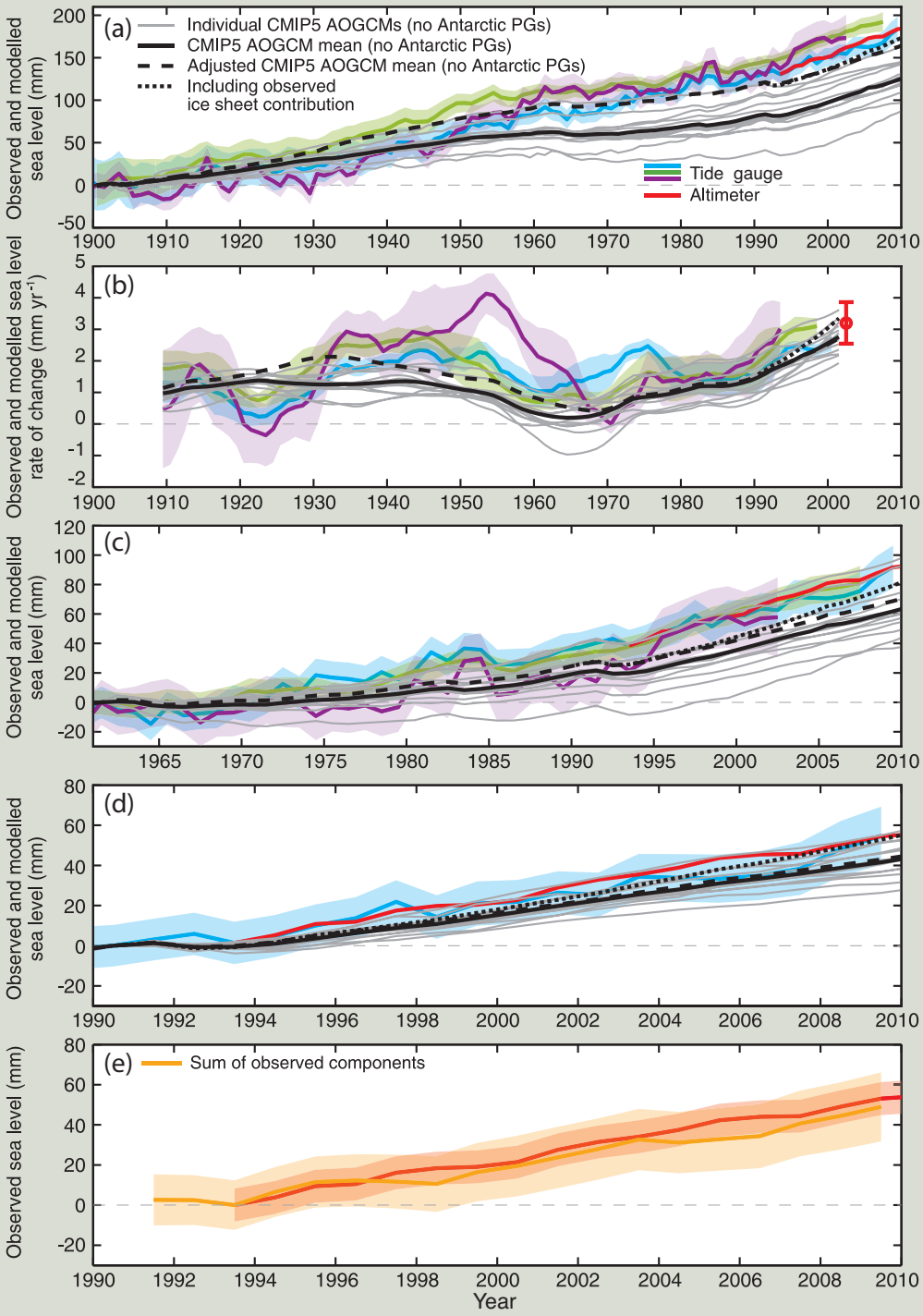

TFE.2, Figure 1 | (a) The observed and modelled sea level for 1900 to 2010. (b) The rates of sea level change for the same period, with the satellite altimeter data shown as a red dot for the rate. (c) The observed and modelled sea level for 1961 to 2010. (d) The observed and modelled sea level for 1990 to 2010. Panel (e) compares the sum of the observed contributions (orange) and the observed sea level from the satellite altimeter data (red). Estimates of GMSL from different sources are given, with the shading indicating the uncertainty estimates (two standard deviations). The satellite altimeter data since 1993 are shown in red. The grey lines in panels (a)-(d) are the sums of the contributions from modelled ocean thermal expansion and glaciers (excluding glaciers peripheral to the Antarctic ice sheet), plus changes in land-water storage (see Figure 13.4). The black line is the mean of the grey lines plus a correction of thermal expansion for the omission of volcanic forcing in the Atmosphere–Ocean General Circulation Model (AOGCM) control experiments (see Section 13.3.1). The dashed black line (adjusted model mean) is the sum of the corrected model mean thermal expansion, the change in land water storage, the glacier estimate using observed (rather than modelled) climate (see Figure 13.4), and an illustrative long-term ice-sheet contribution (of 0.1 mm yr^{-1}). The dotted black line is the adjusted model mean but now including the observed ice-sheet contributions, which begin in 1993. Because the observational ice-sheet estimates include the glaciers peripheral to the Greenland and Antarctic ice sheets (from Section 4.4), the contribution from glaciers to the adjusted model mean excludes the peripheral glaciers (PGs) to avoid double counting. {13.3; Figure 13.7}

TFE.2 (continued)

When calibrated appropriately, recently improved dynamical ice sheet models can reproduce the observed rapid changes in ice sheet outflow for individual glacier systems (e.g., Pine Island Glacier in Antarctica; *medium confidence*). However, models of ice sheet response to global warming and particularly ice sheet–ocean interactions are incomplete and the omission of ice sheet models, especially of dynamics, from the model budget of the past means that they have not been as critically evaluated as other contributions. {13.3, 13.4}

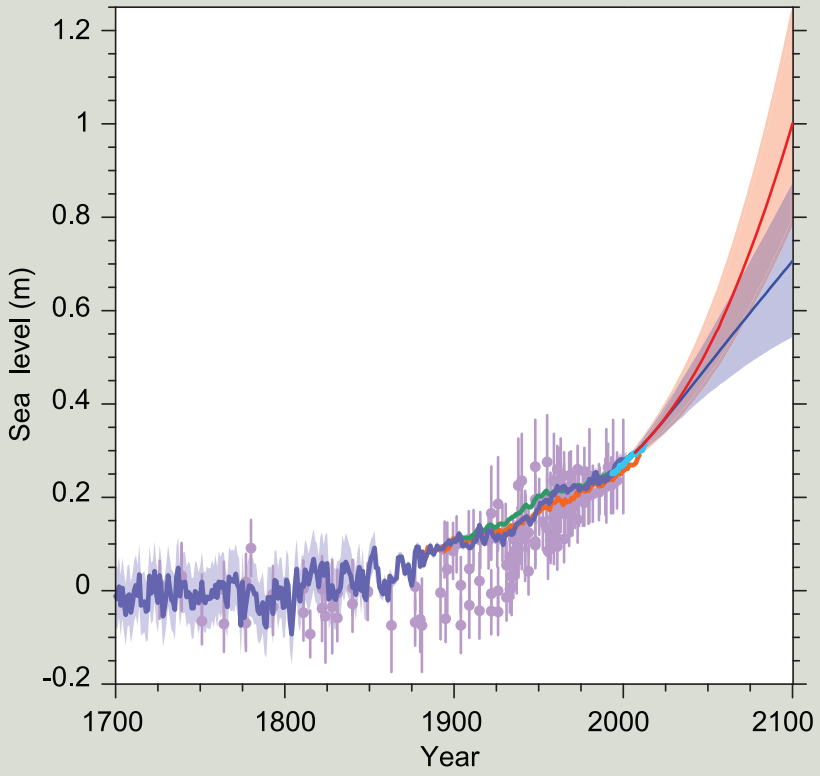

TFE.2, Figure 2 | Compilation of paleo sealevel data (purple), tide gauge data (blue, red and green), altimeter data (light blue) and central estimates and *likely* ranges for projections of global mean sea level rise from the combination of CMIP5 and process-based models for RCP2.6 (blue) and RCP8.5 (red) scenarios, all relative to pre-industrial values. {Figures 13.3, 13.11, 13.27}

GMSL rise for 2081–2100 (relative to 1986–2005) for the Representative Concentration Pathways (RCPs) will *likely* be in the 5 to 95% ranges derived from Coupled Model Intercomparison Project Phase 5 (CMIP5) climate projections in combination with process-based models of other contributions (*medium confidence*), that is, 0.26 to 0.55 m (RCP2.6), 0.32 to 0.63 m (RCP4.5), 0.33 to 0.63 m (RCP6.0), 0.45 to 0.82 (RCP8.5) m (see Table TS.1 and Figure TS.15 for RCP forcing). For RCP8.5 the range at 2100 is 0.52 to 0.98 m. Confidence in the projected *likely* ranges comes from the consistency of process-based models with observations and physical understanding. It is assessed that there is currently insufficient evidence to evaluate the probability of specific levels above the *likely* range. Based on current understanding, only the collapse of marine-based sectors of the Antarctic ice sheet, if initiated, could cause GMSL to rise substantially above the *likely* range during the 21st century. There is a lack of consensus on the probability for such a collapse, and the potential additional contribution to GMSL rise cannot be precisely quantified, but there is *medium confidence* that it would not exceed several tenths of a metre of sea level rise during the 21st century. It is *virtually certain* that GMSL rise will continue beyond 2100. {13.5.1, 13.5.3}

Many semi-empirical models projections of GMSL rise are higher than process-based model projections, but there is no consensus in the scientific community about their reliability and there is thus *low confidence* in their projections. {13.5.2, 13.5.3}

TFE.2, Figure 2 combines the paleo, tide gauge and altimeter observations of sea level rise from 1700 with the projected GMSL change to 2100. {13.5, 13.7, 13.8}

There is *low confidence* in a global-scale observed trend in drought or dryness (lack of rainfall), owing to lack of direct observations, dependencies of inferred trends on the index choice and geographical inconsistencies in the trends. However, this masks important regional changes and, for example, the frequency and intensity of drought have *likely* increased in the Mediterranean and West Africa and *likely* decreased in central North America and northwest Australia since 1950. {2.6.2; Table 2.13}

There is *high confidence* for droughts during the last millennium of greater magnitude and longer duration than those observed since the beginning of the 20th century in many regions. There is *medium confidence* that more megadroughts occurred in monsoon Asia and wetter conditions prevailed in arid Central Asia and the South American monsoon region during the Little Ice Age (1450–1850) compared to the Medieval Climate Anomaly (950–1250). {5.5.4, 5.5.5}

Confidence remains *low* for long-term (centennial) changes in tropical cyclone activity, after accounting for past changes in observing capabilities. However, for the years since the 1970s, it is *virtually certain* that the frequency and intensity of storms in the North Atlantic have increased although the reasons for this increase are debated (see TFE.9). There is *low confidence* of large-scale trends in storminess over the last century and there is still insufficient evidence to determine whether robust trends exist in small-scale severe weather events such as hail or thunderstorms. {2.6.2–2.6.4}

With *high confidence*, floods larger than recorded since the 20th century occurred during the past five centuries in northern and central Europe, the western Mediterranean region and eastern Asia. There is *medium confidence* that in the Near East, India and central North America, modern large floods are comparable or surpass historical floods in magnitude and/or frequency. {5.5.5}

TS.2.7.2 Oceans

It is *likely* that the magnitude of extreme high sea level events has increased since 1970 (see TFE.9, Table 1). Most of the increase in extreme sea level can be explained by the mean sea level rise: changes in extreme high sea levels are reduced to less than 5 mm yr^{-1} at 94% of tide gauges once the rise in mean sea level is accounted for. There is *medium confidence* based on reanalysis forced model hindcasts and ship observations that mean significant wave height has increased since the 1950s over much of the North Atlantic north of 45°N, with typical winter season trends of up to 20 cm per decade. {3.4.5, 3.7.5}

TS.2.8 Changes in Carbon and Other Biogeochemical Cycles

Concentrations of the atmospheric greenhouse gases (GHGs) carbon dioxide (CO_2), methane (CH_4) and nitrous oxide (N_2O) in 2011 exceed the range of concentrations recorded in ice cores during the past 800 kyr. Past changes in atmospheric GHG concentrations are determined with *very high confidence* from polar ice cores. Since AR4 these records have been extended from 650 ka to 800 ka. {5.2.2}

With *very high confidence*, the current rates of CO_2, CH_4 and N_2O rise in atmospheric concentrations and the associated increases in RF are unprecedented with respect to the 'highest resolution' ice core records of the last 22 kyr. There is *medium confidence* that the rate of change of the observed GHG rise is also unprecedented compared with the lower resolution records of the past 800 kyr. {2.2.1, 5.2.2}

In several periods characterized by high atmospheric CO_2 concentrations, there is *medium confidence* that global mean temperature was significantly above pre-industrial level. During the mid-Pliocene (3.3 to 3.0 Ma), atmospheric CO_2 concentration between 350 ppm and 450 ppm (*medium confidence*) occurred when GMST was 1.9°C to 3.6°C warmer (*medium confidence*) than for pre-industrial climate. During the Early Eocene (52 to 48 Ma), atmospheric CO_2 concentration exceeded about 1000 ppm when GMST was 9°C to 14°C higher (*medium confidence*) than for pre-industrial conditions. {5.3.1}

TS.2.8.1 Carbon Dioxide

Between 1750 and 2011, CO_2 emissions from fossil fuel combustion and cement production are estimated from energy and fuel use statistics to have released 375 [345 to 405] PgC[9]. In 2002–2011, average fossil fuel and cement manufacturing emissions were 8.3 [7.6 to 9.0] PgC yr^{-1} (*high confidence*), with an average growth rate of 3.2% yr^{-1} (Figure TS.4). This rate of increase of fossil fuel emissions is higher than during the 1990s (1.0% yr^{-1}). In 2011, fossil fuel emissions were 9.5 [8.7 to 10.3] PgC. {2.2.1, 6.3.1; Table 6.1}

Between 1750 and 2011, land use change (mainly deforestation), derived from land cover data and modelling, is estimated to have released 180 [100 to 260] PgC. Land use change emissions between 2002 and 2011 are dominated by tropical deforestation, and are estimated at 0.9 [0.1 to 1.7] PgC yr^{-1} (*medium confidence*), with possibly a small decrease from the 1990s due to lower reported forest loss during this decade. This estimate includes gross deforestation emissions of around 3 PgC yr^{-1} compensated by around 2 PgC yr^{-1} of forest regrowth in some regions, mainly abandoned agricultural land. {6.3.2; Table 6.2}

Of the 555 [470 to 640] PgC released to the atmosphere from fossil fuel and land use emissions from 1750 to 2011, 240 [230 to 250] PgC accumulated in the atmosphere, as estimated with very high accuracy from the observed increase of atmospheric CO_2 concentration from 278 [273 to 283] ppm[10] in 1750 to 390.5 [390.4 to 390.6] ppm in 2011. The amount of CO_2 in the atmosphere grew by 4.0 [3.8 to 4.2] PgC yr^{-1} in the first decade of the 21st century. The distribution of observed atmospheric CO_2 increases with latitude clearly shows that the increases are driven by anthropogenic emissions that occur primarily in the industrialized countries north of the equator. Based on annual average concentrations, stations in the NH show slightly higher concentrations than stations in the SH. An independent line of evidence

[9] 1 Petagram of carbon = 1 PgC = 10^{15} grams of carbon = 1 Gigatonne of carbon = 1 GtC. This corresponds to 3.667 $GtCO_2$.

[10] ppm (parts per million) or ppb (parts per billion, 1 billion = 1000 million) is the ratio of the number of greenhouse gas molecules to the total number of molecules of dry air. For example, 300 ppm means 300 molecules of a greenhouse gas per million molecules of dry air.

for the anthropogenic origin of the observed atmospheric CO_2 increase comes from the observed consistent decrease in atmospheric oxygen (O_2) content and a decrease in the stable isotopic ratio of CO_2 ($^{13}C/^{12}C$) in the atmosphere (Figure TS.5). {2.2.1, 6.1.3}

The remaining amount of carbon released by fossil fuel and land use emissions has been re-absorbed by the ocean and terrestrial ecosystems. Based on high agreement between independent estimates using different methods and data sets (e.g., oceanic carbon, oxygen and transient tracer data), it is *very likely* that the global ocean inventory of anthropogenic carbon increased from 1994 to 2010. In 2011, it is estimated to be 155 [125 to 185] PgC. The annual global oceanic uptake rates calculated from independent data sets (from changes in the oceanic inventory of anthropogenic carbon, from measurements of the atmospheric oxygen to nitrogen ratio (O_2/N_2) or from CO_2 partial pressure (pCO_2) data) and for different time periods agree with each other within their uncertainties, and *very likely* are in the range of 1.0 to 3.2 PgC yr^{-1}. Regional observations of the storage rate of anthropogenic carbon in the ocean are in broad agreement with the expected rate resulting from the increase in atmospheric CO_2

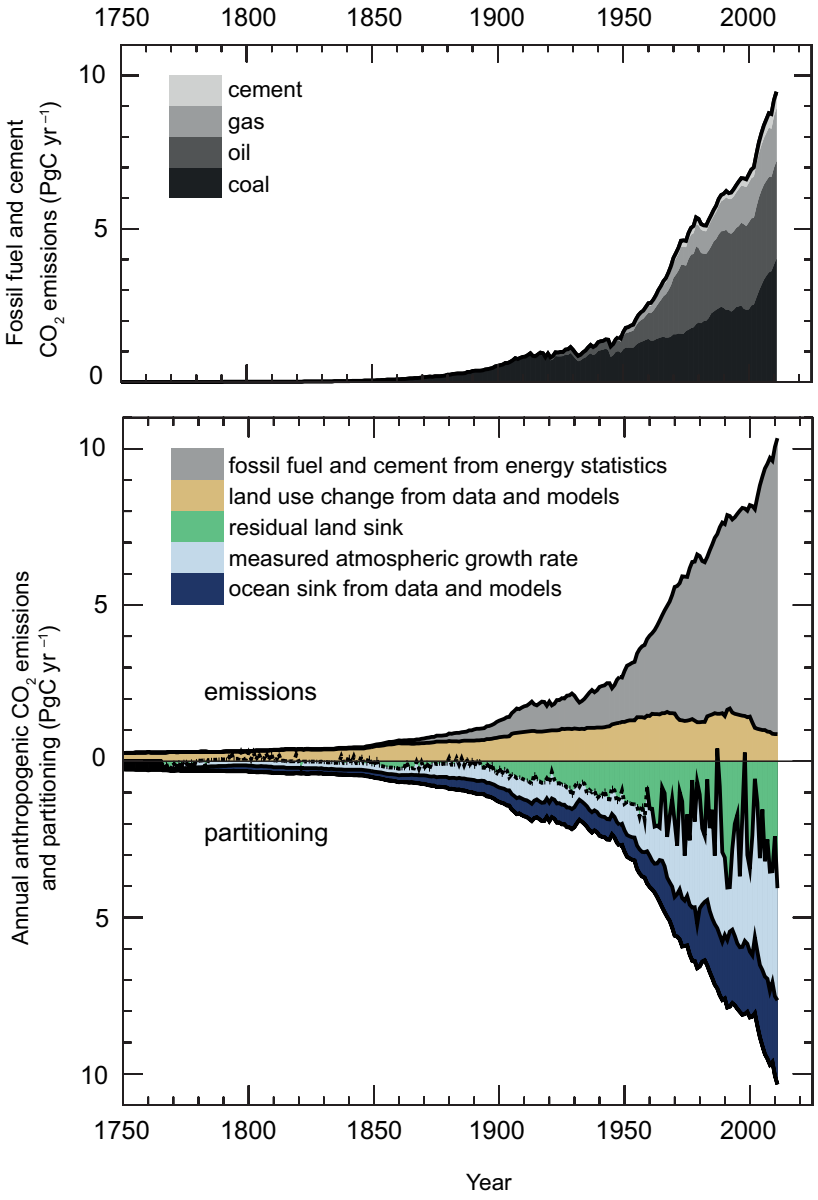

Figure TS.4 | Annual anthropogenic CO_2 emissions and their partitioning among the atmosphere, land and ocean (PgC yr^{-1}) from 1750 to 2011. (Top) Fossil fuel and cement CO_2 emissions by category, estimated by the Carbon Dioxide Information Analysis Center (CDIAC). (Bottom) Fossil fuel and cement CO_2 emissions as above. CO_2 emissions from net land use change, mainly deforestation, are based on land cover change data (see Table 6.2). The atmospheric CO_2 growth rate prior to 1959 is based on a spline fit to ice core observations and a synthesis of atmospheric measurements from 1959. The fit to ice core observations does not capture the large interannual variability in atmospheric CO_2 and is represented with a dashed line. The ocean CO_2 sink is from a combination of models and observations. The residual land sink (term in green in the figure) is computed from the residual of the other terms. The emissions and their partitioning include only the fluxes that have changed since 1750, and not the natural CO_2 fluxes (e.g., atmospheric CO_2 uptake from weathering, outgassing of CO_2 from lakes and rivers and outgassing of CO_2 by the ocean from carbon delivered by rivers; see Figure 6.1) between the atmosphere, land and ocean reservoirs that existed before that time and still exist today. The uncertainties in the various terms are discussed in Chapter 6 and reported in Table 6.1 for decadal mean values. {Figure 6.8}

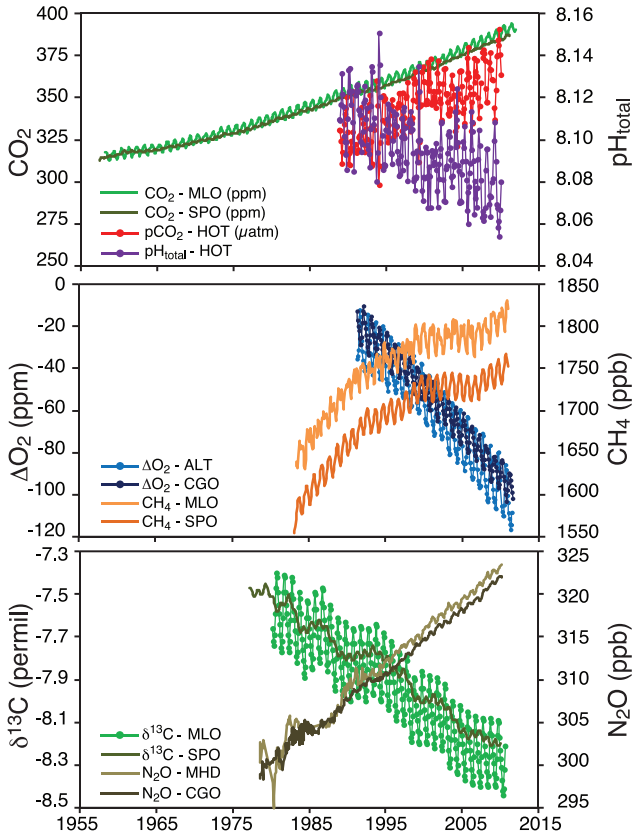

Figure TS.5 | Atmospheric concentration of CO_2, oxygen, $^{13}C/^{12}C$ stable isotope ratio in CO_2, as well as CH_4 and N_2O atmospheric concentrations and oceanic surface observations of CO_2 partial pressure (pCO_2) and pH, recorded at representative time series stations in the Northern and the Southern Hemispheres. MLO: Mauna Loa Observatory, Hawaii; SPO: South Pole; HOT: Hawaii Ocean Time-Series station; MHD: Mace Head, Ireland; CGO: Cape Grim, Tasmania; ALT: Alert, Northwest Territories, Canada. Further detail regarding the related Figure SPM.4 is given in the TS Supplementary Material. {Figures 3.18, 6.3; FAQ 3.3, Figure 1}

concentrations, but with significant spatial and temporal variations. {3.8.1, 6.3}

Natural terrestrial ecosystems (those not affected by land use change) are estimated by difference from changes in other reservoirs to have accumulated 160 [70 to 250] PgC between 1750 and 2011. The gain of carbon by natural terrestrial ecosystems is estimated to take place mainly through the uptake of CO_2 by enhanced photosynthesis at higher CO_2 levels and nitrogen deposition and longer growing seasons in mid and high latitudes. Natural carbon sinks vary regionally owing to physical, biological and chemical processes acting on different time scales. An excess of atmospheric CO_2 absorbed by land ecosystems gets stored as organic matter in diverse carbon pools, from short-lived (leaves, fine roots) to long-lived (stems, soil carbon). {6.3; Table 6.1}

TS.2.8.2 Carbon and Ocean Acidification

Oceanic uptake of anthropogenic CO_2 results in gradual acidification of the ocean. The pH[11] of ocean surface water has decreased by 0.1 since the beginning of the industrial era (*high confidence*), corresponding to a 26% increase in hydrogen ion concentration. The observed pH trends range between –0.0014 and –0.0024 per year in surface waters. In the ocean interior, natural physical and biological processes, as well as uptake of anthropogenic CO_2, can cause changes in pH over decadal and longer time scales. {3.8.2; Box 3.2; Table 3.2; FAQ 3.3}

TS.2.8.3 Methane

The concentration of CH_4 has increased by a factor of 2.5 since pre-industrial times, from 722 [697 to 747] ppb in 1750 to 1803 [1799 to 1807] ppb in 2011 (Figure TS.5). There is *very high confidence* that the atmospheric CH_4 increase during the Industrial Era is caused by anthropogenic activities. The massive increase in the number of ruminants, the emissions from fossil fuel extraction and use, the expansion of rice paddy agriculture and the emissions from landfills and waste are the dominant anthropogenic CH_4 sources. Anthropogenic emissions account for 50 to 65% of total emissions. By including natural geological CH_4 emissions that were not accounted for in previous budgets, the fossil component of the total CH_4 emissions (i.e., anthropogenic emissions related to leaks in the fossil fuel industry and natural geological leaks) is now estimated to amount to about 30% of the total CH_4 emissions (*medium confidence*). {2.2.1, 6.1, 6.3.3}

In recent decades, CH_4 growth in the atmosphere has been variable. CH_4 concentrations were relatively stable for about a decade in the 1990s, but then started growing again starting in 2007. The exact drivers of this renewed growth are still debated. Climate-driven fluctuations of CH_4 emissions from natural wetlands (177 to 284 $\times 10^{12}$ g (CH_4) yr^{-1} for 2000–2009 based on bottom-up estimates) are the main drivers of the global interannual variability of CH_4 emissions (*high confidence*), with a smaller contribution from biomass burning emissions during high fire years {2.2.1, 6.3.3; Table 6.8}.

TS.2.8.4 Nitrous Oxide

Since pre-industrial times, the concentration of N_2O in the atmosphere has increased by a factor of 1.2 (Figure TS.5). Changes in the nitrogen cycle, in addition to interactions with CO_2 sources and sinks, affect emissions of N_2O both on land and from the ocean. {2.2.1, 6.4.6}

TS.2.8.5 Oceanic Oxygen

High agreement among analyses provides *medium confidence* that oxygen concentrations have decreased in the open ocean thermocline in many ocean regions since the 1960s. The general decline is consistent with the expectation that warming-induced stratification leads to a decrease in the supply of oxygen to the thermocline from near surface waters, that warmer waters can hold less oxygen and that changes in wind-driven circulation affect oxygen concentrations. It is *likely* that the tropical oxygen minimum zones have expanded in recent decades. {3.8.3}

[11] pH is a measure of acidity: a decrease in pH value means an increase in acidity, that is, acidification.

TS.3 Drivers of Climate Change

TS.3.1 Introduction

Human activities have changed and continue to change the Earth's surface and atmospheric composition. Some of these changes have a direct or indirect impact on the energy balance of the Earth and are thus drivers of climate change. Radiative forcing (RF) is a measure of the net change in the energy balance of the Earth system in response to some external perturbation (see Box TS.2), with positive RF leading to a warming and negative RF to a cooling. The RF concept is valuable for comparing the influence on GMST of most individual agents affecting the Earth's radiation balance. The quantitative values provided in AR5 are consistent with those in previous IPCC reports, though there have been some important revisions (Figure TS.6). Effective radiative forcing (ERF) is now used to quantify the impact of some forcing agents that involve rapid adjustments of components of the atmosphere and surface that are assumed constant in the RF concept (see Box TS.2). RF and ERF are estimated from the change between 1750 and 2011, referred to as 'Industrial Era', if other time periods are not explicitly stated. Uncertainties are given associated with the best estimates of RF and ERF, with values representing the 5 to 95% (90%) confidence range. {8.1, 7.1}

In addition to the global mean RF or ERF, the spatial distribution and temporal evolution of forcing, as well as climate feedbacks, play a role in determining the eventual impact of various drivers on climate. Land surface changes may also impact the local and regional climate through processes that are not radiative in nature. {8.1, 8.3.5, 8.6}

TS.3.2 Radiative Forcing from Greenhouse Gases

Human activity leads to change in the atmospheric composition either directly (via emissions of gases or particles) or indirectly (via atmospheric chemistry). Anthropogenic emissions have driven the changes in well-mixed greenhouse gas (WMGHG) concentrations during the Industrial Era (see Section TS.2.8 and TFE.7). As historical WMGHG concentrations since the pre-industrial are well known based on direct measurements and ice core records, and WMGHG radiative properties are also well known, the computation of RF due to concentration changes provides tightly constrained values (Figure TS.6). There has not been significant change in our understanding of WMGHG radiative impact, so that the changes in RF estimates relative to AR4 are due essentially to concentration increases. The best estimate for WMGHG ERF is the same as RF, but the uncertainty range is twice as large due to the poorly constrained cloud responses. Owing to high-quality observations, it is certain that increasing atmospheric burdens of most WMGHGs, especially CO_2, resulted in a further increase in their RF from 2005 to 2011. Based on concentration changes, the RF of all WMGHGs in 2011 is 2.83 [2.54 to 3.12] W m^{-2} (*very high confidence*). This is an increase since AR4 of 0.20 [0.18 to 0.22] W m^{-2}, with nearly all of the increase due to the increase in the abundance of CO_2 since 2005. The Industrial Era RF for CO_2 alone is 1.82 [1.63 to 2.01] W m^{-2}. Over the last 15 years, CO_2 has been the dominant contributor to the increase in RF from the WMGHGs, with RF of CO_2 having an average growth rate slightly less than 0.3 W m^{-2} per decade. The uncertainty in the WMGHG RF is due in part to its radiative properties but mostly to the full accounting of atmospheric radiative transfer including clouds. {2.2.1, 5.2, 6.3, 8.3, 8.3.2; Table 6.1}

After a decade of near stability, the recent increase of CH_4 concentration led to an enhanced RF compared to AR4 by 2% to 0.48 [0.43 to 0.53] W m^{-2}. It is *very likely* that the RF from CH_4 is now larger than that of all halocarbons combined. {2.2.1, 8.3.2}

Atmospheric N_2O has increased by 6% since AR4, causing an RF of 0.17 [0.14 to 0.20] W m^{-2}. N_2O concentrations continue to rise while those of dichlorodifluoromethane (CF_2Cl_2, CFC-12), the third largest WMGHG contributor to RF for several decades, are decreasing due to phase-out of emissions of this chemical under the Montreal Protocol. Since

Box TS.2 | Radiative Forcing and Effective Radiative Forcing

RF and ERF are used to quantify the change in the Earth's energy balance that occurs as a result of an externally imposed change. They are expressed in watts per square metre (W m^{-2}). RF is defined in AR5, as in previous IPCC assessments, as the change in net downward flux (shortwave + longwave) at the tropopause after allowing for stratospheric temperatures to readjust to radiative equilibrium, while holding other state variables such as tropospheric temperatures, water vapour and cloud cover fixed at the unperturbed values (see Glossary). {8.1.1}

Although the RF concept has proved very valuable, improved understanding has shown that including rapid adjustments of the Earth's surface and troposphere can provide a better metric for quantifying the climate response. These rapid adjustments occur over a variety of time scales, but are relatively distinct from responses to GMST change. Aerosols in particular impact the atmosphere temperature profile and cloud properties on a time scale much shorter than adjustments of the ocean (even the upper layer) to forcings. The ERF concept defined in AR5 allows rapid adjustments to perturbations, for all variables except for GMST or ocean temperature and sea ice cover. The ERF and RF values are significantly different for the anthropogenic aerosols, owing to their influence on clouds and on snow or ice cover. For other components that drive the Earth's energy balance, such as GHGs, ERF and RF are fairly similar, and RF may have comparable utility given that it requires fewer computational resources to calculate and is not affected by meteorological variability and hence can better isolate small forcings. In cases where RF and ERF differ substantially, ERF has been shown to be a better indicator of the GMST response and is therefore emphasized in AR5. {7.1, 8.1; Box 8.1}

AR4, N_2O has overtaken CFC-12 to become the third largest WMGHG contributor to RF. The RF from halocarbons is very similar to the value in AR4, with a reduced RF from CFCs but increases in many of their replacements. Four of the halocarbons (trichlorofluoromethane ($CFCl_3$, CFC-11), CFC-12, trichlorotrifluoroethane ($CF_2ClCFCl_2$, CFC-113) and chlorodifluoromethane (CHF_2Cl, HCFC-22) account for 85% of the total halocarbon RF. The former three compounds have declining RF over the last 5 years but are more than compensated for by the increased RF from HCFC-22. There is *high confidence* that the growth rate in RF from all WMGHG is weaker over the last decade than in the 1970s and 1980s owing to a slower increase in the non-CO_2 RF. {2.2.1, 8.3.2}

The short-lived GHGs ozone (O_3) and stratospheric water vapour also contribute to anthropogenic forcing. Observations indicate that O_3 *likely* increased at many undisturbed (background) locations through the 1990s. These increases have continued mainly over Asia (though

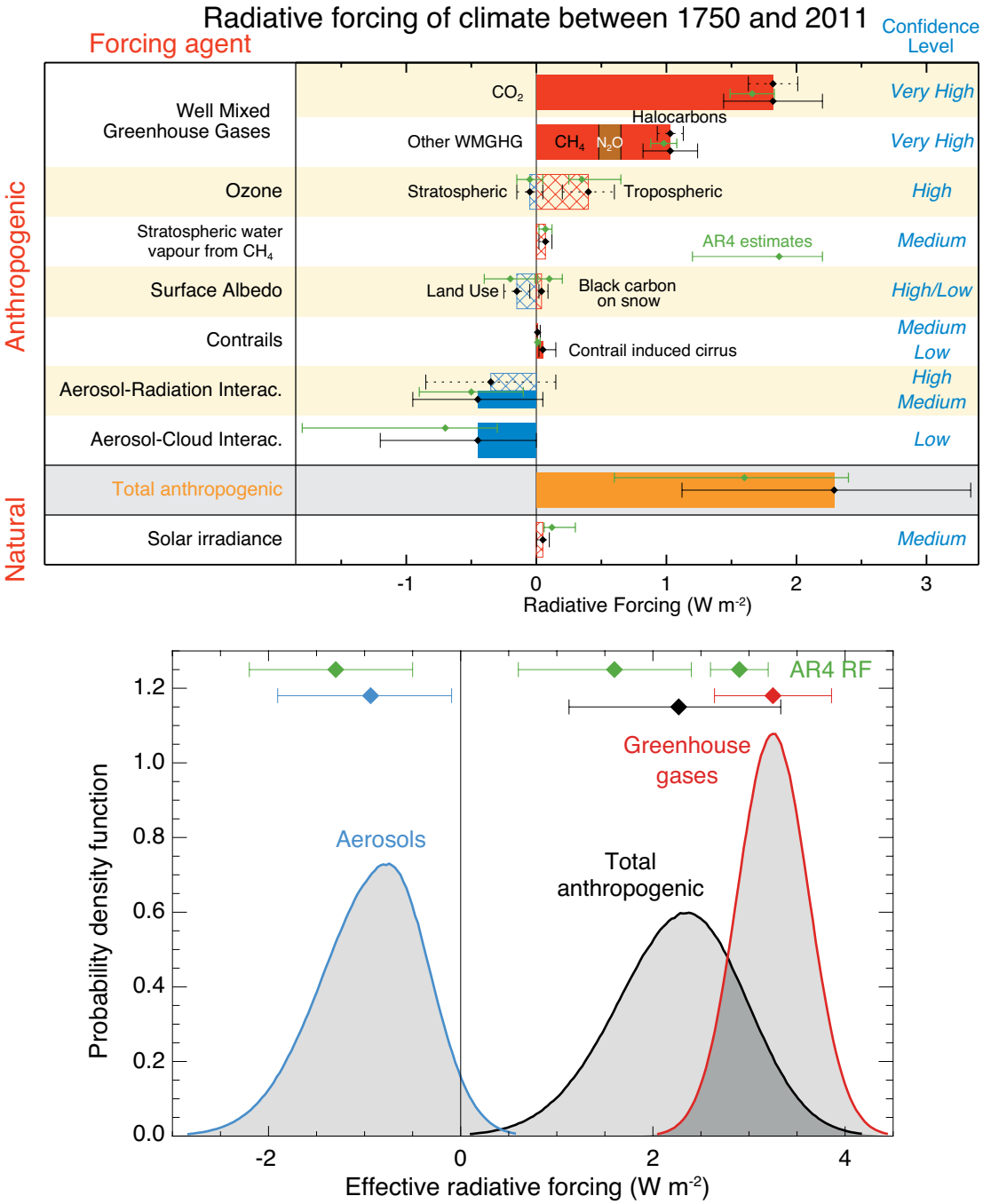

Figure TS.6 | Radiative forcing (RF) and Effective radiative forcing (ERF) of climate change during the Industrial Era. (Top) Forcing by concentration change between 1750 and 2011 with associated uncertainty range (solid bars are ERF, hatched bars are RF, green diamonds and associated uncertainties are for RF assessed in AR4). (Bottom) Probability density functions (PDFs) for the ERF, for the aerosol, greenhouse gas (GHG) and total. The green lines show the AR4 RF 90% confidence intervals and can be compared with the red, blue and black lines which show the AR5 ERF 90% confidence intervals (although RF and ERF differ, especially for aerosols). The ERF from surface albedo changes and combined contrails and contrail-induced cirrus is included in the total anthropogenic forcing, but not shown as a separate PDF. For some forcing mechanisms (ozone, land use, solar) the RF is assumed to be representative of the ERF but an additional uncertainty of 17% is added in quadrature to the RF uncertainty. {Figures 8.15, 8.16}

observations cover a limited area) and flattened over Europe during the last decade. The total RF due to changes in O_3 is 0.35 [0.15 to 0.55] W m^{-2} (*high confidence*), with RF due to tropospheric O_3 of 0.40 [0.20 to 0.60] W m^{-2} (*high confidence*) and due to stratospheric O_3 of –0.05 [–0.15 to +0.05] W m^{-2} (*high confidence*). O_3 is not emitted directly into the atmosphere; instead it is formed by photochemical reactions. In the troposphere these reactions involve precursor compounds that are emitted into the atmosphere from a variety of natural and anthropogenic sources. Tropospheric O_3 RF is largely attributed to increases in emissions of CH_4, carbon monoxide, volatile organics and nitrogen oxides, while stratospheric RF results primarily from O_3 depletion by anthropogenic halocarbons. However, there is now strong evidence for substantial links between the changes in tropospheric and stratospheric O_3 and a total O_3 RF of 0.50 [0.30 to 0.70] W m^{-2} is attributed to tropospheric O_3 precursor emissions and –0.15 [–0.30 to 0.00] W m^{-2} to O_3 depletion by halocarbons. There is strong evidence that tropospheric O_3 also has a detrimental impact on vegetation physiology, and therefore on its CO_2 uptake. This reduced uptake leads to an indirect increase in the atmospheric CO_2 concentration. Thus a fraction of the CO_2 RF should be attributed to ozone or its precursors rather than direct emission of CO_2, but there is a *low confidence* on the quantitative estimates. RF for stratospheric water vapour produced from CH_4 oxidation is 0.07 [0.02 to 0.12] W m^{-2}. Other changes in stratospheric water vapour, and all changes in water vapour in the troposphere, are regarded as a feedback rather than a forcing. {2.2.2, 8.1–8.3; FAQ 8.1}

TS.3.3 Radiative Forcing from Anthropogenic Aerosols

Anthropogenic aerosols are responsible for an RF of climate through multiple processes which can be grouped into two types: aerosol–radiation interactions (ari) and aerosol–cloud interactions (aci). There has been progress since AR4 on observing and modelling climate-relevant aerosol properties (including their size distribution, hygroscopicity, chemical composition, mixing state, optical and cloud nucleation properties) and their atmospheric distribution. Nevertheless, substantial uncertainties remain in assessments of long-term trends of global aerosol optical depth and other global properties of aerosols due to difficulties in measurement and lack of observations of some relevant parameters, high spatial and temporal variability and the relatively short observational records that exist. The anthropogenic RFari is given a best estimate of –0.35 [–0.85 to +0.15] W m^{-2} (*high confidence*) using evidence from aerosol models and some constraints from observations. The RFari is caused by multiple aerosol types (see Section TS3.6). The rapid adjustment to RFari leads to further negative forcing, in particular through cloud adjustments, and is attributable primarily to black carbon. As a consequence, the ERFari is more negative than the RFari (*low confidence*) and given a best estimate of –0.45 [–0.95 to +0.05] W m^{-2}. The assessment for RFari is less negative than reported in AR4 because of a re-evaluation of aerosol absorption. The uncertainty estimate is wider but more robust. {2.2.3, 7.3, 7.5.2}

Improved understanding of aerosol–cloud interactions has led to a reduction in the magnitude of many global aerosol–cloud forcings estimates. The total ERF due to aerosols (ERFari+aci, excluding the effect of absorbing aerosol on snow and ice) is assessed to be –0.9 [–1.9 to –0.1] W m^{-2} (*medium confidence*). This estimate encompasses all rapid adjustments, including changes to the cloud lifetime and aerosol microphysical effects on mixed-phase, ice and convective clouds. This range was obtained by giving equal weight to satellite-based studies and estimates from climate models. It is consistent with multiple lines of evidence suggesting less negative estimates for aerosol–cloud interactions than those discussed in AR4. {7.4, 7.5, 8.5}

The RF from black carbon (BC) on snow and ice is assessed to be 0.04 [0.02 to 0.09] W m^{-2} (*low confidence*). Unlike in the previous IPCC assessment, this estimate includes the effects on sea ice, accounts for more physical processes and incorporates evidence from both models and observations. This RF causes a two to four times larger GMST change per unit forcing than CO_2 primarily because all of the forcing energy is deposited directly into the cryosphere, whose evolution drives a positive albedo feedback on climate. This effect thus can represent a significant forcing mechanism in the Arctic and other snow- or ice-covered regions. {7.3, 7.5.2, 8.3.4, 8.5}

Despite the large uncertainty ranges on aerosol forcing, there is a *high confidence* that aerosols have offset a substantial portion of GHG forcing. Aerosol–cloud interactions can influence the character of individual storms, but evidence for a systematic aerosol effect on storm or precipitation intensity is more limited and ambiguous. {7.4, 7.6, 8.5}

TS.3.4 Radiative Forcing from Land Surface Changes and Contrails

There is robust evidence that anthropogenic land use changes such as deforestation have increased the land surface albedo, which leads to an RF of –0.15 [–0.25 to –0.05] W m^{-2}. There is still a large spread of quantitative estimates owing to different assumptions for the albedo of natural and managed surfaces (e.g., croplands, pastures). In addition, the time evolution of the land use change, and in particular how much was already completed in the reference year 1750, are still debated. Furthermore, land use change causes other modifications that are not radiative but impact the surface temperature, including modifications in the surface roughness, latent heat flux, river runoff and irrigation. These are more uncertain and they are difficult to quantify, but they tend to offset the impact of albedo changes at the global scale. As a consequence, there is low agreement on the sign of the net change in global mean temperature as a result of land use change. Land use change, and in particular deforestation, also has significant impacts on WMGHG concentrations. It contributes to the corresponding RF associated with CO_2 emissions or concentration changes. {8.3.5}

Persistent contrails from aviation contribute a positive RF of 0.01 [0.005 to 0.03] W m^{-2} (*medium confidence*) for year 2011, and the combined contrail and contrail-cirrus ERF from aviation is assessed to be 0.05 [0.02 to 0.15] W m^{-2} (*low confidence*). This forcing can be much larger regionally but there is now *medium confidence* that it does not produce observable regional effects on either the mean or diurnal range of surface temperature. {7.2.7}

TS.3.5 Radiative Forcing from Natural Drivers of Climate Change

Solar and volcanic forcings are the two dominant natural contributors to global climate change during the Industrial Era. Satellite observations

of total solar irradiance (TSI) changes since 1978 show quasi-periodic cyclical variation with a period of roughly 11 years. Longer term forcing is typically estimated by comparison of solar minima (during which variability is least). This gives an RF change of –0.04 [–0.08 to 0.00] W m^{-2} between the most recent (2008) minimum and the 1986 minimum. There is some diversity in the estimated trends of the composites of various satellite data, however. Secular trends of TSI before the start of satellite observations rely on a number of indirect proxies. The best estimate of RF from TSI changes over the industrial era is 0.05 [0.00 to 0.10] W m^{-2} (*medium confidence*), which includes greater RF up to around 1980 and then a small downward trend. This RF estimate is substantially smaller than the AR4 estimate due to the addition of the latest solar cycle and inconsistencies in how solar RF was estimated in earlier IPCC assessments. The recent solar minimum appears to have been unusually low and long-lasting and several projections indicate lower TSI for the forthcoming decades. However, current abilities to project solar irradiance are extremely limited so that there is *very low confidence* concerning future solar forcing. Nonetheless, there is a *high confidence* that 21st century solar forcing will be much smaller than the projected increased forcing due to WMGHGs. {5.2.1, 8.4.1; FAQ 5.1}

Changes in solar activity affect the cosmic ray flux impinging upon the Earth's atmosphere, which has been hypothesized to affect climate through changes in cloudiness. Cosmic rays enhance aerosol nucleation and thus may affect cloud condensation nuclei production in the free troposphere, but the effect is too weak to have any climatic influence during a solar cycle or over the last century (medium evidence, high agreement). No robust association between changes in cosmic rays and cloudiness has been identified. In the event that such an association existed, a mechanism other than cosmic ray–induced nucleation of new aerosol particles would be needed to explain it. {7.3, 7.4.6}

The RF of stratospheric volcanic aerosols is now well understood and there is a large RF for a few years after major volcanic eruptions (Box TS.5, Figure 1). Although volcanic eruptions inject both mineral particles and sulphate aerosol precursors into the atmosphere, it is the latter, because of their small size and long lifetimes, that are responsible for RF important for climate. The emissions of CO_2 from volcanic eruptions are at least 100 times smaller than anthropogenic emissions, and inconsequential for climate on century time scales. Large tropical volcanic eruptions have played an important role in driving annual to decadal scale climate change during the Industrial Era owing to their sometimes very large negative RF. There has not been any major volcanic eruption since Mt Pinatubo in 1991, which caused a 1-year RF of about –3.0 W m^{-2}, but several smaller eruptions have caused an RF averaged over the years 2008–2011 of –0.11 [–0.15 to –0.08] W m^{-2} (*high confidence*), twice as strong in magnitude compared to the 1999–2002 average. The smaller eruptions have led to better understanding of the dependence of RF on the amount of material from high-latitude injections as well as the time of the year when they take place. {5.2.1, 5.3.5, 8.4.2; Annex II}

TS.3.6 Synthesis of Forcings; Spatial and Temporal Evolution

A synthesis of the Industrial Era forcing finds that among the forcing agents, there is a *very high confidence* only for the WMGHG RF. Relative to AR4, the confidence level has been elevated for seven forcing agents owing to improved evidence and understanding. {8.5; Figure 8.14}

The time evolution of the total anthropogenic RF shows a nearly continuous increase from 1750, primarily since about 1860. The total anthropogenic RF increase rate since 1960 has been much greater than during earlier Industrial Era periods, driven primarily by the continuous increase in most WMGHG concentrations. There is still low agreement on the time evolution of the total aerosol ERF, which is the primary factor for the uncertainty in the total anthropogenic forcing. The fractional uncertainty in the total anthropogenic forcing decreases gradually after 1950 owing to the smaller offset of positive WMGHG forcing by negative aerosol forcing. There is robust evidence and high agreement that natural forcing is a small fraction of the WMGHG forcing. Natural forcing changes over the last 15 years have *likely* offset a substantial fraction (at least 30%) of the anthropogenic forcing increase during this period (Box TS.3). Forcing by CO_2 is the largest single contributor to the total forcing during the Industrial Era and from 1980–2011. Compared to the entire Industrial Era, the dominance of CO_2 forcing is larger for the 1980–2011 change with respect to other WMGHGs, and there is *high confidence* that the offset from aerosol forcing to WMGHG forcing during this period was much smaller than over the 1950–1980 period. {8.5.2}

Forcing can also be attributed to emissions rather than to the resulting concentration changes (Figure TS.7). Carbon dioxide is the largest single contributor to historical RF from either the perspective of changes in the atmospheric concentration of CO_2 or the impact of changes in net emissions of CO_2. The relative importance of other forcing agents can vary markedly with the perspective chosen, however. In particular, CH_4 emissions have a much larger forcing (about 1.0 W m^{-2} over the Industrial Era) than CH_4 concentration increases (about 0.5 W m^{-2}) due to several indirect effects through atmospheric chemistry. In addition, carbon monoxide emissions are *virtually certain* to cause a positive forcing, while emissions of reactive nitrogen oxides *likely* cause a net negative forcing but uncertainties are large. Emissions of ozone-depleting halocarbons *very likely* cause a net positive forcing as their direct radiative effect is larger than the impact of the stratospheric ozone depletion that they induce. Emissions of SO_2, organic carbon and ammonia cause a negative forcing, while emissions of black carbon lead to positive forcing via aerosol–radiation interactions. Note that mineral dust forcing may include a natural component or a climate feedback effect. {7.3, 7.5.2, 8.5.1}

Although the WMGHGs show a spatially fairly homogeneous forcing, other agents such as aerosols, ozone and land use changes are highly heterogeneous spatially. RFari showed maximum negative values over eastern North America and Europe during the early 20th century, with large negative values extending to East and Southeast Asia, South America and central Africa by 1980. Since then, however, the magnitude has decreased over eastern North America and Europe due to pollution control, and the peak negative forcing has shifted to South and East Asia primarily as a result of economic growth and the resulting increase in emissions in those areas. Total aerosol ERF shows similar behaviour for locations with maximum negative forcing, but also shows substantial positive forcing over some deserts and the Arctic. In contrast, the global mean whole atmosphere ozone forcing increased throughout

the 20th century, and has peak positive amplitudes around 15°N to 30°N but negative values over Antarctica. Negative land use forcing by albedo changes has been strongest in industrialized and biomass burning regions. The inhomogeneous nature of these forcings can cause them to have a substantially larger influence on the hydrologic cycle than an equivalent global mean homogeneous forcing. {8.3.5, 8.6}

Over the 21st century, anthropogenic RF is projected to increase under the Representative Concentration Pathways (RCPs; see Box TS.6). Simple model estimates of the RF resulting from the RCPs, which include WMGHG emissions spanning a broad range of possible futures, show anthropogenic RF relative to 1750 increasing to 3.0 to 4.8 W m^{-2} in 2050, and 2.7 to 8.4 W m^{-2} at 2100. In the near term, the RCPs are quite similar to one another (and emissions of near-term climate forcers do not span the literature range of possible futures), with RF at 2030 ranging only from 2.9 to 3.3 W m^{-2} (additional 2010 to 2030 RF of 0.7 to 1.1 W m^{-2}), but they show highly diverging values for the second half of the 21st century driven largely by CO_2. Results based on the RCP scenarios suggest only small changes in aerosol ERF between 2000 and 2030, followed by a strong reduction in the aerosols and a substantial weakening of the negative total aerosol ERF. Nitrate aerosols are an exception to this reduction, with a substantially increased negative forcing which is a robust feature among the few available models. The divergence across the RCPs indicates that, although a certain amount of future climate change is already 'in the system' due to the current radiative imbalance caused by historical emissions and the long lifetime of some atmospheric forcing agents, societal choices can still have a very large effect on future RF, and hence on climate change. {8.2, 8.5.3, 12.3; Figures 8.22, 12.4}

TS.3.7 Climate Feedbacks

Feedbacks will also play an important role in determining future climate change. Indeed, climate change may induce modification in the water, carbon and other biogeochemical cycles which may reinforce (positive feedback) or dampen (negative feedback) the expected

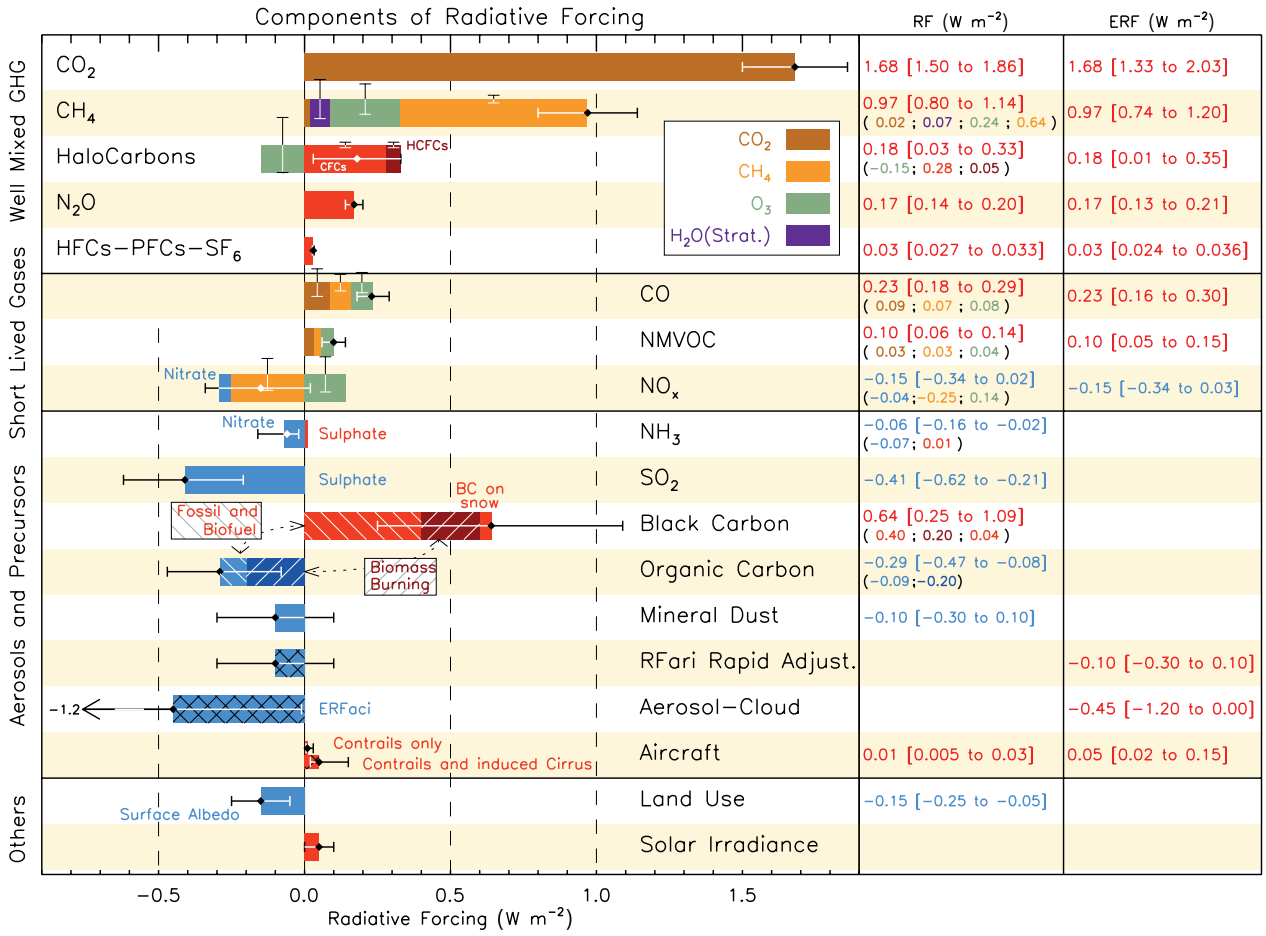

Figure TS.7 | Radiative forcing (RF) of climate change during the Industrial Era shown by emitted components from 1750 to 2011. The horizontal bars indicate the overall uncertainty, while the vertical bars are for the individual components (vertical bar lengths proportional to the relative uncertainty, with a total length equal to the bar width for a ±50% uncertainty). Best estimates for the totals and individual components (from left to right) of the response are given in the right column. Values are RF except for the effective radiative forcing (ERF) due to aerosol–cloud interactions (ERFaci) and rapid adjustment associated with the RF due to aerosol-radiation interaction (RFari Rapid Adjust.). Note that the total RF due to aerosol-radiation interaction (–0.35 Wm^{-2}) is slightly different from the sum of the RF of the individual components (–0.33 Wm^{-2}). The total RF due to aerosol-radiation interaction is the basis for Figure SPM.5. Secondary organic aerosol has not been included since the formation depends on a variety of factors not currently sufficiently quantified. The ERF of contrails includes contrail induced cirrus. Combining ERFaci –0.45 [–1.2 to 0.0] Wm^{-2} and rapid adjustment of ari –0.1 [–0.3 to +0.1] Wm^{-2} results in an integrated component of adjustment due to aerosols of –0.55 [–1.33 to –0.06] Wm^{-2}. CFCs = chlorofluorocarbons, HCFCs = hydrochlorofluorocarbons, HFCs = hydrofluorocarbons, PFCs = perfluorocarbons, NMVOC = Non-Methane Volatile Organic Compounds, BC = black carbon. Further detail regarding the related Figure SPM.5 is given in the TS Supplementary Material. {Figure 8.17}

temperature increase. Snow and ice albedo feedbacks are known to be positive. The combined water vapour and lapse rate feedback is *extremely likely* to be positive and now fairly well quantified, while cloud feedbacks continue to have larger uncertainties (see TFE.6). In addition, the new Coupled Model Intercomparison Project Phase 5 (CMIP5) models consistently estimate a positive carbon-cycle feedback, that is, reduced natural CO_2 sinks in response to future climate change. In particular, carbon-cycle feedbacks in the oceans are positive in the models. Carbon sinks in tropical land ecosystems are less consistent, and may be susceptible to climate change via processes such as drought and fire that are sometimes not yet fully represented. A key update since AR4 is the introduction of nutrient dynamics in some of the CMIP5 land carbon models, in particular the limitations on plant growth imposed by nitrogen availability. The net effect of accounting for the nitrogen cycle is a smaller projected land sink for a given trajectory of anthropogenic CO_2 emissions (see TFE.7). {6.4, Box 6.1, 7.2}

Models and ecosystem warming experiments show high agreement that wetland CH_4 emissions will increase per unit area in a warmer climate, but wetland areal extent may increase or decrease depending on regional changes in temperature and precipitation affecting wetland hydrology, so that there is *low confidence* in quantitative projections of wetland CH_4 emissions. Reservoirs of carbon in hydrates and permafrost are very large, and thus could potentially act as very powerful feedbacks. Although poorly constrained, the 21st century global release of CH_4 from hydrates to the atmosphere is *likely* to be low due to the under-saturated state of the ocean, long ventilation time of the ocean and slow propagation of warming through the seafloor. There is *high confidence* that release of carbon from thawing permafrost provides a positive feedback, but there is *low confidence* in quantitative projections of its strength. {6.4.7}

Aerosol-climate feedbacks occur mainly through changes in the source strength of natural aerosols or changes in the sink efficiency of natural and anthropogenic aerosols; a limited number of modelling studies have assessed the magnitude of this feedback to be small with a *low confidence*. There is *medium confidence* for a weak feedback (of uncertain sign) involving dimethylsulphide, cloud condensation nuclei and cloud albedo due to a weak sensitivity of cloud condensation nuclei population to changes in dimethylsulphide emissions. {7.3.5}

TS.3.8 Emission Metrics

Different metrics can be used to quantify and communicate the relative and absolute contributions to climate change of emissions of different substances, and of emissions from regions/countries or sources/sectors. Up to AR4, the most common metric has been the Global Warming Potential (GWP) that integrates RF out to a particular time horizon. This metric thus accounts for the radiative efficiencies of the various substances, and their lifetimes in the atmosphere, and gives values relative to those for the reference gas CO_2. There is now increasing focus on the Global Temperature change Potential (GTP), which is based on the change in GMST at a chosen point in time, again relative to that caused by the reference gas CO_2, and thus accounts for climate response along with radiative efficiencies and atmospheric lifetimes. Both the GWP and the GTP use a time horizon (Figure TS.8 top), the choice of which is subjective and context dependent. In general, GWPs for near-term climate forcers are higher than GTPs due to the equal time weighting in the integrated forcing used in the GWP. Hence the choice of metric can greatly affect the relative importance of near-term climate forcers and WMGHGs, as can the choice of time horizon. Analysis of the impact of current emissions (1-year pulse of emissions) shows that near-term climate forcers, such as black carbon, sulphur dioxide or CH_4, can have contributions comparable to that of CO_2 for short time horizons (of either the same or opposite sign), but their impacts become progressively less for longer time horizons over which emissions of CO_2 dominate (Figure TS.8 top). {8.7}

A large number of other metrics may be defined down the driver–response–impact chain. No single metric can accurately compare all consequences (i.e., responses in climate parameters over time) of different emissions, and a metric that establishes equivalence with regard to one effect will not give equivalence with regard to other effects. The choice of metric therefore depends strongly on the particular consequence one wants to evaluate. It is important to note that the metrics do not define policies or goals, but facilitate analysis and implementation of multi-component policies to meet particular goals. All choices of metric contain implicit value-related judgements such as type of effect considered and weighting of effects over time. Whereas GWP integrates the effects up to a chosen time horizon (i.e., giving equal weight to all times up to the horizon and zero weight thereafter), the GTP gives the temperature just for one chosen year with no weight on years before or after. {8.7}

The GWP and GTP have limitations and suffer from inconsistencies related to the treatment of indirect effects and feedbacks, for instance, if climate–carbon feedbacks are included for the reference gas CO_2 but not for the non-CO_2 gases. The uncertainty in the GWP increases with time horizon, and for the 100-year GWP of WMGHGs the uncertainty can be as large as ±40%. Several studies also point out that this metric is not well suited for policies with a maximum temperature target. Uncertainties in GTP also increase with time as they arise from the same factors contributing to GWP uncertainties along with additional contributions from it being further down the driver–response–impact chain and including climate response. The GTP metric is better suited to target-based policies, but is again not appropriate for every goal. Updated metric values accounting for changes in knowledge of lifetimes and radiative efficiencies and for climate–carbon feedbacks are now available. {8.7, Table 8.7, Table 8.A.1, Chapter 8 Supplementary Material Table 8.SM.16}

With these emission metrics, the climate impact of past or current emissions attributable to various activities can be assessed. Such activity-based accounting can provide additional policy-relevant information, as these activities are more directly affected by particular societal choices than overall emissions. A single year's worth of emissions (a pulse) is often used to quantify the impact on future climate. From this perspective and with the absolute GTP metric used to illustrate the results, energy and industry have the largest contributions to warming over the next 50 to 100 years (Figure TS.8, bottom). Household fossil and biofuel, biomass burning and on-road transportation are also relatively large contributors to warming over these time scales, while current emissions from sectors that emit large amounts of CH_4 (animal husbandry, waste/landfills and agriculture) are also important over

shorter time horizons (up to about 20 years). Another useful perspective is to examine the effect of sustained current emissions. Because emitted substances are removed according to their residence time, short-lived species remain at nearly constant values while long-lived gases accumulate in this analysis. In both cases, the sectors that have the greatest long-term warming impacts (energy and industry) lead to cooling in the near term (primarily due to SO_2 emissions), and thus emissions from those sectors can lead to opposite global mean temperature responses at short and long time scales. The relative importance of the other sectors depends on the time and perspective chosen. As with RF or ERF, uncertainties in aerosol impacts are large, and in particular attribution of aerosol–cloud interactions to individual components is poorly constrained. {8.7; Chapter 8 Supplementary Material Figures 8.SM.9, 8.SM.10}

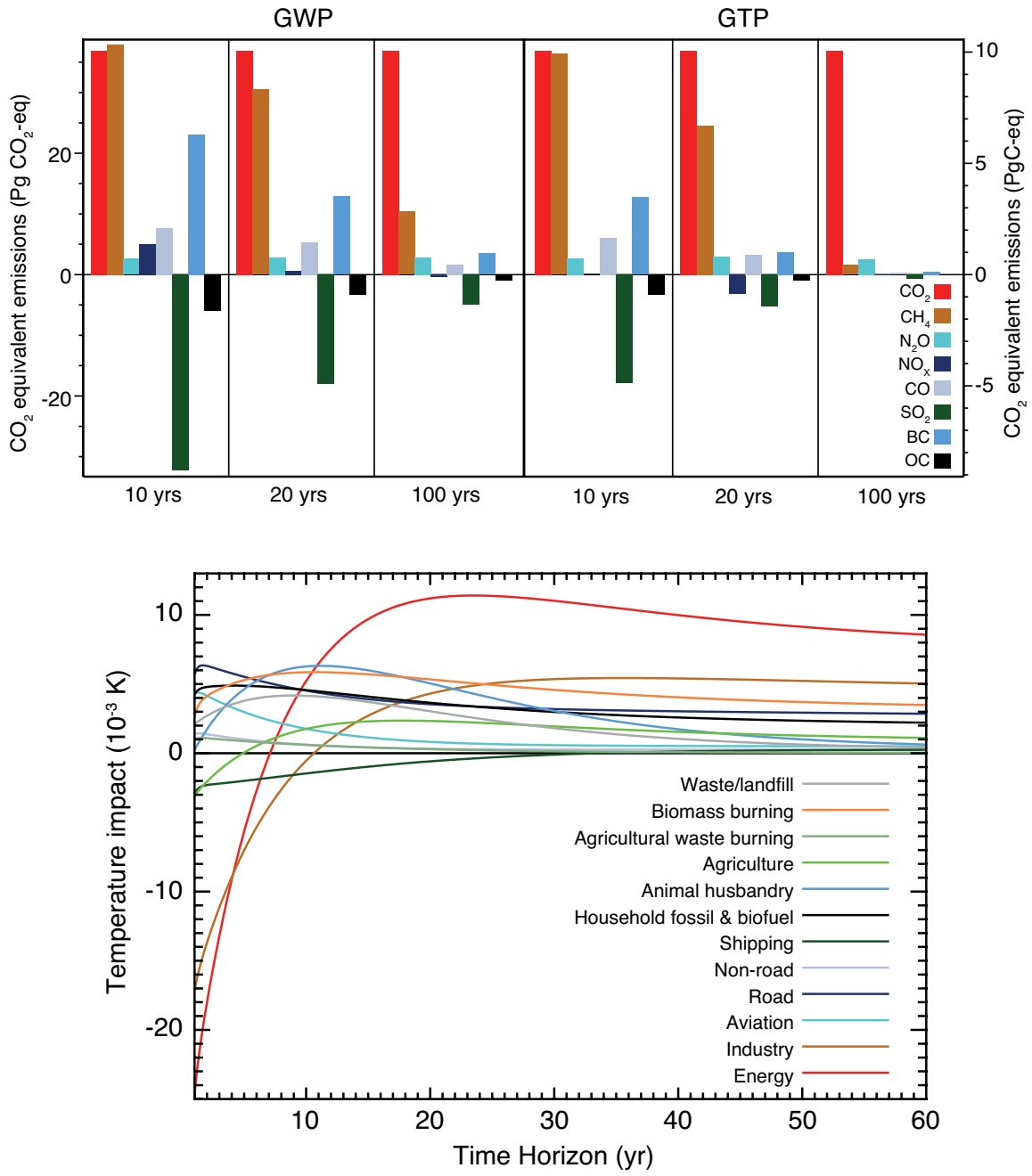

Figure TS.8 | (Upper) Global anthropogenic present-day emissions weighted by the Global Warming Potential (GWP) and the Global Temperature change Potential (GTP) for the chosen time horizons. Year 2008 (single-year pulse) emissions weighted by GWP, which is the global mean radiative forcing (RF) per unit mass emitted integrated over the indicated number of years relative to the forcing from CO_2 emissions, and GTP which estimates the impact on global mean temperature based on the temporal evolution of both RF and climate response per unit mass emitted relative to the impact of CO_2 emissions. The units are 'CO_2 equivalents', which reflects equivalence only in the impact parameter of the chosen metric (integrated RF over the chosen time horizon for GWP; temperature change at the chosen point in time for GTP), given as Pg(CO_2)eq (left axis) and PgCeq (right axis). (Bottom) The Absolute GTP (AGTP) as a function of time multiplied by the present-day emissions of all compounds from the indicated sectors is used to estimate global mean temperature response (AGTP is the same as GTP, except is not normalized by the impact of CO_2 emissions). There is little change in the relative values for the sectors over the 60 to 100-year time horizon. The effects of aerosol–cloud interactions and contrail-induced cirrus are not included in the upper panel. {Figures 8.32, 8.33}

TS.4 Understanding the Climate System and Its Recent Changes

TS.4.1 Introduction

Understanding of the climate system results from combining observations, theoretical studies of feedback processes and model simulations. Compared to AR4, more detailed observations and improved climate models (see Box TS.4) now enable the attribution of detected changes to human influences in more climate system components. The consistency of observed and modelled changes across the climate system, including in regional temperatures, the water cycle, global energy budget, cryosphere and oceans (including ocean acidification), points to global climate change resulting primarily from anthropogenic increases in WMGHG concentrations. {10}

TS.4.2 Surface Temperature

Several advances since the AR4 have allowed a more robust quantification of human influence on surface temperature changes. Observational uncertainty has been explored much more thoroughly than previously and the assessment now considers observations from the first decade of the 21st century and simulations from a new generation of climate models whose ability to simulate historical climate has improved in many respects relative to the previous generation of models considered in AR4. Observed GMST anomalies relative to 1880–1919 in recent years lie well outside the range of GMST anomalies in CMIP5 simulations with natural forcing only, but are consistent with the ensemble of CMIP5 simulations including both anthropogenic and natural forcing (Figure TS.9) even though some individual models overestimate the warming trend, while others underestimate it. Simulations with WMGHG changes only, and no aerosol changes, generally exhibit stronger warming than has been observed (Figure TS.9). Observed temperature trends over the period 1951–2010, which are characterized by warming over most of the globe with the most intense warming over the NH continents, are, at most observed locations, consistent with the temperature trends in CMIP5 simulations including anthropogenic and natural forcings and inconsistent with the temperature trends in CMIP5 simulations including natural forcings only. A number of studies have investigated the effects of the Atlantic Multi-decadal Oscillation (AMO) on GMST. Although some studies find a significant role for the AMO in driving multi-decadal variability in GMST, the AMO exhibited little trend over the period 1951–2010 on which the current assessments are based, and the AMO is assessed with *high confidence* to have made little contribution to the GMST trend between 1951 and 2010 (considerably less than 0.1°C). {2.4, 9.8.1, 10.3; FAQ 9.1}

It is *extremely likely* that human activities caused more than half of the observed increase in global average surface temperature from 1951 to 2010. This assessment is supported by robust evidence from multiple studies using different methods. In particular, the temperature trend attributable to all anthropogenic forcings combined can be more closely constrained in multi-signal detection and attribution analyses. Uncertainties in forcings and in climate models' responses to those forcings, together with difficulty in distinguishing the patterns of temperature response due to WMGHGs and other anthropogenic forcings, prevent as precise a quantification of the temperature changes attributable to

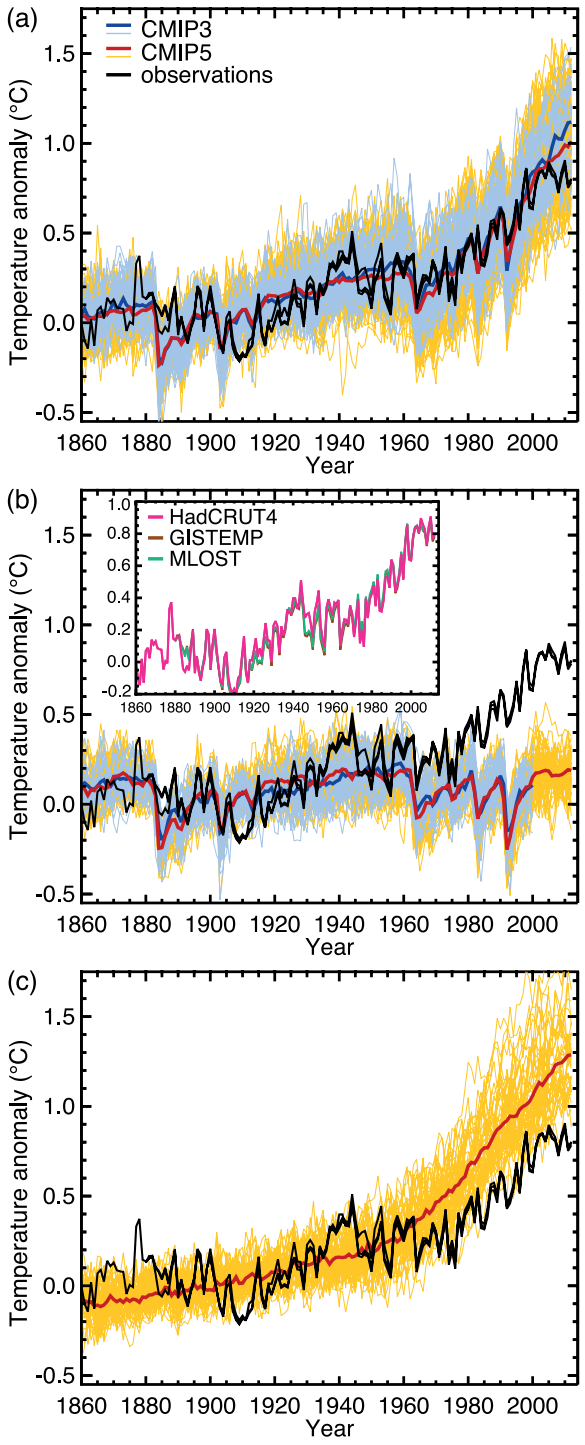

Figure TS.9 | Three observational estimates of global mean surface temperature (black lines) from the Hadley Centre/Climatic Research Unit gridded surface temperature data set 4 (HadCRUT4), Goddard Institute for Space Studies Surface Temperature Analysis (GISTEMP), and Merged Land–Ocean Surface Temperature Analysis (MLOST), compared to model simulations (CMIP3 models— thin blue lines and CMIP5 models—thin yellow lines) with anthropogenic and natural forcings (a), natural forcings only (b) and greenhouse gas forcing only (c). Thick red and blue lines are averages across all available CMIP5 and CMIP3 simulations respectively. All simulated and observed data were masked using the HadCRUT4 coverage (as this data set has the most restricted spatial coverage), and global average anomalies are shown with respect to 1880–1919, where all data are first calculated as anomalies relative to 1961–1990 in each grid box. Inset to (b) shows the three observational data sets distinguished by different colours. {Figure 10.1}

Box TS.3 | Climate Models and the Hiatus in Global Mean Surface Warming of the Past 15 Years

The observed GMST has shown a much smaller increasing linear trend over the past 15 years than over the past 30 to 60 years (Box TS.3, Figure 1a, c). Depending on the observational data set, the GMST trend over 1998–2012 is estimated to be around one third to one half of the trend over 1951–2012. For example, in HadCRUT4 the trend is 0.04°C per decade over 1998–2012, compared to 0.11°C per decade over 1951–2012. The reduction in observed GMST trend is most marked in NH winter. Even with this 'hiatus' in GMST trend, the decade of the 2000s has been the warmest in the instrumental record of GMST. Nevertheless, the occurrence of the hiatus in GMST trend during the past 15 years raises the two related questions of what has caused it and whether climate models are able to reproduce it. {2.4.3, 9.4.1; Box 9.2; Table 2.7}

Fifteen-year-long hiatus periods are common in both the observed and CMIP5 historical GMST time series. However, an analysis of the full suite of CMIP5 historical simulations (augmented for the period 2006–2012 by RCP4.5 simulations) reveals that 111 out of 114 realizations show a GMST trend over 1998–2012 that is higher than the entire HadCRUT4 trend ensemble (Box TS.3, Figure 1a; CMIP5 ensemble mean trend is 0.21°C per decade). This difference between simulated and observed trends could be caused by some combination of (a) internal climate variability, (b) missing or incorrect RF, and (c) model response error. These potential sources of the difference, which are not mutually exclusive, are assessed below, as is the cause of the observed GMST trend hiatus. {2.4.3, 9.3.2, 9.4.1; Box 9.2}

Internal Climate Variability

Hiatus periods of 10 to 15 years can arise as a manifestation of internal decadal climate variability, which sometimes enhances and sometimes counteracts the long-term externally forced trend. Internal variability thus diminishes the relevance of trends over periods as short as 10 to 15 years for long-term climate change. Furthermore, the timing of internal decadal climate variability is not expected to be matched by the CMIP5 historical simulations, owing to the predictability horizon of at most 10 to 20 years (CMIP5 historical simulations are typically started around nominally 1850 from a control run). However, climate models exhibit individual decades of GMST trend hiatus even during a prolonged phase of energy uptake of the climate system, in which case the energy budget would be balanced by increasing subsurface–ocean heat uptake. {2.4.3, 9.3.2, 11.2.2; Boxes 2.2, 9.2}

Owing to sampling limitations, it is uncertain whether an increase in the rate of subsurface–ocean heat uptake occurred during the past 15 years. However, it is *very likely* that the climate system, including the ocean below 700 m depth, has continued to accumulate energy over the period 1998–2010. Consistent with this energy accumulation, GMSL has continued to rise during 1998–2012, at a rate only slightly and insignificantly lower than during 1993–2012. The consistency between observed heat content and sea level changes yields *high confidence* in the assessment of continued ocean energy accumulation, which is in turn consistent with the positive radiative imbalance of the climate system. By contrast, there is limited evidence that the hiatus in GMST trend has been accompanied by a slower rate of increase in ocean heat content over the depth range 0 to 700 m, when comparing the period 2003–2010 against 1971–2010. There is low agreement on this slowdown, as three of five analyses show a slowdown in the rate of increase while the other two show the increase continuing unabated. {3.2.3, 3.2.4, 3.7, 8.5.1, 13.3; Boxes 3.1, 13.1}

During the 15-year period beginning in 1998, the ensemble of HadCRUT4 GMST trends lies below almost all model-simulated trends (Box TS.3, Figure 1a), whereas during the 15-year period ending in 1998, it lies above 93 out of 114 modelled trends (Box TS.3, Figure 1b; HadCRUT4 ensemble mean trend 0.26°C per decade, CMIP5 ensemble mean trend 0.16°C per decade). Over the 62-year period 1951–2012, observed and CMIP5 ensemble mean trend agree to within 0.02°C per decade (Box TS.3, Figure 1c; CMIP5 ensemble mean trend 0.13°C per decade). There is hence *very high confidence* that the CMIP5 models show long-term GMST trends consistent with observations, despite the disagreement over the most recent 15-year period. Due to internal climate variability, in any given 15-year period the observed GMST trend sometimes lies near one end of a model ensemble, an effect that is pronounced in Box TS.3, Figure 1a, b as GMST was influenced by a very strong El Niño event in 1998. {Box 9.2}

Unlike the CMIP5 historical simulations referred to above, some CMIP5 predictions were initialized from the observed climate state during the late 1990s and the early 21st century. There is medium evidence that these initialized predictions show a GMST lower by about 0.05°C to 0.1°C compared to the historical (uninitialized) simulations and maintain this lower GMST during the first few years of the simulation. In some initialized models this lower GMST occurs in part because they correctly simulate a shift, around 2000, from a positive to a negative phase of the Inter-decadal Pacific Oscillation (IPO). However, the improvement of this phasing of the IPO through initialization is not universal across the CMIP5 predictions. Moreover, although part of the GMST reduction through initialization indeed results from initializing at the correct phase of internal variability, another part may result from correcting a model bias that was caused by incorrect past forcing or incorrect model response to past forcing, especially in the ocean. The relative magnitudes of these effects are at present unknown; moreover, the quality of a forecasting system cannot be evaluated from a single prediction (here, a 10-year prediction within

(continued on next page)

Box TS.3 (continued)

the period 1998–2012). Overall, there is *medium confidence* that initialization leads to simulations of GMST during 1998–2012 that are more consistent with the observed trend hiatus than are the uninitialized CMIP5 historical simulations, and that the hiatus is in part a consequence of internal variability that is predictable on the multi-year time scale. {11.1, 11.2.3; Boxes 2.5, 9.2, 11.1, 11.2}

Radiative Forcing

On decadal to interdecadal time scales and under continually increasing ERF, the forced component of the GMST trend responds to the ERF trend relatively rapidly and almost linearly (*medium confidence*). The expected forced-response GMST trend is related to the ERF trend by a factor that has been estimated for the 1% per year CO_2 increases in the CMIP5 ensemble as 2.0 [1.3 to 2.7] W m^{-2} °C^{-1} (90% uncertainty range). Hence, an ERF trend can be approximately converted to a forced-response GMST trend, permitting an assessment of how much of the change in the GMST trends shown in Box TS.3, Figure 1 is due to a change in ERF trend. {Box 9.2}

The AR5 best-estimate ERF trend over 1998–2011 is 0.22 [0.10 to 0.34] W m^{-2} per decade (90% uncertainty range), which is substantially lower than the trend over 1984–1998 (0.32 [0.22 to 0.42] W m^{-2} per decade; note that there was a strong volcanic eruption in 1982) and the trend over 1951–2011 (0.31 [0.19 to 0.40] W m^{-2} per decade; Box TS.3, Figure 1d–f; the end year 2011 is chosen because data availability is more limited than for GMST). The resulting forced-response GMST trend would approximately be 0.12 [0.05 to 0.29] °C per decade, 0.19 [0.09 to 0.39] °C per decade, and 0.18 [0.08 to 0.37] °C per decade for the periods 1998–2011, 1984–1998, and 1951–2011, respectively (the uncertainty ranges assume that the range of the conversion factor to GMST trend and the range of ERF trend itself are independent). The AR5 best-estimate ERF forcing trend difference between 1998–2011 and 1951–2011 thus might explain about one-half (0.05 °C per decade) of the observed GMST trend difference between these periods (0.06 to 0.08 °C per decade, depending on observational data set). {8.5.2}

The reduction in AR5 best-estimate ERF trend over 1998–2011 compared to both 1984–1998 and 1951–2011 is mostly due to decreasing trends in the natural forcings, –0.16 [–0.27 to –0.06] W m^{-2} per decade over 1998–2011 compared to 0.01 [–0.00 to +0.01] W m^{-2} per decade over 1951–2011. Solar forcing went from a relative maximum in 2000 to a relative minimum in 2009, with a peak-to-peak difference of around 0.15 W m^{-2} and a linear trend over 1998–2011 of around –0.10 W m^{-2} per decade. Furthermore, a series of small volcanic eruptions has increased the observed stratospheric aerosol loading after 2000, leading to an additional negative ERF linear-trend contribution of around –0.06 W m^{-2} per decade over 1998–2011 (Box TS.3, Figure 1d, f). By contrast, satellite-derived estimates of tropospheric aerosol optical depth suggests little overall trend in global mean aerosol optical depth over the last 10 years, implying little change in ERF due to aerosol–radiative interaction (*low confidence* because of *low confidence* in aerosol optical depth trend itself). Moreover, because there is only *low confidence* in estimates of ERF due to aerosol–cloud interaction, there is likewise *low confidence* in its trend over the last 15 years. {2.2.3, 8.4.2, 8.5.1, 8.5.2, 10.3.1; Box 10.2; Table 8.5}

For the periods 1984–1998 and 1951–2011, the CMIP5 ensemble mean ERF trend deviates from the AR5 best-estimate ERF trend by only 0.01 W m^{-2} per decade (Box TS.3, Figure 1e, f). After 1998, however, some contributions to a decreasing ERF trend are missing in the CMIP5 models, such as the increasing stratospheric aerosol loading after 2000 and the unusually low solar minimum in 2009. Nonetheless, over 1998–2011 the CMIP5 ensemble mean ERF trend is lower than the AR5 best-estimate ERF trend by 0.03 W m^{-2} per decade (Box TS.3, Figure 1d). Furthermore, global mean aerosol optical depth in the CMIP5 models shows little trend over 1998–2012, similar to the observations. Although the forcing uncertainties are substantial, there are no apparent incorrect or missing global mean forcings in the CMIP5 models over the last 15 years that could explain the model–observations difference during the warming hiatus. {9.4.6}

Model Response Error

The discrepancy between simulated and observed GMST trends during 1998–2012 could be explained in part by a tendency for some CMIP5 models to simulate stronger warming in response to increases in greenhouse-gas concentration than is consistent with observations. Averaged over the ensembles of models assessed in Section 10.3.1, the best-estimate GHG and other anthropogenic scaling factors are less than one (though not significantly so, Figure 10.4), indicating that the model-mean GHG and other anthropogenic responses should be scaled down to best match observations. This finding provides evidence that some CMIP5 models show a larger response to GHGs and other anthropogenic factors (dominated by the effects of aerosols) than the real world (*medium confidence*). As a consequence, it is argued in Chapter 11 that near-term model projections of GMST increase should be scaled down by about 10%. This downward scaling is, however, not sufficient to explain the model mean overestimate of GMST trend over the hiatus period. {10.3.1, 11.3.6}

Another possible source of model error is the poor representation of water vapour in the upper atmosphere. It has been suggested that a reduction in stratospheric water vapour after 2000 caused a reduction in downward longwave radiation and hence a surface-cooling contribution, possibly missed by the models. However, this effect is assessed here to be small, because there was a recovery in stratospheric water vapour after 2005. {2.2.2, 9.4.1; Box 9.2} *(continued on next page)*

Box TS.3 (continued)

In summary, the observed recent warming hiatus, defined as the reduction in GMST trend during 1998–2012 as compared to the trend during 1951–2012, is attributable in roughly equal measure to a cooling contribution from internal variability and a reduced trend in external forcing (expert judgement, *medium confidence*). The forcing trend reduction is due primarily to a negative forcing trend from both volcanic eruptions and the downward phase of the solar cycle. However, there is *low confidence* in quantifying the role of forcing trend in causing the hiatus, because of uncertainty in the magnitude of the volcanic forcing trend and *low confidence* in the aerosol forcing trend. {Box 9.2}

Almost all CMIP5 historical simulations do not reproduce the observed recent warming hiatus. There is *medium confidence* that the GMST trend difference between models and observations during 1998–2012 is to a substantial degree caused by internal variability, with possible contributions from forcing error and some CMIP5 models overestimating the response to increasing GHG forcing. The CMIP5 model trend in ERF shows no apparent bias against the AR5 best estimate over 1998–2012. However, *confidence* in this assessment of CMIP5 ERF trend is *low*, primarily because of the uncertainties in model aerosol forcing and processes, which through spatial heterogeneity might well cause an undetected global mean ERF trend error even in the absence of a trend in the global mean aerosol loading. {Box 9.2}

The causes of both the observed GMST trend hiatus and of the model–observation GMST trend difference during 1998–2012 imply that, barring a major volcanic eruption, most 15-year GMST trends in the near-term future will be larger than during 1998–2012 (*high confidence*; see Section 11.3.6 for a full assessment of near-term projections of GMST). The reasons for this implication are fourfold: first, anthropogenic GHG concentrations are expected to rise further in all RCP scenarios; second, anthropogenic aerosol concentration is expected to decline in all RCP scenarios, and so is the resulting cooling effect; third, the trend in solar forcing is expected to be larger over most near-term 15-year periods than over 1998–2012 (*medium confidence*), because 1998–2012 contained the full downward phase of the solar cycle; and fourth, it is *more likely than not* that internal climate variability in the near term will enhance and not counteract the surface warming expected to arise from the increasing anthropogenic forcing. {Box 9.2}

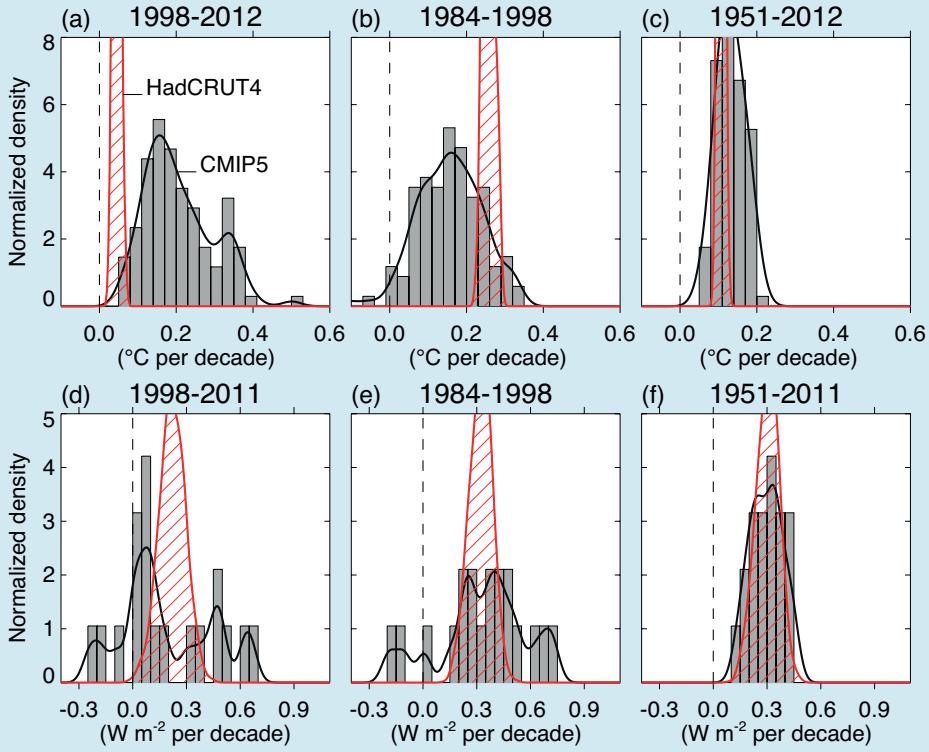

Box TS.3, Figure 1 | (Top) Observed and simulated GMST trends in °C per decade, over the periods 1998–2012 (a), 1984–1998 (b), and 1951–2012 (c). For the observations, 100 realizations of the Hadley Centre/Climatic Research Unit gridded surface temperature data set 4 (HadCRUT4) ensemble are shown (red, hatched). The uncertainty displayed by the ensemble width is that of the statistical construction of the global average only, in contrast to the trend uncertainties quoted in Section 2.4.3, which include an estimate of internal climate variability. Here, by contrast, internal variability is characterized through the width of the model ensemble. For the models, all 114 available CMIP5 historical realizations are shown, extended after 2005 with the RCP4.5 scenario and through 2012 (grey, shaded). (Bottom) Trends in effective radiative forcing (ERF, in W m^{-2} per decade) over the periods 1998–2011 (d), 1984–1998 (e), and 1951–2011 (f). The figure shows AR5 best-estimate ERF trends (red, hatched) and CMIP5 ERF (grey, shaded). Black lines are smoothed versions of the histograms. Each histogram is normalized so that its area sums up to one. {2.4.3, 8.5.2; Box 9.2; Figure 8.18; Box 9.2, Figure 1}

Thematic Focus Elements

TFE.3 | Comparing Projections from Previous IPCC Assessments with Observations

Verification of projections is arguably the most convincing way of establishing the credibility of climate change science. Results of projected changes in carbon dioxide (CO_2), global mean surface temperature (GMST) and global mean sea level (GMSL) from previous IPCC assessment reports are quantitatively compared with the best available observational estimates. The comparison between the four previous reports highlights the evolution in our understanding of how the climate system responds to changes in both natural and anthropogenic forcing and provides an assessment of how the projections compare with observational estimates. TFE.3, Figure 1, for example, shows the projected and observed estimates of: (1) CO_2 changes (top row), (2) GMST anomaly relative to 1961–1990 (middle row) and (3) GMSL relative to 1961–1990 (bottom row). Results from previous assessment reports are in the left-hand column, and for completeness results from current assessment are given in the right-hand column. {2.4, 3.7, 6.3, 11.3, 13.3} *(continued on next page)*

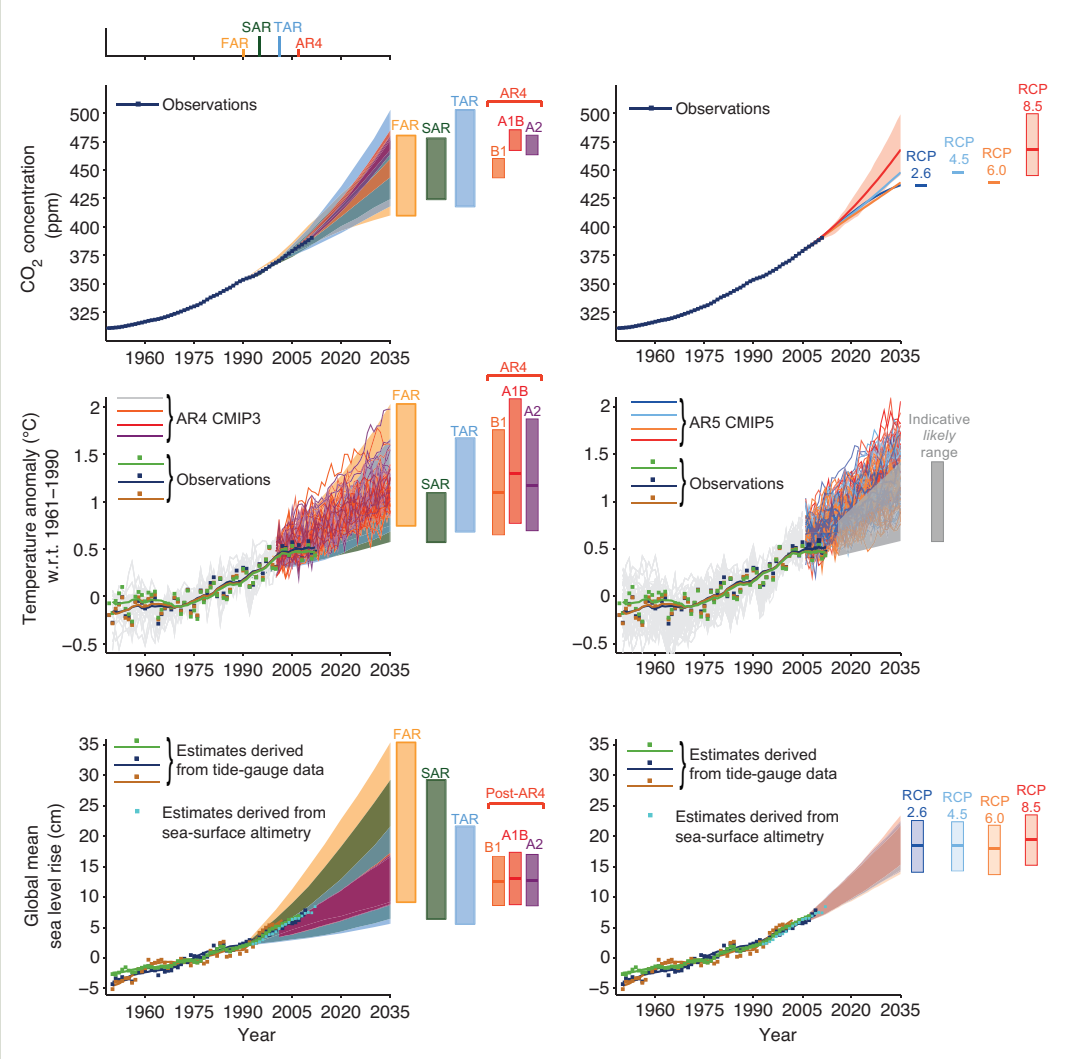

TFE.3, Figure 1 | (Top left) Observed globally and annually averaged CO_2 concentrations in parts per million (ppm) since 1950 compared with projections from the previous IPCC assessments. Observed global annual CO_2 concentrations are shown in dark blue. The shading shows the largest model projected range of global annual CO_2 concentrations from 1950 to 2035 from FAR (First Assessment Report; Figure A.3 in the Summary for Policymakers (SPM) of IPCC 1990), SAR (Second Assessment Report; Figure 5b in the TS of IPCC 1996), TAR (Third Assessment Report; Appendix II of IPCC 2001), and for the IPCC Special Report on Emission Scenarios (SRES) A2, A1B and B1 scenarios presented in the AR4 (Fourth Assessment Report; Figure 10.26). The publication years of the assessment reports are shown. (Top right) Same observed globally averaged CO_2 concentrations and the projections from this report. Only RCP8.5 has a range of values because the emission-driven senarios were carried out only for this RCP. For the other RCPs the best estimate is given. (Middle left) Estimated changes in the observed globally and annually averaged surface temperature anomaly relative to 1961–1990 (in °C) since 1950 compared with the range of projections from the previous IPCC assessments. Values are harmonized

TFE.3 (continued)

to start from the same value at 1990. Observed global annual temperature anomaly, relative to 1961–1990, from three data sets is shown as squares and smoothed time series as solid lines from the Hadley Centre/Climatic Research Unit gridded surface temperature data set 4 (HadCRUT4; bright green), Merged Land–Ocean Surface Temperature Analysis (MLOST; warm mustard) and Goddard Institute for Space Studies Surface Temperature Analysis (GISTEMP; dark blue) data sets. The coloured shading shows the projected range of global annual mean near surface temperature change from 1990 to 2035 for models used in FAR (Figure 6.11), SAR (Figure 19 in the TS of IPCC 1996), TAR (full range of TAR, Figure 9.13(b)). TAR results are based on the simple climate model analyses presented in this assessment and not on the individual full three-dimensional climate model simulations. For the AR4 results are presented as single model runs of the CMIP3 ensemble for the historical period from 1950 to 2000 (light grey lines) and for three SRES scenarios (A2, A1B and B1) from 2001 to 2035. For the three SRES scenarios the bars show the CMIP3 ensemble mean and the *likely* range given by –40 % to +60% of the mean as assessed in Chapter 10 of AR4. (Middle right) Projections of annual mean global mean surface air temperature (GMST) for 1950–2035 (anomalies relative to 1961–1990) under different RCPs from CMIP5 models (light grey and coloured lines, one ensemble member per model), and observational estimates the same as the middle left panel. The grey shaded region shows the indicative *likely* range for annual mean GMST during the period 2016–2035 for all RCPs (see Figure TS.14 for more details). The grey bar shows this same indicative *likely* range for the year 2035. (Bottom left) Estimated changes in the observed global annual mean sea level (GMSL) since 1950. Different estimates of changes in global annual sea level anomalies from tide gauge data (dark blue, warm mustard, dark green) and based on annual averages of altimeter data (light blue) starting in 1993 (the values have been aligned to fit the 1993 value of the tide gauge data). Squares indicate annual mean values, solid lines smoothed values. The shading shows the largest model projected range of global annual sea level rise from 1950 to 2035 for FAR (Figures 9.6 and 9.7), SAR (Figure 21 in TS of IPCC, 1996), TAR (Appendix II of IPCC, 2001) and based on the CMIP3 model results available at the time of AR4 using the SRES A1B scenario. Note that in the AR4 no full range was given for the sea level projections for this period. Therefore, the figure shows results that have been published subsequent to the AR4. The bars at the right hand side of each graph show the full range given for 2035 for each assessment report. (Bottom right) Same observational estimate as bottom left. The bars are the *likely* ranges (*medium confidence*) for global mean sea level rise at 2035 with respect to 1961–1990 following the four RCPs. Appendix 1.A provides details on the data and calculations used to create these figures. See Chapters 1, 11 and 13 for more details. {Figures 1.4, 1.5, 1.10, 11.9, 11.19, 11.25, 13.11}

Carbon Dioxide Changes

From 1950 to 2011 the observed concentrations of atmospheric CO_2 have steadily increased. Considering the period 1990–2011, the observed CO_2 concentration changes lie within the envelope of the scenarios used in the four assessment reports. As the most recent assessment prior to the current, the IPCC Fourth Assessment Report (AR4) (TFE.3.Figure 1; top left) has the narrowest scenario range and the observed concentration follows this range. The results from the IPCC Fifth Assessment Report (AR5) (TFE.3, Figure 1; top right) are consistent with AR4, and during 2002–2011, atmospheric CO_2 concentrations increased at a rate of 1.9 to 2.1 ppm yr^{-1}. {2.2.1, 6.3; Table 6.1}

Global Mean Temperature Anomaly

Relative to the 1961–1990 mean, the GMST anomaly has been positive and larger than 0.25°C since 2001. Observations are generally well within the range of the extent of the earlier IPCC projections (TFE.3, Figure1, middle left) This is also true for the Coupled Model Intercomparison Project Phase 5 (CMIP5) results (TFE.3, Figure 1; middle right) in the sense that the observed record lies within the range of the model projections, but on the lower end of the plume. Mt Pinatubo erupted in 1991 (see FAQ 11.2 for discussion of how volcanoes impact the climate system), leading to a brief period of relative global mean cooling during the early 1990s. The IPCC First, Second and Third Assessment Reports (FAR, SAR and TAR) did not include the effects of volcanic eruptions and thus failed to include the cooling associated with the Pinatubo eruption. AR4 and AR5, however, did include the effects from volcanoes and did simulate successfully the associated cooling. During 1995–2000 the global mean temperature anomaly was quite variable—a significant fraction of this variability was due to the large El Niño in 1997–1998 and the strong back-to-back La Niñas in 1999–2001. The projections associated with these assessment reports do not attempt to capture the actual evolution of these El Niño and La Niña events, but include them as a source of uncertainty due to natural variability as encompassed by, for example, the range given by the individual CMIP3 and CMIP5 simulations and projection (TFE.3, Figure 1). The grey wedge in TFE.3, Figure 1 (middle right) corresponds to the indicative *likely* range for annual temperatures, which is determined from the Representative Concentration Pathways (RCPs) assessed value for the 20-year mean 2016–2035 (see discussion of Figure TS.14 and Section 11.3.6 for details). From 1998 to 2012 the observational estimates have largely been on the low end of the range given by the scenarios alone in previous assessment reports and CMIP3 and CMIP5 projections. {2.4; Box 9.2}

Global Mean Sea Level

Based on both tide gauge and satellite altimetry data, relative to 1961–1990, the GMSL has continued to rise. While the increase is fairly steady, both observational records show short periods of either no change or a slight decrease. The observed estimates lie within the envelope of all the projections except perhaps in the very early 1990s. The sea level rise uncertainty due to scenario-related uncertainty is smallest for the most recent assessments (AR4 and AR5) and observed estimates lie well within this scenario-related uncertainty. It is *virtually certain* that over the 20th century sea level rose. The mean rate of sea level increase was 1.7 mm yr^{-1} with a *very likely* range between 1.5 to 1.9 between 1901 and 2010 and this rate increased to 3.2 with a *likely* range of 2.8 to 3.6 mm yr^{-1} between 1993 and 2010 (see TFE.2). {3.7.2, 3.7.4}

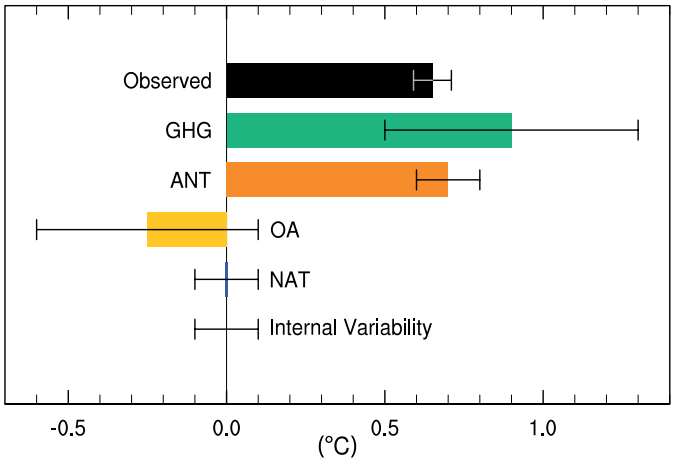

Figure TS.10 | Assessed *likely* ranges (whiskers) and their midpoints (bars) for warming trends over the 1951–2010 period due to well-mixed greenhouse gases (GHG), anthropogenic forcings (ANT) anthropogenic forcings other than well-mixed greenhouse gases (OA), natural forcings (NAT) and internal variability. The trend in the Hadley Centre/Climatic Research Unit gridded surface temperature data set 4 (HadCRUT4) observations is shown in black with its 5 to 95% uncertainty range due only to observational uncertainty in this record. {Figure 10.5}

WMGHGs and other anthropogenic forcings individually. Consistent with AR4, it is assessed that more than half of the observed increase in global average surface temperature from 1951 to 2010 is *very likely* due to the observed anthropogenic increase in WMGHG concentrations. WMGHGs contributed a global mean surface warming *likely* to be between 0.5°C and 1.3°C over the period between 1951 and 2010, with the contributions from other anthropogenic forcings *likely* to be between –0.6°C and 0.1°C and from natural forcings *likely* to be between –0.1°C and 0.1°C. Together these assessed contributions are consistent with the observed warming of approximately 0.6°C over this period (Figure TS.10). {10.3}

Solar forcing is the only known natural forcing acting to warm the climate over the 1951–2010 period but it has increased much less than WMGHG forcing, and the observed pattern of long-term tropospheric warming and stratospheric cooling is not consistent with the expected response to solar irradiance variations. Considering this evidence together with the assessed contribution of natural forcings to observed trends over this period, it is assessed that the contribution from solar forcing to the observed global warming since 1951 is *extremely unlikely* to be larger than that from WMGHGs. Because solar forcing has *very likely* decreased over a period with direct satellite measurements of solar output from 1986 to 2008, there is *high confidence* that changes in total solar irradiance have not contributed to global warming during that period. However, there is *medium confidence* that the 11-year cycle of solar variability influences decadal climate fluctuations in some regions through amplifying mechanisms. {8.4, 10.3; Box 10.2}

Observed warming over the past 60 years is far outside the range of internal climate variability estimated from pre-instrumental data, and it is also far outside the range of internal variability simulated in climate models. Model-based simulations of internal variability are assessed to be adequate to make this assessment. Further, the spatial pattern of observed warming differs from those associated with internal variability. Based on this evidence, the contribution of internal variability to the 1951–2010 GMST trend was assessed to be *likely* between –0.1°C and 0.1°C, and it is *virtually certain* that warming since 1951 cannot be explained by internal variability alone. {9.5, 10.3, 10.7}

The instrumental record shows a pronounced warming during the first half of the 20th century. Consistent with AR4, it is assessed that the early 20th century warming is *very unlikely* to be due to internal variability alone. It remains difficult to quantify the contributions to this early century warming from internal variability, natural forcing and anthropogenic forcing, due to forcing and response uncertainties and incomplete observational coverage. {10.3}

TS.4.3 Atmospheric Temperature

A number of studies since the AR4 have investigated the consistency of simulated and observed trends in free tropospheric temperatures (see section TS.2). Most, though not all, CMIP3 and CMIP5 models overestimate the observed warming trend in the tropical troposphere during the satellite period 1979–2012. Roughly one half to two thirds of this difference from the observed trend is due to an overestimate of the SST trend, which is propagated upward because models attempt to maintain static stability. There is *low confidence* in these assessments, however, owing to the *low confidence* in observed tropical tropospheric trend rates and vertical structure. Outside the tropics, and over the period of the radiosonde record beginning in 1961, the discrepancy between simulated and observed trends is smaller. {2.4.4, 9.4, 10.3}

Analysis of both radiosonde and satellite data sets, combined with CMIP5 and CMIP3 simulations, continues to find that observed tropospheric warming is inconsistent with internal variability and simulations of the response to natural forcings alone. Over the period 1961–2010 CMIP5 models simulate tropospheric warming driven by WMGHG changes, with only a small offsetting cooling due to the combined effects of changes in reflecting and absorbing aerosols and tropospheric ozone. Taking this evidence together with the results of multi-signal detection and attribution analyses, it is *likely* that anthropogenic forcings, dominated by WMGHGs, have contributed to the warming of the troposphere since 1961. Uncertainties in radiosonde and satellite records makes assessment of causes of observed trends in the upper troposphere less confident than an assessment of the overall atmospheric temperature changes. {2.4.4, 9.4, 10.3}

CMIP5 simulations including WMGHGs, ozone and natural forcing changes broadly reproduce the observed evolution of lower stratospheric temperature, with some tendency to underestimate the observed cooling trend over the satellite era (see Section TS.2). New studies of stratospheric temperature, considering the responses to natural forcings, WMGHGs and ozone-depleting substances, demonstrate that it is *very likely* that anthropogenic forcings, dominated by the depletion of the ozone layer due to ozone depleting substances have contributed to the cooling of the lower stratosphere since 1979. CMIP5 models simulate only a very weak cooling of the lower stratosphere in response to historical WMGHG changes, and the influence of WMGHGs on lower stratospheric temperature has not been formally detected. Considering both regions together, it is *very likely* that anthropogenic

Thematic Focus Elements

TFE.4 | The Changing Energy Budget of the Global Climate System

The global energy budget is a fundamental aspect of the Earth's climate system and depends on many phenomena within it. The ocean has stored about 93% of the increase in energy in the climate system over recent decades, resulting in ocean thermal expansion and hence sea level rise. The rate of storage of energy in the Earth system must be equal to the net downward radiative flux at the top of the atmosphere, which is the difference between effective radiative forcing (ERF) due to changes imposed on the system and the radiative response of the system. There are also significant transfers of energy between components of the climate system and from one location to another. The focus here is on the Earth's global energy budget since 1970, when better global observational data coverage is available. {3.7, 9.4, 13.4; Box 3.1}

The ERF of the climate system has been positive as a result of increases in well-mixed (long-lived) greenhouse gas (GHG) concentrations, changes in short-lived GHGs (tropospheric and stratospheric ozone and stratospheric water vapour), and an increase in solar irradiance (TFE.4, Figure 1a). This has been partly compensated by a negative contribution to the ERF of the climate system as a result of changes in tropospheric aerosol, which predominantly reflect sunlight and furthermore enhance the brightness of clouds, although black carbon produces positive forcing. Explosive volcanic eruptions (such as El Chichón in Mexico in 1982 and Mt Pinatubo in the Philippines in 1991)

(continued on next page)

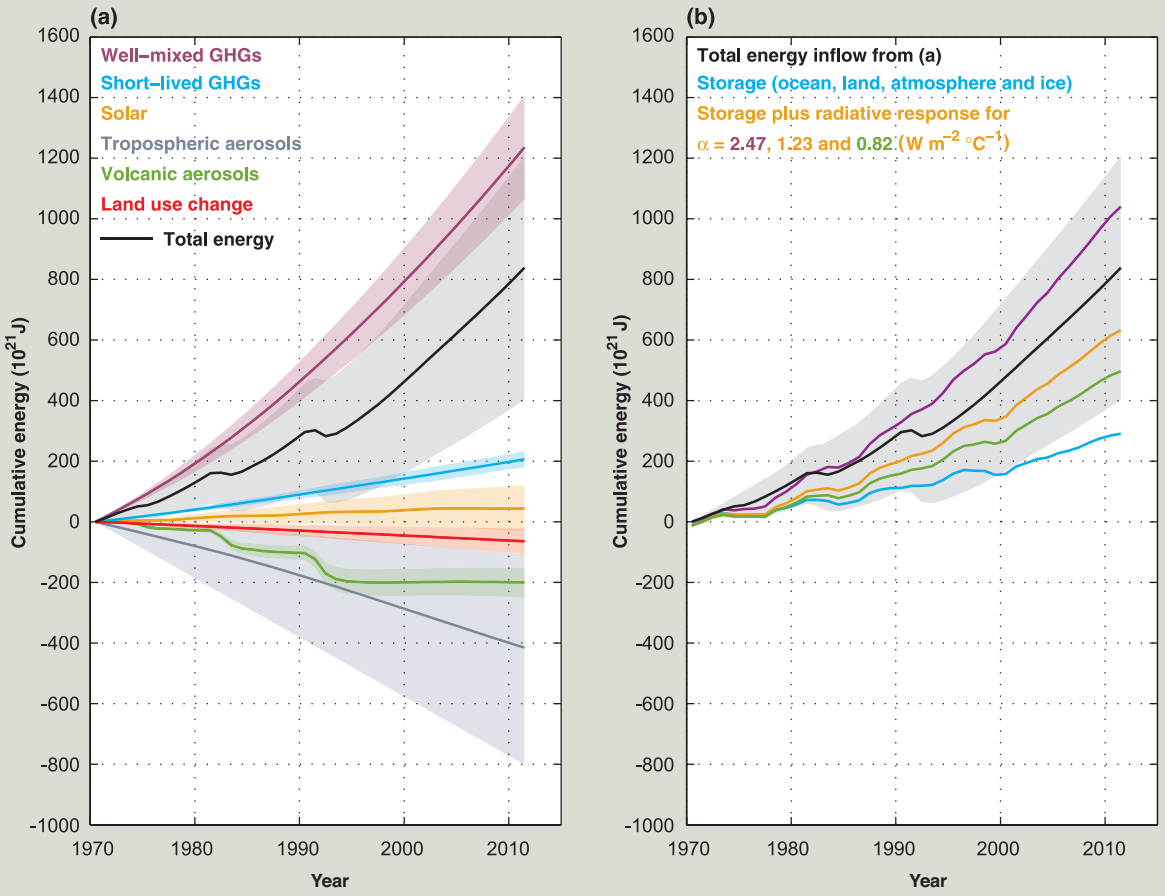

TFE.4, Figure 1 | The Earth's energy budget from 1970 through 2011. (a) The cumulative energy inflow into the Earth system from changes in well-mixed and short-lived greenhouse gases, solar forcing, tropospheric aerosol forcing, volcanic forcing and changes in surface albedo due to land use change (all relative to 1860–1879) are shown by the coloured lines; these contributions are added to give the total energy inflow (black; contributions from black carbon on snow and contrails as well as contrail-induced cirrus are included but not shown separately). (b) The cumulative total energy inflow from (a, black) is balanced by the sum of the energy uptake of the Earth system (blue; energy absorbed in warming the ocean, the atmosphere and the land, as well as in the melting of ice) and an increase in outgoing radiation inferred from changes in the global mean surface temperature. The sum of these two terms is given for a climate feedback parameter α of 2.47, 1.23 and 0.82 W m^{-2} °C^{-1}, corresponding to an equilibrium climate sensitivity of 1.5°C, 3.0°C and 4.5°C, respectively; 1.5°C to 4.5°C is assessed to be the *likely* range of equilibrium climate sensitivity. The energy budget would be closed for a particular value of α if the corresponding line coincided with the total energy inflow. For clarity, all uncertainties (shading) shown are *likely* ranges. {Box 12.2; Box 13.1, Figure 1}

TFE.4 (continued)

can inject sulphur dioxide into the stratosphere, giving rise to stratospheric aerosol, which persists for several years. Stratospheric aerosol reflects some of the incoming solar radiation and thus gives a negative forcing. Changes in surface albedo from land use change have also led to a greater reflection of shortwave radiation back to space and hence a negative forcing. Since 1970, the net ERF of the climate system has increased, and the integrated impact of these forcings is an energy inflow over this period (TFE.4, Figure 1a). {2.3, 8.5; Box 13.1}

As the climate system warms, energy is lost to space through increased outgoing radiation. This radiative response by the system is due predominantly to increased thermal radiation, but it is modified by climate feedbacks such as changes in water vapour, clouds and surface albedo, which affect both outgoing longwave and reflected shortwave radiation. The top of the atmosphere fluxes have been measured by the Earth Radiation Budget Experiment (ERBE) satellites from 1985 to 1999 and the Cloud and the Earth's Radiant Energy System (CERES) satellites from March 2000 to the present. The top of the atmosphere radiative flux measurements are highly precise, allowing identification of changes in the Earth's net energy budget from year to year within the ERBE and CERES missions, but the absolute calibration of the instruments is not sufficiently accurate to allow determination of the absolute top of the atmosphere energy flux or to provide continuity across missions. TFE.4, Figure 1b relates the cumulative total energy change of the Earth system to the change in energy storage and the cumulative outgoing radiation. Calculation of the latter is based on the observed global mean surface temperature multiplied by the climate feedback parameter α, which in turn is related to the equilibrium climate sensitivity. The mid-range value for α, 1.23 W m^{-2} °C^{-1}, corresponds to an ERF for a doubled carbon dioxide (CO_2) concentration of 3.7 [2.96 to 4.44] W m^{-2} combined with an equilibrium climate sensitivity of 3.0°C. The climate feedback parameter α is *likely* to be in the range from 0.82 to 2.47 W m^{-2} °C^{-1} (corresponding to the *likely* range in equilibrium climate sensitivity of 1.5°C to 4.5°C). {9.7.1; Box 12.2}

If ERF were fixed, the climate system would eventually warm sufficiently that the radiative response would balance the ERF, and there would be no further change in energy storage in the climate system. However, the forcing is increasing, and the ocean's large heat capacity means that the climate system is not in radiative equilibrium and its energy content is increasing (TFE.4, Figure 1b). This storage provides strong evidence of a changing climate. The majority of this additional heat is in the upper 700 m of the ocean, but there is also warming in the deep and abyssal ocean. The associated thermal expansion of the ocean has contributed about 40% of the observed sea level rise since 1970. A small amount of additional heat has been used to warm the continents, warm and melt glacial and sea ice and warm the atmosphere. {13.4.2; Boxes 3.1, 13.1}

In addition to these forced variations in the Earth's energy budget, there is also internal variability on decadal time scales. Observations and models indicate that, because of the comparatively small heat capacity of the atmosphere, a decade of steady or even decreasing surface temperature can occur in a warming world. Climate model simulations suggest that these periods are associated with a transfer of heat from the upper to the deeper ocean, of the order 0.1 W m^{-2}, with a near-steady or an increased radiation to space, again of the order 0.1 W m^{-2}. Although these natural fluctuations represent a large amount of heat, they are significantly smaller than the anthropogenic forcing of the Earth's energy budget, particularly on time scales of several decades or longer. {9.4; Boxes 9.2, 13.1}

The available independent estimates of ERF, of observed heat storage, and of surface warming combine to give an energy budget for the Earth that is consistent with the assessed *likely* range of equilibrium climate sensitivity to within estimated uncertainties (*high confidence*). Quantification of the terms in the Earth's energy budget and verification that these terms balance over recent decades provides strong evidence for our understanding of anthropogenic climate change. {Box 13.1}

forcing, particularly WMGHGs and stratospheric ozone depletion, has led to a detectable observed pattern of tropospheric warming and lower stratospheric cooling since 1961. {2.4, 9.4, 10.3}

TS.4.4 Oceans

The observed upper-ocean warming during the late 20th and early 21st centuries and its causes have been assessed more completely since AR4 using updated observations and more simulations (see Section TS.2.2). The long term trends and variability in the observations are most consistent with simulations of the response to both anthropogenic forcing and volcanic forcing. The anthropogenic fingerprint in observed upper-ocean warming, consisting of global mean and basin-scale pattern changes, has also been detected. This result is robust to a number of observational, model and methodological or structural uncertainties. It is *very likely* that anthropogenic forcings have made

a substantial contribution to upper ocean warming (above 700 m) observed since the 1970s. This anthropogenic ocean warming has contributed to global sea level rise over this period through thermal expansion. {3.2.2, 3.2.3, 3.7.2, 10.4.1, 10.4.3; Box 3.1}

Observed surface salinity changes also suggest a change in the global water cycle has occurred (see TFE.1). The long-term trends show that there is a strong positive correlation between the mean climate of the surface salinity and the temporal changes of surface salinity from 1950 to 2000. This correlation shows an enhancement of the climatological salinity pattern—so fresh areas have become fresher and salty areas saltier. The strongest anthropogenic signals are in the tropics (30°S to 30°N) and the Western Pacific. The salinity contrast between the Pacific and Atlantic Oceans has also increased with significant contributions from anthropogenic forcing. {3.3, 10.3.2, 10.4.2; FAQ 3.2}

On a global scale, surface and subsurface salinity changes (1955–2004) over the upper 250 m of the water column do not match changes expected from natural variability but do match the modelled distribution of forced changes (WMGHGs and tropospheric aerosols). Natural external variability taken from the simulations with just the variations in solar and volcanic forcing does not match the observations at all, thus excluding the hypothesis that observed trends can be explained by just solar or volcanic variations. These lines of evidence and our understanding of the physical processes leads to the conclusion that it is *very likely* that anthropogenic forcings have made a discernible contribution to surface and subsurface oceanic salinity changes since the 1960s. {10.4.2; Table 10.1}

Oxygen is an important physical and biological tracer in the ocean. Global analyses of oxygen data from the 1960s to 1990s extend the spatial coverage from local to global scales and have been used in attribution studies with output from a limited range of Earth System Models (ESMs). It is concluded that there is *medium confidence* that the observed global pattern of decrease in dissolved oxygen in the oceans can be attributed in part to human influences. {3.8.3, 10.4.4; Table 10.1}

The observations show distinct trends for ocean acidification (which is observed to be between –0.0014 and –0.0024 pH units per year). There is *high confidence* that the pH of ocean surface seawater decreased by about 0.1 since the beginning of the industrial era as a consequence of the oceanic uptake of anthropogenic CO_2. {3.8.2, 10.4.4; Box 3.2; Table 10.1}

TS.4.5 Cryosphere

The reductions in Arctic sea ice extent and NH snow cover extent and widespread glacier retreat and increased surface melt of Greenland are all evidence of systematic changes in the cryosphere. All of these changes in the cryosphere have been linked to anthropogenic forcings. {4.2.2, 4.4–4.6, 10.5.1, 10.5.3; Table 10.1}

Attribution studies, comparing the seasonal evolution of Arctic sea ice extent from observations from the 1950s with that simulated by coupled model simulations, demonstrate that human influence on the sea ice extent changes can be robustly detected since the early 1990s. The anthropogenic signal is also detectable for individual months from May to December, suggesting that human influence, strongest in late summer, now also extends into colder seasons. From these simulations of sea ice and observed sea ice extent from the instrumental record with high agreement between studies, it is concluded that anthropogenic forcings are *very likely* to have contributed to Arctic sea ice loss since 1979 (Figure TS.12). {10.5.1}

For Antarctic sea ice extent, the shortness of the observed record and differences in simulated and observed variability preclude an assessment of whether or not the observed increase since 1979 is inconsistent with internal variability. Untangling the processes involved with trends and variability in Antarctica and surrounding waters remains complex and several studies are contradictory. In conclusion, there is *low confidence* in the scientific understanding of the observed increase in Antarctic sea ice extent since 1979, due to the large differences between sea ice simulations from CMIP5 models and to the incomplete and competing scientific explanations for the causes of change and *low confidence* in estimates of internal variability (Figure TS.12). {9.4.3, 10.5.1; Table 10.1}

The Greenland ice sheet shows recent major melting episodes in response to record temperatures relative to the 20th century associated with persistent shifts in early summer atmospheric circulation, and these shifts have become more pronounced since 2007. Although many Greenland instrumental records are relatively short (two decades), regional modelling and observations tell a consistent story of the response of Greenland temperatures and ice sheet runoff to shifts in regional atmospheric circulation associated with larger scale flow patterns and global temperature increases. Mass loss and melt is also occurring in Greenland through the intrusion of warm water into the major fjords containing glaciers such as Jacobshaven Glacier. It is *likely* that anthropogenic forcing has contributed to surface melting of the Greenland ice sheet since 1993. {10.5.2; Table 10.1}

Estimates of ice mass in Antarctica since 2000 show that the greatest losses are at the edges. An analysis of observations underneath a floating ice shelf off West Antarctica leads to the conclusion that ocean warming in this region and increased transport of heat by ocean circulation are largely responsible for accelerating melt rates. The observational record of Antarctic mass loss is short and the internal variability of the ice sheet is poorly understood. Due to a low level of scientific understanding there is *low confidence* in attributing the causes of the observed loss of mass from the Antarctic ice sheet since 1993. {3.2, 4.2, 4.4.3, 10.5.2}

The evidence for the retreat of glaciers due to warming and moisture change is now more complete than at the time of AR4. There is *high confidence* in the estimates of observed mass loss and the estimates of natural variations and internal variability from long-term glacier records. Based on these factors and our understanding of glacier response to climatic drivers there is *high confidence* that a substantial part of the mass loss of glaciers is *likely* due to human influence. It is *likely* that there has been an anthropogenic component to observed reductions in NH snow cover since 1970. {4.3.3, 10.5.2, 10.5.3; Table 10.1}

Thematic Focus Elements

TFE.5 | Irreversibility and Abrupt Change

A number of components or phenomena within the climate system have been proposed as potentially exhibiting threshold behaviour. Crossing such thresholds can lead to an abrupt or irreversible transition into a different state of the climate system or some of its components.

Abrupt climate change is defined in this IPCC Fifth Assessment Report (AR5) as a large-scale change in the climate system that takes place over a few decades or less, persists (or is anticipated to persist) for at least a few decades and causes substantial disruptions in human and natural systems. There is information on potential consequences of some abrupt changes, but in general there is *low confidence* and little consensus on the likelihood of such events over the 21st century. Examples of components susceptible to such abrupt change are the strength of the Atlantic Meridional Overturning Circulation (AMOC), clathrate methane release, tropical and boreal forest dieback, disappearance of summer sea ice in the Arctic Ocean, long-term drought and monsoonal circulation. {5.7, 6.4.7, 12.5.5; Table 12.4}

A change is said to be *irreversible* if the recovery time scale from this state due to natural processes is significantly longer than the time it takes for the system to reach this perturbed state. Such behaviour may arise because the time scales for perturbations and recovery processes are different, or because climate change may persist due to the long residence time of a carbon dioxide (CO_2) perturbation in the atmosphere (see TFE.8). Whereas changes in Arctic Ocean summer sea ice extent, long-term droughts and monsoonal circulation are assessed to be reversible within years to decades, tropical or boreal forest dieback may be reversible only within centuries. Changes in clathrate methane and permafrost carbon release, Greenland and Antarctic ice sheet collapse may be irreversible during millennia after the causal perturbation. {5.8, 6.4.7, 12.5.5, 13.4.3, 13.4.4; Table 12.4}

Abrupt Climate Change Linked with AMOC

New transient climate model simulations have confirmed with *high confidence* that strong changes in the strength of the AMOC produce abrupt climate changes at global scale with magnitude and pattern resembling past glacial Dansgaard–Oeschger events and Heinrich stadials. Confidence in the link between changes in North Atlantic climate and low-latitude precipitation has increased since the IPCC Fourth Assessment Report (AR4). From new paleoclimate reconstructions and modelling studies, there is *very high confidence* that a reduced strength of the AMOC and the associated surface cooling in the North Atlantic region caused southward shifts of the Atlantic Intertropical Convergence Zone and affected the American (north and south), African and Asian monsoons. {5.7}

The interglacial mode of the AMOC can recover (*high confidence*) from a short-lived freshwater input into the subpolar North Atlantic. Approximately 8.2 ka, a sudden freshwater release occurred during the final stages of North America ice sheet melting. Paleoclimate observations and model results indicate, with *high confidence*, a marked reduction in the strength of the AMOC followed by a rapid recovery, within approximately 200 years after the perturbation. {5.8.2}

Although many more model simulations have been conducted since AR4 under a wide range of future forcing scenarios, projections of the AMOC behaviour have not changed. It remains *very likely* that the AMOC will weaken over the 21st century relative to 1850-1900 values. Best estimates and ranges for the reduction from the Coupled Model Intercomparison Project Phase 5 (CMIP5) are 11% (1 to 24%) for the Representative Concentration Pathway RCP2.6 and 34% (12 to 54%) for RCP8.5, but there is *low confidence* on the magnitude of weakening. It also remains *very unlikely* that the AMOC will undergo an abrupt transition or collapse in the 21st century for the scenarios considered (*high confidence*) (TFE.5, Figure 1). For an abrupt transition of the AMOC to occur, the sensitivity of the AMOC to forcing would have to be far greater than seen in current models, or would require meltwater flux from the Greenland ice sheet greatly exceeding even the highest of current projections. Although neither possibility can be excluded entirely, it is *unlikely* that the AMOC will collapse beyond the end of the 21st century for the scenarios considered, but a collapse beyond the 21st century for large sustained warming cannot be excluded. There is *low confidence* in assessing the evolution of AMOC beyond the 21st century because of limited number of analyses and equivocal results. {12.4.7, 12.5.5}

Potential Irreversibility of Changes in Permafrost, Methane Clathrates and Forests

In a warming climate, permafrost thawing may induce decomposition of carbon accumulated in frozen soils which could persist for hundreds to thousands of years, leading to an increase of atmospheric CO_2 and/or methane (CH_4)

(continued on next page)

TFE.5 (continued)

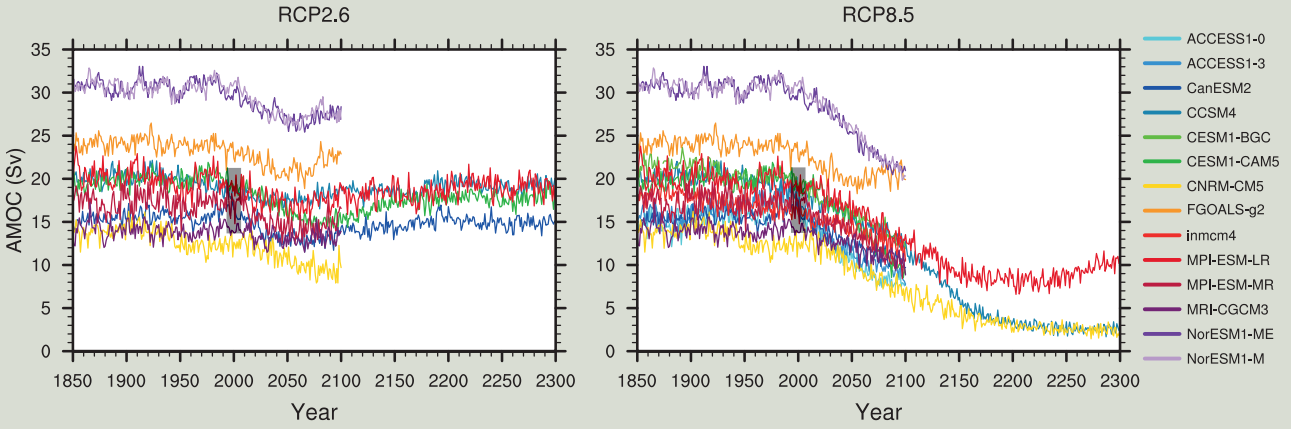

TFE.5, Figure 1 | Atlantic Meridional Overturning Circulation (AMOC) strength at 30°N (Sv) as a function of year, from 1850 to 2300 as simulated by different Atmosphere–Ocean General Circulation Models in response to scenario RCP2.6 (left) and RCP8.5 (right). The vertical black bar shows the range of AMOC strength measured at 26°N, from 2004 to 2011 {Figures 3.11, 12.35}

concentrations. The existing modelling studies of permafrost carbon balance under future warming that take into account at least some of the essential permafrost-related processes do not yield consistent results, beyond the fact that present-day permafrost will become a net emitter of carbon during the 21st century under plausible future warming scenarios (*low confidence*). This also reflects an insufficient understanding of the relevant soil processes during and after permafrost thaw, including processes leading to stabilization of unfrozen soil carbon, and precludes any quantitative assessment of the amplitude of irreversible changes in the climate system potentially related to permafrost degassing and associated feedbacks. {6.4.7, 12.5.5}

Anthropogenic warming will *very likely* lead to enhanced CH_4 emissions from both terrestrial and oceanic clathrates. Deposits of CH_4 clathrates below the sea floor are susceptible to destabilization via ocean warming. However, sea level rise due to changes in ocean mass enhances clathrate stability in the ocean. While difficult to formally assess, initial estimates of the 21st century feedback from CH_4 clathrate destabilization are small but not insignificant. It is *very unlikely* that CH_4 from clathrates will undergo catastrophic release during the 21st century (*high confidence*). On multi-millennial time scales, such CH_4 emissions may provide a positive feedback to anthropogenic warming and may be irreversible, due to the diffference between release and accumulation time scales. {6.4.7, 12.5.5}

The existence of critical climate change driven dieback thresholds in the Amazonian and other tropical rainforests purely driven by climate change remains highly uncertain. The possibility of a critical threshold being crossed in precipitation volume and duration of dry seasons cannot be ruled out. The response of boreal forest to projected climate change is also highly uncertain, and the existence of critical thresholds cannot at present be ruled out. There is *low confidence* in projections of the collapse of large areas of tropical and/or boreal forests. {12.5.5}

Potential Irreversibility of Changes in the Cryosphere

The reversibility of sea ice loss has been directly assessed in sensitivity studies to CO_2 increase and decrease with Atmosphere–Ocean General Circulation Models (AOGCMs) or Earth System Models (ESMs). None of them show evidence of an irreversible change in Arctic sea ice at any point. By contrast, as a result of the strong coupling between surface and deep waters in the Southern Ocean, the Antarctic sea ice in some models integrated with ramp-up and ramp-down atmospheric CO_2 concentration exhibits some hysteresis behaviour. {12.5.5}

At present, both the Greenland and Antarctic ice sheets have a positive surface mass balance (snowfall exceeds melting), although both are losing mass because ice outflow into the sea exceeds the net surface mass balance. A positive feedback operates to reduce ice sheet volume and extent when a decrease of the surface elevation of the ice sheet induces a decreased surface mass balance. This arises generally through increased surface melting, and therefore applies in the 21st century to Greenland, but not to Antarctica, where surface melting is currently very small. Surface melting in Antarctica is projected to become important after several centuries under high well-mixed greenhouse gas radiative forcing scenarios. {4.4, 13.4.4; Boxes 5.2, 13.2}

Abrupt change in ice sheet outflow to the sea may be caused by unstable retreat of the grounding line in regions where the bedrock is below sea level and slopes downwards towards the interior of the ice sheet. This mainly

(continued on next page)

TFE.5 (continued)

applies to West Antarctica, but also to parts of East Antarctica and Greenland. Grounding line retreat can be triggered by ice shelf decay, due to warmer ocean water under ice shelves enhancing submarine ice shelf melt, or melt water ponds on the surface of the ice shelf promoting ice shelf fracture. Because ice sheet growth is a slow process, such changes would be irreversible in the definition adopted here. {4.4.5; Box 13.2}

There is *high confidence* that the volumes of the Greenland and West Antarctic ice sheets were reduced during periods of the past few million years that were globally warmer than present. Ice sheet model simulations and geological data suggest that the West Antarctic ice sheet is very sensitive to subsurface ocean warming and imply with *medium confidence* a West Antarctic ice sheet retreat if atmospheric CO_2 concentration stays within, or above, the range of 350–450 ppm for several millennia. {5.8.1, 13.4.4; Box 13.2}

The available evidence indicates that global warming beyond a threshold would lead to the near-complete loss of the Greenland ice sheet over a millennium or longer, causing a global mean sea level rise of approximately 7 m. Studies with fixed present-day ice sheet topography indicate that the threshold is greater than 2°C but less than 4°C (*medium confidence*) of global mean surface temperature rise above pre-industrial. The one study with a dynamical ice sheet suggests the threshold is greater than about 1°C (*low confidence*) global mean warming with respect to pre-industrial. Considering the present state of scientific uncertainty, a *likely* range cannot be quantified. The complete loss of the Greenland ice sheet is not inevitable because this would take a millennium or more; if temperatures decline before the ice sheet has completely vanished, the ice sheet might regrow. However, some part of the mass loss might be irreversible, depending on the duration and degree of exceedance of the threshold, because the ice sheet may have multiple steady states, due to its interaction with regional climate. {13.4.3, 13.4.4}

TS.4.6 Water Cycle

Since the AR4, new evidence has emerged of a detectable human influence on several aspects of the water cycle. There is *medium confidence* that observed changes in near-surface specific humidity since 1973 contain a detectable anthropogenic component. The anthropogenic water vapour fingerprint simulated by an ensemble of climate models has been detected in lower tropospheric moisture content estimates derived from Special Sensor Microwave/Imager (SSM/I) data covering the period 1988–2006. An anthropogenic contribution to increases in tropospheric specific humidity is found with *medium confidence*. {2.5, 10.3}

Attribution studies of global zonal mean terrestrial precipitation and Arctic precipitation both find a detectable anthropogenic influence. Overall there is *medium confidence* in a significant human influence on global scale changes in precipitation patterns, including increases in NH mid-to-high latitudes. Remaining observational and modelling uncertainties and the large effect of internal variability on observed precipitation preclude a more confident assessment. {2.5, 7.6, 10.3}

Based on the collected evidence for attributable changes (with varying levels of confidence and likelihood) in specific humidity, terrestrial precipitation and ocean surface salinity through its connection to precipitation and evaporation, and from physical understanding of the water cycle, it is *likely* that human influence has affected the global water cycle since 1960. This is a major advance since AR4. {2.4, 2.5, 3.3, 9.4.1, 10.3, 10.4.2; Table 10.1; FAQ 3.2}

TS.4.7 Climate Extremes

Several new attribution studies have found a detectable anthropogenic influence in the observed increased frequency of warm days and nights and decreased frequency of cold days and nights. Since the AR4 and SREX, there is new evidence for detection of human influence on extremely warm daytime temperature and there is new evidence that the influence of anthropogenic forcing may be detected separately from the influence of natural forcing at global scales and in some continental and sub-continental regions. This strengthens the conclusions from both AR4 and SREX, and it is now *very likely* that anthropogenic forcing has contributed to the observed changes in the frequency and intensity of daily temperature extremes on the global scale since the mid-20th century. It is *likely* that human influence has significantly increased the probability of occurrence of heat waves in some locations. See TFE.9 and TFE.9, Table 1 for a summary of the assessment of extreme weather and climate events. {10.6}

Since the AR4, there is some new limited direct evidence for an anthropogenic influence on extreme precipitation, including a formal detection and attribution study and indirect evidence that extreme precipitation would be expected to have increased given the evidence of anthropogenic influence on various aspects of the global hydrological cycle and *high confidence* that the intensity of extreme precipitation events will increase with warming, at a rate well exceeding that of the mean precipitation. In land regions where observational coverage is sufficient for assessment, there is *medium confidence* that anthropogenic forcing has contributed to a global-scale intensification of heavy precipitation over the second half of the 20th century. {7.6, 10.6}

Globally, there is *low confidence* in attribution of changes in tropical cyclone activity to human influence. This is due to insufficient observational evidence, lack of physical understanding of the links between anthropogenic drivers of climate and tropical cyclone activity, and the low level of agreement between studies as to the relative importance of internal variability, and anthropogenic and natural forcings. In the North Atlantic region there is *medium confidence* that a reduction in aerosol forcing over the North Atlantic has contributed at least in part to the observed increase in tropical cyclone activity there since the 1970s. There remains substantial disagreement on the relative importance of internal variability, WMGHG forcing and aerosols for this observed trend. {2.6, 10.6, 14.6}

Although the AR4 concluded that it is *more likely than not* that anthropogenic influence has contributed to an increased risk of drought in the second half of the 20th century, an updated assessment of the observational evidence indicates that the AR4 conclusions regarding global increasing trends in hydrological droughts since the 1970s are no longer supported. Owing to the *low confidence* in observed large-scale trends in dryness combined with difficulties in distinguishing decadal-scale variability in drought from long-term climate change, there is now *low confidence* in the attribution of changes in drought over global land since the mid-20th century to human influence. {2.6, 10.6}

TS.4.8 From Global to Regional

Taking a longer term perspective shows the substantial role played by external forcings in driving climate variability on hemispheric scales in pre-industrial times (Box TS.5). It is *very unlikely* that NH temperature variations from 1400 to 1850 can be explained by internal variability alone. There is *medium confidence* that external forcing contributed to NH temperature variability from 850 to 1400 and that external forcing contributed to European temperature variations over the last 5 centuries. {5.3.3, 5.5.1, 10.7.2, 10.7.5; Table 10.1}

Changes in atmospheric circulation are important for local climate change because they could lead to greater or smaller changes in climate in a particular region than elsewhere. It is *likely* that human influence has altered sea level pressure patterns globally. There is *medium confidence* that stratospheric ozone depletion has contributed to the observed poleward shift of the southern Hadley Cell border during austral summer. It is *likely* that stratospheric ozone depletion has contributed to the positive trend in the SAM seen in austral summer since the mid-20th century which corresponds to sea level pressure reductions over the high latitudes and increase in the subtropics (Figure TS.11). {10.3}

The evidence is stronger that observed changes in the climate system can now be attributed to human activities on global and regional scales in many components (Figure TS.12). Observational uncertainty has been explored much more thoroughly than previously, and fingerprints of human influence have been deduced from a new generation of climate models. There is improved understanding of ocean changes, including salinity changes, that are consistent with large scale intensification of the water cycle predicted by climate models. The changes in near surface temperatures, free atmosphere temperatures, ocean temperatures and NH snow cover and sea ice extent, when taken together, show not just global mean changes, but also distinctive regional patterns consistent with the expected fingerprints of change from anthropogenic forcings and the expected responses from volcanic eruptions (Figure TS.12). {10.3–10.6, 10.9}

Human influence has been detected in nearly all of the major assessed components of the climate system (Figure TS.12). Taken together, the combined evidence increases the overall level of confidence in the attribution of observed climate change, and reduces the uncertainties associated with assessment based on a single climate variable. From this combined evidence it is *virtually certain* that human influence has warmed the global climate system. Anthropogenic influence has been identified in changes in temperature near the surface of the Earth, in the atmosphere and in the oceans, as well as in changes in the cryosphere, the water cycle and some extremes. There is strong evidence that excludes solar forcing, volcanoes and internal variability as the strongest drivers of warming since 1950. {10.9; Table 10.1; FAQ 5.1}

Over every continent except Antarctica, anthropogenic influence has *likely* made a substantial contribution to surface temperature increases since the mid-20th century (Figure TS.12). It is *likely* that there has been a significant anthropogenic contribution to the very substantial warming in Arctic land surface temperatures over the past 50 years. For Antarctica large observational uncertainties result in *low confidence* that anthropogenic influence has contributed to observed warming averaged over available stations. Detection and attribution at regional

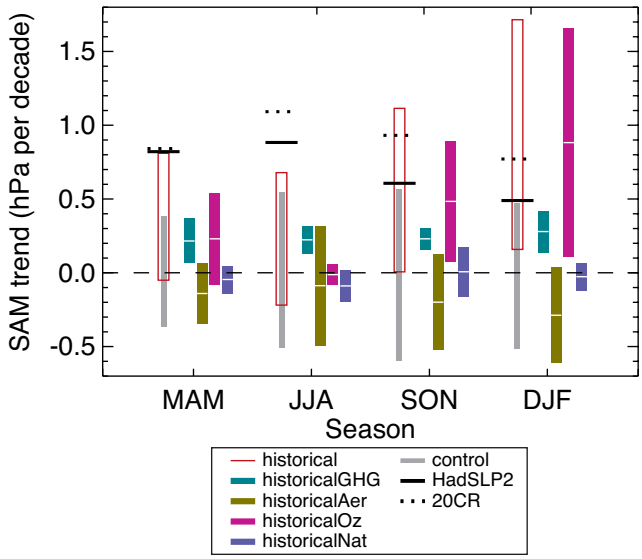

Figure TS.11 | Simulated and observed 1951–2011 trends in the Southern Annular Mode (SAM) index by season. The SAM index is a difference between zonal mean sea level pressure (SLP) at 40°S and 65°S. The SAM index is defined without normalization, so that the magnitudes of simulated and observed trends can be compared. Black lines show observed trends from the Hadley Centre Sea Level Pressure 2r (HadSLP2r) data set (solid), and the 20th Century Reanalysis (dotted). Grey bars show 5th to 95th percentile ranges of control trends, and red boxes show the 5th to 95th percentile range of trends in historical simulations including anthropogenic and natural forcings. Coloured bars show ensemble mean trends and their associated 5 to 95% confidence ranges simulated in response to well-mixed greenhouse gas (light green), aerosol (dark green), ozone (magenta) and natural forcing changes (blue) in CMIP5 individual-forcing simulations. {Figure 10.13b}

scales is complicated by the greater role played by dynamical factors (circulation changes), a greater range of forcings that may be regionally important, and the greater difficulty of modelling relevant processes at regional scales. Nevertheless, human influence has *likely* contributed to temperature increases in many sub-continental regions. {10.3; Box 5.1}

The coherence of observed changes with simulations of anthropogenic and natural forcing in the physical system is remarkable (Figure TS.12), particularly for temperature-related variables. Surface temperature and ocean heat content show emerging anthropogenic and natural signals in both records, and a clear separation from the alternative hypothesis of just natural variations. These signals do not appear just in the global means, but also appear at regional scales on continents and in ocean basins in each of these variables. Sea ice extent emerges clearly from the range of internal variability for the Arctic. At sub-continental scales human influence is *likely* to have substantially increased the probability of occurrence of heat waves in some locations. {Table 10.1}

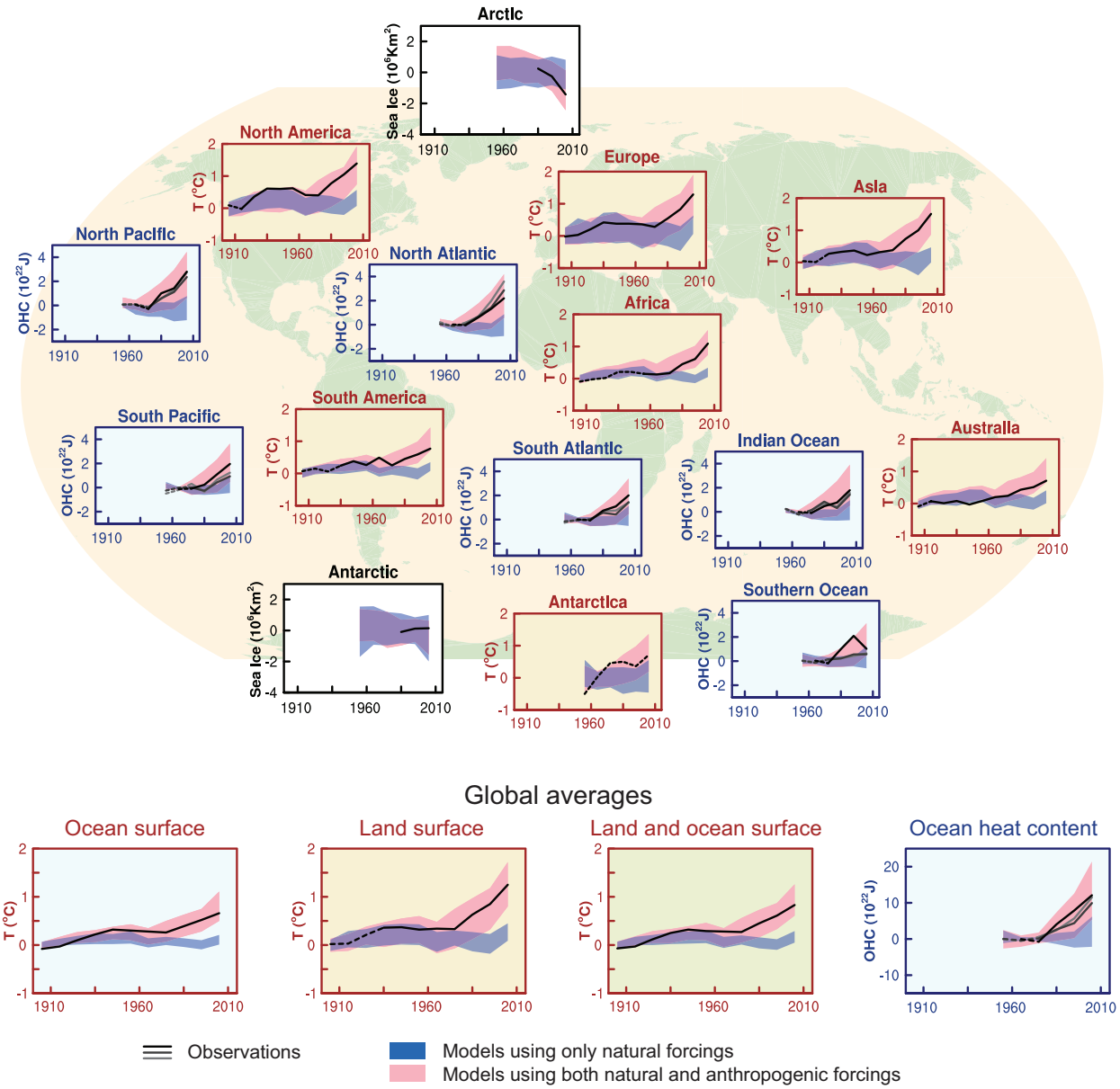

Figure TS.12 | Comparison of observed and simulated change in the climate system, at regional scales (top panels) and global scales (bottom four panels). Brown panels are land surface temperature time series, blue panels are ocean heat content time series and white panels are sea ice time series (decadal averages). Each panel shows observations (black or black and shades of grey), and the 5 to 95% range of the simulated response to natural forcings (blue shading) and natural and anthropogenic forcings (pink shading), together with the corresponding ensemble means (dark blue and dark red respectively). The observed surface temperature is from the Hadley Centre/Climatic Research Unit gridded surface temperature data set 4 (HadCRUT4). Three observed records of ocean heat content (OHC) are shown. Sea ice anomalies (rather than absolute values) are plotted and based on models in Figure 10.16. The observations lines are either solid or dashed and indicate the quality of the observations and estimates. For land and ocean surface temperatures panels and precipitation panels, solid observation lines indicate where spatial coverage of areas being examined is above 50% coverage and dashed observation lines where coverage is below 50%. For example, data coverage of Antarctica never goes above 50% of the land area of the continent. For ocean heat content and sea ice panels the solid observations line is where the coverage of data is good and higher in quality, and the dashed line is where the data coverage is only adequate. This figure is based on Figure 10.21 except presented as decadal averages rather than yearly averages. Further detail regarding the related Figure SPM.6 is given in the TS Supplementary Material. {Figure 10.21}

Box TS.4 | Model Evaluation

Climate models have continued to be improved since the AR4, and many models have been extended into Earth System Models (ESMs) by including the representation of biogeochemical cycles important to climate change. Box TS.4, Figure 1 provides a partial overview of model capabilities as assessed in this report, including improvements or lack thereof relative to models that were assessed in the AR4 or that were available at the time of the AR4. {9.1, 9.8.1; Box 9.1}

The ability of climate models to simulate surface temperature has improved in many, though not all, important aspects relative to the generation of models assessed in the AR4. There continues to be *very high confidence* that models reproduce the observed large-scale time-mean surface temperature patterns (pattern correlation of about 0.99), although systematic errors of several degrees Celsius are found in some regions. There is *high confidence* that on the regional scale (sub-continental and smaller), time-mean surface temperature is better simulated than at the time of the AR4; however, confidence in model capability is lower than for the large scale. Models are able to reproduce the magnitude of the observed global mean or northern-hemisphere-mean temperature variability on interannual to centennial time scales. Models are also able to reproduce the large-scale patterns of temperature during the Last Glacial Maximum indicating an ability to simulate a climate state much different from the present (see also Box TS.5). {9.4.1, 9.6.1}

There is *very high confidence* that models reproduce the general features of the global and annual mean surface temperature changes over the historical period, including the warming in the second half of the 20th century and the cooling immediately following large volcanic eruptions. Most simulations of the historical period do not reproduce the observed reduction in global mean surface warming trend over the last 10 to 15 years (see Box TS.3). There is *medium confidence* that the trend difference between models and observations during 1998–2012 is to a substantial degree caused by internal variability, with possible contributions from forcing inadequacies in models and some models overestimating the response to increasing greenhouse gas forcing. Most, though not all, models overestimate the observed warming trend in the tropical troposphere over the last 30 years, and tend to underestimate the long-term lower-stratospheric cooling trend. {9.4.1; Box 9.2}

The simulation of large-scale patterns of precipitation has improved somewhat since the AR4, although models continue to perform less well for precipitation than for surface temperature. The spatial pattern correlation between modelled and observed annual mean precipitation has increased from 0.77 for models available at the time of the AR4 to 0.82 for current models. At regional scales, precipitation is not simulated as well, and the assessment remains difficult owing to observational uncertainties. {9.4.1, 9.6.1}

Many models are able to reproduce the observed changes in upper-ocean heat content from 1961 to 2005. The time series of the multi-model mean falls within the range of the available observational estimates for most of the period. {9.4.2}

There is robust evidence that the downward trend in Arctic summer sea ice extent is better simulated than at the time of the AR4. About one quarter of the models show a trend as strong as, or stronger, than the trend in observations over the satellite era 1979–2012. Most models simulate a small decreasing trend in Antarctic sea ice extent, albeit with large inter-model spread, in contrast to the small increasing trend in observations. {9.4.3}

There has been substantial progress since the AR4 in the assessment of model simulations of extreme events. Changes in the frequency of extreme warm and cold days and nights over the second half of the 20th century are consistent between models and observations, with the ensemble mean global mean time series generally falling within the range of observational estimates. The majority of models underestimate the sensitivity of extreme precipitation to temperature variability or trends, especially in the tropics. {9.5.4}

In the majority of the models that include an interactive carbon cycle, the simulated global land and ocean carbon sinks over the latter part of the 20th century fall within the range of observational estimates. However, models systematically underestimate the NH land sink implied by atmospheric inversion techniques. {9.4.5}

Regional downscaling methods provide climate information at the smaller scales needed for many climate impact studies. There is *high confidence* that downscaling adds value both in regions with highly variable topography and for various small-scale phenomena. {9.6.4}

The model spread in equilibrium climate sensitivity ranges from 2.1°C to 4.7°C and is very similar to the assessment in the AR4. There is *very high confidence* that the primary factor contributing to the spread in equilibrium climate sensitivity continues to be the cloud feedback. This applies to both the modern climate and the last glacial maximum. There is likewise *very high confidence* that, consistent with observations, models show a strong positive correlation between tropospheric temperature and water vapour on regional to global scales, implying a positive water vapour feedback in both models and observations. {5.3.3, 9.4.1, 9.7} *(continued on next page)*

Box TS.4 (continued)

Climate models are based on physical principles, and they reproduce many important elements of observed climate. Both aspects contribute to our confidence in the models' suitability for their application in detection and attribution studies (see Chapter 10) and for quantitative future predictions and projections (see Chapters 11 to 14). There is increasing evidence that some elements of observed variability or trends are well correlated with inter-model differences in model projections for quantities such as Arctic summer sea ice trends, the snow–albedo feedback, and the carbon loss from tropical land. However, there is still no universal strategy for transferring a model's past performance to a relative weight of this model in a multi-model-ensemble mean of climate projections. {9.8.3}

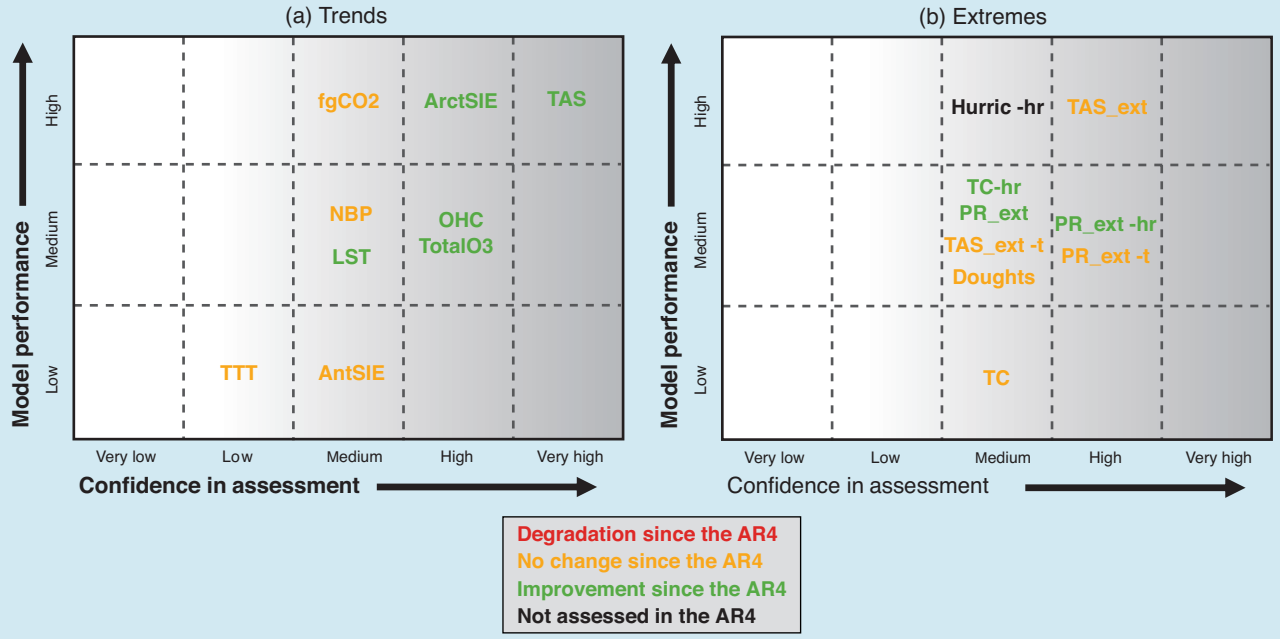

Box TS.4, Figure1 | Summary of how well the current-generation climate models simulate important features of the climate of the 20th century. Confidence in the assessment increases towards the right as suggested by the increasing strength of shading. Model quality increases from bottom to top. The colour coding indicates improvements from the models available at the time of the AR4 to the current assessment. There have been a number of improvements since the AR4, and some some modelled quantities are not better simulated. The major climate quantities are listed in this summary and none shows degradation. The assessment is based mostly on the multi-model mean, not excluding that deviations for individual models could exist. Assessed model quality is simplified for representation in this figure; details of each assessment are found in Chapter 9. {9.8.1; Figure 9.44}

The figure highlights the following key features, with the sections that back up the assessment added in brackets:

(a) Trends in:

AntSIE	Antarctic sea ice extent {9.4.3}
ArctSIE	Arctic sea ice extent {9.4.3}
fgCO2	Global ocean carbon sink {9.4.5}
LST	Lower-stratospheric temperature {9.4.1.}
NBP	Global land carbon sink {9.4.5}
OHC	Global ocean heat content {9.4.2}
TotalO3	Total-column ozone {9.4.1}
TAS	Surface air temperature {9.4.1}
TTT	Tropical tropospheric temperature {9.4.1}

(b) Extremes:

Droughts	Droughts {9.5.4}
Hurric-hr	Year-to-year count of Atlantic hurricanes in high-resolution AGCMs {9.5.4}
PR_ext	Global distribution of precipitation extremes {9.5.4}
PR_ext-hr	Global distribution of precipitation extremes in high-resolution AGCMs {9.5.4}
PR_ext-t	Global trends in precipitation extremes {9.5.4}
TAS_ext	Global distributions of surface air temperature extremes {9.5.4}
TAS_ext-t	Global trends in surface air temperature extremes {9.5.4}
TC	Tropical cyclone tracks and intensity {9.5.4}
TC-hr	Tropical cyclone tracks and intensity in high-resolution AGCMs {9.5.4}

Box TS.5 | Paleoclimate

Reconstructions from paleoclimate archives allow current changes in atmospheric composition, sea level and climate (including extreme events such as droughts and floods), as well as future projections, to be placed in a broader perspective of past climate variability (see Section TS.2). {5.2–5.6, 6.2, 10.7}

Past climate information also documents the behaviour of slow components of the climate system including the carbon cycle, ice sheets and the deep ocean for which instrumental records are short compared to their characteristic time scales of responses to perturbations, thus informing on mechanisms of abrupt and irreversible changes. Together with the knowledge of past external climate forcings, syntheses of paleoclimate data have documented polar amplification, characterized by enhanced temperature changes in the Arctic compared to the global mean, in response to high or low CO_2 concentrations. {5.2.1, 5.2.2, 5.6, 5.7, 5.8, 6.2, 8.4.2, 13.2.1, 13.4; Boxes 5.1, 5.2}

Since AR4, the inclusion of paleoclimate simulations in the PMIP3 (Paleoclimate Modelling Intercomparison Project)/CMIP5 framework has enabled paleoclimate information to be more closely linked with future climate projections. Paleoclimate information for the mid-Holocene (6 ka), the Last Glacial Maximum (approximately 21 ka), and last millennium has been used to test the ability of models to simulate realistically the magnitude and large-scale patterns of past changes. Combining information from paleoclimate simulations and reconstructions enables to quantify the response of the climate system to radiative perturbations, constraints to be placed on the range of equilibrium climate sensitivity, and past patterns of internal climate variability to be documented on inter-annual to multi-centennial scales. {5.3.1–5.3.5, 5.4, 5.5.1, 9.4.1, 9.4.2, 9.5.3, 9.7.2, 10.7.2, 14.1.2}

Box TS.5, Figure 1 illustrates the comparison between the last millennium Paleoclimate Modelling Intercomparison Project Phase 3 (PMIP3)/CMIP5 simulations and reconstructions, together with the associated solar, volcanic and WMGHG RFs. For average annual NH temperatures, the period 1983–2012 was *very likely* the warmest 30-year period of the last 800 years (*high confidence*) and *likely* the warmest 30-year period of the last 1400 years (*medium confidence*). This is supported by comparison of instrumental temperatures with multiple reconstructions from a variety of proxy data and statistical methods, and is consistent with AR4. In response to solar, volcanic and anthropogenic radiative changes, climate models simulate multi-decadal temperature changes in the last 1200 years in the NH that are generally consistent in magnitude and timing with reconstructions, within their uncertainty ranges. Continental-scale temperature reconstructions show, with *high confidence*, multi-decadal periods during the Medieval Climate Anomaly (about 950 to 1250) that were in some regions as warm as the mid-20th century and in others as warm as in the late 20th century. With *high confidence*, these regional warm periods were not as synchronous across regions as the warming since the mid-20th century. Based on the comparison between reconstructions and simulations, there is *high confidence* that not only external orbital, solar and volcanic forcing but also internal variability contributed substantially to the spatial pattern and timing of surface temperature changes between the Medieval Climate Anomaly and the Little Ice Age (about 1450 to 1850). However, there is only *very low confidence* in quantitative estimates of their relative contributions. It is *very unlikely* that NH temperature variations from 1400 to 1850 can be explained by internal variability alone. There is *medium confidence* that external forcing contributed to Northern Hemispheric temperature variability from 850 to 1400 and that external forcing contributed to European temperature variations over the last 5 centuries. {5.3.5, 5.5.1, 10.7.2, 10.7.5; Table 10.1} *(continued on next page)*

Box TS.5 (continued)

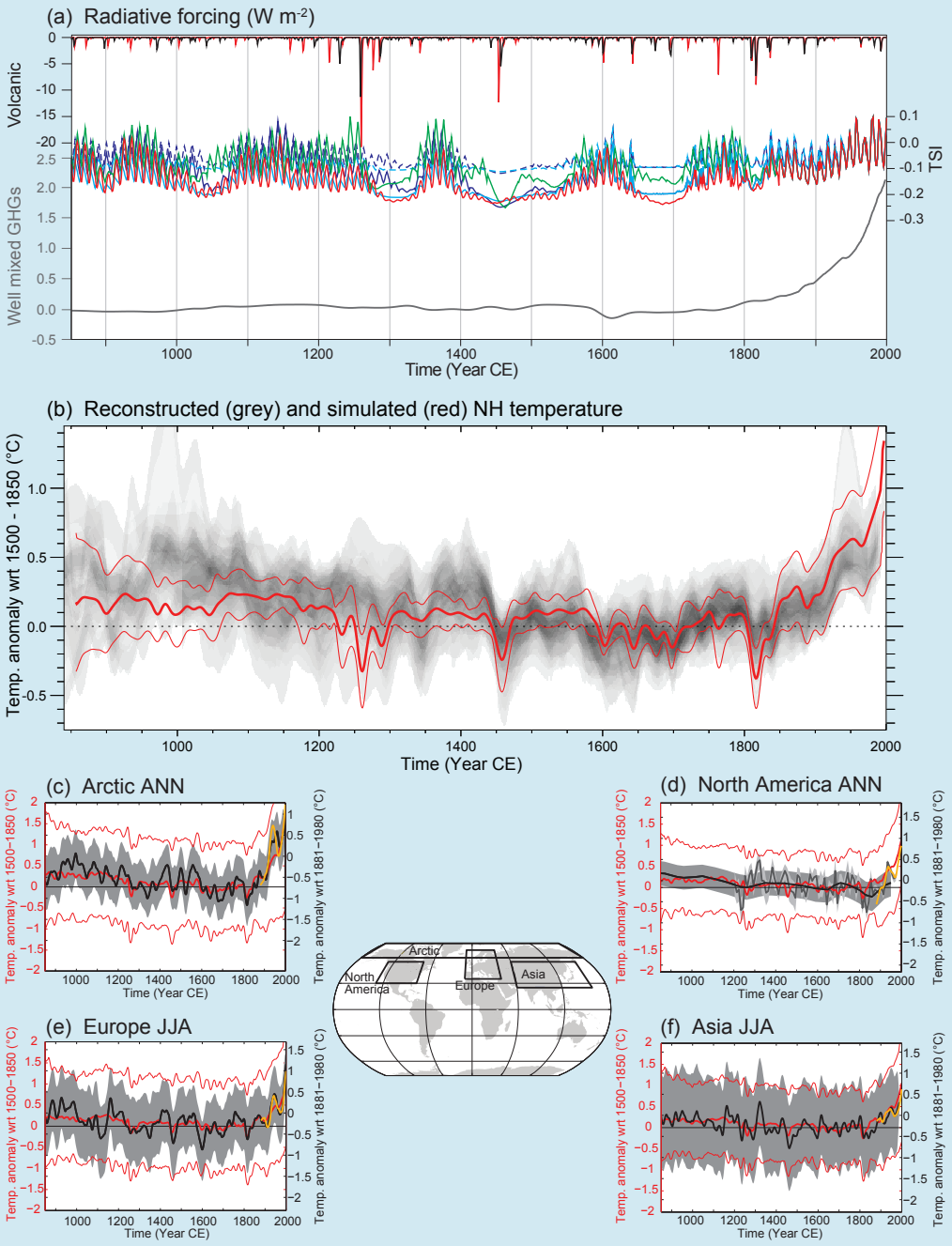

Box TS.5, Figure 1 | Last-millennium simulations and reconstructions. (a) 850–2000 PMIP3/CMIP5 radiative forcing due to volcanic, solar and well-mixed greenhouse gases. Different colours illustrate the two existing data sets for volcanic forcing and four estimates of solar forcing. For solar forcing, solid (dashed) lines stand for reconstruction variants in which background changes in irradiance are (not) considered; (b) 850–2000 PMIP3/CMIP5 simulated (red) and reconstructed (shading) Northern Hemisphere (NH) temperature changes. The thick red line depicts the multi-model mean while the thin red lines show the multi-model 90% range. The overlap of reconstructed temperatures is shown by grey shading; all data are expressed as anomalies from their 1500–1850 mean and smoothed with a 30-year filter. Note that some reconstructions represent a smaller spatial domain than the full NH or a specific season, while annual temperatures for the full NH mean are shown for the simulations. (c), (d), (e) and (f) Arctic and North America annual mean temperature, and Europe and Asia June, July and August (JJA) temperature, from 950 to 2000 from reconstructions (black line), and PMIP3/CMIP5 simulations (thick red, multi-model mean; thin red, 90% multi-model range). All red curves are expressed as anomalies from their 1500–1850 mean and smoothed with a 30-year filter. The shaded envelope depicts the uncertainties from each reconstruction (Arctic: 90% confidence bands, North American: ±2 standard deviation. Asia: ±2 root mean square error. Europe: 95% confidence bands). For comparison with instrumental record, the Climatic Research Unit land station Temperature (CRUTEM4) data set is shown (yellow line). These instrumental data are not necessarily those used in calibration of the reconstrctions, and thus may show greater or lesser correspondence with the reconstructions than the instrumental data actually used for calibration; cutoff timing may also lead to end effects for smoothed data shown. All lines are smoothed by applying a 30-year moving average. Map shows the individual regions for each reconstruction. {5.3.5; Table 5.A.1; Figures 5.1, 5.8, 5.12}

TS.5 Projections of Global and Regional Climate Change

TS.5.1 Introduction

Projections of changes in the climate system are made using a hierarchy of climate models ranging from simple climate models, to models of intermediate complexity, to comprehensive climate models, and Earth System Models (ESMs). These models simulate changes based on a set of scenarios of anthropogenic forcings. A new set of scenarios, the Representative Concentration Pathways (RCPs), was used for the new climate model simulations carried out under the framework of the Coupled Model Intercomparison Project Phase 5 (CMIP5) of the World Climate Research Programme. A large number of comprehensive climate models and ESMs have participated in CMIP5, whose results form the core of the climate system projections.

This section summarizes the assessment of these climate change projections. First, future forcing and scenarios are presented. The following subsections then address various aspects of projections of global and regional climate change, including near-term (up to about mid-century) and long-term (end of the 21st century) projections in the atmosphere, ocean and cryosphere; projections of carbon and other biogeochemical cycles; projections in sea level change; and finally changes to climate phenomena and other aspects of regional climate over the 21st century. Projected changes are given relative to the 1986–2005 average unless indicated otherwise. Projections of climate change on longer term and information on climate stabilization and targets are provided in TFE.8. Methods to counter climate change, termed geoengineering, have been proposed and an overview is provided in Box TS.7. {11.3, 12.3–12.5, 13.5–13.7, 14.1–14.6, Annex I}

TS.5.2 Future Forcing and Scenarios

In this assessment report a series of new RCPs are used that largely replace the IPCC Special Report on Emission Scenarios (SRES) scenarios (see Box TS.6 and Annex II for Climate System Scenario Tables). They produce a range of responses from ongoing warming, to approximately stabilized forcing, to a stringent mitigation scenario (RCP2.6) that stabilizes and then slowly reduces the RF after mid-21st century. In contrast to the AR4, the climate change from the RCP scenarios in the AR5 is framed as a combination of adaptation and mitigation. Mitigation actions starting now in the various RCP scenarios do not produce discernibly different climate change outcomes for the next 30 years or so, whereas long-term climate change after mid-century is appreciably different across the RCPs. {Box 1.1}

Box TS.6 | The New Representative Concentration Pathway Scenarios and Coupled Model Intercomparison Project Phase 5 Models

Future anthropogenic emissions of GHGs, aerosol particles and other forcing agents such as land use change are dependent on socioeconomic factors, and may be affected by global geopolitical agreements to control those emissions to achieve mitigation. AR4 made extensive use of the SRES scenarios that do not include additional climate initiatives, which means that no scenarios were available that explicitly assume implementation of the United Nations Framework Convention on Climate Change (UNFCCC) or the emissions targets of the Kyoto Protocol. However, GHG emissions are directly affected by non-climate change policies designed for a wide range of other purposes. The SRES scenarios were developed using a sequential approach, that is, socioeconomic factors fed into emissions scenarios, which were then used in simple climate models to determine concentrations of GHGs, and other agents required to drive the more complex AOGCMs. In this report, outcomes of climate simulations that use new scenarios (some of which include implied policy actions to achieve mitigation) referred to as RCPs are assessed. These RCPs represent a larger set of mitigation scenarios and were selected to have different targets in terms of radiative forcing at 2100 (about 2.6, 4.5, 6.0 and 8.5 W m^{-2}; Figure TS.15). The scenarios should be considered plausible and illustrative, and do not have probabilities attached to them. {12.3.1; Box 1.1}

The RCPs were developed using Integrated Assessment Models (IAMs) that typically include economic, demographic, energy, and simple climate components. The emission scenarios they produce are then run through a simple model to produce time series of GHG concentrations that can be run in AOGCMs. The emission time series from the RCPs can then be used directly in ESMs that include interactive biogeochemistry (at least a land and ocean carbon cycle). {12.3.1; Box 1.1}

The CMIP5 multi-model experiment (coordinated through the World Climate Research Programme) presents an unprecedented level of information on which to base assessments of climate variability and change. CMIP5 includes new ESMs in addition to AOGCMs, new model experiments and more diagnostic output. CMIP5 is much more comprehensive than the preceding CMIP3 multi-model experiment that was available at the time of the IPCC AR4. CMIP5 has more than twice as many models, many more experiments (that also include experiments to address understanding of the responses in the future climate change scenario runs), and nearly 2×10^{15} bytes of data (as compared to over 30×10^{12} bytes of data in CMIP3). A larger number of forcing agents are treated more completely in the CMIP5 models, with respect to aerosols and land use particularly. Black carbon aerosol is now a commonly included forcing agent. Considering CO_2, both 'concentrations-driven' projections and 'emissions-driven' projections are assessed from CMIP5. These allow quantification of the physical response uncertainties as well as climate–carbon cycle interactions. {1.5.2}

(continued on next page)

Box TS.6 (continued)

The assessment of the mean values and ranges of global mean temperature changes in AR4 would not have been substantially different if the CMIP5 models had been used in that report. The differences in global temperature projections can largely be attributed to the different scenarios. The global mean temperature response simulated by CMIP3 and CMIP5 models is very similar, both in the mean and the model range, transiently and in equilibrium. The range of temperature change across all scenarios is wider because the RCPs include a strong mitigation scenario (RCP2.6) that had no equivalent among the SRES scenarios used in CMIP3. For each scenario, the 5 to 95% range of the CMIP5 projections is obtained by approximating the CMIP5 distributions by a normal distribution with same mean and standard deviation and assessed as being *likely* for projections of global temperature change for the end of the 21st century. Probabilistic projections with simpler models calibrated to span the range of equilibrium climate sensitivity assessed by the AR4 provide uncertainty ranges that are consistent with those from CMIP5. In AR4 the uncertainties in global temperature projections were found to be approximately constant when expressed as a fraction of the model mean warming (constant fractional uncertainty). For the higher RCPs, the uncertainty is now estimated to be smaller than with the AR4 method for long-term climate change, because the carbon cycle–climate feedbacks are not relevant for the concentration-driven RCP projections (in contrast, the assessed projection uncertainties of global temperature in AR4 did account of carbon cycle–climate feedbacks, even though these were not part of the CMIP3 models). When forced with RCP8.5, CO_2 emissions, as opposed to the RCP8.5 CO_2 concentrations, CMIP5 ESMs with interactive carbon cycle simulate, on average, a 50 (–140 to +210) ppm (CMIP5 model spread) larger atmospheric CO_2 concentration and 0.2°C larger global surface temperature increase by 2100. For the low RCPs the fractional uncertainty is larger because internal variability and non-CO_2 forcings make a larger relative contribution to the total uncertainty. {12.4.1, 12.4.8, 12.4.9} *(continued on next page)*

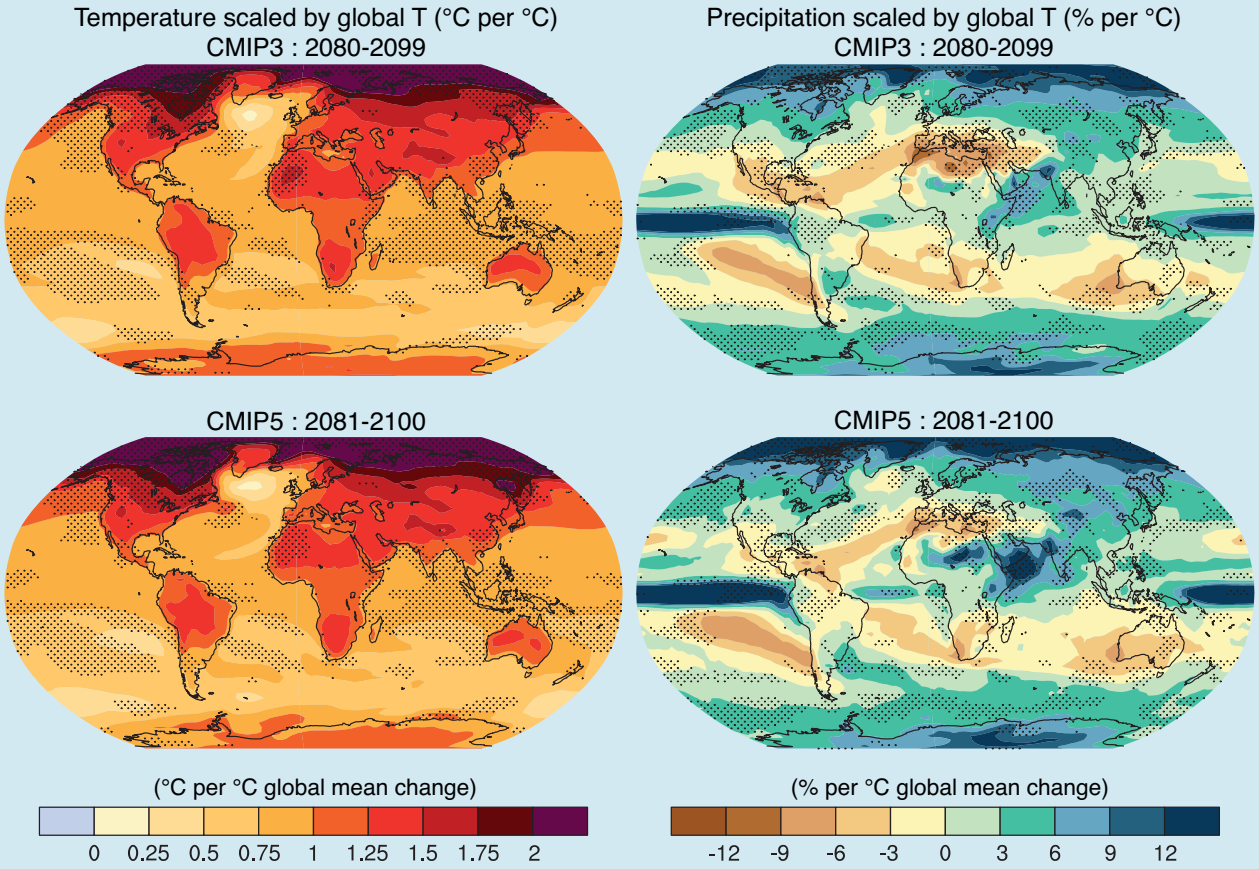

Box TS.6, Figure 1 | Patterns of temperature (left column) and percent precipitation change (right column) for the CMIP3 models average (first row) and CMIP5 models average (second row), scaled by the corresponding global average temperature changes. The patterns are computed in both cases by taking the difference between the averages over the last 20 years of the 21st century experiments (2080–2099 for CMIP3 and 2081–2100 for CMIP5) and the last 20 years of the historic experiments (1980–1999 for CMIP3, 1986–2005 for CMIP5) and rescaling each difference by the corresponding change in global average temperature. This is done first for each individual model, then the results are averaged across models. Stippling indicates a measure of significance of the difference between the two corresponding patterns obtained by a bootstrap exercise. Two subsets of the pooled set of CMIP3 and CMIP5 ensemble members of the same size as the original ensembles, but without distinguishing CMIP3 from CMIP5 members, were randomly sampled 500 times. For each random sample the corresponding patterns and their difference are computed, then the true difference is compared, grid-point by grid-point, to the distribution of the bootstrapped differences, and only grid-points at which the value of the difference falls in the tails of the bootstrapped distribution (less than the 2.5th percentiles or the 97.5th percentiles) are stippled. {Figure 12.41}

Box TS.6 (continued)

There is overall consistency between the projections of temperature and precipitation based on CMIP3 and CMIP5, both for large-scale patterns and magnitudes of change (Box TS.6, Figure 1). Model agreement and confidence in projections depends on the variable and on spatial and temporal averaging, with better agreement for larger scales. Confidence is higher for temperature than for those quantities related to the water cycle or atmospheric circulation. Improved methods to quantify and display model robustness have been developed to indicate where lack of agreement across models on local trends is a result of internal variability, rather than models actually disagreeing on their forced response. Understanding of the sources and means of characterizing uncertainties in long-term large scale projections of climate change has not changed significantly since AR4, but new experiments and studies have continued to work towards a more complete and rigorous characterization. {9.7.3, 12.2, 12.4.1, 12.4.4, 12.4.5, 12.4.9; Box 12.1}

The well-established stability of geographical patterns of temperature and precipitation change during a transient experiment remains valid in the CMIP5 models (Box TS.6, Figure 1). Patterns are similar over time and across scenarios and to first order can be scaled by the global mean temperature change. There remain limitations to the validity of this technique when it is applied to strong mitigation scenarios, to scenarios where localized forcings (e.g., aerosols) are significant and vary in time and for variables other than average seasonal mean temperature and precipitation. {12.4.2}

The range in anthropogenic aerosol emissions across all scenarios has a larger impact on near-term climate projections than the corresponding range in long-lived GHGs, particularly on regional scales and for hydrological cycle variables. The RCP scenarios do not span the range of future aerosol emissions found in the SRES and alternative scenarios (Box TS.6). {11.3.1, 11.3.6}

If rapid reductions in sulphate aerosol are undertaken for improving air quality or as part of decreasing fossil-fuel CO_2 emissions, then there is *medium confidence* that this could lead to rapid near-term warming. There is evidence that accompanying controls on CH_4 emissions would offset some of this sulphate-induced warming, although the cooling from CH_4 mitigation will emerge more slowly than the warming from sulphate mitigation due to the different time scales over which atmospheric concentrations of these substances decrease in response to decreases in emissions. Although removal of black carbon aerosol could also counter warming associated with sulphate removal, uncertainties are too large to constrain the net sign of the global temperature response to black carbon emission reductions, which depends on reduction of co-emitted (reflective) aerosols and on aerosol indirect effects. {11.3.6}

Including uncertainties in projecting the chemically reactive GHGs CH_4 and N_2O from RCP emissions gives a range in abundance pathways that is *likely* 30% larger than the range in RCP concentrations used to force the CMIP5 climate models. Including uncertainties in emission estimates from agricultural, forest and land use sources, in atmospheric lifetimes, and in chemical feedbacks, results in a much wider range of abundances for N_2O, CH_4 and HFCs and their RF. In the case of CH_4, by year 2100 the *likely* range of RCP8.5 CH_4 abundance extends 520 ppb above the single-valued RCP8.5 CH_4 abundance, and RCP2.6 CH_4 extends 230 ppb below RCP2.6 CH_4. {11.3.5}

There is *very low confidence* in projections of natural forcing. Major volcanic eruptions cause a negative RF up to several watts per square metre, with a typical lifetime of one year, but the possible occurrence and timing of future eruptions is unknown. Except for the 11-year solar cycle, changes in the total solar irradiance are uncertain. Except where explicitly indicated, future volcanic eruptions and changes in total solar irradiance additional to a repeating 11-year solar cycle are not included in the projections of near- and long-term climate assessed. {8, 11.3.6}

TS.5.3 Quantification of Climate System Response

Estimates of the equilibrium climate sensitivity (ECS) based on observed climate change, climate models and feedback analysis, as well as paleoclimate evidence indicate that ECS is positive, *likely* in the range 1.5°C to 4.5°C with *high confidence*, *extremely unlikely* less than 1°C (*high confidence*) and *very unlikely* greater than 6°C (*medium confidence*). Earth system sensitivity over millennia time scales including long-term feedbacks not typically included in models could be significantly higher than ECS (see TFE.6 for further details). {5.3.1, 10.8; Box 12.2}

With *high confidence* the transient climate response (TCR) is positive, *likely* in the range 1°C to 2.5°C and *extremely unlikely* greater than 3°C, based on observed climate change and climate models (see TFE.6 for further details). {10.8; Box 12.2}

The ratio of GMST change to total cumulative anthropogenic carbon emissions is relatively constant and independent of the scenario, but is model dependent, as it is a function of the model cumulative airborne fraction of carbon and the transient climate response. For any given temperature target, higher emissions in earlier decades therefore imply lower emissions by about the same amount later on. The transient climate response to cumulative carbon emission (TCRE) is *likely* between 0.8°C to 2.5°C per 1000 PgC (*high confidence*), for cumulative carbon emissions less than about 2000 PgC until the time at which temperatures peak (see TFE.8 for further details). {10.8, 12.5.4; Box 12.2}

Thematic Focus Elements

TFE.6 | Climate Sensitivity and Feedbacks

The description of climate change as a response to a forcing that is amplified by feedbacks goes back many decades. The concepts of radiative forcing (RF) and climate feedbacks continue to be refined, and limitations are now better understood; for instance, feedbacks may be much faster than the surface warming, feedbacks depend on the type of forcing agent (e.g., greenhouse gas (GHG) vs. solar forcing), or may have intrinsic time scales (associated mainly with vegetation change and ice sheets) of several centuries to millennia. The analysis of physical feedbacks in models and from observations remains a powerful framework that provides constraints on transient future warming for different scenarios, on climate sensitivity and, combined with estimates of carbon cycle feedbacks (see TFE.5), determines the GHG emissions that are compatible with climate stabilization or targets (see TFE.8). {7.1, 9.7.2, 12.5.3; Box 12.2}

The water vapour/lapse rate, albedo and cloud feedbacks are the principal determinants of equilibrium climate sensitivity. All of these feedbacks are assessed to be positive, but with different levels of likelihood assigned ranging from *likely* to *extremely likely*. Therefore, there is *high confidence* that the net feedback is positive and the black body response of the climate to a forcing will therefore be amplified. Cloud feedbacks continue to be the largest uncertainty. The net feedback from water vapour and lapse rate changes together is *extremely likely* positive and approximately doubles the black body response. The mean value and spread of these two processes in climate models are essentially unchanged from the IPCC Fourth Assessment Report (AR4), but are now supported by stronger observational evidence and better process understanding of what determines relative humidity distributions. Clouds respond to climate forcing mechanisms in multiple ways and individual cloud feedbacks can be positive or negative. Key issues include the representation of both deep and shallow cumulus convection, microphysical processes in ice clouds and partial cloudiness that results from small-scale variations of cloud-producing and cloud-dissipating processes. New approaches to diagnosing cloud feedback in General Circulation Models (GCMs) have clarified robust cloud responses, while continuing to implicate low cloud cover as the most important source of intermodel spread in simulated cloud feedbacks. The net radiative feedback due to all cloud types is *likely* positive. This conclusion is reached by considering a plausible range for unknown contributions by processes yet to be accounted for, in addition to those occurring in current climate models. Observations alone do not currently provide a robust, direct constraint, but multiple lines of evidence now indicate positive feedback contributions from changes in both the height of high clouds and the horizontal distribution of clouds. The additional feedback from low cloud amount is also positive in most climate models, but that result is not well understood, nor effectively constrained by observations, so *confidence* in it is *low*. {7.2.4–7.2.6, 9.7.2}

The representation of aerosol–cloud processes in climate models continues to be a challenge. Aerosol and cloud variability at scales significantly smaller than those resolved in climate models, and the subtle responses of clouds to aerosol at those scales, mean that, for the foreseeable future, climate models will continue to rely on parameterizations of aerosol–cloud interactions or other methods that represent subgrid variability. This implies large uncertainties for estimates of the forcings associated with aerosol–cloud interactions. {7.4, 7.5.3, 7.5.4}

Equilibrium climate sensitivity (ECS) and transient climate response (TCR) are useful metrics summarising the global climate system's temperature response to an externally imposed RF. ECS is defined as the equilibrium change in annual mean global mean surface temperature (GMST) following a doubling of the atmospheric carbon dioxide (CO_2) concentration, while TCR is defined as the annual mean GMST change at the time of CO_2 doubling following a linear increase in CO_2 forcing over a period of 70 years (see Glossary). Both metrics have a broader application than these definitions imply: ECS determines the eventual warming in response to stabilisation of atmospheric composition on multi-century time scales, while TCR determines the warming expected at a given time following any steady increase in forcing over a 50- to 100-year time scale. {Box 12.2; 12.5.3}

ECS and TCR can be estimated from various lines of evidence (TFE.6, Figures 1 and 2). The estimates can be based on the values of ECS and TCR diagnosed from climate models, or they can be constrained by analysis of feedbacks in climate models, patterns of mean climate and variability in models compared to observations, temperature fluctuations as reconstructed from paleoclimate archives, observed and modelled short term perturbations of the energy balance like those caused by volcanic eruptions, and the observed surface and ocean temperature trends since pre-industrial. For many applications, the limitations of the forcing-feedback analysis framework and the dependence of feedbacks on time scales and the climate state must be kept in mind. {5.3.1, 5.3.3, 9.7.1–9.7.3, 10.8.1, 10.8.2, 12.5.3; Box 5.2; Table 9.5} *(continued on next page)*

TFE.6 (continued)

Newer studies of constraints on ECS are based on the observed warming since pre-industrial, analysed using simple and intermediate complexity models, improved statistical methods and several different and newer data sets. Together with paleoclimate constraints but without considering the CMIP based evidence these studies show ECS is *likely* between 1.5°C to 4.5°C (*medium confidence*) and *extremely unlikely* less than 1.0°C. {5.3.1, 5.3.3, 10.8.2; Boxes 5.2, 12.2}

Estimates based on Atmosphere–Ocean General Circulation Models (AOGCMs) and feedback analysis indicate a range of 2°C to 4.5°C, with the Coupled Model Intercomparison Project Phase 5 (CMIP5) model mean at 3.2°C, similar to CMIP3. High climate sensitivities are found in some perturbed parameter ensembles models, but recent comparisons of perturbed-physics ensembles against the observed climate find that models with ECS values in the range 3°C to 4°C show the smallest errors for many fields. Relationships between climatological quantities and climate sensitivity are often found within a specific perturbed parameter ensemble model but in many cases the relationship is not robust across perturbed parameter ensembles models from different models or in CMIP3 and CMIP5. The assessed literature suggests that the range of climate sensitivities and transient responses covered by CMIP3 and CMIP5 cannot be narrowed significantly by constraining the models with observations of the mean climate and variability. Studies based on perturbed parameter ensembles models and CMIP3 support the conclusion that a credible representation of the mean climate and variability is very difficult to achieve with ECSs below 2°C. {9.2.2, 9.7.3; Box 12.2}

New estimates of ECS based on reconstructions and simulations of the Last Glacial Maximum (21 ka to 19 ka) show that values below 1°C as well as above 6°C are *very unlikely*. In some models climate sensitivity differs between warm and cold climates because of differences in the representation of cloud feedbacks. Estimates of an Earth system sensitivity including slow feedbacks (e.g., ice sheets or vegetation) are even more difficult to relate to climate sensitivity of the current climate state. The main limitations of ECS estimates from paleoclimate states are uncertainties in proxy data, spatial coverage of the data, uncertainties in some forcings, and structural limitations in models used in model–data comparisons. {5.3, 10.8.2, 12.5.3}

Bayesian methods to constrain ECS or TCR are sensitive to the assumed prior distributions. They can in principle yield narrower estimates by combining constraints from the observed warming trend, volcanic eruptions, model climatology and paleoclimate, and that has been done in some studies, but there is no consensus on how this should be done robustly. This approach is sensitive to the assumptions regarding the independence of the various lines of evidence, the possibility of shared biases in models or feedback estimates and the assumption that each individual line of evidence is unbiased. The combination of different estimates in this assessment is based on expert judgement. {10.8.2; Box 12.2}

Based on the combined evidence from observed climate change including the observed 20th century warming, climate models, feedback analysis and paleoclimate, as discussed above, ECS is *likely* in the range 1.5°C to 4.5°C with *high confidence*. ECS is positive, *extremely unlikely*

(continued on next page)

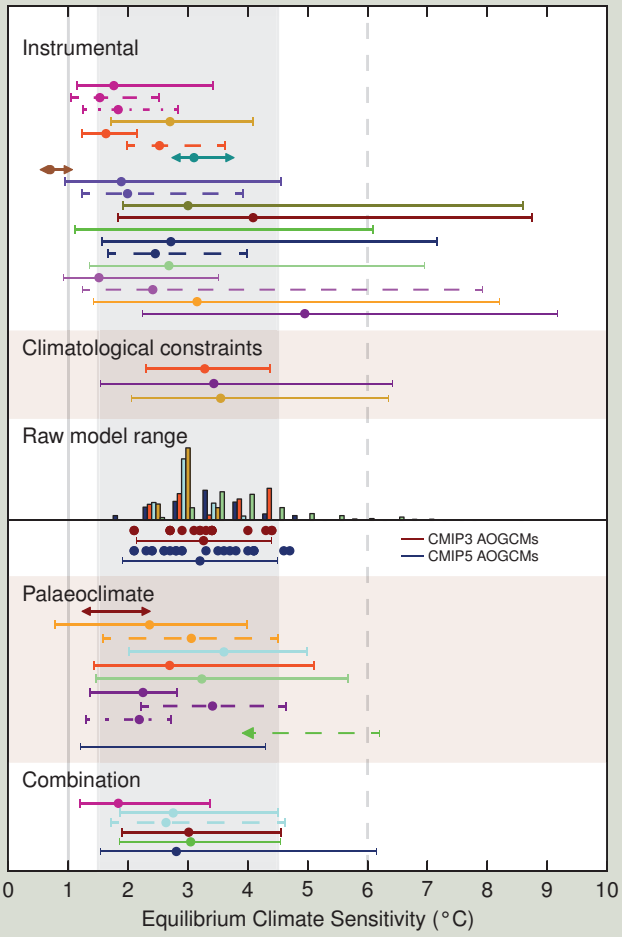

TFE.6, Figure 1 | Probability density functions, distributions and ranges for equilibrium climate sensitivity, based on Figure 10.20b plus climatological constraints shown in IPCC AR4 (Box AR4 10.2 Figure 1), and results from CMIP5 (Table 9.5). The grey shaded range marks the *likely* 1.5°C to 4.5°C range, grey solid line the *extremely unlikely* less than 1°C, the grey dashed line the *very unlikely* greater than 6°C. See Figure 10.20b and Chapter 10 Supplementary Material for full caption and details. {Box 12.2, Figure 1}

TFE.6 (continued)

less than 1°C (*high confidence*), and *very unlikely* greater than 6°C (*medium confidence*). The tails of the ECS distribution are now better understood. Multiple lines of evidence provide *high confidence* that an ECS value less than 1°C is *extremely unlikely*. The upper limit of the *likely* range is unchanged compared to AR4. The lower limit of the *likely* range of 1.5°C is less than the lower limit of 2°C in AR4. This change reflects the evidence from new studies of observed temperature change, using the extended records in atmosphere and ocean. These studies suggest a best fit to the observed surface and ocean warming for ECS values in the lower part of the *likely* range. Note that these studies are not purely observational, because they require an estimate of the response to RF from models. In addition, the uncertainty in ocean heat uptake remains substantial. Accounting for short-term variability in simple models remains challenging, and it is important not to give undue weight to any short time period which might be strongly affected by internal variability. On the other hand, AOGCMs with observed climatology with ECS values in the upper part of the 1.5 to 4.5°C range show very good agreement with observed climatology, but the simulation of key feedbacks like clouds remains challenging in those models. The estimates from the observed warming, paleoclimate, and from climate models are consistent within their uncertainties, each is supported by many studies and multiple data sets, and in combination they provide *high confidence* for the assessed *likely* range. Even though this assessed range is similar to previous reports, confidence today is much higher as a result of high quality and longer observational records with a clearer anthropogenic signal, better process understanding, more and better understood evidence from paleoclimate reconstructions, and better climate models with higher resolution that capture many more processes more realistically. All these lines of evidence individually support the assessed *likely* range of 1.5°C to 4.5°C. {3.2, 9.7.3, 10.8; Boxes 9.2, 13.1}

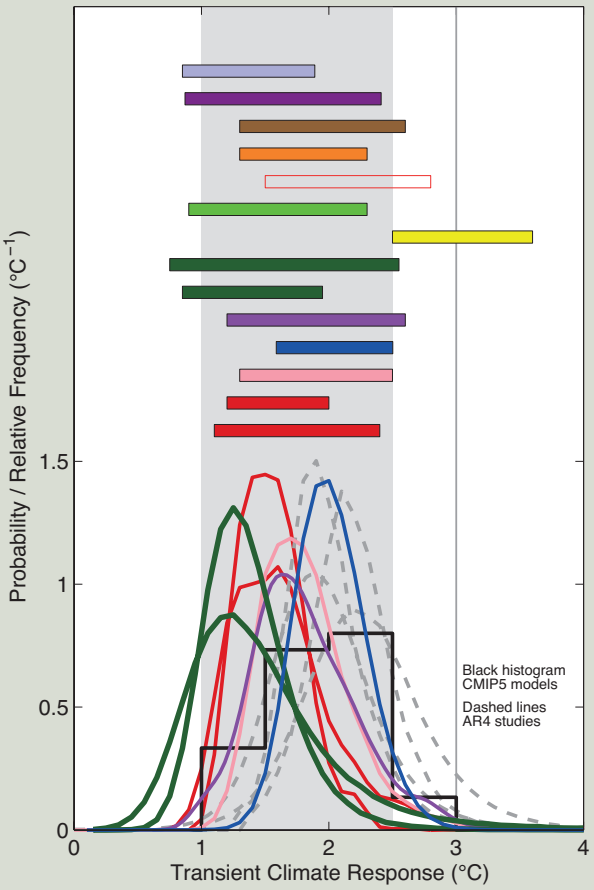

TFE.6, Figure 2 | Probability density functions, distributions and ranges (5 to 95%) for the transient climate response from different studies, based on Figure 10.20a, and results from CMIP5 (black histogram, Table 9.5). The grey shaded range marks the *likely* 1°C to 2.5°C range, the grey solid line marks the *extremely unlikely* greater than 3°C. See Figure 10.20a and Chapter 10 Supplementary Material for full caption and details. {Box 12.2, Figure 2}

On time scales of many centuries and longer, additional feedbacks with their own intrinsic time scales (e.g., vegetation, ice sheets) may become important but are not usually modelled in AOGCMs. The resulting equilibrium temperature response to a doubling of CO_2 on millennial time scales or Earth system sensitivity is less well constrained but *likely* to be larger than ECS, implying that lower atmospheric CO_2 concentrations are compatible with limiting warming to below a given temperature level. These slow feedbacks are less likely to be proportional to global mean temperature change, implying that Earth system sensitivity changes over time. Estimates of Earth system sensitivity are also difficult to relate to climate sensitivity of the current climate state. {5.3.3, 10.8.2, 12.5.3}

For scenarios of increasing RF, TCR is a more informative indicator of future climate change than ECS. This assessment concludes with *high confidence* that the TCR is *likely* in the range 1°C to 2.5°C, close to the estimated 5 to 95% range of CMIP5 (1.2°C to 2.4°C), is positive and *extremely unlikely* greater than 3°C. As with the ECS, this is an expert-assessed range, supported by several different and partly independent lines of evidence, each based on multiple studies, models and data sets. TCR is estimated from the observed global changes in surface temperature, ocean heat uptake and RF including detection/attribution studies identifying the response patterns to increasing GHG concentrations, and the results of CMIP3 and CMIP5. Estimating TCR suffers from fewer difficulties in terms of state- or time-dependent feedbacks, and is less affected by uncertainty as to how much energy is taken up by the

(continued on next page)

TFE.6 (continued)

ocean. Unlike ECS, the ranges of TCR estimated from the observed warming and from AOGCMs agree well, increasing our confidence in the assessment of uncertainties in projections over the 21st century.

The assessed ranges of ECS and TCR are largely consistent with the observed warming, the estimated forcing and the projected future warming. In contrast to AR4, no best estimate for ECS is given because of a lack of agreement on the best estimate across lines of evidence and studies and an improved understanding of the uncertainties in estimates based on the observed warming. Climate models with ECS values in the upper part of the *likely* range show very good agreement with observed climatology, whereas estimates derived from observed climate change tend to best fit the observed surface and ocean warming for ECS values in the lower part of the *likely* range. In estimates based on the observed warming the most likely value is sensitive to observational and model uncertainties, internal climate variability and to assumptions about the prior distribution of ECS. In addition, "best estimate" and "most likely value" are defined in various ways in different studies. {9.7.1, 10.8.1, 12.5.3; Table 9.5}

TS.5.4 Near-term Climate Change

Near-term decadal climate prediction provides information not available from existing seasonal to interannual (months to a year or two) predictions or from long-term (mid 21st century and beyond) climate change projections. Prediction efforts on seasonal to interannual time scales require accurate estimates of the initial climate state with less focus extended to changes in external forcing[12], whereas long-term climate projections rely more heavily on estimations of external forcing with little reliance on the initial state of internal variability. Estimates of near-term climate depend on the committed warming (caused by the inertia of the oceans as they respond to historical external forcing) the time evolution of internally generated climate variability, and the future path of external forcing. Near-term predictions out to about a decade (Figure TS.13) depend more heavily on an accurate depiction of the internally generated climate variability. {11.1, 12, 14}

Further near-term warming from past emissions is unavoidable owing to thermal inertia of the oceans. This warming will be increased by ongoing emissions of GHGs over the near term, and the climate observed in the near term will also be strongly influenced by the internally generated variability of the climate system. Previous IPCC Assessments only described climate-change projections wherein the externally forced component of future climate was included but no attempt was made to initialize the internally generated climate variability. Decadal climate predictions, on the other hand, are intended to predict both the externally forced component of future climate change, and the internally generated component. Near-term predictions do not provide detailed information of the evolution of weather. Instead they can provide estimated changes in the time evolution of the statistics of near-term climate. {11.1, 11.2.2; Box 11.1; FAQ 11.1}

Retrospective prediction experiments have been used to assess forecast quality. There is *high confidence* that the retrospective prediction experiments for forecast periods of up to 10 years exhibit positive skill when verified against observations over large regions of the planet and of the global mean. Observation-based initialization of the forecasts contributes to the skill of predictions of annual mean temperature for the first couple of years and to the skill of predictions of the GMST and the temperature over the North Atlantic, regions of the South Pacific and the tropical Indian Ocean up to 10 years (*high confidence*) partly due to a correction of the forced response. Probabilistic temperature predictions are statistically reliable (see Section 11.2.3 for definition of reliability) owing to the correct representation of global trends, but still unreliable at the regional scale when probabilities are computed from the multi-model ensemble. Predictions initialized over 2000–2005 improve estimates of the recent global mean temperature hiatus. Predictions of precipitation over continental areas with large forced trends also exhibit positive skill. {11.2.2, 11.2.3; Box 9.2}

TS.5.4.1 Projected Near-term Changes in Climate

Projections of near-term climate show small sensitivity to GHG scenarios compared to model spread, but substantial sensitivity to uncertainties in aerosol emissions, especially on regional scales and for hydrological cycle variables. In some regions, the local and regional responses in precipitation and in mean and extreme temperature to land use change will be larger than those due to large-scale GHGs and aerosol forcing. These scenarios presume that there are no major volcanic eruptions and that anthropogenic aerosol emissions are rapidly reduced during the near term. {11.3.1, 11.3.2, 11.3.6}

TS.5.4.2 Projected Near-term Changes in Temperature

In the absence of major volcanic eruptions—which would cause significant but temporary cooling—and, assuming no significant future long-term changes in solar irradiance, it is *likely* that the GMST anomaly for the period 2016–2035, relative to the reference period of 1986–2005 will be in the range 0.3°C to 0.7°C (*medium confidence*). This is based on multiple lines of evidence. This range is consistent

[12] Seasonal-to-interannual predictions typically include the impact of external forcing.

with the range obtained by using CMIP5 5 to 95% model trends for 2012–2035. It is also consistent with the CMIP5 5 to 95% range for all four RCP scenarios of 0.36°C to 0.79°C, using the 2006–2012 reference period, after the upper and lower bounds are reduced by 10% to take into account the evidence that some models may be too sensitive to anthropogenic forcing (see Table TS.1 and Figure TS.14). {11.3.6}

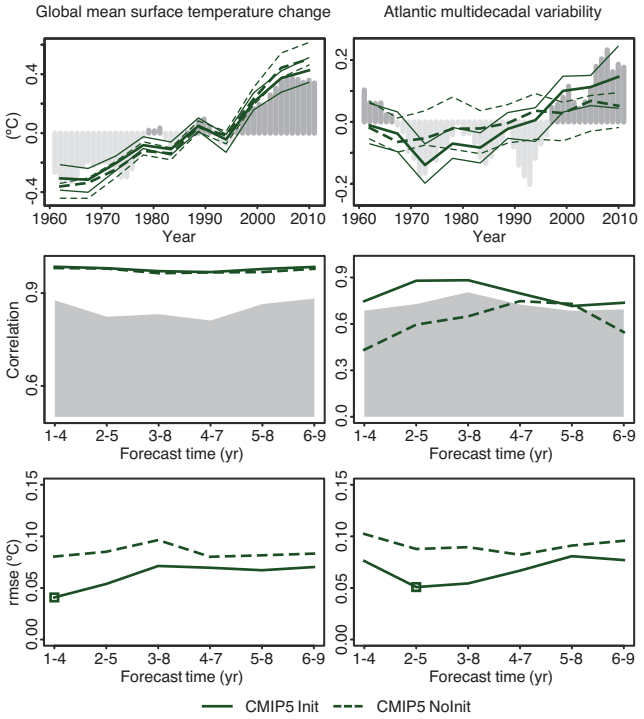

Figure TS.13 | Decadal prediction forecast quality of several climate indices. (Top row) Time series of the 2- to 5-year average ensemble mean initialized hindcast anomalies and the corresponding non-initialized experiments for three climate indices: global mean surface temperature (GMST, left) and the Atlantic Multi-decadal Variability (AMV, right). The observational time series, Goddard Institute of Space Studies Goddard Institute for Space Studies Surface Temperature Analysis (GISTEMP) global mean temperature and Extended Reconstructed Sea Surface Tempearture (ERSST) for the AMV, are represented with dark grey (positive anomalies) and light grey (negative anomalies) vertical bars, where a 4-year running mean has been applied for consistency with the time averaging of the predictions. Predicted time series are shown for the CMIP5 Init (solid) and NoInit (dotted) simulations with hindcasts started every 5 years over the period 1960–2005. The lower and upper quartile of the multi-model ensemble are plotted using thin lines. The AMV index was computed as the sea surface temperature (SST) anomalies averaged over the region Equator to 60ºN and 80ºW to 0ºW minus the SST anomalies averaged over 60ºS to 60ºN. Note that the vertical axes are different for each time series. (Middle row) Correlation of the ensemble mean prediction with the observational reference along the forecast time for 4-year averages of the three sets of CMIP5 hindcasts for Init (solid) and NoInit (dashed). The one-sided 95% confidence level with a *t* distribution is represented in grey. The effective sample size has been computed taking into account the autocorrelation of the observational time series. A two-sided *t* test (where the effective sample size has been computed taking into account the autocorrelation of the observational time series) has been used to test the differences between the correlation of the initialized and non-initialized experiments, but no differences were found statistically significant with a confidence equal or higher than 90%. (Bottom row) Root mean square error (RMSE) of the ensemble mean prediction along the forecast time for 4-year averages of the CMIP5 hindcasts for Init (solid) and NoInit (dashed). A two-sided *F* test (where the effective sample size has been computed taking into account the autocorrelation of the observational time series) has been used to test the ratio between the RMSE of the Init and NoInit, and those forecast times with differences statistically significant with a confidence equal or higher than 90% are indicated with an open square. {Figure 11.3}

Higher concentrations of GHGs and lower amounts of sulphate aerosol lead to greater warming. In the near-term, differences in global mean surface air temperature across RCP scenarios for a single climate model are typically smaller than across climate models for a single RCP scenario. In 2030, the CMIP5 ensemble median values for global mean temperature differ by at most 0.2°C between the RCP scenarios, whereas the model spread (defined as the 17 to 83% range) for each RCP is around 0.4°C. The inter-scenario spread increases in time and by 2050 is comparable to the model spread. Regionally, the largest differences in surface air temperature between RCP scenarios are found in the Arctic. {11.3.2. 11.3.6}

The projected warming of global mean temperatures implies *high confidence* that new levels of warming relative to 1850-1900 mean climate will be crossed, particularly under higher GHG emissions scenarios. Relative to a reference period of 1850–1900, under RCP4.5 or RCP6.0, it is *more likely than not* that the mean GMST for the period 2016–2035 will be more than 1°C above the mean for 1850–1900, and *very unlikely* that it will be more than 1.5°C above the 1850–1900 mean (*medium confidence*). {11.3.6}

A future volcanic eruption similar in size to the 1991 eruption of Mt Pinatubo would cause a rapid drop in global mean surface air temperature of about 0.5°C in the following year, with recovery over the next few years. Larger eruptions, or several eruptions occurring close together in time, would lead to larger and more persistent effects. {11.3.6}

Possible future changes in solar irradiance could influence the rate at which GMST increases, but there is *high confidence* that this influence will be small in comparison to the influence of increasing concentrations of GHGs in the atmosphere. {11.3.6}

The spatial patterns of near-term warming projected by the CMIP5 models following the RCP scenarios (Figure TS.15) are broadly consistent with the AR4. It is *very likely* that anthropogenic warming of surface air temperature over the next few decades will proceed more rapidly over land areas than over oceans, and it is *very likely* that the anthropogenic warming over the Arctic in winter will be greater than the global mean warming, consistent with the AR4. Relative to background levels of internally generated variability there is *high confidence* that the anthropogenic warming relative to the reference period is expected to be larger in the tropics and subtropics than in mid-latitudes. {11.3.2}

It is *likely* that in the next decades the frequency of warm days and warm nights will increase in most land regions, while the frequency of cold days and cold nights will decrease. Models also project increases in the duration, intensity and spatial extent of heat waves and warm spells for the near term. These changes may proceed at a different rate than the mean warming. For example, several studies project that European high-percentile summer temperatures are projected to warm faster than mean temperatures (see also TFE.9). {11.3.2}

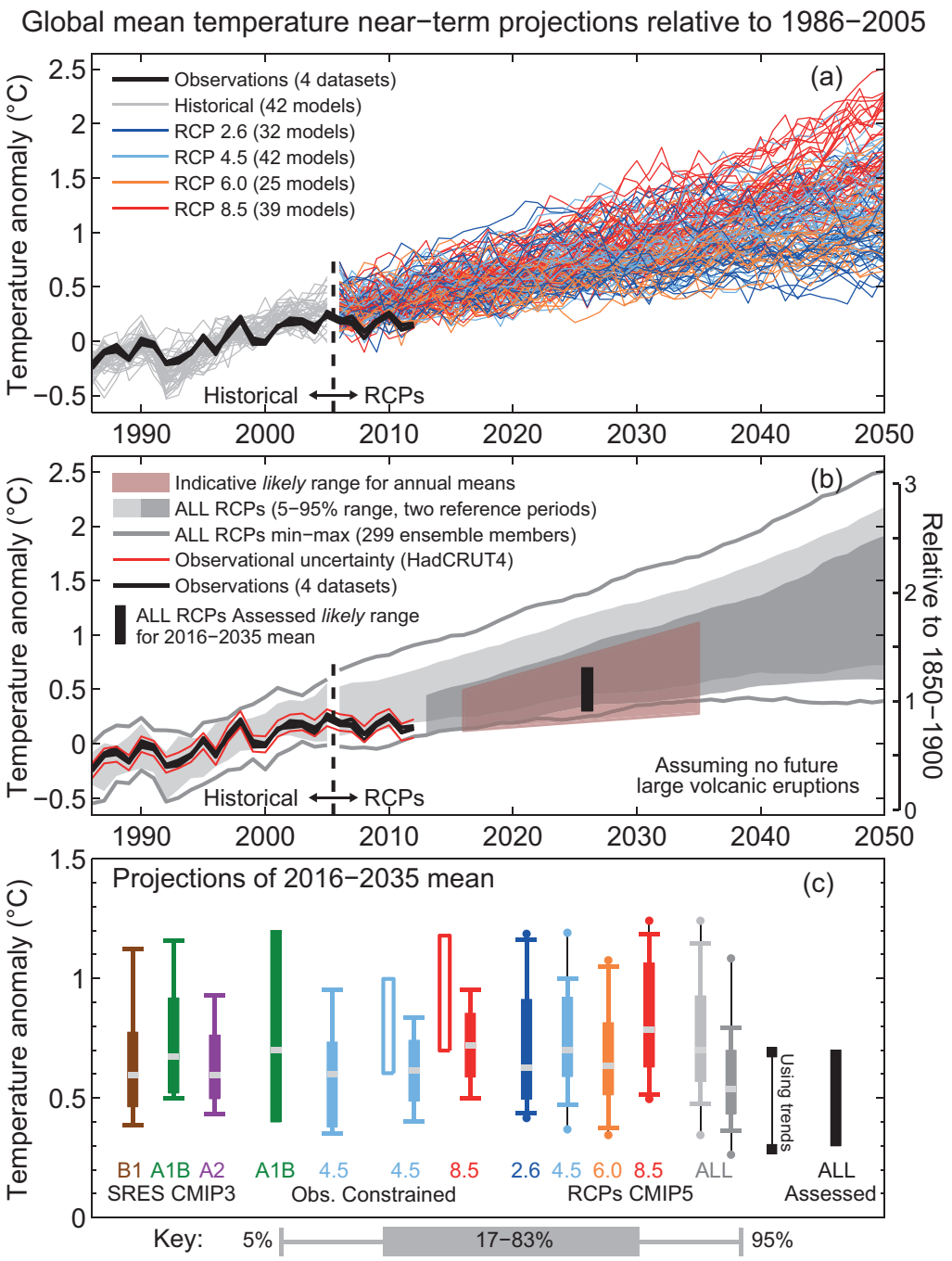

Figure TS.14 | Synthesis of near-term projections of global mean surface air temperature (GMST). (a) Projections of annual mean GMST 1986–2050 (anomalies relative to 1986–2005) under all RCPs from CMIP5 models (grey and coloured lines, one ensemble member per model), with four observational estimates (Hadley Centre/Climatic Research Unit gridded surface temperature data set 4 (HadCRUT4), European Centre for Medium Range Weather Forecasts (ECMWF) interim re-analysis of the global atmosphere and surface conditions (ERA-Interim), Goddard Institute for Space Studies Surface Temperature Analysis (GISTEMP), National Oceanic and Atmospheric Administration (NOAA)) for the period 1986–2012 (black lines). (b) As (a) but showing the 5 to 95% range of annual mean CMIP5 projections (using one ensemble member per model) for all RCPs using a reference period of 1986–2005 (light grey shade) and all RCPs using a reference period of 2006–2012, together with the observed anomaly for (2006–2012) minus (1986–2005) of 0.16°C (dark grey shade). The percentiles for 2006 onwards have been smoothed with a 5-year running mean for clarity. The maximum and minimum values from CMIP5 using all ensemble members and the 1986–2005 reference period are shown by the grey lines (also smoothed). Black lines show annual mean observational estimates. The red shaded region shows the indicative *likely* range for annual mean GMST during the period 2016–2035 based on the 'ALL RCPs Assessed' *likely* range for the 20-year mean GMST anomaly for 2016–2035, which is shown as a black bar in both (b) and (c) (see text for details). The temperature scale relative to 1850-1900 mean climate on the right-hand side assumes a warming of GMST prior to 1986–2005 of 0.61°C estimated from HadCRUT4. (c) A synthesis of projections for the mean GMST anomaly for 2016–2035 relative to 1986–2005. The box and whiskers represent the 66% and 90% ranges. Shown are: unconstrained SRES CMIP3 and RCP CMIP5 projections; observationally constrained projections for the SRES A1B and, the RCP4.5 and 8.5 scenarios; unconstrained projections for all four RCP scenarios using two reference periods as in (b) (light grey and dark grey shades), consistent with (b); 90% range estimated using CMIP5 trends for the period 2012–2035 and the observed GMST anomaly for 2012; an overall *likely* (>66%) assessed range for all RCP scenarios. The dots for the CMIP5 estimates show the maximum and minimum values using all ensemble members. The medians (or maximum likelihood estimate; green filled bar) are indicated by a grey band. (Adapted from Figure 11.25.) See Section 11.3.6 for details. {Figure 11.25}

TS.5.4.3 Projected Near-term Changes in the Water Cycle

Zonal mean precipitation will *very likely* increase in high and some of the mid latitudes, and will *more likely than not* decrease in the subtropics. At more regional scales precipitation changes may be dominated by a combination of natural internal variability, volcanic forcing and anthropogenic aerosol effects. {11.3.2}

Over the next few decades increases in near-surface specific humidity are *very likely*. It is *likely* that there will be increases in evaporation in many regions. There is *low confidence* in projected changes in soil moisture and surface runoff. {11.3.2}

In the near term, it is *likely* that the frequency and intensity of heavy precipitation events will increase over land. These changes are primarily driven by increases in atmospheric water vapour content, but also affected by changes in atmospheric circulation. The impact of anthropogenic forcing at regional scales is less obvious, as regional-scale changes are strongly affected by natural variability and also depend on the course of future aerosol emissions, volcanic forcing and land use changes (see also TFE.9). {11.3.2}

TS.5.4.4 Projected Near-term Changes in Atmospheric Circulation

Internally generated climate variability and multiple RF agents (e.g., volcanoes, GHGs, ozone and anthropogenic aerosols) will all contribute to near-term changes in the atmospheric circulation. For example, it is *likely* that the annual mean Hadley Circulation and the SH mid-latitude westerlies will shift poleward, while it is *likely* that the projected recovery of stratospheric ozone and increases in GHG concentrations will have counteracting impacts on the width of the Hadley Circulation and the meridional position of the SH storm track. Therefore it is *unlikely* that they will continue to expand poleward as rapidly as in recent decades. {11.3.2}

There is *low confidence* in near-term projections of the position and strength of NH storm tracks. Natural variations are larger than the projected impact of GHGs in the near term. {11.3.2}

There is *low confidence* in basin-scale projections of changes in intensity and frequency of tropical cyclones in all basins to the mid-21st century. This *low confidence* reflects the small number of studies exploring near-term tropical cyclone activity, the differences across published projections of tropical cyclone activity, and the large role for natural variability. There is *low confidence* in near-term projections for increased tropical cyclone intensity in the Atlantic; this projection is in part due to projected reductions in aerosol loading. {11.3.2}

TS.5.4.5 Projected Near-term Changes in the Ocean

It is *very likely* that globally averaged surface and vertically averaged ocean temperatures will increase in the near-term. In the absence of multiple major volcanic eruptions, it is *very likely* that globally averaged surface and depth-averaged temperatures averaged for 2016–2035 will be warmer than those averaged over 1986–2005. {11.3.3}

It is *likely* that salinity will increase in the tropical and (especially) subtropical Atlantic, and decrease in the western tropical Pacific over the next few decades. Overall, it is *likely* that there will be some decline in the Atlantic Meridional Overturning Circulation by 2050 (*medium confidence*). However, the rate and magnitude of weakening is very uncertain and decades when this circulation increases are also to be expected. {11.3.3}

TS.5.4.6 Projected Near-term Changes in the Cryosphere

A nearly ice-free Arctic Ocean (sea ice extent less than 10^6 km^2 for at least five consecutive years) in September is *likely* before mid-century under RCP8.5 (*medium confidence*). This assessment is based on a subset of models that most closely reproduce the climatological mean state and 1979 to 2012 trend of Arctic sea ice cover. It is *very likely* that there will be further shrinking and thinning of Arctic sea ice cover, and decreases of northern high-latitude spring time snow cover and near surface permafrost as GMST rises (Figures TS.17 and TS.18). There is *low confidence* in projected near-term decreases in the Antarctic sea ice extent and volume. {11.3.4}

TS.5.4.7 Possibility of Near-term Abrupt Changes in Climate

There are various mechanisms that could lead to changes in global or regional climate that are abrupt by comparison with rates experienced in recent decades. The likelihood of such changes is generally lower for the near term than for the long term. For this reason the relevant mechanisms are primarily assessed in the TS.5 sections on long-term changes and in TFE.5. {11.3.4}

TS.5.4.8 Projected Near-term Changes in Air Quality

The range in projections of air quality (O_3 and $PM_{2.5}$ in surface air) is driven primarily by emissions (including CH_4), rather than by physical climate change (*medium confidence*). The response of air quality to climate-driven changes is more uncertain than the response to emission-driven changes (*high confidence*). Globally, warming decreases background surface O_3 (*high confidence*). High CH_4 levels (such as RCP8.5 and SRES A2) can offset this decrease, raising 2100 background surface O_3 on average by about 8 ppb (25% of current levels) relative to scenarios with small CH_4 changes (such as RCP4.5 and RCP6.0) (*high confidence*). On a continental scale, projected air pollution levels are lower under the new RCP scenarios than under the SRES scenarios because the SRES did not incorporate air quality legislation (*high confidence*). {11.3.5, 11.3.5.2; Figures 11.22 and 11.23ab, AII.4.2, AII.7.1–AII.7.4}

Observational and modelling evidence indicates that, all else being equal, locally higher surface temperatures in polluted regions will trigger regional feedbacks in chemistry and local emissions that will increase peak levels of O_3 and $PM_{2.5}$ (*medium confidence*). Local emissions combined with background levels and with meteorological conditions conducive to the formation and accumulation of pollution are known to produce extreme pollution episodes on local and regional scales. There is *low confidence* in projecting changes in meteorological blocking associated with these extreme episodes. For $PM_{2.5}$, climate change may alter natural aerosol sources (wildfires, wind-lofted

dust, biogenic precursors) as well as precipitation scavenging, but no confidence level is attached to the overall impact of climate change on $PM_{2.5}$ distributions. {11.3.5, 11.3.5.2; Box 14.2}

TS.5.5 Long-term Climate Change

TS.5.5.1 Projected Long-term Changes in Global Temperature

Global mean temperatures will continue to rise over the 21st century under all of the RCPs. From around the mid-21st century, the rate of global warming begins to be more strongly dependent on the scenario (Figure TS.15). {12.4.1}

Under the assumptions of the concentration-driven RCPs, GMSTs for 2081–2100, relative to 1986–2005 will *likely* be in the 5 to 95% range of the CMIP5 models; 0.3°C to 1.7°C (RCP2.6), 1.1 to 2.6°C (RCP4.5), 1.4°C to 3.1°C (RCP6.0), 2.6°C to 4.8°C (RCP8.5) (see Table TS.1). With *high confidence*, the 5 to 95% range of CMIP5 is assessed as *likely* rather than *very likely* based on the assessment of TCR (see TFE.6). The 5 to 95% range of CMIP5 for global mean temperature change is also assessed as *likely* for mid-21st century, but only with *medium confidence*. With respect to 1850–1900 mean conditions, global temperatures averaged in the period 2081–2100 are projected to *likely* exceed 1.5°C above 1850–1900 values for RCP4.5, RCP6.0 and RCP8.5 (*high confidence*) and are *likely* to exceed 2°C above 1850–1900 values for RCP6.0 and RCP8.5 (*high confidence*). Temperature change above 2°C relative to 1850–1900 under RCP2.6 is *unlikely* (*medium confidence*). Warming above 4°C by 2081–2100 is *unlikely* in all RCPs (*high confidence*) except for RCP8.5, where it is *about as likely as not* (*medium confidence*). {12.4.1; Tables 12.2, 12.3}

TS.5.5.2 Projected Long-term Changes in Regional Temperature

There is *very high confidence* that globally averaged changes over land will exceed changes over the ocean at the end of the 21st century by a factor that is *likely* in the range 1.4 to 1.7. In the absence of a strong reduction in the Atlantic Meridional Overturning, the Arctic region is projected to warm most (*very high confidence*) (Figure TS.15). As

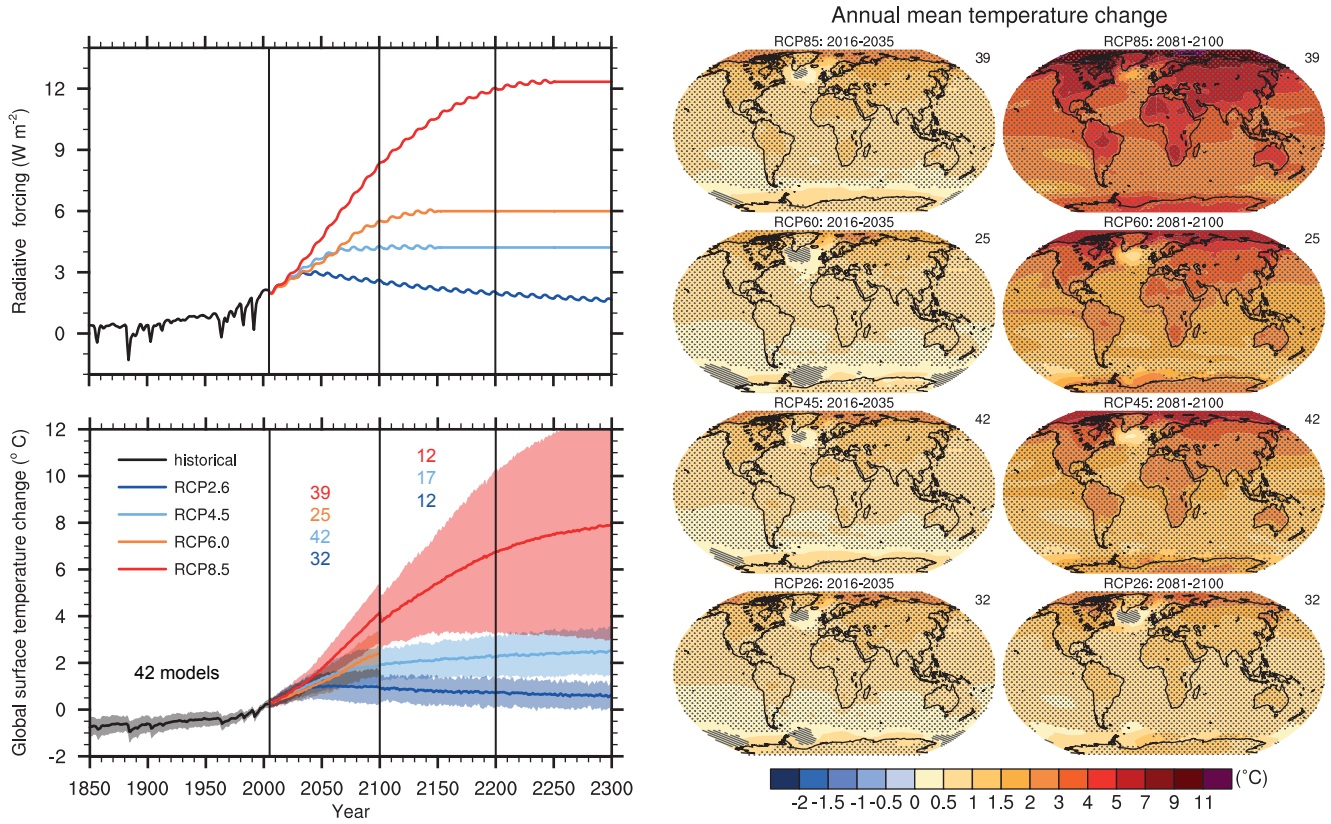

Figure TS.15 | (Top left) Total global mean radiative forcing for the four RCP scenarios based on the Model for the Assessment of Greenhouse-gas Induced Climate Change (MAGICC) energy balance model. Note that the actual forcing simulated by the CMIP5 models differs slightly between models. (Bottom left) Time series of global annual mean surface air temperature anomalies (relative to 1986–2005) from CMIP5 concentration-driven experiments. Projections are shown for each RCP for the multi-model mean (solid lines) and ±1.64 standard deviation (5 to 95%) across the distribution of individual models (shading), based on annual means. The 1.64 standard deviation range based on the 20 yr averages 2081–2100, relative to 1986–2005, are interpreted as *likely* changes for the end of the 21st century. Discontinuities at 2100 are due to different numbers of models performing the extension runs beyond the 21st century and have no physical meaning. Numbers in the same colours as the lines indicate the number of different models contributing to the different time periods. Maps: Multi-model ensemble average of annual mean surface air temperature change (compared to 1986–2005 base period) for 2016–2035 and 2081–2100, for RCP2.6, 4.5, 6.0 and 8.5. Hatching indicates regions where the multi-model mean signal is less than one standard deviation of internal variability. Stippling indicates regions where the multi-model mean signal is greater than two standard deviations of internal variability and where 90% of the models agree on the sign of change. The number of CMIP5 models used is indicated in the upper right corner of each panel. Further detail regarding the related Figures SPM.7a and SPM.8.a is given in the TS Supplementary Material. {Box 12.1; Figures 12.4, 12.5, 12.11; Annex I}

Table TS.1 | Projected change in global mean surface air temperature and global mean sea level rise for the mid- and late 21st century relative to the reference period of 1986–2005. {12.4.1; Tables 12.2,13.5}

		2046–2065		2081–2100	
	Scenario	**Mean**	***Likely* range[c]**	**Mean**	***Likely* range[c]**
Global Mean Surface Temperature Change (°C)[a]	RCP2.6	1.0	0.4 to 1.6	1.0	0.3 to 1.7
	RCP4.5	1.4	0.9 to 2.0	1.8	1.1 to 2.6
	RCP6.0	1.3	0.8 to 1.8	2.2	1.4 to 3.1
	RCP8.5	2.0	1.4 to 2.6	3.7	2.6 to 4.8
	Scenario	**Mean**	***Likely* range[d]**	**Mean**	***Likely* range[d]**
Global Mean Sea Level Rise (m)[b]	RCP2.6	0.24	0.17 to 0.32	0.40	0.26 to 0.55
	RCP4.5	0.26	0.19 to 0.33	0.47	0.32 to 0.63
	RCP6.0	0.25	0.18 to 0.32	0.48	0.33 to 0.63
	RCP8.5	0.30	0.22 to 0.38	0.63	0.45 to 0.82

Notes:

[a] Based on the CMIP5 ensemble; anomalies calculated with respect to 1986–2005. Using HadCRUT4 and its uncertainty estimate (5–95% confidence interval), the observed warming to the reference period 1986–2005 is 0.61 [0.55 to 0.67] °C from 1850–1900, and 0.11 [0.09 to 0.13] °C from 1980–1999, the reference period for projections used in AR4. *Likely* ranges have not been assessed here with respect to earlier reference periods because methods are not generally available in the literature for combining the uncertainties in models and observations. Adding projected and observed changes does not account for potential effects of model biases compared to observations, and for natural internal variability during the observational reference period. {2.4; 11.2; Tables 12.2 and 12.3}

[b] Based on 21 CMIP5 models; anomalies calculated with respect to 1986–2005. Where CMIP5 results were not available for a particular AOGCM and scenario, they were estimated as explained in Chapter 13, Table 13.5. The contributions from ice sheet rapid dynamical change and anthropogenic land water storage are treated as having uniform probability distributions, and as largely independent of scenario. This treatment does not imply that the contributions concerned will not depend on the scenario followed, only that the current state of knowledge does not permit a quantitative assessment of the dependence. Based on current understanding, only the collapse of marine-based sectors of the Antarctic ice sheet, if initiated, could cause global mean sea level to rise substantially above the *likely* range during the 21st century. There is *medium confidence* that this additional contribution would not exceed several tenths of a metre of sea level rise during the 21st century.

[c] Calculated from projections as 5–95% model ranges. These ranges are then assessed to be *likely* ranges after accounting for additional uncertainties or different levels of confidence in models. For projections of global mean surface temperature change in 2046–2065 *confidence* is *medium*, because the relative importance of natural internal variability, and uncertainty in non-greenhouse gas forcing and response, are larger than for 2081–2100. The *likely* ranges for 2046–2065 do not take into account the possible influence of factors that lead to the assessed range for near-term (2016–2035) global mean surface temperature change that is lower than the 5–95% model range, because the influence of these factors on longer term projections has not been quantified due to insufficient scientific understanding. {11.3}

[d] Calculated from projections as 5–95% model ranges. These ranges are then assessed to be *likely* ranges after accounting for additional uncertainties or different levels of confidence in models. For projections of global mean sea level rise *confidence* is *medium* for both time horizons.

GMST rises, the pattern of atmospheric zonal mean temperatures show warming throughout the troposphere and cooling in the stratosphere, consistent with previous assessments. The consistency is especially clear in the tropical upper troposphere and the northern high latitudes. {12.4.3; Box 5.1}

It is *virtually certain* that, in most places, there will be more hot and fewer cold temperature extremes as global mean temperatures increase. These changes are expected for events defined as extremes on both daily and seasonal time scales. Increases in the frequency, duration and magnitude of hot extremes along with heat stress are expected; however, occasional cold winter extremes will continue to occur. Twenty-year return values of low-temperature events are projected to increase at a rate greater than winter mean temperatures in most regions, with the largest changes in the return values of low temperatures at high latitudes. Twenty-year return values for high-temperature events are projected to increase at a rate similar to or greater than the rate of increase of summer mean temperatures in most regions. Under RCP8.5 it is *likely* that, in most land regions, a current 20-year high-temperature event will occur more frequently by the end of the 21st century (at least doubling its frequency, but in many regions becoming an annual or 2-year event) and a current 20-year low-temperature event will become exceedingly rare (See also TFE.9). {12.4.3}

Models simulate a decrease in cloud amount in the future over most of the tropics and mid-latitudes, due mostly to reductions in low clouds. Changes in marine boundary layer clouds are most uncertain. Increases in cloud fraction and cloud optical depth and therefore cloud reflection are simulated in high latitudes, poleward of 50°. {12.4.3}

TS.5.5.3 Projected Long-term Changes in Atmospheric Circulation

Mean sea level pressure is projected to decrease in high latitudes and increase in the mid-latitudes as global temperatures rise. In the tropics, the Hadley and Walker Circulations are *likely* to slow down. Poleward shifts in the mid-latitude jets of about 1 to 2 degrees latitude are *likely* at the end of the 21st century under RCP8.5 in both hemispheres (*medium confidence*), with weaker shifts in the NH. In austral summer, the additional influence of stratospheric ozone recovery in the SH opposes changes due to GHGs there, though the net response varies strongly across models and scenarios. Substantial uncertainty and thus *low confidence* remains in projecting changes in NH storm tracks, especially for the North Atlantic basin. The Hadley Cell is *likely* to widen, which translates to broader tropical regions and a poleward encroachment of subtropical dry zones. In the stratosphere, the Brewer–Dobson circulation is *likely* to strengthen. {12.4.4}

TS.5.5.4 Projected Long-term Changes in the Water Cycle

On the planetary scale, relative humidity is projected to remain roughly constant, but specific humidity to increase in a warming climate. The projected differential warming of land and ocean promotes changes in atmospheric moistening that lead to small decreases in near-surface relative humidity over most land areas with the notable exception of parts of tropical Africa (*medium confidence*) (see TFE.1, Figure 1). {12.4.5}

It is *virtually certain* that, in the long term, global precipitation will increase with increased GMST. Global mean precipitation will increase at a rate per °C smaller than that of atmospheric water vapour. It will *likely* increase by 1 to 3% $°C^{-1}$ for scenarios other than RCP2.6. For RCP2.6 the range of sensitivities in the CMIP5 models is 0.5 to 4% $°C^{-1}$ at the end of the 21st century. {7.6.2, 7.6.3, 12.4.1}

Changes in average precipitation in a warmer world will exhibit substantial spatial variation under RCP8.5. Some regions will experience increases, other regions will experience decreases and yet others will not experience significant changes at all (see Figure TS.16). There is *high confidence* that the contrast of annual mean precipitation between dry and wet regions and that the contrast between wet and dry seasons will increase over most of the globe as temperatures increase. The general pattern of change indicates that high latitudes are *very likely* to experience greater amounts of precipitation due to the increased specific humidity of the warmer troposphere as well as increased transport of water vapour from the tropics by the end of this century under the RCP8.5 scenario. Many mid-latitude and subtropical arid and semi-arid regions will *likely* experience less precipitation and many moist mid-latitude regions will *likely* experience more precipitation by the end of this century under the RCP8.5 scenario. Maps of precipitation change for the four RCP scenarios are shown in Figure TS.16. {12.4.2, 12.4.5}

Globally, for short-duration precipitation events, a shift to more intense individual storms and fewer weak storms is *likely* as temperatures increase. Over most of the mid-latitude land masses and over wet tropical regions, extreme precipitation events will *very likely* be more intense and more frequent in a warmer world. The global average sensitivity of the 20-year return value of the annual maximum daily precipitation ranges from 4% $°C^{-1}$ of local temperature increase (average of CMIP3 models) to 5.3% $°C^{-1}$ of local temperature increase (average of CMIP5 models), but regionally there are wide variations. {12.4.2, 12.4.5}

Annual surface evaporation is projected to increase as global temperatures rise over most of the ocean and is projected to change over land following a similar pattern as precipitation. Decreases in annual runoff are *likely* in parts of southern Europe, the Middle East and southern Africa by the end of this century under the RCP8.5 scenario. Increases in annual runoff are *likely* in the high northern latitudes corresponding to large increases in winter and spring precipitation by the end of the 21st century under the RCP8.5 scenario. Regional to global-scale projected decreases in soil moisture and increased risk of agricultural drought are *likely* in presently dry regions and are projected with *medium confidence* by the end of this century under the RCP8.5 scenario. Prominent

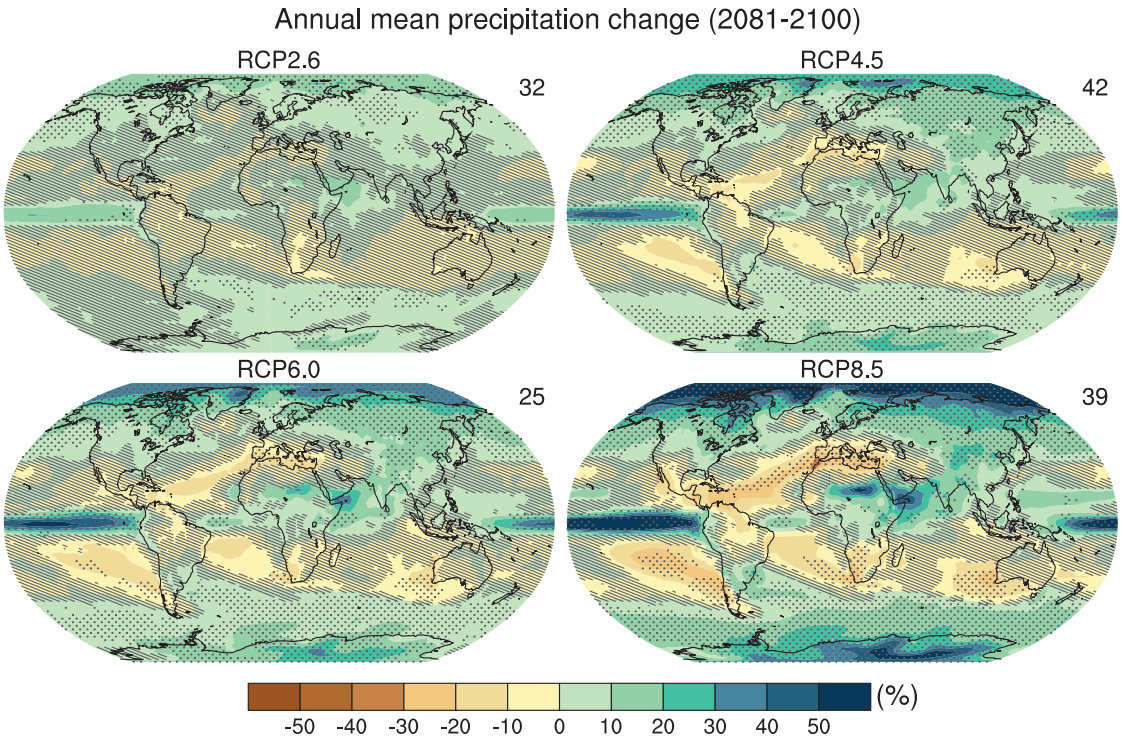

Figure TS.16 | Maps of multi-model results for the scenarios RCP2.6, RCP4.5, RCP6.0 and RCP8.5 in 2081–2100 of average percent change in mean precipitation. Changes are shown relative to 1986–2005. The number of CMIP5 models to calculate the multi-model mean is indicated in the upper right corner of each panel. Hatching indicates regions where the multi- model mean signal is less than 1 standard deviation of internal variability. Stippling indicates regions where the multi- model mean signal is greater than 2 standard deviations of internal variability and where 90% of models agree on the sign of change (see Box 12.1). Further detail regarding the related Figure SPM.8b is given in the TS Supplementary Material. {Figure 12.22; Annex I}

areas of projected decreases in evaporation include southern Africa and northwestern Africa along the Mediterranean. Soil moisture drying in the Mediterranean and southern African regions is consistent with projected changes in Hadley Circulation and increased surface temperatures, so surface drying in these regions as global temperatures increase is *likely* with *high confidence* by the end of this century under the RCP8.5 scenario. In regions where surface moistening is projected, changes are generally smaller than natural variability on the 20-year time scale. A summary of the projected changes in the water cycle from the CMIP5 models is shown in TFE.1, Figure 1. {12.4.5; Box 12.1}

TS.5.5.5 Projected Long-term Changes in the Cryosphere

It is *very likely* that the Arctic sea ice cover will continue shrinking and thinning year-round in the course of the 21st century as GMST rises. At the same time, in the Antarctic, a decrease in sea ice extent and volume is expected, but with *low confidence*. The CMIP5 multi-model projections give average reductions in Arctic sea ice extent for 2081–2100 compared to 1986–2005 ranging from 8% for RCP2.6 to 34% for RCP8.5 in February and from 43% for RCP2.6 to 94% for RCP8.5 in September (*medium confidence*) (Figure TS.17). A nearly ice-free Arctic Ocean (sea ice extent less than 10^6 km^2 for at least five consecutive years) in September before mid-century is *likely* under RCP8.5 (*medium confidence*), based on an assessment of a subset of models that most closely reproduce the climatological mean state and 1979–2012 trend of the Arctic sea ice cover. Some climate projections exhibit 5- to 10-year periods of sharp summer Arctic sea ice decline—even steeper than observed over the last decade—and it is *likely* that such instances of rapid ice loss will occur in the future. There is little evidence in global climate models of a tipping point (or critical threshold) in the transition from a perennially ice-covered to a seasonally ice-free Arctic Ocean beyond which further sea ice loss is unstoppable and irreversible. In the Antarctic, the CMIP5 multi-model mean projects a decrease in sea ice extent that ranges from 16% for RCP2.6 to 67% for RCP8.5 in February and from 8% for RCP2.6 to 30% for RCP8.5 in September for 2081–2100 compared to 1986–2005. There is, however, *low confidence* in those projections because of the wide inter-model spread and the inability of almost all of the available models to reproduce the overall increase of the Antarctic sea ice areal coverage observed during the satellite era. {12.4.6, 12.5.5}

It is *very likely* that NH snow cover will reduce as global temperatures rise over the coming century. A retreat of permafrost extent with rising global temperatures is *virtually certain*. Snow cover changes result from precipitation and ablation changes, which are sometimes opposite. Projections of the NH spring snow covered area by the end of the 21st century vary between a decrease of 7 [3 to 10] % (RCP2.6) and 25 [18 to 32] % (RCP8.5) (Figure TS.18), but *confidence* is those numbers is only *medium* because snow processes in global climate models are strongly simplified. The projected changes in permafrost are a response not only to warming, but also to changes in snow cover, which exerts a control on the underlying soil. By the end of the 21st century, diagnosed near-surface permafrost area is projected to decrease by between 37% (RCP2.6) to 81% (RCP8.5) (*medium confidence*). {12.4.6}

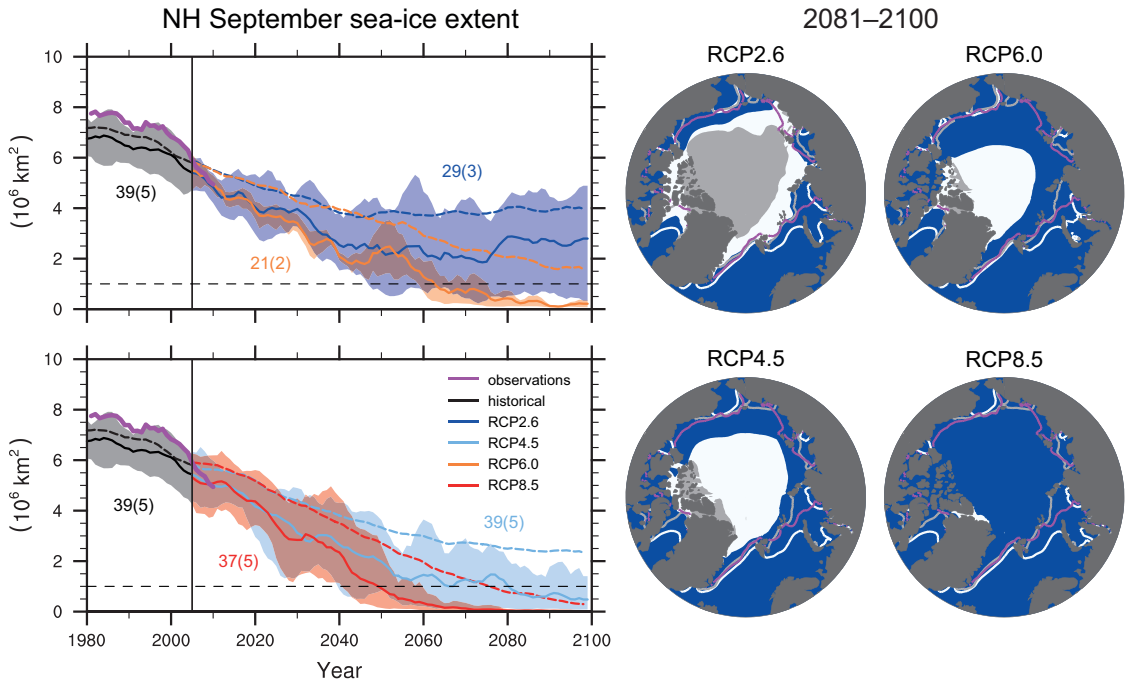

Figure TS.17 | Northern Hemisphere (NH) sea ice extent in September over the late 20th century and the whole 21st century for the scenarios RCP2.6, RCP4.5, RCP6.0 and RCP8.5 in the CMIP5 models, and corresponding maps of multi-model results in 2081–2100 of NH September sea ice extent. In the time series, the number of CMIP5 models to calculate the multi-model mean is indicated (subset in brackets). Time series are given as 5-year running means. The projected mean sea ice extent of a subset of models that most closely reproduce the climatological mean state and 1979–2012 trend of the Arctic sea ice is given (solid lines), with the minimum to maximum range of the subset indicated with shading. Black (grey shading) is the modelled historical evolution using historical reconstructed forcings. The CMIP5 multi-model mean is indicated with dashed lines. In the maps, the CMIP5 multi-model mean is given in white and the results for the subset in grey. Filled areas mark the averages over the 2081–2100 period, lines mark the sea ice extent averaged over the 1986–2005 period. The observed sea ice extent is given in pink as a time series and averaged over 1986–2005 as a pink line in the map. Further detail regarding the related Figures SPM.7b and SPM.8c is given in the TS Supplementary Material. {Figures 12.18, 12.29, 12.31}

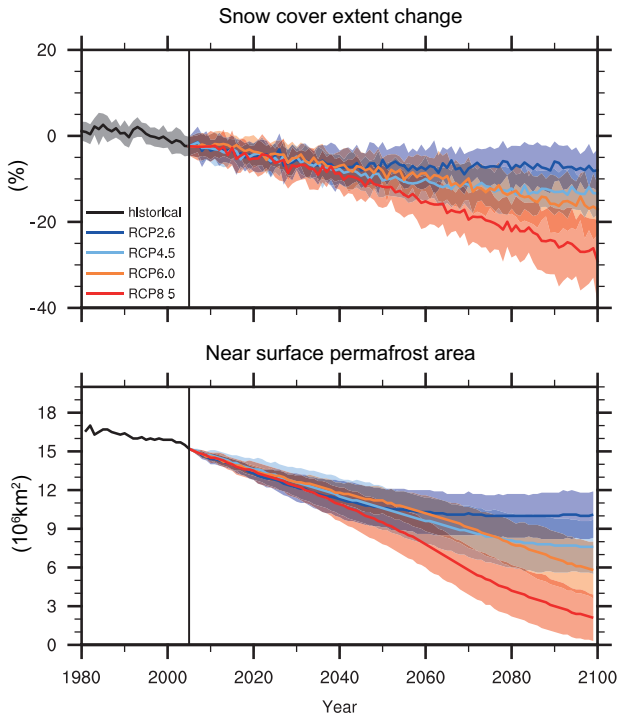

Figure TS.18 | (Top) Northern Hemisphere (NH) spring (March to April average) relative snow-covered area (RSCA) in CMIP5, obtained by dividing the simulated 5-year box smoothed spring snow-covered area (SCA) by the simulated average spring SCA of 1986–2005 reference period. (Bottom) NH diagnosed near-surface permafrost area in CMIP5, using 20-year average monthly surface air temperatures and snow depths. Lines indicate the multi model average, shading indicates the inter-model spread (one standard deviation). {Figures 12.32, 12.33}

TS.5.5.6 Projected Long-term Changes in the Ocean

Over the course of the 21st century, the global ocean will warm in all RCP scenarios. The strongest ocean warming is projected for the surface in subtropical and tropical regions. At greater depth the warming is projected to be most pronounced in the Southern Ocean. Best estimates of ocean warming in the top one hundred metres are about 0.6°C (RCP2.6) to 2.0°C (RCP8.5), and 0.3°C (RCP2.6) to 0.6°C (RCP8.5) at a depth of about 1 km by the end of the 21st century. For RCP4.5 by the end of the 21st century, half of the energy taken up by the ocean is in the uppermost 700 m, and 85% is in the uppermost 2000 m. Due to the long time scales of this heat transfer from the surface to depth, ocean warming will continue for centuries, even if GHG emissions are decreased or concentrations kept constant, and will result in a continued contribution to sea level rise (see Section TS5.7). {12.4.3, 12.4.7}

TS.5.6 Long-term Projections of Carbon and Other Biogeochemical Cycles

Projections of the global carbon cycle to 2100 using the CMIP5 ESMs represent a wider range of complex interactions between the carbon cycle and the physical climate system. {6}

With *very high confidence*, ocean carbon uptake of anthropogenic CO_2 will continue under all four RCPs through to 2100, with higher uptake in higher concentration pathways. The future evolution of the land carbon uptake is much more uncertain. A majority of CMIP5 ESMs project a continued net carbon uptake by land ecosystems through 2100. Yet, a minority of models simulate a net CO_2 source to the atmosphere by 2100 due to the combined effect of climate change and land use change. In view of the large spread of model results and incomplete process representation, there is *low confidence* on the magnitude of modelled future land carbon changes. {6.4.3}

There is *high confidence* that climate change will partially offset increases in global land and ocean carbon sinks caused by rising atmospheric CO_2. Yet, there are regional differences among CMIP5 ESMs in the response of ocean and land CO_2 fluxes to climate. There is high agreement between models that tropical ecosystems will store less carbon in a warmer climate. There is medium agreement between the CMIP5 ESMs that at high latitudes warming will increase land carbon storage, although none of these models accounts for decomposition of carbon in permafrost which may offset increased land carbon storage. There is *high confidence* that reductions in permafrost extent due to warming will cause thawing of some currently frozen carbon. However, there is *low confidence* on the magnitude of carbon losses through CO_2 and CH_4 emissions to the atmosphere with a range from 50 to 250 PgC between 2000 and 2100 for RCP8.5. {6.4.2, 6.4.3}

The loss of carbon from frozen soils constitutes a positive radiative feedback that is missing in current coupled ESM projections. There is high agreement between CMIP5 ESMs that ocean warming and circulation changes will reduce the rate of ocean carbon uptake in the Southern Ocean and North Atlantic, but that carbon uptake will nevertheless persist in those regions. {6.4.2}

It is *very likely*, based on new experimental results and modelling, that nutrient shortage will limit the effect of rising atmospheric CO_2 on future land carbon sinks for the four RCP scenarios. There is *high confidence* that low nitrogen availability will limit carbon storage on land even when considering anthropogenic nitrogen deposition. The role of phosphorus limitation is more uncertain. {6.4.6}

For the ESMs simulations driven by CO_2 concentrations, representation of the land and ocean carbon cycle allows quantification of the fossil fuel emissions compatible with the RCP scenarios. Between 2012 and 2100, ESM results imply cumulative compatible fossil fuel emissions of 270 [140 to 410] PgC for RCP2.6, 780 [595 to 1005] PgC for RCP4.5, 1060 [840 to 1250] PgC for RCP6.0 and 1685 [1415 to 1910] PgC for RCP8.5 (values quoted to nearest 5 PgC, range ±1 standard deviation derived from CMIP5 model results) (Figure TS.19). For RCP2.6, the models project an average 50% (range 14 to 96%) emission reduction by 2050 relative to 1990 levels. By the end of the 21st century, about half of the models infer emissions slightly above zero, while the other half infer a net removal of CO_2 from the atmosphere (see also Box TS.7). {6.4.3; Table 6.12}

When forced with RCP8.5 CO_2 emissions, as opposed to the RCP8.5 CO_2 concentrations, CMIP5 ESMs with interactive carbon cycles simulate, on average, a 50 (–140 to +210) ppm larger atmospheric CO_2 concentration and a 0.2 (–0.4 to +0.9) °C larger global surface temperature increase by 2100 (CMIP5 model spread). {12.4.8}

It is *virtually certain* that the increased storage of carbon by the ocean will increase acidification in the future, continuing the observed trends of the past decades. Ocean acidification in the surface ocean will follow atmospheric CO_2 and it will also increase in the deep ocean as CO_2 continues to penetrate the abyss. The CMIP5 models consistently project worldwide increased ocean acidification to 2100 under all RCPs. The corresponding decrease in surface ocean pH by the end of 21st century is 0.065 (0.06 to 0.07) for RCP2.6, 0.145 (0.14 to 0.15) for RCP4.5, 0.203 (0.20 to 0.21) for RCP6.0 and 0.31 (0.30 to 0.32) for RCP8.5 (CMIP5 model spread) (Figure TS.20). Surface waters are projected to become seasonally corrosive to aragonite in parts of the Arctic and in some coastal upwelling systems within a decade, and

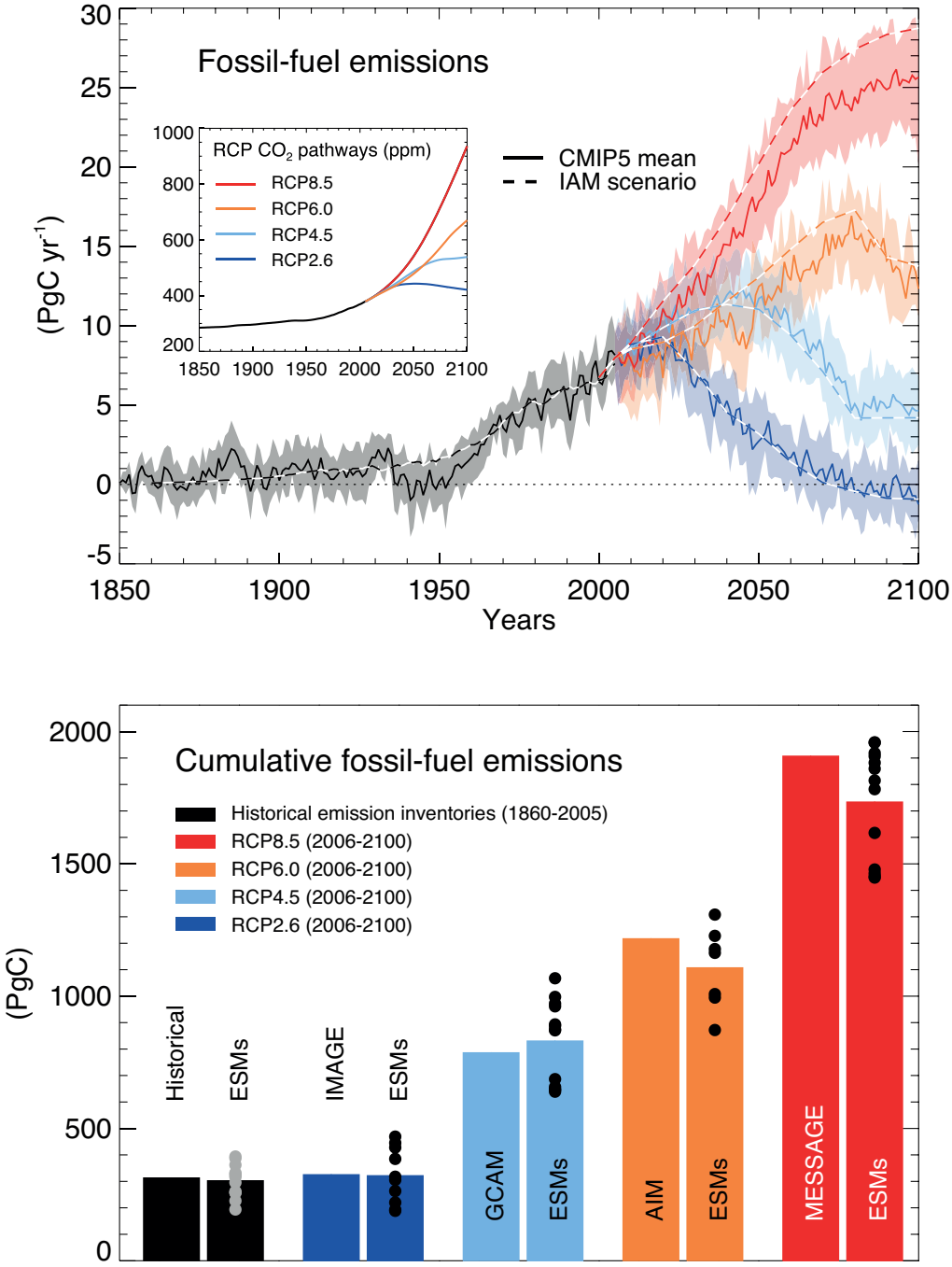

Figure TS.19 | Compatible fossil fuel emissions simulated by the CMIP5 models for the four RCP scenarios. (Top) Time series of annual emission (PgC yr^{-1}). Dashed lines represent the historical estimates and RCP emissions calculated by the Integrated Assessment Models (IAMs) used to define the RCP scenarios, solid lines and plumes show results from CMIP5 Earth System Models (ESMs, model mean, with one standard deviation shaded). (Bottom) Cumulative emissions for the historical period (1860–2005) and 21st century (defined in CMIP5 as 2006–2100) for historical estimates and RCP scenarios. Left bars are cumulative emissions from the IAMs, right bars are the CMIP5 ESMs multi-model mean estimate and dots denote individual ESM results. From the CMIP5 ESMs results, total carbon in the land-atmosphere–ocean system can be tracked and changes in this total must equal fossil fuel emissions to the system. Hence the compatible emissions are given by cumulative emissions = $\Delta C_A + \Delta C_L + \Delta C_O$, while emission rate = d/dt [$C_A + C_L + C_O$], where C_A, C_L, C_O are carbon stored in atmosphere, land and ocean respectively. Other sources and sinks of CO_2 such as from volcanism, sedimentation or rock weathering, which are very small on centennial time scales are not considered here. {Box 6.4; Figure 6.25}

in parts of the Southern Ocean within one to three decades in most scenarios. Aragonite, a less stable form of calcium carbonate, undersaturation becomes widespread in these regions at atmospheric CO_2 levels of 500 to 600 ppm. {6.4.4}

It is *very likely* that the dissolved oxygen content of the ocean will decrease by a few percent during the 21st century in response to surface warming. CMIP5 models suggest that this decrease in dissolved oxygen will predominantly occur in the subsurface mid-latitude oceans, caused by enhanced stratification, reduced ventilation and warming. However, there is no consensus on the future development of the volume of hypoxic and suboxic waters in the open ocean because of large uncertainties in potential biogeochemical effects and in the evolution of tropical ocean dynamics. {6.4.5}

With *very high confidence*, the carbon cycle in the ocean and on land will continue to respond to climate change and atmospheric CO_2 increases that arise during the 21st century (see TFE.7 and TFE 8). {6.4}

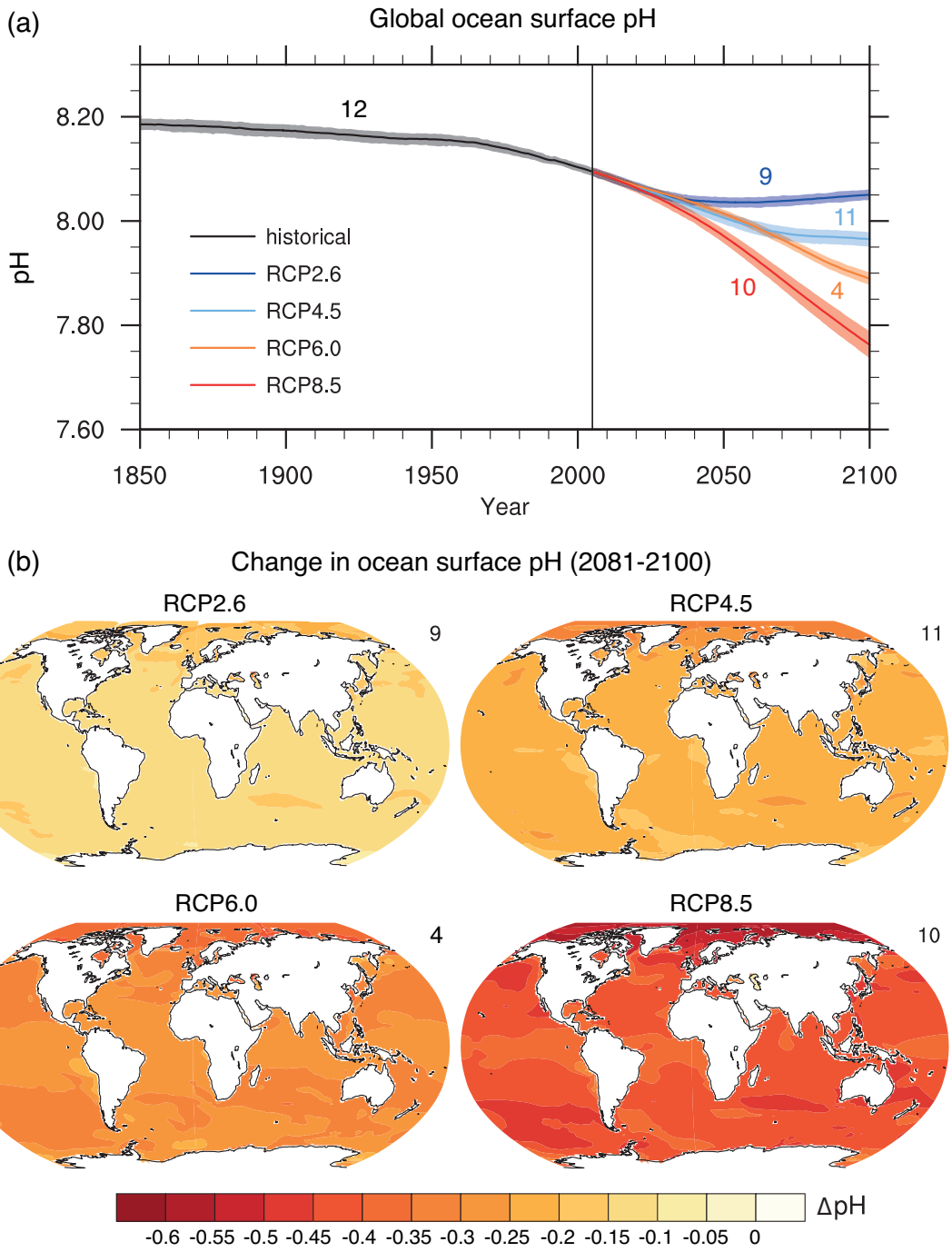

Figure TS.20 | (a) Time series (model averages and minimum to maximum ranges) and (b) maps of multi-model surface ocean pH for the scenarios RCP2.6, RCP4.5, RCP6.0 and RCP8.5 in 2081–2100. The maps in (b) show change in global ocean surface pH in 2081–2100 relative to 1986–2005. The number of CMIP5 models to calculate the multi-model mean is indicated in the upper right corner of each panel. Further detail regarding the related Figures SPM.7c and SPM.8.d is given in the TS Supplementary Material. {Figure 6.28}

Thematic Focus Elements

TFE.7 | Carbon Cycle Perturbation and Uncertainties

The natural carbon cycle has been perturbed since the beginning of the Industrial Revolution (about 1750) by the anthropogenic release of carbon dioxide (CO_2) to the atmosphere, virtually all from fossil fuel combustion and land use change, with a small contribution from cement production. Fossil fuel burning is a process related to energy production. Fossil fuel carbon comes from geological deposits of coal, oil and gas that were buried in the Earth crust for millions of years. Land use change CO_2 emissions are related to the conversion of natural ecosystems into managed ecosystems for food, feed and timber production with CO_2 being emitted from the burning of plant material or from the decomposition of dead plants and soil organic carbon. For instance when a forest is cleared, the plant material may be released to the atmosphere quickly through burning or over many years as the dead biomass and soil carbon decay on their own. {6.1, 6.3; Table 6.1}

The human caused excess of CO_2 in the atmosphere is partly removed from the atmosphere by carbon sinks in land ecosystems and in the ocean, currently leaving less than half of the CO_2 emissions in the atmosphere. Natural carbon sinks are due to physical, biological and chemical processes acting on different time scales. An excess of atmospheric CO_2 supports photosynthetic CO_2 fixation by plants that is stored as plant biomass or in the soil. The residence times of stored carbon on land depends on the compartments (plant/soil) and composition of the organic carbon, with time horizons varying from days to centuries. The increased storage in terrestrial ecosystems not affected by land use change is *likely* to be caused by enhanced photosynthesis at higher CO_2 levels and nitrogen deposition, and changes in climate favoring carbon sinks such as longer growing seasons in mid-to-high latitudes. {6.3, 6.3.1}

The uptake of anthropogenic CO_2 by the ocean is primarily a response to increasing CO_2 in the atmosphere. Excess atmospheric CO_2 absorbed by the surface ocean or transported to the ocean through aquatic systems (e.g., rivers, groundwaters) gets buried in coastal sediments or transported to deep waters where it is stored for decades to centuries. The deep ocean carbon can dissolve ocean carbonate sediments to store excess CO_2 on time scales of centuries to millennia. Within a 1 kyr, the remaining atmospheric fraction of the CO_2 emissions will be between 15 and 40%, depending on the amount of carbon released (TFE.7, Figure 1). On geological time scales of 10 kyr or longer, additional CO_2 is removed very slowly from the atmosphere by rock weathering, pulling the remaining atmospheric CO_2 fraction down to 10 to 25% after 10 kyr. {Box 6.1}

The carbon cycle response to future climate and CO_2 changes can be viewed as two strong and opposing feedbacks. The concentration–carbon feedback determines changes in storage due to elevated CO_2, and the climate–carbon feedback determines changes in carbon storage due to changes in climate. There is *high confidence* that increased atmospheric CO_2 will lead to increased land and ocean carbon uptake but by an uncertain amount. Models agree on the positive sign of land and ocean response to rising CO_2 but show only medium and low agreement for the magnitude of ocean and land carbon uptake respectively (TFE.7, Figure 2). Future climate change will decrease land and ocean carbon uptake compared to the case with constant climate (*medium confidence*). This is further supported by paleoclimate observations and modelling indicating that there is a positive feedback between climate and the carbon cycle on century to millennial time scales. Models agree on the sign, globally negative, of land and ocean response to climate change but show low agreement on the magnitude of this response, especially for the land (TFE.7, Figure 2). A key update since the IPCC Fourth Assessment Report (AR4) is the introduction of nutrient dynamics in some land carbon models, in particular the limitations on plant growth imposed by nitrogen availability. There is *high confidence* that, at the global scale, relative to the Coupled Model Intercomparison Project Phase 5 (CMIP5) carbon-only Earth System

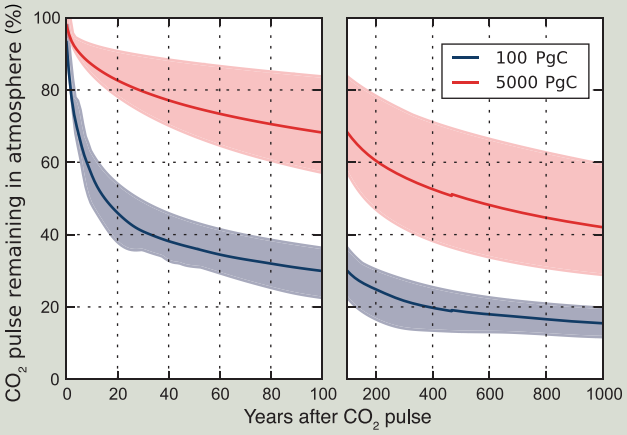

TFE.7, Figure 1 | Percentage of initial atmospheric CO_2 perturbation remaining in the atmosphere in response to an idealized instantaneous CO_2 emission pulse in year 0 as calculated by a range of coupled climate–carbon cycle models. Multi-model mean (line) and the uncertainty interval (maximum model range, shading) simulated during 100 years (left) and 1 kyr (right) following the instantaneous emission pulse of 100 PgC (blue) and 5,000 PgC (red). {Box 6.1, Figure 1}

(continued on next page)

TFE.7 (continued)

Models (ESMs), CMIP5 ESMs including a land nitrogen cycle will reduce the strength of both the concentration–carbon feedback and the climate–carbon feedback of land ecosystems (TFE.7, Figure 2). Inclusion of nitrogen-cycle processes increases the spread across the CMIP5 ensemble. The CMIP5 spread in ocean sensitivity to CO_2 and climate appears reduced compared to AR4 (TFE.7, Figure 2). {6.2.3, 6.4.2}

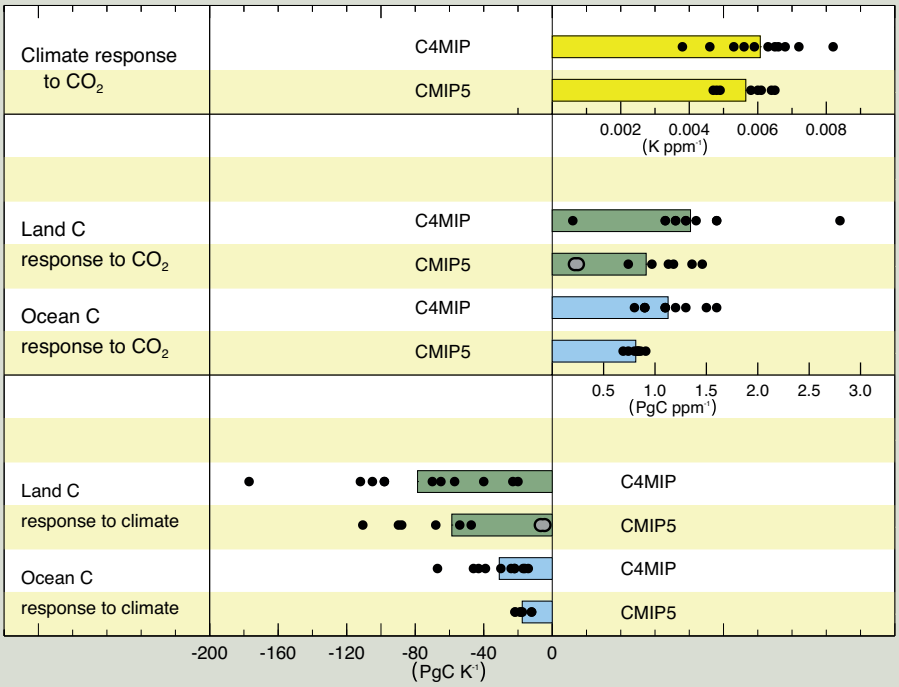

TFE.7, Figure 2 | Comparison of carbon cycle feedback metrics between the ensemble of seven General Circulation Models (GCMs) and four Earth System Models of Intermediate Complexity (EMICs) at the time of AR4 (Coupled Carbon Cycle Climate Model Intercomparison Project (C^4MIP)) under the SRES A2 scenario and the eight CMIP5 models under the 140-year 1% CO_2 increase per year scenario. Black dots represent a single model simulation and coloured bars the mean of the multi-model results, grey dots are used for models with a coupled terrestrial nitrogen cycle. The comparison with C^4MIP models is for context, but these metrics are known to be variable across different scenarios and rates of change (see Section 6.4.2). The SRES A2 scenario is closer in rate of change to a 0.5% CO_2 increase per year scenario and as such it should be expected that the CMIP5 climate–carbon sensitivity terms are comparable, but the concentration–carbon sensitivity terms are *likely* to be around 20% smaller for CMIP5 than for C^4MIP due to lags in the ability of the land and ocean to respond to higher rates of CO_2 increase. This dependence on scenario reduces confidence in any quantitative statements of how CMIP5 carbon cycle feedbacks differ from C^4MIP. {Figure 6.21}

With *very high confidence*, ocean carbon uptake of anthropogenic CO_2 emissions will continue under all four Representative Concentration Pathways (RCPs) through to 2100, with higher uptake corresponding to higher concentration pathways. The future evolution of the land carbon uptake is much more uncertain, with a majority of models projecting a continued net carbon uptake under all RCPs, but with some models simulating a net loss of carbon by the land due to the combined effect of climate change and land use change. In view of the large spread of model results and incomplete process representation, there is *low confidence* on the magnitude of modelled future land carbon changes. {6.4.3; Figure 6.24}

Biogeochemical cycles and feedbacks other than the carbon cycle play an important role in the future of the climate system, although the carbon cycle represents the strongest of these. Changes in the nitrogen cycle, in addition to interactions with CO_2 sources and sinks, affect emissions of nitrous oxide (N_2O) both on land and from the ocean. The human-caused creation of reactive nitrogen has increased steadily over the last two decades and is dominated by the production of ammonia for fertilizer and industry, with important contributions from legume cultivation and combustion of fossil fuels. {6.3}

Many processes, however, are not yet represented in coupled climate-biogeochemistry models (e.g., other processes involving other biogenic elements such as phosphorus, silicon and iron) so their magnitudes have to be estimated in offline or simpler models, which make their quantitative assessment difficult. It is *likely* that there will be nonlinear interactions between many of these processes, but these are not yet well quantified. Therefore any assessment of the future feedbacks between climate and biogeochemical cycles still contains large uncertainty. {6.4}

Box TS.7 | Climate Geoengineering Methods

Geoengineering is defined as the deliberate large-scale intervention in the Earth system to counter undesirable impacts of climate change on the planet. Carbon Dioxide Reduction (CDR) aims to slow or perhaps reverse projected increases in the future atmospheric CO_2 concentrations, accelerating the natural removal of atmospheric CO_2 and increasing the storage of carbon in land, ocean and geological reservoirs. Solar Radiation Management (SRM) aims to counter the warming associated with increasing GHG concentrations by reducing the amount of sunlight absorbed by the climate system. A related technique seeks to deliberately decrease the greenhouse effect in the climate system by altering high-level cloudiness. {6.5, 7.7; FAQ 7.3}

CDR methods could provide mitigation of climate change if CO_2 can be reduced, but there are uncertainties, side effects and risks, and implementation would depend on technological maturity along with economic, political and ethical considerations. CDR would *likely* need to be deployed at large-scale and over at least one century to be able to significantly reduce CO_2 concentrations. There are biogeochemical, and currently technical limitations that make it difficult to provide quantitative estimates of the potential for CDR. It is *virtually certain* that CO_2 removals from the atmosphere by CDR would be partially offset by outgassing of CO_2 previously stored in ocean and terrestrial carbon reservoirs. Some of the climatic and environmental side effects of CDR methods are associated with altered surface albedo from afforestation, ocean de-oxygenation from ocean fertilization, and enhanced N_2O emissions. Land-based CDR methods would probably face competing demands for land. The level of *confidence* on the effectiveness of CDR methods and their side effects on carbon and other biogeochemical cycles is *low*. {6.5; Box 6.2; FAQ 7.3}

SRM remains unimplemented and untested but, if realizable, could offset a global temperature rise and some of its effects. There is *medium confidence* that SRM through stratospheric aerosol injection is scalable to counter the RF and some of the climate effects expected from a twofold increase in CO_2 concentration. There is no consensus on whether a similarly large RF could be achieved from cloud brightening SRM due to insufficient understanding of aerosol–cloud interactions. It does not appear that land albedo change SRM could produce a large RF. Limited literature on other SRM methods precludes their assessment. {7.7.2, 7.7.3}

Numerous side effects, risks and shortcomings from SRM have been identified. SRM would produce an inexact compensation for the RF by GHGs. Several lines of evidence indicate that SRM would produce a small but significant decrease in global precipitation (with larger differences on regional scales) if the global surface temperature were maintained. Another side effect that is relatively well characterized is the likelihood of modest polar stratospheric ozone depletion associated with stratospheric aerosol SRM. There could also be other as yet unanticipated consequences. {7.6.3, 7.7.3, 7.7.4}

As long as GHG concentrations continued to increase, the SRM would require commensurate increase, exacerbating side effects. In addition, scaling SRM to substantial levels would carry the risk that if the SRM were terminated for any reason, there is *high confidence* that surface temperatures would increase rapidly (within a decade or two) to values consistent with the GHG forcing, which would stress systems sensitive to the rate of climate change. Finally, SRM would not compensate for ocean acidification from increasing CO_2. {7.7.3, 7.7.4}

TS.5.7 Long-term Projections of Sea Level Change

TS.5.7.1 Projections of Global Mean Sea Level Change for the 21st Century

GMSL rise for 2081–2100 (relative to 1986–2005) for the RCPs will *likely* be in the 5 to 95% ranges derived from CMIP5 climate projections in combination with process-based models of glacier and ice sheet surface mass balance, with possible ice sheet dynamical changes assessed from the published literature. These *likely* ranges are 0.26 to 0.55 m (RCP2.6), 0.32 to 0.63 m (RCP4.5), 0.33 to 0.63 m (RCP6.0) and 0.45 to 0.82 m (RCP8.5) (*medium confidence*) (Table TS.1, Figure TS.21). For RCP8.5 the range at 2100 is 0.52 to 0.98 m. The central projections for GMSL rise in all scenarios lie within a range of 0.05 m until the middle of the century, when they begin to diverge; by the late 21st century, they have a spread of 0.25 m. Although RCP4.5 and RCP6.0 are very similar at the end of the century, RCP4.5 has a greater rate of rise earlier in the century than RCP6.0. GMSL rise depends on the pathway of CO_2 emissions, not only on the cumulative total; reducing emissions earlier rather than later, for the same cumulative total, leads to a larger mitigation of sea level rise. {12.4.1, 13.4.1, 13.5.1; Table 13.5}

Confidence in the projected *likely* ranges comes from the consistency of process-based models with observations and physical understanding. The basis for higher projections has been considered and it has been concluded that there is currently insufficient evidence to evaluate the probability of specific levels above the *likely* range. Based on current understanding, only the collapse of marine-based sectors of the Antarctic ice sheet, if initiated, could cause GMSL to rise substantially above the *likely* range during the 21st century. There is a lack of consensus on the probability for such a collapse, and the potential additional contribution to GMSL rise cannot be precisely quantified,

but there is *medium confidence* that it would not exceed several tenths of a metre of sea level rise during the 21st century. {13.5.1, 13.5.3}

Under all the RCP scenarios, the time-mean rate of GMSL rise during the 21st century is *very likely* to exceed the rate observed during 1971–2010. In the projections, the rate of rise initially increases. In RCP2.6 it becomes roughly constant (central projection about 4.5 mm yr^{-1}) before the middle of the century, and subsequently declines slightly. The rate of rise becomes roughly constant in RCP4.5 and RCP6.0 by the end of the 21st century, whereas acceleration continues throughout the century in RCP8.5 (reaching 11 [8 to 16] mm yr^{-1} during 2081–2100). {13.5.1; Table 13.5}

In all RCP scenarios, thermal expansion is the largest contribution, accounting for about 30 to 55% of the total. Glaciers are the next largest, accounting for 15-35%. By 2100, 15 to 55% of the present glacier volume is projected to be eliminated under RCP2.6, and 35 to 85% under RCP8.5 (*medium confidence*). The increase in surface melting in Greenland is projected to exceed the increase in accumulation, and there is *high confidence* that the surface mass balance changes on the Greenland ice sheet will make a positive contribution to sea level rise over the 21st century. On the Antarctic ice sheet, surface melting is projected to remain small, while there is *medium confidence* that snowfall will increase (Figure TS.21). {13.3.3, 13.4.3, 13.4.4, 13.5.1; Table 13.5}

There is *medium confidence* in the ability to model future rapid changes in ice sheet dynamics on decadal time scales. At the time of the AR4, scientific understanding was not sufficient to allow an assessment of the possibility of such changes. Since the publication of the AR4, there has been substantial progress in understanding the relevant processes as well as in developing new ice sheet models that are capable of simulating them. However, the published literature as yet provides only a partially sufficient basis for making projections related to particular scenarios. In our projections of GMSL rise by 2081–2100, the *likely* range from rapid changes in ice outflow is 0.03 to 0.20 m from the two ice sheets combined, and its inclusion is the most important reason why the projections are greater than those given in the AR4. {13.1.5, 13.5.1, 13.5.3}

Semi-empirical models are designed to reproduce the observed sea level record over their period of calibration, but do not attribute sea level rise to its individual physical components. For RCPs, some semi-empirical models project a range that overlaps the process-based *likely* range while others project a median and 95-percentile that are about twice as large as the process-based models. In nearly every case, the semi-empirical model 95th percentile is higher than the process-based *likely* range. For 2081–2100 (relative to 1986–2005) under RCP4.5, semi-empirical models give median projections in the range 0.56 to 0.97 m, and their 95th percentiles extend to about 1.2 m. This difference implies either that there is some contribution which is presently

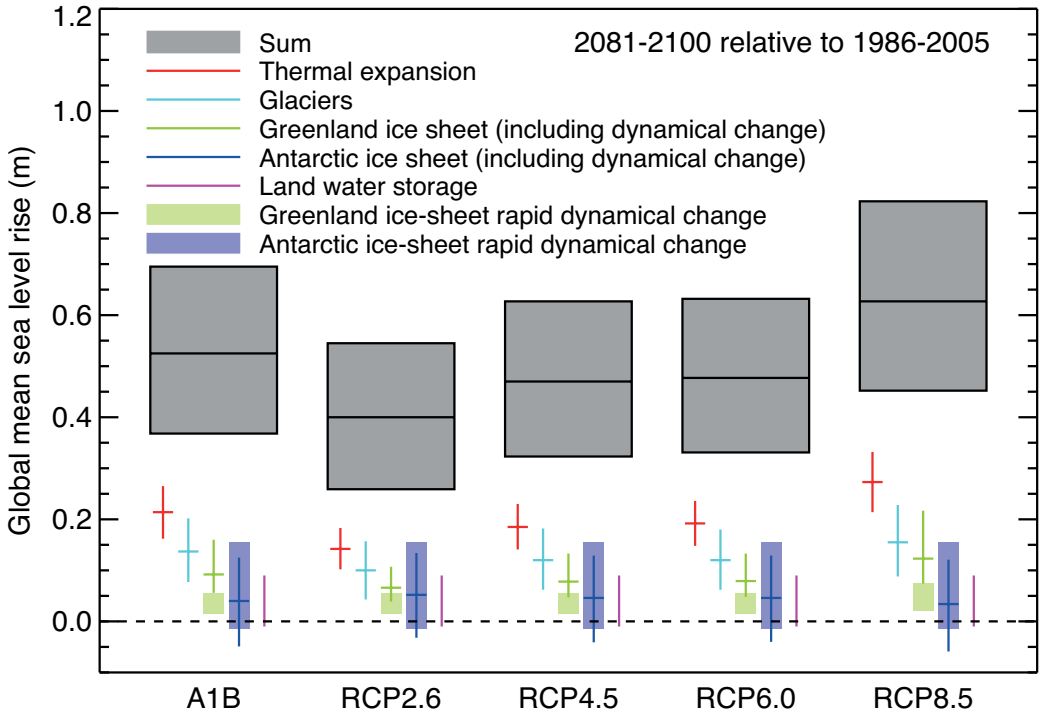

Figure TS.21 | Projections from process-based models with *likely* ranges and median values for global mean sea level (GMSL) rise and its contributions in 2081–2100 relative to 1986–2005 for the four RCP scenarios and scenario SRES A1B used in the AR4. The contributions from ice sheets include the contributions from ice sheet rapid dynamical change, which are also shown separately. The contributions from ice sheet rapid dynamics and anthropogenic land water storage are treated as having uniform probability distributions, and as independent of scenario (except that a higher rate of change is used for Greenland ice sheet outflow under RCP8.5). This treatment does not imply that the contributions concerned will not depend on the scenario followed, only that the current state of knowledge does not permit a quantitative assessment of the dependence. See discussion in Sections 13.5.1 and 13.5.3 and Supplementary Material for methods. Based on current understanding, only the collapse of the marine-based sectors of the Antarctic ice sheet, if initiated, could cause GMSL to rise substantially above the *likely* range during the 21st century. This potential additional contribution cannot be precisely quantified but there is *medium confidence* that it would not exceed several tenths of a metre during the 21st century. {Figure 13.10}

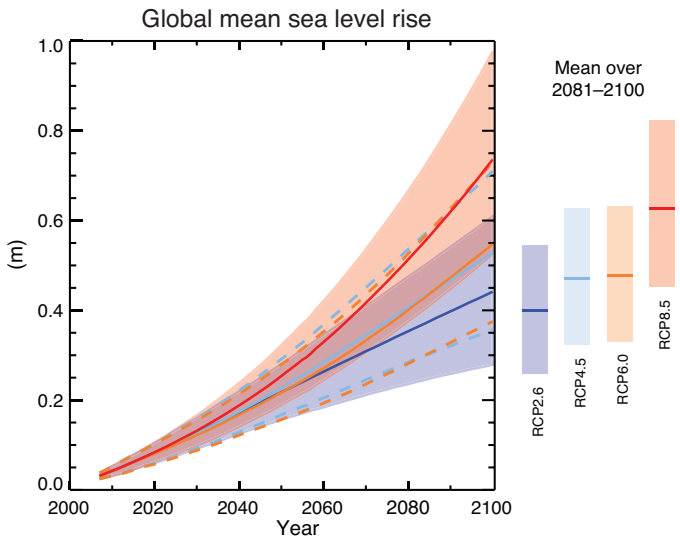

Figure TS.22 | Projections from process-based models of global mean sea level (GMSL) rise relative to 1986–2005 for the four RCP scenarios. The solid lines show the median projections, the dashed lines show the *likely* ranges for RCP4.5 and RCP6.0, and the shading the *likely* ranges for RCP2.6 and RCP8.5. The time means for 2081–2100 are shown as coloured vertical bars. See Sections 13.5.1 and 13.5.3 and Supplementary Material for methods. Based on current understanding, only the collapse of the marine-based sectors of the Antarctic ice sheet, if initiated, could cause GMSL to rise substantially above the *likely* range during the 21st century. This potential additional contribution cannot be precisely quantified but there is *medium confidence* that it would not exceed several tenths of a metre during the 21st century. Further detail regarding the related Figure SPM.9 is given in the TS Supplementary Material. {Table 13.5; Figures 13.10, 13.11}

unidentified or underestimated by process-based models, or that the projections of semi-empirical models are overestimates. Making projections with a semi-empirical model assumes that sea level change in the future will have the same relationship as it has had in the past to RF or global mean temperature change. This may not hold if potentially nonlinear physical processes do not scale in the future in ways which can be calibrated from the past. There is no consensus in the scientific community about the reliability of semi-empirical model projections, and *confidence* in them is assessed to be *low*. {13.5.2, 13.5.3}

TS.5.7.2 Projections of Global Mean Sea Level Change Beyond 2100

It is *virtually certain* that GMSL rise will continue beyond 2100. The few available model results that go beyond 2100 indicate global mean sea level rise above the pre-industrial level (defined here as an equilibrium 280 ppm atmospheric CO_2 concentration) by 2300 to be less than 1 m for a RF that corresponds to CO_2 concentrations that peak and decline and remain below 500 ppm, as in the scenario RCP2.6. For a RF that corresponds to a CO_2 concentration that is above 700 ppm but below 1500 ppm, as in the scenario RCP8.5, the projected rise is 1 m to more than 3 m (*medium confidence*). {13.5.4}

Sea level rise due to ocean thermal expansion will continue for centuries to millennia. The amount of ocean thermal expansion increases with global warming (models give a range of 0.2 to 0.6 m $°C^{-1}$). The glacier contribution decreases over time as their volume (currently about 0.43 m sea level equivalent) decreases. In Antarctica, beyond 2100 and with higher GHG scenarios, the increase in surface melting could exceed the increase in accumulation. {13.5.2, 13.5.4}

The available evidence indicates that global warming greater than a certain threshold would lead to the near-complete loss of the Greenland ice sheet over a millennium or more, causing a GMSL rise of about 7 m. Studies with fixed present-day ice sheet topography indicate the threshold is greater than 2°C but less than 4°C of GMST rise with respect to pre-industrial (*medium confidence*). The one study with a dynamical ice sheet suggests the threshold is greater than about 1°C (*low confidence*) global mean warming with respect to pre-industrial. Considering the present state of scientific uncertainty, a *likely* range cannot be quantified. The complete loss of the ice sheet is not inevitable because this would take a millennium or more; if temperatures decline before the ice sheet is eliminated, the ice sheet might regrow. However, some part of the mass loss might be irreversible, depending on the duration and degree of exceedance of the threshold, because the ice sheet may have multiple steady states, due to its interaction with its regional climate. {13.4.3, 13.5.4}

Currently available information indicates that the dynamical contribution of the ice sheets will continue beyond 2100, but *confidence* in projections is *low*. In Greenland, ice outflow induced from interaction with the ocean is self-limiting as the ice sheet margin retreats inland from the coast. By contrast, the bedrock topography of Antarctica is such that there may be enhanced rates of mass loss as the ice retreats. About 3.3 m of equivalent global sea level of the West Antarctic ice sheet is grounded on areas with downward sloping bedrock, which may be subject to potential ice loss via the marine ice sheet instability. Abrupt and irreversible ice loss from a potential instability of marine-based sectors of the Antarctic Ice Sheet in response to climate forcing is possible, but current evidence and understanding is insufficient to make a quantitative assessment. Due to relatively weak snowfall on Antarctica and the slow ice motion in its interior, it can be expected that the West Antarctic ice sheet would take at least several thousand years to regrow if it was eliminated by dynamic ice discharge. Consequently any significant ice loss from West Antarctic that occurs within the next century will be irreversible on a multi-centennial to millennial time scale. {5.8, 13.4.3, 13.4.4, 13.5.4}

TS.5.7.3 Projections of Regional Sea Level Change

Regional sea level will change due to dynamical ocean circulation changes, changes in the heat content of the ocean, mass redistribution in the entire Earth system and changes in atmospheric pressure. Ocean dynamical change results from changes in wind and buoyancy forcing (heat and freshwater), associated changes in the circulation, and redistribution of heat and freshwater. Over time scales longer than a few days, regional sea level also adjusts nearly isostatically to regional changes in sea level atmospheric pressure relative to its mean over the ocean. Ice sheet mass loss (both contemporary and past), glacier mass loss and changes in terrestrial hydrology cause water mass redistribution among the cryosphere, the land and the oceans, giving rise to distinctive regional changes in the solid Earth, Earth rotation and the gravity field. In some coastal locations, changes in the hydrological cycle, ground subsidence associated with anthropogenic activity,

tectonic processes and coastal processes can dominate the relative sea level change, that is, the change in sea surface height relative to the land. {13.1.3, 13.6.2, 13.6.3, 13.6.4}

By the end of the 21st century, sea level change will have a strong regional pattern, which will dominate over variability, with many regions *likely* experiencing substantial deviations from the global mean change (Figure TS.23). It is *very likely* that over about 95% of the ocean will experience regional relative sea level rise, while most regions experiencing a sea level fall are located near current and former glaciers and ice sheets. Local sea level changes deviate more than 10% and 25% from the global mean projection for as much as 30% and 9% of the ocean area, respectively, indicating that spatial variations can be large. Regional changes in sea level reach values of up to 30% above the global mean value in the Southern Ocean and around North America, between 10% and 20% in equatorial regions, and up to 50% below the global mean in the Arctic region and some regions near Antarctica. About 70% of the coastlines worldwide are projected to experience a relative sea level change within 20% of the GMSL change. Over decadal periods, the rates of regional relative sea level change as a result of climate variability can differ from the global average rate by more than 100%. {13.6.5}

TS.5.7.4 Projections of Change in Sea Level Extremes and Waves During the 21st Century

It is *very likely* that there will be a significant increase in the occurrence of future sea level extremes by the end of the 21st century, with a *likely* increase in the early 21st century (see TFE.9, Table 1). This increase will primarily be the result of an increase in mean sea level (*high confidence*), with extreme return periods decreasing by at least an order of magnitude in some regions by the end of the 21st century. There is *low confidence* in region-specific projections of storminess and associated storm surges. {13.7.2}

It is *likely* (*medium confidence*) that annual mean significant wave heights will increase in the Southern Ocean as a result of enhanced wind speeds. Southern Ocean–generated swells are *likely* to affect heights, periods and directions of waves in adjacent basins. It is *very likely* that wave heights and the duration of the wave season will increase in the Arctic Ocean as a result of reduced sea ice extent. In general, there is *low confidence* in region-specific projections due to the *low confidence* in tropical and extratropical storm projections, and to the challenge of down-scaling future wind states from coarse resolution climate models. {13.7.3}

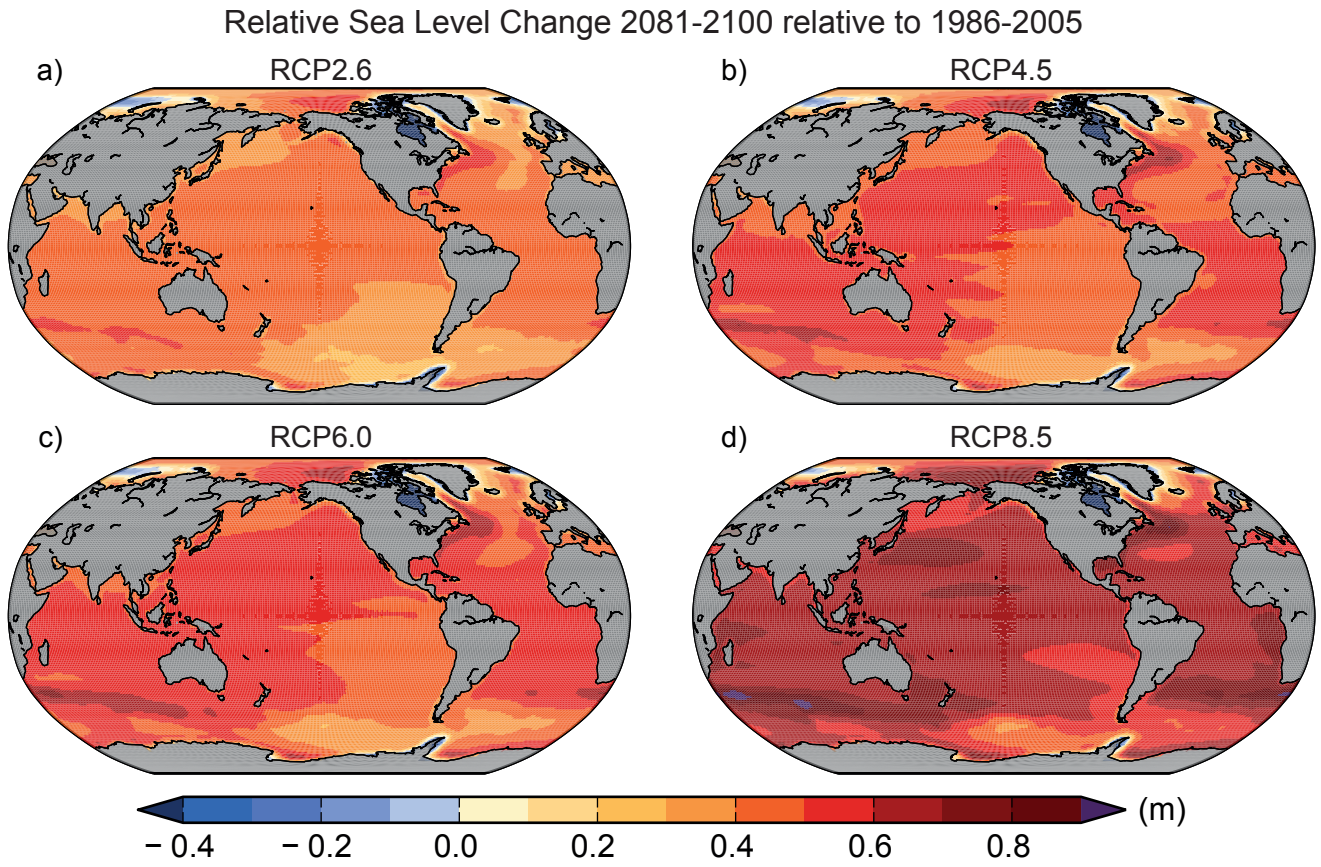

Figure TS.23 | Ensemble mean net regional relative sea level change (metres) evaluated from 21 CMIP5 models for the RCP scenarios (a) 2.6, (b) 4.5, (c) 6.0 and (d) 8.5 between 1986–2005 and 2081–2100. Each map includes effects of atmospheric loading, plus land-ice, glacial isostatic adjustment (GIA) and terrestrial water sources. {Figure 13.20}

Thematic Focus Elements

TFE.8 | Climate Targets and Stabilization

The concept of stabilization is strongly linked to the ultimate objective of the United Nations Framework Convention on Climate Change (UNFCCC), which is 'to achieve […] stabilization of greenhouse gas concentrations in the atmosphere at a level that would prevent dangerous anthropogenic interference with the climate system'. Recent policy discussions focused on limits to a global temperature increase, rather than to greenhouse gas (GHG) concentrations, as climate targets in the context of the UNFCCC objectives. The most widely discussed is that of 2°C, that is, to limit global temperature increase relative to pre-industrial times to below 2°C, but targets other than 2°C have been proposed (e.g., returning warming to well below 1.5°C global warming relative to pre-industrial, or returning below an atmospheric carbon dioxide (CO_2) concentration of 350 ppm). Climate targets generally mean avoiding a warming beyond a predefined threshold. Climate impacts, however, are geographically diverse and sector specific, and no objective threshold defines when dangerous interference is reached. Some changes may be delayed or irreversible, and some impacts could be beneficial. It is thus not possible to define a single critical objective threshold without value judgements and without assumptions on how to aggregate current and future costs and benefits. This TFE does not advocate or defend any threshold or objective, nor does it judge the economic or political feasibility of such goals, but assesses, based on the current understanding of climate and carbon cycle feedbacks, the climate projections following the Representative Concentration Pathways (RCPs) in the context of climate targets, and the implications of different long-term temperature stabilization objectives on allowed carbon emissions. Further below it is highlighted that temperature stabilization does not necessarily imply stabilization of the entire Earth system. {12.5.4}

Temperature targets imply an upper limit on the total radiative forcing (RF). Differences in RF between the four RCP scenarios are relatively small up to 2030, but become very large by the end of the 21st century and dominated by CO_2 forcing. Consequently, in the near term, global mean surface temperatures (GMSTs) are projected to continue to rise at a similar rate for the four RCP scenarios. Around the mid-21st century, the rate of global warming begins to be more strongly dependent on the scenario. By the end of the 21st century, global mean temperatures will be warmer than present day under all the RCPs, global temperature change being largest (>0.3°C per decade) in the highest RCP8.5 and significantly lower in RCP2.6, particularly after about 2050 when global surface temperature response stabilizes (and declines thereafter) (see Figure TS.15). {11.3.1, 12.3.3, 12.4.1}

In the near term (2016–2035), global mean surface warming is *more likely than not* to exceed 1°C and *very unlikely* to be more than 1.5°C relative to the average from year 1850 to 1900 (assuming 0.61°C warming from 1850-1900 to 1986–2005) (*medium confidence*). By the end of the 21st century (2081–2100), global mean surface warming, relative to 1850-1900, is *likely* to exceed 1.5°C for RCP4.5, RCP6.0 and RCP8.5 (*high confidence*) and is *likely* to exceed 2°C for RCP6.0 and RCP8.5 (*high confidence*). It is *more likely than not* to exceed 2°C for RCP4.5 (*medium confidence*). Global mean surface warming above 2°C under RCP2.6 is *unlikely* (*medium confidence*). Global mean surface warming above 4°C by 2081–2100 is *unlikely* in all RCPs (*high confidence*) except for RCP8.5 where it is *about as likely as not* (*medium confidence*). {11.3.6, 12.4.1; Table 12.3}

Continuing GHG emissions beyond 2100 as in the RCP8.5 extension induces a total RF above 12 W m^{-2} by 2300, with global warming reaching 7.8 [3.0 to 12.6] °C for 2281–2300 relative to 1986–2005. Under the RCP4.5 extension, where radiative forcing is kept constant (around 4.5 W m^{-2}) beyond 2100, global warming reaches 2.5 [1.5 to 3.5] °C. Global warming reaches 0.6 [0.0 to 1.2] °C under the RCP2.6 extension where sustained negative emissions lead to a further decrease in RF, reaching values below present-day RF by 2300. See also Box TS.7. {12.3.1, 12.4.1, 12.5.1}

The total amount of anthropogenic CO_2 released in the atmosphere since pre-industrial (often termed cumulative carbon emission, although it applies only to CO_2 emissions) is a good indicator of the atmospheric CO_2 concentration and hence of the global warming response. The ratio of GMST change to total cumulative anthropogenic CO_2 emissions is relatively constant over time and independent of the scenario. This near-linear relationship between total CO_2 emissions and global temperature change makes it possible to define a new quantity, the transient climate response to cumulative carbon emission (TCRE), as the transient GMST change for a given amount of cumulated anthropogenic CO_2 emissions, usually 1000 PgC (TFE.8, Figure 1). TCRE is model dependent, as it is a function of the cumulative CO_2 airborne fraction and the transient climate response, both quantities varying significantly across models. Taking into account the available information from multiple lines of evidence (observations, models and process understanding), the near linear relationship between cumulative CO_2 emissions and peak global mean temperature is

(continued on next page)

TFE.8 (continued)

well established in the literature and robust for cumulative total CO_2 emissions up to about 2000 PgC. It is consistent with the relationship inferred from past cumulative CO_2 emissions and observed warming, is supported by process understanding of the carbon cycle and global energy balance, and emerges as a robust result from the entire hierarchy of models. Expert judgment based on the available evidence suggests that TCRE is *likely* between 0.8°C and 2.5°C per 1000 PgC, for cumulative emissions less than about 2000 PgC until the time at which temperature peaks (TFE.8, Figure 1a). {6.4.3, 12.5.4; Box 12.2}

CO_2-induced warming is projected to remain approximately constant for many centuries following a complete cessation of emissions. A large fraction of climate change is thus irreversible on a human time scale, except if net anthropogenic CO_2 emissions were strongly negative over a sustained period. Based on the assessment of TCRE (assuming a normal distribution with a ±1 standard deviation range of 0.8 to 2.5°C per 1000 PgC), limiting the warming caused by anthropogenic CO_2 emissions alone (i.e., ignoring other radiative forcings) to less than 2°C since the period 1861–1880 with a probability of >33%, >50% and >66%, total CO_2 emissions from all anthropogenic sources would need to be below a cumulative budget of about 1570 PgC, 1210 PgC and 1000 PgC since 1870, respectively. An amount of 515 [445 to 585] PgC was emitted between 1870 and 2011 (TFE.8, Figure 1a,b). Higher emissions in earlier decades therefore imply lower or even negative emissions later on. Accounting for non-CO_2 forcings contributing to peak warming implies lower cumulated CO_2 emissions. Non-CO_2 forcing constituents are important, requiring either assumptions on how CO_2 emission reductions are linked to changes in other forcings, or separate emission budgets and climate modelling for short-lived and long-lived gases. So far, not many studies have considered non-CO_2 forcings. Those that do consider them found significant effects, in particular warming of several tenths of a degree for abrupt reductions in emissions of short-lived species, like aerosols. Accounting for an unanticipated release of GHGs from permafrost or methane hydrates, not included in studies assessed here, would also reduce the anthropogenic CO_2 emissions compatible with a given temperature target. Requiring a higher likelihood of temperatures remaining below a given temperature target would further reduce the compatible emissions (TFE.8, Figure 1c). When accounting for the non-CO_2 forcings as in the RCP scenarios, compatible carbon emissions since 1870 are reduced to about 900 PgC, 820 PgC and 790 PgC to limit warming to less than 2°C since the period 1861–1880 with a probability of >33%, >50%, and >66%, respectively. These estimates were derived by computing the fraction of the Coupled Model Intercomparison Project Phase 5 (CMIP5) Earth System Models (ESMs) and Earth System Models of Intermediate Complexity (EMICs) that stay below 2°C for given cumulative emissions following RCP8.5, as shown in TFE.8 Fig. 1c. The non-CO_2 forcing in RCP8.5 is higher than in RCP2.6. Because all likelihood statements in calibrated IPCC language are open intervals, the estimates provided are thus both conservative and consistent choices valid for non-CO_2 forcings across all RCP scenarios. There is no RCP scenario which limits warming to 2°C with probabilities of >33% or >50%, and which could be used to directly infer compatible cumulative emissions. For a probability of >66% RCP2.6 can be used as a comparison. Combining the average back-calculated fossil fuel carbon emissions for RCP2.6 between 2012 and 2100 (270 PgC) with the average historical estimate of 515 PgC gives a total of 785 PgC, i.e., 790 PgC when rounded to 10 PgC. As the 785 PgC estimate excludes an explicit assessment of future land-use change emissions, the 790 PgC value also remains a conservative estimate consistent with the overall likelihood assessment. The ranges of emissions for these three likelihoods based on the RCP scenarios are rather narrow, as they are based on a single scenario and on the limited sample of models available (TFE.8 Fig. 1c). In contrast to TCRE they do not include observational constraints or account for sources of uncertainty not sampled by the models. The concept of a fixed cumulative CO_2 budget holds not just for 2°C, but for any temperature level explored with models so far (up to about 5°C, see Figures 12.44 to 12.46). Higher temperature targets would allow larger cumulative budgets, while lower temperature target would require lower cumulative budgets (TFE.8, Figure 1). {6.3.1, 12.5.2, 12.5.4}

The climate system has multiple time scales, ranging from annual to multi-millennial, associated with different thermal and carbon reservoirs. These long time scales induce a commitment warming 'already in the pipe-line'. Stabilization of the forcing would not lead to an instantaneous stabilization of the warming. For the RCP scenarios and their extensions to 2300, the fraction of realized warming, at that time when RF stabilizes, would be about 75 to 85% of the equilibrium warming. For a 1% yr^{-1} CO_2 increase to 2 × CO_2 or 4 × CO_2 and constant forcing thereafter, the fraction of realized warming would be much smaller, about 40 to 70% at the time when the forcing is kept constant. Owing to the long time scales in the deep ocean, full equilibrium is reached only after hundreds to thousands of years. {12.5.4}

(continued on next page)

TFE.8 (continued)

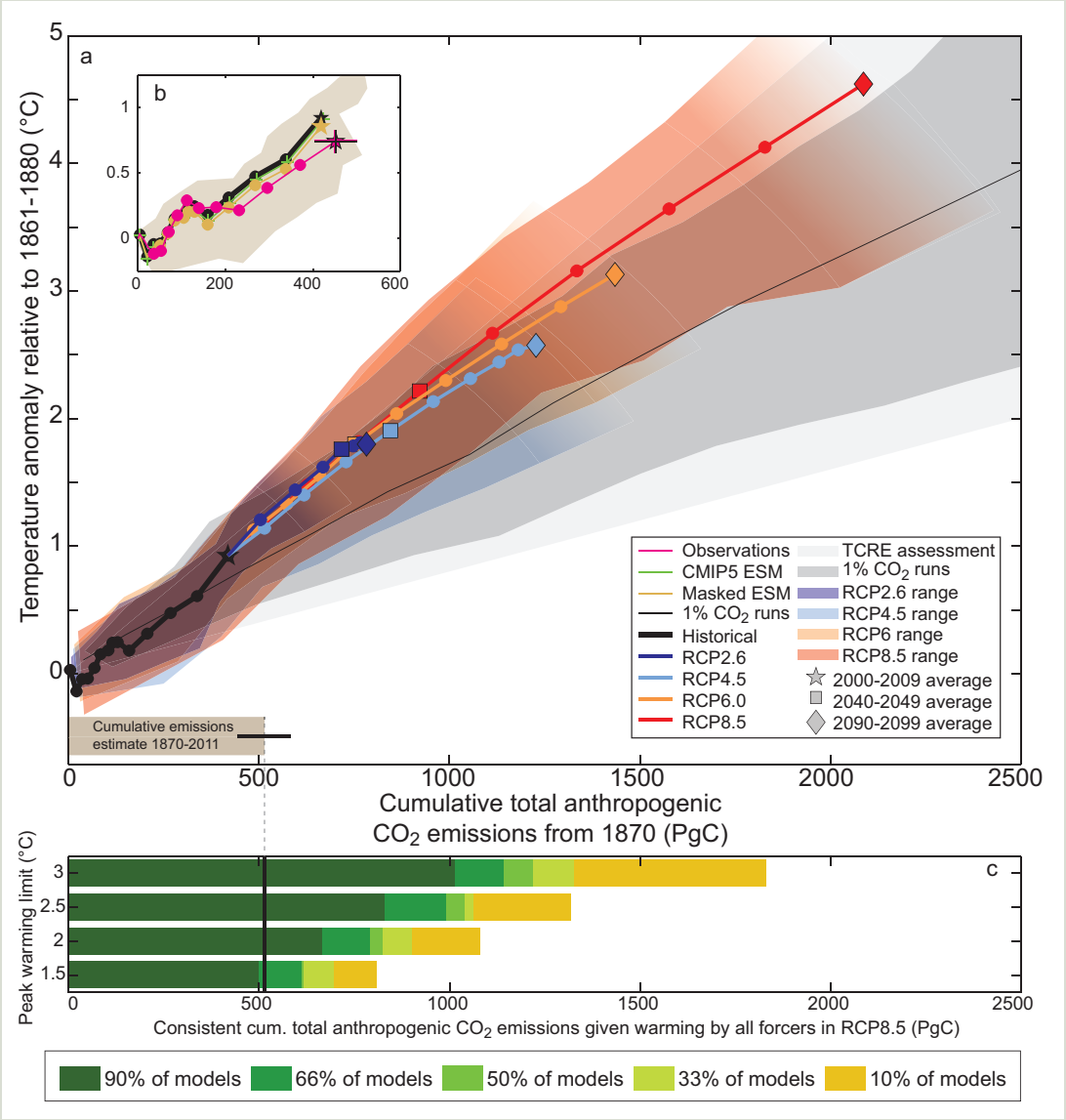

TFE.8, Figure 1 | Global mean temperature increase since 1861–1880 as a function of cumulative total global CO_2 emissions from various lines of evidence. (a) Decadal average results are shown over all CMIP5 Earth System Model of Intermediate Complexity (EMICs) and Earth System Models (ESMs) for each RCP respectively, with coloured lines (multi-model average), decadal markers (dots) and with three decades (2000–2009, 2040–2049 and 2090–2099) highlighted with a star, square and diamond, respectively. The historical time period up to decade 2000–2009 is taken from the CMIP5 historical runs prolonged by RCP8.5 for 2006–2010 and is indicated with a black thick line and black symbols. Coloured ranges illustrate the model spread (90% range) over all CMIP5 ESMs and EMICs and do not represent a formal uncertainty assessment. Ranges are filled as long as data of all models is available and until peak temperature. They are faded out for illustrative purposes afterward. CMIP5 simulations with 1% yr^{-1} CO_2 increase only are illustrated by the dark grey area (range definition similar to RCPs above) and the black thin line (multi-model average). The light grey cone represents this Report's assessment of the transient climate response to emissions (TCRE) from CO_2 only. Estimated cumulative historical CO_2 emissions from 1870 to 2011 with associated uncertainties are illustrated by the grey bar at the bottom of (a). (b) Comparison of historical model results with observations. The magenta line and uncertainty ranges are based on observed emissions from Carbon Dioxide Information Analysis Center (CDIAC) extended by values of the Global Carbon project until 2010 and observed temperature estimates of the Hadley Centre/Climatic Research Unit gridded surface temperature data set 4 (HadCRUT4). The uncertainties in the last decade of observations are based on the assessment in this report. The black thick line is identical to the one in (a). The thin green line with crosses is as the black line but for ESMs only. The yellow-brown line and range show these ESM results until 2010, when corrected for HadCRUT4's incomplete geographical coverage over time. All values are given relative to the 1861–1880 base period. All time-series are derived from decadal averages to illustrate the long-term trends. Note that observations are in addition subject to internal climate variability, adding an uncertainty of about 0.1°C. (c) Cumulative CO_2 emissions over the entire industrial era, consistent with four illustrative peak global temperature limits (1.5°C, 2°C, 2.5°C and 3°C, respectively) when taking into account warming by all forcers. Horizontal bars indicate consistent cumulative emission budgets as a function of the fraction of models (CMIP5 ESMs and EMICs) that at least hold warming below a given temperature limit. Note that the fraction of models cannot be interpreted as a probability. The budgets are derived from the RCP8.5 runs, with relative high non-CO_2 forcing over the 21st century. If non-CO_2 are significantly reduced, the CO_2 emissions compatible with a specific temperature limit might be slightly higher, but only to a very limited degree, as illustrated by the other coloured lines in (a), which assume significantly lower non-CO_2 forcing. Further detail regarding the related Figure SPM.10 is given in the TS Supplementary Material. {Figure 12.45}

TFE.8 (continued)

The commitment to past emissions is a persistent warming for hundreds of years, continuing at about the level of warming that has been realized when emissions were ceased. The persistence of this CO_2-induced warming after emission have ceased results from a compensation between the delayed commitment warming described above and the slow reduction in atmospheric CO_2 resulting from ocean and land carbon uptake. This persistence of warming also results from the nonlinear dependence of RF on atmospheric CO_2, that is, the relative decrease in forcing being smaller than the relative decrease in CO_2 concentration. For high climate sensitivities, and in particular if sulphate aerosol emissions are eliminated at the same time as GHG emissions, the commitment from past emission can be strongly positive, and is a superposition of a fast response to reduced aerosols emissions and a slow response to reduced CO_2. {12.5.4}

Stabilization of global temperature does not imply stabilization for all aspects of the climate system. Processes related to vegetation change, changes in the ice sheets, deep ocean warming and associated sea level rise and potential feedbacks linking, for example, ocean and the ice sheets have their own intrinsic long time scales. Ocean acidification will *very likely* continue in the future as long as the oceans will continue to take up atmospheric CO_2. Committed land ecosystem carbon cycle changes will manifest themselves further beyond the end of the 21st century. It is *virtually certain* that global mean sea level rise will continue beyond 2100, with sea level rise due to thermal expansion to continue for centuries to millennia. Global mean sea level rise depends on the pathway of CO_2 emissions, not only on the cumulative total; reducing emissions earlier rather than later, for the same cumulative total, leads to a larger mitigation of sea level rise. {6.4.4, 12.5.4, 13.5.4}

TS.5.8 Climate Phenomena and Regional Climate Change

This section assesses projected changes over the 21st century in large-scale climate phenomena that affect regional climate (Table TS.2). Some of these phenomena are defined by climatology (e.g., monsoons), and some by interannual variability (e.g., El Niño), the latter affecting climate extremes such as floods, droughts and heat waves. Changes in statistics of weather phenomena such as tropical cyclones and extratropical storms are also summarized here. {14.8}

TS.5.8.1 Monsoon Systems

Global measures of monsoon by the area and summer precipitation are *likely* to increase in the 21st century, while the monsoon circulation weakens. Monsoon onset dates are *likely* to become earlier or not to change much while monsoon withdrawal dates are *likely* to delay, resulting in a lengthening of the monsoon season in many regions (Figure TS.24). The increase in seasonal mean precipitation is pronounced in the East and South Asian summer monsoons while the change in other monsoon regions is subject to larger uncertainties. {14.2.1}

There is *medium confidence* that monsoon-related interannual rainfall variability will increase in the future. Future increase in precipitation extremes related to the monsoon is *very likely* in South America, Africa, East Asia, South Asia, Southeast Asia and Australia. {14.2.1, 14.8.5, 14.8.7, 14.8.9, 14.8.11–14.8.13}

There is *medium confidence* that overall precipitation associated with the Asian-Australian monsoon will increase but with a north–south asymmetry: Indian monsoon rainfall is projected to increase, while projected changes in the Australian summer monsoon rainfall are small. There is *medium confidence* in that the Indian summer monsoon circulation weakens, but this is compensated by increased atmospheric moisture content, leading to more rainfall. For the East Asian summer monsoon, both monsoon circulation and rainfall are projected to increase. {14.2.2, 14.8.9, 14.8.11, 14.8.13}

There is *low confidence* in projections of the North American and South American monsoon precipitation changes, but *medium confidence* that the North American monsoon will arrive and persist later in the annual cycle, and *high confidence* in expansion of South American Monsoon area. {14.2.3, 14.8.3–14.8.5}

There is *low confidence* in projections of a small delay in the West African rainy season, with an intensification of late-season rains. The limited skills of model simulations for the region suggest *low confidence* in the projections. {14.2.4, 14.8.7}

TS.5.8.2 Tropical Phenomena

Precipitation change varies in space, increasing in some regions and decreasing in some others. The spatial distribution of tropical rainfall changes is *likely* shaped by the current climatology and ocean warming pattern. The first effect is to increase rainfall near the currently rainy regions, and the second effect increases rainfall where the ocean warming exceeds the tropical mean. There is *medium confidence* that tropical rainfall projections are more reliable for the seasonal than annual mean changes. {7.6.2, 12.4.5, 14.3.1}

There is *medium confidence* in future increase in seasonal mean precipitation on the equatorial flank of the Intertropical Convergence Zone and a decrease in precipitation in the subtropics including parts

Table TS.2 | Overview of projected regional changes and their relation to major climate phenomena. A phenomenon is considered relevant when there is both sufficient confidence that it has an influence on the given region, and when there is sufficient confidence that the phenomenon will change, particularly under the RCP4.5 or higher end scenarios. See Section 14.8 and Tables 14.2 and 14.3 for full assessment of the confidence in these changes, and their relevance for regional climate. {14.8; Tables 14.2, 14.3}

Regions	Projected Major Changes in Relation to Phenomena
Arctic {14.8.2}	Wintertime changes in temperature and precipitation resulting from the small projected increase in North Atlantic Oscillation (NAO); enhanced warming and sea ice melting; significant increase in precipitation by mid-century due mostly to enhanced precipitation in extratropical cyclones.
North America {14.8.3}	Monsoon precipitation will shift later in the annual cycle; increased precipitation in extratropical cyclones will lead to large increases in wintertime precipitation over the northern third of the continent; extreme precipitation increases in tropical cyclones making landfall along the western coast of USA and Mexico, the Gulf Mexico, and the eastern coast of USA and Canada.
Central America and Caribbean {14.8.4}	Projected reduction in mean precipitation and increase in extreme precipitation; more extreme precipitation in tropical cyclones making landfall along the eastern and western coasts.
South America {14.8.5}	A southward displaced South Atlantic Convergence Zone increases precipitation in the southeast; positive trend in the Southern Annular Mode displaces the extratropical storm track southward, decreasing precipitation in central Chile and increasing it at the southern tip of South America.
Europe and Mediterranean {14.8.6}	Enhanced extremes of storm-related precipitation and decreased frequency of storm-related precipitation over the eastern Mediterranean.
Africa {14.8.7}	Enhanced summer monsoon precipitation in West Africa; increased short rain in East Africa due to the pattern of Indian Ocean warming; increased rainfall extremes of landfall cyclones on the east coast (including Madagascar).
Central and North Asia {14.8.8}	Enhanced summer precipitation; enhanced winter warming over North Asia.
East Asia {14.8.9}	Enhanced summer monsoon precipitation; increased rainfall extremes of landfall typhoons on the coast; reduction in the midwinter suppression of extratropical cyclones.
West Asia {14.8.10}	Increased rainfall extremes of landfall cyclones on the Arabian Peninsula; decreased precipitation in northwest Asia due to a northward shift of extratropical storm tracks.
South Asia {14.8.11}	Enhanced summer monsoon precipitation; increased rainfall extremes of landfall cyclones on the coasts of the Bay of Bengal and Arabian Sea.
Southeast Asia {14.8.12}	Reduced precipitation in Indonesia during July to October due to the pattern of Indian Ocean warming; increased rainfall extremes of landfall cyclones on the coasts of the South China Sea, Gulf of Thailand and Andaman Sea.
Australia and New Zealand {14.8.13}	Summer monsoon precipitation may increase over northern Australia; more frequent episodes of the zonal South Pacific Convergence Zone may reduce precipitation in northeastern Australia; increased warming and reduced precipitation in New Zealand and southern Australia due to projected positive trend in the Southern Annular Mode; increased extreme precipitation associated with tropical and extratropical storms
Pacific Islands {14.8.14}	Tropical convergence zone changes affect rainfall and its extremes; more extreme precipitation associated with tropical cyclones
Antarctica {14.8.15}	Increased warming over Antarctic Peninsula and West Antarctic related to the positive trend in the Southern Annular Mode; increased precipitation in coastal areas due to a poleward shift of storm track.

of North and Central Americas, the Caribbean, South America, Africa and West Asia. There is *medium confidence* that the interannual occurrence of zonally oriented South Pacific Convergence Zone events will increase, leading possibly to more frequent droughts in the southwest Pacific. There is *medium confidence* that the South Atlantic Convergence Zone will shift southwards, leading to a precipitation increase over southeastern South America and a reduction immediately north of the convergence zone. {14.3.1, 14.8.3–14.8.5, 14.8.7, 14.8.11, 14.8.14}

The tropical Indian Ocean is *likely* to feature a zonal pattern with reduced warming and decreased rainfall in the east (including Indonesia), and enhanced warming and increased rainfall in the west (including East Africa). The Indian Ocean dipole mode of interannual variability is *very likely* to remain active, affecting climate extremes in East Africa, Indonesia and Australia. {14.3.3, 14.8.7, 14.8.12}

There is *low confidence* in the projections for the tropical Atlantic—both for the mean and interannual modes, because of large errors in model simulations in the region. Future projections in Atlantic hurricanes and tropical South American and West African precipitation are therefore of *low confidence*. {14.3.4, 14.6.1, 14.8.5,14.8.7}

It is currently not possible to assess how the Madden–Julian Oscillation will change owing to the poor skill in model simulations of this intraseasonal phenomenon and the sensitivity to ocean warming patterns. Future projections of regional climate extremes in West Asia, Southeast Asia and Australia are therefore of *low confidence*. {9.5.2, 14.3.4, 14.8.10, 14.8.12, 14.8.13}

TS.5.8.3 El Niño-Southern Oscillation

There is *high confidence* that the El Niño-Southern Oscillation (ENSO) will remain the dominant mode of natural climate variability in the 21st century with global influences in the 21st century, and that regional rainfall variability it induces *likely* intensifies. Natural variations of the amplitude and spatial pattern of ENSO are so large that *confidence* in any projected change for the 21st century remains *low*. The projected change in El Niño amplitude is small for both RCP4.5 and RCP8.5 compared to the spread of the change among models (Figure TS.25). Over the North Pacific and North America, patterns of temperature and precipitation anomalies related to El Niño and La Niña (teleconnections) are *likely* to move eastwards in the future (*medium confidence*), while *confidence* is *low* in changes in climate impacts on other regions including Central and South Americas, the Caribbean, Africa, most of Asia, Australia and most Pacific Islands. In a warmer climate, the increase in atmospheric moisture intensifies temporal variability

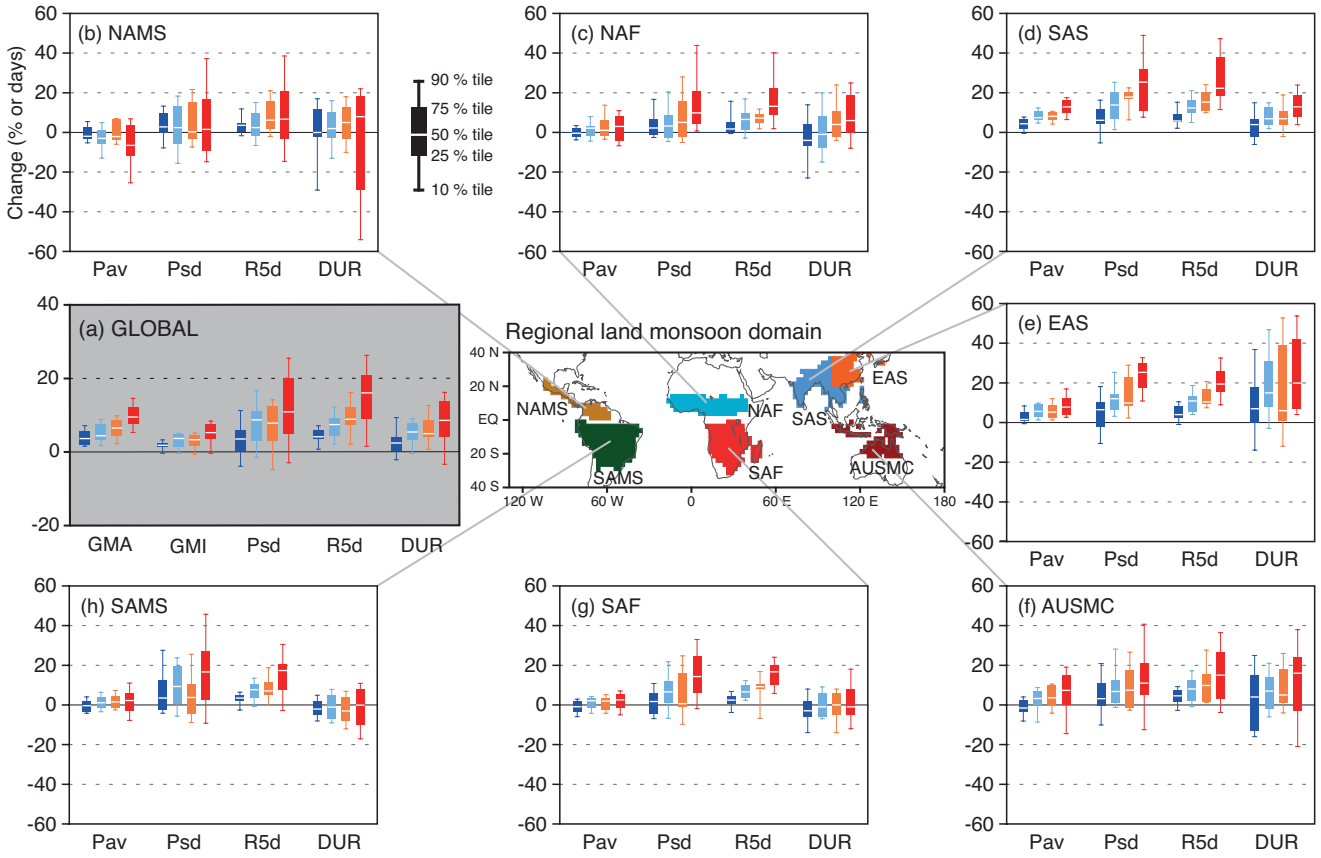

Figure TS.24 | Future change in monsoon statistics between the present-day (1986–2005) and the future (2080–2099) based on CMIP5 ensemble from RCP2.6 (dark blue; 18 models), RCP4.5 (blue; 24), RCP6.0 (yellow; 14), and RCP8.5 (red; 26) simulations. (a) GLOBAL: Global monsoon area (GMA), global monsoon intensity (GMI), standard deviation of inter-annual variability in seasonal precipitation (Psd), seasonal maximum 5-day precipitation total (R5d) and monsoon season duration (DUR). Regional land monsoon domains determined by 24 multi-model mean precipitation in the present-day. (b)–(h) Future change in regional land monsoon statistics: seasonal average precipitation (Pav), Psd, R5d, and DUR in (b) North America (NAMS), (c) North Africa (NAF), (d) South Asia (SAS), (e) East Asia (EAS), (f) Australia-Maritime continent (AUSMC), (g) South Africa (SAF) and (h) South America (SAMS). Units are % except for DUR (days). Box-and-whisker plots show the 10th, 25th, 50th, 75th and 90th percentiles. All the indices are calculated for the summer season (May to September for the Northern, and November to March for the Southern Hemisphere) over each model's monsoon domains. {Figures 14.3, 14.4, 14.6, 14.7}

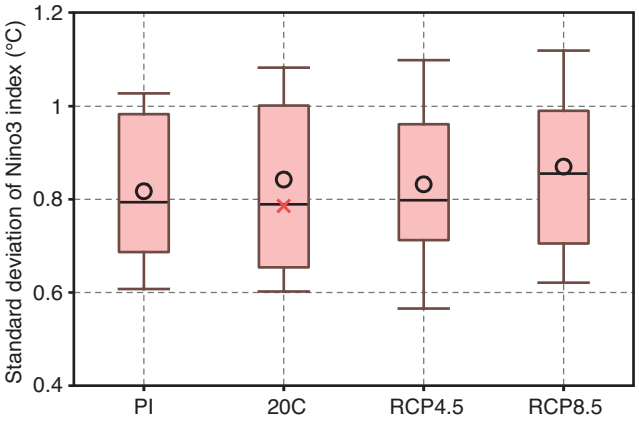

Figure TS.25 | Standard deviation in CMIP5 multi-model ensembles of sea surface temperature variability over the eastern equatorial Pacific Ocean (Nino3 region: 5°S to 5°N, 150°W to 90°W), a measure of El Niño amplitude, for the pre-industrial (PI) control and 20th century (20C) simulations, and 21st century projections using RCP4.5 and RCP8.5. Open circles indicate multi-model ensemble means, and the red cross symbol is the observed standard deviation for the 20th century. Box-and-whisker plots show the 16th, 25th, 50th, 75th and 84th percentiles. {Figure 14.14}

of precipitation even if atmospheric circulation variability remains the same. This applies to ENSO-induced precipitation variability but the possibility of changes in ENSO teleconnections complicates this general conclusion, making it somewhat regional-dependent. {12.4.5, 14.4, 14.8.3–14.8.5, 14.8.7, 14.8.9, 14.8.11–14.8.14}

TS.5.8.4 Cyclones

Projections for the 21st century indicate that it is *likely* that the global frequency of tropical cyclones will either decrease or remain essentially unchanged, concurrent with a *likely* increase in both global mean tropical cyclone maximum wind speed and rain rates (Figure TS.26). The influence of future climate change on tropical cyclones is *likely* to vary by region, but there is *low confidence* in region-specific projections. The frequency of the most intense storms will *more likely than not* increase in some basins. More extreme precipitation near the centers of tropical cyclones making landfall is projected in North and Central America, East Africa, West, East, South and Southeast Asia as well as in Australia and many Pacific islands (*medium confidence*). {14.6.1, 14.8.3, 14.8.4, 14.8.7, 14.8.9–14.8.14}

The global number of extratropical cyclones is *unlikely* to decrease by more than a few percent and future changes in storms are *likely* to be small compared to natural interannual variability and substantial variations between models. A small poleward shift is *likely* in the SH storm track but the magnitude of this change is model dependent. It is *unlikely* that the response of the North Atlantic storm track in climate projections is a simple poleward shift. There is *medium confidence* in a projected poleward shift in the North Pacific storm track. There is *low confidence* in the impact of storm track changes on regional climate at the surface. More precipitation in extratropical cyclones leads to a winter precipitation increase in Arctic, Northern Europe, North America and the mid-to-high-latitude SH. {11.3.2, 12.4.4, 14.6.2, 14.8.2, 14.8.3, 14.8.5, 14.8.6, 14.8.13, 14.8.15}

TS.5.8.5 Annular and Dipolar Modes of Variability

Future boreal wintertime North Atlantic Oscillation (NAO is *very likely* to exhibit large natural variations as observed in the past. The NAO is *likely* to become slightly more positive (on average), with some, but not very well documented implications for winter conditions in the Arctic, North America and Eurasia. The austral summer/autumn positive trend in Southern Annular Mode (SAM) is *likely* to weaken considerably as stratospheric ozone recovers through the mid-21st century with some, but not very well documented, implications for South America, Africa, Australia, New Zealand and Antarctica. {11.3.2, 14.5.2,14.8.5, 14.8.7, 14.8.13, 14.8.15}

TS.5.8.6 Additional Phenomena

It is *unlikely* that the Atlantic Multi-decadal Oscillation (AMO will change its behaviour as the mean climate changes. However, natural fluctuations in the AMO over the coming few decades are *likely* to influence regional climates at least as strongly as will human-induced changes with implications for Atlantic major hurricane frequency, the West African monsoon and North American and European summer conditions. {14.2.4, 14.5.1, 14.6.1, 14.7.6, 14.8.2, 14.8.3, 14.8.6, 14.8.8}

There is *medium confidence* that the frequency of NH and SH blocking will not increase, while the trends in blocking intensity and persistence remain uncertain. {Box 14.2}

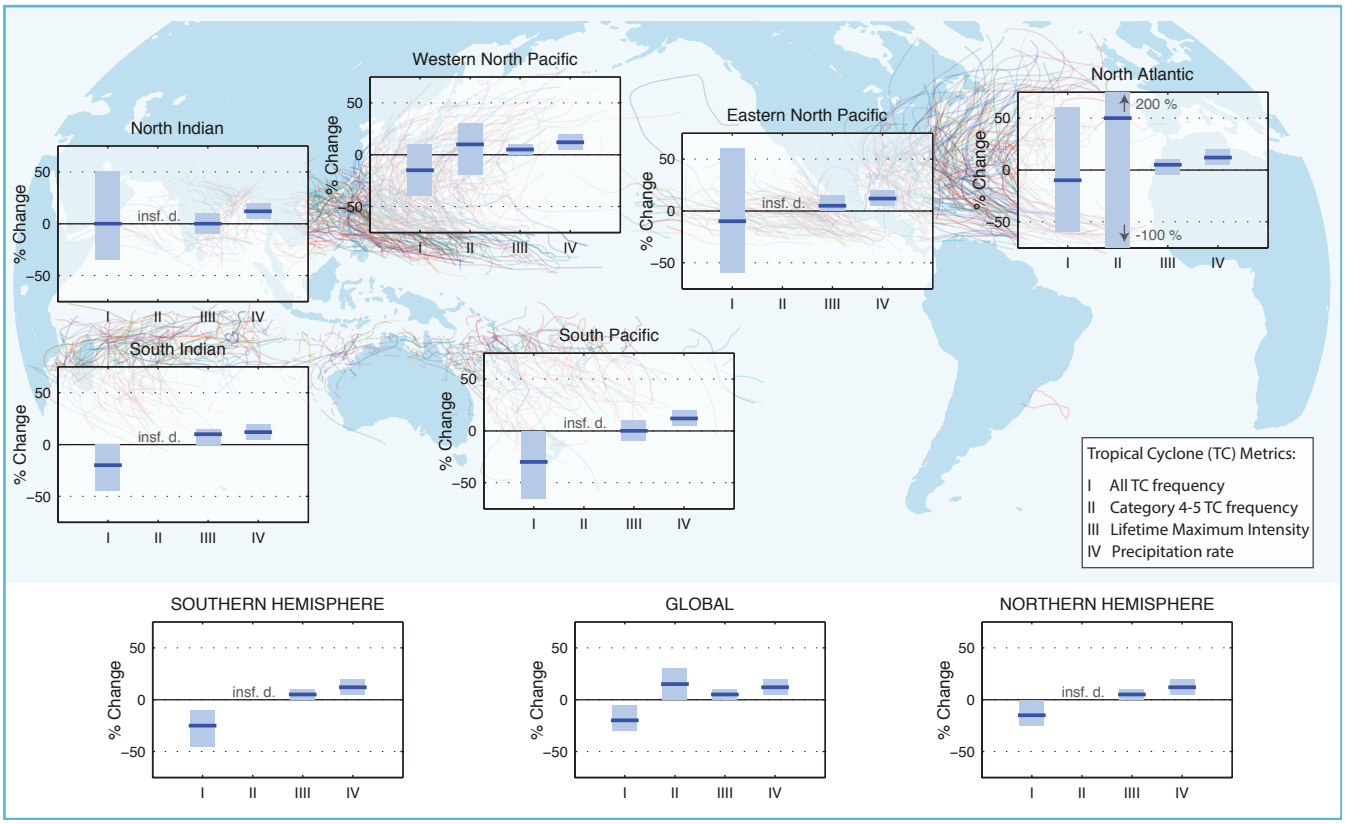

Figure TS.26 | Projected changes in tropical cyclone statistics. All values represent expected percent change in the average over period 2081–2100 relative to 2000–2019, under an A1B-like scenario, based on expert judgement after subjective normalization of the model projections. Four metrics were considered: the percent change in I) the total annual frequency of tropical storms, II) the annual frequency of Category 4 and 5 storms, III) the mean Lifetime Maximum Intensity (LMI; the maximum intensity achieved during a storm's lifetime) and IV) the precipitation rate within 200 km of storm center at the time of LMI. For each metric plotted, the solid blue line is the best guess of the expected percent change, and the coloured bar provides the 67% (*likely*) confidence interval for this value (note that this interval ranges across –100% to +200% for the annual frequency of Category 4 and 5 storms in the North Atlantic). Where a metric is not plotted, there are insufficient data (denoted X) available to complete an assessment. A randomly drawn (and coloured) selection of historical storm tracks are underlaid to identify regions of tropical cyclone activity. See Section 14.6.1 for details. {14.6.1}

Thematic Focus Elements

TFE.9 | Climate Extremes

Assessing changes in climate extremes poses unique challenges, not just because of the intrinsically rare nature of these events, but because they invariably happen in conjunction with disruptive conditions. They are strongly influenced by both small- and large-scale weather patterns, modes of variability, thermodynamic processes, land–atmosphere feedbacks and antecedent conditions. Much progress has been made since the IPCC Fourth Assessment Report (AR4) including the comprehensive assessment of extremes undertaken by the IPCC Special Report on Managing the Risk of Extreme Events and Disasters to Advance Climate Change Adaptation (SREX) but also because of the amount of observational evidence available, improvements in our understanding and the ability of models to simulate extremes. {1.3.3, 2.6, 7.6, 9.5.4}

For some climate extremes such as droughts, floods and heat waves, several factors need to be combined to produce an extreme event. Analyses of rarer extremes such as 1-in-20- to 1-in-100-year events using Extreme Value Theory are making their way into a growing body of literature. Other recent advances concern the notion of 'fraction of attributable risk' that aims to link a particular extreme event to specific causal relationships. {1.3.3, 2.6.1, 2.6.2, 10.6.2, 12.4.3; Box 2.4}

TFE.9, Table 1 indicates the changes that have been observed in a range of weather and climate extremes over the last 50 years, the assessment of the human contribution to those changes, and how those extremes are expected to change in the future. The table also compares the current assessment with that of the AR4 and the SREX where applicable. {2.6, 3.7, 10.6, 11.3, 12.4, 14.6}

Temperature Extremes, Heat Waves and Warm Spells

It is *very likely* that both maximum and minimum temperature extremes have warmed over most land areas since the mid-20th century. These changes are well simulated by current climate models, and it is *very likely* that anthropogenic forcing has affected the frequency of these extremes and *virtually certain* that further changes will occur. This supports AR4 and SREX conclusions although with greater confidence in the anthropogenic forcing component. {2.6.1, 9.5.4, 10.6.1, 12.4.3}

For land areas with sufficient data there has been an overall increase in the number of warm days and nights. Similar decreases are seen in the number of cold days and nights. It is *very likely* that increases in unusually warm days and nights and/or reductions in unusually cold days and nights including frosts have occurred over this period across most continents. Warm spells or heat waves containing consecutive extremely hot days or nights are often associated with quasi-stationary anticyclonic circulation anomalies and are also affected by pre-existing soil conditions and the persistence of soil moisture anomalies that can amplify or dampen heat waves particularly in moisture-limited regions. Most global land areas, with a few exceptions, have experienced more heat waves since the middle of the 20th century. Several studies suggest that increases in mean temperature account for most of the changes in heat wave frequency, however, heat wave intensity/amplitude is highly sensitive to changes in temperature variability and the shape of the temperature distribution and heat wave definition also plays a role. Although in some regions instrumental periods prior to the 1950s had more heat waves (e.g., USA), for other regions such as Europe, an increase in heat wave frequency in the period since the 1950s stands out in long historical temperature series. {2.6, 2.6.1, 5.5.1; Box 2.4; Tables 2.12, 2.13; FAQ 2.2}

The observed features of temperature extremes and heat waves are well simulated by climate models and are similar to the spread among observationally based estimates in most regions. Regional downscaling now offers credible information on the spatial scales required for assessing extremes and improvements in the simulation of the El Niño-Southern Oscillation from Coupled Model Intercomparison Project Phase 3 (CMIP3) to Phase 5 (CMIP5) and other large-scale phenomena is crucial. However simulated changes in frequency and intensity of extreme events is limited by observed data availability and quality issues and by the ability of models to reliably simulate certain feedbacks and mean changes in key features of circulation such as blocking. {2.6, 2.7, 9.4, 9.5.3, 9.5.4, 9.6, 9.6.1, 10.3, 10.6, 14.4; Box 14.2}

Since AR4, the understanding of mechanisms and feedbacks leading to changes in extremes has improved. There continues to be strengthening evidence for a human influence on the observed frequency of extreme temperatures and heat waves in some regions. Near-term (decadal) projections suggest *likely* increases in temperature extremes but with little distinguishable separation between emissions scenarios (TFE.9, Figure 1). Changes may proceed at

(continued on next page)

TFE.9, Table 1 | Extreme weather and climate events: Global-scale assessment of recent observed changes, human contribution to the changes and projected further changes for the early (2016–2035) and late (2081–2100) 21st century. Bold indicates where the AR5 (black) provides a revised* global-scale assessment from the Special Report on Managing the Risk of Extreme Events and Disasters to Advance Climate Change Adaptation (SREX, blue) or AR4 (red). Projections for early 21st century were not provided in previous assessment reports. Projections in the AR5 are relative to the reference period of 1986–2005, and use the new RCP scenarios unless otherwise specified. See the Glossary for definitions of extreme weather and climate events.

Phenomenon and direction of trend	Assessment that changes occurred (typically since 1950 unless otherwise indicated)	Assessment of a human contribution to observed changes	Likelihood of further changes	
			Early 21st century	Late 21st century
Warmer and/or fewer cold days and nights over most land areas	*Very likely* {2.6} *Very likely* *Very likely*	***Very likely*** {10.6} *Likely* *Likely*	*Likely* {11.3}	*Virtually certain* {12.4} *Virtually certain* *Virtually certain*
Warmer and/or more frequent hot days and nights over most land areas	*Very likely* {2.6} *Very likely* *Very likely*	***Very likely*** {10.6} *Likely* *Likely* (nights only)	*Likely* {11.3}	*Virtually certain* {12.4} *Virtually certain* *Virtually certain*
Warm spells/heat waves. Frequency and/or duration increases over most land areas	***Medium confidence*** on a global scale *Likely* in large parts of Europe, Asia and Australia {2.6} *Medium confidence* in many (but not all) regions *Likely*	***Likely***[a] {10.6} Not formally assessed *More likely than not*	Not formally assessed[b] {11.3}	*Very likely* {12.4} *Very likely* *Very likely*
Heavy precipitation events. Increase in the frequency, intensity, and/or amount of heavy precipitation	*Likely* more land areas with increases than decreases[c] {2.6} *Likely* more land areas with increases than decreases *Likely* over most land areas	***Medium confidence*** {7.6, 10.6} *Medium confidence* *More likely than not*	*Likely* over many land areas {11.3}	***Very likely*** over most of the mid-latitude land masses and over wet tropical regions {12.4} *Likely* over many areas *Very likely* over most land areas
Increases in intensity and/or duration of drought	***Low confidence*** on a global scale *Likely* changes in some regions[d] {2.6} *Medium confidence* in some regions *Likely* in many regions, since 1970[e]	***Low confidence*** {10.6} *Medium confidence*[f] *More likely than not*	*Low confidence*[g] {11.3}	***Likely*** *(medium confidence)* on a regional to global scale[h] {12.4} *Medium confidence* in some regions *Likely*[e]
Increases in intense tropical cyclone activity	***Low confidence*** in long term (centennial) changes *Virtually certain* in North Atlantic since 1970 {2.6} *Low confidence* *Likely* in some regions, since 1970	***Low confidence***[i] {10.6} *Low confidence* *More likely than not*	*Low confidence* {11.3}	***More likely than not*** in the Western North Pacific and North Atlantic[j] {14.6} *More likely than not* in some basins *Likely*
Increased incidence and/or magnitude of extreme high sea level	*Likely* (since 1970) {3.7} *Likely* (late 20th century) *Likely*	***Likely***[k] {3.7} *Likely*[k] *More likely than not*[k]	*Likely*[l] {13.7}	***Very likely***[l] {13.7} *Very likely*[m] *Likely*

* The direct comparison of assessment findings between reports is difficult. For some climate variables, different aspects have been assessed, and the revised guidance note on uncertainties has been used for the SREX and AR5. The availability of new information, improved scientific understanding, continued analyses of data and models, and specific differences in methodologies applied in the assessed studies, all contribute to revised assessment findings.

Notes:

[a] Attribution is based on available case studies. It is *likely* that human influence has more than doubled the probability of occurrence of some observed heat waves in some locations.

[b] Models project near-term increases in the duration, intensity and spatial extent of heat waves and warm spells.

[c] In most continents, *confidence* in trends is not higher than *medium* except in North America and Europe where there have been *likely* increases in either the frequency or intensity of heavy precipitation with some seasonal and/or regional variation. It is *very likely* that there have been increases in central North America.

[d] The frequency and intensity of drought has *likely* increased in the Mediterranean and West Africa and *likely* decreased in central North America and north-west Australia.

[e] AR4 assessed the area affected by drought.

[f] SREX assessed *medium confidence* that anthropogenic influence had contributed to some changes in the drought patterns observed in the second half of the 20th century, based on its attributed impact on precipitation and temperature changes. SREX assessed *low confidence* in the attribution of changes in droughts at the level of single regions.

[g] There is *low confidence* in projected changes in soil moisture.

[h] Regional to global-scale projected decreases in soil moisture and increased agricultural drought are *likely* (*medium confidence*) in presently dry regions by the end of this century under the RCP8.5 scenario. Soil moisture drying in the Mediterranean, Southwest USA and southern African regions is consistent with projected changes in Hadley circulation and increased surface temperatures, so there is *high confidence* in *likely* surface drying in these regions by the end of this century under the RCP8.5 scenario.

[i] There is *medium confidence* that a reduction in aerosol forcing over the North Atlantic has contributed at least in part to the observed increase in tropical cyclone activity since the 1970s in this region.

[j] Based on expert judgment and assessment of projections which use an SRES A1B (or similar) scenario.

[k] Attribution is based on the close relationship between observed changes in extreme and mean sea level.

[l] There is *high confidence* that this increase in extreme high sea level will primarily be the result of an increase in mean sea level. There is *low confidence* in region-specific projections of storminess and associated storm surges.

[m] SREX assessed it to be *very likely* that mean sea level rise will contribute to future upward trends in extreme coastal high water levels.

TFE.9 (continued)

a different rate than the mean warming however, with several studies showing that projected European high-percentile summer temperatures will warm faster than mean temperatures. Future changes associated with the warming of temperature extremes in the long-term are *virtually certain* and scale with the strength of emissions scenario, that is, greater anthropogenic emissions correspond to greater warming of extremes (TFE.9, Figure 1). For high-emissions scenarios, it is *likely* that, in most land regions, a current 1-in-20-year maximum temperature event

(continued on next page)

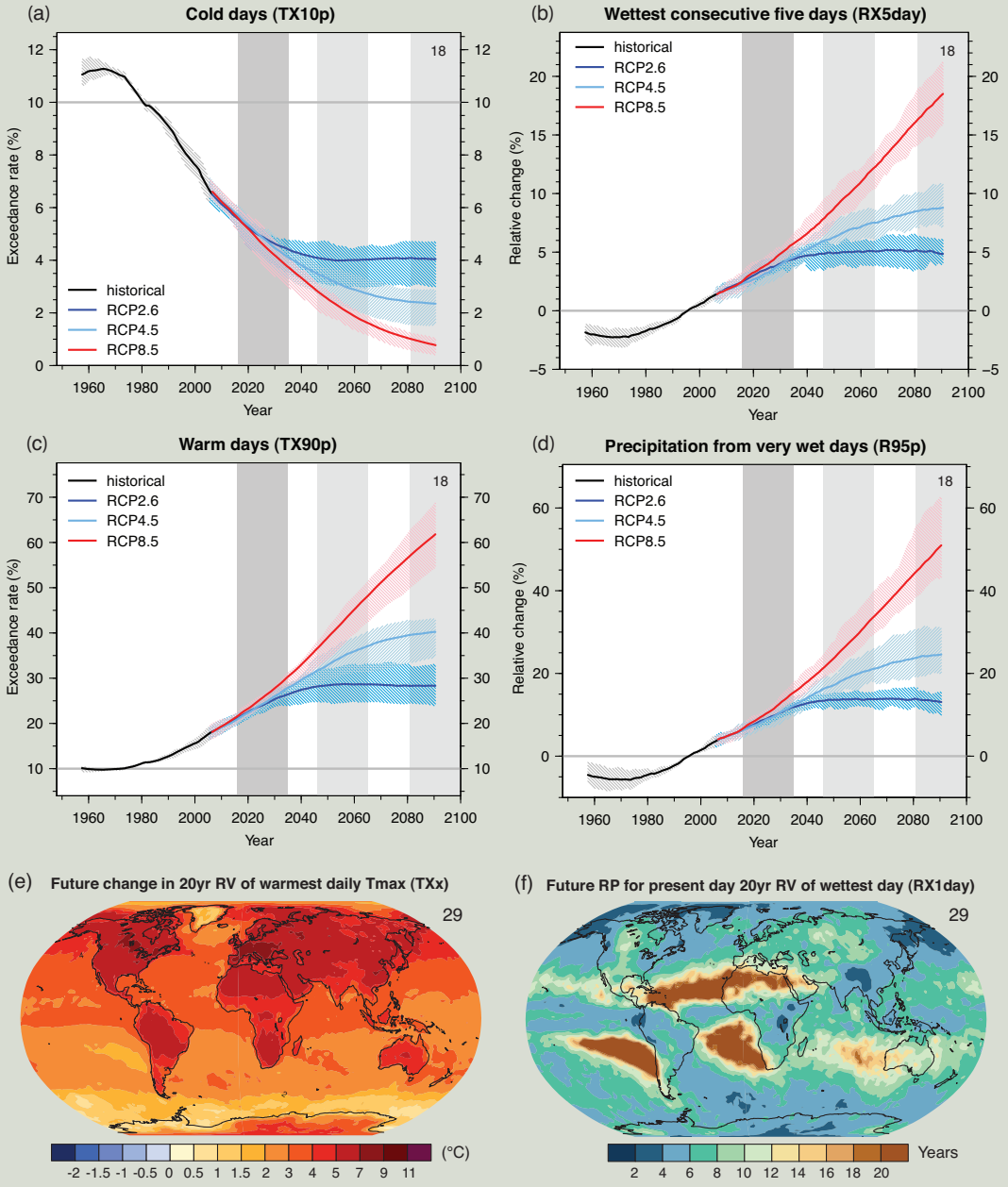

TFE.9, Figure 1 | Global projections of the occurrence of (a) cold days (TX10p)- percentage of days annually with daily maximum surface air temperature (Tmax) below the 10th percentile of Tmax for 1961 to 1990, (b) wettest consecutive 5 days (RX5day) —percentage change relative to 1986–2005 in annual maximum consecutive 5-day precipitation totals, (c) warm days (TX90p)—percentage of days annually with daily maximum surface air temperature (Tmax) exceeding the 90th percentile of Tmax for 1961 to 1990 and (d) very wet day precipitation (R95p)—percentage change relative to 1986–2005 of annual precipitation from days >95th percentile. Results are shown from CMIP5 for the RCP2.6, RCP4.5 and RCP8.5 scenarios. Solid lines indicate the ensemble median and shading indicates the interquartile spread between individual projections (25th and 75th percentiles). Maps show (e) the change from 1986–2005 to 2081–2100 in 20-year return values (RV) of daily maximum temperatures, TXx, and (f) the 2081–2100 return period (RP) for rare daily precipitation values, RX1day, that have a 20-year return period during 1986–2005. Both maps are based on the CMIP5 RCP8.5 scenario. The number of models used to calculate the multi-model mean is indicated in each panel. See Box 2.4, Table 1 for index definitions. {Figures 11.17, 12.14, 12.26, 12.27}

TFE.9 (continued)

will at least double in frequency but in many regions will become an annual or a 1-in-2-year event by the end of the 21st century. The magnitude of both high and low temperature extremes is expected to increase at least at the same rate as the mean, but with 20-year return values for low temperature events projected to increase at a rate greater than winter mean temperatures in most regions. {10.6.1, 11.3.2, 12.4.3}

Precipitation Extremes

It is *likely* that the number of heavy precipitation events over land has increased in more regions than it has decreased in since the mid-20th century, and there is *medium confidence* that anthropogenic forcing has contributed to this increase. {2.6.2, 10.6.1}

There has been substantial progress between CMIP3 and CMIP5 in the ability of models to simulate more realistic precipitation extremes. However, evidence suggests that the majority of models underestimate the sensitivity of extreme precipitation to temperature variability or trends especially in the tropics, which implies that models may underestimate the projected increase in extreme precipitation in the future. While progress has been made in understanding the processes that drive extreme precipitation, challenges remain in quantifying cloud and convective effects in models for example. The complexity of land surface and atmospheric processes limits confidence in regional projections of precipitation change, especially over land, although there is a component of a 'wet-get-wetter' and 'dry-get-drier' response over oceans at the large scale. Even so, there is *high confidence* that, as the climate warms, extreme precipitation rates (e.g., on daily time scales) will increase faster than the time average. Changes in local extremes on daily and sub-daily time scales are expected to increase by roughly 5 to 10% per °C of warming (*medium confidence*). {7.6, 9.5.4}

For the near and long term, CMIP5 projections confirm a clear tendency for increases in heavy precipitation events in the global mean seen in the AR4, but there are substantial variations across regions (TFE.9, Figure 1). Over most of the mid-latitude land masses and over wet tropical regions, extreme precipitation will *very likely* be more intense and more frequent in a warmer world. {11.3.2, 12.4.5}

Floods and Droughts

There continues to be a lack of evidence and thus *low confidence* regarding the sign of trend in the magnitude and/or frequency of floods on a global scale over the instrumental record. There is *high confidence* that past floods larger than those recorded since 1900 have occurred during the past five centuries in northern and central Europe, western Mediterranean region, and eastern Asia. There is *medium confidence* that modern large floods are comparable to or surpass historical floods in magnitude and/or frequency in the Near East, India and central North America. {2.6.2, 5.5.5}

Compelling arguments both for and against significant increases in the land area affected by drought and/or dryness since the mid-20th century have resulted in a *low confidence* assessment of observed and attributable large-scale trends. This is due primarily to a lack and quality of direct observations, dependencies of inferred trends on the index choice, geographical inconsistencies in the trends and difficulties in distinguishing decadal scale variability from long term trends. On millennial time scales, there is *high confidence* that proxy information provides evidence of droughts of greater magnitude and longer duration than observed during the 20th century in many regions. There is *medium confidence* that more megadroughts occurred in monsoon Asia and wetter conditions prevailed in arid Central Asia and the South American monsoon region during the Little Ice Age (1450 to 1850) compared to the Medieval Climate Anomaly (950 to 1250). {2.6.2, 5.5.4, 5.5.5, 10.6.1}

Under the Representative Concentration Pathway RCP8.5, projections by the end of the century indicate an increased risk of drought is *likely* (*medium confidence*) in presently dry regions linked to regional to global-scale projected decreases in soil moisture. Soil moisture drying is most prominent in the Mediterranean, Southwest USA, and southern Africa, consistent with projected changes in the Hadley Circulation and increased surface temperatures, and surface drying in these regions is *likely* (*high confidence*) by the end of the century under RCP8.5. {12.4.5}

Extreme Sea Level

It is *likely* that the magnitude of extreme high sea level events has increased since 1970 and that most of this rise can be explained by increases in mean sea level. When mean sea level changes is taken into account, changes in extreme high sea levels are reduced to less than 5 mm y^{r-1} at 94% of tide gauges. In the future it is *very likely* that there will be a significant increase in the occurrence of sea level extremes and similarly to past observations, this increase will primarily be the result of an increase in mean sea level. {3.7.5, 13.7.2}

(continued on next page)

TFE.9 (continued)

Tropical and Extratropical Cyclones

There is *low confidence* in long-term (centennial) changes in tropical cyclone activity, after accounting for past changes in observing capabilities. However over the satellite era, increases in the frequency and intensity of the strongest storms in the North Atlantic are robust (*very high confidence*). However, the cause of this increase is debated and there is *low confidence* in attribution of changes in tropical cyclone activity to human influence owing to insufficient observational evidence, lack of physical understanding of the links between anthropogenic drivers of climate and tropical cyclone activity and the low level of agreement between studies as to the relative importance of internal variability, and anthropogenic and natural forcings. {2.6.3, 10.6.1, 14.6.1}

Some high-resolution atmospheric models have realistically simulated tracks and counts of tropical cyclones and models generally are able to capture the general characteristics of storm tracks and extratropical cyclones with evidence of improvement since the AR4. Storm track biases in the North Atlantic have improved slightly, but models still produce a storm track that is too zonal and underestimate cyclone intensity. {9.4.1, 9.5.4}

While projections indicate that it is *likely* that the global frequency of tropical cyclones will either decrease or remain essentially unchanged, concurrent with a *likely* increase in both global mean tropical cyclone maximum wind speed and rainfall rates, there is lower confidence in region-specific projections of frequency and intensity. However, due to improvements in model resolution and downscaling techniques, it is *more likely than not* that the frequency of the most intense storms will increase substantially in some basins under projected 21st century warming (see Figure TS.26). {11.3.2, 14.6.1}

Research subsequent to the AR4 and SREX continues to support a *likely* poleward shift of storm tracks since the 1950s. However over the last century there is *low confidence* of a clear trend in storminess due to inconsistencies between studies or lack of long-term data in some parts of the world (particularly in the Southern Hemisphere (SH)). {2.6.4, 2.7.6}

Despite systematic biases in simulating storm tracks, most models and studies are in agreement that the global number of extratropical cyclones is *unlikely* to decrease by more than a few per cent. A small poleward shift is *likely* in the SH storm track. It is *more likely than not* (*medium confidence*) for a projected poleward shift in the North Pacific storm track but it is *unlikely* that the response of the North Atlantic storm track is a simple poleward shift. There is *low confidence* in the magnitude of regional storm track changes, and the impact of such changes on regional surface climate. {14.6.2}

TS.6 Key Uncertainties

This final section of the Technical Summary provides readers with a short overview of key uncertainties in the understanding of the climate system and the ability to project changes in response to anthropogenic influences. The overview is not comprehensive and does not describe in detail the basis for these findings. These are found in the main body of this Technical Summary and in the underlying chapters to which each bullet points in the curly brackets.

TS.6.1 Key Uncertainties in Observation of Changes in the Climate System

- There is only *medium* to *low confidence* in the rate of change of tropospheric warming and its vertical structure. Estimates of tropospheric warming rates encompass surface temperature warming rate estimates. There is *low confidence* in the rate and vertical structure of the stratospheric cooling. {2.4.4}

- *Confidence* in global precipitation change over land is *low* prior to 1951 and *medium* afterwards because of data incompleteness. {2.5.1}

- Substantial ambiguity and therefore *low confidence* remains in the observations of global-scale cloud variability and trends. {2.5.6}

- There is *low confidence* in an observed global-scale trend in drought or dryness (lack of rainfall), due to lack of direct observations, methodological uncertainties and choice and geographical inconsistencies in the trends. {2.6.2}

- There is *low confidence* that any reported long-term (centennial) changes in tropical cyclone characteristics are robust, after accounting for past changes in observing capabilities. {2.6.3}

- Robust conclusions on long-term changes in large-scale atmospheric circulation are presently not possible because of large variability on interannual to decadal time scales and remaining differences between data sets. {2.7}

- Different global estimates of sub-surface ocean temperatures have variations at different times and for different periods, suggesting that sub-decadal variability in the temperature and upper heat content (0 to to 700 m) is still poorly characterized in the historical record. {3.2}

- Below ocean depths of 700 m the sampling in space and time is too sparse to produce annual global ocean temperature and heat content estimates prior to 2005. {3.2.4}

- Observational coverage of the ocean deeper than 2000 m is still limited and hampers more robust estimates of changes in global ocean heat content and carbon content. This also limits the quantification of the contribution of deep ocean warming to sea level rise. {3.2, 3.7, 3.8; Box 3.1}

- The number of continuous observational time series measuring the strength of climate relevant ocean circulation features (e.g., the meridional overturning circulation) is limited and the existing time series are still too short to assess decadal and longer trends. {3.6}.

- In Antarctica, available data are inadequate to assess the status of change of many characteristics of sea ice (e.g., thickness and volume). {4.2.3}

- On a global scale the mass loss from melting at calving fronts and iceberg calving are not yet comprehensively assessed. The largest uncertainty in estimated mass loss from glaciers comes from the Antarctic, and the observational record of ice–ocean interactions around both ice sheets remains poor. {4.3.3, 4.4}

TS.6.2 Key Uncertainties in Drivers of Climate Change

- Uncertainties in aerosol–cloud interactions and the associated radiative forcing remain large. As a result, uncertainties in aerosol forcing remain the dominant contributor to the overall uncertainty in net anthropogenic forcing, despite a better understanding of some of the relevant atmospheric processes and the availability of global satellite monitoring. {2.2, 7.3–7.5, 8.5}

- The cloud feedback is *likely* positive but its quantification remains difficult. {7.2}

- Paleoclimate reconstructions and Earth System Models indicate that there is a positive feedback between climate and the carbon cycle, but *confidence* remains *low* in the strength of this feedback, particularly for the land. {6.4}

TS.6.3 Key Uncertainties in Understanding the Climate System and Its Recent Changes

- The simulation of clouds in AOGCMs has shown modest improvement since AR4; however, it remains challenging. {7.2, 9.2.1, 9.4.1, 9.7.2}

- Observational uncertainties for climate variables other than temperature, uncertainties in forcings such as aerosols, and limits in process understanding continue to hamper attribution of changes in many aspects of the climate system. {10.1, 10.3, 10.7}

- Changes in the water cycle remain less reliably modelled in both their changes and their internal variability, limiting confidence in attribution assessments. Observational uncertainties and the large effect of internal variability on observed precipitation also precludes a more confident assessment of the causes of precipitation changes. {2.5.1, 2.5.4, 10.3.2}

- Modelling uncertainties related to model resolution and incorporation of relevant processes become more important at regional scales, and the effects of internal variability become more significant. Therefore, challenges persist in attributing observed change to external forcing at regional scales. {2.4.1, 10.3.1}

- The ability to simulate changes in frequency and intensity of extreme events is limited by the ability of models to reliably simulate mean changes in key features. {10.6.1}

- In some aspects of the climate system, including changes in drought, changes in tropical cyclone activity, Antarctic warming, Antarctic sea ice extent, and Antarctic mass balance, *confidence* in attribution to human influence remains *low* due to modelling uncertainties and low agreement between scientific studies. {10.3.1, 10.5.2, 10.6.1}

TS.6.4 Key Uncertainties in Projections of Global and Regional Climate Change

- Based on model results there is limited confidence in the predictability of yearly to decadal averages of temperature both for the global average and for some geographical regions. Multi-model results for precipitation indicate a generally low predictability. Short-term climate projection is also limited by the uncertainty in projections of natural forcing. {11.1, 11.2, 11.3.1, 11.3.6; Box 11.1}

- There is *medium confidence* in near-term projections of a northward shift of NH storm track and westerlies. {11.3.2}

- There is generally *low confidence* in basin-scale projections of significant trends in tropical cyclone frequency and intensity in the 21st century. {11.3.2, 14.6.1}

- Projected changes in soil moisture and surface run off are not robust in many regions. {11.3.2, 12.4.5}

- Several components or phenomena in the climate system could potentially exhibit abrupt or nonlinear changes, but for many phenomena there is *low confidence* and little consensus on the likelihood of such events over the 21st century. {12.5.5}

- There is *low confidence* on magnitude of carbon losses through CO_2 or CH_4 emissions to the atmosphere from thawing permafrost. There is *low confidence* in projected future CH_4 emissions from natural sources due to changes in wetlands and gas hydrate release from the sea floor. {6.4.3, 6.4.7}

- There is *medium confidence* in the projected contributions to sea level rise by models of ice sheet dynamics for the 21st century, and *low confidence* in their projections beyond 2100. {13.3.3}

- There is *low confidence* in semi-empirical model projections of global mean sea level rise, and no consensus in the scientific community about their reliability. {13.5.2, 13.5.3}

- There is *low confidence* in projections of many aspects of climate phenomena that influence regional climate change, including changes in amplitude and spatial pattern of modes of climate variability. {9.5.3, 14.2–14.7}

Frequently Asked Questions

FAQ

Frequently Asked Questions

These Frequently Asked Questions have been extracted from the chapters of the underlying report and are compiled here. When referencing specific FAQs, please reference the corresponding chapter in the report from where the FAQ originated (e.g., FAQ 3.1 is part of Chapter 3).

Table of Contents

Frequently Asked Questions

Frequently Asked Questions

FAQ 1.1 | If Understanding of the Climate System Has Increased, Why Hasn't the Range of Temperature Projections Been Reduced?

The models used to calculate the IPCC's temperature projections agree on the direction of future global change, but the projected size of those changes cannot be precisely predicted. Future greenhouse gas (GHG) emission rates could take any one of many possible trajectories, and some underlying physical processes are not yet completely understood, making them difficult to model. Those uncertainties, combined with natural year-to-year climate variability, produce an 'uncertainty range' in temperature projections.

The uncertainty range around projected GHG and aerosol precursor emissions (which depend on projections of future social and economic conditions) cannot be materially reduced. Nevertheless, improved understanding and climate models—along with observational constraints—may reduce the uncertainty range around some factors that influence the climate's response to those emission changes. The complexity of the climate system, however, makes this a slow process. (FAQ1.1, Figure 1)

Climate science has made many important advances since the last IPCC assessment report, thanks to improvements in measurements and data analysis in the cryosphere, atmosphere, land, biosphere and ocean systems. Scientists also have better understanding and tools to model the role of clouds, sea ice, aerosols, small-scale ocean mixing, the carbon cycle and other processes. More observations mean that models can now be evaluated more thoroughly, and projections can be better constrained. For example, as models and observational analysis have improved, projections of sea level rise have become more accurate, balancing the current sea level rise budget.

Despite these advances, there is still a range in plausible projections for future global and regional climate—what scientists call an 'uncertainty range'. These uncertainty ranges are specific to the variable being considered (precipitation vs. temperature, for instance) and the spatial and temporal extent (such as regional vs. global averages). Uncertainties in climate projections arise from natural variability and uncertainty around the rate of future emissions and the climate's response to them. They can also occur because representations of some known processes are as yet unrefined, and because some processes are not included in the models.

There are fundamental limits to just how precisely annual temperatures can be projected, because of the chaotic nature of the climate system. Furthermore, decadal-scale projections are sensitive to prevailing conditions—such as the temperature of the deep ocean—that are less well known. Some natural variability over decades arises from interactions between the ocean, atmosphere, land, biosphere and cryosphere, and is also linked to phenomena such as the El Niño-Southern Oscillation (ENSO) and the North Atlantic Oscillation (see Box 2.5 for details on patterns and indices of climate variability).

Volcanic eruptions and variations in the sun's output also contribute to natural variability, although they are externally forced and explainable. This natural variability can be viewed as part of the 'noise' in the climate record, which provides the backdrop against which the 'signal' of anthropogenic climate change is detected.

Natural variability has a greater influence on uncertainty at regional and local scales than it does over continental or global scales. It is inherent in the Earth system, and more knowledge will not eliminate the uncertainties it brings. However, some progress is possible—particularly for projections up to a few years ahead—which exploit advances in knowledge of, for instance, the cryosphere or ocean state and processes. This is an area of active research. When climate variables are averaged over decadal timescales or longer, the relative importance of internal variability diminishes, making the long-term signals more evident (FAQ1.1, Figure 1). This long-term perspective is consistent with a common definition of climate as an average over 30 years.

A second source of uncertainty stems from the many possible trajectories that future emission rates of GHGs and aerosol precursors might take, and from future trends in land use. Nevertheless, climate projections rely on input from these variables. So to obtain these estimates, scientists consider a number of alternative scenarios for future human society, in terms of population, economic and technological change, and political choices. They then estimate the likely emissions under each scenario. The IPCC informs policymaking, therefore climate projections for different emissions scenarios can be useful as they show the possible climatic consequences of different policy choices. These scenarios are intended to be compatible with the full range of emissions scenarios described in the current scientific literature, with or without climate policy. As such, they are designed to sample uncertainty in future scenarios. *(continued on next page)*

FAQ 1.1 (continued)

Projections for the next few years and decades are sensitive to emissions of short-lived compounds such as aerosols and methane. More distant projections, however, are more sensitive to alternative scenarios around long-lived GHG emissions. These scenario-dependent uncertainties will not be reduced by improvements in climate science, and will become the dominant uncertainty in projections over longer timescales (e.g., 2100) (FAQ 1.1, Figure 1).

The final contribution to the uncertainty range comes from our imperfect knowledge of how the climate will respond to future anthropogenic emissions and land use change. Scientists principally use computer-based global climate models to estimate this response. A few dozen global climate models have been developed by different groups of scientists around the world. All models are built on the same physical principles, but some approximations are needed because the climate system is so complex. Different groups choose slightly different approximations to represent specific processes in the atmosphere, such as clouds. These choices produce differences in climate projections from different models. This contribution to the uncertainty range is described as 'response uncertainty' or 'model uncertainty'.

The complexity of the Earth system means that future climate could follow many different scenarios, yet still be consistent with current understanding and models. As observational records lengthen and models improve, researchers should be able, within the limitations of the range of natural variability, to narrow that range in probable temperature in the next few decades (FAQ 1.1, Figure 1). It is also possible to use information about the current state of the oceans and cryosphere to produce better projections up to a few years ahead.

As science improves, new geophysical processes can be added to climate models, and representations of those already included can be improved. These developments can appear to increase model-derived estimates of climate response uncertainty, but such increases merely reflect the quantification of previously unmeasured sources of uncertainty (FAQ1.1, Figure 1). As more and more important processes are added, the influence of unquantified processes lessens, and there can be more confidence in the projections.

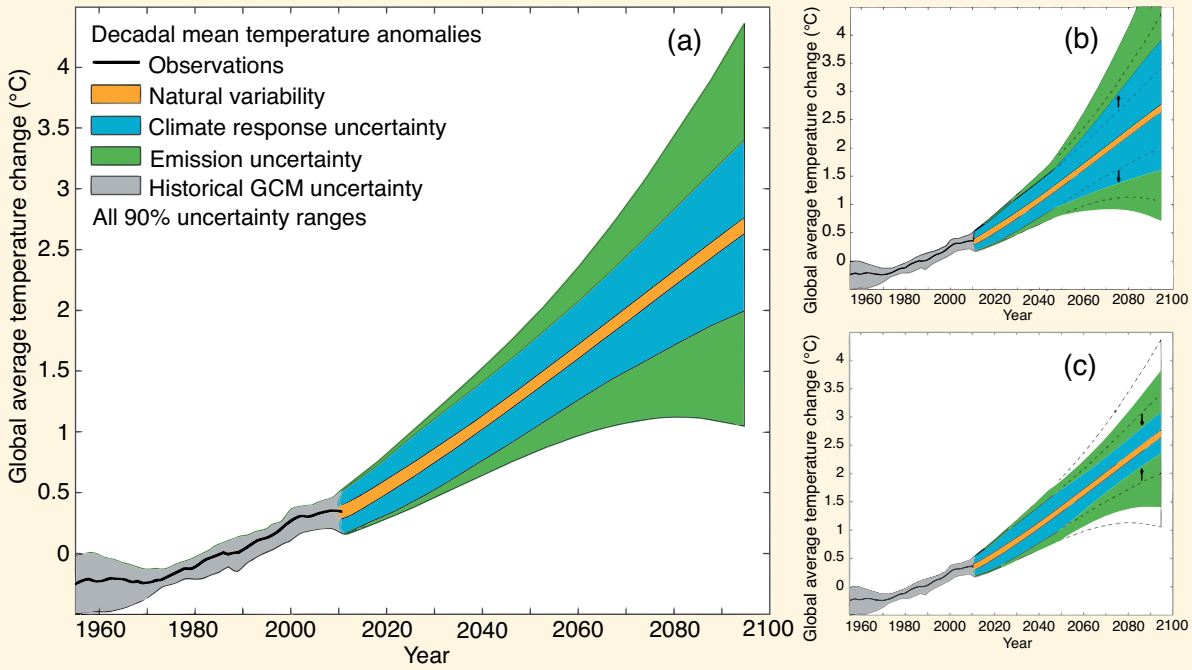

FAQ 1.1, Figure 1 | Schematic diagram showing the relative importance of different uncertainties, and their evolution in time. (a) Decadal mean surface temperature change (°C) from the historical record (black line), with climate model estimates of uncertainty for historical period (grey), along with future climate projections and uncertainty. Values are normalised by means from 1961 to 1980. Natural variability (orange) derives from model interannual variability, and is assumed constant with time. Emission uncertainty (green) is estimated as the model mean difference in projections from different scenarios. Climate response uncertainty (blue-solid) is based on climate model spread, along with added uncertainties from the carbon cycle, as well as rough estimates of additional uncertainty from poorly modelled processes. Based on Hawkins and Sutton (2011) and Huntingford et al. (2009). (b) Climate response uncertainty can appear to increase when a new process is discovered to be relevant, but such increases reflect a quantification of previously unmeasured uncertainty, or (c) can decrease with additional model improvements and observational constraints. The given uncertainty range of 90% means that the temperature is estimated to be in that range, with a probability of 90%.

Frequently Asked Questions

FAQ 2.1 | How Do We Know the World Has Warmed?

Evidence for a warming world comes from multiple independent climate indicators, from high up in the atmosphere to the depths of the oceans. They include changes in surface, atmospheric and oceanic temperatures; glaciers; snow cover; sea ice; sea level and atmospheric water vapour. Scientists from all over the world have independently verified this evidence many times. That the world has warmed since the 19th century is unequivocal.

Discussion about climate warming often centres on potential residual biases in temperature records from land-based weather stations. These records are very important, but they only represent one indicator of changes in the climate system. Broader evidence for a warming world comes from a wide range of independent physically consistent measurements of many other, strongly interlinked, elements of the climate system (FAQ 2.1, Figure 1).

A rise in global average surface temperatures is the best-known indicator of climate change. Although each year and even decade is not always warmer than the last, global surface temperatures have warmed substantially since 1900.

Warming land temperatures correspond closely with the observed warming trend over the oceans. Warming oceanic air temperatures, measured from aboard ships, and temperatures of the sea surface itself also coincide, as borne out by many independent analyses.

The atmosphere and ocean are both fluid bodies, so warming at the surface should also be seen in the lower atmosphere, and deeper down into the upper oceans, and observations confirm that this is indeed the case. Analyses of measurements made by weather balloon radiosondes and satellites consistently show warming of the troposphere, the active weather layer of the atmosphere. More than 90% of the excess energy absorbed by the climate system since at least the 1970s has been stored in the oceans as can be seen from global records of ocean heat content going back to the 1950s. *(continued on next page)*

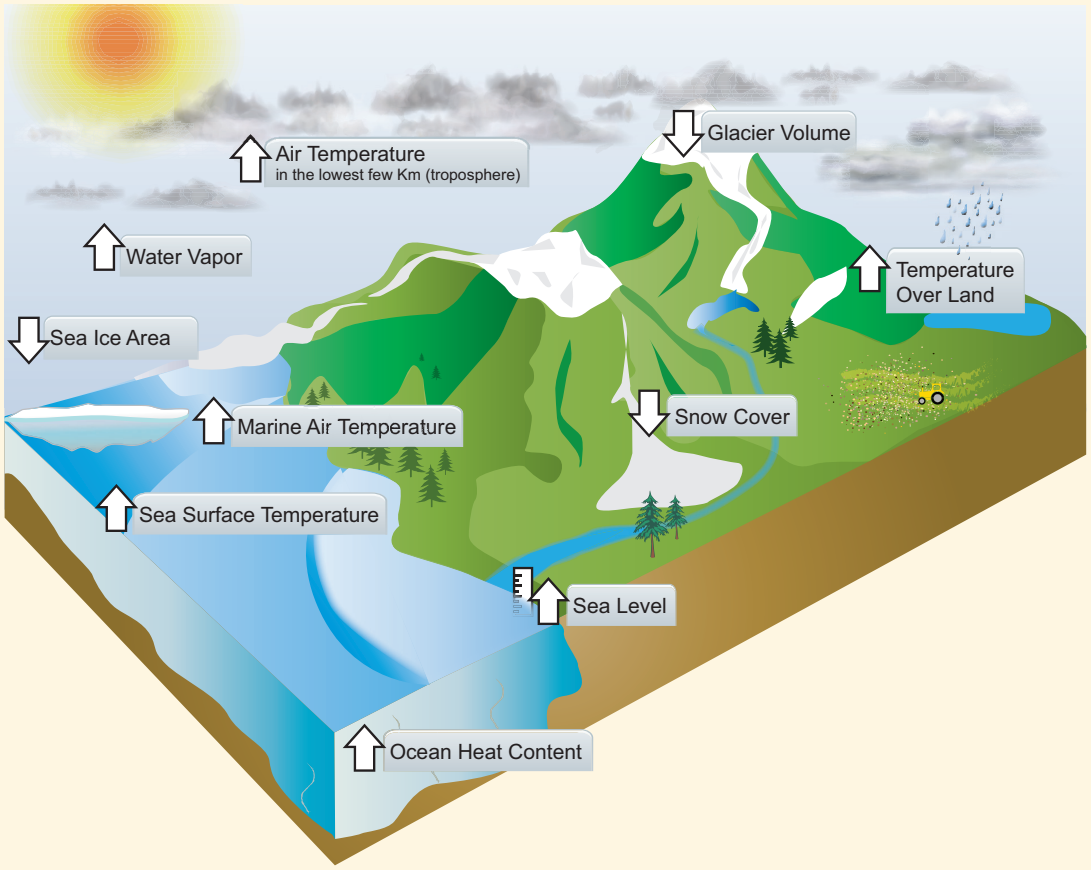

FAQ 2.1, Figure 1 | Independent analyses of many components of the climate system that would be expected to change in a warming world exhibit trends consistent with warming (arrow direction denotes the sign of the change), as shown in FAQ 2.1, Figure 2.

FAQ 2.1 (continued)

As the oceans warm, the water itself expands. This expansion is one of the main drivers of the independently observed rise in sea levels over the past century. Melting of glaciers and ice sheets also contribute, as do changes in storage and usage of water on land.

A warmer world is also a moister one, because warmer air can hold more water vapour. Global analyses show that specific humidity, which measures the amount of water vapour in the atmosphere, has increased over both the land and the oceans.

The frozen parts of the planet—known collectively as the cryosphere—affect, and are affected by, local changes in temperature. The amount of ice contained in glaciers globally has been declining every year for more than 20 years, and the lost mass contributes, in part, to the observed rise in sea level. Snow cover is sensitive to changes in temperature, particularly during the spring, when snow starts to melt. Spring snow cover has shrunk across the NH since the 1950s. Substantial losses in Arctic sea ice have been observed since satellite records began, particularly at the time of the mimimum extent, which occurs in September at the end of the annual melt season. By contrast, the increase in Antarctic sea ice has been smaller.

Individually, any single analysis might be unconvincing, but analysis of these different indicators and independent data sets has led many independent research groups to *all* reach the same conclusion. From the deep oceans to the top of the troposphere, the evidence of warmer air and oceans, of melting ice and rising seas all points unequivocally to one thing: the world has warmed since the late 19th century (FAQ 2.1, Figure 2).

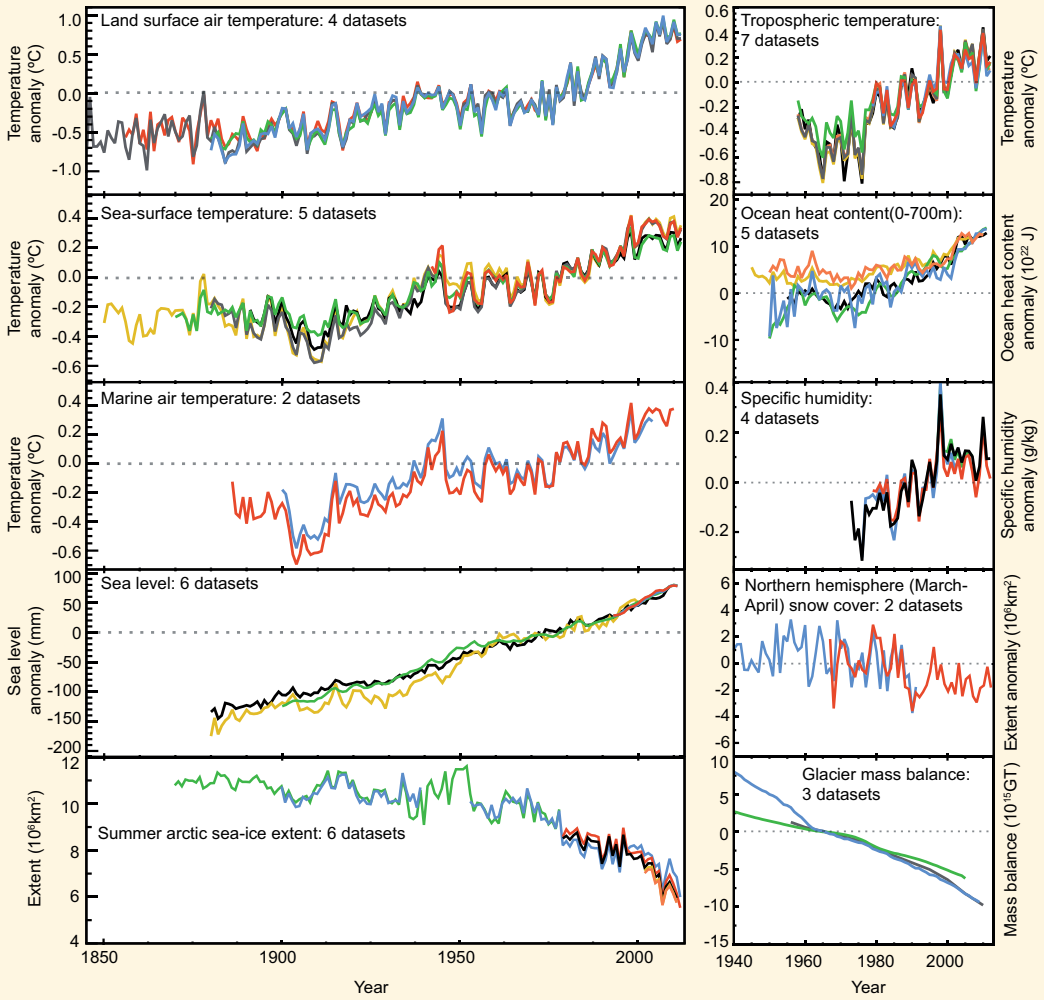

FAQ 2.1, Figure 2 | Multiple independent indicators of a changing global climate. Each line represents an independently derived estimate of change in the climate element. In each panel all data sets have been normalized to a common period of record. A full detailing of which source data sets go into which panel is given in the Supplementary Material 2.SM.5.

Frequently Asked Questions

FAQ 2.2 | Have There Been Any Changes in Climate Extremes?

There is strong evidence that warming has lead to changes in temperature extremes—including heat waves—since the mid-20th century. Increases in heavy precipitation have probably also occurred over this time, but vary by region. However, for other extremes, such as tropical cyclone frequency, we are less certain, except in some limited regions, that there have been discernable changes over the observed record.

From heat waves to cold snaps or droughts to flooding rains, recording and analysing climate extremes poses unique challenges, not just because these events are rare, but also because they invariably happen in conjunction with disruptive conditions. Furthermore, there is no consistent definition in the scientific literature of what constitutes an extreme climatic event, and this complicates comparative global assessments.

Although, in an absolute sense, an extreme climate event will vary from place to place—a hot day in the tropics, for instance, may be a different temperature to a hot day in the mid-latitudes—international efforts to monitor extremes have highlighted some significant global changes.

For example, using consistent definitions for cold (<10th percentile) and warm (>90th percentile) days and nights it is found that warm days and nights have increased and cold days and nights have decreased for most regions of the globe; a few exceptions being central and eastern North America, and southern South America but mostly only related to daytime temperatures. Those changes are generally most apparent in minimum temperature extremes, for example, warm nights. Data limitations make it difficult to establish a causal link to increases in average temperatures, but FAQ 2.2, Figure 1 indicates that daily global temperature extremes have indeed changed. Whether these changes are simply associated with the average of daily temperatures increasing (the dashed lines in FAQ 2.2, Figure 1) or whether other changes in the distribution of daytime and nighttime temperatures have occurred is still under debate.

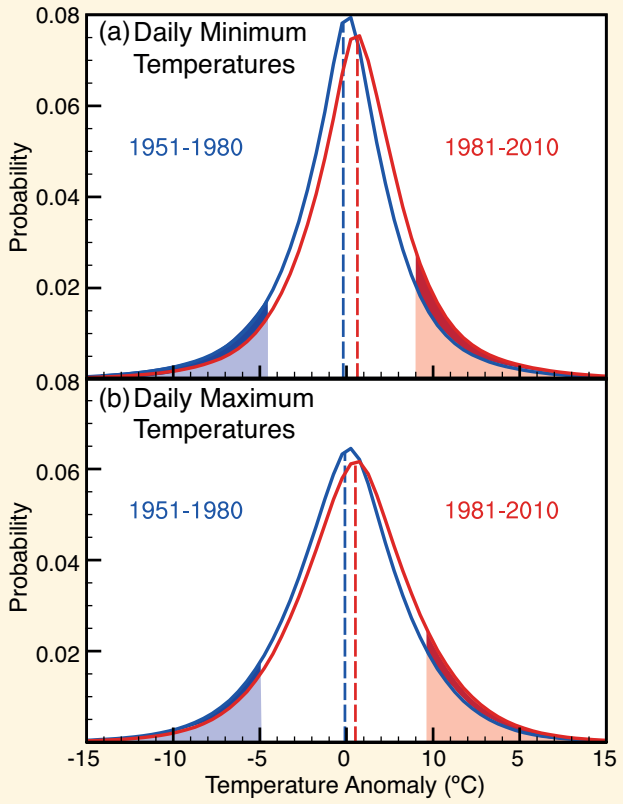

FAQ 2.2, Figure 1 | Distribution of (a) daily minimum and (b) daily maximum temperature anomalies relative to a 1961–1990 climatology for two periods: 1951–1980 (blue) and 1981–2010 (red) using the HadGHCND data set. The shaded blue and red areas represent the coldest 10% and warmest 10% respectively of (a) nights and (b) days during the 1951–1980 period. The darker shading indicates by how much the number of the coldest days and nights has reduced (dark blue) and by how much the number of the warmest days and nights has increased (dark red) during the 1981–2010 period compared to the 1951–1980 period.

Warm spells or heat waves, that is, periods containing consecutive extremely hot days or nights, have also been assessed, but there are fewer studies of heat wave characteristics than those that compare changes in merely warm days or nights. Most global land areas with available data have experienced more heat waves since the middle of the 20th century. One exception is the south-eastern USA, where heat wave frequency and duration measures generally show decreases. This has been associated with a so-called 'warming hole' in this region, where precipitation has also increased and may be related to interactions between the land and the atmosphere and long-term variations in the Atlantic and Pacific Oceans. However, for large regions, particularly in Africa and South America, information on changes in heatwaves is limited.

For regions such as Europe, where historical temperature reconstructions exist going back several hundreds of years, indications are that some areas have experienced a disproportionate number of extreme heat waves in recent decades. *(continued on next page)*

FAQ 2.2 (continued)

Changes in extremes for other climate variables are generally less coherent than those observed for temperature, owing to data limitations and inconsistencies between studies, regions and/or seasons. However, increases in precipitation extremes, for example, are consistent with a warmer climate. Analyses of land areas with sufficient data indicate increases in the frequency and intensity of extreme precipitation events in recent decades, but results vary strongly between regions and seasons. For instance, evidence is most compelling for increases in heavy precipitation in North America, Central America and Europe, but in some other regions—such as southern Australia and western Asia—there is evidence of decreases. Likewise, drought studies do not agree on the sign of the global trend, with regional inconsistencies in trends also dependent on how droughts are defined. However, indications exist that droughts have increased in some regions (e.g., the Mediterranean) and decreased in others (e.g., central North America) since the middle of the 20th century.

Considering other extremes, such as tropical cyclones, the latest assessments show that due to problems with past observing capabilities, it is difficult to make conclusive statements about long-term trends. There is very strong evidence, however, that storm activity has increased in the North Atlantic since the 1970s.

Over periods of a century or more, evidence suggests slight decreases in the frequency of tropical cyclones making landfall in the North Atlantic and the South Pacific, once uncertainties in observing methods have been considered. Little evidence exists of any longer-term trend in other ocean basins. For extratropical cyclones, a poleward shift is evident in both hemispheres over the past 50 years, with further but limited evidence of a decrease in wind storm frequency at mid-latitudes. Several studies suggest an increase in intensity, but data sampling issues hamper these assessments.

FAQ

FAQ 2.2, Figure 2 summarizes some of the observed changes in climate extremes. Overall, the most robust global changes in climate extremes are seen in measures of daily temperature, including to some extent, heat waves. Precipitation extremes also appear to be increasing, but there is large spatial variability, and observed trends in droughts are still uncertain except in a few regions. While robust increases have been seen in tropical cyclone frequency and activity in the North Atlantic since the 1970s, the reasons for this are still being debated. There is limited evidence of changes in extremes associated with other climate variables since the mid-20th century.

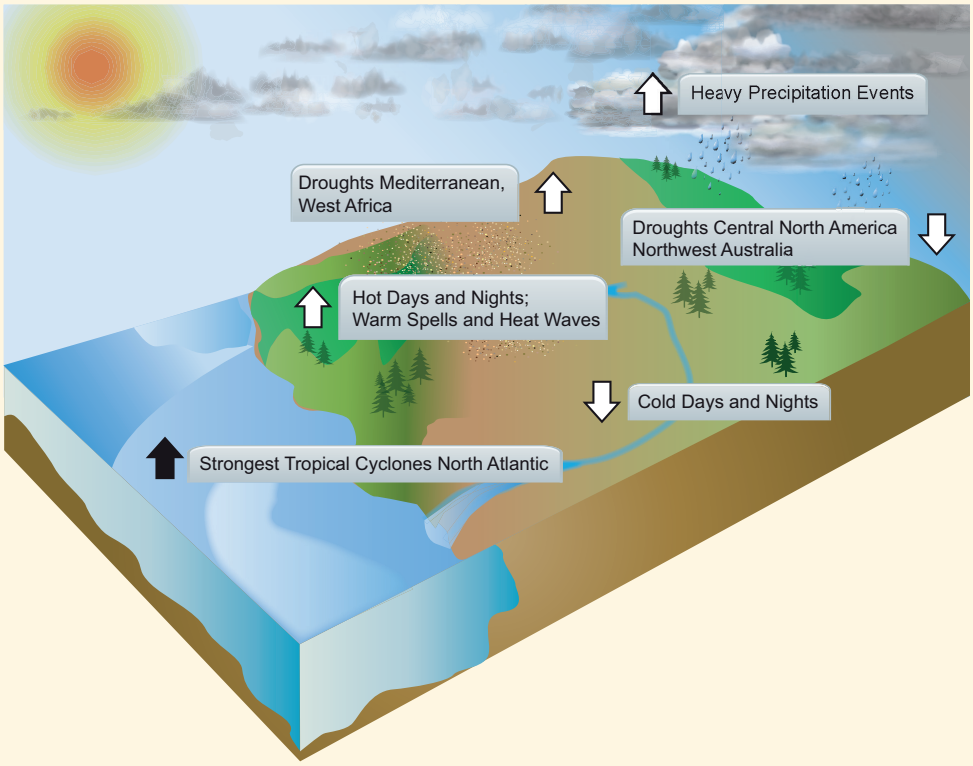

FAQ 2.2, Figure 2 | Trends in the frequency (or intensity) of various climate extremes (arrow direction denotes the sign of the change) since the middle of the 20th century (except for North Atlantic storms where the period covered is from the 1970s).

Frequently Asked Questions

FAQ 3.1 | Is the Ocean Warming?

Yes, the ocean is warming over many regions, depth ranges and time periods, although neither everywhere nor constantly. The signature of warming emerges most clearly when considering global, or even ocean basin, averages over time spans of a decade or more.

Ocean temperature at any given location can vary greatly with the seasons. It can also fluctuate substantially from year to year—or even decade to decade—because of variations in ocean currents and the exchange of heat between ocean and atmosphere.

Ocean temperatures have been recorded for centuries, but it was not until around 1971 that measurements were sufficiently comprehensive to estimate the average global temperature of the upper several hundred meters of the ocean confidently for any given year. In fact, before the international Argo temperature/salinity profiling float array first achieved worldwide coverage in 2005, the global average upper ocean temperature for any given year was sensitive to the methodology used to estimate it.

Global mean upper ocean temperatures have increased over decadal time scales from 1971 to 2010. Despite large uncertainty in most yearly means, this warming is a robust result. In the upper 75 m of the ocean, the global average warming trend has been 0.11 [0.09 to 0.13]°C per decade over this time. That trend generally lessens from the surface to mid-depth, reducing to about 0.04°C per decade by 200 m, and to less than 0.02°C per decade by 500 m.

Temperature anomalies enter the subsurface ocean by paths in addition to mixing from above (FAQ3.1, Figure 1). Colder—hence denser—waters from high latitudes can sink from the surface, then spread toward the equator beneath warmer, lighter, waters at lower latitudes. At a few locations—the northern North Atlantic Ocean and the Southern Ocean around Antarctica—ocean water is cooled so much that it sinks to great depths, even to the sea floor. This water then spreads out to fill much of the rest of the deep ocean. As ocean surface waters warm, these sinking waters also warm with time, increasing temperatures in the ocean interior much more quickly than would downward mixing of surface heating alone.

In the North Atlantic, the temperature of these deep waters varies from decade to decade—sometimes warming, sometimes cooling—depending on prevailing winter atmospheric patterns. Around Antarctica, bottom waters have warmed detectably from about 1992–2005, perhaps due to the strengthening and southward shift of westerly winds around the Southern Ocean over the last several decades. This warming signal in the deepest coldest bottom waters of the world ocean is detectable, although it weakens northward in the Indian, Atlantic and Pacific Oceans. Deep warming rates are generally less pronounced than ocean surface rates (around 0.03ºC per decade since the 1990s in the deep and bottom waters around Antarctica, and smaller in many other locations). However, they occur over a large volume, so deep ocean warming contributes significantly to the total increase in ocean heat.

Estimates of historical changes in global average ocean temperature have become more accurate over the past several years, largely thanks to the recognition, and reduction, of systematic measurement errors. By carefully comparing less accurate measurements with sparser, more accurate ones at adjacent locations and similar times, scientists have reduced some spurious instrumental biases in the historical record. These improvements revealed that the global average ocean temperature has increased much more steadily from year to year than was reported prior to 2008. Nevertheless, the global average warming rate may not be uniform in time. In some years, the ocean appears to warm faster than average; in others, the warming rate seems to slow.

The ocean's large mass and high heat capacity allow it to store huge amounts of energy—more than 1000 times that in the atmosphere for an equivalent increase in temperature. The Earth is absorbing more heat than it is emitting back into space, and nearly all this excess heat is entering the oceans and being stored there. The ocean has absorbed about 93% of the combined heat stored by warmed air, sea, and land, and melted ice between 1971 and 2010.

The ocean's huge heat capacity and slow circulation lend it significant thermal inertia. It takes about a decade for near-surface ocean temperatures to adjust in response to climate forcing (Section 12.5), such as changes in greenhouse gas concentrations. Thus, if greenhouse gas concentrations could be held at present levels into the future, increases in the Earth's surface temperature would begin to slow within about a decade. However, deep ocean temperature would continue to warm for centuries to millennia (Section 12.5), and thus sea levels would continue to rise for centuries to millennia as well (Section 13.5). *(continued on next page)*

FAQ 3.1 (continued)

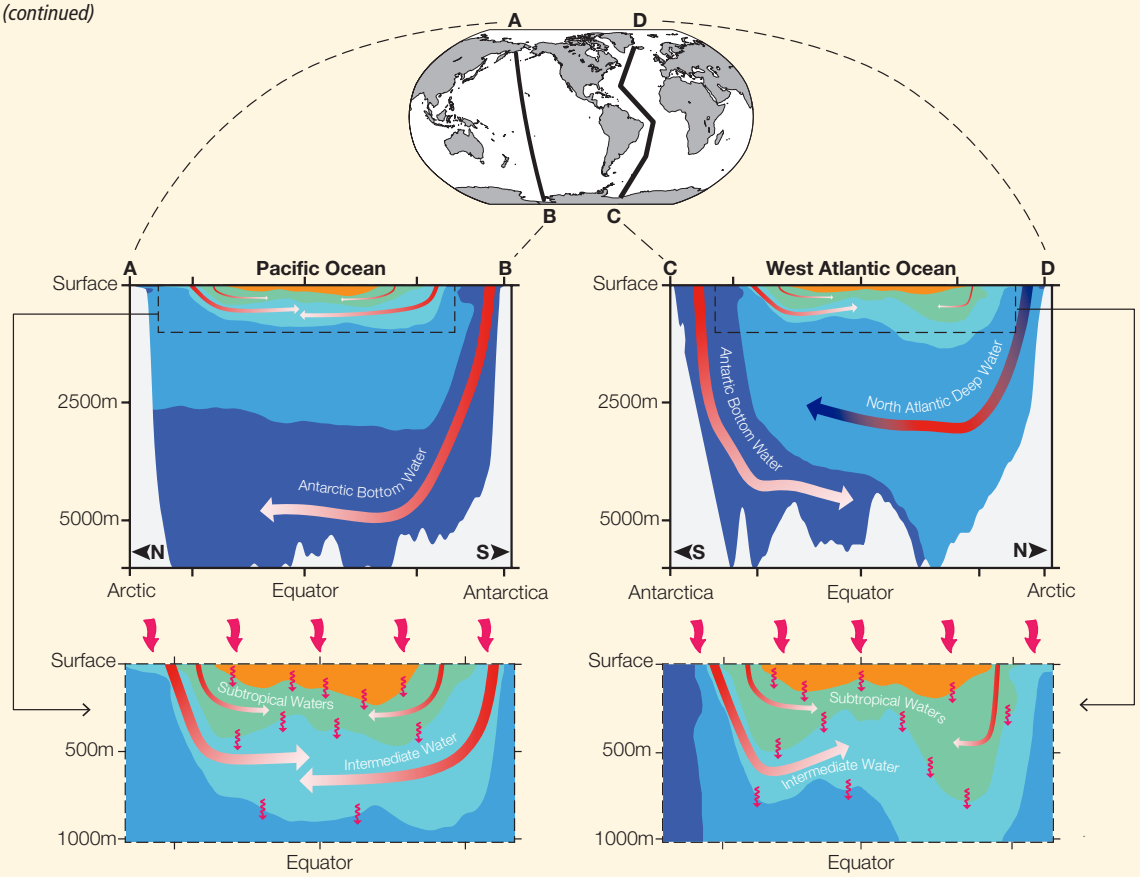

FAQ 3.1, Figure 1 | Ocean heat uptake pathways. The ocean is stratified, with the coldest, densest water in the deep ocean (upper panels: use map at top for orientation). Cold Antarctic Bottom Water (dark blue) sinks around Antarctica then spreads northward along the ocean floor into the central Pacific (upper left panel: red arrows fading to white indicate stronger warming of the bottom water most recently in contact with the ocean surface) and western Atlantic oceans (upper right panel), as well as the Indian Ocean (not shown). Less cold, hence lighter, North Atlantic Deep Water (lighter blue) sinks in the northern North Atlantic Ocean (upper right panel: red and blue arrow in the deep water indicates decadal warming and cooling), then spreads south above the Antarctic Bottom Water. Similarly, in the upper ocean (lower left panel shows Pacific Ocean detail, lower right panel the Atlantic), cool Intermediate Waters (cyan) sink in sub-polar regions (red arrows fading to white indicating warming with time), before spreading toward the equator under warmer Subtropical Waters (green), which in turn sink (red arrows fading to white indicate stronger warming of the intermediate and subtropical waters most recently in contact with the surface) and spread toward the equator under tropical waters, the warmest and lightest (orange) in all three oceans. Excess heat or cold entering at the ocean surface (top curvy red arrows) also mixes slowly downward (sub-surface wavy red arrows).

Frequently Asked Questions

FAQ 3.2 | Is There Evidence for Changes in the Earth's Water Cycle?

The Earth's water cycle involves evaporation and precipitation of moisture at the Earth's surface. Changes in the atmosphere's water vapour content provide strong evidence that the water cycle is already responding to a warming climate. Further evidence comes from changes in the distribution of ocean salinity, which, due to a lack of long-term observations of rain and evaporation over the global oceans, has become an important proxy rain gauge.

The water cycle is expected to intensify in a warmer climate, because warmer air can be moister: the atmosphere can hold about 7% more water vapour for each degree Celsius of warming. Observations since the 1970s show increases in surface and lower atmospheric water vapour (FAQ 3.2, Figure 1a), at a rate consistent with observed warming. Moreover, evaporation and precipitation are projected to intensify in a warmer climate.

Recorded changes in ocean salinity in the last 50 years support that projection. Seawater contains both salt and fresh water, and its salinity is a function of the weight of dissolved salts it contains. Because the total amount of salt—which comes from the weathering of rocks—does not change over human time scales, seawater's salinity can only be altered—over days or centuries—by the addition or removal of fresh water.

The atmosphere connects the ocean's regions of net fresh water loss to those of fresh water gain by moving evaporated water vapour from one place to another. The distribution of salinity at the ocean surface largely reflects the spatial pattern of evaporation minus precipitation, runoff from land, and sea ice processes. There is some shifting of the patterns relative to each other, because of the ocean's currents.

Subtropical waters are highly saline, because evaporation exceeds rainfall, whereas seawater at high latitudes and in the tropics—where more rain falls than evaporates—is less so (FAQ 3.2, Figure 1b, d). The Atlantic, the saltiest ocean basin, loses more freshwater through evaporation than it gains from precipitation, while the Pacific is nearly neutral (i.e., precipitation gain nearly balances evaporation loss), and the Southern Ocean (region around Antarctica) is dominated by precipitation.

Changes in surface salinity and in the upper ocean have reinforced the mean salinity pattern. The evaporation-dominated subtropical regions have become saltier, while the precipitation-dominated subpolar and tropical regions have become fresher. When changes over the top 500 m are considered, the evaporation-dominated Atlantic has become saltier, while the nearly neutral Pacific and precipitation-dominated Southern Ocean have become fresher (FAQ 3.2, Figure 1c).

Observing changes in precipitation and evaporation directly and globally is difficult, because most of the exchange of fresh water between the atmosphere and the surface happens over the 70% of the Earth's surface covered by ocean. Long-term precipitation records are available only from over the land, and there are no long-term measurements of evaporation.

Land-based observations show precipitation increases in some regions, and decreases in others, making it difficult to construct a globally integrated picture. Land-based observations have shown more extreme rainfall events, and more flooding associated with earlier snow melt at high northern latitudes, but there is strong regionality in the trends. Land-based observations are so far insufficient to provide evidence of changes in drought.

Ocean salinity, on the other hand, acts as a sensitive and effective rain gauge over the ocean. It naturally reflects and smoothes out the difference between water gained by the ocean from precipitation, and water lost by the ocean through evaporation, both of which are very patchy and episodic. Ocean salinity is also affected by water runoff from the continents, and by the melting and freezing of sea ice or floating glacial ice. Fresh water added by melting ice on land will change global-averaged salinity, but changes to date are too small to observe.

Data from the past 50 years show widespread salinity changes in the upper ocean, which are indicative of systematic changes in precipitation and runoff minus evaporation, as illustrated in FAQ 3.2, Figure 1.

FAQ 3.2 is based on observations reported in Chapters 2 and 3, and on model analyses in Chapters 9 and 12.

(continued on next page)

FAQ 3.2 (continued)

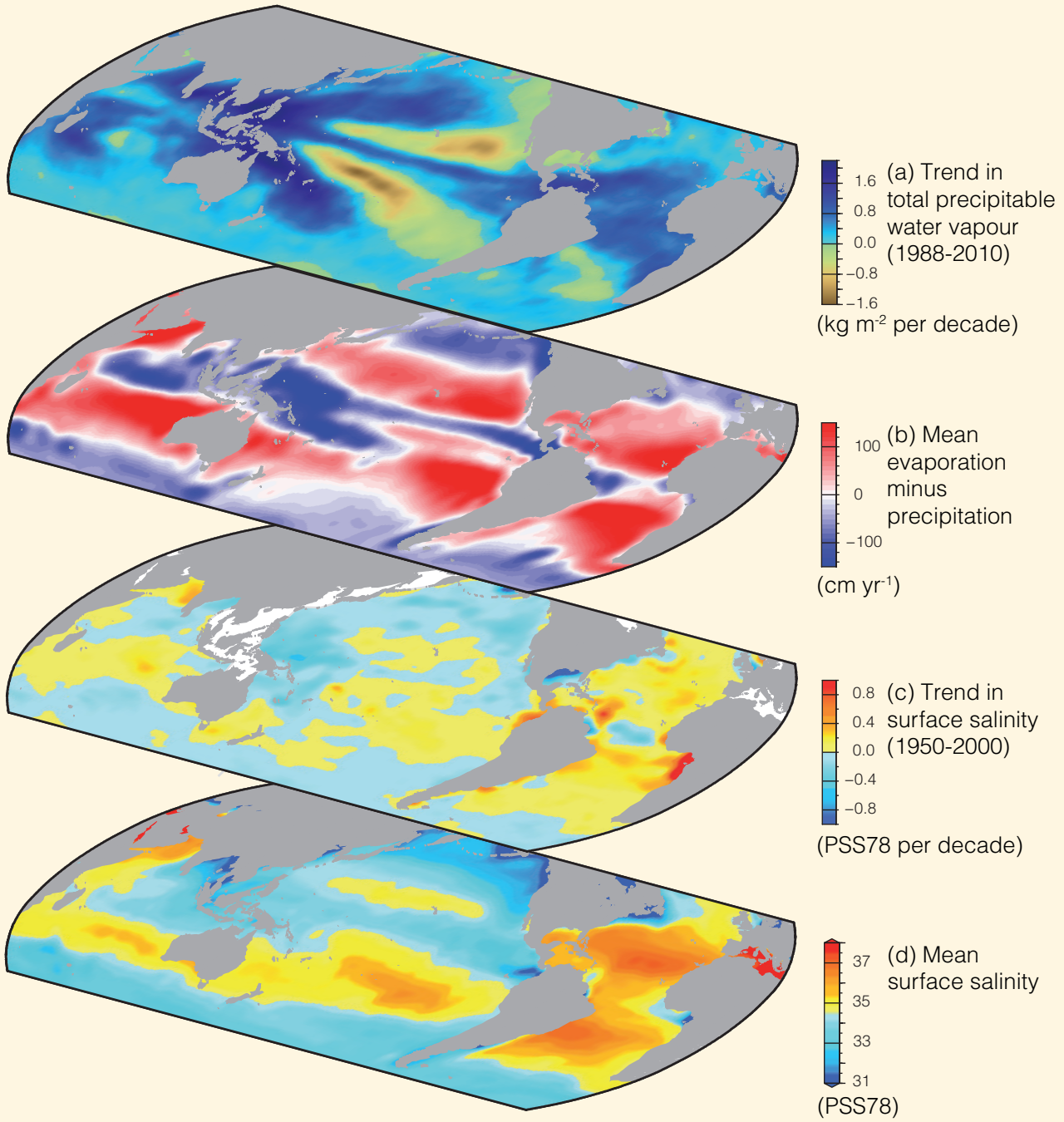

FAQ 3.2, Figure 1 | Changes in sea surface salinity are related to the atmospheric patterns of evaporation minus precipitation (E – P) and trends in total precipitable water: (a) Linear trend (1988–2010) in total precipitable water (water vapor integrated from the Earth's surface up through the entire atmosphere) (kg m^{-2} per decade) from satellite observations (Special Sensor Microwave Imager) (after Wentz et al., 2007) (blues: wetter; yellows: drier). (b) The 1979–2005 climatological mean net E –P (cm yr^{-1}) from meteorological reanalysis (National Centers for Environmental Prediction/National Center for Atmospheric Research; Kalnay et al., 1996) (reds: net evaporation; blues: net precipitation). (c) Trend (1950–2000) in surface salinity (PSS78 per 50 years) (after Durack and Wijffels, 2010) (blues freshening; yellows-reds saltier). (d) The climatological-mean surface salinity (PSS78) (blues: <35; yellows–reds: >35).

Frequently Asked Questions

FAQ 3.3 | How Does Anthropogenic Ocean Acidification Relate to Climate Change?

Both anthropogenic climate change and anthropogenic ocean acidification are caused by increasing carbon dioxide concentrations in the atmosphere. Rising levels of carbon dioxide (CO_2), along with other greenhouse gases, indirectly alter the climate system by trapping heat as it is reflected back from the Earth's surface. Anthropogenic ocean acidification is a direct consequence of rising CO_2 concentrations as seawater currently absorbs about 30% of the anthropogenic CO_2 from the atmosphere.

Ocean acidification refers to a reduction in pH over an extended period, typically decades or longer, caused primarily by the uptake of CO_2 from the atmosphere. pH is a dimensionless measure of acidity. Ocean acidification describes the direction of pH change rather than the end point; that is, ocean pH is decreasing but is not expected to become acidic (pH < 7). Ocean acidification can also be caused by other chemical additions or subtractions from the oceans that are natural (e.g., increased volcanic activity, methane hydrate releases, long-term changes in net respiration) or human-induced (e.g., release of nitrogen and sulphur compounds into the atmosphere). Anthropogenic ocean acidification refers to the component of pH reduction that is caused by human activity.

Since about 1750, the release of CO_2 from industrial and agricultural activities has resulted in global average atmospheric CO_2 concentrations that have increased from 278 to 390.5 ppm in 2011. The atmospheric concentration of CO_2 is now higher than experienced on the Earth for at least the last 800,000 years and is expected to continue to rise because of our dependence on fossil fuels for energy. To date, the oceans have absorbed approximately 155 ± 30 PgC from the atmosphere, which corresponds to roughly one-fourth of the total amount of CO_2 emitted (555 ± 85 PgC) by human activities since preindustrial times. This natural process of absorption has significantly reduced the greenhouse gas levels in the atmosphere and minimized some of the impacts of global warming. However, the ocean's uptake of CO_2 is having a significant impact on the chemistry of seawater. The average pH of ocean surface waters has already fallen by about 0.1 units, from about 8.2 to 8.1 since the beginning of the Industrial Revolution. Estimates of projected future atmospheric and oceanic CO_2 concentrations indicate that, by the end of this century, the average surface ocean pH could be 0.2 to 0.4 lower than it is today. The pH scale is logarithmic, so a change of 1 unit corresponds to a 10-fold change in hydrogen ion concentration.

When atmospheric CO_2 exchanges across the air–sea interface it reacts with seawater through a series of four chemical reactions that increase the concentrations of the carbon species: dissolved carbon dioxide ($CO_{2(aq)}$), carbonic acid (H_2CO_3) and bicarbonate (HCO_3^-):

$$CO_{2(atmos)} \rightleftarrows CO_{2(aq)} \quad (1)$$

$$CO_{2(aq)} + H_2O \rightleftarrows H_2CO_3 \quad (2)$$

$$H_2CO_3 \rightleftarrows H^+ + HCO_3^- \quad (3)$$

$$HCO_3^- \rightleftarrows H^+ + CO_3^{2-} \quad (4)$$

Hydrogen ions (H^+) are produced by these reactions. This increase in the ocean's hydrogen ion concentration corresponds to a reduction in pH, or an increase in acidity. Under normal seawater conditions, more than 99.99% of the hydrogen ions that are produced will combine with carbonate ion (CO_3^{2-}) to produce additional HCO_3^-. Thus, the addition of anthropogenic CO_2 into the oceans lowers the pH and consumes carbonate ion. These reactions are fully reversible and the basic thermodynamics of these reactions in seawater are well known, such that at a pH of approximately 8.1 approximately 90% the carbon is in the form of bicarbonate ion, 9% in the form of carbonate ion, and only about 1% of the carbon is in the form of dissolved CO_2. Results from laboratory, field, and modeling studies, as well as evidence from the geological record, clearly indicate that marine ecosystems are highly susceptible to the increases in oceanic CO_2 and the corresponding decreases in pH and carbonate ion.

Climate change and anthropogenic ocean acidification do not act independently. Although the CO_2 that is taken up by the ocean does not contribute to greenhouse warming, ocean warming reduces the solubility of carbon dioxide in seawater; and thus reduces the amount of CO_2 the oceans can absorb from the atmosphere. For example, under doubled preindustrial CO_2 concentrations and a 2°C temperature increase, seawater absorbs about 10% less CO_2 (10% less total carbon, C_T) than it would with no temperature increase (compare columns 4 and 6 in Table 1), but the pH remains almost unchanged. Thus, a warmer ocean has less capacity to remove CO_2 from the atmosphere, yet still experiences ocean acidification. The reason for this is that bicarbonate is converted to carbonate in a warmer ocean, releasing a hydrogen ion thus stabilizing the pH. *(continued on next page)*

FAQ 3.3 (continued)

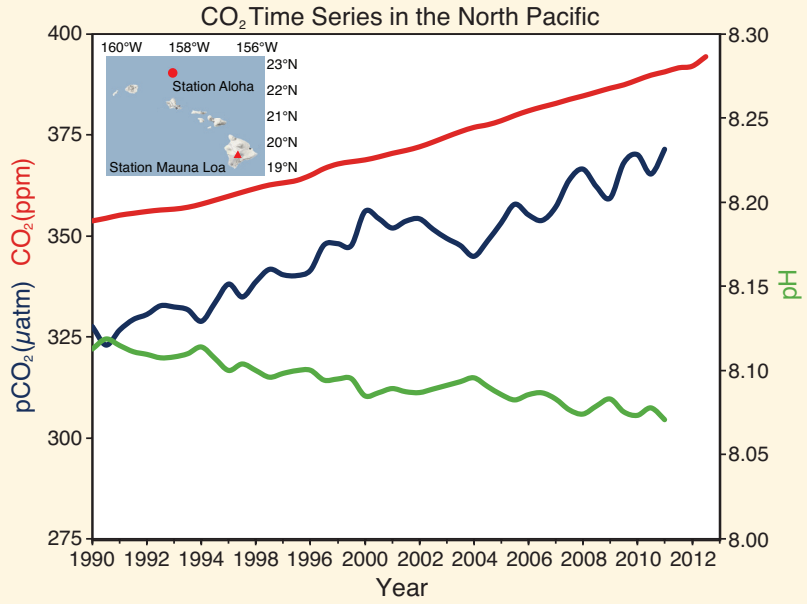

FAQ 3.3, Figure 1 | A smoothed time series of atmospheric CO_2 mole fraction (in ppm) at the atmospheric Mauna Loa Observatory (top red line), surface ocean partial pressure of CO_2 (pCO_2; middle blue line) and surface ocean pH (bottom green line) at Station ALOHA in the subtropical North Pacific north of Hawaii for the period from1990–2011 (after Doney et al., 2009; data from Dore et al., 2009). The results indicate that the surface ocean pCO_2 trend is generally consistent with the atmospheric increase but is more variable due to large-scale interannual variability of oceanic processes.

FAQ 3.3, Table 1 | Oceanic pH and carbon system parameter changes in surface water for a CO_2 doubling from the preindustrial atmosphere without and with a 2°C warming[a].

Parameter	Pre-industrial (280 ppmv) 20°C	2 × Pre-industrial (560 ppmv) 20°C	(% change relative to pre-industrial)	2 × Pre-industrial (560 ppmv) 22°C	(% change relative to pre-industrial)
pH	8.1714	7.9202	–	7.9207	–
H^+ (mol kg^{-1})	$6.739e^{-9}$	$1.202e^{-8}$	(78.4)	$1.200e^{-8}$	(78.1)
$CO_{2(aq)}$ (µmol kg^{-1})	9.10	18.10	(98.9)	17.2	(89.0)
HCO_3^- (µmol kg^{-1})	1723.4	1932.8	(12.15)	1910.4	(10.9)
CO_3^{2-} (µmol kg^{-1})	228.3	143.6	(-37.1)	152.9	(–33.0)
C_T (µmol kg^{-1})	1960.8	2094.5	(6.82)	2080.5	(6.10)

Notes:

[a] $CO_{2(aq)}$ = dissolved CO_2, H_2CO_3 = carbonic acid, HCO_3^- = bicarbonate, CO_3^{2-} = carbonate, C_T = total carbon = $CO_{2(aq)} + HCO_3^- + CO_3^{2-}$).

Frequently Asked Questions

FAQ 4.1 | How Is Sea Ice Changing in the Arctic and Antarctic?

The sea ice covers on the Arctic Ocean and on the Southern Ocean around Antarctica have quite different characteristics, and are showing different changes with time. Over the past 34 years (1979–2012), there has been a downward trend of 3.8% per decade in the annual average extent of sea ice in the Arctic. The average winter thickness of Arctic Ocean sea ice has thinned by approximately 1.8 m between 1978 and 2008, and the total volume (mass) of Arctic sea ice has decreased at all times of year. The more rapid decrease in the extent of sea ice at the summer minimum is a consequence of these trends. In contrast, over the same 34-year period, the total extent of Antarctic sea ice shows a small increase of 1.5% per decade, but there are strong regional differences in the changes around the Antarctic. Measurements of Antarctic sea ice thickness are too few to be able to judge whether its total volume (mass) is decreasing, steady, or increasing.

A large part of the total Arctic sea ice cover lies above 60°N (FAQ 4.1, Figure 1) and is surrounded by land to the south with openings to the Canadian Arctic Archipelago, and the Bering, Barents and Greenland seas. Some of the ice within the Arctic Basin survives for several seasons, growing in thickness by freezing of seawater at the base and by deformation (ridging and rafting). Seasonal sea ice grows to only ~2 m in thickness but sea ice that is more than 1 year old (perennial ice) can be several metres thicker. Arctic sea ice drifts within the basin, driven by wind and ocean currents: the mean drift pattern is dominated by a clockwise circulation pattern in the western Arctic and a Transpolar Drift Stream that transports Siberian sea ice across the Arctic and exports it from the basin through the Fram Strait.

Satellites with the capability to distinguish ice and open water have provided a picture of the sea ice cover changes. Since 1979, the annual average extent of ice in the Arctic has decreased by 3.8% per decade. The decline in extent at the end of summer (in late September) has been even greater at 11% per decade, reaching a record minimum in 2012. The decadal average extent of the September minimum Arctic ice cover has decreased for each decade since satellite records began. Submarine and satellite records suggest that the thickness of Arctic ice, and hence the total volume, is also decreasing. Changes in the relative amounts of perennial and seasonal ice are contributing to the reduction in ice volume. Over the 34-year record, approximately 17% of this type of sea ice per decade has been lost to melt and export out of the basin since 1979 and 40% since 1999. Although the area of Arctic sea ice coverage can fluctuate from year to year because of variable seasonal production, the proportion of thick perennial ice, and the total sea ice volume, can recover only slowly.

Unlike the Arctic, the sea ice cover around Antarctica is constrained to latitudes north of 78°S because of the presence of the continental land mass. The Antarctic sea ice cover is largely seasonal, with an average thickness of only ~1 m at the time of maximum extent in September. Only a small fraction of the ice cover survives the summer minimum in February, and very little Antarctic sea ice is more than 2 years old. The ice edge is exposed to the open ocean and the snowfall rate over Antarctic sea ice is higher than in the Arctic. When the snow load from snowfall is sufficient to depress the ice surface below sea level, seawater infiltrates the base of the snow pack and snow-ice is formed when the resultant slush freezes. Consequently, snow-to-ice conversion (as well as basal freezing as in the Arctic) contributes to the seasonal growth in ice thickness and total ice volume in the Antarctic. Snow-ice formation is sensitive to changes in precipitation and thus changes in regional climate. The consequence of changes in precipitation on Antarctic sea ice thickness and volume remains a focus for research.

Unconstrained by land boundaries, the latitudinal extent of the Antarctic sea ice cover is highly variable. Near the Antarctic coast, sea ice drift is predominantly from east to west, but further north, it is from west to east and highly divergent. Distinct clockwise circulation patterns that transport ice northward can be found in the Weddell and Ross seas, while the circulation is more variable around East Antarctica. The northward extent of the sea ice cover is controlled in part by the divergent drift that is conducive in winter months to new ice formation in persistent open water areas (polynyas) along the coastlines. These zones of ice formation result in saltier and thus denser ocean water and become one of the primary sources of the deepest water found in the global oceans.

Over the same 34-year satellite record, the annual extent of sea ice in the Antarctic increased at about 1.5% per decade. However, there are regional differences in trends, with decreases seen in the Bellingshausen and Amundsen seas, but a larger increase in sea ice extent in the Ross Sea that dominates the overall trend. Whether the smaller overall increase in Antarctic sea ice extent is meaningful as an indicator of climate is uncertain because the extent

(continued on next page)

FAQ 4.1 (continued)

varies so much from year to year and from place to place around the continent. Results from a recent study suggest that these contrasting trends in ice coverage may be due to trends in regional wind speed and patterns. Without better ice thickness and ice volume estimates, it is difficult to characterize how Antarctic sea ice cover is responding to changing climate, or which climate parameters are most influential.

There are large differences in the physical environment and processes that affect the state of Arctic and Antarctic sea ice cover and contribute to their dissimilar responses to climate change. The long, and unbroken, record of satellite observations have provided a clear picture of the decline of the Arctic sea ice cover, but available evidence precludes us from making robust statements about overall changes in Antarctic sea ice and their causes.

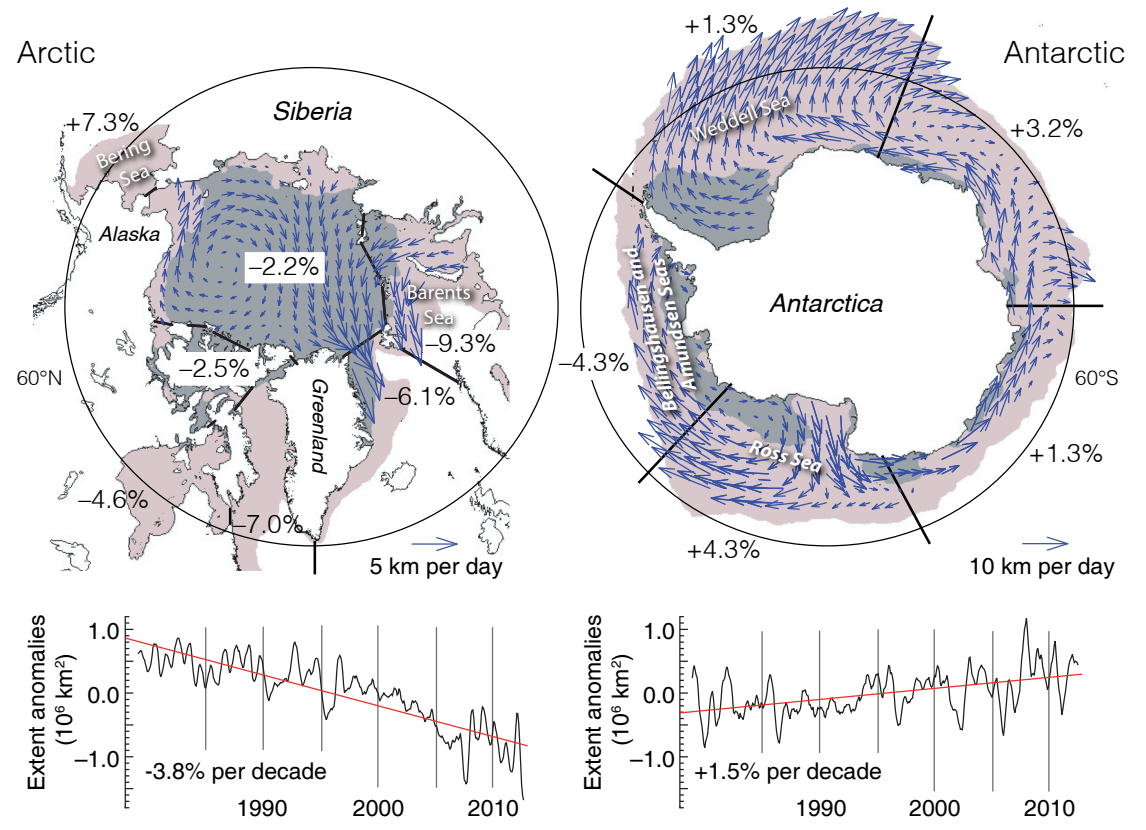

FAQ 4.1, Figure 1 | The mean circulation pattern of sea ice and the decadal trends (%) in annual anomalies in ice extent (i.e., after removal of the seasonal cycle), in different sectors of the Arctic and Antarctic. Arrows show the average direction and magnitude of ice drift. The average sea ice cover for the period 1979 through 2012, from satellite observations, at maximum (minimum) extent is shown as orange (grey) shading.

Frequently Asked Questions

FAQ 4.2 | Are Glaciers in Mountain Regions Disappearing?

In many mountain ranges around the world, glaciers are disappearing in response to the atmospheric temperature increases of past decades. Disappearing glaciers have been reported in the Canadian Arctic and Rocky Mountains; the Andes; Patagonia; the European Alps; the Tien Shan; tropical mountains in South America, Africa and Asia and elsewhere. In these regions, more than 600 glaciers have disappeared over the past decades. Even if there is no further warming, many more glaciers will disappear. It is also likely that some mountain ranges will lose most, if not all, of their glaciers.

In all mountain regions where glaciers exist today, glacier volume has decreased considerably over the past 150 years. Over that time, many small glaciers have disappeared. With some local exceptions, glacier shrinkage (area and volume reduction) was globally widespread already and particularly strong during the 1940s and since the 1980s. However, there were also phases of relative stability during the 1890s, 1920s and 1970s, as indicated by long-term measurements of length changes and by modelling of mass balance. Conventional *in situ* measurements—and increasingly, airborne and satellite measurements—offer robust evidence in most glacierized regions that the rate of reduction in glacier area was higher over the past two decades than previously, and that glaciers continue to shrink. In a few regions, however, individual glaciers are behaving differently and have advanced while most others were in retreat (e.g., on the coasts of New Zealand, Norway and Southern Patagonia (Chile), or in the Karakoram range in Asia). In general, these advances are the result of special topographic and/or climate conditions (e.g., increased precipitation).

It can take several decades for a glacier to adjust its extent to an instantaneous change in climate, so most glaciers are currently larger than they would be if they were in balance with current climate. Because the time required for the adjustment increases with glacier size, larger glaciers will continue to shrink over the next few decades, even if temperatures stabilise. Smaller glaciers will also continue to shrink, but they will adjust their extent faster and many will ultimately disappear entirely.

Many factors influence the future development of each glacier, and whether it will disappear: for instance, its size, slope, elevation range, distribution of area with elevation, and its surface characteristics (e.g., the amount of debris cover). These factors vary substantially from region to region, and also between neighbouring glaciers. External factors, such as the surrounding topography and the climatic regime, are also important for future glacier evolution. Over shorter time scales (one or two decades), each glacier responds to climate change individually and differently in detail.

Over periods longer than about 50 years, the response is more coherent and less dependent on local environmental details, which means that long-term trends in glacier development can be well modelled. Such models are built on an understanding of basic physical principles. For example, an increase in local mean air temperature, with no change in precipitation, will cause an upward shift of the equilibrium line altitude (ELA; see Glossary) by about 150 m for each degree Celsius of atmospheric warming. Such an upward shift and its consequences for glaciers of different size and elevation range are illustrated in FAQ 4.2, Figure 1.

Initially, all glaciers have an accumulation area (white) above and an ablation area (light blue) below the ELA (FAQ 4.2, Figure 1a). As the ELA shifts upwards, the accumulation area shrinks and the ablation area expands, thus increasing the area over which ice is lost through melt (FAQ 4.2, Figure 1b). This imbalance results in an overall loss of ice. After several years, the glacier front retreats, and the ablation area shrinks until the glacier has adjusted its extent to the new climate (FAQ 4.2, Figure 1c). Where climate change is sufficiently strong to raise the ELA permanently above the glacier's highest point (FAQ 4.2, Figure 1b, right) the glacier will eventually disappear entirely (FAQ 4.2, Figure 1c, right). Higher glaciers, which retain their accumulation areas, will shrink but not disappear (FAQ 4.2, Figure 1c, left and middle). A large valley glacier might lose much of its tongue, probably leaving a lake in its place (FAQ 4.2, Figure 1c, left). Besides air temperature, changes in the quantity and seasonality of precipitation influence the shift of the ELA as well. Glacier dynamics (e.g., flow speed) also plays a role, but is not considered in this simplified scheme.

Many observations have confirmed that different glacier types do respond differently to recent climate change. For example, the flat, low-lying tongues of large valley glaciers (such as in Alaska, Canada or the Alps) currently show the strongest mass losses, largely independent of aspect, shading or debris cover. This type of glacier is slow in

(continued on next page)

FAQ 4.2 (continued)

adjusting its extent to new climatic conditions and reacts mainly by thinning without substantial terminus retreat. In contrast, smaller mountain glaciers, with fairly constant slopes, adjust more quickly to the new climate by changing the size of their ablation area more rapidly (FAQ 4.2, Figure 1c, middle).

The long-term response of most glacier types can be determined very well with the approach illustrated in FAQ 4.2, Figure 1. However, modelling short-term glacier response, or the long-term response of more complex glacier types (e.g., those that are heavily debris-covered, fed by avalanche snow, have a disconnected accumulation area, are of surging type, or calve into water), is difficult. These cases require detailed knowledge of other glacier characteristics, such as mass balance, ice thickness distribution, and internal hydraulics. For the majority of glaciers worldwide, such data are unavailable, and their response to climate change can thus only be approximated with the simplified scheme shown in FAQ 4.2, Figure 1.

The Karakoram–Himalaya mountain range, for instance, has a large variety of glacier types and climatic conditions, and glacier characteristics are still only poorly known. This makes determining their future evolution particularly uncertain. However, gaps in knowledge are expected to decrease substantially in coming years, thanks to increased use of satellite data (e.g., to compile glacier inventories or derive flow velocities) and extension of the ground-based measurement network.

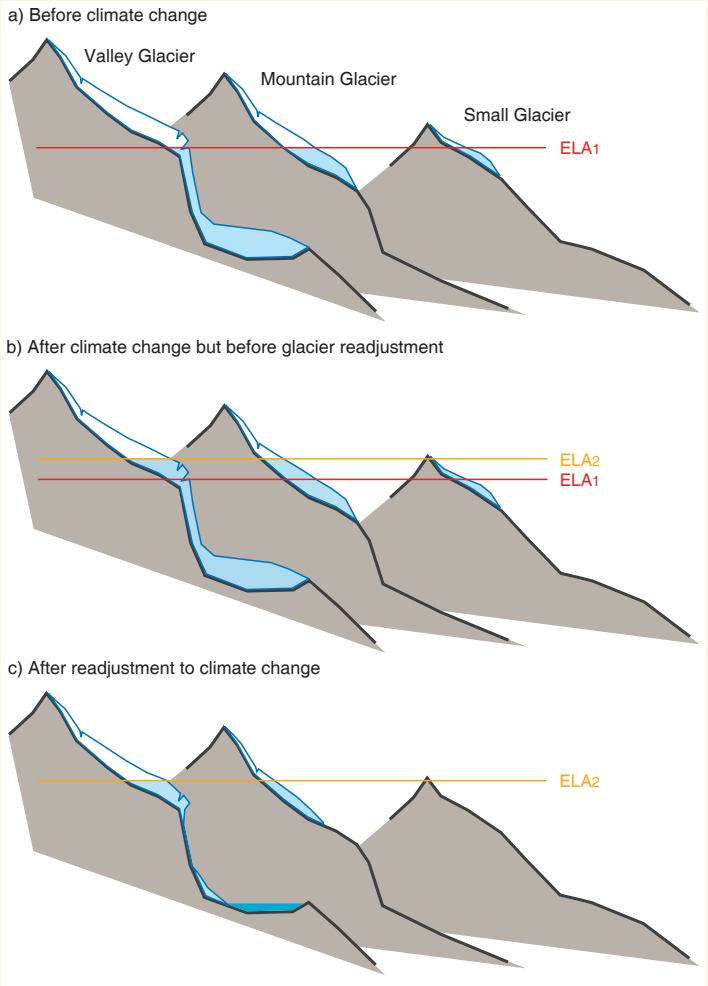

FAQ 4.2, Figure 1 | Schematic of three types of glaciers located at different elevations, and their response to an upward shift of the equilibrium line altitude (ELA). (a) For a given climate, the ELA has a specific altitude (ELA1), and all glaciers have a specific size. (b) Due to a temperature increase, the ELA shifts upwards to a new altitude (ELA2), initially resulting in reduced accumulation and larger ablation areas for all glaciers. (c) After glacier size has adjusted to the new ELA, the valley glacier (left) has lost its tongue and the small glacier (right) has disappeared entirely.

In summary, the fate of glaciers will be variable, depending on both their specific characteristics and future climate conditions. More glaciers will disappear; others will lose most of their low-lying portions and others might not change substantially. Where the ELA is already above the highest elevation on a particular glacier, that glacier is destined to disappear entirely unless climate cools. Similarly, all glaciers will disappear in those regions where the ELA rises above their highest elevation in the future.

Frequently Asked Questions

FAQ 5.1 | Is the Sun a Major Driver of Recent Changes in Climate?

Total solar irradiance (TSI, Chapter 8) is a measure of the total energy received from the sun at the top of the atmosphere. It varies over a wide range of time scales, from billions of years to just a few days, though variations have been relatively small over the past 140 years. Changes in solar irradiance are an important driver of climate variability (Chapter 1; Figure 1.1) along with volcanic emissions and anthropogenic factors. As such, they help explain the observed change in global surface temperatures during the instrumental period (FAQ 5.1, Figure 1; Chapter 10) and over the last millennium. While solar variability may have had a discernible contribution to changes in global surface temperature in the early 20th century, it cannot explain the observed increase since TSI started to be measured directly by satellites in the late 1970s (Chapters 8, 10).

The Sun's core is a massive nuclear fusion reactor that converts hydrogen into helium. This process produces energy that radiates throughout the solar system as electromagnetic radiation. The amount of energy striking the top of Earth's atmosphere varies depending on the generation and emission of electromagnetic energy by the Sun and on the Earth's orbital path around the Sun.

Satellite-based instruments have directly measured TSI since 1978, and indicate that on average, ~1361 W m^{-2} reaches the top of the Earth's atmosphere. Parts of the Earth's surface and air pollution and clouds in the atmosphere act as a mirror and reflect about 30% of this power back into space. Higher levels of TSI are recorded when the Sun is more active. Irradiance variations follow the roughly 11-year sunspot cycle: during the last cycles, TSI values fluctuated by an average of around 0.1%.

For pre-satellite times, TSI variations have to be estimated from sunspot numbers (back to 1610), or from radioisotopes that are formed in the atmosphere, and archived in polar ice and tree rings. Distinct 50- to 100-year periods of very low solar activity—such as the Maunder Minimum between 1645 and 1715—are commonly referred to as grand solar minima. Most estimates of TSI changes between the Maunder Minimum and the present day are in the order of 0.1%, similar to the amplitude of the 11-year variability.

How can solar variability help explain the observed global surface temperature record back to 1870? To answer this question, it is important to understand that other climate drivers are involved, each producing characteristic patterns of regional climate responses. However, it is the combination of them all that causes the observed climate change. Solar variability and volcanic eruptions are natural factors. Anthropogenic (human-produced) factors, on the other hand, include changes in the concentrations of greenhouse gases, and emissions of visible air pollution (aerosols) and other substances from human activities. 'Internal variability' refers to fluctuations within the climate system, for example, due to weather variability or phenomena like the El Niño-Southern Oscillation.

The relative contributions of these natural and anthropogenic factors change with time. FAQ 5.1, Figure 1 illustrates those contributions based on a very simple calculation, in which the mean global surface temperature variation represents the sum of four components linearly related to solar, volcanic, and anthropogenic forcing, and to internal variability. Global surface temperature has increased by approximately 0.8°C from 1870 to 2010 (FAQ 5.1, Figure 1a). However, this increase has not been uniform: at times, factors that cool the Earth's surface—volcanic eruptions, reduced solar activity, most anthropogenic aerosol emissions—have outweighed those factors that warm it, such as greenhouse gases, and the variability generated within the climate system has caused further fluctuations unrelated to external influences.

The solar contribution to the record of global surface temperature change is dominated by the 11-year solar cycle, which can explain global temperature fluctuations up to approximately 0.1°C between minima and maxima (FAQ 5.1, Figure 1b). A long-term increasing trend in solar activity in the early 20th century may have augmented the warming recorded during this interval, together with internal variability, greenhouse gas increases and a hiatus in volcanism. However, it cannot explain the observed increase since the late 1970s, and there was even a slight decreasing trend of TSI from 1986 to 2008 (Chapters 8 and 10).

Volcanic eruptions contribute to global surface temperature change by episodically injecting aerosols into the atmosphere, which cool the Earth's surface (FAQ 5.1, Figure 1c). Large volcanic eruptions, such as the eruption of Mt. Pinatubo in 1991, can cool the surface by around 0.1°C to 0.3°C for up to three years. *(continued on next page)*

FAQ 5.1 (continued)

The most important component of internal climate variability is the El Niño Southern Oscillation, which has a major effect on year-to-year variations of tropical and global mean temperature (FAQ 5.1, Figure 1d). Relatively high annual temperatures have been encountered during El Niño events, such as in 1997–1998.

The variability of observed global surface temperatures from 1870 to 2010 (Figure 1a) reflects the combined influences of natural (solar, volcanic, internal; FAQ 5.1, Figure 1b–d) factors, superimposed on the multi-decadal warming trend from anthropogenic factors (FAQ 5.1, Figure 1e).

Prior to 1870, when anthropogenic emissions of greenhouse gases and aerosols were smaller, changes in solar and volcanic activity and internal variability played a more important role, although the specific contributions of these individual factors to global surface temperatures are less certain. Solar minima lasting several decades have often been associated with cold conditions. However, these periods are often also affected by volcanic eruptions, making it difficult to quantify the solar contribution.

At the regional scale, changes in solar activity have been related to changes in surface climate and atmospheric circulation in the Indo-Pacific, Northern Asia and North Atlantic areas. The mechanisms that amplify the regional effects of the relatively small fluctuations of TSI in the roughly 11-year solar cycle involve dynamical interactions between the upper and the lower atmosphere, or between the ocean sea surface temperature and atmosphere, and have little effect on global mean temperatures (see Box 10.2).

Finally, a decrease in solar activity during the past solar minimum a few years ago (FAQ 5.1, Figure 1b) raises the question of its future influence on climate. Despite uncertainties in future solar activity, there is *high confidence* that the effects of solar activity within the range of grand solar maxima and minima will be much smaller than the changes due to anthropogenic effects.

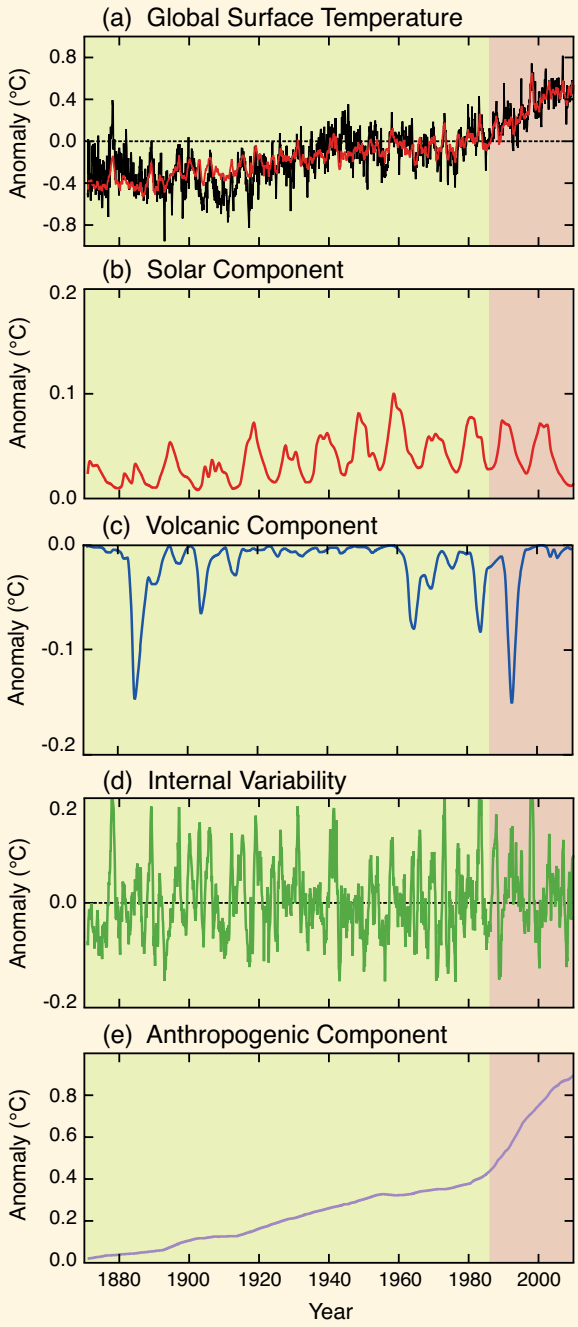

FAQ 5.1, Figure 1 | Global surface temperature anomalies from 1870 to 2010, and the natural (solar, volcanic, and internal) and anthropogenic factors that influence them. (a) Global surface temperature record (1870–2010) relative to the average global surface temperature for 1961–1990 (black line). A model of global surface temperature change (a: red line) produced using the sum of the impacts on temperature of natural (b, c, d) and anthropogenic factors (e). (b) Estimated temperature response to solar forcing. (c) Estimated temperature response to volcanic eruptions. (d) Estimated temperature variability due to internal variability, here related to the El Niño-Southern Oscillation. (e) Estimated temperature response to anthropogenic forcing, consisting of a warming component from greenhouse gases, and a cooling component from most aerosols.

Frequently Asked Questions

FAQ 5.2 | How Unusual is the Current Sea Level Rate of Change?

The rate of mean global sea level change—averaging 1.7 ± 0.2 mm yr^{-1} for the entire 20th century and between 2.8 and 3.6 mm yr^{-1} since 1993 (Chapter 13)—is unusual in the context of centennial-scale variations of the last two millennia. However, much more rapid rates of sea level change occurred during past periods of rapid ice sheet disintegration, such as transitions between glacial and interglacial periods. Exceptional tectonic effects can also drive very rapid local sea level changes, with local rates exceeding the current global rates of change.

'Sea level' is commonly thought of as the point where the ocean meets the land. Earth scientists define sea level as a measure of the position of the sea surface relative to the land, both of which may be moving relative to the center of the Earth. A measure of sea level therefore reflects a combination of geophysical and climate factors. Geophysical factors affecting sea level include land subsidence or uplift and glacial isostatic adjustments—the earth–ocean system's response to changes in mass distribution on the Earth, specifically ocean water and land ice.

Climate influences include variations in ocean temperatures, which cause sea water to expand or contract, changes in the volume of glaciers and ice sheets, and shifts in ocean currents. Local and regional changes in these climate and geophysical factors produce significant deviations from the global estimate of the mean rate of sea level change. For example, *local* sea level is falling at a rate approaching 10 mm yr^{-1} along the northern Swedish coast (Gulf of Bothnia), due to ongoing uplift caused by continental ice that melted after the last glacial period. In contrast, *local* sea level rose at a rate of ~20 mm yr^{-1} from 1960 to 2005 south of Bangkok, mainly in response to subsidence due to ground water extraction.

For the past ~150 years, sea level change has been recorded at tide gauge stations, and for the past ~20 years, with satellite altimeters. Results of these two data sets are consistent for the overlapping period. The globally averaged rate of sea level rise of ~1.7 ± 0.2 mm yr^{-1} over the 20th century—and about twice that over the past two decades—may seem small compared with observations of wave and tidal oscillations around the globe that can be orders of magnitude larger. However, if these rates persist over long time intervals, the magnitude carries important consequences for heavily populated, low-lying coastal regions, where even a small increase in sea level can inundate large land areas.

Prior to the instrumental period, local rates of sea level change are estimated from indirect measures recorded in sedimentary, fossil and archaeological archives. These proxy records are spatially limited and reflect both local and global conditions. Reconstruction of a global signal is strengthened, though, when individual proxy records from widely different environmental settings converge on a common signal. It is important to note that geologic archives—particularly those before about 20,000 years ago—most commonly only capture millennial-scale changes in sea level. Estimates of century-scale rates of sea level change are therefore based on millennial-scale information, but it must be recognised that such data do not necessarily preclude more rapid rates of century-scale changes in sea level.

Sea level reconstructions for the last two millennia offer an opportunity to use proxy records to overlap with, and extend beyond, the instrumental period. A recent example comes from salt-marsh deposits on the Atlantic Coast of the United States, combined with sea level reconstructions based on tide-gauge data and model predictions, to document an average rate of sea level change since the late 19th century of 2.1 ± 0.2 mm yr^{-1}. This century-long rise exceeds any other century-scale change rate in the entire 2000-year record for this same section of coast.

On longer time scales, much larger rates and amplitudes of sea level changes have sometimes been encountered. Glacial–interglacial climate cycles over the past 500,000 years resulted in global sea level changes of up to about 120 to 140 m. Much of this sea level change occurred in 10,000 to 15,000 years, during the transition from a full glacial period to an interglacial period, at average rates of 10 to 15 mm yr^{-1}. These high rates are only sustainable when the Earth is emerging from periods of extreme glaciation, when large ice sheets contact the oceans. For example, during the transition from the last glacial maximum (about 21,000 years ago) to the present interglacial (Holocene, last 11,650 years), fossil coral reef deposits indicate that global sea level rose abruptly by 14 to 18 m in less than 500 years. This event is known as Meltwater Pulse 1A, in which the rate of sea level rise reached more than 40 mm yr^{-1}.

These examples from longer time scales indicate rates of sea level change greater than observed today, but it should be remembered that they all occurred in special circumstances: at times of transition from full glacial to interglacial condition; at locations where the long-term after-effects of these transitions are still occurring; at locations of

(continued on next page)

FAQ 5.2 (continued)

major tectonic upheavals or in major deltas, where subsidence due to sediment compaction—sometimes amplified by ground-fluid extraction—dominates.

The instrumental and geologic record support the conclusion that the current rate of mean global sea level change is unusual relative to that observed and/or estimated over the last two millennia. Higher rates have been observed in the geological record, especially during times of transition between glacial and interglacial periods.

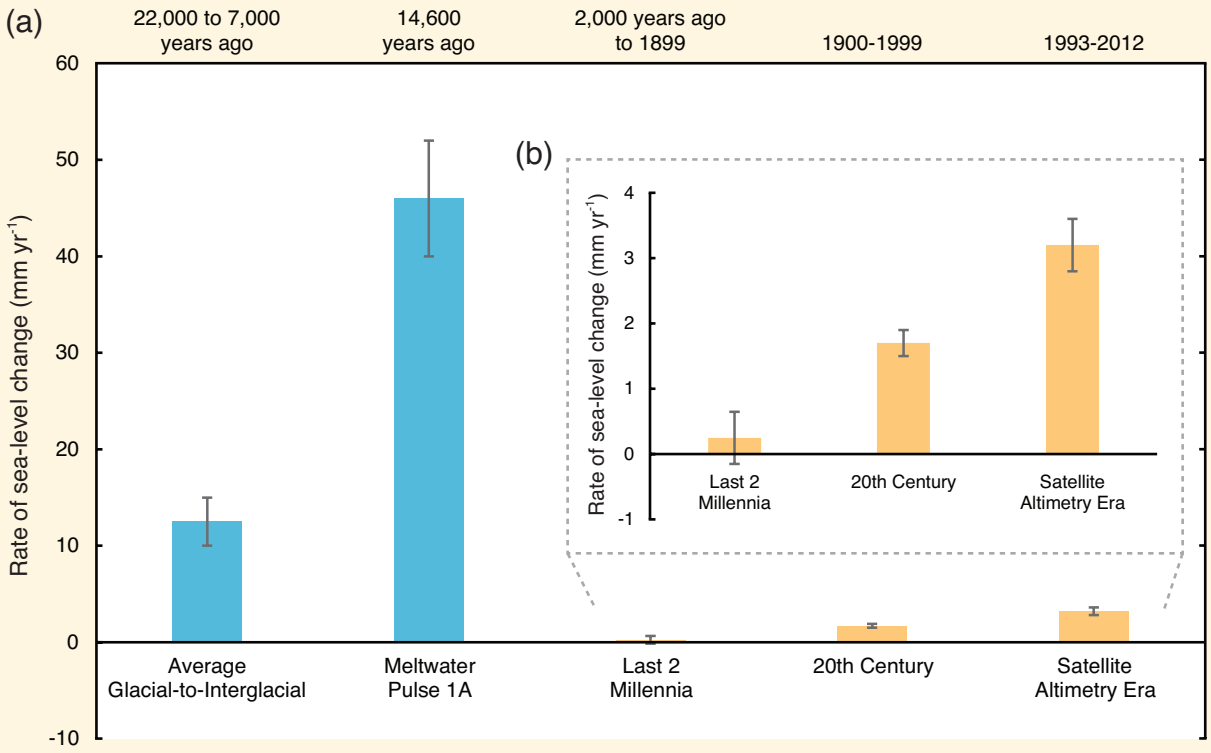

FAQ 5.2, Figure 1 | (a) Estimates of the average rate of global mean sea level change (in mm yr^{-1}) for five selected time intervals: last glacial-to-interglacial transition; Meltwater Pulse 1A; last 2 millennia; 20th century; satellite altimetry era (1993–2012). Blue columns denote time intervals of transition from a glacial to an interglacial period, whereas orange columns denote the current interglacial period. Black bars indicate the range of likely values of the average rate of global mean sea level change. Note the overall higher rates of global mean sea level change characteristic of times of transition between glacial and interglacial periods. (b) Expanded view of the rate of global mean sea level change during three time intervals of the present interglacial.

Frequently Asked Questions

FAQ 6.1 | Could Rapid Release of Methane and Carbon Dioxide from Thawing Permafrost or Ocean Warming Substantially Increase Warming?

Permafrost is permanently frozen ground, mainly found in the high latitudes of the Arctic. Permafrost, including the sub-sea permafrost on the shallow shelves of the Arctic Ocean, contains old organic carbon deposits. Some are relicts from the last glaciation, and hold at least twice the amount of carbon currently present in the atmosphere as carbon dioxide (CO_2). Should a sizeable fraction of this carbon be released as methane and CO_2, it would increase atmospheric concentrations, which would lead to higher atmospheric temperatures. That in turn would cause yet more methane and CO_2 to be released, creating a positive feedback, which would further amplify global warming.

The Arctic domain presently represents a net sink of CO_2—sequestering around 0.4 ± 0.4 PgC yr^{-1} in growing vegetation representing about 10% of the current global land sink. It is also a modest source of methane (CH_4): between 15 and 50 Tg(CH_4) yr^{-1} are emitted mostly from seasonally unfrozen wetlands corresponding to about 10% of the global wetland methane source. There is no clear evidence yet that thawing contributes significantly to the current global budgets of these two greenhouse gases. However, under sustained Arctic warming, modelling studies and expert judgments indicate with medium agreement that a potential combined release totalling up to 350 PgC as CO_2 equivalent could occur by the year 2100.

Permafrost soils on land, and in ocean shelves, contain large pools of organic carbon, which must be thawed and decomposed by microbes before it can be released—mostly as CO_2. Where oxygen is limited, as in waterlogged soils, some microbes also produce methane.

On land, permafrost is overlain by a surface 'active layer', which thaws during summer and forms part of the tundra ecosystem. If spring and summer temperatures become warmer on average, the active layer will thicken, making more organic carbon available for microbial decomposition. However, warmer summers would also result in greater uptake of carbon dioxide by Arctic vegetation through photosynthesis. That means the net Arctic carbon balance is a delicate one between enhanced uptake and enhanced release of carbon.

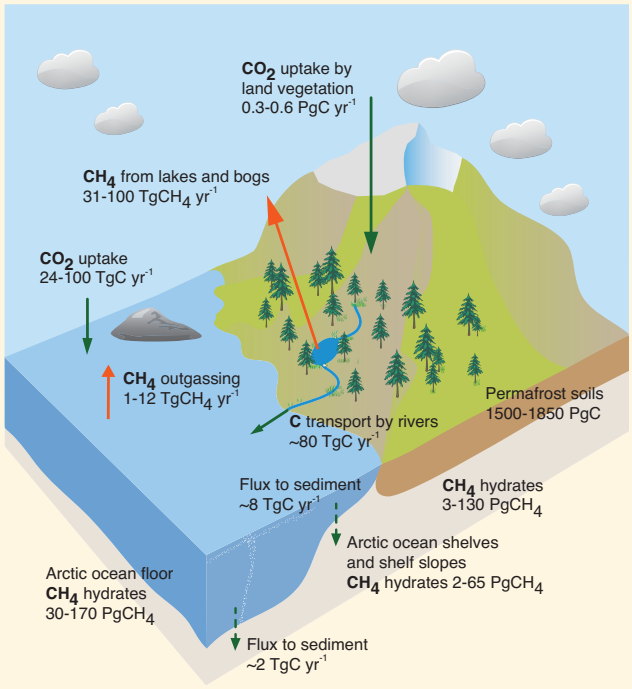

FAQ 6.1, Figure 1 | A simplified graph of current major carbon pools and flows in the Arctic domain, including permafrost on land, continental shelves and ocean. (Adapted from McGuire et al., 2009; and Tarnocai et al., 2009.) TgC = 10^{12} gC, and PgC = 10^{15} gC.

Hydrological conditions during the summer thaw are also important. The melting of bodies of excess ground ice may create standing water conditions in pools and lakes, where lack of oxygen will induce methane production. The complexity of Arctic landscapes under climate warming means we have *low confidence* in which of these different processes might dominate on a regional scale. Heat diffusion and permafrost melting takes time—in fact, the deeper Arctic permafrost can be seen as a relict of the last glaciation, which is still slowly eroding—so any significant loss of permafrost soil carbon will happen over long time scales.

Given enough oxygen, decomposition of organic matter in soil is accompanied by the release of heat by microbes (similar to compost), which, during summer, might stimulate further permafrost thaw. Depending on carbon and ice content of the permafrost, and the hydrological regime, this mechanism could, under warming, trigger relatively fast local permafrost degradation. *(continued on next page)*

FAQ 6.1 (continued)

Modelling studies of permafrost dynamics and greenhouse gas emissions indicate a relatively slow positive feedback, on time scales of hundreds of years. Until the year 2100, up to 250 PgC could be released as CO_2, and up to 5 Pg as CH_4. Given methane's stronger greenhouse warming potential, that corresponds to a further 100 PgC of equivalent CO_2 released until the year 2100. These amounts are similar in magnitude to other biogeochemical feedbacks, for example, the additional CO_2 released by the global warming of terrestrial soils. However, current models do not include the full complexity of Arctic processes that occur when permafrost thaws, such as the formation of lakes and ponds.

Methane hydrates are another form of frozen carbon, occurring in deep permafrost soils, ocean shelves, shelf slopes and deeper ocean bottom sediments. They consist of methane and water molecule clusters, which are only stable in a specific window of low temperatures and high pressures. On land and in the ocean, most of these hydrates originate from marine or terrestrial biogenic carbon, decomposed in the absence of oxygen and trapped in an aquatic environment under suitable temperature–pressure conditions.

Any warming of permafrost soils, ocean waters and sediments and/or changes in pressure could destabilise those hydrates, releasing their CH_4 to the ocean. During larger, more sporadic releases, a fraction of that CH_4 might also be outgassed to the atmosphere. There is a large pool of these hydrates: in the Arctic alone, the amount of CH_4 stored as hydrates could be more than 10 times greater than the CH_4 presently in the global atmosphere.

Like permafrost thawing, liberating hydrates on land is a slow process, taking decades to centuries. The deeper ocean regions and bottom sediments will take still longer—between centuries and millennia to warm enough to destabilise the hydrates within them. Furthermore, methane released in deeper waters has to reach the surface and atmosphere before it can become climatically active, but most is expected to be consumed by microorganisms before it gets there. Only the CH_4 from hydrates in shallow shelves, such as in the Arctic Ocean north of Eastern Siberia, may actually reach the atmosphere to have a climate impact.

Several recent studies have documented locally significant CH_4 emissions over the Arctic Siberian shelf and from Siberian lakes. How much of this CH_4 originates from decomposing organic carbon or from destabilizing hydrates is not known. There is also no evidence available to determine whether these sources have been stimulated by recent regional warming, or whether they have always existed—it may be possible that these CH_4 seepages have been present since the last deglaciation. In any event, these sources make a very small contribution to the global CH_4 budget—less than 5%. This is also confirmed by atmospheric methane concentration observations, which do not show any substantial increases over the Arctic.

However modelling studies and expert judgment indicate that CH_4 and CO_2 emissions will increase under Arctic warming, and that they will provide a positive climate feedback. Over centuries, this feedback will be moderate: of a magnitude similar to other climate–terrestrial ecosystem feedbacks. Over millennia and longer, however, CO_2 and CH_4 releases from permafrost and shelves/shelf slopes are much more important, because of the large carbon and methane hydrate pools involved.

Frequently Asked Questions

FAQ 6.2 | What Happens to Carbon Dioxide After It Is Emitted into the Atmosphere?

Carbon dioxide (CO_2), after it is emitted into the atmosphere, is firstly rapidly distributed between atmosphere, the upper ocean and vegetation. Subsequently, the carbon continues to be moved between the different reservoirs of the global carbon cycle, such as soils, the deeper ocean and rocks. Some of these exchanges occur very slowly. Depending on the amount of CO_2 released, between 15% and 40% will remain in the atmosphere for up to 2000 years, after which a new balance is established between the atmosphere, the land biosphere and the ocean. Geological processes will take anywhere from tens to hundreds of thousands of years—perhaps longer—to redistribute the carbon further among the geological reservoirs. Higher atmospheric CO_2 concentrations, and associated climate impacts of present emissions, will, therefore, persist for a very long time into the future.

CO_2 is a largely non-reactive gas, which is rapidly mixed throughout the entire troposphere in less than a year. Unlike reactive chemical compounds in the atmosphere that are removed and broken down by sink processes, such as methane, carbon is instead redistributed among the different reservoirs of the global carbon cycle and ultimately recycled back to the atmosphere on a multitude of time scales. FAQ 6.2, Figure 1 shows a simplified diagram of the global carbon cycle. The open arrows indicate typical timeframes for carbon atoms to be transferred through the different reservoirs.

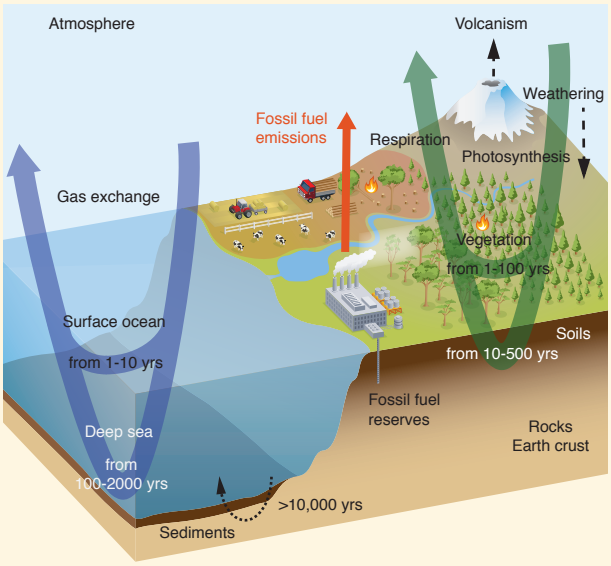

FAQ 6.2, Figure 1 | Simplified schematic of the global carbon cycle showing the typical turnover time scales for carbon transfers through the major reservoirs.

Before the Industrial Era, the global carbon cycle was roughly balanced. This can be inferred from ice core measurements, which show a near constant atmospheric concentration of CO_2 over the last several thousand years prior to the Industrial Era. Anthropogenic emissions of carbon dioxide into the atmosphere, however, have disturbed that equilibrium. As global CO_2 concentrations rise, the exchange processes between CO_2 and the surface ocean and vegetation are altered, as are subsequent exchanges within and among the carbon reservoirs on land, in the ocean and eventually, the Earth crust. In this way, the added carbon is redistributed by the global carbon cycle, until the exchanges of carbon between the different carbon reservoirs have reached a new, approximate balance.

Over the ocean, CO_2 molecules pass through the air-sea interface by gas exchange. In seawater, CO_2 interacts with water molecules to form carbonic acid, which reacts very quickly with the large reservoir of dissolved inorganic carbon—bicarbonate and carbonate ions—in the ocean. Currents and the formation of sinking dense waters transport the carbon between the surface and deeper layers of the ocean. The marine biota also redistribute carbon: marine organisms grow organic tissue and calcareous shells in surface waters, which, after their death, sink to deeper waters, where they are returned to the dissolved inorganic carbon reservoir by dissolution and microbial decomposition. A small fraction reaches the sea floor, and is incorporated into the sediments.

The extra carbon from anthropogenic emissions has the effect of increasing the atmospheric partial pressure of CO_2, which in turn increases the air-to-sea exchange of CO_2 molecules. In the surface ocean, the carbonate chemistry quickly accommodates that extra CO_2. As a result, shallow surface ocean waters reach balance with the atmosphere within 1 or 2 years. Movement of the carbon from the surface into the middle depths and deeper waters takes longer—between decades and many centuries. On still longer time scales, acidification by the invading CO_2 dissolves carbonate sediments on the sea floor, which further enhances ocean uptake. However, current understanding suggests that, unless substantial ocean circulation changes occur, plankton growth remains roughly unchanged because it is limited mostly by environmental factors, such as nutrients and light, and not by the availability of inorganic carbon it does not contribute significantly to the ocean uptake of anthropogenic CO_2. *(continued on next page)*

FAQ 6.2 (continued)

On land, vegetation absorbs CO_2 by photosynthesis and converts it into organic matter. A fraction of this carbon is immediately returned to the atmosphere as CO_2 by plant respiration. Plants use the remainder for growth. Dead plant material is incorporated into soils, eventually to be decomposed by microorganisms and then respired back into the atmosphere as CO_2. In addition, carbon in vegetation and soils is also converted back into CO_2 by fires, insects, herbivores, as well as by harvest of plants and subsequent consumption by livestock or humans. Some organic carbon is furthermore carried into the ocean by streams and rivers.

An increase in atmospheric CO_2 stimulates photosynthesis, and thus carbon uptake. In addition, elevated CO_2 concentrations help plants in dry areas to use ground water more efficiently. This in turn increases the biomass in vegetation and soils and so fosters a carbon sink on land. The magnitude of this sink, however, also depends critically on other factors, such as water and nutrient availability.

Coupled carbon-cycle climate models indicate that less carbon is taken up by the ocean and land as the climate warms constituting a positive climate feedback. Many different factors contribute to this effect: warmer seawater, for instance, has a lower CO_2 solubility, so altered chemical carbon reactions result in less oceanic uptake of excess atmospheric CO_2. On land, higher temperatures foster longer seasonal growth periods in temperate and higher latitudes, but also faster respiration of soil carbon.

The time it takes to reach a new carbon distribution balance depends on the transfer times of carbon through the different reservoirs, and takes place over a multitude of time scales. Carbon is first exchanged among the 'fast' carbon reservoirs, such as the atmosphere, surface ocean, land vegetation and soils, over time scales up to a few thousand years. Over longer time scales, very slow secondary geological processes—dissolution of carbonate sediments and sediment burial into the Earth's crust—become important.

FAQ 6.2, Figure 2 illustrates the decay of a large excess amount of CO_2 (5000 PgC, or about 10 times the cumulative CO_2 emitted so far since the beginning of the industrial Era) emitted into the atmosphere, and how it is redistributed among land and the ocean over time. During the first 200 years, the ocean and land take up similar amounts of carbon. On longer time scales, the ocean uptake dominates mainly because of its larger reservoir size (~38,000 PgC) as compared to land (~4000 PgC) and atmosphere (589 PgC prior to the Industrial Era). Because of ocean chemistry the size of the initial input is important: higher emissions imply that a larger fraction of CO_2 will remain in the atmosphere. After 2000 years, the atmosphere will still contain between 15% and 40% of those initial CO_2 emissions. A further reduction by carbonate sediment dissolution, and reactions with igneous rocks, such as silicate weathering and sediment burial, will take anything from tens to hundreds of thousands of years, or even longer.

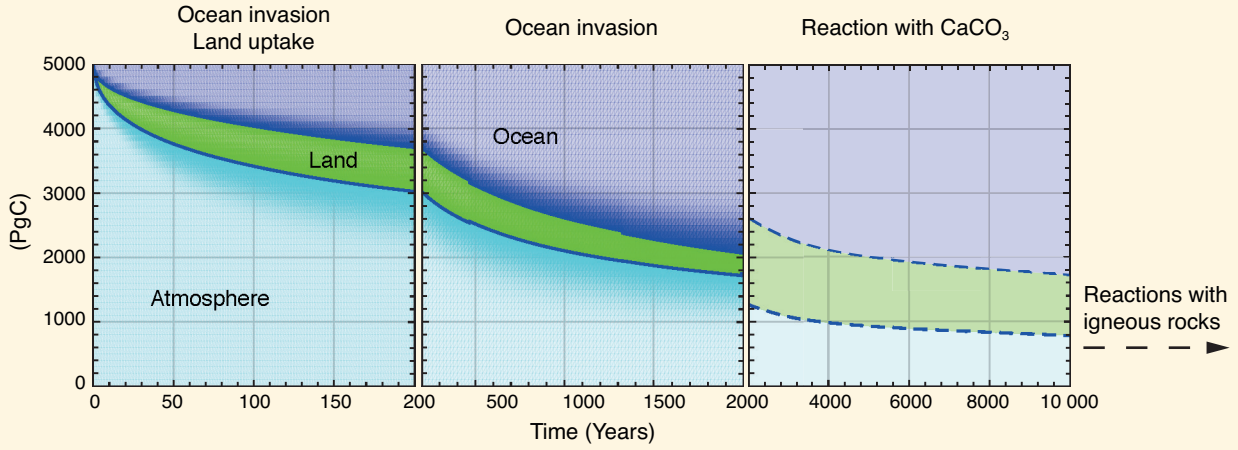

FAQ 6.2, Figure 2 | Decay of a CO_2 excess amount of 5000 PgC emitted at time zero into the atmosphere, and its subsequent redistribution into land and ocean as a function of time, computed by coupled carbon-cycle climate models. The sizes of the colour bands indicate the carbon uptake by the respective reservoir. The first two panels show the multi-model mean from a model intercomparison project (Joos et al., 2013). The last panel shows the longer term redistribution including ocean dissolution of carbonaceous sediments as computed with an Earth System Model of Intermediate Complexity (after Archer et al., 2009b).

Frequently Asked Questions

FAQ 7.1 | How Do Clouds Affect Climate and Climate Change?

Clouds strongly affect the current climate, but observations alone cannot yet tell us how they will affect a future, warmer climate. Comprehensive prediction of changes in cloudiness requires a global climate model. Such models simulate cloud fields that roughly resemble those observed, but important errors and uncertainties remain. Different climate models produce different projections of how clouds will change in a warmer climate. Based on all available evidence, it seems likely that the net cloud–climate feedback amplifies global warming. If so, the strength of this amplification remains uncertain.

Since the 1970s, scientists have recognized the critical importance of clouds for the climate system, and for climate change. Clouds affect the climate system in a variety of ways. They produce precipitation (rain and snow) that is necessary for most life on land. They warm the atmosphere as water vapour condenses. Although some of the condensed water re-evaporates, the precipitation that reaches the surface represents a net warming of the air. Clouds strongly affect the flows of both sunlight (warming the planet) and infrared light (cooling the planet as it is radiated to space) through the atmosphere. Finally, clouds contain powerful updraughts that can rapidly carry air from near the surface to great heights. The updraughts carry energy, moisture, momentum, trace gases, and aerosol particles. For decades, climate scientists have been using both observations and models to study how clouds change with the daily weather, with the seasonal cycle, and with year-to-year changes such as those associated with El Niño.

All cloud processes have the potential to change as the climate state changes. Cloud feedbacks are of intense interest in the context of climate change. Any change in a cloud process that is caused by climate change—and in turn influences climate—represents a cloud–climate feedback. Because clouds interact so strongly with both sunlight and infrared light, small changes in cloudiness can have a potent effect on the climate system.

Many possible types of cloud–climate feedbacks have been suggested, involving changes in cloud amount, cloud-top height and/or cloud reflectivity (see FAQ7.1, Figure 1). The literature shows consistently that high clouds amplify global warming as they interact with infrared light emitted by the atmosphere and surface. There is more uncertainty, however, about the feedbacks associated with low-altitude clouds, and about cloud feedbacks associated with amount and reflectivity in general.

Thick high clouds efficiently reflect sunlight, and both thick and thin high clouds strongly reduce the amount of infrared light that the atmosphere and surface emit to space. The compensation between these two effects makes

(continued on next page)

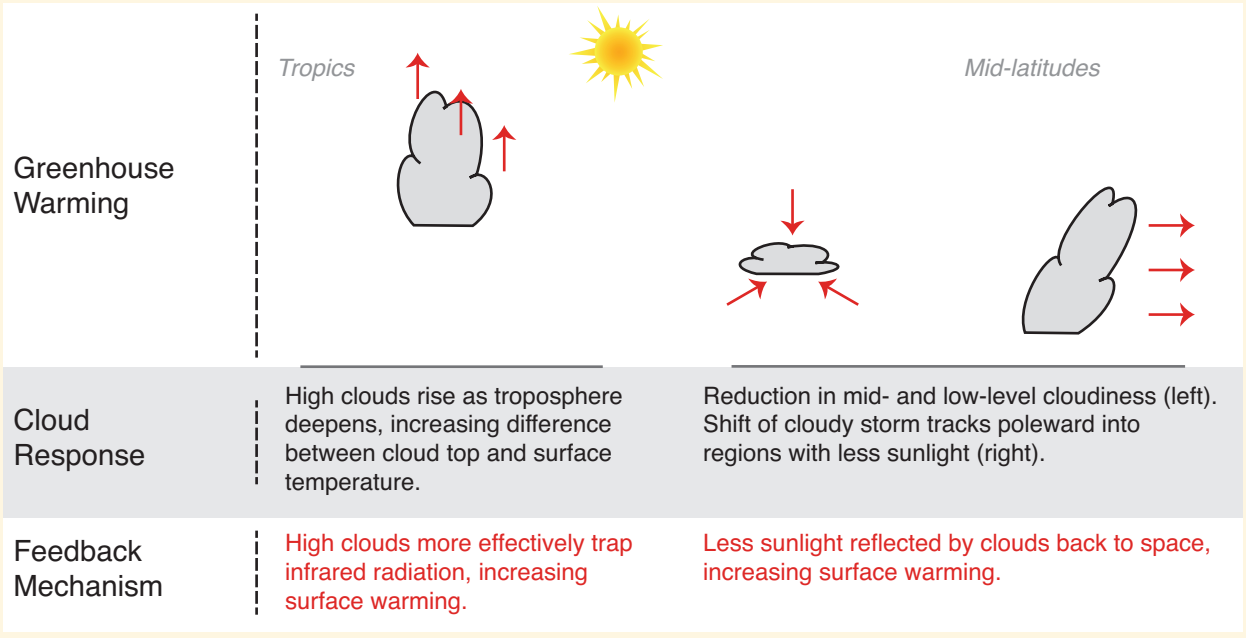

FAQ 7.1, Figure 1 | Schematic of important cloud feedback mechanisms.

FAQ 7.1 (continued)

the surface temperature somewhat less sensitive to changes in high cloud amount than to changes in low cloud amount. This compensation could be disturbed if there were a systematic shift from thick high cloud to thin cirrus cloud or vice versa; while this possibility cannot be ruled out, it is not currently supported by any evidence. On the other hand, changes in the altitude of high clouds (for a given high-cloud amount) can strongly affect surface temperature. An upward shift in high clouds reduces the infrared light that the surface and atmosphere emit to space, but has little effect on the reflected sunlight. There is strong evidence of such a shift in a warmer climate. This amplifies global warming by preventing some of the additional infrared light emitted by the atmosphere and surface from leaving the climate system.

Low clouds reflect a lot of sunlight back to space but, for a given state of the atmosphere and surface, they have only a weak effect on the infrared light that is emitted to space by the Earth. As a result, they have a net cooling effect on the present climate; to a lesser extent, the same holds for mid-level clouds. In a future climate warmed by increasing greenhouse gases, most IPCC-assessed climate models simulate a decrease in low and mid-level cloud amount, which would increase the absorption of sunlight and so tend to increase the warming. The extent of this decrease is quite model-dependent, however.

There are also other ways that clouds may change in a warmer climate. Changes in wind patterns and storm tracks could affect the regional and seasonal patterns of cloudiness and precipitation. Some studies suggest that the signal of one such trend seen in climate models—a poleward migration of the clouds associated with mid-latitude storm tracks—is already detectable in the observational record. By shifting clouds into regions receiving less sunlight, this could also amplify global warming. More clouds may be made of liquid drops, which are small but numerous and reflect more sunlight back to space than a cloud composed of the same mass of larger ice crystals. Thin cirrus cloud, which exerts a net warming effect and is very hard for climate models to simulate, could change in ways not simulated by models although there is no evidence for this. Other processes may be regionally important, for example, interactions between clouds and the surface can change over the ocean where sea ice melts, and over land where plant transpiration is reduced.

There is as yet no broadly accepted way to infer global cloud feedbacks from observations of long-term cloud trends or shorter-time scale variability. Nevertheless, all the models used for the current assessment (and the preceding two IPCC assessments) produce net cloud feedbacks that either enhance anthropogenic greenhouse warming or have little overall effect. Feedbacks are not 'put into' the models, but emerge from the functioning of the clouds in the simulated atmosphere and their effects on the flows and transformations of energy in the climate system. The differences in the strengths of the cloud feedbacks produced by the various models largely account for the different sensitivities of the models to changes in greenhouse gas concentrations.

Frequently Asked Questions

FAQ 7.2 | How Do Aerosols Affect Climate and Climate Change?

Atmospheric aerosols are composed of small liquid or solid particles suspended in the atmosphere, other than larger cloud and precipitation particles. They come from natural and anthropogenic sources, and can affect the climate in multiple and complex ways through their interactions with radiation and clouds. Overall, models and observations indicate that anthropogenic aerosols have exerted a cooling influence on the Earth since pre-industrial times, which has masked some of the global mean warming from greenhouse gases that would have occurred in their absence. The projected decrease in emissions of anthropogenic aerosols in the future, in response to air quality policies, would eventually unmask this warming.

Atmospheric aerosols have a typical lifetime of one day to two weeks in the troposphere, and about one year in the stratosphere. They vary greatly in size, chemical composition and shape. Some aerosols, such as dust and sea spray, are mostly or entirely of natural origin, while other aerosols, such as sulphates and smoke, come from both natural and anthropogenic sources.

Aerosols affect climate in many ways. First, they scatter and absorb sunlight, which modifies the Earth's radiative balance (see FAQ.7.2, Figure 1). Aerosol scattering generally makes the planet more reflective, and tends to cool the climate, while aerosol absorption has the opposite effect, and tends to warm the climate system. The balance between cooling and warming depends on aerosol properties and environmental conditions. Many observational studies have quantified local radiative effects from anthropogenic and natural aerosols, but determining their

(continued on next page)

Aerosol-radiation interactions

Scattering aerosols

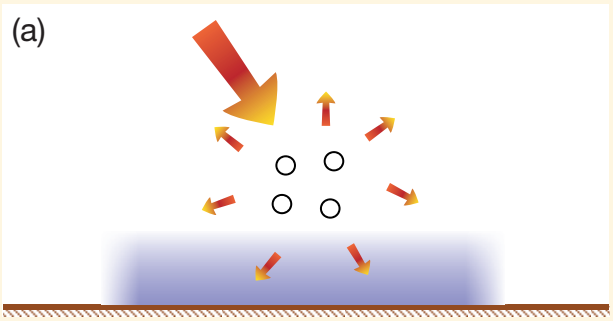

Aerosols scatter solar radiation. Less solar radiation reaches the surface, which leads to a localised cooling.

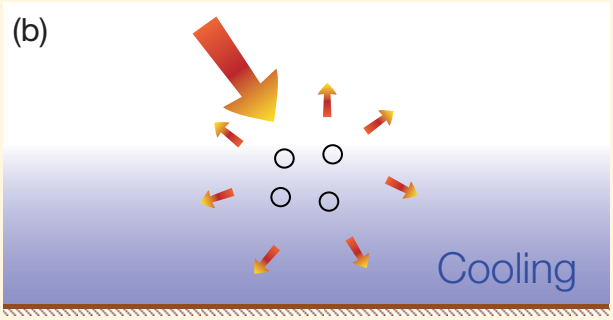

The atmospheric circulation and mixing processes spread the cooling regionally and in the vertical.

Absorbing aerosols

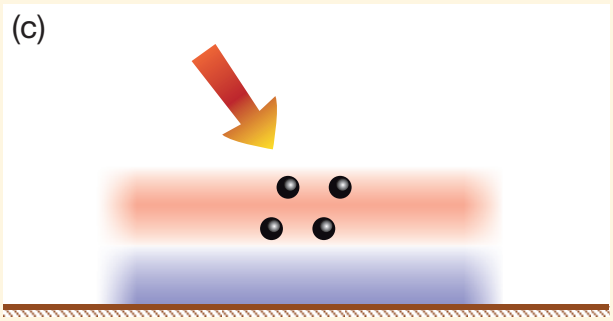

Aerosols absorb solar radiation. This heats the aerosol layer but the surface, which receives less solar radiation, can cool locally.

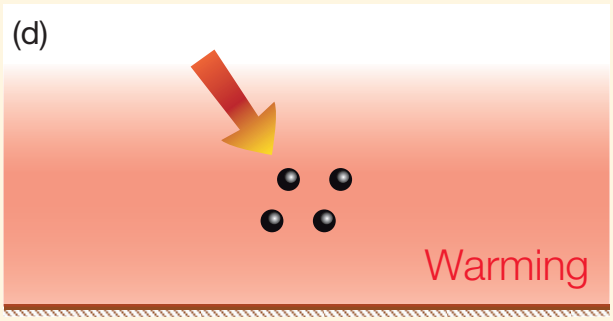

At the larger scale there is a net warming of the surface and atmosphere because the atmospheric circulation and mixing processes redistribute the thermal energy.

FAQ 7.2, Figure 1 | Overview of interactions between aerosols and solar radiation and their impact on climate. The left panels show the instantaneous radiative effects of aerosols, while the right panels show their overall impact after the climate system has responded to their radiative effects.

FAQ 7.2 (continued)

global impact requires satellite data and models. One of the remaining uncertainties comes from black carbon, an absorbing aerosol that not only is more difficult to measure than scattering aerosols, but also induces a complicated cloud response. Most studies agree, however, that the overall radiative effect from anthropogenic aerosols is to cool the planet.

Aerosols also serve as condensation and ice nucleation sites, on which cloud droplets and ice particles can form (see FAQ.7.2, Figure 2). When influenced by more aerosol particles, clouds of liquid water droplets tend to have more, but smaller droplets, which causes these clouds to reflect more solar radiation. There are however many other pathways for aerosol–cloud interactions, particularly in ice—or mixed liquid and ice—clouds, where phase changes between liquid and ice water are sensitive to aerosol concentrations and properties. The initial view that an increase in aerosol concentration will also increase the amount of low clouds has been challenged because a number of counteracting processes come into play. Quantifying the overall impact of aerosols on cloud amounts and properties is understandably difficult. Available studies, based on climate models and satellite observations, generally indicate that the net effect of anthropogenic aerosols on clouds is to cool the climate system.

Because aerosols are distributed unevenly in the atmosphere, they can heat and cool the climate system in patterns that can drive changes in the weather. These effects are complex, and hard to simulate with current models, but several studies suggest significant effects on precipitation in certain regions.

Because of their short lifetime, the abundance of aerosols—and their climate effects—have varied over time, in rough concert with anthropogenic emissions of aerosols and their precursors in the gas phase such as sulphur dioxide (SO_2) and some volatile organic compounds. Because anthropogenic aerosol emissions have increased substantially over the industrial period, this has counteracted some of the warming that would otherwise have occurred from increased concentrations of well mixed greenhouse gases. Aerosols from large volcanic eruptions that enter the stratosphere, such as those of El Chichón and Pinatubo, have also caused cooling periods that typically last a year or two.

Over the last two decades, anthropogenic aerosol emissions have decreased in some developed countries, but increased in many developing countries. The impact of aerosols on the global mean surface temperature over this particular period is therefore thought to be small. It is projected, however, that emissions of anthropogenic aerosols will ultimately decrease in response to air quality policies, which would suppress their cooling influence on the Earth's surface, thus leading to increased warming.

Aerosol-cloud interactions

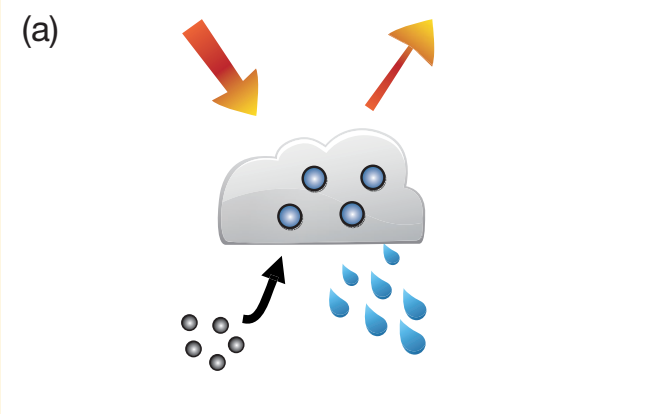

Aerosols serve as cloud condensation nuclei upon which liquid droplets can form.

More aerosols result in a larger concentration of smaller droplets, leading to a brighter cloud. However there are many other possible aerosol–cloud–precipitation processes which may amplify or dampen this effect.

FAQ 7.2, Figure 2 | Overview of aerosol–cloud interactions and their impact on climate. Panels (a) and (b) represent a clean and a polluted low-level cloud, respectively.

Frequently Asked Questions

FAQ 7.3 | Could Geoengineering Counteract Climate Change and What Side Effects Might Occur?

Geoengineering—also called climate engineering—is defined as a broad set of methods and technologies that aim to deliberately alter the climate system in order to alleviate impacts of climate change. Two distinct categories of geoengineering methods are usually considered: Solar Radiation Management (SRM, assessed in Section 7.7) aims to offset the warming from anthropogenic greenhouse gases by making the planet more reflective while Carbon Dioxide Removal (CDR, assessed in Section 6.5) aims at reducing the atmospheric CO_2 concentration. The two categories operate on different physical principles and on different time scales. Models suggest that if SRM methods were realizable they would be effective in countering increasing temperatures, and would be less, but still, effective in countering some other climate changes. SRM would not counter all effects of climate change, and all proposed geoengineering methods also carry risks and side effects. Additional consequences cannot yet be anticipated as the level of scientific understanding about both SRM and CDR is low. There are also many (political, ethical, and practical) issues involving geoengineering that are beyond the scope of this report.

Carbon Dioxide Removal Methods

CDR methods aim at removing CO_2 from the atmosphere by deliberately modifying carbon cycle processes, or by industrial (e.g., chemical) approaches. The carbon withdrawn from the atmosphere would then be stored in land, ocean or in geological reservoirs. Some CDR methods rely on biological processes, such as large-scale afforestation/reforestation, carbon sequestration in soils through biochar, bioenergy with carbon capture and storage (BECCS) and ocean fertilization. Others would rely on geological processes, such as accelerated weathering of silicate and carbonate rocks—on land or in the ocean (see FAQ.7.3, Figure 1). The CO_2 removed from the atmosphere would

(continued on next page)

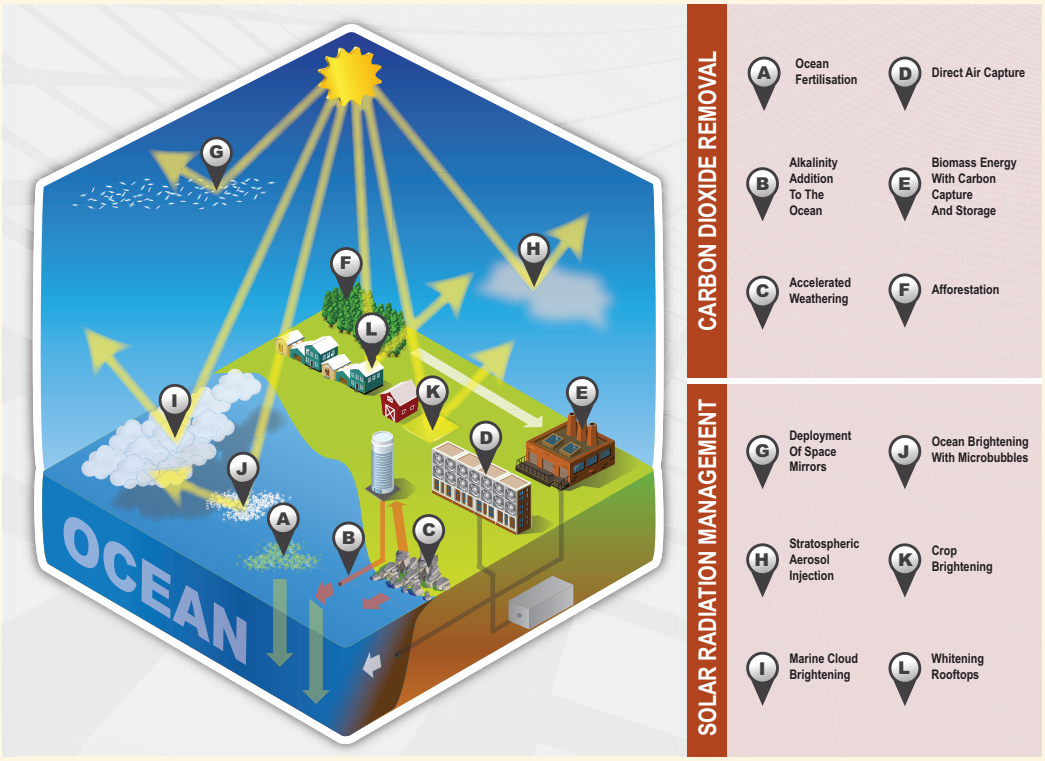

FAQ 7.3, Figure 1 | Overview of some proposed geoengineering methods as they have been suggested. Carbon Dioxide Removal methods (see Section 6.5 for details): (A) nutrients are added to the ocean (ocean fertilization), which increases oceanic productivity in the surface ocean and transports a fraction of the resulting biogenic carbon downward; (B) alkalinity from solid minerals is added to the ocean, which causes more atmospheric CO_2 to dissolve in the ocean; (C) the weathering rate of silicate rocks is increased, and the dissolved carbonate minerals are transported to the ocean; (D) atmospheric CO_2 is captured chemically, and stored either underground or in the ocean; (E) biomass is burned at an electric power plant with carbon capture, and the captured CO_2 is stored either underground or in the ocean; and (F) CO_2 is captured through afforestation and reforestation to be stored in land ecosystems. Solar Radiation Management methods (see Section 7.7 for details): (G) reflectors are placed in space to reflect solar radiation; (H) aerosols are injected in the stratosphere; (I) marine clouds are seeded in order to be made more reflective; (J) microbubbles are produced at the ocean surface to make it more reflective; (K) more reflective crops are grown; and (L) roofs and other built structures are whitened.

FAQ 7.3 (continued)

then be stored in organic form in land reservoirs, or in inorganic form in oceanic and geological reservoirs, where it would have to be stored for at least hundreds of years for CDR to be effective.

CDR methods would reduce the radiative forcing of CO_2 inasmuch as they are effective at removing CO_2 from the atmosphere and keeping the removed carbon away from the atmosphere. Some methods would also reduce ocean acidification (see FAQ 3.2), but other methods involving oceanic storage might instead increase ocean acidification if the carbon is sequestered as dissolved CO_2. A major uncertainty related to the effectiveness of CDR methods is the storage capacity and the permanence of stored carbon. Permanent carbon removal and storage by CDR would decrease climate warming in the long term. However, non-permanent storage strategies would allow CO_2 to return back to the atmosphere where it would once again contribute to warming. An intentional removal of CO_2 by CDR methods will be partially offset by the response of the oceanic and terrestrial carbon reservoirs if the CO_2 atmospheric concentration is reduced. This is because some oceanic and terrestrial carbon reservoirs will outgas to the atmosphere the anthropogenic CO_2 that had previously been stored. To completely offset past anthropogenic CO_2 emissions, CDR techniques would therefore need to remove not just the CO_2 that has accumulated in the atmosphere since pre-industrial times, but also the anthropogenic carbon previously taken up by the terrestrial biosphere and the ocean.

Biological and most chemical weathering CDR methods cannot be scaled up indefinitely and are necessarily limited by various physical or environmental constraints such as competing demands for land. Assuming a maximum CDR sequestration rate of 200 PgC per century from a combination of CDR methods, it would take about one and half centuries to remove the CO_2 emitted in the last 50 years, making it difficult—even for a suite of additive CDR methods—to mitigate climate change rapidly. Direct air capture methods could in principle operate much more rapidly, but may be limited by large-scale implementation, including energy use and environmental constraints.

CDR could also have climatic and environmental side effects. For instance, enhanced vegetation productivity may increase emissions of N_2O, which is a more potent greenhouse gas than CO_2. A large-scale increase in vegetation coverage, for instance through afforestation or energy crops, could alter surface characteristics, such as surface reflectivity and turbulent fluxes. Some modelling studies have shown that afforestation in seasonally snow-covered boreal regions could in fact accelerate global warming, whereas afforestation in the tropics may be more effective at slowing global warming. Ocean-based CDR methods that rely on biological production (i.e., ocean fertilization) would have numerous side effects on ocean ecosystems, ocean acidity and may produce emissions of non-CO_2 greenhouse gases.

Solar Radiation Management Methods

The globally averaged surface temperature of the planet is strongly influenced by the amount of sunlight absorbed by the Earth's atmosphere and surface, which warms the planet, and by the existence of the greenhouse effect, the process by which greenhouse gases and clouds affect the way energy is eventually radiated back to space. An increase in the greenhouse effect leads to a surface temperature rise until a new equilibrium is found. If less incoming sunlight is absorbed because the planet has been made more reflective, or if energy can be emitted to space more effectively because the greenhouse effect is reduced, the average global surface temperature will be reduced.

Suggested geoengineering methods that aim at managing the Earth's incoming and outgoing energy flows are based on this fundamental physical principle. Most of these methods propose to either reduce sunlight reaching the Earth or increase the reflectivity of the planet by making the atmosphere, clouds or the surface brighter (see FAQ 7.3, Figure 1). Another technique proposes to suppress high-level clouds called cirrus, as these clouds have a strong greenhouse effect. Basic physics tells us that if any of these methods change energy flows as expected, then the planet will cool. The picture is complicated, however, because of the many and complex physical processes which govern the interactions between the flow of energy, the atmospheric circulation, weather and the resulting climate.

While the globally averaged surface temperature of the planet will respond to a change in the amount of sunlight reaching the surface or a change in the greenhouse effect, the temperature at any given location and time is influenced by many other factors and the amount of cooling from SRM will not in general equal the amount of warming caused by greenhouse gases. For example, SRM will change heating rates only during daytime, but increasing greenhouse gases can change temperatures during both day and night. This inexact compensation can influence

(continued on next page)

FAQ 7.3 (continued)

the diurnal cycle of surface temperature, even if the average surface temperature is unchanged. As another example, model calculations suggest that a uniform decrease in sunlight reaching the surface might offset global mean CO_2-induced warming, but some regions will cool less than others. Models suggest that if anthropogenic greenhouse warming were completely compensated by stratospheric aerosols, then polar regions would be left with a small residual warming, while tropical regions would become a little cooler than in pre-industrial times.

SRM could theoretically counteract anthropogenic climate change rapidly, cooling the Earth to pre-industrial levels within one or two decades. This is known from climate models but also from the climate records of large volcanic eruptions. The well-observed eruption of Mt Pinatubo in 1991 caused a temporary increase in stratospheric aerosols and a rapid decrease in surface temperature of about 0.5°C.

Climate consists of many factors besides surface temperature. Consequences for other climate features, such as rainfall, soil moisture, river flow, snowpack and sea ice, and ecosystems may also be important. Both models and theory show that compensating an increased greenhouse effect with SRM to stabilize surface temperature would somewhat lower the globally averaged rainfall (see FAQ 7.3, Figure 2 for an idealized model result), and there also could be regional changes. Such imprecise compensation in regional and global climate patterns makes it improbable that SRM will produce a future climate that is 'just like' the one we experience today, or have experienced in the past. However, available climate models indicate that a geoengineered climate with SRM and high atmospheric CO_2 levels would be generally closer to 20th century climate than a future climate with elevated CO_2 concentrations and no SRM.

SRM techniques would probably have other side effects. For example, theory, observation and models suggest that stratospheric sulphate aerosols from volcanic eruptions and natural emissions deplete stratospheric ozone, especially while chlorine from chlorofluorocarbon emissions resides in the atmosphere. Stratospheric aerosols introduced for SRM are expected to have the same effect. Ozone depletion would increase the amount of ultraviolet light reaching the surface damaging terrestrial and marine ecosystems. Stratospheric aerosols would also increase the ratio of direct to diffuse sunlight reaching the surface, which generally increases plant productivity. There has also been some concern that sulphate aerosol SRM would increase acid rain, but model studies suggest that acid rain is probably not a major concern since the rate of acid rain production from stratospheric aerosol SRM would be much smaller than values currently produced by pollution sources. SRM will also not address the ocean acidification associated with increasing atmospheric CO_2 concentrations and its impacts on marine ecosystems.

Without conventional mitigation efforts or potential CDR methods, high CO_2 concentrations from anthropogenic emissions will persist in the atmosphere for as long as a thousand years, and SRM would have to be maintained as long as CO_2 concentrations were high. Stopping SRM while CO_2 concentrations are still high would lead to a very rapid warming over one or two decades (see FAQ7.3, Figure 2), severely stressing ecosystem and human adaptation.

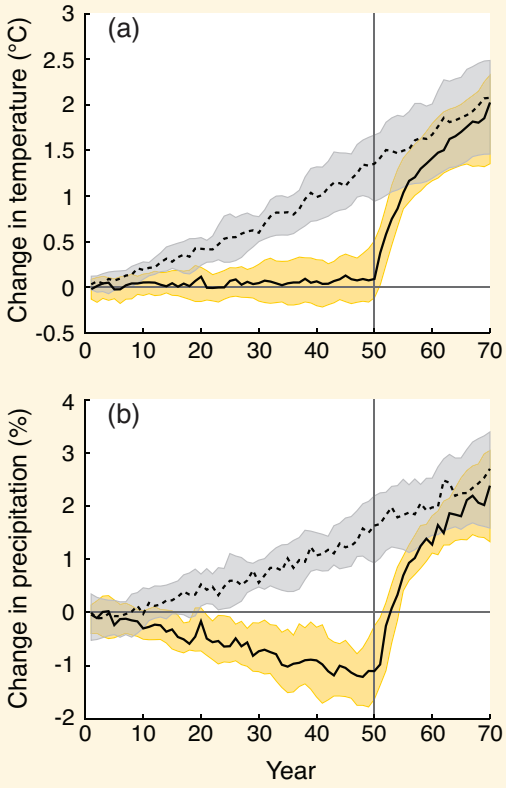

FAQ 7.3, Figure 2 | Change in globally averaged (a) surface temperature (°C) and (b) precipitation (%) in two idealized experiments. Solid lines are for simulations using Solar Radiation Management (SRM) to balance a 1% yr^{-1} increase in CO_2 concentration until year 50, after which SRM is stopped. Dashed lines are for simulations with a 1% yr^{-1} increase in CO_2 concentration and no SRM. The yellow and grey envelopes show the 25th to 75th percentiles from eight different models.

If SRM were used to avoid some consequences of increasing CO_2 concentrations, the risks, side effects and shortcomings would clearly increase as the scale of SRM increase. Approaches have been proposed to use a time-limited amount of SRM along with aggressive strategies for reducing CO_2 concentrations to help avoid transitions across climate thresholds or tipping points that would be unavoidable otherwise; assessment of such approaches would require a very careful risk benefit analysis that goes much beyond this Report.

Frequently Asked Questions

FAQ 8.1 | How Important Is Water Vapour to Climate Change?

As the largest contributor to the natural greenhouse effect, water vapour plays an essential role in the Earth's climate. However, the amount of water vapour in the atmosphere is controlled mostly by air temperature, rather than by emissions. For that reason, scientists consider it a feedback agent, rather than a forcing to climate change. Anthropogenic emissions of water vapour through irrigation or power plant cooling have a negligible impact on the global climate.

Water vapour is the primary greenhouse gas in the Earth's atmosphere. The contribution of water vapour to the natural greenhouse effect relative to that of carbon dioxide (CO_2) depends on the accounting method, but can be considered to be approximately two to three times greater. Additional water vapour is injected into the atmosphere from anthropogenic activities, mostly through increased evaporation from irrigated crops, but also through power plant cooling, and marginally through the combustion of fossil fuel. One may therefore question why there is so much focus on CO_2, and not on water vapour, as a forcing to climate change.

Water vapour behaves differently from CO_2 in one fundamental way: it can condense and precipitate. When air with high humidity cools, some of the vapour condenses into water droplets or ice particles and precipitates. The typical residence time of water vapour in the atmosphere is ten days. The flux of water vapour into the atmosphere from anthropogenic sources is considerably less than from 'natural' evaporation. Therefore, it has a negligible impact on overall concentrations, and does not contribute significantly to the long-term greenhouse effect. This is the main reason why tropospheric water vapour (typically below 10 km altitude) is not considered to be an anthropogenic gas contributing to radiative forcing.

Anthropogenic emissions do have a significant impact on water vapour in the stratosphere, which is the part of the atmosphere above about 10 km. Increased concentrations of methane (CH_4) due to human activities lead to an additional source of water, through oxidation, which partly explains the observed changes in that atmospheric layer. That stratospheric water change has a radiative impact, is considered a forcing, and can be evaluated. Stratospheric concentrations of water have varied significantly in past decades. The full extent of these variations is not well understood and is probably less a forcing than a feedback process added to natural variability. The contribution of stratospheric water vapour to warming, both forcing and feedback, is much smaller than from CH_4 or CO_2.

The maximum amount of water vapour in the air is controlled by temperature. A typical column of air extending from the surface to the stratosphere in polar regions may contain only a few kilograms of water vapour per square metre, while a similar column of air in the tropics may contain up to 70 kg. With every extra degree of air temperature, the atmosphere can retain around 7% more water vapour (see upper-left insert in the FAQ 8.1, Figure 1). This increase in concentration amplifies the greenhouse effect, and therefore leads to more warming. This process, referred to as the water vapour feedback, is well understood and quantified. It occurs in all models used to estimate climate change, where its strength is consistent with observations. Although an increase in atmospheric water vapour has been observed, this change is recognized as a climate feedback (from increased atmospheric temperature) and should not be interpreted as a radiative forcing from anthropogenic emissions. *(continued on next page)*

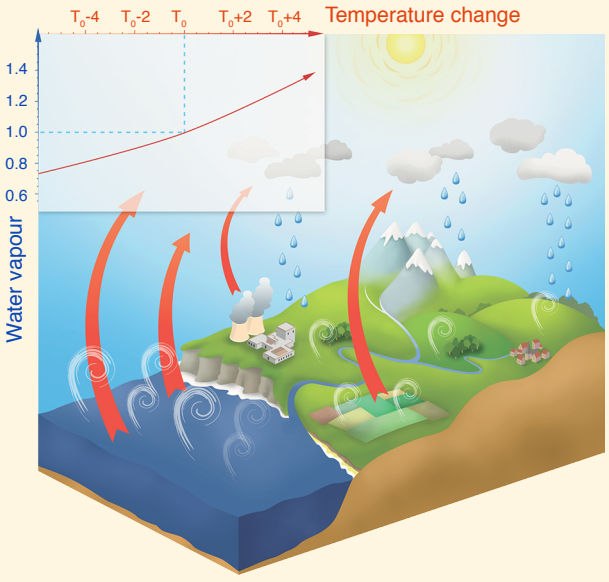

FAQ 8.1, Figure 1 | Illustration of the water cycle and its interaction with the greenhouse effect. The upper-left insert indicates the relative increase of potential water vapour content in the air with an increase of temperature (roughly 7% per degree). The white curls illustrate evaporation, which is compensated by precipitation to close the water budget. The red arrows illustrate the outgoing infrared radiation that is partly absorbed by water vapour and other gases, a process that is one component of the greenhouse effect. The stratospheric processes are not included in this figure.

FAQ 8.1 (continued)

Currently, water vapour has the largest greenhouse effect in the Earth's atmosphere. However, other greenhouse gases, primarily CO_2, are necessary to sustain the presence of water vapour in the atmosphere. Indeed, if these other gases were removed from the atmosphere, its temperature would drop sufficiently to induce a decrease of water vapour, leading to a runaway drop of the greenhouse effect that would plunge the Earth into a frozen state. So greenhouse gases other than water vapour provide the temperature structure that sustains current levels of atmospheric water vapour. Therefore, although CO_2 is the main anthropogenic control knob on climate, water vapour is a strong and fast feedback that amplifies any initial forcing by a typical factor between two and three. Water vapour is not a significant initial forcing, but is nevertheless a fundamental agent of climate change.

Frequently Asked Questions

FAQ 8.2 | Do Improvements in Air Quality Have an Effect on Climate Change?

Yes they do, but depending on which pollutant(s) they limit, they can either cool or warm the climate. For example, whereas a reduction in sulphur dioxide (SO_2) emissions leads to more warming, nitrogen oxide (NO_x) emission control has both a cooling (through reducing of tropospheric ozone) and a warming effect (due to its impact on methane lifetime and aerosol production). Air pollution can also affect precipitation patterns.

Air quality is nominally a measure of airborne surface pollutants, such as ozone, carbon monoxide, NO_x and aerosols (solid or liquid particulate matter). Exposure to such pollutants exacerbates respiratory and cardiovascular diseases, harms plants and damages buildings. For these reasons, most major urban centres try to control discharges of airborne pollutants.

Unlike carbon dioxide (CO_2) and other well-mixed greenhouse gases, tropospheric ozone and aerosols may last in the atmosphere only for a few days to a few weeks, though indirect couplings within the Earth system can prolong their impact. These pollutants are usually most potent near their area of emission or formation, where they can force local or regional perturbations to climate, even if their globally averaged effect is small.

Air pollutants affect climate differently according to their physical and chemical characteristics. Pollution-generated greenhouse gases will impact climate primarily through shortwave and longwave radiation, while aerosols can in addition affect climate through cloud–aerosol interactions.

Controls on anthropogenic emissions of methane (FAQ 8.2, Figure 1) to lower surface ozone have been identified as 'win–win' situations. Consequences of controlling other ozone precursors are not always as clear. NO_x emission controls, for instance, might be expected to have a cooling effect as they reduce tropospheric ozone, but their impact on CH_4 lifetime and aerosol formation is more likely instead to cause overall warming.

Satellite observations have identified increasing atmospheric concentrations of SO_2 (the primary precursor to scattering sulphate aerosols) from coal-burning power plants over eastern Asia during the last few decades. The most recent power plants use scrubbers to reduce such emissions (albeit not the concurrent CO_2 emissions and associated long-term climate warming). This improves air quality, but also reduces the cooling effect of sulphate aerosols and therefore exacerbates warming. Aerosol cooling occurs through aerosol–radiation and aerosol–cloud interactions and is estimated at –0.9 W m^{-2} (all aerosols combined, Section 8.3.4.3) since pre-industrial, having grown especially during the second half of the 20th century when anthropogenic emissions rose sharply. *(continued on next page)*

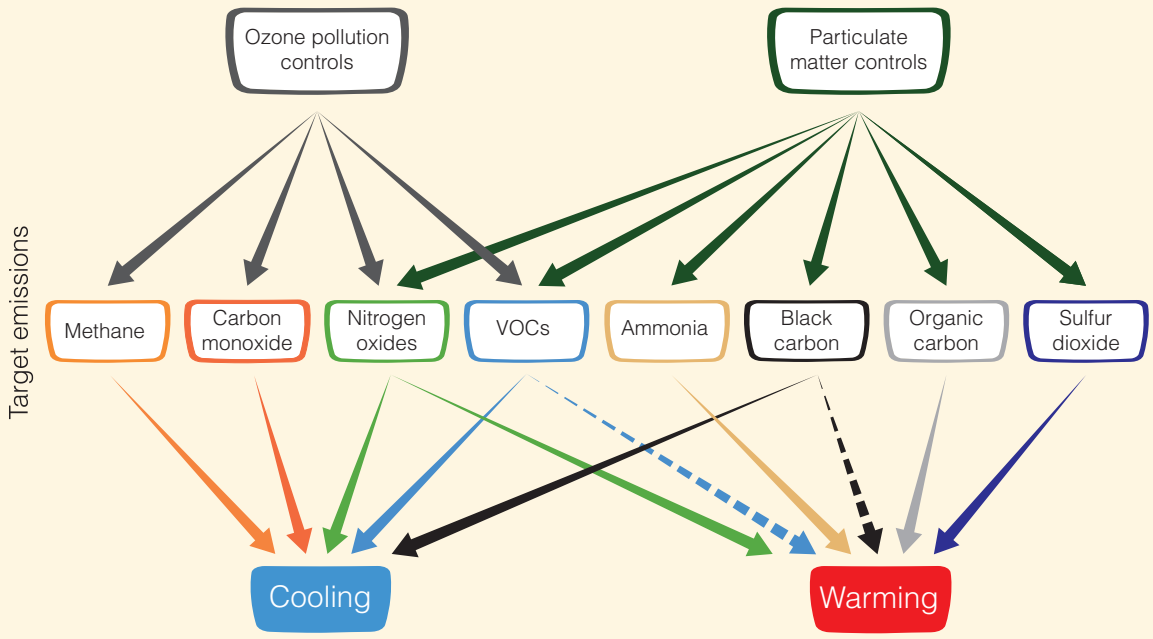

FAQ 8.2, Figure 1 | Schematic diagram of the impact of pollution controls on specific emissions and climate impact. Solid black line indicates known impact; dashed line indicates uncertain impact.

FAQ 8.2 (continued)

Black carbon or soot, on the other hand, absorbs heat in the atmosphere (leading to a 0.4 W m^{-2} radiative forcing from anthropogenic fossil and biofuel emissions) and, when deposited on snow, reduces its albedo, or ability to reflect sunlight. Reductions of black carbon emissions can therefore have a cooling effect, but the additional interaction of black carbon with clouds is uncertain and could lead to some counteracting warming.

Air quality controls might also target a specific anthropogenic activity sector, such as transportation or energy production. In that case, co-emitted species within the targeted sector lead to a complex mix of chemistry and climate perturbations. For example, smoke from biofuel combustion contains a mixture of both absorbing and scattering particles as well as ozone precursors, for which the combined climate impact can be difficult to ascertain.

Thus, surface air quality controls will have some consequences on climate. Some couplings between the targeted emissions and climate are still poorly understood or identified, including the effects of air pollutants on precipitation patterns, making it difficult to fully quantify these consequences. There is an important twist, too, in the potential effect of climate change on air quality. In particular, an observed correlation between surface ozone and temperature in polluted regions indicates that higher temperatures from climate change alone could worsen summertime pollution, suggesting a 'climate penalty'. This penalty implies stricter surface ozone controls will be required to achieve a specific target. In addition, projected changes in the frequency and duration of stagnation events could impact air quality conditions. These features will be regionally variable and difficult to assess, but better understanding, quantification and modelling of these processes will clarify the overall interaction between air pollutants and climate.

Frequently Asked Questions

FAQ 9.1 | Are Climate Models Getting Better, and How Would We Know?

Climate models are extremely sophisticated computer programs that encapsulate our understanding of the climate system and simulate, with as much fidelity as currently feasible, the complex interactions between the atmosphere, ocean, land surface, snow and ice, the global ecosystem and a variety of chemical and biological processes.

The complexity of climate models—the representation of physical processes like clouds, land surface interactions and the representation of the global carbon and sulphur cycles in many models—has increased substantially since the IPCC First Assessment Report in 1990, so in that sense, current Earth System Models are vastly 'better' than the models of that era. This development has continued since the Fourth Assessment, while other factors have also contributed to model improvement. More powerful supercomputers allow current models to resolve finer spatial detail. Today's models also reflect improved understanding of how climate processes work—understanding that has come from ongoing research and analysis, along with new and improved observations.

Climate models of today are, in principle, better than their predecessors. However, every bit of added complexity, while intended to improve some aspect of simulated climate, also introduces new sources of possible error (e.g., via uncertain parameters) and new interactions between model components that may, if only temporarily, degrade a model's simulation of other aspects of the climate system. Furthermore, despite the progress that has been made, scientific uncertainty regarding the details of many processes remains.

An important consideration is that model performance can be evaluated only relative to past observations, taking into account natural internal variability. To have confidence in the future projections of such models, historical climate—and its variability and change—must be well simulated. The scope of model evaluation, in terms of the kind and quantity of observations available, the availability of better coordinated model experiments, and the expanded use of various performance metrics, has provided much more quantitative information about model performance. But this alone may not be sufficient. Whereas weather and seasonal climate predictions can be regularly verified, climate projections spanning a century or more cannot. This is particularly the case as anthropogenic forcing is driving the climate system toward conditions not previously observed in the instrumental record, and it will always be a limitation.

Quantifying model performance is a topic that has featured in all previous IPCC Working Group I Reports. Reading back over these earlier assessments provides a general sense of the improvements that have been made. Past reports have typically provided a rather broad survey of model performance, showing differences between model-calculated versions of various climate quantities and corresponding observational estimates.

Inevitably, some models perform better than others for certain climate variables, but no individual model clearly emerges as 'the best' overall. Recently, there has been progress in computing various performance metrics, which synthesize model performance relative to a range of different observations according to a simple numerical score. Of course, the definition of such a score, how it is computed, the observations used (which have their

(continued on next page)

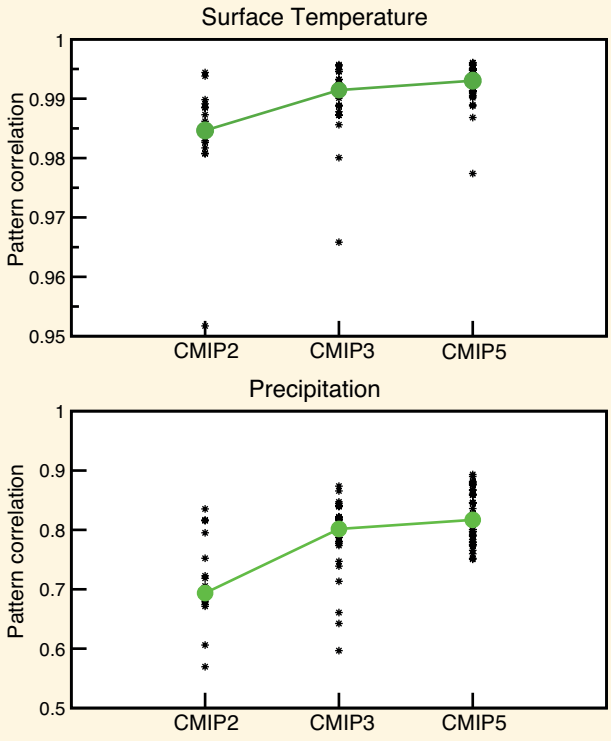

FAQ 9.1, Figure 1 | Model capability in simulating annual mean temperature and precipitation patterns as illustrated by results of three recent phases of the Coupled Model Intercomparison Project (CMIP2, models from about year 2000; CMIP3, models from about 2005; and CMIP5, the current generation of models). The figure shows the correlation (a measure of pattern similarity) between observed and modelled temperature (upper panel) and precipitation (lower panel). Larger values indicate better correspondence between modelled and observed spatial patterns. The black symbols indicate correlation coefficient for individual models, and the large green symbols indicate the median value (i.e., half of the model results lie above and the other half below this value). Improvement in model performance is evident by the increase in correlation for successive model generations.

FAQ 9.1 (continued)

own uncertainties), and the manner in which various scores are combined are all important, and will affect the end result.

Nevertheless, if the metric is computed consistently, one can compare different generations of models. Results of such comparisons generally show that, although each generation exhibits a range in performance, the average model performance index has improved steadily between each generation. An example of changes in model performance over time is shown in FAQ 9.1, Figure 1, and illustrates the ongoing, albeit modest, improvement. It is interesting to note that both the poorest and best performing models demonstrate improvement, and that this improvement comes in parallel with increasing model complexity and an elimination of artificial adjustments to atmosphere and ocean coupling (so-called 'flux adjustment'). Some of the reasons for this improvement include increased understanding of various climate processes and better representation of these processes in climate models. More comprehensive Earth observations are also driving improvements.

So, yes, climate models are getting better, and we can demonstrate this with quantitative performance metrics based on historical observations. Although future climate projections cannot be directly evaluated, climate models are based, to a large extent, on verifiable physical principles and are able to reproduce many important aspects of past response to external forcing. In this way, they provide a scientifically sound preview of the climate response to different scenarios of anthropogenic forcing.

Frequently Asked Questions

FAQ 10.1 | Climate Is Always Changing. How Do We Determine the Causes of Observed Changes?

The causes of observed long-term changes in climate (on time scales longer than a decade) are assessed by determining whether the expected 'fingerprints' of different causes of climate change are present in the historical record. These fingerprints are derived from computer model simulations of the different patterns of climate change caused by individual climate forcings. On multi-decade time scales, these forcings include processes such as greenhouse gas increases or changes in solar brightness. By comparing the simulated fingerprint patterns with observed climate changes, we can determine whether observed changes are best explained by those fingerprint patterns, or by natural variability, which occurs without any forcing.

The fingerprint of human-caused greenhouse gas increases is clearly apparent in the pattern of observed 20th century climate change. The observed change cannot be otherwise explained by the fingerprints of natural forcings or natural variability simulated by climate models. Attribution studies therefore support the conclusion that 'it is extremely likely *that human activities have caused more than half of the observed increase in global mean surface temperatures from 1951 to 2010.'*

The Earth's climate is always changing, and that can occur for many reasons. To determine the principal causes of observed changes, we must first ascertain whether an observed change in climate is different from other fluctuations that occur without any forcing at all. Climate variability without forcing—called internal variability—is the consequence of processes within the climate system. Large-scale oceanic variability, such as El Niño-Southern Oscillation (ENSO) fluctuations in the Pacific Ocean, is the dominant source of internal climate variability on decadal to centennial time scales.

Climate change can also result from natural forcings external to the climate system, such as volcanic eruptions, or changes in the brightness of the sun. Forcings such as these are responsible for the huge changes in climate that are clearly documented in the geological record. Human-caused forcings include greenhouse gas emissions or atmospheric particulate pollution. Any of these forcings, natural or human caused, could affect internal variability as well as causing a change in average climate. Attribution studies attempt to determine the causes of a detected change in observed climate. Over the past century we know that global average temperature has increased, so if the observed change is forced then the principal forcing must be one that causes warming, not cooling.

Formal climate change attribution studies are carried out using controlled experiments with climate models. The model-simulated responses to specific climate forcings are often called the fingerprints of those forcings. A climate model must reliably simulate the fingerprint patterns associated with individual forcings, as well as the patterns of unforced internal variability, in order to yield a meaningful climate change attribution assessment. No model can perfectly reproduce all features of climate, but many detailed studies indicate that simulations using current models are indeed sufficiently reliable to carry out attribution assessments.

FAQ 10.1, Figure 1 illustrates part of a fingerprint assessment of global temperature change at the surface during the late 20th century. The observed change in the latter half of the 20th century, shown by the black time series in the left panels, is larger than expected from just internal variability. Simulations driven only by natural forcings (yellow and blue lines in the upper left panel) fail to reproduce late 20th century global warming at the surface with a spatial pattern of change (upper right) completely different from the observed pattern of change (middle right). Simulations including both natural and human-caused forcings provide a much better representation of the time rate of change (lower left) and spatial pattern (lower right) of observed surface temperature change.

Both panels on the left show that computer models reproduce the naturally forced surface cooling observed for a year or two after major volcanic eruptions, such as occurred in 1982 and 1991. Natural forcing simulations capture the short-lived temperature changes following eruptions, but only the natural + human caused forcing simulations simulate the longer-lived warming trend.

A more complete attribution assessment would examine temperature above the surface, and possibly other climate variables, in addition to the surface temperature results shown in FAQ 10.1, Figure 1. The fingerprint patterns associated with individual forcings become easier to distinguish when more variables are considered in the assessment.

(continued on next page)

FAQ 10.1 (continued)

Overall, FAQ 10.1, Figure 1 shows that the pattern of observed temperature change is significantly different than the pattern of response to natural forcings alone. The simulated response to all forcings, including human-caused forcings, provides a good match to the observed changes at the surface. We cannot correctly simulate recent observed climate change without including the response to human-caused forcings, including greenhouse gases, stratospheric ozone, and aerosols. Natural causes of change are still at work in the climate system, but recent trends in temperature are largely attributable to human-caused forcing.

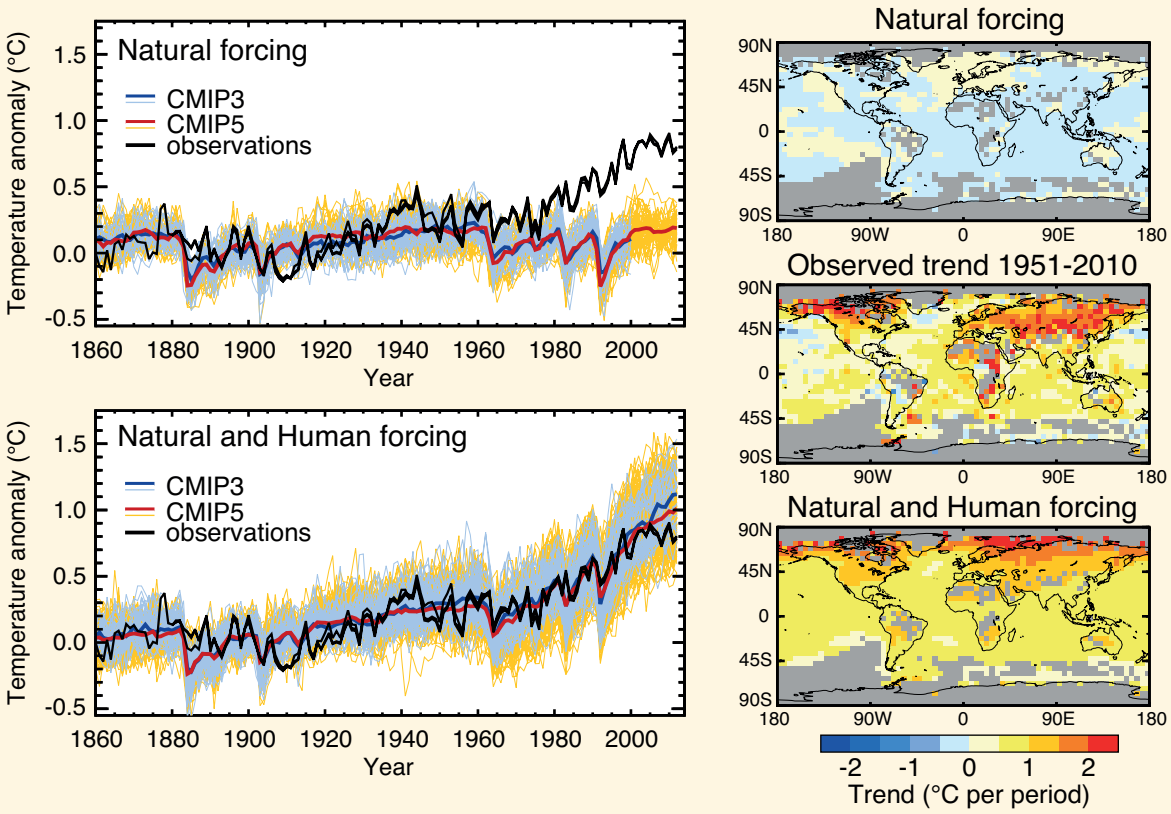

FAQ 10.1, Figure 1 | (Left) Time series of global and annual-averaged surface temperature change from 1860 to 2010. The top left panel shows results from two ensemble of climate models driven with just natural forcings, shown as thin blue and yellow lines; ensemble average temperature changes are thick blue and red lines. Three different observed estimates are shown as black lines. The lower left panel shows simulations by the same models, but driven with both natural forcing and human-induced changes in greenhouse gases and aerosols. (Right) Spatial patterns of local surface temperature trends from 1951 to 2010. The upper panel shows the pattern of trends from a large ensemble of Coupled Model Intercomparison Project Phase 5 (CMIP5) simulations driven with just natural forcings. The bottom panel shows trends from a corresponding ensemble of simulations driven with natural + human forcings. The middle panel shows the pattern of observed trends from the Hadley Centre/Climatic Research Unit gridded surface temperature data set 4 (HadCRUT4) during this period.

Frequently Asked Questions

FAQ 10.2 | When Will Human Influences on Climate Become Obvious on Local Scales?

Human-caused warming is already becoming locally obvious on land in some tropical regions, especially during the warm part of the year. Warming should become obvious in middle latitudes—during summer at first—within the next several decades. The trend is expected to emerge more slowly there, especially during winter, because natural climate variability increases with distance from the equator and during the cold season. Temperature trends already detected in many regions have been attributed to human influence. Temperature-sensitive climate variables, such as Arctic sea ice, also show detected trends attributable to human influence.

Warming trends associated with global change are generally more evident in averages of global temperature than in time series of local temperature ('local' here refers generally to individual locations, or small regional averages). This is because most of the local variability of local climate is averaged away in the global mean. Multi-decadal warming trends detected in many regions are considered to be outside the range of trends one might expect from natural internal variability of the climate system, but such trends will only become obvious when the local mean climate emerges from the 'noise' of year-to-year variability. How quickly this happens depends on both the rate of the warming trend and the amount of local variability. Future warming trends cannot be predicted precisely, especially at local scales, so estimates of the future time of emergence of a warming trend cannot be made with precision.

In some tropical regions, the warming trend has already emerged from local variability (FAQ 10.2, Figure 1). This happens more quickly in the tropics because there is less temperature variability there than in other parts of the globe. Projected warming may not emerge in middle latitudes until the mid-21st century—even though warming trends there are larger—because local temperature variability is substantially greater there than in the tropics. On a seasonal basis, local temperature variability tends to be smaller in summer than in winter. Warming therefore tends to emerge first in the warm part of the year, even in regions where the warming trend is larger in winter, such as in central Eurasia in FAQ 10.2, Figure 1.

Variables other than land surface temperature, including some oceanic regions, also show rates of long-term change different from natural variability. For example, Arctic sea ice extent is declining very rapidly, and already shows a human influence. On the other hand, local precipitation trends are very hard to detect because at most locations the variability in precipitation is quite large. The probability of record-setting warm summer temperatures has increased throughout much of the Northern Hemisphere . High temperatures presently considered extreme are projected to become closer to the norm over the coming decades. The probabilities of other extreme events, including some cold spells, have lessened.

In the present climate, individual extreme weather events cannot be unambiguously ascribed to climate change, since such events could have happened in an unchanged climate. However the probability of occurrence of such events could have changed significantly at a particular location. Human-induced increases in greenhouse gases are estimated to have contributed substantially to the probability of some heatwaves. Similarly, climate model studies suggest that increased greenhouse gases have contributed to the observed intensification of heavy precipitation events found over parts of the Northern Hemisphere. However, the probability of many other extreme weather events may not have changed substantially. Therefore, it is incorrect to ascribe every new weather record to climate change.

The date of future emergence of projected warming trends also depends on local climate variability, which can temporarily increase or decrease temperatures. Furthermore, the projected local temperature curves shown in FAQ 10.2, Figure 1 are based on multiple climate model simulations forced by the same assumed future emissions scenario. A different rate of atmospheric greenhouse gas accumulation would cause a different warming trend, so the spread of model warming projections (the coloured shading in FAQ 10.2, Figure 1) would be wider if the figure included a spread of greenhouse gas emissions scenarios. The increase required for summer temperature change to emerge from 20th century local variability (regardless of the rate of change) is depicted on the central map in FAQ 10.2, Figure 1.

A full answer to the question of when human influence on local climate will become obvious depends on the strength of evidence one considers sufficient to render something 'obvious'. The most convincing scientific evidence for the effect of climate change on local scales comes from analysing the global picture, and from the wealth of evidence from across the climate system linking many observed changes to human influence. *(continued on next page)*

FAQ 10.2 (continued)

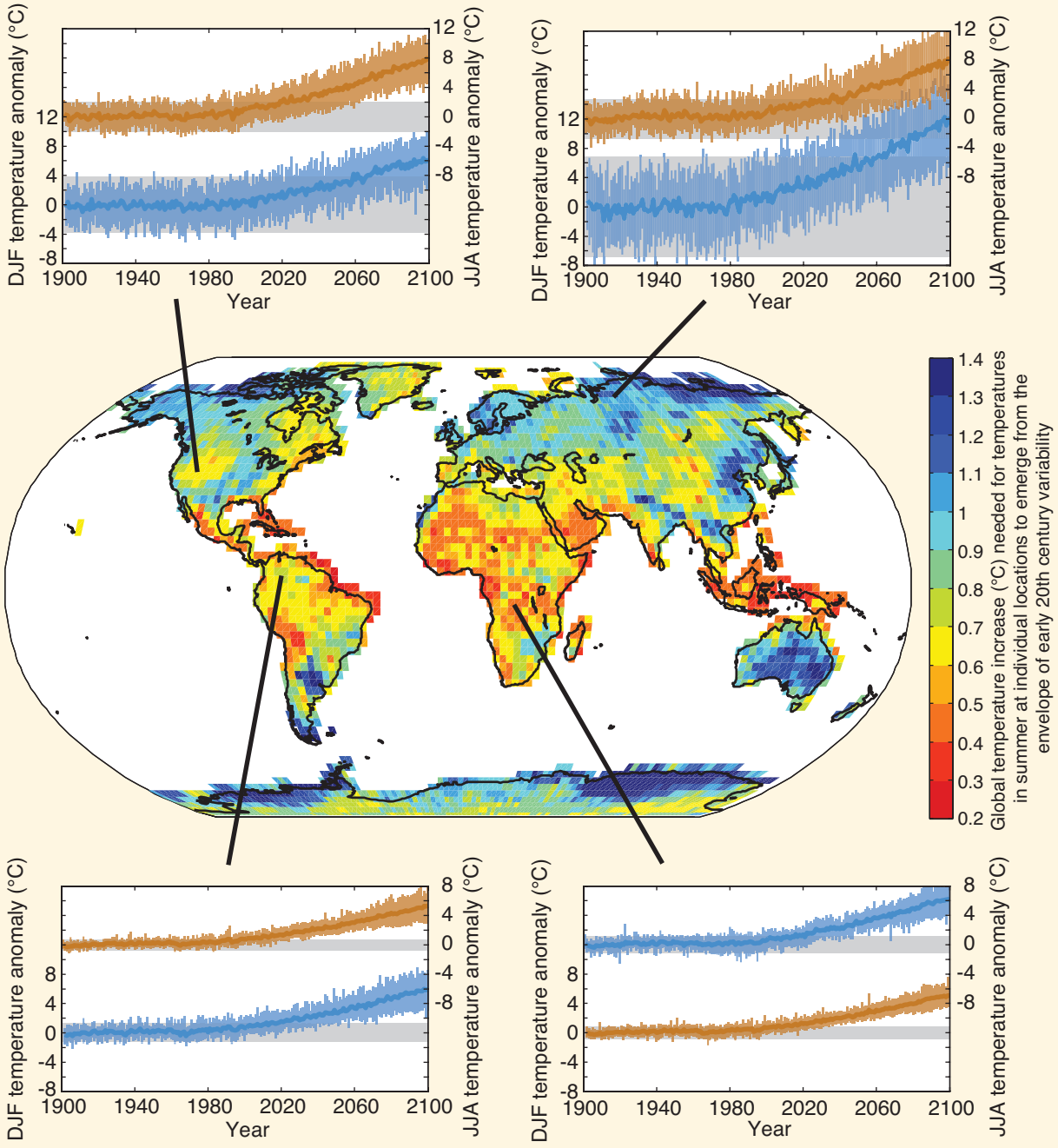

FAQ 10.2, Figure 1 | Time series of projected temperature change shown at four representative locations for summer (red curves, representing June, July and August at sites in the tropics and Northern Hemisphere or December, January and February in the Southern Hemisphere) and winter (blue curves). Each time series is surrounded by an envelope of projected changes (pink for the local warm season, blue for the local cold season) yielded by 24 different model simulations, emerging from a grey envelope of natural local variability simulated by the models using early 20th century conditions. The warming signal emerges first in the tropics during summer. The central map shows the global temperature increase (°C) needed for temperatures in summer at individual locations to emerge from the envelope of early 20th century variability. Note that warm colours denote the smallest needed temperature increase, hence earliest time of emergence. All calculations are based on Coupled Model Intercomparison Project Phase 5 (CMIP5) global climate model simulations forced by the Representative Concentration Pathway 8.5 (RCP8.5) emissions scenario. Envelopes of projected change and natural variability are defined as ±2 standard deviations. (Adapted and updated from Mahlstein et al., 2011.)

Frequently Asked Questions

FAQ 11.1 | If You Cannot Predict the Weather Next Month, How Can You Predict Climate for the Coming Decade?

Although weather and climate are intertwined, they are in fact different things. Weather is defined as the state of the atmosphere at a given time and place, and can change from hour to hour and day to day. Climate, on the other hand, generally refers to the statistics of weather conditions over a decade or more.

An ability to predict future climate without the need to accurately predict weather is more commonplace that it might first seem. For example, at the end of spring, it can be accurately predicted that the average air temperature over the coming summer in Melbourne (for example) will very likely be higher than the average temperature during the most recent spring—even though the day-to-day weather during the coming summer cannot be predicted with accuracy beyond a week or so. This simple example illustrates that factors exist—in this case the seasonal cycle in solar radiation reaching the Southern Hemisphere—that can underpin skill in predicting changes in climate over a coming period that does not depend on accuracy in predicting weather over the same period.

The statistics of weather conditions used to define climate include long-term averages of air temperature and rainfall, as well as statistics of their variability, such as the standard deviation of year-to-year rainfall variability from the long-term average, or the frequency of days below 5°C. Averages of climate variables over long periods of time are called climatological averages. They can apply to individual months, seasons or the year as a whole. A climate prediction will address questions like: 'How likely will it be that the average temperature during the coming summer will be higher than the long-term average of past summers?' or: 'How likely will it be that the next decade will be warmer than past decades?' More specifically, a climate prediction might provide an answer to the question: 'What is the probability that temperature (in China, for instance) averaged over the next ten years will exceed the temperature in China averaged over the past 30 years?' Climate predictions do not provide forecasts of the detailed day-to-day evolution of future weather. Instead, they provide probabilities of long-term changes to the statistics of future climatic variables.

Weather forecasts, on the other hand, provide predictions of day-to-day weather for specific times in the future. They help to address questions like: 'Will it rain tomorrow?' Sometimes, weather forecasts are given in terms of probabilities. For example, the weather forecast might state that: 'the likelihood of rainfall in Apia tomorrow is 75%'.

To make accurate weather predictions, forecasters need highly detailed information about the current state of the atmosphere. The chaotic nature of the atmosphere means that even the tiniest error in the depiction of 'initial conditions' typically leads to inaccurate forecasts beyond a week or so. This is the so-called 'butterfly effect'.

Climate scientists do not attempt or claim to predict the detailed future evolution of the weather over coming seasons, years or decades. There is, on the other hand, a sound scientific basis for supposing that aspects of climate can be predicted, albeit imprecisely, despite the butterfly effect. For example, increases in long-lived atmospheric greenhouse gas concentrations tend to increase surface temperature in future decades. Thus, information from the past can and does help predict future climate.

Some types of naturally occurring so-called 'internal' variability can—in theory at least—extend the capacity to predict future climate. Internal climatic variability arises from natural instabilities in the climate system. If such variability includes or causes extensive, long-lived, upper ocean temperature anomalies, this will drive changes in the overlying atmosphere, both locally and remotely. The El Niño-Southern Oscillation phenomenon is probably the most famous example of this kind of internal variability. Variability linked to the El Niño-Southern Oscillation unfolds in a partially predictable fashion. The butterfly effect is present, but it takes longer to strongly influence some of the variability linked to the El Nino-Southern Oscillation.

Meteorological services and other agencies have exploited this. They have developed seasonal-to-interannual prediction systems that enable them to routinely predict seasonal climate anomalies with demonstrable predictive skill. The skill varies markedly from place to place and variable to variable. Skill tends to diminish the further the prediction delves into the future and in some locations there is no skill at all. 'Skill' is used here in its technical sense: it is a measure of how much greater the accuracy of a prediction is, compared with the accuracy of some typically simple prediction method like assuming that recent anomalies will persist during the period being predicted.

Weather, seasonal-to-interannual and decadal prediction systems are similar in many ways (e.g., they all incorporate the same mathematical equations for the atmosphere, they all need to specify initial conditions to kick-start

(continued on next page)

FAQ 11.1 (continued)

predictions, and they are all subject to limits on forecast accuracy imposed by the butterfly effect). However, decadal prediction, unlike weather and seasonal-to-interannual prediction, is still in its infancy. Decadal prediction systems nevertheless exhibit a degree of skill in *hindcasting* near-surface temperature over much of the globe out to at least nine years. A 'hindcast' is a prediction of a past event in which only observations prior to the event are fed into the prediction system used to make the prediction. The bulk of this skill is thought to arise from *external forcing*. 'External forcing' is a term used by climate scientists to refer to a forcing agent outside the climate system causing a change in the climate system. This includes increases in the concentration of long-lived greenhouse gases.

Theory indicates that skill in predicting decadal precipitation should be less than the skill in predicting decadal surface temperature, and hindcast performance is consistent with this expectation.

Current research is aimed at improving decadal prediction systems, and increasing the understanding of the reasons for any apparent skill. Ascertaining the degree to which the extra information from internal variability actually translates to increased skill is a key issue. While prediction systems are expected to improve over coming decades, the chaotic nature of the climate system and the resulting butterfly effect will always impose unavoidable limits on predictive skill. Other sources of uncertainty exist. For example, as volcanic eruptions can influence climate but their timing and magnitude cannot be predicted, future eruptions provide one of a number of other sources of uncertainty. Additionally, the shortness of the period with enough oceanic data to initialize and assess decadal predictions presents a major challenge.

Finally, note that decadal prediction systems are designed to exploit both externally forced and internally generated sources of predictability. Climate scientists distinguish between decadal predictions and decadal projections. Projections exploit only the predictive capacity arising from external forcing. While previous IPCC Assessment Reports focussed exclusively on projections, this report also assesses decadal prediction research and its scientific basis.

Frequently Asked Questions

FAQ 11.2 | How Do Volcanic Eruptions Affect Climate and Our Ability to Predict Climate?

Large volcanic eruptions affect the climate by injecting sulphur dioxide gas into the upper atmosphere (also called stratosphere), which reacts with water to form clouds of sulphuric acid droplets. These clouds reflect sunlight back to space, preventing its energy from reaching the Earth's surface, thus cooling it, along with the lower atmosphere. These upper atmospheric sulphuric acid clouds also locally absorb energy from the Sun, the Earth and the lower atmosphere, which heats the upper atmosphere (see FAQ 11.2, Figure 1). In terms of surface cooling, the 1991 Mt Pinatubo eruption in the Philippines, for example, injected about 20 million tons of sulphur dioxide (SO_2) into the stratosphere, cooling the Earth by about 0.5°C for up to a year. Globally, eruptions also reduce precipitation, because the reduced incoming shortwave at the surface is compensated by a reduction in latent heating (i.e., in evaporation and hence rainfall).

For the purposes of predicting climate, an eruption causing significant global surface cooling and upper atmospheric heating for the next year or so can be expected. The problem is that, while a volcano that has become more active can be detected, the precise timing of an eruption, or the amount of SO_2 injected into the upper atmosphere and how it might disperse cannot be predicted. This is a source of uncertainty in climate predictions.

Large volcanic eruptions produce lots of particles, called ash or tephra. However, these particles fall out of the atmosphere quickly, within days or weeks, so they do not affect the global climate. For example, the 1980 Mount St. Helens eruption affected surface temperatures in the northwest USA for several days but, because it emitted little SO_2 into the stratosphere, it had no detectable global climate impacts. If large, high-latitude eruptions inject sulphur into the stratosphere, they will have an effect only in the hemisphere where they erupted, and the effects will only last a year at most, as the stratospheric cloud they produce only has a lifetime of a few months.

Tropical or subtropical volcanoes produce more global surface or tropospheric cooling. This is because the resulting sulphuric acid cloud in the upper atmosphere lasts between one and two years, and can cover much of the globe. However, their regional climatic impacts are difficult to predict, because dispersion of stratospheric sulphate aerosols depends heavily on atmospheric wind conditions at the time of eruption. Furthermore, the surface cooling effect is typically not uniform: because continents cool more than the ocean, the summer monsoon can weaken, reducing rain over Asia and Africa. The climatic response is complicated further by the fact that upper atmospheric clouds from tropical eruptions also absorb sunlight and heat from the Earth, which produces more upper atmosphere warming in the tropics than at high latitudes.

The largest volcanic eruptions of the past 250 years stimulated scientific study. After the 1783 Laki eruption in Iceland, there were record warm summer temperatures in Europe, followed by a very cold winter. Two large eruptions, an unidentified one in 1809, and the 1815 Tambora eruption caused the 'Year Without a Summer' in 1816. Agricultural failures in Europe and the USA that year led to food shortages, famine and riots.

The largest eruption in more than 50 years, that of Agung in 1963, led to many modern studies, including observations and climate model calculations. Two subsequent large eruptions, El Chichón in 1982 and Pinatubo in 1991, inspired the work that led to our current understanding of the effects of volcanic eruptions on climate.

(continued on next page)

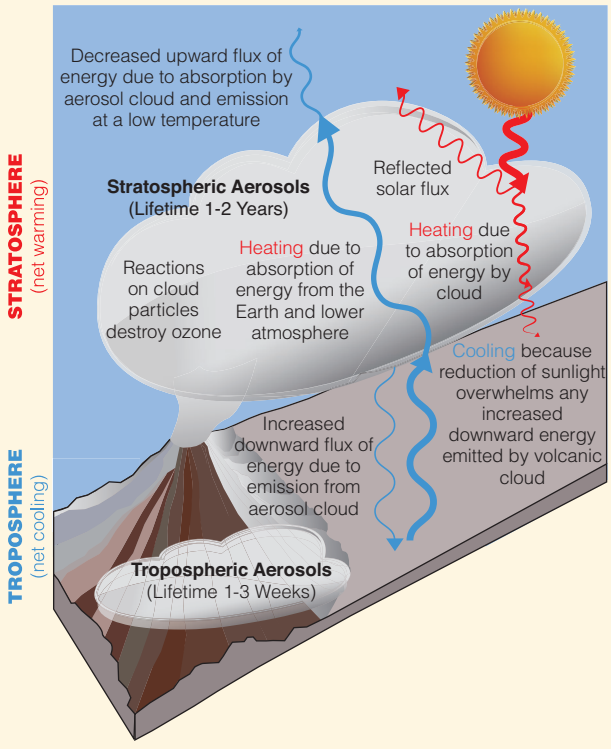

FAQ 11.2, Figure 1 | Schematic of how large tropical or sub-tropical volcanoes impact upper atmospheric (stratospheric) and lower atmospheric (tropospheric) temperatures.

FAQ 11.2 (continued)

Volcanic clouds remain in the stratosphere only for a couple of years, so their impact on climate is correspondingly short. But the impacts of consecutive large eruptions can last longer: for example, at the end of the 13th century there were four large eruptions—one every ten years. The first, in 1258 CE, was the largest in 1000 years. That sequence of eruptions cooled the North Atlantic Ocean and Arctic sea ice. Another period of interest is the three large, and several lesser, volcanic events during 1963–1991 (see Chapter 8 for how these eruptions affected atmospheric composition and reduced shortwave radiation at the ground.

Volcanologists can detect when a volcano becomes more active, but they cannot predict whether it will erupt, or if it does, how much sulphur it might inject into the stratosphere. Nevertheless, volcanoes affect the ability to predict climate in three distinct ways. First, if a violent eruption injects significant volumes of sulphur dioxide into the stratosphere, this effect can be included in climate predictions. There are substantial challenges and sources of uncertainty involved, such as collecting good observations of the volcanic cloud, and calculating how it will move and change during its lifetime. But, based on observations, and successful modelling of recent eruptions, some of the effects of large eruptions can be included in predictions.

The second effect is that volcanic eruptions are a potential source of uncertainty in our predictions. Eruptions cannot be predicted in advance, but they will occur, causing short-term climatic impacts on both local and global scales. In principle, this potential uncertainty can be accounted for by including random eruptions, or eruptions based on some scenario in our near-term ensemble climate predictions. This area of research needs further exploration. The future projections in this report do not include future volcanic eruptions.

Third, the historical climate record can be used, along with estimates of observed sulphate aerosols, to test the fidelity of our climate simulations. While the climatic response to explosive volcanic eruptions is a useful analogue for some other climatic forcings, there are limitations. For example, successfully simulating the impact of one eruption can help validate models used for seasonal and interannual predictions. But in this way not all the mechanisms involved in global warming over the next century can be validated, because these involve long term oceanic feedbacks, which have a longer time scale than the response to individual volcanic eruptions.

Frequently Asked Questions

FAQ 12.1 | Why Are So Many Models and Scenarios Used to Project Climate Change?

Future climate is partly determined by the magnitude of future emissions of greenhouse gases, aerosols and other natural and man-made forcings. These forcings are external to the climate system, but modify how it behaves. Future climate is shaped by the Earth's response to those forcings, along with internal variability inherent in the climate system. A range of assumptions about the magnitude and pace of future emissions helps scientists develop different emission scenarios, upon which climate model projections are based. Different climate models, meanwhile, provide alternative representations of the Earth's response to those forcings, and of natural climate variability. Together, ensembles of models, simulating the response to a range of different scenarios, map out a range of possible futures, and help us understand their uncertainties.

Predicting socioeconomic development is arguably even more difficult than predicting the evolution of a physical system. It entails predicting human behaviour, policy choices, technological advances, international competition and cooperation. The common approach is to use scenarios of plausible future socioeconomic development, from which future emissions of greenhouse gases and other forcing agents are derived. It has not, in general, been possible to assign likelihoods to individual forcing scenarios. Rather, a set of alternatives is used to span a range of possibilities. The outcomes from different forcing scenarios provide policymakers with alternatives and a range of possible futures to consider.

Internal fluctuations in climate are spontaneously generated by interactions between components such as the atmosphere and the ocean. In the case of near-term climate change, they may eclipse the effect of external perturbations, like greenhouse gas increases (see Chapter 11). Over the longer term, however, the effect of external forcings is expected to dominate instead. Climate model simulations project that, after a few decades, different scenarios of future anthropogenic greenhouse gases and other forcing agents—and the climate system's response to them—will differently affect the change in mean global temperature (FAQ 12.1, Figure 1, left panel). Therefore, evaluating the consequences of those various scenarios and responses is of paramount importance, especially when policy decisions are considered.

Climate models are built on the basis of the physical principles governing our climate system, and empirical understanding, and represent the complex, interacting processes needed to simulate climate and climate change, both past and future. Analogues from past observations, or extrapolations from recent trends, are inadequate strategies for producing projections, because the future will not necessarily be a simple continuation of what we have seen thus far.

Although it is possible to write down the equations of fluid motion that determine the behaviour of the atmosphere and ocean, it is impossible to solve them without using numerical algorithms through computer model simulation, similarly to how aircraft engineering relies on numerical simulations of similar types of equations. Also, many small-scale physical, biological and chemical processes, such as cloud processes, cannot be described by those equations, either because we lack the computational ability to describe the system at a fine enough resolution to directly simulate these processes or because we still have a partial scientific understanding of the mechanisms driving these processes. Those need instead to be approximated by so-called parameterizations within the climate models, through which a mathematical relation between directly simulated and approximated quantities is established, often on the basis of observed behaviour.

There are various alternative and equally plausible numerical representations, solutions and approximations for modelling the climate system, given the limitations in computing and observations. This diversity is considered a healthy aspect of the climate modelling community, and results in a range of plausible climate change projections at global and regional scales. This range provides a basis for quantifying uncertainty in the projections, but because the number of models is relatively small, and the contribution of model output to public archives is voluntary, the sampling of possible futures is neither systematic nor comprehensive. Also, some inadequacies persist that are common to all models; different models have different strength and weaknesses; it is not yet clear which aspects of the quality of the simulations that can be evaluated through observations should guide our evaluation of future model simulations. *(continued on next page)*

FAQ 12.1 (continued)

Models of varying complexity are commonly used for different projection problems. A faster model with lower resolution, or a simplified description of some climate processes, may be used in cases where long multi-century simulations are required, or where multiple realizations are needed. Simplified models can adequately represent large-scale average quantities, like global average temperature, but finer details, like regional precipitation, can be simulated only by complex models.

The coordination of model experiments and output by groups such as the Coupled Model Intercomparison Project (CMIP), the World Climate Research Program and its Working Group on Climate Models has seen the science community step up efforts to evaluate the ability of models to simulate past and current climate and to compare future climate change projections. The 'multi-model' approach is now a standard technique used by the climate science community to assess projections of a specific climate variable.

FAQ 12.1, Figure 1, right panels, shows the temperature response by the end of the 21st century for two illustrative models and the highest and lowest RCP scenarios. Models agree on large-scale patterns of warming at the surface, for example, that the land is going to warm faster than ocean, and the Arctic will warm faster than the tropics. But they differ both in the magnitude of their global response for the same scenario, and in small scale, regional aspects of their response. The magnitude of Arctic amplification, for instance, varies among different models, and a subset of models show a weaker warming or slight cooling in the North Atlantic as a result of the reduction in deepwater formation and shifts in ocean currents.

There are inevitable uncertainties in future external forcings, and the climate system's response to them, which are further complicated by internally generated variability. The use of multiple scenarios and models have become a standard choice in order to assess and characterize them, thus allowing us to describe a wide range of possible future evolutions of the Earth's climate.

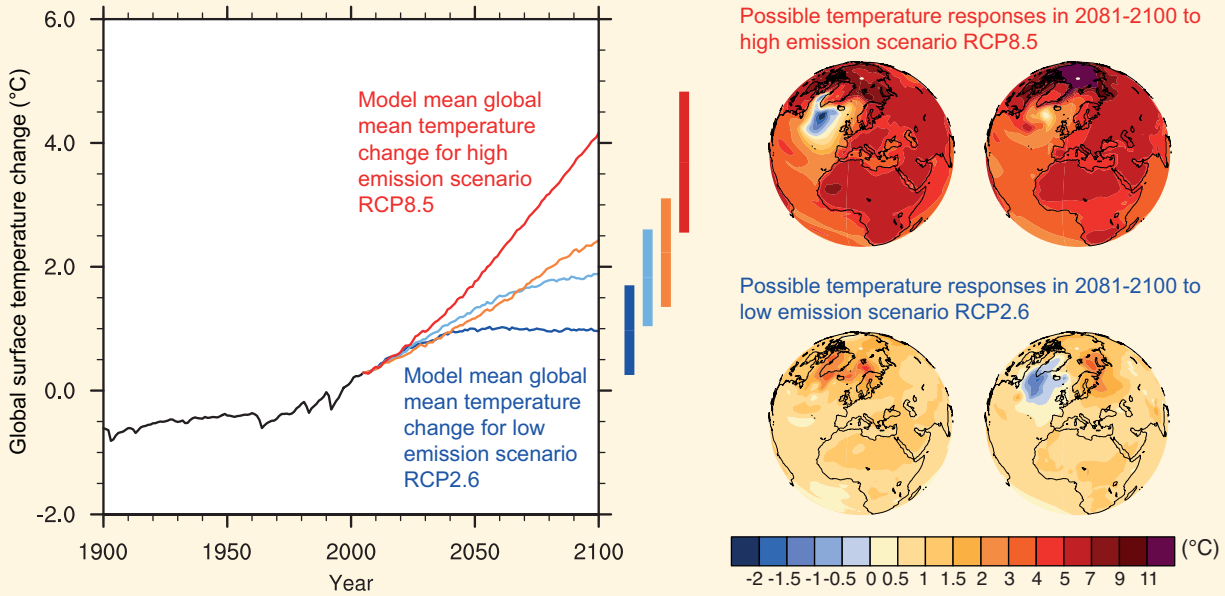

FAQ 12.1, Figure 1 | Global mean temperature change averaged across all Coupled Model Intercomparison Project Phase 5 (CMIP5) models (relative to 1986–2005) for the four Representative Concentration Pathway (RCP) scenarios: RCP2.6 (dark blue), RCP4.5 (light blue), RCP6.0 (orange) and RCP8.5 (red); 32, 42, 25 and 39 models were used respectively for these 4 scenarios. *Likely* ranges for global temperature change by the end of the 21st century are indicated by vertical bars. Note that these ranges apply to the difference between two 20-year means, 2081–2100 relative to 1986–2005, which accounts for the bars being centred at a smaller value than the end point of the annual trajectories. For the highest (RCP8.5) and lowest (RCP2.6) scenario, illustrative maps of surface temperature change at the end of the 21st century (2081–2100 relative to 1986–2005) are shown for two CMIP5 models. These models are chosen to show a rather broad range of response, but this particular set is not representative of any measure of model response uncertainty.

Frequently Asked Questions

FAQ 12.2 | How Will the Earth's Water Cycle Change?

The flow and storage of water in the Earth's climate system are highly variable, but changes beyond those due to natural variability are expected by the end of the current century. In a warmer world, there will be net increases in rainfall, surface evaporation and plant transpiration. However, there will be substantial differences in the changes between locations. Some places will experience more precipitation and an accumulation of water on land. In others, the amount of water will decrease, due to regional drying and loss of snow and ice cover.

The water cycle consists of water stored on the Earth in all its phases, along with the movement of water through the Earth's climate system. In the atmosphere, water occurs primarily as a gas—water vapour—but it also occurs as ice and liquid water in clouds. The ocean, of course, is primarily liquid water, but the ocean is also partly covered by ice in polar regions. Terrestrial water in liquid form appears as surface water—such as lakes and rivers—soil moisture and groundwater. Solid terrestrial water occurs in ice sheets, glaciers, snow and ice on the surface and in permafrost and seasonally frozen soil.

Statements about future climate sometimes say that the water cycle will accelerate, but this can be misleading, for strictly speaking, it implies that the cycling of water will occur more and more quickly with time and at all locations. Parts of the world will indeed experience intensification of the water cycle, with larger transports of water and more rapid movement of water into and out of storage reservoirs. However, other parts of the climate system will experience substantial depletion of water, and thus less movement of water. Some stores of water may even vanish.

As the Earth warms, some general features of change will occur simply in response to a warmer climate. Those changes are governed by the amount of energy that global warming adds to the climate system. Ice in all forms will melt more rapidly, and be less pervasive. For example, for some simulations assessed in this report, summer Arctic sea ice disappears before the middle of this century. The atmosphere will have more water vapour, and observations and model results indicate that it already does. By the end of the 21st century, the average amount of water vapour in the atmosphere could increase by 5 to 25%, depending on the amount of human emissions of greenhouse gases and radiatively active particles, such as smoke. Water will evaporate more quickly from the surface. Sea level will rise due to expansion of warming ocean waters and melting land ice flowing into the ocean (see FAQ 13.2).

These general changes are modified by the complexity of the climate system, so that they should not be expected to occur equally in all locations or at the same pace. For example, circulation of water in the atmosphere, on land and in the ocean can change as climate changes, concentrating water in some locations and depleting it in others. The changes also may vary throughout the year: some seasons tend to be wetter than others. Thus, model simulations assessed in this report show that winter precipitation in northern Asia may increase by more than 50%, whereas summer precipitation there is projected to hardly change. Humans also intervene directly in the water cycle, through water management and changes in land use. Changing population distributions and water practices would produce further changes in the water cycle.

Water cycle processes can occur over minutes, hours, days and longer, and over distances from metres to kilometres and greater. Variability on these scales is typically greater than for temperature, so climate changes in precipitation are harder to discern. Despite this complexity, projections of future climate show changes that are common across many models and climate forcing scenarios. Similar changes were reported in the AR4. These results collectively suggest well understood mechanisms of change, even if magnitudes vary with model and forcing. We focus here on changes over land, where changes in the water cycle have their largest impact on human and natural systems.

Projected climate changes from simulations assessed in this report (shown schematically in FAQ 12.2, Figure 1) generally show an increase in precipitation in parts of the deep tropics and polar latitudes that could exceed 50% by the end of the 21st century under the most extreme emissions scenario. In contrast, large areas of the subtropics could have decreases of 30% or more. In the tropics, these changes appear to be governed by increases in atmospheric water vapour and changes in atmospheric circulation that further concentrate water vapour in the tropics and thus promote more tropical rainfall. In the subtropics, these circulation changes simultaneously promote less rainfall despite warming in these regions. Because the subtropics are home to most of the world's deserts, these changes imply increasing aridity in already dry areas, and possible expansion of deserts. *(continued on next page)*

FAQ 12.2 (continued)

Increases at higher latitudes are governed by warmer temperatures, which allow more water in the atmosphere and thus, more water that can precipitate. The warmer climate also allows storm systems in the extratropics to transport more water vapour into the higher latitudes, without requiring substantial changes in typical wind strength. As indicated above, high latitude changes are more pronounced during the colder seasons.

Whether land becomes drier or wetter depends partly on precipitation changes, but also on changes in surface evaporation and transpiration from plants (together called evapotranspiration). Because a warmer atmosphere can have more water vapour, it can induce greater evapotranspiration, given sufficient terrestrial water. However, increased carbon dioxide in the atmosphere reduces a plant's tendency to transpire into the atmosphere, partly counteracting the effect of warming.

In the tropics, increased evapotranspiration tends to counteract the effects of increased precipitation on soil moisture, whereas in the subtropics, already low amounts of soil moisture allow for little change in evapotranspiration. At higher latitudes, the increased precipitation generally outweighs increased evapotranspiration in projected climates, yielding increased annual mean runoff, but mixed changes in soil moisture. As implied by circulation changes in FAQ 12.2, Figure 1, boundaries of high or low moisture regions may also shift.

A further complicating factor is the character of rainfall. Model projections show rainfall becoming more intense, in part because more moisture will be present in the atmosphere. Thus, for simulations assessed in this report, over much of the land, 1-day precipitation events that currently occur on average every 20 years could occur every 10 years or even more frequently by the end of the 21st century. At the same time, projections also show that precipitation events overall will tend to occur less frequently. These changes produce two seemingly contradictory effects: more intense downpours, leading to more floods, yet longer dry periods between rain events, leading to more drought.

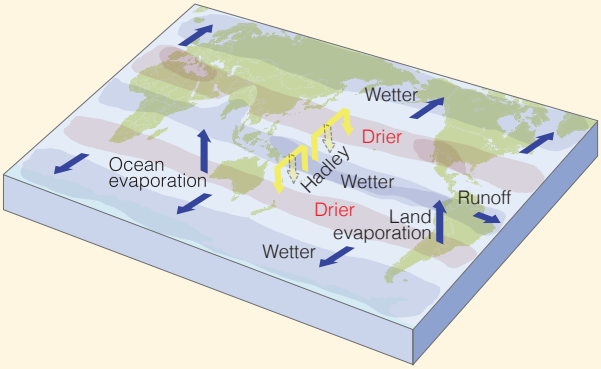

FAQ 12.2, Figure 1 | Schematic diagram of projected changes in major components of the water cycle. The blue arrows indicate major types of water movement changes through the Earth's climate system: poleward water transport by extratropical winds, evaporation from the surface and runoff from the land to the oceans. The shaded regions denote areas more likely to become drier or wetter. Yellow arrows indicate an important atmospheric circulation change by the Hadley Circulation, whose upward motion promotes tropical rainfall, while suppressing subtropical rainfall. Model projections indicate that the Hadley Circulation will shift its downward branch poleward in both the Northern and Southern Hemispheres, with associated drying. Wetter conditions are projected at high latitudes, because a warmer atmosphere will allow greater precipitation, with greater movement of water into these regions.

At high latitudes and at high elevation, further changes occur due to the loss of frozen water. Some of these are resolved by the present generation of global climate models (GCMs), and some changes can only be inferred because they involve features such as glaciers, which typically are not resolved or included in the models. The warmer climate means that snow tends to start accumulating later in the fall, and melt earlier in the spring. Simulations assessed in this report show March to April snow cover in the Northern Hemisphere is projected to decrease by approximately 10 to 30% on average by the end of this century, depending on the greenhouse gas scenario. The earlier spring melt alters the timing of peak springtime flow in rivers receiving snowmelt. As a result, later flow rates will decrease, potentially affecting water resource management. These features appear in GCM simulations.

Loss of permafrost will allow moisture to seep more deeply into the ground, but it will also allow the ground to warm, which could enhance evapotranspiration. However, most current GCMs do not include all the processes needed to simulate well permafrost changes. Studies analysing soils freezing or using GCM output to drive more detailed land models suggest substantial permafrost loss by the end of this century. In addition, even though current GCMs do not explicitly include glacier evolution, we can expect that glaciers will continue to recede, and the volume of water they provide to rivers in the summer may dwindle in some locations as they disappear. Loss of glaciers will also contribute to a reduction in springtime river flow. However, if annual mean precipitation increases—either as snow or rain—then these results do not necessarily mean that annual mean river flow will decrease.

Frequently Asked Questions

FAQ 12.3 | What Would Happen to Future Climate if We Stopped Emissions Today?

Stopping emissions today is a scenario that is not plausible, but it is one of several idealized cases that provide insight into the response of the climate system and carbon cycle. As a result of the multiple time scales in the climate system, the relation between change in emissions and climate response is quite complex, with some changes still occurring long after emissions ceased. Models and process understanding show that as a result of the large ocean inertia and the long lifetime of many greenhouse gases, primarily carbon dioxide, much of the warming would persist for centuries after greenhouse gas emissions have stopped.

When emitted in the atmosphere, greenhouse gases get removed through chemical reactions with other reactive components or, in the case of carbon dioxide (CO_2), get exchanged with the ocean and the land. These processes characterize the lifetime of the gas in the atmosphere, defined as the time it takes for a concentration pulse to decrease by a factor of e (2.71). How long greenhouse gases and aerosols persist in the atmosphere varies over a wide range, from days to thousands of years. For example, aerosols have a lifetime of weeks, methane (CH_4) of about 10 years, nitrous oxide (N_2O) of about 100 years and hexafluoroethane (C_2F_6) of about 10,000 years. CO_2 is more complicated as it is removed from the atmosphere through multiple physical and biogeochemical processes in the ocean and the land; all operating at different time scales. For an emission pulse of about 1000 PgC, about half is removed within a few decades, but the remaining fraction stays in the atmosphere for much longer. About 15 to 40% of the CO_2 pulse is still in the atmosphere after 1000 years.

As a result of the significant lifetimes of major anthropogenic greenhouse gases, the increased atmospheric concentration due to past emissions will persist long after emissions are ceased. Concentration of greenhouse gases would not return immediately to their pre-industrial levels if emissions were halted. Methane concentration would return to values close to pre-industrial level in about 50 years, N_2O concentrations would need several centuries, while CO_2 would essentially never come back to its pre-industrial level on time scales relevant for our society. Changes in emissions of short-lived species like aerosols on the other hand would result in nearly instantaneous changes in their concentrations.

The climate system response to the greenhouse gases and aerosols forcing is characterized by an inertia, driven mainly by the ocean. The ocean has a very large capacity of absorbing heat and a slow mixing between the surface and the deep ocean. This means that it will take several centuries for the whole ocean to warm up and to reach equilibrium with the altered radiative forcing. The surface ocean (and hence the continents) will continue to warm until it reaches a surface temperature in equilibrium with this new radiative forcing. The AR4 showed that if concentration of greenhouse gases were held constant at present day level, the Earth surface would still continue to warm by about 0.6°C over the 21st century relative to the year 2000. This is the climate commitment to current concentrations (or constant composition commitment), shown in grey in FAQ 12.3, Figure 1. Constant emissions at current levels would further increase the atmospheric concentration and result in much more warming than observed so far (FAQ 12.3, Figure 1, red lines).

Even if anthropogenic greenhouses gas emissions were halted now, the radiative forcing due to these long-lived greenhouse gases concentrations would only slowly decrease in the future, at a rate determined by the lifetime of the gas (see above). Moreover, the

(continued on next page)

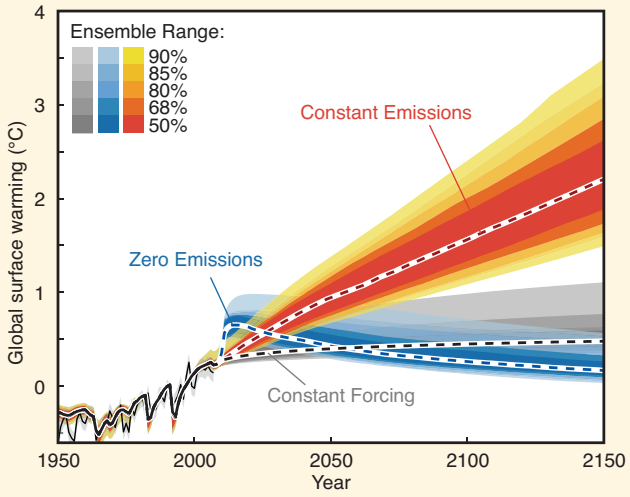

FAQ 12.3, Figure 1 | Projections based on the energy balance carbon cycle model Model for the Assessment of Greenhouse Gas-Induced Climate Change (MAGICC) for constant atmospheric composition (constant forcing, grey), constant emissions (red) and zero future emissions (blue) starting in 2010, with estimates of uncertainty. Figure adapted from Hare and Meinshausen (2006) based on the calibration of a simple carbon cycle climate model to all Coupled Model Intercomparison Project Phase 3 (CMIP3) and Coupled Climate Carbon Cycle Model Intercomparison Project (C4MIP) models (Meinshausen et al., 2011a; Meinshausen et al., 2011b). Results are based on a full transient simulation starting from pre-industrial and using all radiative forcing components. The thin black line and shading denote the observed warming and uncertainty.

FAQ 12.3 (continued)

climate response of the Earth System to that radiative forcing would be even slower. Global temperature would not respond quickly to the greenhouse gas concentration changes. Eliminating CO_2 emissions only would lead to near constant temperature for many centuries. Eliminating short-lived negative forcings from sulphate aerosols at the same time (e.g., by air pollution reduction measures) would cause a temporary warming of a few tenths of a degree, as shown in blue in FAQ 12.3, Figure 1. Setting all emissions to zero would therefore, after a short warming, lead to a near stabilization of the climate for multiple centuries. This is called the commitment from past emissions (or zero future emission commitment). The concentration of GHG would decrease and hence the radiative forcing as well, but the inertia of the climate system would delay the temperature response.

As a consequence of the large inertia in the climate and carbon cycle, the long-term global temperature is largely controlled by total CO_2 emissions that have accumulated over time, irrespective of the time when they were emitted. Limiting global warming below a given level (e.g., 2°C above pre-industrial) therefore implies a given budget of CO_2, that is, higher emissions earlier implies stronger reductions later. A higher climate target allows for a higher CO_2 concentration peak, and hence larger cumulative CO_2 emissions (e.g., permitting a delay in the necessary emission reduction).

Global temperature is a useful aggregate number to describe the magnitude of climate change, but not all changes will scale linearly global temperature. Changes in the water cycle for example also depend on the type of forcing (e.g., greenhouse gases, aerosols, land use change), slower components of the Earth system such as sea level rise and ice sheet would take much longer to respond, and there may be critical thresholds or abrupt or irreversible changes in the climate system.

Frequently Asked Questions

FAQ 13.1 | Why Does Local Sea Level Change Differ from the Global Average?

Shifting surface winds, the expansion of warming ocean water, and the addition of melting ice can alter ocean currents which, in turn, lead to changes in sea level that vary from place to place. Past and present variations in the distribution of land ice affect the shape and gravitational field of the Earth, which also cause regional fluctuations in sea level. Additional variations in sea level are caused by the influence of more localized processes such as sediment compaction and tectonics.

Along any coast, vertical motion of either the sea or land surface can cause changes in sea level relative to the land (known as relative sea level). For example, a local change can be caused by an increase in sea surface height, or by a decrease in land height. Over relatively short time spans (hours to years), the influence of tides, storms and climatic variability—such as El Niño—dominates sea level variations. Earthquakes and landslides can also have an effect by causing changes in land height and, sometimes, tsunamis. Over longer time spans (decades to centuries), the influence of climate change—with consequent changes in volume of ocean water and land ice—is the main contributor to sea level change in most regions. Over these longer time scales, various processes may also cause vertical motion of the land surface, which can also result in substantial changes in relative sea level.

Since the late 20th century, satellite measurements of the height of the ocean surface relative to the center of the Earth (known as geocentric sea level) show differing rates of geocentric sea level change around the world (see FAQ 13.1, Figure 1). For example, in the western Pacific Ocean, rates were about three times greater than the global mean value of about 3 mm per year from 1993 to 2012. In contrast, those in the eastern Pacific Ocean are lower than the global mean value, with much of the west coast of the Americas experiencing a fall in sea surface height over the same period. *(continued on next page)*

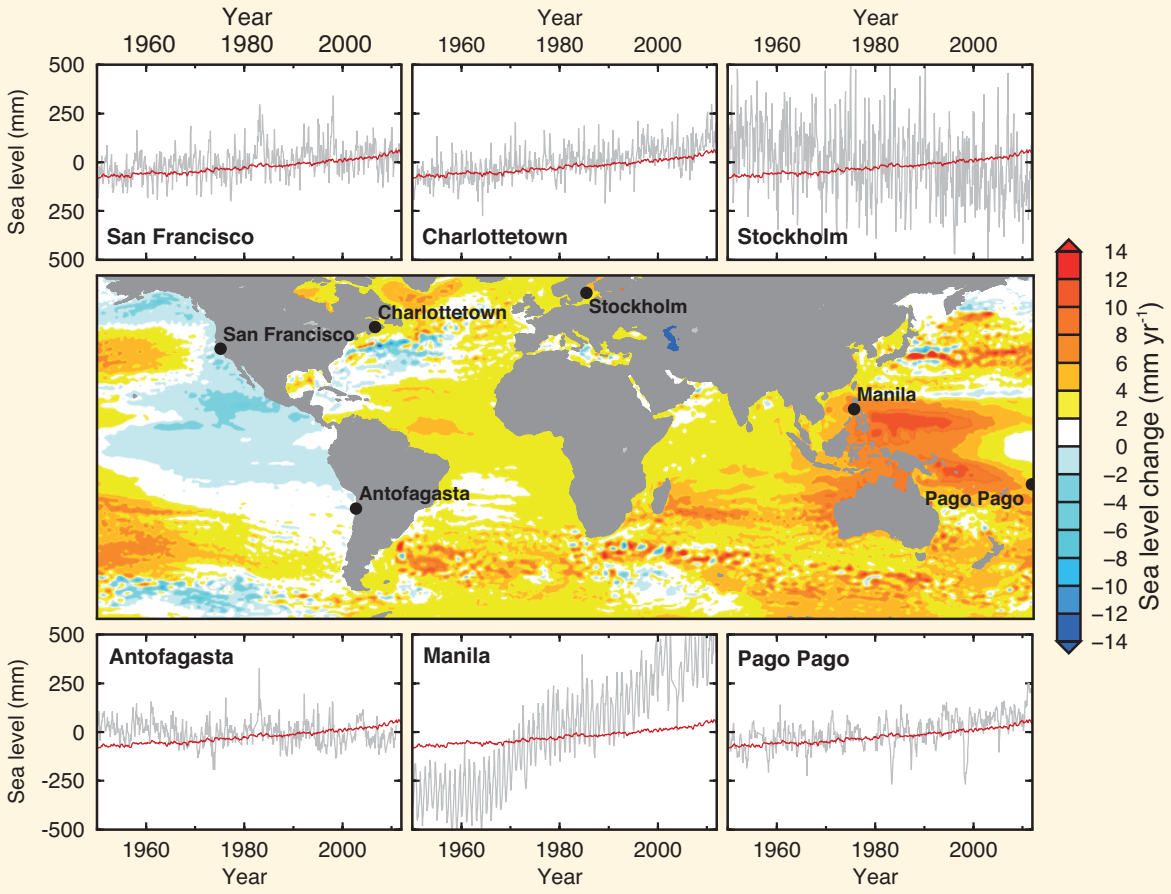

FAQ13.1, Figure 1 | Map of rates of change in sea surface height (geocentric sea level) for the period 1993–2012 from satellite altimetry. Also shown are relative sea level changes (grey lines) from selected tide gauge stations for the period 1950–2012. For comparison, an estimate of global mean sea level change is also shown (red lines) with each tide gauge time series. The relatively large, short-term oscillations in local sea level (grey lines) are due to the natural climate variability described in the main text. For example, the large, regular deviations at Pago Pago are associated with the El Niño-Southern Oscillation.

FAQ 13.1 (continued)

Much of the spatial variation shown in FAQ 13.1, Figure 1 is a result of natural climate variability—such as El Niño and the Pacific Decadal Oscillation—over time scales from about a year to several decades. These climate variations alter surface winds, ocean currents, temperature and salinity, and hence affect sea level. The influence of these processes will continue during the 21st century, and will be superimposed on the spatial pattern of sea level change associated with longer term climate change, which also arises through changes in surface winds, ocean currents, temperature and salinity, as well as ocean volume. However, in contrast to the natural variability, the longer term trends accumulate over time and so are expected to dominate over the 21st century. The resulting rates of geocentric sea level change over this longer period may therefore exhibit a very different pattern from that shown in FAQ 13.1, Figure 1.

Tide gauges measure relative sea level, and so they include changes resulting from vertical motion of both the land and the sea surface. Over many coastal regions, vertical land motion is small, and so the long-term rate of sea level change recorded by coastal and island tide gauges is similar to the global mean value (see records at San Francisco and Pago Pago in FAQ 13.1, Figure 1). In some regions, vertical land motion has had an important influence. For example, the steady fall in sea level recorded at Stockholm (FAQ 13.1, Figure 1) is caused by uplift of this region after the melting of a large (>1 km thick) continental ice sheet at the end of the last Ice Age, between ~20,000 and ~9000 years ago. Such ongoing land deformation as a response to the melting of ancient ice sheets is a significant contributor to regional sea level changes in North America and northwest Eurasia, which were covered by large continental ice sheets during the peak of the last Ice Age.

In other regions, this process can also lead to land subsidence, which elevates relative sea levels, as it has at Charlottetown, where a relatively large increase has been observed, compared to the global mean rate (FAQ 13.1, Figure 1). Vertical land motion due to movement of the Earth's tectonic plates can also cause departures from the global mean sea level trend in some areas—most significantly, those located near active subduction zones, where one tectonic plate slips beneath another. For the case of Antofagasta (FAQ 13.1, Figure 1) this appears to result in steady land uplift and therefore relative sea level fall.

In addition to regional influences of vertical land motion on relative sea level change, some processes lead to land motion that is rapid but highly localized. For example, the greater rate of rise relative to the global mean at Manila (FAQ 13.1, Figure 1) is dominated by land subsidence caused by intensive groundwater pumping. Land subsidence due to natural and anthropogenic processes, such as the extraction of groundwater or hydrocarbons, is common in many coastal regions, particularly in large river deltas.

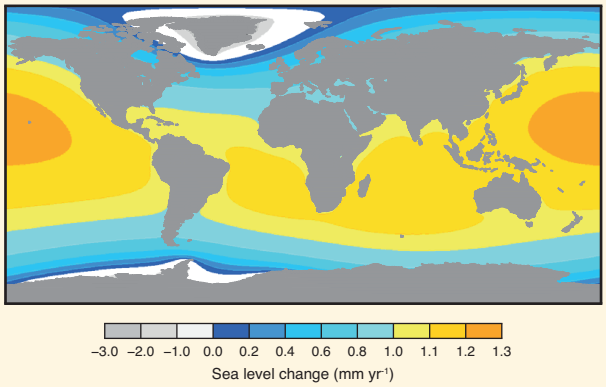

FAQ13.1, Figure 2 | Model output showing relative sea level change due to melting of the Greenland ice sheet and the West Antarctic ice sheet at rates of 0.5 mm yr^{-1} each (giving a global mean value for sea level rise of 1 mm yr^{-1}). The modelled sea level changes are less than the global mean value in areas near the melting ice but enhanced further afield. (Adapted from Milne et al., 2009)

It is commonly assumed that melting ice from glaciers or the Greenland and Antarctic ice sheets would cause globally uniform sea level rise, much like filling a bath tub with water. In fact, such melting results in regional variations in sea level due to a variety of processes, including changes in ocean currents, winds, the Earth's gravity field and land height. For example, computer models that simulate these latter two processes predict a regional fall in relative sea level around the melting ice sheets, because the gravitational attraction between ice and ocean water is reduced, and the land tends to rise as the ice melts (FAQ 13.1, Figure 2). However, further away from the ice sheet melting, sea level rise is enhanced, compared to the global average value.

In summary, a variety of processes drive height changes of the ocean surface and ocean floor, resulting in distinct spatial patterns of sea level change at local to regional scales. The combination of these processes produces a complex pattern of total sea level change, which varies through time as the relative contribution of each process changes. The global average change is a useful single value that reflects the contribution of climatic processes (e.g., land-ice melting and ocean warming), and represents a good estimate of sea level change at many coastal locations. At the same time, however, where the various regional processes result in a strong signal, there can be large departures from the global average value.

Frequently Asked Questions

FAQ 13.2 | Will the Greenland and Antarctic Ice Sheets Contribute to Sea Level Change over the Rest of the Century?

The Greenland, West and East Antarctic ice sheets are the largest reservoirs of freshwater on the planet. As such, they have contributed to sea level change over geological and recent times. They gain mass through accumulation (snowfall) and lose it by surface ablation (mostly ice melt) and outflow at their marine boundaries, either to a floating ice shelf, or directly to the ocean through iceberg calving. Increases in accumulation cause global mean sea level to fall, while increases in surface ablation and outflow cause it to rise. Fluctuations in these mass fluxes depend on a range of processes, both within the ice sheet and without, in the atmosphere and oceans. Over the course of this century, however, sources of mass loss appear set to exceed sources of mass gain, so that a continuing positive contribution to global sea level can be expected. This FAQ summarizes current research on the topic and provides indicative magnitudes for the various end-of-century (2081-2100 with respect to 1986-2005) sea level contributions from the full assessment, which are reported as the two-in-three probability level across all emission scenarios.

Over millennia, the slow horizontal flow of an ice sheet carries mass from areas of net accumulation (generally, in the high-elevation interior) to areas of net loss (generally, the low-elevation periphery and the coastal perimeter). At present, Greenland loses roughly half of its accumulated ice by surface ablation, and half by calving. Antarctica, on the other hand, loses virtually all its accumulation by calving and submarine melt from its fringing ice shelves. Ice shelves are floating, so their loss has only a negligible direct effect on sea level, although they can affect sea level indirectly by altering the mass budget of their parent ice sheet (see below).

In East Antarctica, some studies using satellite radar altimetry suggest that snowfall has increased, but recent atmospheric modelling and satellite measurements of changes in gravity find no significant increase. This apparent disagreement may be because relatively small long-term trends are masked by the strong interannual variability of snowfall. Projections suggest a substantial increase in 21st century Antarctic snowfall, mainly because a warmer atmosphere would be able to carry more moisture into polar regions. Regional changes in atmospheric circulation probably play a secondary role. For the whole of the Antarctic ice sheet, this process is projected to contribute between 0 and 70 mm to sea level fall.

Currently, air temperatures around Antarctica are too cold for substantial surface ablation. Field and satellite-based observations, however, indicate enhanced outflow—manifested as ice-surface lowering—in a few localized coastal regions. These areas (Pine Island and Thwaites Glaciers in West Antarctica, and Totten and Cook Glaciers in East Antarctica) all lie within kilometre-deep bedrock troughs towards the edge of Antarctica's continental shelf. The increase in outflow is thought to have been triggered by regional changes in ocean circulation, bringing warmer water in contact with floating ice shelves.

On the more northerly Antarctic Peninsula, there is a well-documented record of ice-shelf collapse, which appears to be related to the increased surface melting caused by atmospheric warming over recent decades. The subsequent thinning of glaciers draining into these ice shelves has had a positive—but minor—effect on sea level, as will any further such events on the Peninsula. Regional projections of 21st century atmospheric temperature change suggest that this process will probably not affect the stability of the large ice shelves of both the West and East Antarctica, although these ice shelves may be threatened by future oceanic change (see below).

Estimates of the contribution of the Antarctic ice sheets to sea level over the last few decades vary widely, but great strides have recently been made in reconciling the observations. There are strong indications that enhanced outflow (primarily in West Antarctica) currently outweighs any increase in snow accumulation (mainly in East Antarctica), implying a tendency towards sea level rise. Before reliable projections of outflow over the 21st century can be made with greater confidence, models that simulate ice flow need to be improved, especially of any changes in the grounding line that separates floating ice from that resting on bedrock and of interactions between ice shelves and the ocean. The concept of 'marine ice-sheet instability' is based on the idea that the outflow from an ice sheet resting on bedrock below sea level increases if ice at the grounding line is thicker and, therefore, faster flowing. On bedrock that slopes downward towards the ice-sheet interior, this creates a vicious cycle of increased outflow, causing ice at the grounding line to thin and go afloat. The grounding line then retreats down slope into thicker ice that, in turn, drives further increases in outflow. This feedback could potentially result in the rapid loss of parts of the ice sheet, as grounding lines retreat along troughs and basins that deepen towards the ice sheet's interior.

(continued on next page)

FAQ 13.2 (continued)

Future climate forcing could trigger such an unstable collapse, which may then continue independently of climate. This potential collapse might unfold over centuries for individual bedrock troughs in West Antarctica and sectors of East Antarctica. Much research is focussed on understanding how important this theoretical concept is for those ice sheets. Sea level could rise if the effects of marine instability become important, but there is not enough evidence at present to unambiguously identify the precursor of such an unstable retreat. Change in outflow is projected to contribute between –20 (i.e., fall) and 185 mm to sea level rise by year 2100, although the uncertain impact of marine ice-sheet instability could increase this figure by several tenths of a metre. Overall, increased snowfall seems set to only partially offset sea level rise caused by increased outflow.

In Greenland, mass loss through more surface ablation and outflow dominates a possible recent trend towards increased accumulation in the interior. Estimated mass loss due to surface ablation has doubled since the early 1990s. This trend is expected to continue over the next century as more of the ice sheet experiences surface ablation for longer periods. Indeed, projections for the 21st century suggest that increasing mass loss will dominate over weakly increasing accumulation. The refreezing of melt water within the snow pack high up on the ice sheet offers an important (though perhaps temporary) dampening effect on the relation between atmospheric warming and mass loss.

Although the observed response of outlet glaciers is both complex and highly variable, iceberg calving from many of Greenland's major outlet glaciers has increased substantially over the last decade, and constitutes an appreciable additional mass loss. This seems to be related to the intrusion of warm water into the coastal seas around Greenland, but it is not clear whether this phenomenon is related to inter-decadal variability, such as the North Atlantic

(continued on next page)

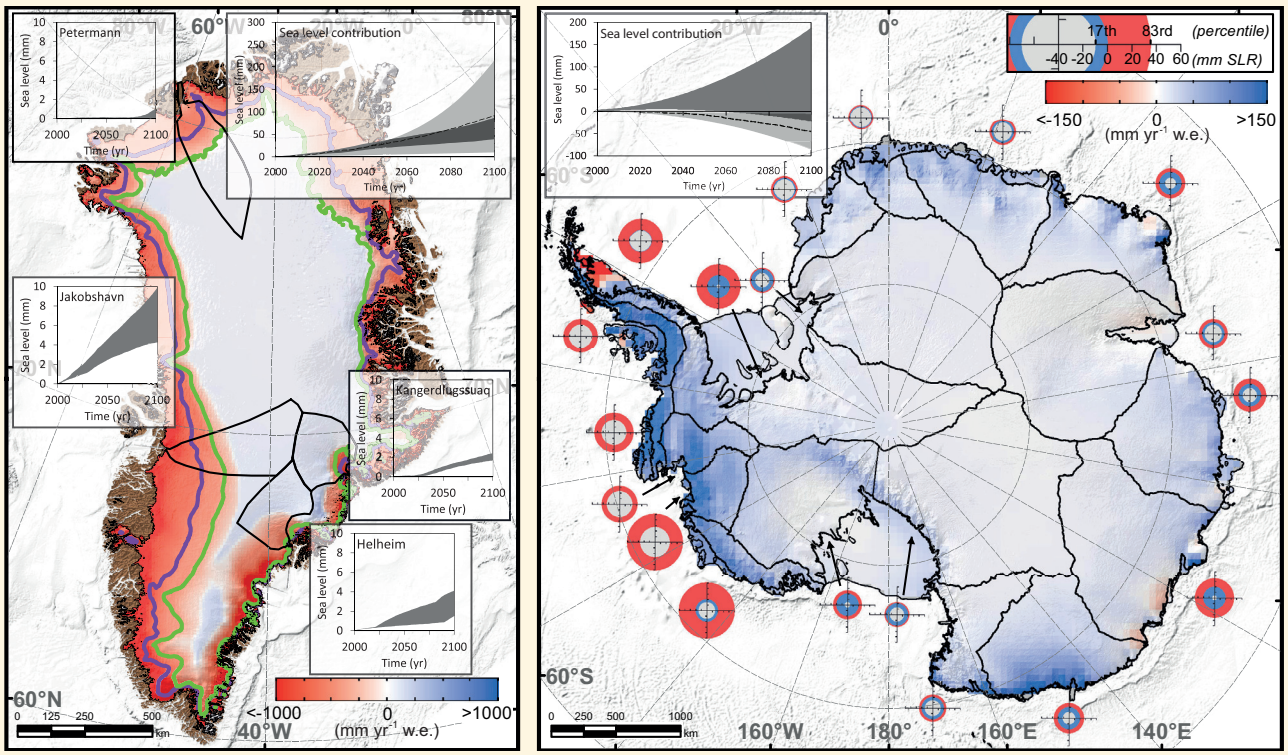

FAQ 13.2, Figure 1 | Illustrative synthesis of projected changes in SMB and outflow by 2100 for (a) Greenland and (b) Antarctic ice sheets. Colours shown on the maps refer to projected SMB change between the start and end of the 21st century using the RACMO2 regional atmospheric climate model under future warming scenarios A1B (Antarctic) and RCP4.5 (Greenland). For Greenland, average equilibrium line locations during both these time periods are shown in purple and green, respectively. Ice-sheet margins and grounding lines are shown as black lines, as are ice-sheet sectors. For Greenland, results of flowline modelling for four major outlet glaciers are shown as inserts, while for Antarctica the coloured rings reflect projected change in outflow based on a probabilistic extrapolation of observed trends. The outer and inner radius of each ring indicate the upper and lower bounds of the two-thirds probability range of the contribution, respectively (scale in upper right); red refers to mass loss (sea level rise) while blue refers to mass gain (sea level fall). Finally, the sea level contribution is shown for each ice sheet (insert located above maps) with light grey referring to SMB (model experiment used to generate the SMB map is shown as a dashed line) and dark grey to outflow. All projections refer to the two-in-three probability range across all scenarios.

FAQ 13.2 (continued)

Oscillation, or a longer term trend associated with greenhouse gas–induced warming. Projecting its effect on 21st century outflow is therefore difficult, but it does highlight the apparent sensitivity of outflow to ocean warming. The effects of more surface melt water on the lubrication of the ice sheet's bed, and the ability of warmer ice to deform more easily, may lead to greater rates of flow, but the link to recent increases in outflow is unclear. Change in the net difference between surface ablation and accumulation is projected to contribute between 10 and 160 mm to sea level rise in 2081-2100 (relative to 1986-2005), while increased outflow is projected to contribute a further 10 to 70 mm (Table 13.5).

The Greenland ice sheet has contributed to a rise in global mean sea level over the last few decades, and this trend is expected to increase during this century. Unlike Antarctica, Greenland has no known large-scale instabilities that might generate an abrupt increase in sea level rise over the 21st century. A threshold may exist, however, so that continued shrinkage might become irreversible over multi-centennial time scales, even if the climate were to return to a pre-industrial state over centennial time scales. Although mass loss through the calving of icebergs may increase in future decades, this process will eventually end when the ice margin retreats onto bedrock above sea level where the bulk of the ice sheet resides.

Frequently Asked Questions

FAQ 14.1 | How is Climate Change Affecting Monsoons?

Monsoons are the most important mode of seasonal climate variation in the tropics, and are responsible for a large fraction of the annual rainfall in many regions. Their strength and timing is related to atmospheric moisture content, land–sea temperature contrast, land cover and use, atmospheric aerosol loadings and other factors. Overall, monsoonal rainfall is projected to become more intense in future, and to affect larger areas, because atmospheric moisture content increases with temperature. However, the localized effects of climate change on regional *monsoon strength and variability are complex and more uncertain.*

Monsoon rains fall over all tropical continents: Asia, Australia, the Americas and Africa. The monsoon circulation is driven by the difference in temperature between land and sea, which varies seasonally with the distribution of solar heating. The duration and amount of rainfall depends on the moisture content of the air, and on the configuration and strength of the atmospheric circulation. The regional distribution of land and ocean also plays a role, as does topography. For example, the Tibetan Plateau—through variations in its snow cover and surface heating—modulates the strength of the complex Asian monsoon systems. Where moist on-shore winds rise over mountains, as they do in southwest India, monsoon rainfall is intensified. On the lee side of such mountains, it lessens.

Since the late 1970s, the East Asian summer monsoon has been weakening and not extending as far north as it used to in earlier times , as a result of changes in the atmospheric circulation. That in turn has led to increasing drought in northern China, but floods in the Yangtze River Valley farther south. In contrast, the Indo-Australian and Western Pacific monsoon systems show no coherent trends since the mid-20th century, but are strongly modulated by the El Niño-Southern Oscillation (ENSO). Similarly, changes observed in the South American monsoon system over the last few decades are strongly related to ENSO variability. Evidence of trends in the North American monsoon system is limited, but a tendency towards heavier rainfalls on the northern side of the main monsoon region has been observed. No systematic long-term trends have been observed in the behaviour of the Indian or the African monsoons.

The land surface warms more rapidly than the ocean surface, so that surface temperature contrast is increasing in most regions. The tropical atmospheric overturning circulation, however, slows down on average as the climate warms due to energy balance constraints in the tropical atmosphere. These changes in the atmospheric circulation lead to regional changes in monsoon intensity, area and timing. There are a number of other effects as to how

(continued on next page)

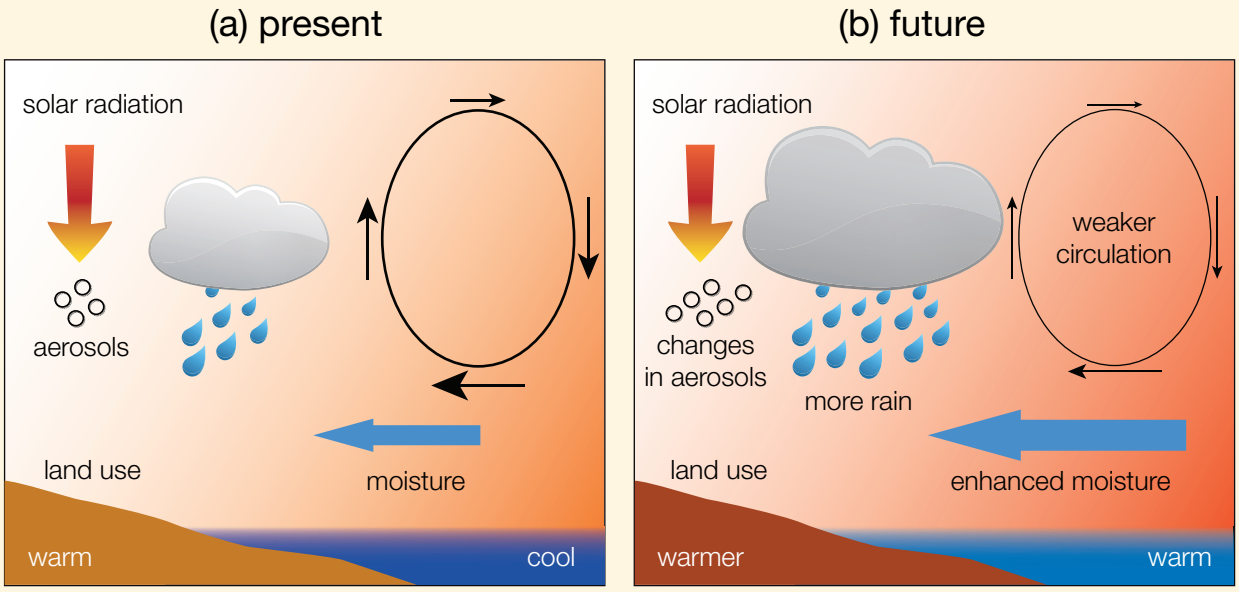

FAQ 14.1, Figure 1 | Schematic diagram illustrating the main ways that human activity influences monsoon rainfall. As the climate warms, increasing water vapour transport from the ocean into land increases because warmer air contains more water vapour. This also increases the potential for heavy rainfalls. Warming-related changes in large-scale circulation influence the strength and extent of the overall monsoon circulation. Land use change and atmospheric aerosol loading can also affect the amount of solar radiation that is absorbed in the atmosphere and land, potentially moderating the land–sea temperature difference.

FAQ 14.1 (continued)

climate change can influence monsoons. Surface heating varies with the intensity of solar radiation absorption, which is itself affected by any land use changes that alter the reflectivity (albedo) of the land surface. Also, changing atmospheric aerosol loadings, such as air pollution, affect how much solar radiation reaches the ground, which can change the monsoon circulation by altering summer solar heating of the land surface. Absorption of solar radiation by aerosols, on the other hand, warms the atmosphere, changing the atmospheric heating distribution.

The strongest effect of climate change on the monsoons is the increase in atmospheric moisture associated with warming of the atmosphere, resulting in an increase in total monsoon rainfall even if the strength of the monsoon circulation weakens or does not change.

Climate model projections through the 21st century show an increase in total monsoon rainfall, largely due to increasing atmospheric moisture content. The total surface area affected by the monsoons is projected to increase, along with the general poleward expansion of the tropical regions. Climate models project from 5% to an approximately 15% increase of global monsoon rainfall depending on scenarios. Though total tropical monsoon rainfall increases, some areas will receive less monsoon rainfall, due to weakening tropical wind circulations. Monsoon onset dates are *likely* to be early or not to change much and the monsoon retreat dates are *likely* to delay, resulting in lengthening of the monsoon season.

Future regional trends in monsoon intensity and timing remain uncertain in many parts of the world. Year-to-year variations in the monsoons in many tropical regions are affected by ENSO. How ENSO will change in future—and how its effects on monsoon will change—also remain uncertain. However, the projected overall increase in monsoon rainfall indicates a corresponding increase in the risk of extreme rain events in most regions.

Frequently Asked Questions

FAQ 14.2 | How Are Future Projections in Regional Climate Related to Projections of Global Means?

The relationship between regional climate change and global mean change is complex. Regional climates vary strongly with location and so respond differently to changes in global-scale influences. The global mean change is, in effect, a convenient summary of many diverse regional climate responses.

Heat and moisture, and changes in them, are not evenly distributed across the globe for several reasons:

- External forcings vary spatially (e.g., solar radiation depends on latitude, aerosol emissions have local sources, land use changes regionally, etc.).
- Surface conditions vary spatially, for example, land/sea contrast, topography, sea surface temperatures, soil moisture content.
- Weather systems and ocean currents redistribute heat and moisture from one region to another.

Weather systems are associated with regionally important climate phenomena such as monsoons, tropical convergence zones, storm tracks and important modes of climate variability (e.g., El Niño-Southern Oscillation (ENSO), North Atlantic Oscillation (NAO), Southern Annular Mode (SAM), etc.). In addition to modulating regional warming, some climate phenomena are also projected to change in the future, which can lead to further impacts on regional climates (see Table 14.3).

Projections of change in surface temperature and precipitation show large regional variations (FAQ 14.2, Figure 1). Enhanced surface warming is projected to occur over the high-latitude continental regions and the Arctic ocean,

(continued on next page)

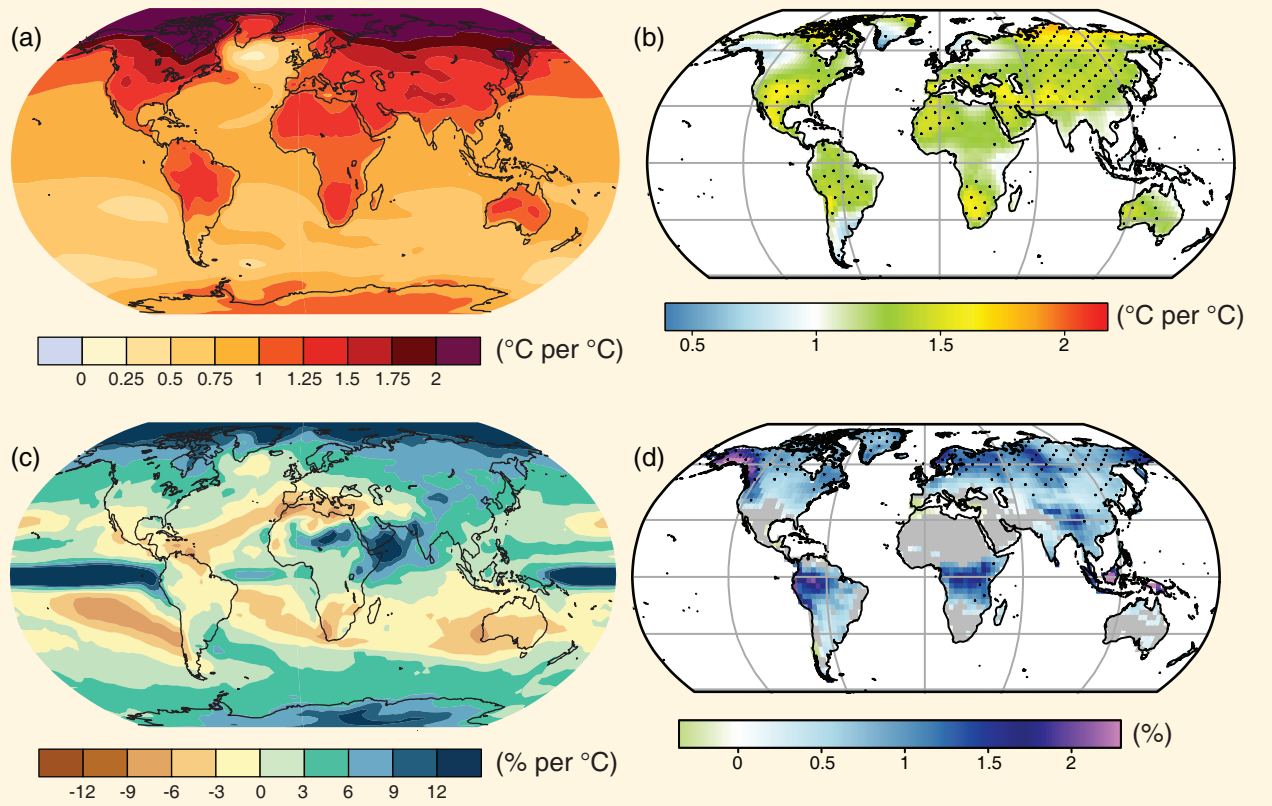

FAQ 14.2, Figure 1 | Projected 21st century changes in annual mean and annual extremes (over land) of surface air temperature and precipitation: (a) mean surface temperature per °C of global mean change, (b) 90th percentile of daily maximum temperature per °C of global average maximum temperature, (c) mean precipitation (in % per °C of global mean temperature change), and (d) fraction of days with precipitation exceeding the 95th percentile. Sources: Panels (a) and (c) projected changes in means between 1986–2005 and 2081–2100 from CMIP5 simulations under RCP4.5 scenario (see Chapter 12, Figure 12.41); Panels (b) and (d) projected changes in extremes over land between 1980–1999 and 2081–2100 (adapted from Figures 7 and 12 of Orlowsky and Seneviratne, 2012).

FAQ 14.2 (continued)

while over other oceans and lower latitudes changes are closer to the global mean (FAQ 14.2, Figure 1a). For example, warming near the Great Lakes area of North America is projected to be about 50% greater than that of the global mean warming. Similar large regional variations are also seen in the projected changes of more extreme temperatures (FAQ 14.2, Figure 1b). Projected changes in precipitation are even more regionally variable than changes in temperature (FAQ 14.2, Figure 1c, d), caused by modulation from climate phenomena such as the monsoons and tropical convergence zones. Near-equatorial latitudes are projected to have increased mean precipitation, while regions on the poleward edges of the subtropics are projected to have reduced mean precipitation. Higher latitude regions are projected to have increased mean precipitation and in particular more extreme precipitation from extratropical cyclones.

Polar regions illustrate the complexity of processes involved in regional climate change. Arctic warming is projected to increase more than the global mean, mostly because the melting of ice and snow produces a regional feedback by allowing more heat from the Sun to be absorbed. This gives rise to further warming, which encourages more melting of ice and snow. However, the projected warming over the Antarctic continent and surrounding oceans is less marked in part due to a stronger positive trend in the Southern Annular Mode. Westerly winds over the mid-latitude southern oceans have increased over recent decades, driven by the combined effect of loss of stratospheric ozone over Antarctica, and changes in the atmosphere's temperature structure related to increased greenhouse gas concentrations. This change in the Southern Annular Mode is well captured by climate models and has the effect of reducing atmospheric heat transport to the Antarctic continent. Nevertheless, the Antarctic Peninsula is still warming rapidly, because it extends far enough northwards to be influenced by the warm air masses of the westerly wind belt.

Glossary

Glossary

Editor:
Serge Planton (France)

This Glossary should be cited as:
IPCC, 2013: Annex III: Glossary [Planton, S. (ed.)]. In: *Climate Change 2013: The Physical Science Basis. Contribution of Working Group I to the Fifth Assessment Report of the Intergovernmental Panel on Climate Change* [Stocker, T.F., D. Qin, G.-K. Plattner, M. Tignor, S.K. Allen, J. Boschung, A. Nauels, Y. Xia, V. Bex and P.M. Midgley (eds.)]. Cambridge University Press, Cambridge, United Kingdom and New York, NY, USA.

This glossary defines some specific terms as the Lead Authors intend them to be interpreted in the context of this report. Red, italicized words indicate that the term is defined in the Glossary.

Abrupt climate change A large-scale change in the *climate system* that takes place over a few decades or less, persists (or is anticipated to persist) for at least a few decades and causes substantial disruptions in human and natural systems.

Active layer The layer of ground that is subject to annual thawing and freezing in areas underlain by *permafrost*.

Adjustment time See *Lifetime*. See also *Response time*.

Advection Transport of water or air along with its properties (e.g., temperature, chemical tracers) by winds or currents. Regarding the general distinction between advection and *convection*, the former describes transport by large-scale motions of the *atmosphere* or ocean, while convection describes the predominantly vertical, locally induced motions.

Aerosol A suspension of airborne solid or liquid particles, with a typical size between a few nanometres and 10 µm that reside in the *atmosphere* for at least several hours. For convenience the term *aerosol*, which includes both the particles and the suspending gas, is often used in this report in its plural form to mean *aerosol particles*. Aerosols may be of either natural or *anthropogenic* origin. Aerosols may influence *climate* in several ways: directly through scattering and absorbing radiation (see *Aerosol–radiation interaction*) and indirectly by acting as *cloud condensation nuclei* or *ice nuclei*, modifying the optical properties and *lifetime* of clouds (see *Aerosol–cloud interaction*).

Aerosol–cloud interaction A process by which a perturbation to *aerosol* affects the microphysical properties and evolution of clouds through the aerosol role as *cloud condensation nuclei* or ice nuclei, particularly in ways that affect radiation or precipitation; such processes can also include the effect of clouds and precipitation on aerosol. The aerosol perturbation can be *anthropogenic* or come from some natural *source*. The *radiative forcing* from such interactions has traditionally been attributed to numerous *indirect aerosol effects*, but in this report, only two levels of radiative forcing (or effect) are distinguished:

Radiative forcing (or effect) due to aerosol–cloud interactions (RFaci) The radiative forcing (or *radiative effect*, if the perturbation is internally generated) due to the change in number or size distribution of cloud droplets or ice crystals that is the proximate result of an aerosol perturbation, with other variables (in particular total cloud water content) remaining equal. In liquid clouds, an increase in cloud droplet concentration and surface area would increase the cloud *albedo*. This effect is also known as the *cloud albedo effect*, *first indirect effect,* or *Twomey effect*. It is a largely theoretical concept that cannot readily be isolated in observations or comprehensive process models due to the rapidity and ubiquity of *rapid adjustments*.

Effective radiative forcing (or effect) due to aerosol–cloud interactions (ERFaci) The final radiative forcing (or effect) from the aerosol perturbation including the rapid adjustments to the initial change in droplet or crystal formation rate. These adjustments include changes in the strength of *convection*, precipitation efficiency, cloud fraction, *lifetime* or water content of clouds, and the formation or suppression of clouds in remote areas due to altered circulations.

The total effective radiative forcing due to both aerosol–cloud and aerosol–radiation interactions is denoted *aerosol effective radiative forcing (ERFari+aci).* See also *Aerosol–radiation interaction*.

Aerosol–radiation interaction An interaction of *aerosol* directly with radiation produce *radiative effects*. In this report two levels of radiative forcing (or effect) are distinguished:

Radiative forcing (or effect) due to aerosol–radiation interactions (RFari) The *radiative forcing* (or radiative effect, if the perturbation is internally generated) of an aerosol perturbation due directly to aerosol–radiation interactions, with all environmental variables remaining unaffected. Traditionally known in the literature as the *direct aerosol forcing (or effect)*.

Effective radiative forcing (or effect) due to aerosol-radiation interactions (ERFari) The final radiative forcing (or effect) from the aerosol perturbation including the *rapid adjustments* to the initial change in radiation. These adjustments include changes in cloud caused by the impact of the radiative heating on convective or larger-scale atmospheric circulations, traditionally known as *semi-direct aerosol forcing (or effect)*.

The total effective radiative forcing due to both aerosol–cloud and aerosol–radiation interactions is denoted *aerosol effective radiative forcing (ERFari+aci).* See also *Aerosol–cloud interaction*.

Afforestation Planting of new *forests* on lands that historically have not contained forests. For a discussion of the term *forest* and related terms such as *afforestation*, *reforestation* and *deforestation*, see the IPCC Special Report on Land Use, Land-Use Change and Forestry (IPCC, 2000). See also the report on Definitions and Methodological Options to Inventory Emissions from Direct Human-induced Degradation of Forests and Devegetation of Other Vegetation Types (IPCC, 2003).

Airborne fraction The fraction of total CO_2 emissions (from fossil fuel and land use change) remaining in the *atmosphere*.

Air mass A widespread body of air, the approximately homogeneous properties of which (1) have been established while that air was situated over a particular *region* of the Earth's surface, and (2) undergo specific modifications while in transit away from the source region (AMS, 2000).

Albedo The fraction of *solar radiation* reflected by a surface or object, often expressed as a percentage. Snow-covered surfaces have a high albedo, the albedo of soils ranges from high to low, and vegetation-covered surfaces and oceans have a low albedo. The Earth's planetary albedo varies mainly through varying cloudiness, snow, ice, leaf area and and cover changes.

Alkalinity A measure of the capacity of an aqueous solution to neutralize acids.

Altimetry A technique for measuring the height of the Earth's surface with respect to the geocentre of the Earth within a defined terrestrial reference frame (geocentric sea level).

Annular modes See *Northern Annular Mode (NAM)* and *Southern Annular Mode (SAM)*.

Anthropogenic Resulting from or produced by human activities.

Atlantic Multi-decadal Oscillation/Variability (AMO/AMV) A multi-decadal (65- to 75-year) fluctuation in the North Atlantic, in which *sea surface temperatures* showed warm phases during roughly 1860 to 1880 and 1930 to 1960 and cool phases during 1905 to 1925 and 1970 to 1990 with a range of approximately 0.4°C. See AMO Index, Box 2.5.

Atmosphere The gaseous envelope surrounding the Earth. The dry atmosphere consists almost entirely of nitrogen (78.1% *volume mixing ratio*) and oxygen (20.9% volume mixing ratio), together with a number of trace gases, such as argon (0.93% volume mixing ratio), helium and radiatively active *greenhouse gases* such as *carbon dioxide* (0.035%

volume mixing ratio) and *ozone*. In addition, the atmosphere contains the greenhouse gas water vapour, whose amounts are highly variable but typically around 1% volume mixing ratio. The atmosphere also contains clouds and *aerosols*.

Atmosphere–Ocean General Circulation Model (AOGCM) See *Climate model*.

Atmospheric boundary layer The atmospheric layer adjacent to the Earth's surface that is affected by friction against that boundary surface, and possibly by transport of heat and other variables across that surface (AMS, 2000). The lowest 100 m of the boundary layer (about 10% of the boundary layer thickness), where mechanical generation of turbulence is dominant, is called the *surface boundary layer* or *surface layer*.

Atmospheric lifetime See *Lifetime*.

Attribution See *Detection and attribution*.

Autotrophic respiration *Respiration* by *photosynthetic* (see *photosynthesis*) organisms (e.g., plants and algaes).

Basal lubrication Reduction of friction at the base of an *ice sheet* or *glacier* due to lubrication by meltwater. This can allow the glacier or ice sheet to slide over its base. Meltwater may be produced by pressure-induced melting, friction or geothermal heat, or surface melt may drain to the base through holes in the ice.

Baseline/reference The baseline (or reference) is the state against which change is measured. A *baseline period* is the period relative to which anomalies are computed. The baseline concentration of a trace gas is that measured at a location not influenced by local *anthropogenic* emissions.

Bayesian method/approach A Bayesian method is a method by which a statistical analysis of an unknown or uncertain quantity(ies) is carried out in two steps. First, a prior probability distribution for the uncertain quantity(ies) is formulated on the basis of existing knowledge (either by eliciting expert opinion or by using existing data and studies). At this first stage, an element of subjectivity may influence the choice, but in many cases, the prior probability distribution can be chosen as neutrally as possible, in order not to influence the final outcome of the analysis. In the second step, newly acquired data are used to update the prior distribution into a posterior distribution. The update is carried out either through an analytic computation or though numeric approximation, using a theorem formulated by and named after the British mathematician Thomas Bayes (1702–1761).

Biological pump The process of transporting carbon from the ocean's surface layers to the deep ocean by the primary production of marine phytoplankton, which converts dissolved inorganic carbon (DIC) and nutrients into organic matter through *photosynthesis*. This natural cycle is limited primarily by the availability of light and nutrients such as phosphate, nitrate and silicic acid, and micronutrients, such as iron. See also *Solubility pump*.

Biomass The total mass of living organisms in a given area or volume; dead plant material can be included as dead biomass. *Biomass burning* is the burning of living and dead vegetation.

Biome A biome is a major and distinct regional element of the *biosphere*, typically consisting of several *ecosystems* (e.g., *forests*, rivers, ponds, swamps within a *region*). Biomes are characterized by typical communities of plants and animals.

Biosphere (terrestrial and marine) The part of the Earth system comprising all *ecosystems* and living organisms, in the *atmosphere*, on land (*terrestrial biosphere*) or in the oceans (*marine biosphere*), including derived dead organic matter, such as litter, soil organic matter and oceanic detritus.

Black carbon (BC) Operationally defined *aerosol* species based on measurement of light absorption and chemical reactivity and/or thermal stability. It is sometimes referred to as *soot*.

Blocking Associated with persistent, slow-moving high-pressure systems that obstruct the prevailing westerly winds in the middle and high latitudes and the normal eastward progress of extratropical transient storm systems. It is an important component of the intraseasonal *climate variability* in the extratropics and can cause long-lived weather conditions such as cold spells in winter and summer *heat waves*.

Brewer–Dobson circulation The meridional overturning circulation of the *stratosphere* transporting air upward in the tropics, poleward to the winter hemisphere, and downward at polar and subpolar latitudes. The Brewer–Dobson circulation is driven by the interaction between upward propagating planetary waves and the mean flow.

Burden The total mass of a gaseous substance of concern in the *atmosphere*.

^{13}C Stable *isotope* of carbon having an atomic weight of approximately 13. Measurements of the ratio of $^{13}C/^{12}C$ in *carbon dioxide* molecules are used to infer the importance of different *carbon cycle* and climate processes and the size of the terrestrial carbon *reservoir*.

^{14}C Unstable *isotope* of carbon having an atomic weight of approximately 14, and a half-life of about 5700 years. It is often used for dating purposes going back some 40 kyr. Its variation in time is affected by the magnetic fields of the Sun and Earth, which influence its production from cosmic rays (see *Cosmogenic radioisotopes*).

Calving The breaking off of discrete pieces of ice from a *glacier*, *ice sheet* or an *ice shelf* into lake or seawater, producing icebergs. This is a form of mass loss from an ice body. See also *Mass balance/budget (of glaciers or ice sheets)*.

Carbonaceous aerosol *Aerosol* consisting predominantly of organic substances and *black carbon*.

Carbon cycle The term used to describe the flow of carbon (in various forms, e.g., as *carbon dioxide*) through the *atmosphere*, ocean, terrestrial and marine *biosphere* and *lithosphere*. In this report, the reference unit for the global carbon cycle is GtC or equivalently PgC (10^{15}g).

Carbon dioxide (CO_2) A naturally occurring gas, also a by-product of burning fossil fuels from fossil carbon deposits, such as oil, gas and coal, of *burning biomass*, of *land use* changes and of industrial processes (e.g., cement production). It is the principal *anthropogenic greenhouse gas* that affects the Earth's radiative balance. It is the reference gas against which other greenhouse gases are measured and therefore has a *Global Warming Potential* of 1.

Carbon dioxide (CO_2) fertilization The enhancement of the growth of plants as a result of increased atmospheric *carbon dioxide (CO_2)* concentration.

Carbon Dioxide Removal (CDR) Carbon Dioxide Removal methods refer to a set of techniques that aim to remove CO_2 directly from the *atmosphere* by either (1) increasing natural *sinks* for carbon or (2) using chemical engineering to remove the CO_2, with the intent of reducing the atmospheric CO_2 concentration. CDR methods involve the ocean, land and technical systems, including such methods as *iron fertilization*, large-scale *afforestation* and direct capture of CO_2 from the atmosphere using engineered chemical means. Some CDR methods fall under the category of *geoengineering*, though this may not be the case for others, with the distinction being based on the magnitude, scale, and impact of the particular CDR activities. The boundary between CDR and *mitigation* is not clear and

there could be some overlap between the two given current definitions (IPCC, 2012, p. 2). See also *Solar Radiation Management (SRM)*.

CFC See *Halocarbons*.

Chaotic A *dynamical system* such as the *climate system*, governed by nonlinear deterministic equations (see *Nonlinearity*), may exhibit erratic or chaotic behaviour in the sense that very small changes in the initial state of the system in time lead to large and apparently unpredictable changes in its temporal evolution. Such chaotic behaviour limits the *predictability* of the state of a nonlinear dynamical system at specific future times, although changes in its statistics may still be predictable given changes in the system parameters or boundary conditions.

Charcoal Material resulting from charring of *biomass*, usually retaining some of the microscopic texture typical of plant tissues; chemically it consists mainly of carbon with a disturbed graphitic structure, with lesser amounts of oxygen and hydrogen.

Chronology Arrangement of events according to dates or times of occurrence.

Clathrate (methane) A partly frozen slushy mix of *methane* gas and ice, usually found in sediments.

Clausius–Clapeyron equation/relationship The thermodynamic relationship between small changes in temperature and vapour pressure in an equilibrium system with condensed phases present. For trace gases such as water vapour, this relation gives the increase in equilibrium (or saturation) water vapour pressure per unit change in air temperature.

Climate Climate in a narrow sense is usually defined as the average weather, or more rigorously, as the statistical description in terms of the mean and variability of relevant quantities over a period of time ranging from months to thousands or millions of years. The classical period for averaging these variables is 30 years, as defined by the World Meteorological Organization. The relevant quantities are most often surface variables such as temperature, precipitation and wind. Climate in a wider sense is the state, including a statistical description, of the *climate system*.

Climate–carbon cycle feedback A *climate feedback* involving changes in the properties of land and ocean *carbon cycle* in response to *climate change*. In the ocean, changes in oceanic temperature and circulation could affect the *atmosphere*–ocean CO_2 flux; on the continents, climate change could affect plant *photosynthesis* and soil microbial *respiration* and hence the flux of CO_2 between the atmosphere and the land *biosphere*.

Climate change Climate change refers to a change in the state of the *climate* that can be identified (e.g., by using statistical tests) by changes in the mean and/or the variability of its properties, and that persists for an extended period, typically decades or longer. Climate change may be due to natural internal processes or *external forcings* such as modulations of the *solar cycles*, volcanic eruptions and persistent *anthropogenic* changes in the composition of the *atmosphere* or in *land use*. Note that the *Framework Convention on Climate Change (UNFCCC)*, in its Article 1, defines climate change as: 'a change of climate which is attributed directly or indirectly to human activity that alters the composition of the global atmosphere and which is in addition to natural *climate variability* observed over comparable time periods'. The UNFCCC thus makes a distinction between climate change attributable to human activities altering the atmospheric composition, and climate variability attributable to natural causes. See also *Climate change commitment*, *Detection and Attribution*.

Climate change commitment Due to the thermal inertia of the ocean and slow processes in the *cryosphere* and land surfaces, the *climate* would continue to change even if the atmospheric composition were held fixed at today's values. Past change in atmospheric composition leads to a *committed climate change*, which continues for as long as a radiative imbalance persists and until all components of the *climate system* have adjusted to a new state. The further change in temperature after the composition of the *atmosphere* is held constant is referred to as the *constant composition temperature commitment* or simply *committed warming* or *warming commitment*. Climate change commitment includes other future changes, for example, in the *hydrological cycle*, in *extreme weather events*, in *extreme climate events*, and in *sea level change*. The *constant emission commitment* is the committed climate change that would result from keeping *anthropogenic* emissions constant and the *zero emission commitment* is the climate change commitment when emissions are set to zero. See also *Climate change*.

Climate feedback An interaction in which a perturbation in one climate quantity causes a change in a second, and the change in the second quantity ultimately leads to an additional change in the first. A negative *feedback* is one in which the initial perturbation is weakened by the changes it causes; a positive feedback is one in which the initial perturbation is enhanced. In this Assessment Report, a somewhat narrower definition is often used in which the climate quantity that is perturbed is the *global mean surface temperature*, which in turn causes changes in the global radiation budget. In either case, the initial perturbation can either be externally forced or arise as part of *internal variability*. See also *Climate Feedback Parameter*.

Climate Feedback Parameter A way to quantify the radiative response of the *climate system* to a *global mean surface temperature* change induced by a *radiative forcing*. It varies as the inverse of the *effective climate sensitivity*. Formally, the Climate Feedback Parameter (α; units: W m^{-2} °C^{-1}) is defined as: $\alpha = (\Delta Q - \Delta F)/\Delta T$, where Q is the global mean radiative forcing, T is the global mean air surface temperature, F is the heat flux into the ocean and Δ represents a change with respect to an unperturbed *climate*.

Climate forecast See *Climate prediction*.

Climate index A time series constructed from climate variables that provides an aggregate summary of the state of the *climate system*. For example, the difference between sea level pressure in Iceland and the Azores provides a simple yet useful historical *NAO* index. Because of their optimal properties, climate indices are often defined using *principal components*—linear combinations of climate variables at different locations that have maximum variance subject to certain normalisation constraints (e.g., the *NAM* and *SAM* indices which are principal components of Northern Hemisphere and Southern Hemisphere gridded pressure anomalies, respectively). See Box 2.5 for a summary of definitions for established observational indices. See also *Climate pattern*.

Climate model (spectrum or hierarchy) A numerical representation of the *climate system* based on the physical, chemical and biological properties of its components, their interactions and *feedback* processes, and accounting for some of its known properties. The climate system can be represented by models of varying complexity, that is, for any one component or combination of components a *spectrum* or *hierarchy* of models can be identified, differing in such aspects as the number of spatial dimensions, the extent to which physical, chemical or biological processes are explicitly represented or the level at which empirical *parametrizations* are involved. Coupled *Atmosphere–Ocean General Circulation Models (AOGCMs)* provide a representation of the climate system that is near or at the most comprehensive end of the spectrum currently available. There is an evolution towards more complex models with interactive chemistry and biology. Climate models are applied as a research tool to study and simulate the *climate*, and for operational purposes, including monthly, seasonal and interannual *climate predictions*. See also *Earth System Model*, *Earth-System Model of Intermediate Complexity*, *Energy Balance Model*, *Process-based Model, Regional Climate Model* and *Semi-empirical model*.

Climate pattern A set of spatially varying coefficients obtained by "projection" (regression) of climate variables onto a *climate index* time series. When the climate index is a principal component, the climate pattern is an eigenvector of the covariance matrix, referred to as an *Empirical Orthogonal Function (EOF)* in climate science.

Climate prediction A climate prediction or *climate forecast* is the result of an attempt to produce (starting from a particular state of the *climate system*) an estimate of the actual evolution of the *climate* in the future, for example, at seasonal, interannual or decadal time scales. Because the future evolution of the climate system may be highly sensitive to initial conditions, such predictions are usually probabilistic in nature. See also *Climate projection*, *Climate scenario*, *Model initialization* and *Predictability*.

Climate projection A climate *projection* is the simulated response of the *climate system* to a *scenario* of future emission or concentration of *greenhouse gases* and *aerosols*, generally derived using *climate models*. Climate projections are distinguished from *climate predictions* by their dependence on the emission/concentration/*radiative forcing* scenario used, which is in turn based on assumptions concerning, for example, future socioeconomic and technological developments that may or may not be realized. See also *Climate scenario*.

Climate regime A state of the *climate system* that occurs more frequently than nearby states due to either more persistence or more frequent recurrence. In other words, a cluster in climate state space associated with a local maximum in the *probability density function*.

Climate response See *Climate sensitivity*.

Climate scenario A plausible and often simplified representation of the future *climate*, based on an internally consistent set of climatological relationships that has been constructed for explicit use in investigating the potential consequences of *anthropogenic climate change*, often serving as input to impact models. *Climate projections* often serve as the raw material for constructing climate scenarios, but climate scenarios usually require additional information such as the observed current climate. A *climate change scenario* is the difference between a climate scenario and the current climate. See also *Emission scenario*, *scenario*.

Climate sensitivity In IPCC reports, *equilibrium climate sensitivity* (units: °C) refers to the equilibrium (steady state) change in the annual *global mean surface temperature* following a doubling of the atmospheric *equivalent carbon dioxide concentration*. Owing to computational constraints, the equilibrium climate sensitivity in a *climate model* is sometimes estimated by running an atmospheric general circulation model coupled to a mixed-layer ocean model, because equilibrium climate sensitivity is largely determined by atmospheric processes. Efficient models can be run to equilibrium with a dynamic ocean. The *climate sensitivity parameter* (units: °C $(W\ m^{-2})^{-1}$) refers to the equilibrium change in the annual global mean surface temperature following a unit change in *radiative forcing*.

The *effective climate sensitivity* (units: °C) is an estimate of the global mean surface temperature response to doubled *carbon dioxide* concentration that is evaluated from model output or observations for evolving non-equilibrium conditions. It is a measure of the strengths of the *climate feedbacks* at a particular time and may vary with forcing history and *climate* state, and therefore may differ from equilibrium climate sensitivity.

The *transient climate response* (units: °C) is the change in the global mean surface temperature, averaged over a 20-year period, centred at the time of atmospheric carbon dioxide doubling, in a climate model simulation in which CO_2 increases at 1% yr^{-1}. It is a measure of the strength and rapidity of the surface temperature response to *greenhouse gas* forcing.

Climate sensitivity parameter See *climate sensitivity*.

Climate system The climate system is the highly complex system consisting of five major components: the *atmosphere*, the *hydrosphere*, the *cryosphere*, the *lithosphere* and the *biosphere*, and the interactions between them. The climate system evolves in time under the influence of its own internal dynamics and because of *external forcings* such as volcanic eruptions, solar variations and *anthropogenic* forcings such as the changing composition of the atmosphere and *land use change*.

Climate variability Climate variability refers to variations in the mean state and other statistics (such as standard deviations, the occurrence of extremes, etc.) of the *climate* on all *spatial and temporal scales* beyond that of individual weather events. Variability may be due to natural internal processes within the *climate system* (*internal variability*), or to variations in natural or *anthropogenic external forcing* (*external variability*). See also *Climate change*.

Cloud condensation nuclei (CCN) The subset of *aerosol* particles that serve as an initial site for the condensation of liquid water, which can lead to the formation of cloud droplets, under typical cloud formation conditions. The main factor that determines which aerosol particles are CCN at a given supersaturation is their size.

Cloud feedback A *climate feedback* involving changes in any of the properties of clouds as a response to a change in the local or *global mean surface temperature*. Understanding cloud feedbacks and determining their magnitude and sign require an understanding of how a change in *climate* may affect the spectrum of cloud types, the cloud fraction and height, the radiative properties of clouds, and finally the Earth's radiation budget. At present, cloud feedbacks remain the largest source of *uncertainty* in *climate sensitivity* estimates. See also *Cloud radiative effect*.

Cloud radiative effect The *radiative effect* of clouds relative to the identical situation without clouds. In previous IPCC reports this was called *cloud radiative forcing*, but that terminology is inconsistent with other uses of the forcing term and is not maintained in this report. See also *Cloud feedback*.

CO_2-equivalent See *Equivalent carbon dioxide*.

Cold days/cold nights Days where maximum temperature, or nights where minimum temperature, falls below the 10th *percentile*, where the respective temperature distributions are generally defined with respect to the 1961–1990 *reference* period. For the corresponding indices, see Box 2.4.

Compatible emissions *Earth System Models* that simulate the land and ocean *carbon cycle* can calculate *CO_2* emissions that are compatible with a given atmospheric CO_2 concentration trajectory. The compatible emissions over a given period of time are equal to the increase of carbon over that same period of time in the sum of the three active *reservoirs*: the *atmosphere*, the land and the ocean.

Confidence The validity of a finding based on the type, amount, quality, and consistency of evidence (e.g., mechanistic understanding, theory, data, models, expert judgment) and on the degree of agreement. Confidence is expressed qualitatively (Mastrandrea et al., 2010). See Figure 1.11 for the levels of confidence and Table 1.1 for the list of *likelihood* qualifiers. See also *Uncertainty*.

Convection Vertical motion driven by buoyancy forces arising from static instability, usually caused by near-surface cooling or increases in salinity in the case of the ocean and near-surface warming or cloud-top radiative cooling in the case of the *atmosphere*. In the atmosphere convection gives rise to cumulus clouds and precipitation and is effective at both scavenging and vertically transporting chemical species. In the ocean convection can carry surface waters to deep within the ocean.

Cosmogenic radioisotopes Rare radioactive *isotopes* that are created by the interaction of a high-energy cosmic ray particles with atoms nuclei. They are often used as indicator of *solar activity* which modulates the cosmic rays intensity or as tracers of atmospheric transport processes, and are also called *cosmogenic radionuclides*.

Cryosphere All regions on and beneath the surface of the Earth and ocean where water is in solid form, including *sea ice*, lake ice, river ice, snow cover, *glaciers* and *ice sheets*, and *frozen ground* (which includes *permafrost*).

Dansgaard–Oeschger events Abrupt events characterized in Greenland *ice cores* and in *palaeoclimate* records from the nearby North Atlantic by a cold glacial state, followed by a rapid transition to a warmer phase, and a slow cooling back to glacial conditions. Counterparts of Dansgaard–Oeschger events are observed in other regions as well.

Deforestation Conversion of *forest* to non-forest. For a discussion of the term *forest* and related terms such as *afforestation*, *reforestation*, and *deforestation* see the IPCC Special Report on Land Use, Land-Use Change and Forestry (IPCC, 2000). See also the report on Definitions and Methodological Options to Inventory Emissions from Direct Human-induced Degradation of Forests and Devegetation of Other Vegetation Types (IPCC, 2003).

Deglaciation/glacial termination Transitions from full glacial conditions (*ice age*) to warm *interglacials* characterized by global warming and sea level rise due to change in continental ice volume.

Detection and attribution *Detection of change* is defined as the process of demonstrating that *climate* or a system affected by climate has changed in some defined statistical sense, without providing a reason for that change. An identified change is detected in observations if its *likelihood* of occurrence by chance due to *internal variability* alone is determined to be small, for example, <10%. *Attribution* is defined as the process of evaluating the relative contributions of multiple causal factors to a change or event with an assignment of statistical confidence (Hegerl et al., 2010).

Diatoms Silt-sized algae that live in surface waters of lakes, rivers and oceans and form shells of opal. Their species distribution in ocean cores is often related to past *sea surface temperatures*.

Direct (aerosol) effect See *Aerosol–radiation interaction*.

Direct Air Capture Chemical process by which a pure CO_2 stream is produced by capturing CO_2 from the ambient air.

Diurnal temperature range The difference between the maximum and minimum temperature during a 24-hour period.

Dobson Unit (DU) A unit to measure the total amount of *ozone* in a vertical column above the Earth's surface (*total column ozone*). The number of Dobson Units is the thickness in units of 10^{-5} m that the ozone column would occupy if compressed into a layer of uniform density at a pressure of 1013 hPa and a temperature of 0°C. One DU corresponds to a column of ozone containing 2.69×10^{20} molecules per square metre. A typical value for the amount of ozone in a column of the Earth's *atmosphere*, although very variable, is 300 DU.

Downscaling Downscaling is a method that derives local- to regional-scale (10 to 100 km) information from larger-scale models or data analyses. Two main methods exist: *dynamical downscaling* and *empirical/statistical downscaling*. The dynamical method uses the output of *regional climate models*, global models with variable spatial *resolution* or high-resolution global models. The empirical/statistical methods develop statistical relationships that link the large-scale atmospheric variables with local/regional climate variables. In all cases, the quality of the driving model remains an important limitation on the quality of the downscaled information.

Drought A period of abnormally dry weather long enough to cause a serious hydrological imbalance. Drought is a relative term; therefore any discussion in terms of precipitation deficit must refer to the particular precipitation-related activity that is under discussion. For example, shortage of precipitation during the growing season impinges on crop production or *ecosystem* function in general (due to *soil moisture* drought, also termed *agricultural drought*), and during the *runoff* and percolation season primarily affects water supplies (*hydrological drought*). Storage changes in soil moisture and groundwater are also affected by increases in actual *evapotranspiration* in addition to reductions in precipitation. A period with an abnormal precipitation deficit is defined as a *meteorological drought*. A *megadrought* is a very lengthy and pervasive drought, lasting much longer than normal, usually a decade or more. For the corresponding indices, see Box 2.4.

Dynamical system A process or set of processes whose evolution in time is governed by a set of deterministic physical laws. The *climate system* is a dynamical system. See also *Abrupt climate change*, *Chaotic*, *Nonlinearity* and *Predictability*.

Earth System Model (ESM) A coupled *atmosphere–ocean general circulation model* in which a representation of the *carbon cycle* is included, allowing for interactive calculation of atmospheric CO_2 or *compatible emissions*. Additional components (e.g., atmospheric chemistry, *ice sheets*, dynamic vegetation, nitrogen cycle, but also urban or crop models) may be included. See also *Climate model*.

Earth System Model of Intermediate Complexity (EMIC) A *climate model* attempting to include all the most important earth system processes as in ESMs but at a lower *resolution* or in a simpler, more idealized fashion.

Earth System sensitivity The equilibrium temperature response of the coupled *atmosphere*–ocean–*cryosphere*–vegetation–*carbon cycle* system to a doubling of the atmospheric CO_2 concentration is referred to as Earth System sensitivity. Because it allows slow components (e.g., *ice sheets*, vegetation) of the *climate system* to adjust to the external perturbation, it may differ substantially from the *climate sensitivity* derived from coupled atmosphere–ocean models.

Ecosystem An ecosystem is a functional unit consisting of living organisms, their non-living environment, and the interactions within and between them. The components included in a given ecosystem and its spatial boundaries depend on the purpose for which the ecosystem is defined: in some cases they are relatively sharp, while in others they are diffuse. Ecosystem boundaries can change over time. Ecosystems are nested within other ecosystems, and their scale can range from very small to the entire *biosphere*. In the current era, most ecosystems either contain people as key organisms, or are influenced by the effects of human activities in their environment.

Effective climate sensitivity See *Climate sensitivity*.

Effective radiative forcing See *Radiative forcing*.

Efficacy A measure of how effective a *radiative forcing* from a given *anthropogenic* or natural mechanism is at changing the equilibrium *global mean surface temperature* compared to an equivalent radiative forcing from *carbon dioxide*. A carbon dioxide increase by definition has an efficacy of 1.0. Variations in climate efficacy may result from *rapid adjustments* to the applied forcing, which differ with different forcings.

Ekman pumping Frictional stress at the surface between two fluids (*atmosphere* and ocean) or between a fluid and the adjacent solid surface (the Earth's surface) forces a circulation. When the resulting mass

transport is converging, mass conservation requires a vertical flow away from the surface. This is called Ekman pumping. The opposite effect, in case of divergence, is called *Ekman suction*. The effect is important in both the atmosphere and the ocean.

Ekman transport The total transport resulting from a balance between the Coriolis force and the frictional stress due to the action of the wind on the ocean surface. See also *Ekman pumping*.

Electromagnetic spectrum Wavelength or energy range of all electromagnetic radiation. In terms of *solar radiation*, the *spectral irradiance* is the power arriving at the Earth per unit area, per unit wavelength.

El Niño-Southern Oscillation (ENSO) The term *El Niño* was initially used to describe a warm-water current that periodically flows along the coast of Ecuador and Peru, disrupting the local fishery. It has since become identified with a basin-wide warming of the tropical Pacific Ocean east of the dateline. This oceanic event is associated with a fluctuation of a global-scale tropical and subtropical surface pressure pattern called the *Southern Oscillation*. This coupled *atmosphere*–ocean phenomenon, with preferred time scales of two to about seven years, is known as the El Niño-Southern Oscillation (ENSO). It is often measured by the surface pressure anomaly difference between Tahiti and Darwin or the *sea surface temperatures* in the central and eastern equatorial Pacific. During an ENSO event, the prevailing trade winds weaken, reducing upwelling and altering ocean currents such that the sea surface temperatures warm, further weakening the trade winds. This event has a great impact on the wind, sea surface temperature and precipitation patterns in the tropical Pacific. It has climatic effects throughout the Pacific *region* and in many other parts of the world, through global *teleconnections*. The cold phase of ENSO is called *La Niña*. For the corresponding indices, see Box 2.5.

Emission scenario A plausible representation of the future development of emissions of substances that are potentially radiatively active (e.g., *greenhouse gases*, *aerosols*) based on a coherent and internally consistent set of assumptions about driving forces (such as demographic and socioeconomic development, technological change) and their key relationships. *Concentration scenarios*, derived from emission scenarios, are used as input to a *climate model* to compute *climate projections*. In IPCC (1992) a set of emission scenarios was presented which were used as a basis for the climate projections in IPCC (1996). These emission scenarios are referred to as the IS92 scenarios. In the IPCC Special Report on Emission Scenarios (Nakićenović and Swart, 2000) emission scenarios, the so-called *SRES scenarios*, were published, some of which were used, among others, as a basis for the climate projections presented in Chapters 9 to 11 of IPCC (2001) and Chapters 10 and 11 of IPCC (2007). New emission scenarios for *climate change*, the four *Representative Concentration Pathways*, were developed for, but independently of, the present IPCC assessment. See also *Climate scenario* and *Scenario*.

Energy balance The difference between the total incoming and total outgoing energy. If this balance is positive, warming occurs; if it is negative, cooling occurs. Averaged over the globe and over long time periods, this balance must be zero. Because the *climate system* derives virtually all its energy from the Sun, zero balance implies that, globally, the absorbed *solar radiation*, that is, *incoming solar radiation* minus reflected solar radiation at the top of the *atmosphere* and *outgoing longwave radiation* emitted by the climate system are equal. See also *Energy budget*.

Energy Balance Model (EBM) An energy balance model is a simplified model that analyses the *energy budget* of the Earth to compute changes in the *climate*. In its simplest form, there is no explicit spatial dimension and the model then provides an estimate of the changes in globally averaged temperature computed from the changes in radiation. This zero-dimensional energy balance model can be extended to a one-dimensional or two-dimensional model if changes to the energy budget with respect to latitude, or both latitude and longitude, are explicitly considered. See also *Climate model*.

Energy budget (of the Earth) The Earth is a physical system with an energy budget that includes all gains of incoming energy and all losses of outgoing energy. The Earth's energy budget is determined by measuring how much energy comes into the Earth system from the Sun, how much energy is lost to space, and accounting for the remainder on Earth and its *atmosphere*. *Solar radiation* is the dominant source of energy into the Earth system. Incoming solar energy may be scattered and reflected by clouds and *aerosols* or absorbed in the atmosphere. The transmitted radiation is then either absorbed or reflected at the Earth's surface. The average *albedo* of the Earth is about 0.3, which means that 30% of the incident solar energy is reflected into space, while 70% is absorbed by the Earth. Radiant solar or shortwave energy is transformed into sensible heat, latent energy (involving different water states), potential energy, and kinetic energy before being emitted as *infrared radiation*. With the average *surface temperature* of the Earth of about 15°C (288 K), the main outgoing energy flux is in the infrared part of the spectrum. See also *Energy balance*, *Latent heat flux*, *Sensible heat flux*.

Ensemble A collection of model simulations characterizing a *climate prediction* or *projection*. Differences in initial conditions and model formulation result in different evolutions of the modelled system and may give information on *uncertainty* associated with model error and error in initial conditions in the case of *climate forecasts* and on uncertainty associated with model error and with internally generated *climate variability* in the case of climate projections.

Equilibrium and transient climate experiment An *equilibrium climate experiment* is a *climate model* experiment in which the model is allowed to fully adjust to a change in *radiative forcing*. Such experiments provide information on the difference between the initial and final states of the model, but not on the time-dependent response. If the forcing is allowed to evolve gradually according to a prescribed *emission scenario*, the time-dependent response of a climate model may be analysed. Such an experiment is called a *transient climate experiment*. See also *Climate projection*.

Equilibrium climate sensitivity See *Climate sensitivity*.

Equilibrium line The spatially averaged boundary at a given moment, usually chosen as the seasonal *mass budget* minimum at the end of summer, between the region on a *glacier* where there is a net annual loss of ice mass (*ablation* area) and that where there is a net annual gain (*accumulation* area). The altitude of this boundary is referred to as equilibrium line altitude (ELA).

Equivalent carbon dioxide (CO_2) concentration The concentration of *carbon dioxide* that would cause the same *radiative forcing* as a given mixture of carbon dioxide and other forcing components. Those values may consider only *greenhouse gases*, or a combination of greenhouse gases and *aerosols*. Equivalent carbon dioxide concentration is a *metric* for comparing radiative forcing of a mix of different greenhouse gases at a particular time but does not imply equivalence of the corresponding *climate change* responses nor future forcing. There is generally no connection between *equivalent carbon dioxide emissions* and resulting equivalent carbon dioxide concentrations.

Equivalent carbon dioxide (CO_2) emission The amount of *carbon dioxide* emission that would cause the same integrated *radiative forcing*, over a given time horizon, as an emitted amount of a *greenhouse gas* or a mixture of greenhouse gases. The equivalent carbon dioxide emission is obtained by multiplying the emission of a greenhouse gas by its *Global Warming Potential* for the given time horizon. For a mix of greenhouse

gases it is obtained by summing the equivalent carbon dioxide emissions of each gas. Equivalent carbon dioxide emission is a common scale for comparing emissions of different greenhouse gases but does not imply equivalence of the corresponding *climate change* responses. See also *Equivalent carbon dioxide concentration*.

Evapotranspiration The combined process of evaporation from the Earth's surface and transpiration from vegetation.

Extended Concentration Pathways See *Representative Concentration Pathways*.

External forcing External forcing refers to a forcing agent outside the *climate system* causing a change in the climate system. Volcanic eruptions, solar variations and *anthropogenic* changes in the composition of the *atmosphere* and *land use change* are external forcings. Orbital forcing is also an external forcing as the *insolation* changes with orbital parameters eccentricity, tilt and precession of the equinox.

Extratropical cyclone A large-scale (of order 1000 km) storm in the middle or high latitudes having low central pressure and fronts with strong horizontal gradients in temperature and humidity. A major cause of extreme wind speeds and heavy precipitation especially in wintertime.

Extreme climate event See *Extreme weather event.*

Extreme sea level See *Storm surge.*

Extreme weather event An extreme weather event is an event that is rare at a particular place and time of year. Definitions of *rare* vary, but an extreme weather event would normally be as rare as or rarer than the 10th or 90th *percentile* of a *probability density function* estimated from observations. By definition, the characteristics of what is called *extreme weather* may vary from place to place in an absolute sense. When a pattern of extreme weather persists for some time, such as a season, it may be classed as an *extreme climate event*, especially if it yields an average or total that is itself extreme (e.g., *drought* or heavy rainfall over a season).

Faculae Bright patches on the Sun. The area covered by faculae is greater during periods of high *solar activity*.

Feedback See *Climate feedback*.

Fingerprint The *climate* response pattern in space and/or time to a specific forcing is commonly referred to as a fingerprint. The spatial patterns of sea level response to melting of *glaciers* or *ice sheets* (or other changes in surface loading) are also referred to as fingerprints. Fingerprints are used to detect the presence of this response in observations and are typically estimated using forced *climate model* simulations.

Flux adjustment To avoid the problem of coupled *Atmosphere–Ocean General Circulation Models (AOGCMs)* drifting into some unrealistic *climate* state, adjustment terms can be applied to the atmosphere-ocean fluxes of heat and moisture (and sometimes the surface stresses resulting from the effect of the wind on the ocean surface) before these fluxes are imposed on the model ocean and atmosphere. Because these adjustments are pre-computed and therefore independent of the coupled model integration, they are uncorrelated with the anomalies that develop during the integration.

Forest A vegetation type dominated by trees. Many definitions of the term *forest* are in use throughout the world, reflecting wide differences in biogeophysical conditions, social structure and economics. For a discussion of the term *forest* and related terms such as *afforestation*, *reforestation* and *deforestation* see the IPCC Report on Land Use, Land-Use Change and Forestry (IPCC, 2000). See also the Report on Definitions and Methodological Options to Inventory Emissions from Direct Human-induced Degradation of Forests and Devegetation of Other Vegetation Types (IPCC, 2003).

Fossil fuel emissions Emissions of *greenhouse gases* (in particular *carbon dioxide*), other trace gases and *aerosols* resulting from the combustion of fuels from fossil carbon deposits such as oil, gas and coal.

Framework Convention on Climate Change See *United Nations Framework Convention on Climate Change (UNFCCC)*.

Free atmosphere The atmospheric layer that is negligibly affected by friction against the Earth's surface, and which is above the *atmospheric boundary layer*.

Frozen ground Soil or rock in which part or all of the *pore water* is frozen. Frozen ground includes *permafrost.* Ground that freezes and thaws annually is called *seasonally frozen ground*.

General circulation The large-scale motions of the *atmosphere* and the ocean as a consequence of differential heating on a rotating Earth. General circulation contributes to the *energy balance* of the system through transport of heat and momentum.

General Circulation Model (GCM) See *Climate model*.

Geoengineering Geoengineering refers to a broad set of methods and technologies that aim to deliberately alter the *climate system* in order to alleviate the impacts of *climate change*. Most, but not all, methods seek to either (1) reduce the amount of absorbed solar energy in the climate system (*Solar Radiation Management*) or (2) increase net carbon sinks from the *atmosphere* at a scale sufficiently large to alter *climate* (*Carbon Dioxide Removal*). Scale and intent are of central importance. Two key characteristics of geoengineering methods of particular concern are that they use or affect the climate system (e.g., atmosphere, land or ocean) globally or regionally and/or could have substantive unintended effects that cross national boundaries. Geoengineering is different from weather modification and ecological engineering, but the boundary can be fuzzy (IPCC, 2012, p. 2).

Geoid The equipotential surface having the same geopotential at each latitude and longitude around the world (geodesists denoting this potential W0) that best approximates the *mean sea level*. It is the surface of reference for measurement of altitude. In practice, several variations of definitions of the geoid exist depending on the way the permanent tide (the zero-frequency gravitational tide due to the Sun and Moon) is considered in geodetic studies.

Geostrophic winds or currents A wind or current that is in balance with the horizontal pressure gradient and the Coriolis force, and thus is outside of the influence of friction. Thus, the wind or current is directly parallel to isobars and its speed is proportional to the horizontal pressure gradient.

Glacial–interglacial cycles Phase of the Earth's history marked by large changes in continental ice volume and global sea level. See also *Ice age* and *Interglacials*.

Glacial isostatic adjustment (GIA) The deformation of the Earth and its gravity field due to the response of the earth–ocean system to changes in ice and associated water loads. It is sometimes referred to as *glacio-hydro isostasy*. It includes vertical and horizontal deformations of the Earth's surface and changes in *geoid* due to the redistribution of mass during the ice–ocean mass exchange.

Glacier A perennial mass of land ice that originates from compressed snow, shows evidence of past or present flow (through internal deformation and/or sliding at the base) and is constrained by internal stress and friction at the base and sides. A glacier is maintained by accumulation of snow at high altitudes, balanced by melting at low altitudes and/or discharge into the sea. An ice mass of the same origin as glaciers, but of continental size, is called an *ice sheet*. For the purpose of simplicity in this Assessment Report, all ice masses other than ice sheets are referred to as

glaciers. See also *Equilibrium line* and *Mass balance/budget (of glaciers or ice sheets)*.

Global dimming Global dimming refers to a widespread reduction of *solar radiation* received at the surface of the Earth from about the year 1961 to around 1990.

Global mean surface temperature An estimate of the global mean surface air temperature. However, for changes over time, only anomalies, as departures from a climatology, are used, most commonly based on the area-weighted global average of the *sea surface temperature* anomaly and *land surface air temperature* anomaly.

Global Warming Potential (GWP) An index, based on radiative properties of *greenhouse gases*, measuring the *radiative forcing* following a pulse emission of a unit mass of a given greenhouse gas in the present-day *atmosphere* integrated over a chosen time horizon, relative to that of *carbon dioxide*. The GWP represents the combined effect of the differing times these gases remain in the atmosphere and their relative effectiveness in causing radiative forcing. The *Kyoto Protocol* is based on GWPs from pulse emissions over a 100-year time frame.

Greenhouse effect The infrared *radiative effect* of all infrared-absorbing constituents in the *atmosphere*. *Greenhouse gases*, clouds, and (to a small extent) *aerosols* absorb *terrestrial radiation* emitted by the Earth's surface and elsewhere in the atmosphere. These substances emit *infrared radiation* in all directions, but, everything else being equal, the net amount emitted to space is normally less than would have been emitted in the absence of these absorbers because of the decline of temperature with altitude in the *troposphere* and the consequent weakening of emission. An increase in the concentration of greenhouse gases increases the magnitude of this effect; the difference is sometimes called the enhanced greenhouse effect. The change in a greenhouse gas concentration because of *anthropogenic* emissions contributes to an *instantaneous radiative forcing*. Surface temperature and troposphere warm in response to this forcing, gradually restoring the radiative balance at the top of the atmosphere.

Greenhouse gas (GHG) Greenhouse gases are those gaseous constituents of the *atmosphere*, both natural and *anthropogenic*, that absorb and emit radiation at specific wavelengths within the spectrum of *terrestrial radiation* emitted by the Earth's surface, the atmosphere itself, and by clouds. This property causes the *greenhouse effect.* Water vapour (H_2O), *carbon dioxide (CO_2)*, *nitrous oxide (N_2O)*, *methane (CH_4)* and *ozone* (O_3) are the primary greenhouse gases in the Earth's atmosphere. Moreover, there are a number of entirely human-made greenhouse gases in the atmosphere, such as the *halocarbons* and other chlorine- and bromine-containing substances, dealt with under the *Montreal Protocol.* Beside CO_2, N_2O and CH_4, the *Kyoto Protocol* deals with the greenhouse gases sulphur hexafluoride (SF_6), hydrofluorocarbons (*HFCs*) and perfluorocarbons (PFCs). For a list of *well-mixed greenhouse gases*, see Table 2.A.1.

Gross Primary Production (GPP) The amount of carbon fixed by the autotrophs (e.g. plants and algaes).

Grounding line The junction between a *glacier* or *ice sheet* and *ice shelf*; the place where ice starts to float. This junction normally occurs over a finite zone, rather than at a line.

Gyre Basin-scale ocean horizontal circulation pattern with slow flow circulating around the ocean basin, closed by a strong and narrow (100 to 200 km wide) boundary current on the western side. The subtropical gyres in each ocean are associated with high pressure in the centre of the gyres; the subpolar gyres are associated with low pressure.

Hadley Circulation A direct, thermally driven overturning cell in the *atmosphere* consisting of poleward flow in the upper *troposphere*, subsiding air into the subtropical anticyclones, return flow as part of the trade winds near the surface, and with rising air near the equator in the so-called *Inter-Tropical Convergence Zone*.

Halocarbons A collective term for the group of partially halogenated organic species, which includes the chlorofluorocarbons (*CFCs*), hydrochlorofluorocarbons (*HCFCs*), hydrofluorocarbons (*HFCs*), halons, methyl chloride and methyl bromide. Many of the halocarbons have large *Global Warming Potentials*. The chlorine and bromine-containing halocarbons are also involved in the depletion of the *ozone layer*.

Halocline A layer in the oceanic water column in which salinity changes rapidly with depth. Generally saltier water is denser and lies below less salty water. In some high latitude oceans the surface waters may be colder than the deep waters and the halocline is responsible for maintaining water column stability and isolating the surface waters from the deep waters. See also *Thermocline.*

Halosteric See *Sea level change*.

HCFC See *Halocarbons*.

Heat wave A period of abnormally and uncomfortably hot weather. See also *Warm spell*.

Heterotrophic respiration The conversion of organic matter to *carbon dioxide* by organisms other than autotrophs.

HFC See *Halocarbons*.

Hindcast or retrospective forecast A forecast made for a period in the past using only information available before the beginning of the forecast. A sequence of hindcasts can be used to calibrate the forecast system and/or provide a measure of the average skill that the forecast system has exhibited in the past as a guide to the skill that might be expected in the future.

Holocene The Holocene Epoch is the latter of two epochs in the *Quaternary* System, extending from 11.65 ka (thousand years before 1950) to the present. It is also known as *Marine Isotopic Stage (MIS) 1* or *current interglacial*.

Hydroclimate Part of the *climate* pertaining to the hydrology of a *region*.

Hydrological cycle The cycle in which water evaporates from the oceans and the land surface, is carried over the Earth in atmospheric circulation as water vapour, condenses to form clouds, precipitates over ocean and land as rain or snow, which on land can be intercepted by trees and vegetation, provides *runoff* on the land surface, infiltrates into soils, recharges groundwater, discharges into streams and ultimately flows out into the oceans, from which it will eventually evaporate again. The various systems involved in the hydrological cycle are usually referred to as hydrological systems.

Hydrosphere The component of the *climate system* comprising liquid surface and subterranean water, such as oceans, seas, rivers, fresh water lakes, underground water, etc.

Hypsometry The distribution of land or ice surface as a function of altitude.

Ice age An ice age or *glacial period* is characterized by a long-term reduction in the temperature of the Earth's *climate*, resulting in growth of *ice sheets* and *glaciers*.

Ice–albedo feedback A *climate feedback* involving changes in the Earth's surface *albedo*. Snow and ice have an albedo much higher (up to ~0.8) than the average planetary albedo (~0.3). With increasing temperatures, it is anticipated that snow and ice extent will decrease, the Earth's overall albedo will decrease and more *solar radiation* will be absorbed, warming the Earth further.

Ice core A cylinder of ice drilled out of a *glacier* or *ice sheet*.

Ice sheet A mass of land ice of continental size that is sufficiently thick to cover most of the underlying bed, so that its shape is mainly determined by its dynamics (the flow of the ice as it deforms internally and/or slides at its base). An ice sheet flows outward from a high central ice plateau with a small average surface slope. The margins usually slope more steeply, and most ice is discharged through fast flowing *ice streams* or *outlet glaciers*, in some cases into the sea or into *ice shelves* floating on the sea. There are only two ice sheets in the modern world, one on Greenland and one on Antarctica. During glacial periods there were others.

Ice shelf A floating slab of ice of considerable thickness extending from the coast (usually of great horizontal extent with a very gently sloping surface), often filling embayments in the coastline of an *ice sheet*. Nearly all ice shelves are in Antarctica, where most of the ice discharged into the ocean flows via ice shelves.

Ice stream A stream of ice with strongly enhanced flow that is part of an *ice sheet.* It is often separated from surrounding ice by strongly sheared, crevassed margins. See also *Outlet glacier.*

Incoming solar radiation See *Insolation*.

Indian Ocean Dipole (IOD) Large–scale mode of interannual variability of *sea surface temperature* in the Indian Ocean. This pattern manifests through a zonal gradient of tropical sea surface temperature, which in one extreme phase in boreal autumn shows cooling off Sumatra and warming off Somalia in the west, combined with anomalous easterlies along the equator.

Indirect aerosol effect See *Aerosol-cloud interaction*.

Industrial Revolution A period of rapid industrial growth with far-reaching social and economic consequences, beginning in Britain during the second half of the 18th century and spreading to Europe and later to other countries including the United States. The invention of the steam engine was an important trigger of this development. The industrial revolution marks the beginning of a strong increase in the use of fossil fuels and emission of, in particular, fossil *carbon dioxide*. In this report the terms *pre-industrial* and *industrial* refer, somewhat arbitrarily, to the periods before and after 1750, respectively.

Infrared radiation See *Terrestrial radiation*.

Insolation The amount of *solar radiation* reaching the Earth by latitude and by season measured in W m^{-2}. Usually *insolation* refers to the radiation arriving at the top of the *atmosphere*. Sometimes it is specified as referring to the radiation arriving at the Earth's surface. See also *Total Solar Irradiance*.

Interglacials or interglaciations The warm periods between *ice age* glaciations. Often defined as the periods at which sea levels were close to present sea level. For the *Last Interglacial (LIG)* this occurred between about 129 and 116 ka (thousand years) before present (defined as 1950) although the warm period started in some areas a few thousand years earlier. In terms of the oxygen *isotope* record interglaciations are defined as the interval between the midpoint of the preceding termination and the onset of the next glaciation. The present interglaciation, the *Holocene*, started at 11.65 ka before present although globally sea levels did not approach their present position until about 7 ka before present.

Internal variability See *Climate variability*.

Inter-Tropical Convergence Zone (ITCZ) The Inter-Tropical Convergence Zone is an equatorial zonal belt of low pressure, strong *convection* and heavy precipitation near the equator where the northeast trade winds meet the southeast trade winds. This band moves seasonally.

Iron fertilization Deliberate introduction of iron to the upper ocean intended to enhance biological productivity which can sequester additional atmospheric *carbon dioxide* into the oceans.

Irreversibility A perturbed state of a *dynamical system* is defined as irreversible on a given timescale, if the recovery timescale from this state due to natural processes is significantly longer than the time it takes for the system to reach this perturbed state. In the context of WGI, the time scale of interest is centennial to millennial. See also *Tipping point*.

Isostatic or Isostasy Isostasy refers to the response of the earth to changes in surface load. It includes the deformational and gravitational response. This response is elastic on short time scales, as in the earth–ocean response to recent changes in mountain glaciation, or viscoelastic on longer time scales, as in the response to the last *deglaciation* following the *Last Glacial Maximum*. See also *Glacial Isostatic Adjustment (GIA)*.

Isotopes Atoms of the same chemical element that have the same the number of protons but differ in the number of neutrons. Some proton–neutron configurations are stable (stable isotopes), others are unstable undergoing spontaneous radioactive decay (*radioisotopes*). Most elements have more than one stable isotope. Isotopes can be used to trace transport processes or to study processes that change the isotopic ratio. Radioisotopes provide in addition time information that can be used for radiometric dating.

Kyoto Protocol The Kyoto Protocol to the *United Nations Framework Convention on Climate Change (UNFCCC)* was adopted in 1997 in Kyoto, Japan, at the Third Session of the Conference of the Parties (COP) to the UNFCCC. It contains legally binding commitments, in addition to those included in the UNFCCC. Countries included in Annex B of the Protocol (most Organisation for Economic Cooperation and Development countries and countries with economies in transition) agreed to reduce their *anthropogenic greenhouse gas* emissions (*carbon dioxide*, *methane*, *nitrous oxide*, hydrofluorocarbons, perfluorocarbons, and sulphur hexafluoride) by at least 5% below 1990 levels in the commitment period 2008–2012. The Kyoto Protocol entered into force on 16 February 2005.

Land surface air temperature The surface air temperature as measured in well-ventilated screens over land at 1.5 m above the ground.

Land use and Land use change *Land use* refers to the total of arrangements, activities and inputs undertaken in a certain land cover type (a set of human actions). The term *land use* is also used in the sense of the social and economic purposes for which land is managed (e.g., grazing, timber extraction and conservation). *Land use change* refers to a change in the use or management of land by humans, which may lead to a change in land cover. Land cover and land use change may have an impact on the surface *albedo*, *evapotranspiration*, *sources* and *sinks* of *greenhouse gases*, or other properties of the *climate system* and may thus give rise to *radiative forcing* and/or other impacts on *climate*, locally or globally. See also the IPCC Report on Land Use, Land-Use Change, and Forestry (IPCC, 2000).

Land water storage Water stored on land other than in *glaciers* and *ice sheets* (that is water stored in rivers, lakes, wetlands, the vadose zone, aquifers, reservoirs, snow and *permafrost*). Changes in land water storage driven by *climate* and human activities contribute to *sea level change*.

La Niña See *El Niño-Southern Oscillation*.

Lapse rate The rate of change of an atmospheric variable, usually temperature, with height. The lapse rate is considered positive when the variable decreases with height.

Last Glacial Maximum (LGM) The period during the last *ice age* when the *glaciers* and *ice sheets* reached their maximum extent, approximately

21 ka ago. This period has been widely studied because the *radiative forcings* and boundary conditions are relatively well known.

Last Interglacial (LIG) See *Interglacials*.

Latent heat flux The turbulent flux of heat from the Earth's surface to the *atmosphere* that is associated with evaporation or condensation of water vapour at the surface; a component of the surface *energy budget*.

Lifetime Lifetime is a general term used for various time scales characterizing the rate of processes affecting the concentration of trace gases. The following lifetimes may be distinguished:

Turnover time (T) (also called *global atmospheric lifetime*) is the ratio of the mass M of a *reservoir* (e.g., a gaseous compound in the *atmosphere*) and the total rate of removal S from the reservoir: $T = M/S$. For each removal process, separate turnover times can be defined. In soil carbon biology, this is referred to as *Mean Residence Time*.

Adjustment time or response time (T_a) is the time scale characterizing the decay of an instantaneous pulse input into the reservoir. The term *adjustment time* is also used to characterize the adjustment of the mass of a reservoir following a step change in the *source* strength. *Half-life* or *decay constant* is used to quantify a first-order exponential decay process. See *Response time* for a different definition pertinent to *climate* variations.

The term *lifetime* is sometimes used, for simplicity, as a surrogate for *adjustment time*.

In simple cases, where the global removal of the compound is directly proportional to the total mass of the reservoir, the adjustment time equals the turnover time: $T = T_a$. An example is *CFC*-11, which is removed from the atmosphere only by photochemical processes in the *stratosphere*. In more complicated cases, where several reservoirs are involved or where the removal is not proportional to the total mass, the equality $T = T_a$ no longer holds. *Carbon dioxide (CO_2)* is an extreme example. Its turnover time is only about 4 years because of the rapid exchange between the atmosphere and the ocean and terrestrial biota. However, a large part of that CO_2 is returned to the atmosphere within a few years. Thus, the adjustment time of CO_2 in the atmosphere is actually determined by the rate of removal of carbon from the surface layer of the oceans into its deeper layers. Although an approximate value of 100 years may be given for the adjustment time of CO_2 in the atmosphere, the actual adjustment is faster initially and slower later on. In the case of *methane (CH_4)*, the adjustment time is different from the turnover time because the removal is mainly through a chemical reaction with the hydroxyl radical (OH), the concentration of which itself depends on the CH_4 concentration. Therefore, the CH_4 removal rate S is not proportional to its total mass M.

Likelihood The chance of a specific outcome occurring, where this might be estimated probabilistically. This is expressed in this report using a standard terminology, defined in Table 1.1. See also *Confidence* and *Uncertainty*.

Lithosphere The upper layer of the solid Earth, both continental and oceanic, which comprises all crustal rocks and the cold, mainly elastic part of the uppermost mantle. Volcanic activity, although part of the lithosphere, is not considered as part of the *climate system*, but acts as an *external forcing* factor. See also *Isostatic*.

Little Ice Age (LIA) An interval during the last millennium characterized by a number of extensive expansions of mountain *glaciers* and moderate retreats in between them, both in the Northern and Southern Hemispheres. The timing of glacial advances differs between *regions* and the LIA is, therefore, not clearly defined in time. Most definitions lie in the period 1400 CE and 1900 CE. Currently available *reconstructions* of average Northern Hemisphere temperature indicate that the coolest periods at the hemispheric scale may have occurred from 1450 to 1850 CE.

Longwave radiation See *Terrestrial radiation*.

Madden–Julian Oscillation (MJO) The largest single component of tropical atmospheric intraseasonal variability (periods from 30 to 90 days). The MJO propagates eastwards at around 5 m s^{-1} in the form of a large-scale coupling between atmospheric circulation and deep *convection*. As it progresses, it is associated with large regions of both enhanced and suppressed rainfall, mainly over the Indian and western Pacific Oceans. Each MJO event lasts approximately 30 to 60 days, hence the MJO is also known as the 30- to 60-day wave, or the intraseasonal oscillation.

Marine-based ice sheet An *ice sheet* containing a substantial region that rests on a bed lying below sea level and whose perimeter is in contact with the ocean. The best known example is the West Antarctic ice sheet.

Mass balance/budget (of glaciers or ice sheets) The balance between the mass input to the ice body (*accumulation*) and the mass loss (*ablation* and iceberg *calving*) over a stated period of time, which is often a year or a season. Point mass balance refers to the mass balance at a particular location on the *glacier* or *ice sheet*. Surface mass balance is the difference between surface accumulation and surface ablation. The input and output terms for mass balance are:

Accumulation All processes that add to the mass of a glacier. The main contribution to accumulation is snowfall. Accumulation also includes deposition of hoar, freezing rain, other types of solid precipitation, gain of wind-blown snow, and avalanching.

Ablation Surface processes that reduce the mass of a glacier. The main contributor to ablation is melting with *runoff* but on some glaciers sublimation, loss of wind-blown snow and avalanching are also significant processes of ablation.

Discharge/outflow Mass loss by iceberg calving or ice discharge across the *grounding line* of a floating *ice shelf*. Although often treated as an ablation term, in this report iceberg calving and discharge is considered separately from surface ablation.

Mean sea level The surface level of the ocean at a particular point averaged over an extended period of time such as a month or year. Mean sea level is often used as a national datum to which heights on land are referred.

Medieval Climate Anomaly (MCA) See *Medieval Warm Period*.

Medieval Warm Period (MWP) An interval of relatively warm conditions and other notable *climate* anomalies such as more extensive *drought* in some continental *regions*. The timing of this interval is not clearly defined, with different records showing onset and termination of the warmth at different times, and some showing intermittent warmth. Most definitions lie within the period 900 to 1400 CE. Currently available *reconstructions* of average Northern Hemisphere temperature indicate that the warmest period at the hemispheric scale may have occurred from 950 to 1250 CE. Currently available records and temperature reconstructions indicate that average temperatures during parts of the MWP were indeed warmer in the context of the last 2 kyr, though the warmth may not have been as ubiquitous across seasons and geographical regions as the 20th century warming. It is also called *Medieval Climate Anomaly*.

Meridional Overturning Circulation (MOC) Meridional (north–south) overturning circulation in the ocean quantified by zonal (east–west) sums of mass transports in depth or density layers. In the North Atlantic, away from the subpolar *regions*, the MOC (which is in principle an observable quantity) is often identified with the *thermohaline circulation* (THC),

which is a conceptual and incomplete interpretation. It must be borne in mind that the MOC is also driven by wind, and can also include shallower overturning cells such as occur in the upper ocean in the tropics and subtropics, in which warm (light) waters moving poleward are transformed to slightly denser waters and *subducted* equatorward at deeper levels.

Metadata Information about meteorological and climatological data concerning how and when they were measured, their quality, known problems and other characteristics.

Methane (CH_4) Methane is one of the six *greenhouse gases* to be mitigated under the *Kyoto Protocol* and is the major component of natural gas and associated with all hydrocarbon fuels, animal husbandry and agriculture.

Metric A consistent measurement of a characteristic of an object or activity that is otherwise difficult to quantify. Within the context of the evaluation of *climate models*, this is a quantitative measure of agreement between a simulated and observed quantity which can be used to assess the performance of individual models.

Microwave Sounding Unit (MSU) A microwave sounder on National Oceanic and Atmospheric Administration (NOAA) polar orbiter satellites, that estimates the temperature of thick layers of the *atmosphere* by measuring the thermal emission of oxygen molecules from a complex of emission lines near 60 GHz. A series of nine MSUs began making this kind of measurement in late 1978. Beginning in mid 1998, a follow-on series of instruments, the Advanced Microwave Sounding Units (AMSUs), began operation.

Mineralization/Remineralization The conversion of an element from its organic form to an inorganic form as a result of microbial decomposition. In nitrogen mineralization, organic nitrogen from decaying plant and animal residues (proteins, nucleic acids, amino sugars and urea) is converted to ammonia (NH_3) and ammonium (NH_4^+) by biological activity.

Mitigation A human intervention to reduce the *sources* or enhance the *sinks* of *greenhouse gases*.

Mixing ratio See *Mole fraction*.

Model drift Since model *climate* differs to some extent from observed climate, *climate forecasts* will typically 'drift' from the initial observation-based state towards the model's climate. This drift occurs at different time scales for different variables, can obscure the initial-condition forecast information and is usually removed a posteriori by an empirical, usually linear, adjustment.

Model hierarchy See *Climate model (spectrum or hierarchy)*.

Model initialization A *climate forecast* typically proceeds by integrating a *climate model* forward in time from an initial state that is intended to reflect the actual state of the *climate system*. Available observations of the climate system are 'assimilated' into the model. Initialization is a complex process that is limited by available observations, observational errors and, depending on the procedure used, may be affected by *uncertainty* in the history of climate forcing. The initial conditions will contain errors that grow as the forecast progresses, thereby limiting the time for which the forecast will be useful. See also *Climate prediction*.

Model spread The range or spread in results from *climate models*, such as those assembled for Coupled Model Intercomparison Project Phase 5 (CMIP5). Does not necessarily provide an exhaustive and formal estimate of the *uncertainty* in *feedbacks*, forcing or *projections* even when expressed numerically, for example, by computing a standard deviation of the models' responses. In order to quantify uncertainty, information from observations, physical constraints and expert judgement must be combined, using a statistical framework.

Mode of climate variability Underlying space–time structure with preferred spatial pattern and temporal variation that helps account for the gross features in variance and for *teleconnections*. A mode of variability is often considered to be the product of a spatial *climate pattern* and an associated *climate index* time series.

Mole fraction Mole fraction, or *mixing ratio*, is the ratio of the number of moles of a constituent in a given volume to the total number of moles of all constituents in that volume. It is usually reported for dry air. Typical values for *well-mixed greenhouse gases* are in the order of µmol mol^{-1} (parts per million: *ppm*), nmol mol^{-1} (parts per billion: *ppb*), and fmol mol^{-1} (parts per trillion: *ppt*). Mole fraction differs from *volume mixing ratio*, often expressed in ppmv etc., by the corrections for non-ideality of gases. This correction is significant relative to measurement precision for many greenhouse gases (Schwartz and Warneck, 1995).

Monsoon A monsoon is a tropical and subtropical seasonal reversal in both the surface winds and associated precipitation, caused by differential heating between a continental-scale land mass and the adjacent ocean. Monsoon rains occur mainly over land in summer.

Montreal Protocol The Montreal Protocol on Substances that Deplete the *Ozone Layer* was adopted in Montreal in 1987, and subsequently adjusted and amended in London (1990), Copenhagen (1992), Vienna (1995), Montreal (1997) and Beijing (1999). It controls the consumption and production of chlorine- and bromine-containing chemicals that destroy stratospheric *ozone*, such as chlorofluorocarbons, methyl chloroform, carbon tetrachloride and many others.

Near-surface permafrost A term frequently used in *climate model* applications to refer to *permafrost* at depths close to the ground surface (typically down to 3.5 m). In modelling studies, near-surface permafrost is usually diagnosed from 20 or 30 year climate averages, which is different from the conventional definition of permafrost. Disappearance of near-surface permafrost in a location does not preclude the longer-term persistence of permafrost at greater depth. See also *Active layer*, *Frozen ground* and *Thermokarst*.

Near-term climate forcers (NTCF) Near-term climate forcers (NTCF) refer to those compounds whose impact on *climate* occurs primarily within the first decade after their emission. This set of compounds is primarily composed of those with short *lifetimes* in the atmosphere compared to *well-mixed greenhouse gases*, and has been sometimes referred to as short lived climate forcers or short-lived climate pollutants. However, the common property that is of greatest interest to a climate assessment is the timescale over which their impact on climate is felt. This set of compounds includes *methane*, which is also a well-mixed greenhouse gas, as well as *ozone* and *aerosols*, or their *precursors*, and some halogenated species that are not well-mixed greenhouse gases. These compounds do not accumulate in the atmosphere at decadal to centennial timescales, and so their effect on climate is predominantly in the near term following their emission.

Nitrogen deposition Nitrogen deposition is defined as the nitrogen transferred from the *atmosphere* to the Earth's surface by the processes of wet deposition and dry deposition.

Nitrous oxide (N_2O) One of the six *greenhouse gases* to be mitigated under the *Kyoto Protocol*. The main *anthropogenic source* of nitrous oxide is agriculture (soil and animal manure management), but important contributions also come from sewage treatment, combustion of fossil fuel, and chemical industrial processes. Nitrous oxide is also produced naturally from a wide variety of biological sources in soil and water, particularly microbial action in wet tropical *forests*.

Nonlinearity A process is called *nonlinear* when there is no simple proportional relation between cause and effect. The *climate system* contains many such nonlinear processes, resulting in a system with potentially very complex behaviour. Such complexity may lead to *abrupt climate change*. See also *Chaotic* and *Predictability*.

North Atlantic Oscillation (NAO) The North Atlantic Oscillation consists of opposing variations of surface pressure near Iceland and near the Azores. It therefore corresponds to fluctuations in the strength of the main westerly winds across the Atlantic into Europe, and thus to fluctuations in the embedded *extratropical cyclones* with their associated frontal systems. See NAO Index, Box 2.5.

Northern Annular Mode (NAM) A winter fluctuation in the amplitude of a pattern characterized by low surface pressure in the Arctic and strong mid-latitude westerlies. The NAM has links with the northern polar vortex into the *stratosphere*. Its pattern has a bias to the North Atlantic and its index has a large correlation with the *North Atlantic Oscillation* index. See NAM Index, Box 2.5.

Ocean acidification Ocean acidification refers to a reduction in the *pH* of the ocean over an extended period, typically decades or longer, which is caused primarily by *uptake* of *carbon dioxide* from the *atmosphere*, but can also be caused by other chemical additions or subtractions from the ocean. *Anthropogenic ocean acidification* refers to the component of pH reduction that is caused by human activity (IPCC, 2011, p. 37).

Ocean heat uptake efficiency This is a measure (W m^{-2} $°C^{-1}$) of the rate at which heat storage by the global ocean increases as *global mean surface temperature* rises. It is a useful parameter for *climate change* experiments in which the *radiative forcing* is changing monotonically, when it can be compared with the *Climate Feedback Parameter* to gauge the relative importance of *climate response* and ocean heat *uptake* in determining the rate of climate change. It can be estimated from such an experiment as the ratio of the rate of increase of ocean heat content to the global mean surface air temperature change.

Organic aerosol Component of the *aerosol* that consists of organic compounds, mainly carbon, hydrogen, oxygen and lesser amounts of other elements. See also *Carbonaceous aerosol*.

Outgoing longwave radiation Net outgoing radiation in the infrared part of the spectrum at the top of the *atmosphere*. See also *Terrestrial radiation*.

Outlet glacier A *glacier*, usually between rock walls, that is part of, and drains an *ice sheet*. See also *Ice stream*.

Ozone Ozone, the triatomic form of oxygen (O_3), is a gaseous atmospheric constituent. In the *troposphere*, it is created both naturally and by photochemical reactions involving gases resulting from human activities (*smog*). Tropospheric ozone acts as a *greenhouse gas*. In the *stratosphere*, it is created by the interaction between solar ultraviolet radiation and molecular oxygen (O_2). Stratospheric ozone plays a dominant role in the stratospheric radiative balance. Its concentration is highest in the *ozone layer*.

Ozone hole See *Ozone layer*.

Ozone layer The *stratosphere* contains a layer in which the concentration of *ozone* is greatest, the so-called ozone layer. The layer extends from about 12 to 40 km above the Earth's surface. The ozone concentration reaches a maximum between about 20 and 25 km. This layer has been depleted by human emissions of chlorine and bromine compounds. Every year, during the Southern Hemisphere spring, a very strong depletion of the ozone layer takes place over the Antarctic, caused by *anthropogenic* chlorine and bromine compounds in combination with the specific meteorological conditions of that *region*. This phenomenon is called the *Ozone hole*. See also *Montreal Protocol*.

Pacific Decadal Oscillation (PDO) The pattern and time series of the first empirical orthogonal function of *sea surface temperature* over the North Pacific north of 20°N. The PDO broadened to cover the whole Pacific Basin is known as the Inter-decadal Pacific Oscillation. The PDO and IPO exhibit similar temporal evolution. See also *Pacific Decadal Variability*.

Pacific decadal variability Coupled decadal-to-inter-decadal variability of the atmospheric circulation and underlying ocean in the Pacific Basin. It is most prominent in the North Pacific, where fluctuations in the strength of the winter Aleutian Low pressure system co-vary with North Pacific *sea surface temperatures*, and are linked to decadal variations in atmospheric circulation, sea surface temperatures and ocean circulation throughout the whole Pacific Basin. Such fluctuations have the effect of modulating the *El Niño-Southern Oscillation* cycle. Key measures of Pacific decadal variability are the *North Pacific Index (NPI)*, the *Pacific Decadal Oscillation (PDO)* index and the *Inter-decadal Pacific Oscillation (IPO)* index, all defined in Box 2.5.

Pacific–North American (PNA) pattern An atmospheric large-scale wave pattern featuring a sequence of tropospheric high and low pressure anomalies stretching from the subtropical west Pacific to the east coast of North America. See PNA pattern index, Box 2.5.

Paleoclimate *Climate* during periods prior to the development of measuring instruments, including historic and geologic time, for which only *proxy* climate records are available.

Parameterization In *climate models*, this term refers to the technique of representing processes that cannot be explicitly resolved at the spatial or temporal *resolution* of the model (sub-grid scale processes) by relationships between model-resolved larger-scale variables and the area- or time-averaged effect of such subgrid scale processes.

Percentiles The set of partition values which divides the total population of a distribution into 100 equal parts, the 50th percentile corresponding to the *median* of the population.

Permafrost Ground (soil or rock and included ice and organic material) that remains at or below 0°C for at least two consecutive years. See also *Near-surface permafrost*.

pH pH is a dimensionless measure of the acidity of water (or any solution) given by its concentration of hydrogen ions (H^+). pH is measured on a logarithmic scale where $pH = -\log_{10}(H^+)$. Thus, a pH decrease of 1 unit corresponds to a 10-fold increase in the concentration of H^+, or acidity.

Photosynthesis The process by which plants take *carbon dioxide* from the air (or bicarbonate in water) to build carbohydrates, releasing oxygen in the process. There are several pathways of photosynthesis with different responses to atmospheric carbon dioxide concentrations. See also *Carbon dioxide fertilization*.

Plankton Microorganisms living in the upper layers of aquatic systems. A distinction is made between *phytoplankton*, which depend on *photosynthesis* for their energy supply, and *zooplankton*, which feed on phytoplankton.

Pleistocene The Pleistocene Epoch is the earlier of two epochs in the *Quaternary* System, extending from 2.59 Ma to the beginning of the *Holocene* at 11.65 ka.

Pliocene The Plionece Epoch is the last epoch of the *Neogene* System and extends from 5.33 Ma to the beginning of the *Pleistocene* at 2.59 Ma.

Pollen analysis A technique of both relative dating and environmental *reconstruction*, consisting of the identification and counting of pollen types preserved in peat, lake sediments and other deposits. See also *Proxy*.

Precipitable water The total amount of atmospheric water vapour in a vertical column of unit cross-sectional area. It is commonly expressed in terms of the height of the water if completely condensed and collected in a vessel of the same unit cross section.

Precursors Atmospheric compounds that are not *greenhouse gases* or *aerosols*, but that have an effect on greenhouse gas or aerosol concentrations by taking part in physical or chemical processes regulating their production or destruction rates.

Predictability The extent to which future states of a system may be predicted based on knowledge of current and past states of the system. Because knowledge of the *climate system*'s past and current states is generally imperfect, as are the models that utilize this knowledge to produce a *climate prediction*, and because the climate system is inherently *nonlinear* and *chaotic*, predictability of the climate system is inherently limited. Even with arbitrarily accurate models and observations, there may still be limits to the predictability of such a nonlinear system (AMS, 2000).

Prediction quality/skill Measures of the success of a *prediction* against observationally based information. No single measure can summarize all aspects of forecast quality and a suite of *metrics* is considered. Metrics will differ for forecasts given in deterministic and probabilistic form. See also *Climate prediction*.

Pre-industrial See *Industrial Revolution*.

Probability Density Function (PDF) A probability density function is a function that indicates the relative chances of occurrence of different outcomes of a variable. The function integrates to unity over the domain for which it is defined and has the property that the integral over a sub-domain equals the probability that the outcome of the variable lies within that sub-domain. For example, the probability that a temperature anomaly defined in a particular way is greater than zero is obtained from its PDF by integrating the PDF over all possible temperature anomalies greater than zero. Probability density functions that describe two or more variables simultaneously are similarly defined.

Process-based Model Theoretical concepts and computational methods that represent and simulate the behaviour of real-world systems derived from a set of functional components and their interactions with each other and the system environment, through physical and mechanistic processes occurring over time. See also *Climate model*.

Projection A projection is a potential future evolution of a quantity or set of quantities, often computed with the aid of a model. Unlike predictions, projections are conditional on assumptions concerning, for example, future socioeconomic and technological developments that may or may not be realized. See also *Climate prediction* and *Climate projection*.

Proxy A proxy *climate* indicator is a record that is interpreted, using physical and biophysical principles, to represent some combination of climate-related variations back in time. Climate-related data derived in this way are referred to as proxy data. Examples of proxies include *pollen analysis*, *tree ring* records, speleothems, characteristics of corals and various data derived from marine sediments and *ice cores*. Proxy-data can be calibrated to provide quantitative climate information.

Quasi-Biennal Oscillation (QBO) A near-periodic oscillation of the equatorial zonal wind between easterlies and westerlies in the tropical *stratosphere* with a mean period of around 28 months. The alternating wind maxima descend from the base of the mesosphere down to the *tropopause*, and are driven by wave energy that propagates up from the *troposphere*.

Quaternary The Quaternary System is the latter of three systems that make up the *Cenozoic Era* (65 Ma to present), extending from 2.59 Ma to the present, and includes the *Pleistocene* and *Holocene* epochs.

Radiative effect The impact on a radiation flux or heating rate (most commonly, on the downward flux at the top of *atmosphere*) caused by the interaction of a particular constituent with either the *infrared* or *solar radiation* fields through absorption, scattering and emission, relative to an otherwise identical atmosphere free of that constituent. This quantifies the impact of the constituent on the *climate system*. Examples include the *aerosol–radiation interactions*, *cloud radiative effect*, and *greenhouse effect*. In this report, the portion of any top-of-atmosphere radiative effect that is due to *anthropogenic* or other external influences (e.g., volcanic eruptions or changes in the sun) is termed the *instantaneous radiative forcing*.

Radiative forcing Radiative forcing is the change in the net, downward minus upward, radiative flux (expressed in W m^{-2}) at the *tropopause* or top of *atmosphere* due to a change in an external driver of *climate change*, such as, for example, a change in the concentration of *carbon dioxide* or the output of the Sun. Sometimes internal drivers are still treated as forcings even though they result from the alteration in *climate*, for example *aerosol* or *greenhouse gas* changes in *paleoclimates*. The traditional radiative forcing is computed with all tropospheric properties held fixed at their unperturbed values, and after allowing for stratospheric temperatures, if perturbed, to readjust to radiative-dynamical equilibrium. Radiative forcing is called *instantaneous* if no change in stratospheric temperature is accounted for. The radiative forcing once *rapid adjustments* are accounted for is termed the *effective radiative forcing.* For the purposes of this report, radiative forcing is further defined as the change relative to the year 1750 and, unless otherwise noted, refers to a global and annual average value. Radiative forcing is not to be confused with *cloud radiative forcing*, which describes an unrelated measure of the impact of clouds on the radiative flux at the top of the atmosphere.

Rapid adjustment The response to an agent perturbing the *climate system* that is driven directly by the agent, independently of any change in the *global mean surface temperature*. For example, *carbon dioxide* and *aerosols*, by altering internal heating and cooling rates within the *atmosphere*, can each cause changes to cloud cover and other variables thereby producing a *radiative effect* even in the absence of any surface warming or cooling. Adjustments are *rapid* in the sense that they begin to occur right away, before *climate feedbacks* which are driven by warming (although some adjustments may still take significant time to proceed to completion, for example those involving vegetation or *ice sheets*). It is also called the *rapid response* or *fast adjustment*. For further explanation on the concept, see Sections 7.1 and 8.1.

Rapid climate change See *Abrupt climate change*.

Rapid dynamical change (of glaciers or ice sheets) Changes in *glacier* or *ice sheet* mass controlled by changes in flow speed and *discharge* rather than by *accumulation* or *ablation*. This can result in a rate of mass change larger than that due to any imbalance between accumulation and ablation. Rapid dynamical change may be initiated by a climatic trigger, such as incursion of warm ocean water beneath an *ice shelf*, or thinning of a grounded tidewater terminus, which may lead to reactions within the glacier system, that may result in rapid ice loss. See also *Mass balance/budget (of glaciers or ice sheets)*.

Reanalysis Reanalyses are estimates of historical atmospheric temperature and wind or oceanographic temperature and current, and other quantities, created by processing past meteorological or oceanographic data using fixed state-of-the-art weather forecasting or ocean circulation models with data assimilation techniques. Using fixed data assimilation avoids effects from the changing analysis system that occur in operational analyses. Although continuity is improved, global reanalyses still suffer from changing coverage and biases in the observing systems.

Rebound effect When CO_2 is removed from the *atmosphere*, the CO_2 concentration gradient between atmospheric and land/ocean carbon *reservoirs* is reduced. This leads to a reduction or reversal in subsequent inherent rate of removal of CO_2 from the atmosphere by natural *carbon cycle* processes on land and ocean.

Reconstruction (of climate variable) Approach to reconstructing the past temporal and spatial characteristics of a climate variable from predictors. The predictors can be instrumental data if the reconstruction is used to infill missing data or *proxy* data if it is used to develop *paleoclimate* reconstructions. Various techniques have been developed for this purpose: linear multivariate regression based methods and nonlinear *Bayesian* and analog methods.

Reforestation Planting of *forests* on lands that have previously contained forests but that have been converted to some other use. For a discussion of the term *forest* and related terms such as *afforestation*, *reforestation* and *deforestation*, see the IPCC Report on Land Use, Land-Use Change and Forestry (IPCC, 2000). See also the Report on Definitions and Methodological Options to Inventory Emissions from Direct Human-induced Degradation of Forests and Devegetation of Other Vegetation Types (IPCC, 2003).

Region A region is a territory characterized by specific geographical and climatological features. The *climate* of a region is affected by regional and local scale features like topography, *land use* characteristics and lakes, as well as remote influences from other regions. See also *Teleconnection*.

Regional Climate Model (RCM) A *climate model* at higher *resolution* over a limited area. Such models are used in *downscaling* global *climate* results over specific regional domains.

Relative humidity The relative humidity specifies the ratio of actual water vapour pressure to that at saturation with respect to liquid water or ice at the same temperature. See also *Specific humidity*.

Relative sea level Sea level measured by a *tide gauge* with respect to the land upon which it is situated. See also *Mean sea level* and *Sea level change*.

Representative Concentration Pathways (RCPs) *Scenarios* that include time series of emissions and concentrations of the full suite of *greenhouse gases* and *aerosols* and chemically active gases, as well as *land use*/land cover (Moss et al., 2008). The word *representative* signifies that each RCP provides only one of many possible scenarios that would lead to the specific *radiative forcing* characteristics. The term *pathway* emphasizes that not only the long-term concentration levels are of interest, but also the trajectory taken over time to reach that outcome. (Moss et al., 2010).

RCPs usually refer to the portion of the concentration pathway extending up to 2100, for which Integrated Assessment Models produced corresponding *emission scenarios*. *Extended Concentration Pathways (ECPs)* describe extensions of the RCPs from 2100 to 2500 that were calculated using simple rules generated by stakeholder consultations, and do not represent fully consistent scenarios.

Four RCPs produced from Integrated Assessment Models were selected from the published literature and are used in the present IPCC Assessment as a basis for the *climate predictions* and *projections* presented in Chapters 11 to 14:

RCP2.6 One pathway where radiative forcing peaks at approximately 3 W m^{-2} before 2100 and then declines (the corresponding ECP assuming constant emissions after 2100)

RCP4.5 and RCP6.0 Two intermediate *stabilization pathways* in which radiative forcing is stabilized at approximately 4.5 W m^{-2} and 6.0 W m^{-2} after 2100 (the corresponding ECPs assuming constant concentrations after 2150)

RCP8.5 One high pathway for which radiative forcing reaches greater than 8.5 W m^{-2} by 2100 and continues to rise for some amount of time (the corresponding ECP assuming constant emissions after 2100 and constant concentrations after 2250)

For further description of future scenarios, see Box 1.1.

Reservoir A component of the *climate system*, other than the *atmosphere*, which has the capacity to store, accumulate or release a substance of concern, for example, carbon, a *greenhouse gas* or a *precursor*. Oceans, soils and *forests* are examples of reservoirs of carbon. *Pool* is an equivalent term (note that the definition of pool often includes the atmosphere). The absolute quantity of the substance of concern held within a reservoir at a specified time is called the *stock*.

Resolution In *climate models*, this term refers to the physical distance (metres or degrees) between each point on the grid used to compute the equations. *Temporal resolution* refers to the time step or time elapsed between each model computation of the equations.

Respiration The process whereby living organisms convert organic matter to *carbon dioxide*, releasing energy and consuming molecular oxygen.

Response time The response time or *adjustment time* is the time needed for the *climate system* or its components to re-equilibrate to a new state, following a forcing resulting from external processes. It is very different for various components of the climate system. The response time of the *troposphere* is relatively short, from days to weeks, whereas the *stratosphere* reaches equilibrium on a time scale of typically a few months. Due to their large heat capacity, the oceans have a much longer response time: typically decades, but up to centuries or millennia. The response time of the strongly coupled surface–troposphere system is, therefore, slow compared to that of the stratosphere, and mainly determined by the oceans. The *biosphere* may respond quickly (e.g., to *droughts*), but also very slowly to imposed changes. See *lifetime* for a different definition of response time pertinent to the rate of processes affecting the concentration of trace gases.

Return period An estimate of the average time interval between occurrences of an event (e.g., flood or extreme rainfall) of (or below/above) a defined size or intensity. See also *Return value*.

Return value The highest (or, alternatively, lowest) value of a given variable, on average occurring once in a given period of time (e.g., in 10 years). See also *Return period*.

River discharge See *Streamflow*.

Runoff That part of precipitation that does not evaporate and is not transpired, but flows through the ground or over the ground surface and returns to bodies of water. See also *Hydrological cycle*.

Scenario A plausible description of how the future may develop based on a coherent and internally consistent set of assumptions about key driving forces (e.g., rate of technological change, prices) and relationships. Note that scenarios are neither predictions nor forecasts, but are useful to provide a view of the implications of developments and actions. See also *Climate scenario*, *Emission scenario*, *Representative Concentration Pathways* and *SRES scenarios*.

Sea ice Ice found at the sea surface that has originated from the freezing of seawater. Sea ice may be discontinuous pieces (ice floes) moved on the ocean surface by wind and currents (pack ice), or a motionless sheet attached to the coast (land-fast ice). *Sea ice concentration* is the fraction of the ocean covered by ice. Sea ice less than one year old is called *first-year ice*. *Perennial ice* is sea ice that survives at least one summer. It may be subdivided into *second-year ice* and *multi-year ice*, where multiyear ice has survived at least two summers.

Sea level change Sea level can change, both globally and locally due to (1) changes in the shape of the ocean basins, (2) a change in ocean volume as a result of a change in the mass of water in the ocean, and (3) changes in ocean volume as a result of changes in ocean water density. Global *mean sea level* change resulting from change in the mass of the ocean is called *barystatic*. The amount of barystatic sea level change due to the addition or removal of a mass of water is called its *sea level equivalent (SLE)*. Sea level changes, both globally and locally, resulting from changes in water density are called *steric*. Density changes induced by temperature changes only are called *thermosteric*, while density changes induced by salinity changes are called *halosteric*. Barystatic and steric sea level changes do not include the effect of changes in the shape of ocean basins induced by the change in the ocean mass and its distribution. See also *Relative Sea Level* and *Thermal expansion*.

Sea level equivalent (SLE) The sea level equivalent of a mass of water (ice, liquid or vapour) is that mass, converted to a volume using a density of 1000 kg m^{-3}, and divided by the present-day ocean surface area of 3.625×10^{14} m^2. Thus, 362.5 Gt of water mass added to the ocean will cause 1 mm of global *mean sea level* rise. See also *Sea level change*.

Seasonally frozen ground See *Frozen ground*.

Sea surface temperature (SST) The sea surface temperature is the subsurface bulk temperature in the top few metres of the ocean, measured by ships, buoys and drifters. From ships, measurements of water samples in buckets were mostly switched in the 1940s to samples from engine intake water. Satellite measurements of *skin temperature* (uppermost layer; a fraction of a millimetre thick) in the infrared or the top centimetre or so in the microwave are also used, but must be adjusted to be compatible with the bulk temperature.

Semi-direct (aerosol) effect See *Aerosol–radiation interaction*.

Semi-empirical model Model in which calculations are based on a combination of observed associations between variables and theoretical considerations relating variables through fundamental principles (e.g., conservation of energy). For example, in sea level studies, semi-empirical models refer specifically to transfer functions formulated to project future global *mean sea level change*, or contributions to it, from future *global mean surface temperature* change or *radiative forcing*.

Sensible heat flux The turbulent or conductive flux of heat from the Earth's surface to the *atmosphere* that is not associated with phase changes of water; a component of the surface *energy budget*.

Sequestration See *Uptake*.

Shortwave radiation See *Solar radiation*.

Significant wave height The average trough-to-crest height of the highest one third of the wave heights (sea and swell) occurring in a particular time period.

Sink Any process, activity or mechanism that removes a *greenhouse gas*, an *aerosol* or a *precursor* of a greenhouse gas or aerosol from the *atmosphere*.

Slab-ocean model A simplified representation in a *climate model* of the ocean as a motionless layer of water with a depth of 50 to 100 m. Climate models with a slab ocean can be used only for estimating the equilibrium response of *climate* to a given forcing, not the transient evolution of climate. See also *Equilibrium and transient climate experiment*.

Snow cover extent The areal extent of snow covered ground.

Snow water equivalent (SWE) The depth of liquid water that would result if a mass of snow melted completely.

Soil moisture Water stored in the soil in liquid or frozen form.

Soil temperature The temperature of the soil. This can be measured or modelled at multiple levels within the depth of the soil.

Solar activity General term describing a variety of magnetic phenomena on the Sun such as *sunspots*, *faculae* (bright areas), and flares (emission of high-energy particles). It varies on time scales from minutes to millions of years. See also *Solar cycle*.

Solar ('11-year') cycle A quasi-regular modulation of *solar activity* with varying amplitude and a period of between 8 and 14 years.

Solar radiation Electromagnetic radiation emitted by the Sun with a spectrum close to the one of a black body with a temperature of 5770 K. The radiation peaks in visible wavelengths. When compared to the *terrestrial radiation* it is often referred to as *shortwave radiation*. See also *Insolation* and *Total solar irradiance (TSI)*.

Solar Radiation Management (SRM) Solar Radiation Management refers to the intentional modification of the Earth's shortwave radiative budget with the aim to reduce *climate change* according to a given *metric* (e.g., *surface temperature*, precipitation, regional impacts, etc). Artificial injection of stratospheric *aerosols* and cloud brightening are two examples of SRM techniques. Methods to modify some fast-responding elements of the longwave radiative budget (such as cirrus clouds), although not strictly speaking SRM, can be related to SRM. SRM techniques do not fall within the usual definitions of *mitigation* and adaptation (IPCC, 2012, p. 2). See also *Solar radiation*, *Carbon Dioxide Removal (CDR)* and *Geoengineering*.

Solubility pump Solubility pump is an important physicochemical process that transports dissolved inorganic carbon from the ocean's surface to its interior. This process controls the inventory of carbon in the ocean. The solubility of gaseous *carbon dioxide* can alter carbon dioxide concentrations in the oceans and the overlying *atmosphere*. See also *Biological pump*.

Source Any process, activity or mechanism that releases a *greenhouse gas*, an *aerosol* or a *precursor* of a greenhouse gas or aerosol into the *atmosphere*.

Southern Annular Mode (SAM) The leading mode of variability of Southern Hemisphere geopotential height, which is associated with shifts in the latitude of the midlatitude jet. See SAM Index, Box 2.5.

Southern Oscillation See *El Niño-Southern Oscillation (ENSO)*.

South Pacific Convergence Zone (SPCZ) A band of low-level convergence, cloudiness and precipitation ranging from the west Pacific warm pool south-eastwards towards French Polynesia, which is one of the most significant features of subtropical Southern Hemisphere *climate*. It shares some characteristics with the *ITCZ*, but is more extratropical in nature, especially east of the Dateline.

Spatial and temporal scales *Climate* may vary on a large range of spatial and temporal scales. Spatial scales may range from local (less than 100 000 km^2), through regional (100 000 to 10 million km^2) to continental (10 to 100 million km^2). Temporal scales may range from seasonal to geological (up to hundreds of millions of years).

Specific humidity The specific humidity specifies the ratio of the mass of water vapour to the total mass of moist air. See also *Relative humidity*.

SRES scenarios SRES scenarios are *emission scenarios* developed by Nakićenović and Swart (2000) and used, among others, as a basis for some of the *climate projections* shown in Chapters 9 to 11 of IPCC (2001) and Chapters 10 and 11 of IPCC (2007). The following terms are relevant for a better understanding of the structure and use of the set of SRES scenarios:

> **Scenario family** Scenarios that have a similar demographic, societal, economic and technical change storyline. Four scenario families comprise the SRES scenario set: A1, A2, B1 and B2.

Illustrative Scenario A scenario that is illustrative for each of the six scenario groups reflected in the Summary for Policymakers of Nakićenović and Swart (2000). They include four revised *marker scenarios* for the scenario groups A1B, A2, B1, B2 and two additional scenarios for the A1FI and A1T groups. All scenario groups are equally sound.

Marker Scenario A scenario that was originally posted in draft form on the SRES website to represent a given scenario family. The choice of markers was based on which of the initial quantifications best reflected the storyline, and the features of specific models. Markers are no more likely than other scenarios, but are considered by the SRES writing team as illustrative of a particular storyline. They are included in revised form in Nakićenović and Swart (2000). These scenarios received the closest scrutiny of the entire writing team and via the SRES open process. Scenarios were also selected to illustrate the other two scenario groups.

Storyline A narrative description of a scenario (or family of scenarios), highlighting the main scenario characteristics, relationships between key driving forces and the dynamics of their evolution.

Steric See *Sea level change*.

Stock See *Reservoir*.

Storm surge The temporary increase, at a particular locality, in the height of the sea due to extreme meteorological conditions (low atmospheric pressure and/or strong winds). The storm surge is defined as being the excess above the level expected from the tidal variation alone at that time and place.

Storm tracks Originally, a term referring to the tracks of individual cyclonic weather systems, but now often generalized to refer to the main *regions* where the tracks of extratropical disturbances occur as sequences of low (cyclonic) and high (anticyclonic) pressure systems.

Stratosphere The highly stratified region of the *atmosphere* above the *troposphere* extending from about 10 km (ranging from 9 km at high latitudes to 16 km in the tropics on average) to about 50 km altitude.

Streamflow Water flow within a river channel, for example expressed in $m^3\ s^{-1}$. A synonym for *river discharge*.

Subduction Ocean process in which surface waters enter the ocean interior from the surface mixed layer through *Ekman pumping* and lateral *advection*. The latter occurs when surface waters are advected to a region where the local surface layer is less dense and therefore must slide below the surface layer, usually with no change in density.

Sunspots Dark areas on the Sun where strong magnetic fields reduce the convection causing a temperature reduction of about 1500 K compared to the surrounding regions. The number of sunspots is higher during periods of higher *solar activity*, and varies in particular with the *solar cycle.*

Surface layer See *Atmospheric boundary layer*.

Surface temperature See *Global mean surface temperature*, *Land surface air temperature* and *Sea surface temperature*.

Talik A layer of year-round unfrozen ground that lies in *permafrost* areas.

Teleconnection A statistical association between climate variables at widely separated, geographically-fixed spatial locations. Teleconnections are caused by large spatial structures such as basin-wide coupled modes of ocean–*atmosphere* variability, Rossby wave-trains, mid-latitude jets and *storm tracks*, etc. See also *Teleconnection pattern*.

Teleconnection pattern A correlation map obtained by calculating the correlation between variables at different spatial locations and a *climate index*. It is the special case of a *climate pattern* obtained for standardized variables and a standardized climate index, that is, the variables and index are each centred and scaled to have zero mean and unit variance. One-point teleconnection maps are made by choosing a variable at one of the locations to be the climate index. See also *Teleconnection*.

Terrestrial radiation Radiation emitted by the Earth's surface, the *atmosphere* and the clouds. It is also known as *thermal infrared* or *longwave radiation*, and is to be distinguished from the near-infrared radiation that is part of the solar spectrum. *Infrared radiation*, in general, has a distinctive range of wavelengths (*spectrum*) longer than the wavelength of the red light in the visible part of the spectrum. The spectrum of terrestrial radiation is almost entirely distinct from that of shortwave or *solar radiation* because of the difference in temperature between the Sun and the Earth–atmosphere system. See also *Outgoing longwave radiation*.

Thermal expansion In connection with sea level, this refers to the increase in volume (and decrease in density) that results from warming water. A warming of the ocean leads to an expansion of the ocean volume and hence an increase in sea level. See also *Sea level change*.

Thermocline The layer of maximum vertical temperature gradient in the ocean, lying between the surface ocean and the abyssal ocean. In subtropical regions, its source waters are typically surface waters at higher latitudes that have *subducted* (see *Subduction*) and moved equatorward. At high latitudes, it is sometimes absent, replaced by a *halocline*, which is a layer of maximum vertical salinity gradient.

Thermohaline circulation (THC) Large-scale circulation in the ocean that transforms low-density upper ocean waters to higher-density intermediate and deep waters and returns those waters back to the upper ocean. The circulation is asymmetric, with conversion to dense waters in restricted regions at high latitudes and the return to the surface involving slow upwelling and diffusive processes over much larger geographic regions. The THC is driven by high densities at or near the surface, caused by cold temperatures and/or high salinities, but despite its suggestive though common name, is also driven by mechanical forces such as wind and tides. Frequently, the name THC has been used synonymously with *Meridional Overturning Circulation*.

Thermokarst The process by which characteristic landforms result from the thawing of ice-rich *permafrost* or the melting of massive ground ice.

Thermosteric See *Sea level change*.

Tide gauge A device at a coastal or deep-sea location that continuously measures the level of the sea with respect to the adjacent land. Time averaging of the sea level so recorded gives the observed secular changes of the *relative sea level*.

Tipping point In *climate*, a hypothesized critical threshold when global or regional *climate changes* from one stable state to another stable state. The tipping point event may be irreversible. See also *Irreversibility*.

Total solar irradiance (TSI) The total amount of *solar radiation* in watts per square metre received outside the Earth's *atmosphere* on a surface normal to the incident radiation, and at the Earth's mean distance from the Sun.

Reliable measurements of solar radiation can only be made from space and the precise record extends back only to 1978. The generally accepted value is 1368 W m^{-2} with an accuracy of about 0.2%. It has recently been estimated to 1360.8 ± 0.5 W m^{-2} for the solar minimum of 2008. Variations of a few tenths of a percent are common, usually associated with the passage of *sunspots* across the solar disk. The *solar cycle* variation of TSI is of the order of 0.1% (AMS, 2000). Changes in the ultraviolet part of the spectrum during a solar cycle are comparatively larger (percent) than in TSI. See also *Insolation*.

Transient climate response See *Climate sensitivity*.

Transient climate response to cumulative CO_2 emissions (TCRE) The transient global average *surface temperature* change per unit cumulated *CO_2* emissions, usually 1000 PgC. TCRE combines both information on the *airborne fraction* of cumulated CO_2 emissions (the fraction of the total CO_2 emitted that remains in the *atmosphere*), and on the *transient climate response* (TCR).

Tree rings Concentric rings of secondary wood evident in a cross section of the stem of a woody plant. The difference between the dense, small-celled late wood of one season and the wide-celled early wood of the following spring enables the age of a tree to be estimated, and the ring widths or density can be related to climate parameters such as temperature and precipitation. See also *Proxy*.

Trend In this report, the word *trend* designates a change, generally monotonic in time, in the value of a variable.

Tropopause The boundary between the *troposphere* and the *stratosphere*.

Troposphere The lowest part of the *atmosphere*, from the surface to about 10 km in altitude at mid-latitudes (ranging from 9 km at high latitudes to 16 km in the tropics on average), where clouds and weather phenomena occur. In the troposphere, temperatures generally decrease with height. See also *Stratosphere*.

Turnover time See *Lifetime*.

Uncertainty A state of incomplete knowledge that can result from a lack of information or from disagreement about what is known or even knowable. It may have many types of sources, from imprecision in the data to ambiguously defined concepts or terminology, or uncertain *projections* of human behaviour. Uncertainty can therefore be represented by quantitative measures (e.g., a *probability density function*) or by qualitative statements (e.g., reflecting the judgment of a team of experts) (see Moss and Schneider, 2000; Manning et al., 2004; Mastrandrea et al., 2010). See also *Confidence* and *Likelihood*.

United Nations Framework Convention on Climate Change (UNFCCC) The Convention was adopted on 9 May 1992 in New York and signed at the 1992 Earth Summit in Rio de Janeiro by more than 150 countries and the European Community. Its ultimate objective is the 'stabilisation of *greenhouse gas* concentrations in the *atmosphere* at a level that would prevent dangerous *anthropogenic* interference with the *climate system*'. It contains commitments for all Parties. Under the Convention, Parties included in Annex I (all OECD countries and countries with economies in transition) aim to return greenhouse gas emissions not controlled by the *Montreal Protocol* to 1990 levels by the year 2000. The convention entered in force in March 1994. In 1997, the UNFCCC adopted the *Kyoto Protocol*.

Uptake The addition of a substance of concern to a *reservoir*. The uptake of carbon containing substances, in particular *carbon dioxide*, is often called (carbon) *sequestration*.

Urban heat island (UHI) The relative warmth of a city compared with surrounding rural areas, associated with changes in *runoff*, effects on heat retention, and changes in surface *albedo*.

Ventilation The exchange of ocean properties with the atmospheric *surface layer* such that property concentrations are brought closer to equilibrium values with the *atmosphere* (AMS, 2000), and the processes that propagate these properties into the ocean interior.

Volatile Organic Compounds (VOC) Important class of organic chemical air pollutants that are volatile at ambient air conditions. Other terms used to represent VOCs are *hydrocarbons* (HCs), *reactive organic gases* (ROGs) and *non-methane volatile organic compounds* (NMVOCs). NMVOCs are major contributors (together with NO_x and CO) to the formation of photochemical oxidants such as *ozone*.

Walker Circulation Direct thermally driven zonal overturning circulation in the *atmosphere* over the tropical Pacific Ocean, with rising air in the western and sinking air in the eastern Pacific.

Warm days/warm nights Days where maximum temperature, or nights where minimum temperature, exceeds the 90th *percentile*, where the respective temperature distributions are generally defined with respect to the 1961–1990 *reference* period. For the corresponding indices, see Box 2.4.

Warm spell A period of abnormally hot weather. For the corresponding indices, see Box 2.4. See also *Heat wave*.

Water cycle See *Hydrological cycle*.

Water mass A body of ocean water with identifiable properties (temperature, salinity, density, chemical tracers) resulting from its unique formation process. Water masses are often identified through a vertical or horizontal extremum of a property such as salinity. North Pacific Intermediate Water (NPIW) and Antarctic Intermediate Water (AAIW) are examples of water masses.

Weathering The gradual removal of atmospheric *CO_2* through dissolution of silicate and carbonate rocks. Weathering may involve physical processes (*mechanical weathering*) or chemical activity (*chemical weathering*).

Well-mixed greenhouse gas See *Greenhouse gas*.

Younger Dryas A period 12.85 to 11.65 ka (thousand years before 1950), during the *deglaciation*, characterized by a temporary return to colder conditions in many locations, especially around the North Atlantic.

References

AMS, 2000: *AMS Glossary of Meteorology*, 2nd ed. American Meteorological Society, Boston, MA, http://amsglossary.allenpress.com/glossary/browse.

Hegerl, G. C., O. Hoegh-Guldberg, G. Casassa, M. P. Hoerling, R. S. Kovats, C. Parmesan, D. W. Pierce, and P. A. Stott, 2010: Good practice guidance paper on detection and attribution related to anthropogenic climate change. In: *Meeting Report of the Intergovernmental Panel on Climate Change Expert Meeting on Detection and Attribution of Anthropogenic Climate Change* [T. F. Stocker, C. B. Field, D. Qin, V. Barros, G.-K. Plattner, M. Tignor, P. M. Midgley and K. L. Ebi (eds.)]. IPCC Working Group I Technical Support Unit, University of Bern, Bern, Switzerland.

IPCC, 1992: *Climate Change 1992: The Supplementary Report to the IPCC Scientific Assessment* [J. T. Houghton, B. A. Callander and S. K. Varney (eds.)]. Cambridge University Press, Cambridge, United Kingdom and New York, NY, USA, 116 pp.

IPCC, 1996: *Climate Change 1995: The Science of Climate Change. Contribution of Working Group I to the Second Assessment Report of the Intergovernmental Panel on Climate Change* [J. T. Houghton., L. G. Meira . A. Callander, N. Harris, A. Kattenberg and K. Maskell (eds.)]. Cambridge University Press, Cambridge, United Kingdom and New York, NY, USA, 572 pp.

IPCC, 2000: *Land Use, Land-Use Change, and Forestry. Special Report of the Intergovernmental Panel on Climate Change* [R. T. Watson, I. R. Noble, B. Bolin, N. H. Ravindranath, D. J. Verardo, and D. J. Dokken (eds.)]. Cambridge University Press, Cambridge, United Kingdom and New York, NY, USA, 377 pp.

IPCC, 2001: *Climate Change 2001: The Scientific Basis. Contribution of Working Group I to the Third Assessment Report of the Intergovernmental Panel on Climate Change* [T. Houghton, Y. Ding, D. J. Griggs, M. Noquer, P. J. van der Linden, X. Dai, K. Maskell and C. A. Johnson (eds.)]. Cambridge University Press, Cambridge, United Kingdom and New York, NY, USA, 881 pp.

IPCC, 2003: Definitions and Methodological Options to Inventory Emissions from Direct Human-Induced Degradation of Forests and Devegetation of Other Vegetation Types [Penman, J., M. Gytarsky, T. Hiraishi, T. Krug, D. Kruger, R. Pipatti, L. Buendia, K. Miwa, T. Ngara, K. Tanabe and F. Wagner (eds.)]. The Institute for Global Environmental Strategies (IGES), Japan, 32 pp.

IPCC, 2007: *Climate Change 2007: The Physical Science Basis. Contribution of Working Group I to the Fourth Assessment Report of the Intergovernmental Panel on Climate Change.* [Solomon, S., D. Qin, M. Manning, Z. Chen, M. Marquis, K. B. Averyt, M. Tignor and H. L. Miller (eds.)]. Cambridge University Press, Cambridge, United Kingdom and New York, NY, USA, 996 pp.

IPCC, 2011: *Workshop Report of the Intergovernmental Panel on Climate Change Workshop on Impacts of Ocean Acidification on Marine Biology and Ecosystems* [C. B. Field, V. Barros, T. F. Stocker, D. Qin, K.J. Mach, G.-K. Plattner, M. D. Mastrandrea, M. Tignor and K. L. Ebi (eds.)]. IPCC Working Group II Technical Support Unit, Carnegie Institution, Stanford, CA, USA, 164 pp.

IPCC, 2012: *Meeting Report of the Intergovernmental Panel on Climate Change Expert Meeting on Geoengineering* [O. Edenhofer, R. Pichs-Madruga, Y. Sokona, C. Field, V. Barros, T. F. Stocker, Q. Dahe, J. Minx, K. Mach, G.-K. Plattner, S. Schlömer, G. Hansen and M. Mastrandrea (eds.)]. IPCC Working Group III Technical Support Unit, Potsdam Institute for Climate Impact Research, Potsdam, Germany, 99 pp.

Manning, M., et al., 2004: *IPCC Workshop on Describing Scientific Uncertainties in Climate Change to Support Analysis of Risk of Options*. Workshop Report. IPCC Working Group I Technical Support Unit, Boulder, CO, USA, 138 pp.

Mastrandrea, M. D., C. B. Field, T. F. Stocker, O. Edenhofer, K. L. Ebi, D. J. Frame, H. Held, E. Kriegler, K. J. Mach, P. R. Matschoss, G.-K. Plattner, G. W. Yohe, and F. W. Zwiers, 2010: *Guidance Note for Lead Authors of the IPCC Fifth Assessment Report on Consistent Treatment of Uncertainties*. Intergovernmental Panel on Climate Change (IPCC). http://www.ipcc.ch.

Moss, R., and S. Schneider, 2000: *Uncertainties in the IPCC TAR: Recommendations to Lead Authors for More Consistent Assessment and Reporting*. In: IPCC Supporting Material: Guidance Papers on Cross Cutting Issues in the Third Assessment Report of the IPCC. [Pachauri, R., T. Taniguchi, and K. Tanaka (eds.)]. Intergovernmental Panel on Climate Change, Geneva, pp. 33–51.

Moss, R., et al., 2008: *Towards new scenarios for analysis of emissions, climate change, impacts and response strategies*. Intergovernmental Panel on Climate Change, Geneva, 132 pp.

Moss, R. et al., 2010: The next generation of scenarios for climate change research and assessment. *Nature*, **463**, 747–756.

Nakićenović, N., and R. Swart (eds.), 2000: *Special Report on Emissions Scenarios*. *A Special Report of Working Group III of the Intergovernmental Panel on Climate Change*. Cambridge University Press, Cambridge, United Kingdom and New York, NY, USA, 599 pp.

Schwartz, S.E., and P. Warneck, 1995: Units for use in atmospheric chemistry. *Pure Appl. Chem.*, **67**, 1377–1406.